COST ACTION TU1208

CIVIL ENGINEERING APPLICATIONS OF GROUND PENETRATING RADAR

Second Action's General Meeting - Proceedings

Vienna, Austria, April 30 – May 2, 2014

Editors: Lara Pajewski & A. Benedetto

COST
EUROPEAN COOPERATION
IN SCIENCE AND TECHNOLOGY

TU1208 Basic Info
Start - End of Action: 4 April 2013 - 3 April 2017

Chair of the Action:
Dr. Lara Pajewski
Roma Tre University, IT
lara.pajewski@uniroma3.it

Vice-Chair of the Action:
Prof. Andreas Loizos
National Technical University of Athens, EL

COST TUD DC Chair:
Prof. Cristina Pronello
Politecnico di Torino, IT

COST TUD DC Rapporteur:
Dr. Goran Mladenovic
University of Belgrade, RS

COST Science Officer:
Dr. Mickael Pero
COST Office, BE

COST Administrative Officer:
Ms. Carmencita Malimban
COST Office, BE

Grant Holder:
Roma Tre University, Department of Engineering, IT

Editorial Coordinator of the Action:
Prof. Andrea Benedetto
Roma Tre University, IT

Chairs of Working Groups (WGs):
- WG1: Dr. Guido Manacorda, IDS Ingegneria dei Sistemi, IT
- WG2: Dr. Christina Plati, National Technical University of Athens, EL
- WG3: Dr. Antonis Giannopoulos, University of Edinburgh, UK
- WG4: Dr. Immo Trinks, Ludwig Boltzmann Institute for Archaeological Prospection and Virtual Archaeology, AT

Short-Term Scientific Missions (STSMs) Manager:
Prof. Marian Marciniak
National Institute of Telecommunications, PL

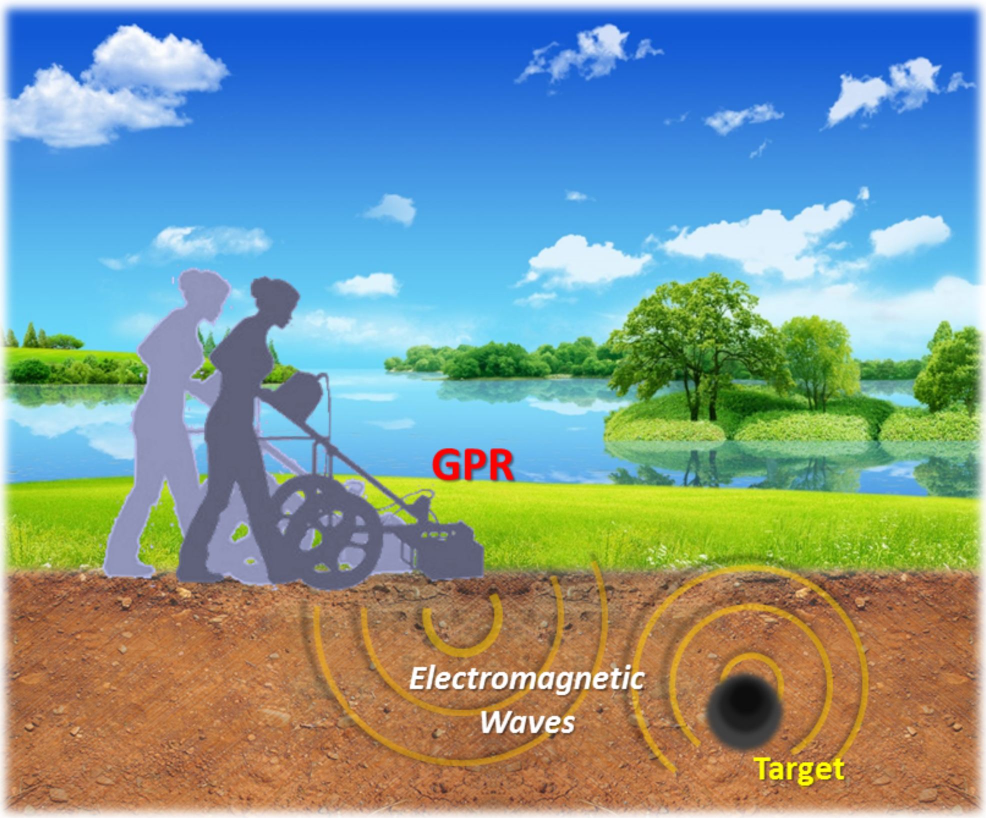

COST ACTION TU1208

CIVIL ENGINEERING APPLICATIONS OF GROUND PENETRATING RADAR

Second General Meeting – Proceedings
Vienna, Austria, April 30 – May 2, 2014
Editors: Lara Pajewski & Andrea Benedetto

PREFACE

TO THE PROCEEDINGS OF THE SECOND GENERAL MEETING

COST ACTION TU1208

"CIVIL ENGINEERING APPLICATIONS OF GROUND PENETRATING RADAR"

The Second General Meeting of the COST Action TU1208 "Civil Engineering Applications of Ground Penetrating Radar" was held in Vienna, Austria, from 30 April to 2 May, 2014. The meeting was organised jointly with the 2014 European Geosciences Union General Assembly (EGU GA, www.egu2014.eu*), the venue was the Austria Center Vienna.*

This special event closed the first year of the Action's activities and overall it included: the GI3.1 Session "Civil Engineering Applications of Ground Penetrating Radar" of the 2014 EGU GA, the Management Committee (MC) Meeting, and the Meetings of the four Working Groups (WGs) composing the general pattern of the scientific programme of the Action. The agenda of the event was very rich, with about 100 presentations. Several new and interesting results were presented and discussed, which were obtained by the Action's Members during the first year of the Action's lifetime. The main focus was on innovative GPR technologies and methodologies, advanced inspection strategies and practices, accurate electromagnetic methods for the modelling of GPR scenarios, inversion and imaging techniques, and data-processing algorithms. Further presentations dealt with the applications of GPR outside from the civil engineering field, as well as with the integration of GPR with other Non-Destructive Testing (NDT) techniques.

The joint organisation of the Second General Meeting with the 2014 EGU GA was complicated, but our efforts were rewarded. The EGU GA brought together 12.437 scientists from 106 countries, of which

27% were students, studying all the Earth disciplines, planetary and space sciences. Being open to such a wide scientific community, the Second General Meeting gave huge visibility to COST and to the Action TU1208, created new synergies and attracted new Members, whilst providing a significant added value to the discussion of the Action's ongoing projects and results.

We were delighted by the participation to our meeting of Dr Diarmad Campbell, Chair of the COST Action TU1206 "SUB-URBAN - A European Network to Improve Understanding and Use of the Ground Beneath our Cities." Points of common interest between TU1206 and TU1208 were identified and ideas for future cooperation were fruitfully discussed. In particular, it was decided to organise together a workshop on 3D Gelogical Modelling, to be held in Edinburgh, on November 19-21, 2014. This event will aim to exchange progress, problems and solutions to understand and communicate the 3D composition and properties of the subsurface, in order to aid science-based decision making.

The Proceedings of the Second General Meeting consist of five parts.

The first part collects contributions of general interest, including reports on the COST Action TU1208, the COST Action TU1206, and the COST initiatives for Early-Stage Researchers. This part of the Proceedings also comprises three papers resuming noteworthy training activities carried out by TU1208 Members: in Estonia, GPR possibilities were shown to elementary-school children and citizens; in the United Kingdom and France, practical training courses were offered to GPR end-users.

The second part of the Proceedings focuses on the development of innovative GPR systems, which is the main objective of WG1. The recent NeTTUN (Leading the Way in New Technology for the Tunnelling Industry) and ORFEUS (Optimised Radar to Find Every

Utility in the Street) FP7 projects are presented, where the use of GPR was experimented in tunnelling works and in the installation of pipes through horisontal directional drilling; both the projects addressed the installation of GPR on the cutting head. Novel GPR systems for the high-resolution inspection of walls and structures are being developed by Action Members and the ongoing activities are presented here. The improvement of GPR energetic properties and the electromagnetic-field exposure of GPR users are being studied. An in-depth comparison of results obtained by pulsed and stepped-frequency radar systems is being performed; results are being confronted in the time, frequency and wavelet domains. Research activities are carried out within the Action, in order to develop tools for accurate electromagnetic modelling of GPR antennas in realistic environments. Finally, the first part of this volume includes a contribution concerned with the importance of accurate positioning in GPR surveys.

The third part of this volume collects contributions on the non-invasive surveying, by using GPR, of pavements, bridges, tunnels, railways and buildings; further contributions deal with the detection of underground utilities and voids, as well as with the determination by using GPR of the volumetric water content in structures, substructures, foundations and soil. These are the main topics faced by WG2 Members. For all the Projects included in WG2 of the COST Action TU1208, the Project Leaders prepared reports, resuming the progress of the scientific activities. Moreover, a number of new case studies carried out by Action Members during the first year of the Action, as a contribution to the various WG2 Projects, were presented during the Second General Meeting and are resumed here.

The subsequent part of the Proceedings includes papers on the development of advanced electromagnetic-modelling, imaging, inversion and data-processing techniques for GPR (WG3 topics). The

part is opened with an introduction to inverse scattering and processing of GPR data, followed by a paper about the finite-difference time-domain modelling of the GPR signal based on data obtained from other NDT methods as an approach to achieve a more exhaustive interpretation of field data, and by a contribution about the full-waveform inversion of GPR data for civil-engineering applications. Next, for all the Projects included in WG3 of the COST Action TU1208, the Project Leaders prepared reports, resuming the progress of the scientific activities. Further papers present more in detail how Members from different Countries contributed to the WG3 Projects during the first year of the Action.

The last part of these Proceedings includes works focusing on the applications of GPR outside from the civil-engineering area, as well as on the integration of different technologies for non-destructive investigations in civil and environmental engineering, archaeology, coastal-region and industrial-site characterisation. This part of the volume also comprises a report resuming the objectives and main results of the COST Action SPLASHCOS - Submerged Prehistoric Archaeology and Landscapes of the Continental Shelf; such Action ended in 2013 and was focused on the preservation, managing and dissemination of the archives of archaeological and palaeoclimatic information locked up on the drowned prehistoric landscapes of the European continental shelf.

We deeply thank COST for funding the COST Action TU1208, the Second General Meeting, and the publication of this volume. We are grateful to the COST Office for its constant and strong support to the COST Action TU1208 during the first year of the Action's lifetime and for exceptionally authorising the organisation of the Second General Meeting inside the 2014 EGU GA. In particular, we would like to thank Prof Tatiana Kovacikova, Head of Science Operations, our previous and present Science Officers, Dr Thierry Goger and Dr

Mickael Pero, and our Administrative Officer, Ms Carmencita Malimban. A very special thank goes from the Chair of the Action to Prof Cristina Pronello, Chair of the COST Transport and Urban Development (TUD) Domain Committee (DC), for appreciating and strongly supporting the idea of this meeting, for her help, encouragement, inspiration, and for all her wise suggestions. We would like to thank Prof Goran Mladenovic, DC Rapporteur for the Action TU1208, for his guidance during this first year of the Action's lifetime. We also wish to thank Prof Walter Schmidt, President of the EGU Division on Geosciences Instrumentation, for the time and efforts spent for the organisation of the GI activities within the 2014 EGU GA, for having fulfilled our requests concerning the scheduling of the GI3.1 oral and poster slots, and for his support to the organisation of the EGU GA Splinter Meetings constituting our MC and WG Meetings. Last but not least, we would like to greatly thank all the TU1208 Members for their proactive and enthusiastic participation to the Second General Meeting and for their continuous efforts to make this COST Action a success.

We look forward to the next TU1208 event: the 15th International Conference on Ground Penetrating Radar (GPR 2014), co-organised by our Action along with the Université catholique de Louvain, to be held in Brussels, Belgium, on June 30 – July 4, 2014.

Lara Pajewski, Chair of the COST Action TU1208
Andrea Benedetto, Editorial Coordinator of the COST Action TU1208

FIRST-YEAR ACTIVITIES AND RESULTS OF THE COST ACTION TU1208 “CIVIL ENGINEERING APPLICATIONS OF GROUND PENETRATING RADAR”

Lara Pajewski (IT), Andrea Benedetto (IT),
Andreas Loizos (GR), Evert Slob (NL), Fabio Tosti (IT)
lara.pajewski@uniroma3.it

The abstract is published in *Geophysical Research Abstracts*, Vol. 16, EGU2014-16933, 2014 and is available on *www.egu2014.eu*

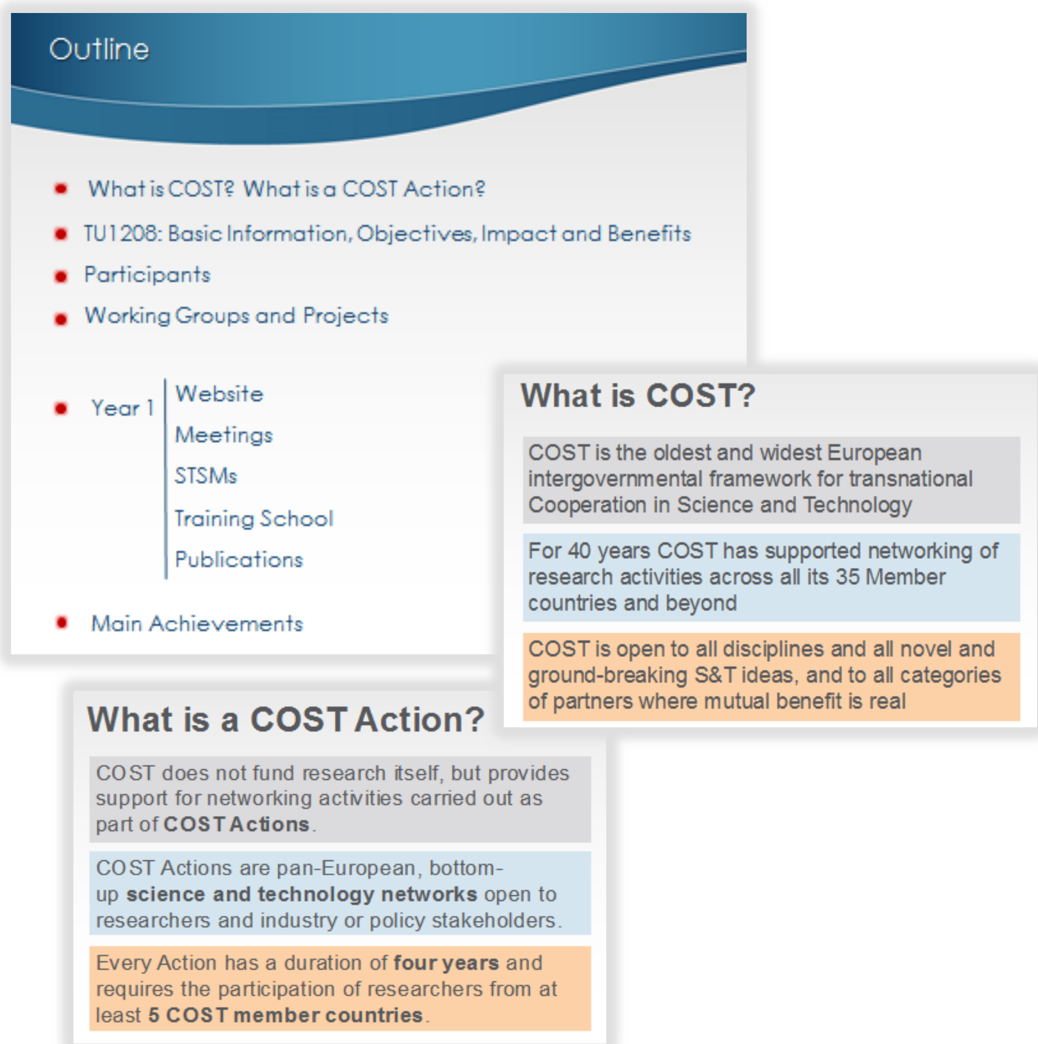

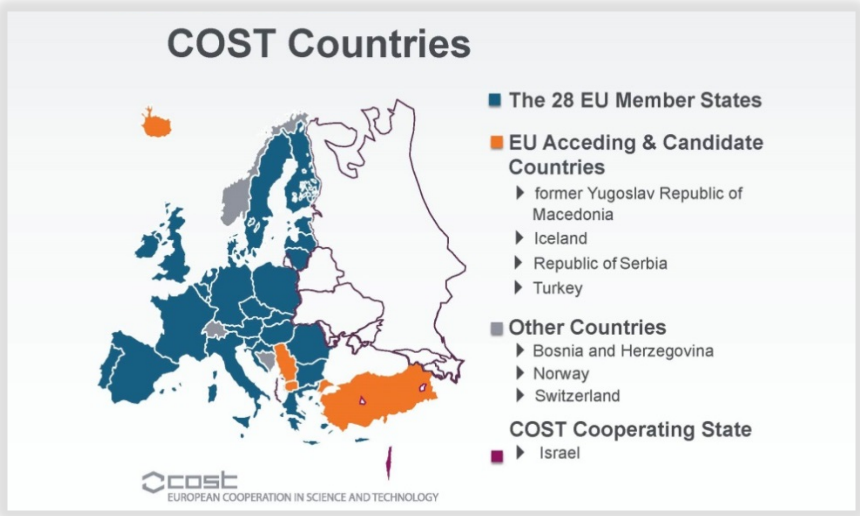
COST Countries
The 28 EU Member States
EU Acceding & Candidate Countries
former Yugoslav Republic of Macedonia
Iceland
Republic of Serbia
Turkey
Other Countries
Bosnia and Herzegovina
Norway
Switzerland
COST Cooperating State
Israel
cost
EUROPEAN COOPERATION IN SCIENCE AND TECHNOLOGY


COST Action TU1208: Basic Information
Chair of the Action
Lara Pajewski
"Roma Tre" University (IT)
lara.pajewski@uniroma3.it
Vice-Chair of the Action
Andreas Loizos
National Technical University of Athens (EL)
DC Rapporteur
Goran Mladenovic
University of Belgrade (RS)
Science and Administrative Officers
Mickael Pero and Carmencita Malimban
COST Office (BE)
Start date – End date
4th April 2013 – 3rd April 2017
www.GPRadar.eu
www.cost.eu/domains_actions/tud/Actions/TU1208


COST Action TU1208: Main Objective
Exchange and increase scientific-technical knowledge and experience of GPR techniques in Civil Engineering, simultaneously promoting throughout Europe the effective use of this safe and non-destructive technique.
The COST Action TU1208 is establishing and strengthening active links between universities, research institutes, companies and end users working in this field, fostering and accelerating its long-term development in Europe.

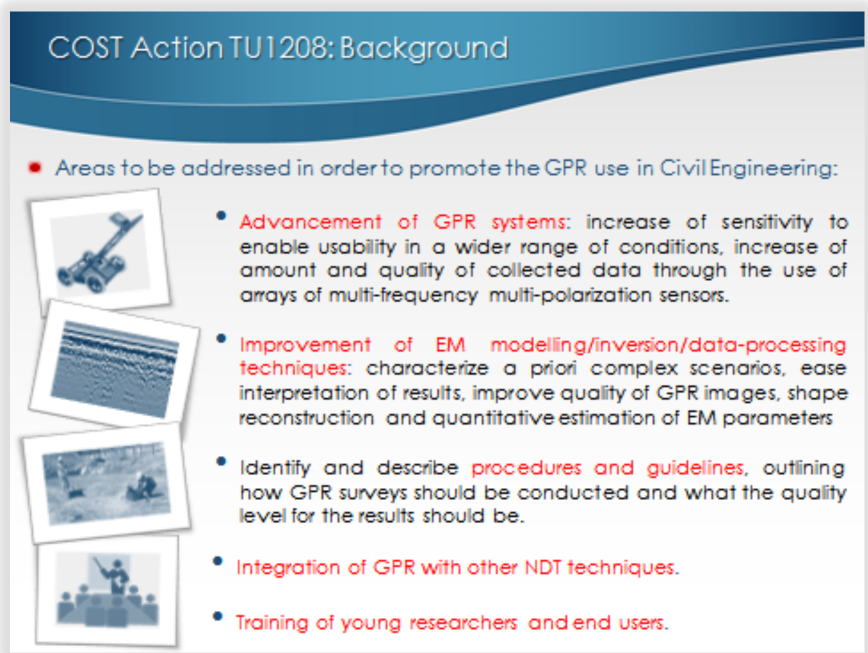
COST Action TU1208: Background
Areas to be addressed in order to promote the GPR use in Civil Engineering:
Advancement of GPR systems: increase of sensitivity to enable usability in a wider range of conditions, increase of amount and quality of collected data through the use of arrays of multi-frequency multi-polarization sensors.
Improvement of EM modelling/inversion/data-processing techniques: characterize a priori complex scenarios, ease interpretation of results, improve quality of GPR images, shape reconstruction and quantitative estimation of EM parameters
Identify and describe procedures and guidelines, outlining how GPR surveys should be conducted and what the quality level for the results should be.
Integration of GPR with other NDT techniques.
Training of young researchers and end users.

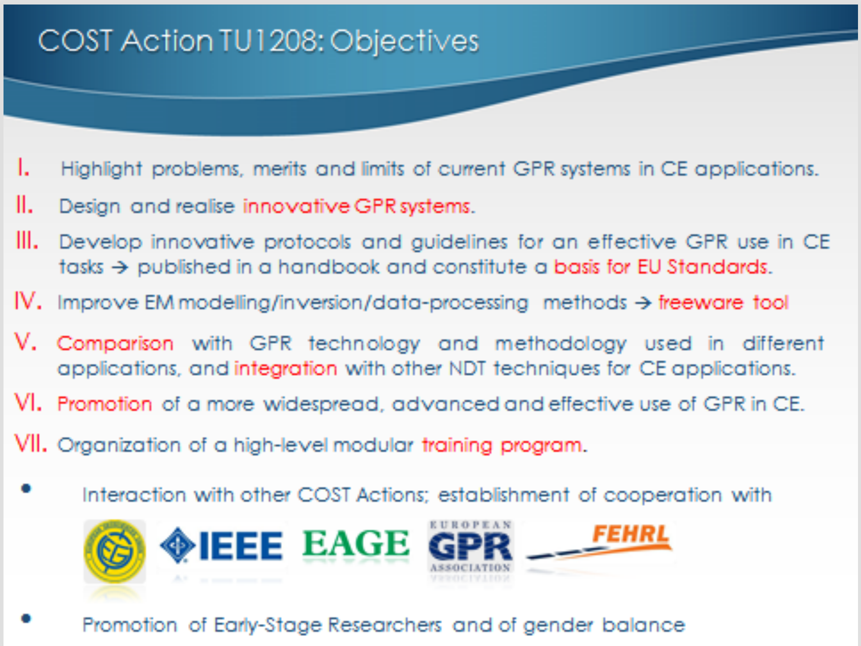
COST Action TU1208: Objectives
I. Highlight problems, merits and limits of current GPR systems in CE applications.
II. Design and realise innovative GPR systems.
III. Develop innovative protocols and guidelines for an effective GPR use in CE tasks → published in a handbook and constitute a basis for EU Standards.
IV. Improve EM modelling/inversion/data-processing methods → freeware tool
V. Comparison with GPR technology and methodology used in different applications, and integration with other NDT techniques for CE applications.
VI. Promotion of a more widespread, advanced and effective use of GPR in CE.
VII. Organization of a high-level modular training program.
• Interaction with other COST Actions; establishment of cooperation with
IEEE
EAGE
EUROPEAN GPR ASSOCIATION
FEHRL
• Promotion of Early-Stage Researchers and of gender balance

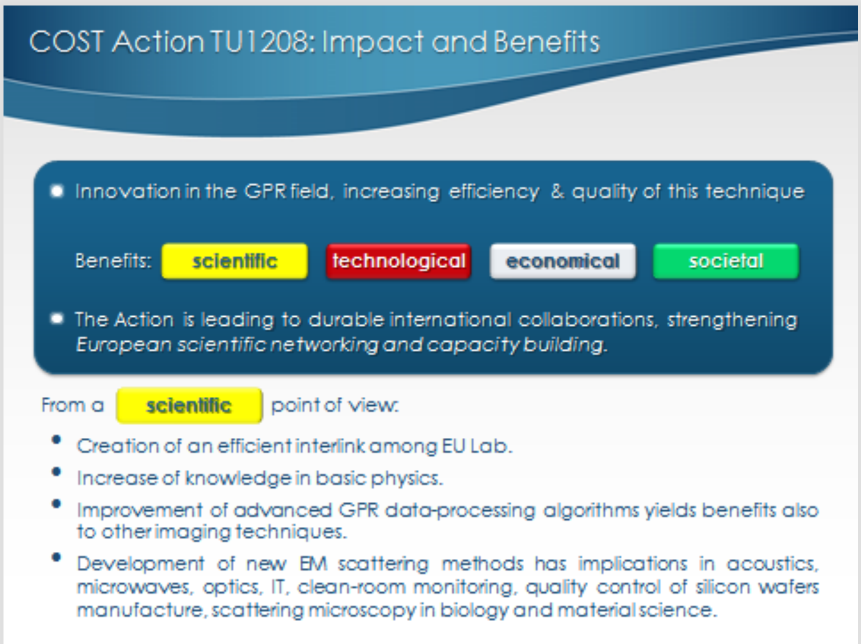
COST Action TU1208: Impact and Benefits
• Innovation in the GPR field, increasing efficiency & quality of this technique
Benefits: scientific technological economical societal
• The Action is leading to durable international collaborations, strengthening European scientific networking and capacity building.
From a scientific point of view:
• Creation of an efficient interlink among EU Lab.
• Increase of knowledge in basic physics.
• Improvement of advanced GPR data-processing algorithms yields benefits also to other imaging techniques.
• Development of new EM scattering methods has implications in acoustics, microwaves, optics, IT, clean-room monitoring, quality control of silicon wafers manufacture, scattering microscopy in biology and material science.

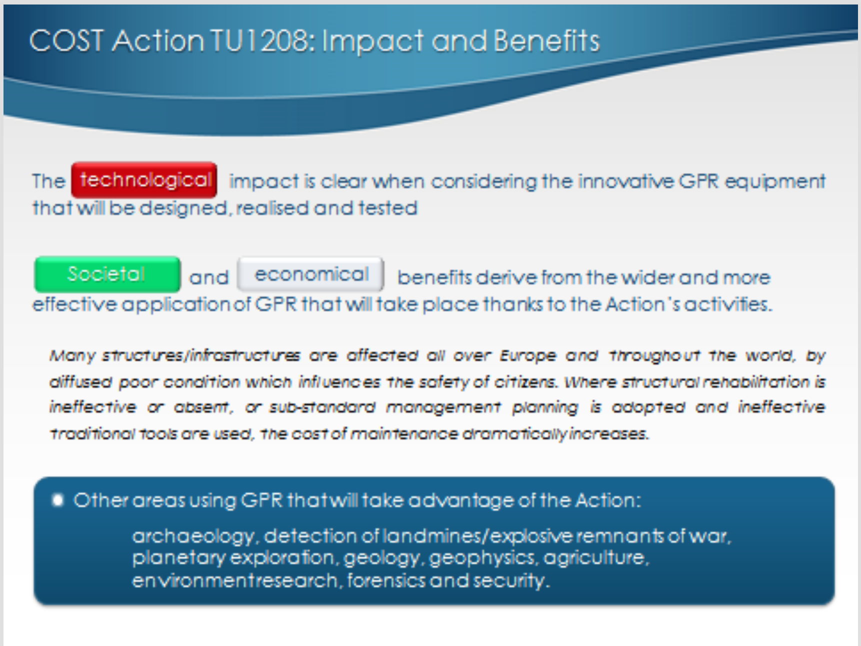
COST Action TU1208: Impact and Benefits
The technological impact is clear when considering the innovative GPR equipment that will be designed, realised and tested
Societal and economical benefits derive from the wider and more effective application of GPR that will take place thanks to the Action's activities.
Many structures/infrastructures are affected all over Europe and throughout the world, by diffused poor condition which influences the safety of citizens. Where structural rehabilitation is ineffective or absent, or sub-standard management planning is adopted and ineffective traditional tools are used, the cost of maintenance dramatically increases.
Other areas using GPR that will take advantage of the Action:
archaeology, detection of landmines/explosive remnants of war, planetary exploration, geology, geophysics, agriculture, environment research, forensics and security.

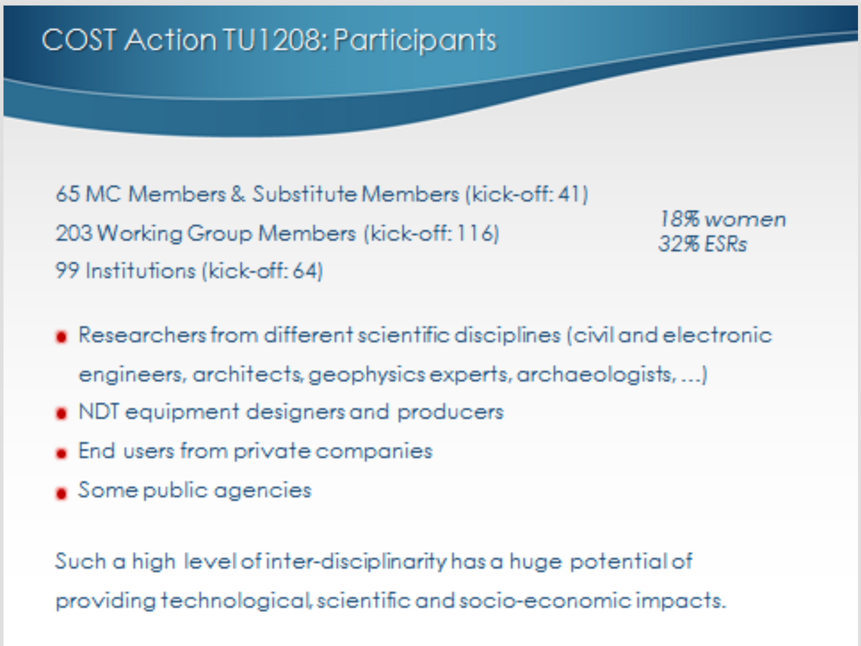
COST Action TU1208: Participants
65 MC Members & Substitute Members (kick-off: 41)
203 Working Group Members (kick-off: 116)
99 Institutions (kick-off: 64)
18% women
32% ESRs
Researchers from different scientific disciplines (civil and electronic engineers, architects, geophysics experts, archaeologists, ...)
NDT equipment designers and producers
End users from private companies
Some public agencies
Such a high level of inter-disciplinarity has a huge potential of providing technological, scientific and socio-economic impacts.

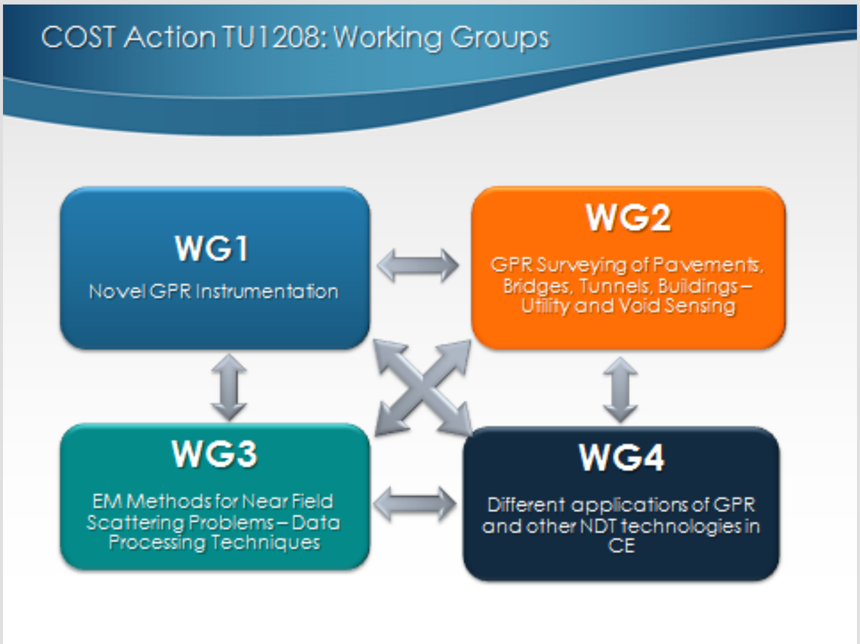
COST Action TU1208: Working Groups
WG1
Novel GPR Instrumentation
WG2
GPR Surveying of Pavements, Bridges, Tunnels, Buildings – Utility and Void Sensing
WG3
EM Methods for Near Field Scattering Problems – Data Processing Techniques
WG4
Different applications of GPR and other NDT technologies in CE

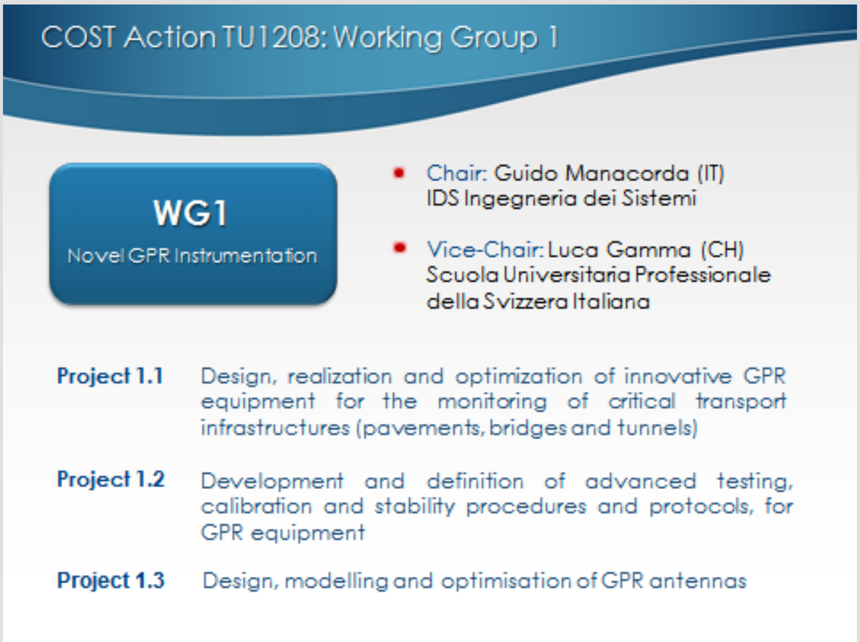
COST Action TU1208: Working Group 1
WG1
Novel GPR Instrumentation
Chair: Guido Manacorda (IT)
IDS Ingegneria dei Sistemi
Vice-Chair: Luca Gamma (CH)
Scuola Universitaria Professionale della Svizzera Italiana
Project 1.1
Design, realization and optimization of innovative GPR equipment for the monitoring of critical transport infrastructures (pavements, bridges and tunnels)
Project 1.2
Development and definition of advanced testing, calibration and stability procedures and protocols, for GPR equipment
Project 1.3
Design, modelling and optimisation of GPR antennas

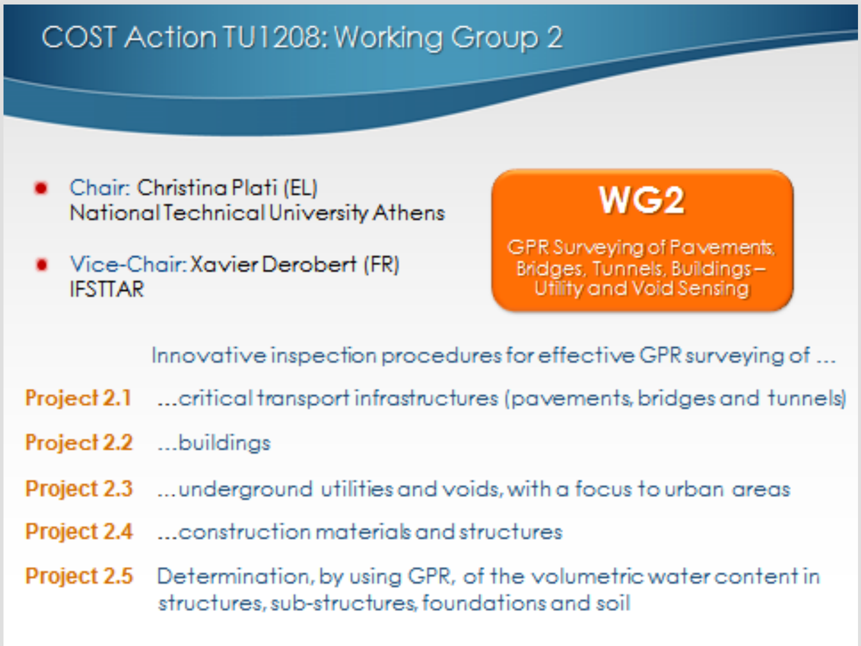
COST Action TU1208: Working Group 2
Chair: Christina Plati (EL)
National Technical University Athens
Vice-Chair: Xavier Derobert (FR)
IFSTTAR
WG2
GPR Surveying of Pavements, Bridges, Tunnels, Buildings – Utility and Void Sensing
Innovative inspection procedures for effective GPR surveying of ...
Project 2.1 ...critical transport infrastructures (pavements, bridges and tunnels)
Project 2.2 ...buildings
Project 2.3 ...underground utilities and voids, with a focus to urban areas
Project 2.4 ...construction materials and structures
Project 2.5 Determination, by using GPR, of the volumetric water content in structures, sub-structures, foundations and soil

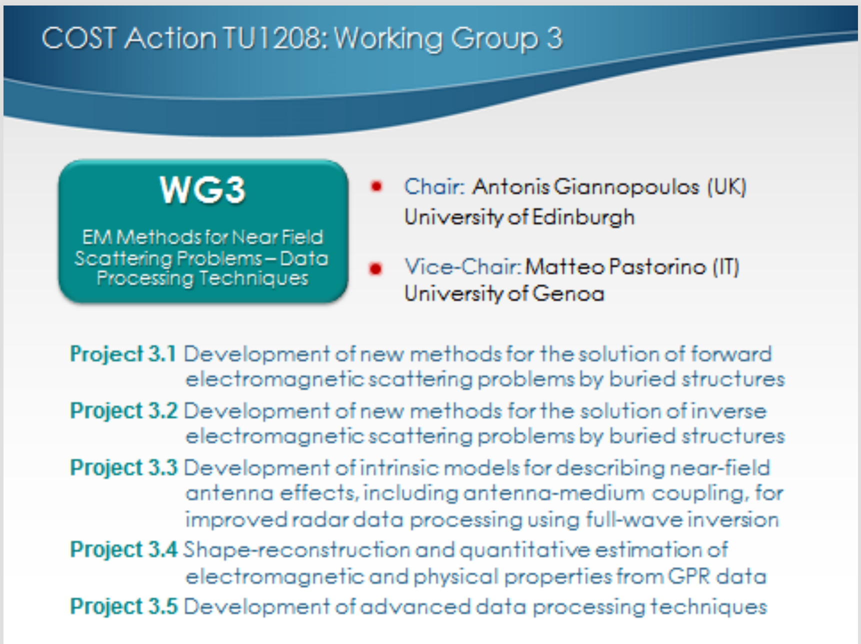
COST Action TU1208: Working Group 3
WG3
EM Methods for Near Field Scattering Problems – Data Processing Techniques
Chair: Antonis Giannopoulos (UK)
University of Edinburgh
Vice-Chair: Matteo Pastorino (IT)
University of Genoa
Project 3.1 Development of new methods for the solution of forward electromagnetic scattering problems by buried structures
Project 3.2 Development of new methods for the solution of inverse electromagnetic scattering problems by buried structures
Project 3.3 Development of intrinsic models for describing near-field antenna effects, including antenna-medium coupling, for improved radar data processing using full-wave inversion
Project 3.4 Shape-reconstruction and quantitative estimation of electromagnetic and physical properties from GPR data
Project 3.5 Development of advanced data processing techniques

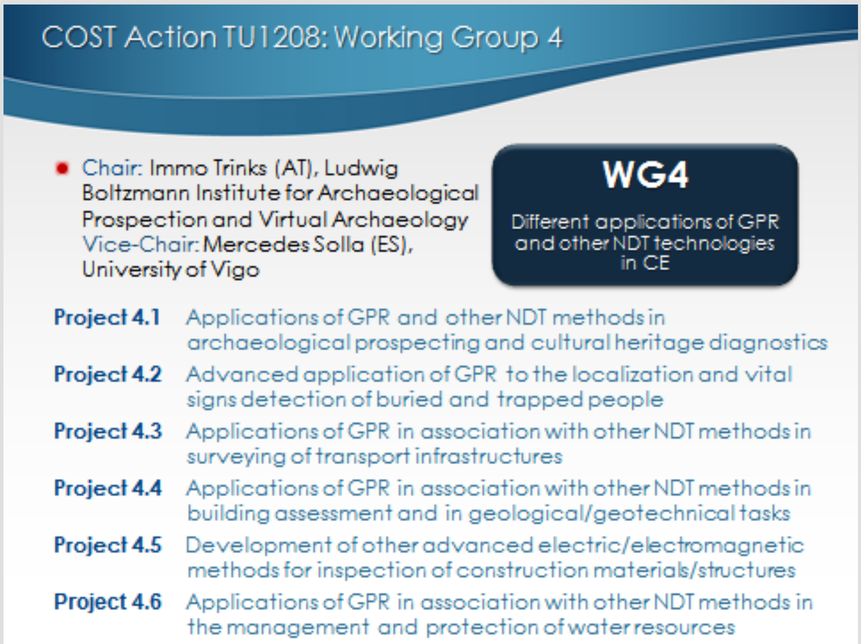
COST Action TU1208: Working Group 4
Chair: Immo Trinks (AT), Ludwig Boltzmann Institute for Archaeological Prospection and Virtual Archaeology
Vice-Chair: Mercedes Solla (ES), University of Vigo
WG4
Different applications of GPR and other NDT technologies in CE
Project 4.1 Applications of GPR and other NDT methods in archaeological prospecting and cultural heritage diagnostics
Project 4.2 Advanced application of GPR to the localization and vital signs detection of buried and trapped people
Project 4.3 Applications of GPR in association with other NDT methods in surveying of transport infrastructures
Project 4.4 Applications of GPR in association with other NDT methods in building assessment and in geological/geotechnical tasks
Project 4.5 Development of other advanced electric/electromagnetic methods for inspection of construction materials/structures
Project 4.6 Applications of GPR in association with other NDT methods in the management and protection of water resources


cost
EUROPEAN COOPERATION IN SCIENCE AND TECHNOLOGY
Action TU1208
Civil Engineering Applications of Ground Penetrating Radar
HOME ABOUT ACTIVITIES RESOURCES PEOPLE LINKS MEMBERS AREA
Austria Belgium Croatia Czech Republic Denmark
Finland France Germany Greece Italy
Latvia Macedonia Malta The Netherlands Norway
Poland Portugal Spain Switzerland Turkey
United Kingdom
Armenia Australia Hong Kong Rwanda U.S.A.
GPR
Electromagnetic Waves
Target
www.GPRadar.eu

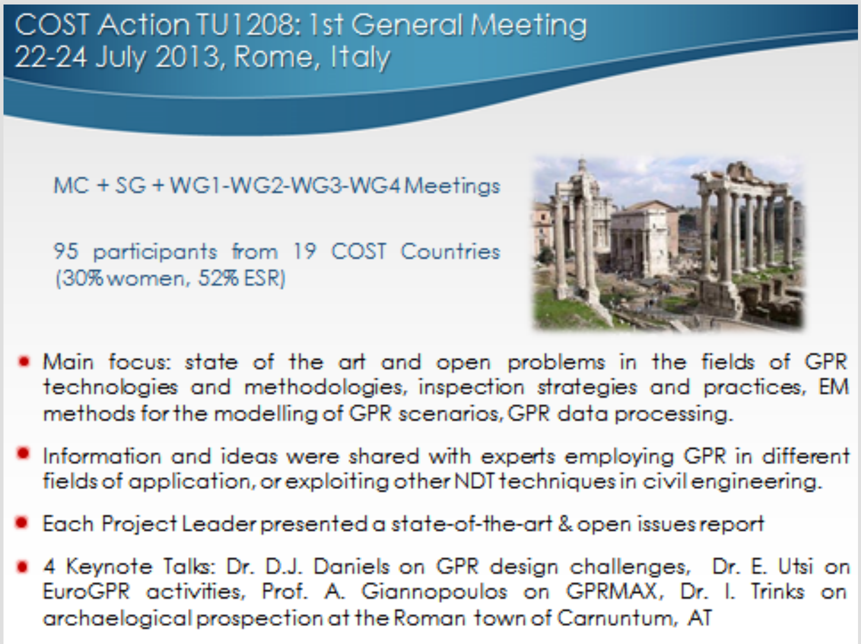
COST Action TU1208: 1st General Meeting
22-24 July 2013, Rome, Italy
MC + SG + WG1-WG2-WG3-WG4 Meetings
95 participants from 19 COST Countries (30% women, 52% ESR)
Main focus: state of the art and open problems in the fields of GPR technologies and methodologies, inspection strategies and practices, EM methods for the modelling of GPR scenarios, GPR data processing.
Information and ideas were shared with experts employing GPR in different fields of application, or exploiting other NDT techniques in civil engineering.
Each Project Leader presented a state-of-the-art & open issues report
4 Keynote Talks: Dr. D.J. Daniels on GPR design challenges, Dr. E. Utsi on EuroGPR activities, Prof. A. Giannopoulos on GPRMAX, Dr. I. Trinks on archaelogical prospection at the Roman town of Carnuntum, AT

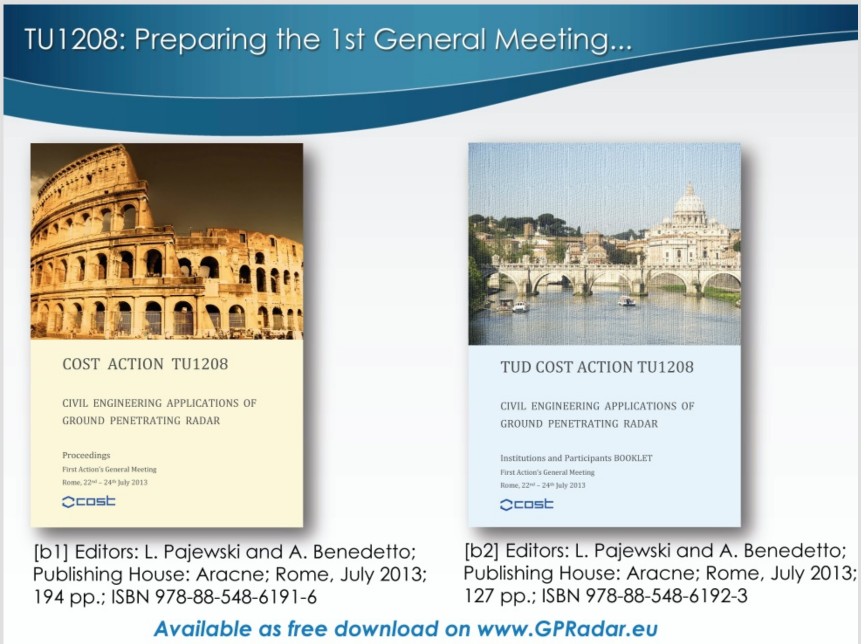
TU1208: Preparing the 1st General Meeting...
COST ACTION TU1208
CIVIL ENGINEERING APPLICATIONS OF GROUND PENETRATING RADAR
Proceedings
First Action's General Meeting
Rome, 22nd - 24th July 2013
TUD COST ACTION TU1208
CIVIL ENGINEERING APPLICATIONS OF GROUND PENETRATING RADAR
Institutions and Participants BOOKLET
First Action's General Meeting
Rome, 22nd - 24th July 2013
[b1] Editors: L. Pajewski and A. Benedetto; Publishing House: Aracne; Rome, July 2013; 194 pp.; ISBN 978-88-548-6191-6
[b2] Editors: L. Pajewski and A. Benedetto; Publishing House: Aracne; Rome, July 2013; 127 pp.; ISBN 978-88-548-6192-3
Available as free download on www.GPRadar.eu

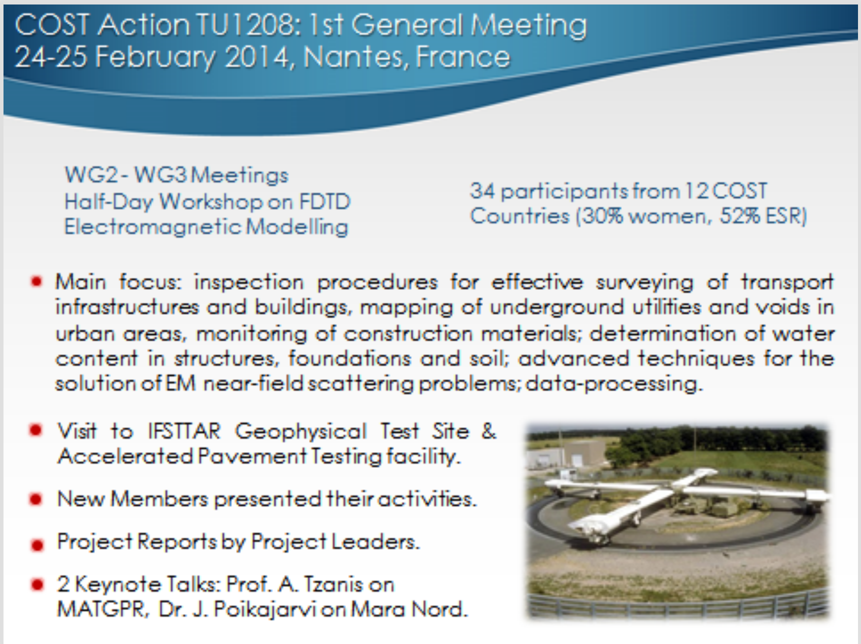
COST Action TU1208: 1st General Meeting
24-25 February 2014, Nantes, France
WG2 - WG3 Meetings
Half-Day Workshop on FDTD
Electromagnetic Modelling
34 participants from 12 COST Countries (30% women, 52% ESR)
Main focus: inspection procedures for effective surveying of transport infrastructures and buildings, mapping of underground utilities and voids in urban areas, monitoring of construction materials; determination of water content in structures, foundations and soil; advanced techniques for the solution of EM near-field scattering problems; data-processing.
Visit to IFSTTAR Geophysical Test Site & Accelerated Pavement Testing facility.
New Members presented their activities.
Project Reports by Project Leaders.
2 Keynote Talks: Prof. A. Tzanis on MATGPR, Dr. J. Poikajarvi on Mara Nord.


COST Action TU1208: 2nd General Meeting
30 April – 2 May 2014, Vienna, Austria
EUROPEAN GEOSCIENCES UNION
cost
30 April:
GI3.1 Session of EGU GA “Civil Engineering Applications of GPR”
1 May:
MC Meeting, WG1 and WG2 Meetings
2 May:
WG3 and WG4 Meetings

COST Action TU1208: Training School 1

Microwave Imaging and Diagnostics: Theory, Techniques and Applications

24-28 March 2014, Madonna di Campiglio, IT

Organised jointly with COST Action TD1301 *Development of a European-based Collaborative Network to Accelerate Technological, Clinical and Commercialization Progress in the Area of Medical Microwave Imaging* and EU School of Antennas

35 Trainees (28.6% women, 100% ESR), 8 Trainers, 6 TU1208 + 6 TD1301 Grants

Beneficiary
Fabio Mangini, "La Sapienza" University, Rome, IT
Laurence Mertens, Université catholique de Louvain, Louvain-La-Neuve, BE
Iraklis Giannakis, The University of Edinburgh, Edinburgh, UK
Saba Adabi, "Roma Tre" University, Rome, IT
Albéric De Coster, Université catholique de Louvain, Louvain-La-Neuve, BE
Belén Larumbe Gonzalo, Public University of Navarra, Pamplona, ES

COST Action TU1208
"Civil Engineering Applications of Ground Penetrating Radar"

Training School Report

Microwave Imaging and Diagnostics:
Theory, Techniques, and Applications

Granted Trainees:
Saba Adabi, "Roma Tre" University, Engineering Department, Rome, Italy
Alberic De Coster, UCL, Louvaine-la-Neuve, Belgium
Iraldis Giannakis, University of Edinburgh, Edinburgh, United Kingdom
Belen Larumbe, , Public University of Navarra, Spain
Fabio Mangini, Sapienza University, Rome, Italy
Laurence Mertens, UCL, Louvaine-la-Neuve, Belgium

Training School Dates: 24 March 2014 – 28 March 2014

1

COST Action TU1208: Training School 2

Future Radar System: Radar2020 – 5-9 May 2014, Karlsruhe, Germany

Time	Monday, May 5.	Tuesday, May 6.	Wed.day, May 7.	Thursday, May 8.	Friday, May 9.
08:30 - 10:00	Registration	RCS Definitions RCS of Targets *Wiesbeck*	Future Radar, OFDM-Radar, *Wiesbeck*	UWB-Radar Basics *Yarovoy*	SAR Systems SAR DBF, Interferr. *Younis*
Break					
10:30 - 12:00	Intro. Overview, Radar History, *Wiesbeck*	Radar Overview Pulse-Radar, *Wiesbeck*	DSSS Coding Dig. Beamforming *Wiesbeck*	Surface Pen. Radar GPR, TWR, ... *Yarovoy*	Discussion 10:30-11:30
Lunch					11:30 – 12:30
13:30 - 15:00	Prop. Phenom., Polarimetry *Wiesbeck*	CW-, FM-CW-Radar, Coding *Zwick*	MIMO Radar Array Imaging *Wiesbeck*	SAR Principles, SAR Processing, *Younis*	Exam 12:30-14:30
Break					
15:30 - 17:00	Radar Equation, Resolution,Accuracy *Wiesbeck*	Automotive Radar Virtual Drive *Zwick*	Exercise + Automotive Radar Demonstration *Daimler, IHE*	Perform. Param., SAR Modes, *Younis*	
17:15- 18:00	*Exercise, Discussion*	*Exercise, Discussion*	Dinner 19:00	*Exercise, Discussion*	

Organised jointly with the EU School of Antennas & EU Microwave Association

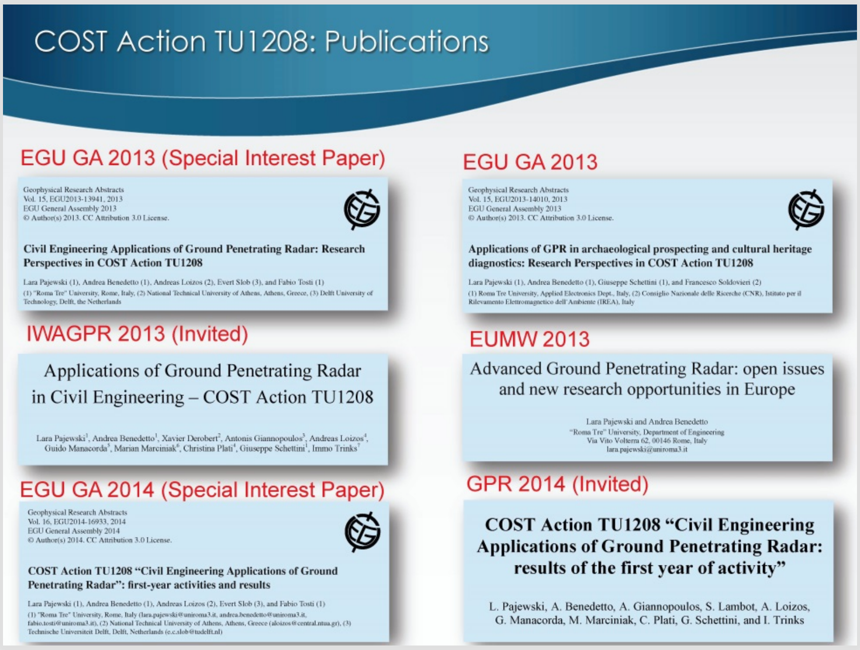
COST Action TU1208: Publications
EGU GA 2013 (Special Interest Paper)
Civil Engineering Applications of Ground Penetrating Radar: Research Perspectives in COST Action TU1208
EGU GA 2013
Applications of GPR in archaeological prospecting and cultural heritage diagnostics: Research Perspectives in COST Action TU1208
IWAGPR 2013 (Invited)
Applications of Ground Penetrating Radar in Civil Engineering – COST Action TU1208
EUMW 2013
Advanced Ground Penetrating Radar: open issues and new research opportunities in Europe
EGU GA 2014 (Special Interest Paper)
COST Action TU1208 "Civil Engineering Applications of Ground Penetrating Radar": first-year activities and results
GPR 2014 (Invited)
COST Action TU1208 "Civil Engineering Applications of Ground Penetrating Radar: results of the first year of activity"
L. Pajewski, A. Benedetto, A. Giannopoulos, S. Lambot, A. Loizos, G. Manacorda, M. Marciniak, C. Plati, G. Schettini, and I. Trinks

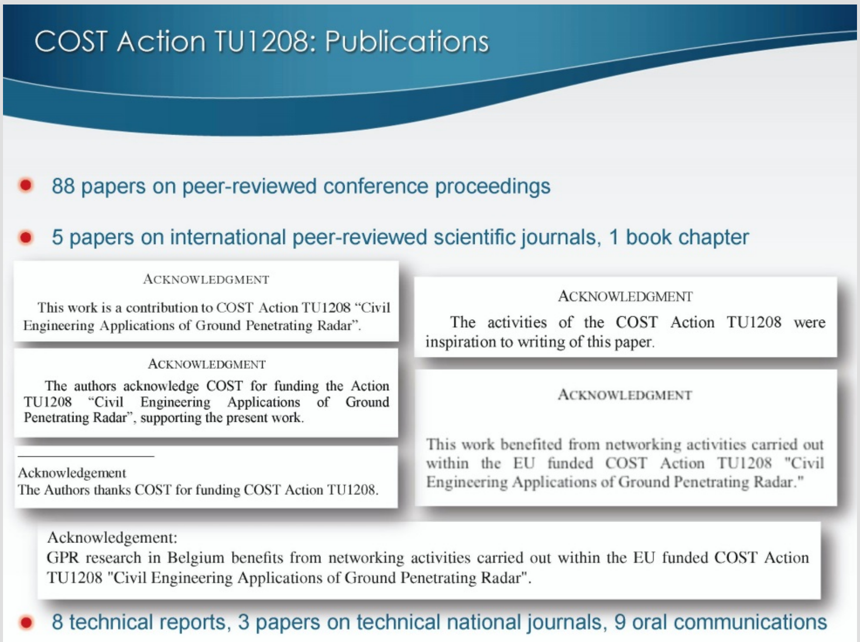
COST Action TU1208: Publications
88 papers on peer-reviewed conference proceedings
5 papers on international peer-reviewed scientific journals, 1 book chapter
ACKNOWLEDGMENT
This work is a contribution to COST Action TU1208 "Civil Engineering Applications of Ground Penetrating Radar".
ACKNOWLEDGMENT
The activities of the COST Action TU1208 were inspiration to writing of this paper.
ACKNOWLEDGMENT
The authors acknowledge COST for funding the Action TU1208 "Civil Engineering Applications of Ground Penetrating Radar", supporting the present work.
ACKNOWLEDGMENT
This work benefited from networking activities carried out within the EU funded COST Action TU1208 "Civil Engineering Applications of Ground Penetrating Radar."
Acknowledgement
The Authors thanks COST for funding COST Action TU1208.
Acknowledgement:
GPR research in Belgium benefits from networking activities carried out within the EU funded COST Action TU1208 "Civil Engineering Applications of Ground Penetrating Radar".
8 technical reports, 3 papers on technical national journals, 9 oral communications

Time-table

Year 2

- Multidisciplinary and multinational application and comparison of GPR equipment, inspection practice, EM and data-processing algorithms.
- Strong human exchange and sharing of resources: numerous Short-Term Scientific Missions.

Year 3

- Outline and test of innovative inspection procedures, on the basis of the activity carried out during the previous years.
- Codification and development of new EM algorithms and of new methods for an effective data-processing.
- Assessment for design of novel GPR equipment and prototype realization.
- Short-Term Scientific Missions!

Time-table

Year 4

- Critical study and review of results obtained during preceding years.
- Coordination and elaboration of a handbook with protocols and guidelines at EU level.
- Optimization of the new EM and data-processing codes. Realization of graphical user interface and manuals. Releasing freeware software for the benefit of GPR community.
- Test and optimization of the new GPR equipment.
- Short-Term Scientific Missions!

COST Action TU1206 "SUB-URBAN - A European network to improve understanding and use of the ground beneath our cities"

Diarmad Campbell (UK), Johannes de Beer (NO), David Lawrence (UK), Michiel van der Meulen (NL), Susie Mielby (DK), David Hay (UK), Ray Scanlon (IE), Ignace Campenhout (NL), Renate Taugs (DE), Ingelov Eriksson (NO) - *sdgc@bgs.ac.uk*

The abstract is published in *Geophysical Research Abstracts*, Vol. 16, EGU2014-11333, 2014 and is available on *www.egu2014.eu*

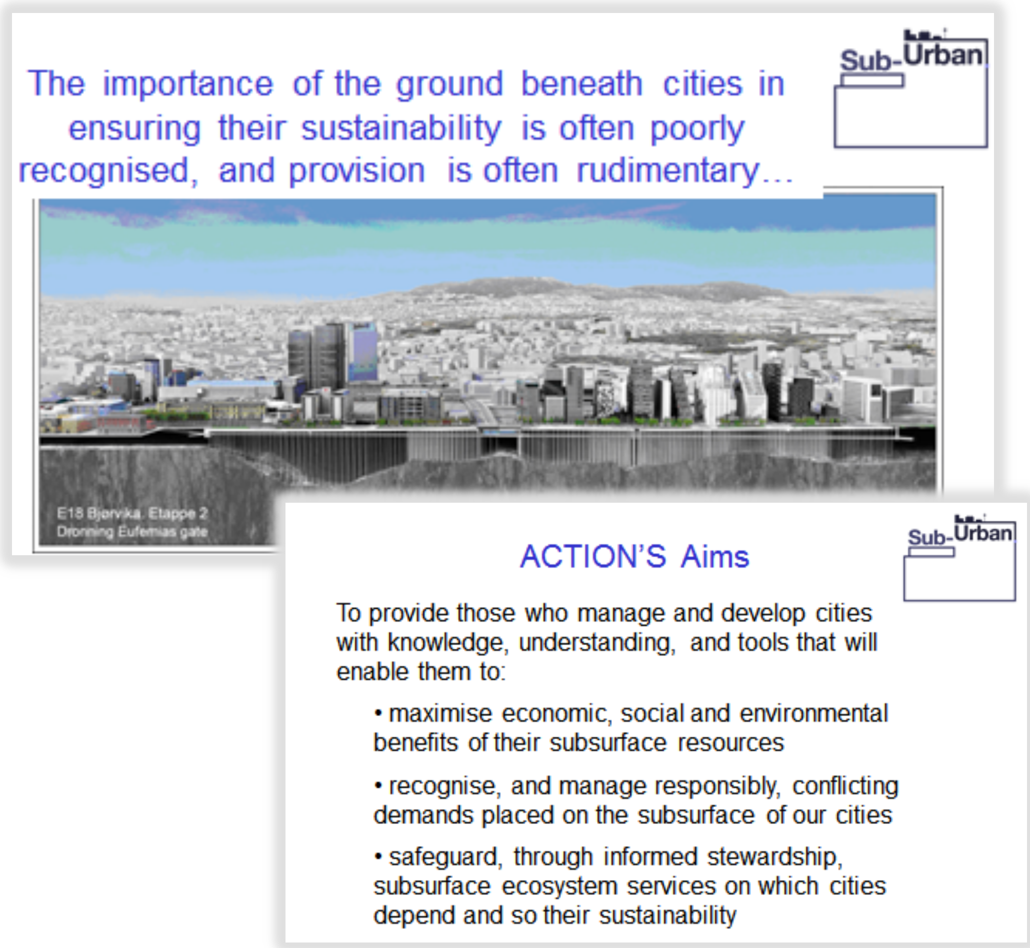

Geothermal energy

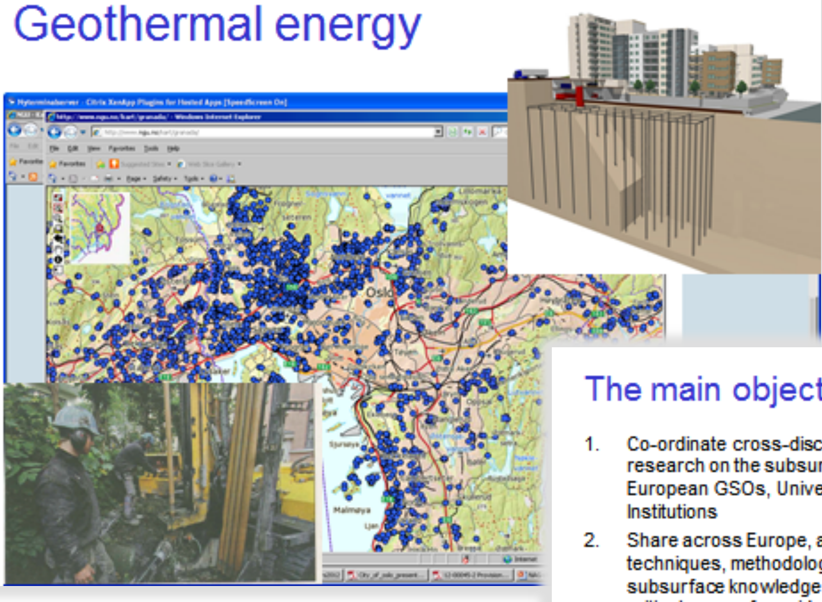

The main objectives:

1. Co-ordinate cross-disciplinary research on the subsurface in European GSOs, Universities, and Institutions
2. Share across Europe, and beyond, techniques, methodologies, and subsurface knowledge to build critical mass of providers/users
3. Inform and Empower policy and decision makers about urban subsurface, provide them with tools and basis to make informed decisions
4. Make subsurface knowledge complementary to, and interoperable with, current above-ground 3D city modelling to broaden its ***relevance and impact*** (economic, environmental and social)

Key Aspiration

Transform relationships between experts who develop urban subsurface knowledge and those who can benefit most from it - urban decision makers, practitioners and the wider research community

Approach

Sub-Urban

- Establish state-of-the-art in urban subsurface knowledge: data acquisition, subsurface modelling, subsurface planning
(WG1 – City-partner focus, case studies, multi-scalar)
- Identify/develop good practice, address gaps and develop a ‘Toolbox’ of guidance for key subsurface issues (Data availability, monitoring, 3D/4D modelling /linkage workflows, knowledge delivery)
(WG2 – Multiple Process-related Subprojects)
- Trial, refine, and rollout toolbox, in and beyond Europe for use in policy, planning, practice
(WG3 – City-partner led)
- Develop Data and Knowledge-based Virtuous Circles involving Practitioners, City-partners, Geological Survey Organisations, and other Researchers (WG4)

Implementation of scientific work plan

Sub-Urban

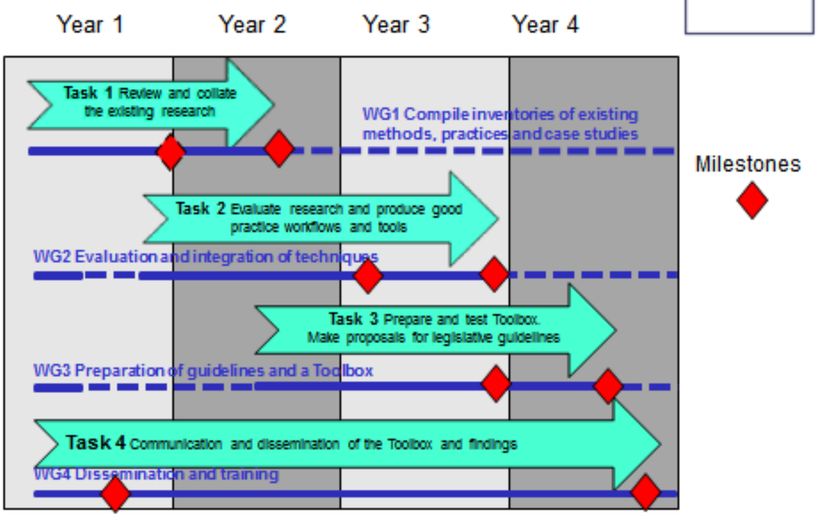

Current State of Urban Sub-Surface Knowledge, Needs and Aims - WG1

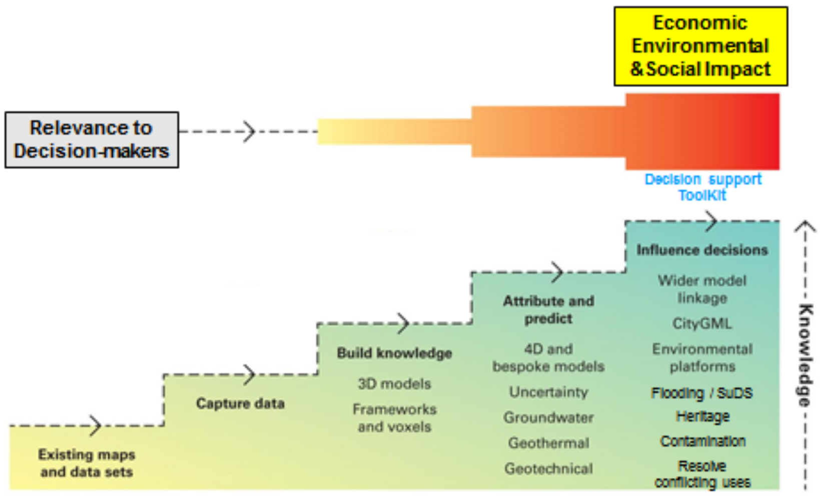

WG1 Task

- 10 key city studies in progress
- Assess, review and collate
  - **current capabilities** in managing / modelling **subsurface data** in an **urban context**
  - related **needs of decision-makers**
- covering
  - legislation
  - methodologies, technologies
  - interactions between GSOs, researchers and decision-makers
  - EU directives and design codes

Scope of Toolbox WG2

Data	Specifications
	Online capture
	Data management
	Data delivery
	Data re-use
3D Model	Workflows for main modelling software and city scenarios
	Deterministic modelling
	Stochastic modelling
	Model uncertainty
Knowledge Development	Physical properties e.g. hydraulic conductivity, aquifers
	Chemical properties
	Groundwater, historical & predictive time series models for aquifer protection, sustainable drainage, climate-change effects
Knowledge Use	City case-studies
	Visualisation
	Monitoring
Knowledge delivery and integration	Building Information modelling (BIM) and CityGML
	Buried infrastructure, Archaeological/cultural assets
	Volumetric planning
	Ecosystem services stewardship
	Aquifer vulnerability/groundwater protection
	Thermal and other mineral resource extraction and storage
	Ground stability and foundation conditions
	Risk management in development/construction
	Protection of cultural heritage
	Hazard identification and risk management
	Burial of services and development of subsurface infrastructure, including underground transport, storage and waste disposal

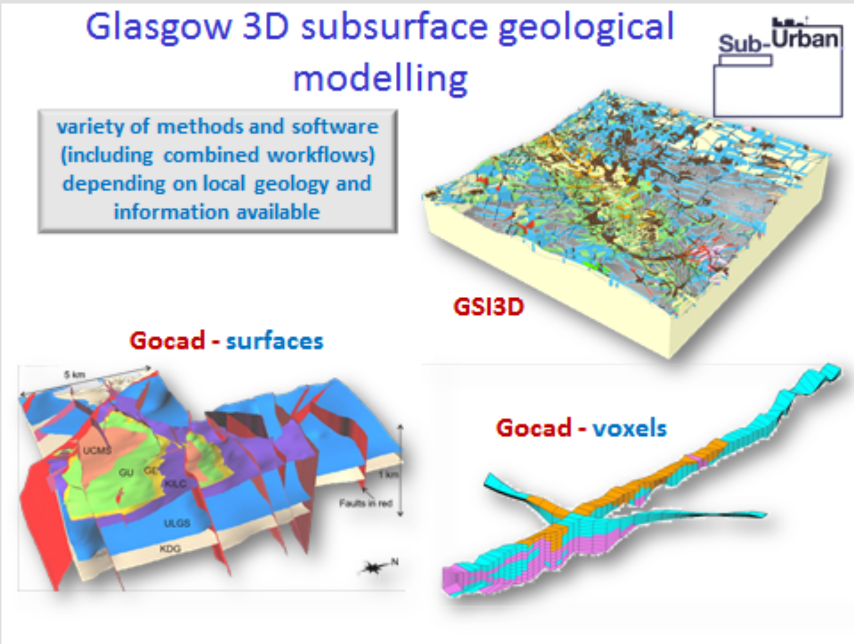
Glasgow 3D subsurface geological modelling
Sub-Urban
variety of methods and software (including combined workflows) depending on local geology and information available
GSI3D
Gocad - surfaces
Gocad - voxels

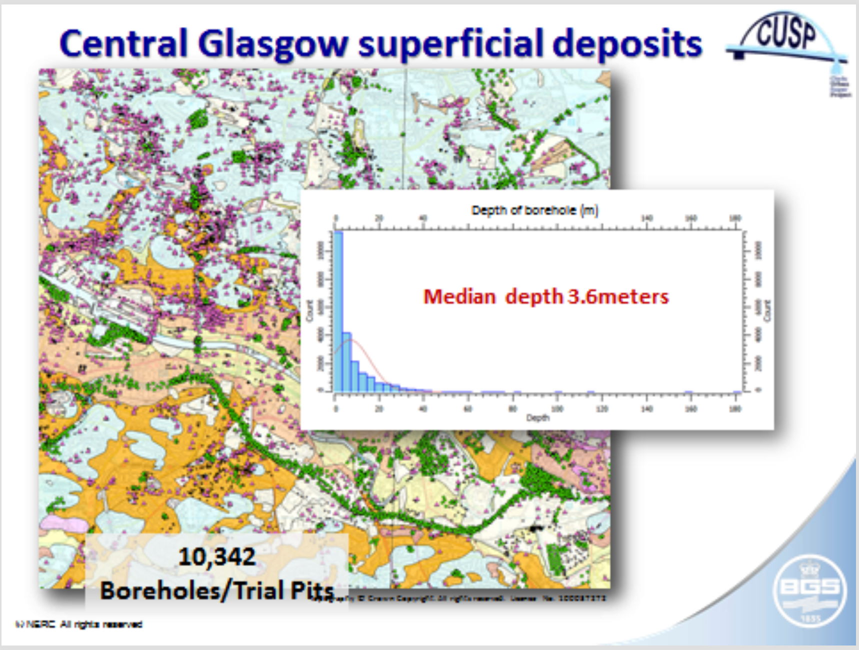
Central Glasgow superficial deposits
CUSP
Depth of borehole (m)
Median depth 3.6meters
Depth
10,342
Boreholes/Trial Pits
© NERC All rights reserved

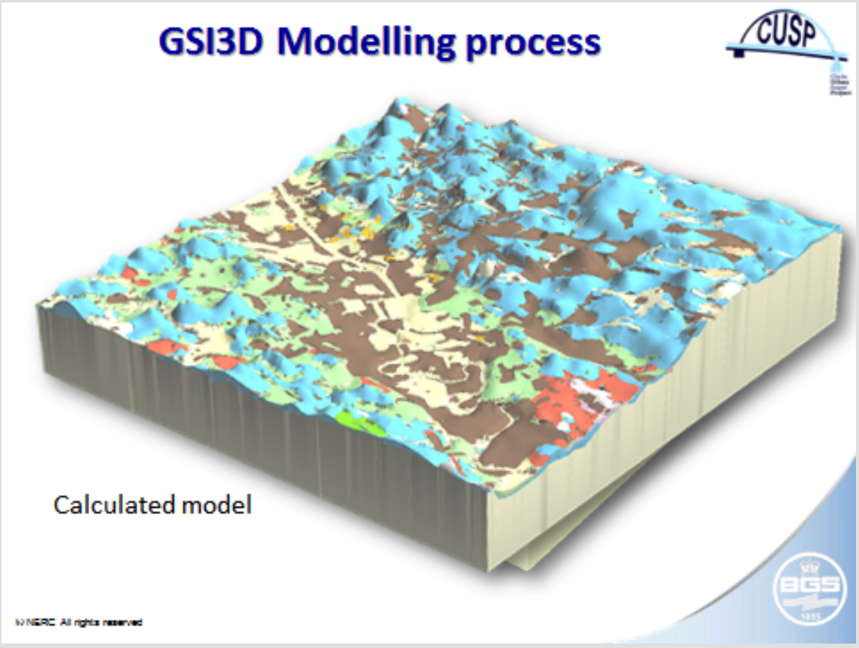
GSI3D Modelling process
CUSP
Calculated model
© NERC All rights reserved
BGS

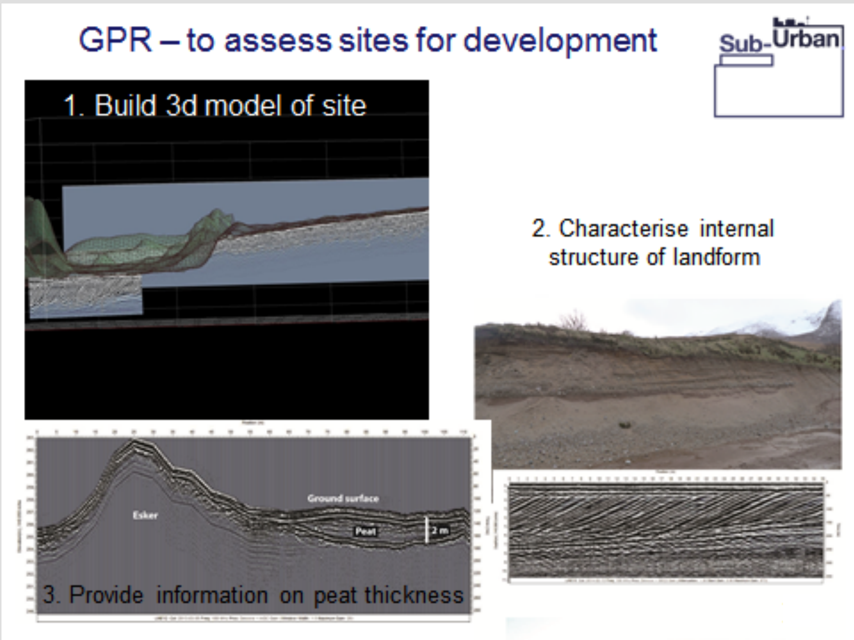
GPR – to assess sites for development
Sub-Urban
1. Build 3d model of site
2. Characterise internal structure of landform
Esker
Ground surface
Peat
2 m
3. Provide information on peat thickness

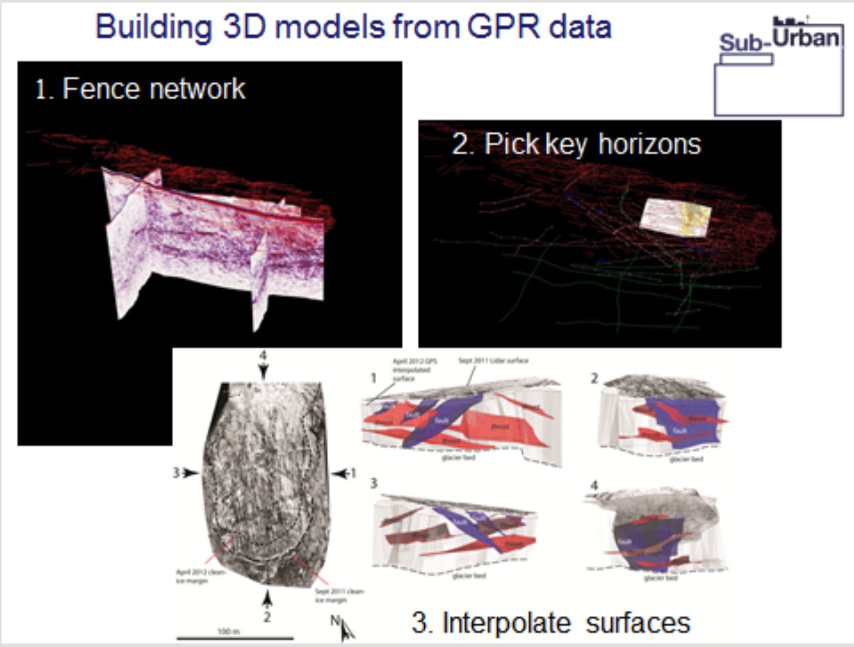
Building 3D models from GPR data
Sub-Urban
1. Fence network
2. Pick key horizons
3. Interpolate surfaces

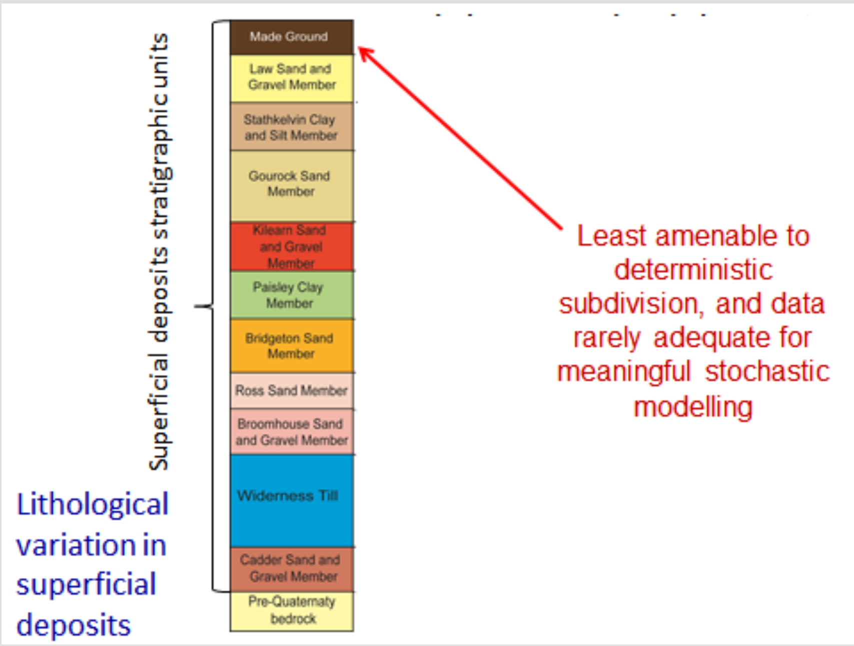
Superficial deposits stratigraphic units
Made Ground
Law Sand and Gravel Member
Stathkelvin Clay and Silt Member
Gourock Sand Member
Kilearn Sand and Gravel Member
Paisley Clay Member
Bridgeton Sand Member
Ross Sand Member
Broomhouse Sand and Gravel Member
Wilderness Till
Cadder Sand and Gravel Member
Pre-Quaternaty bedrock
Least amenable to deterministic subdivision, and data rarely adequate for meaningful stochastic modelling
Lithological variation in superficial deposits

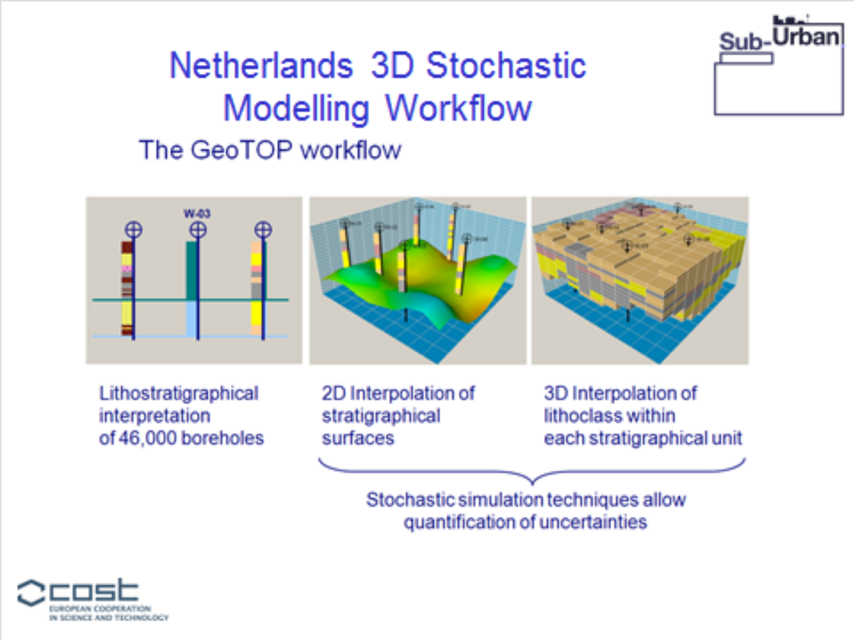
Netherlands 3D Stochastic Modelling Workflow
The GeoTOP workflow
Sub-Urban
W-03
Lithostratigraphical interpretation of 46,000 boreholes
2D Interpolation of stratigraphical surfaces
3D Interpolation of lithoclass within each stratigraphical unit
Stochastic simulation techniques allow quantification of uncertainties
cost
EUROPEAN COOPERATION IN SCIENCE AND TECHNOLOGY

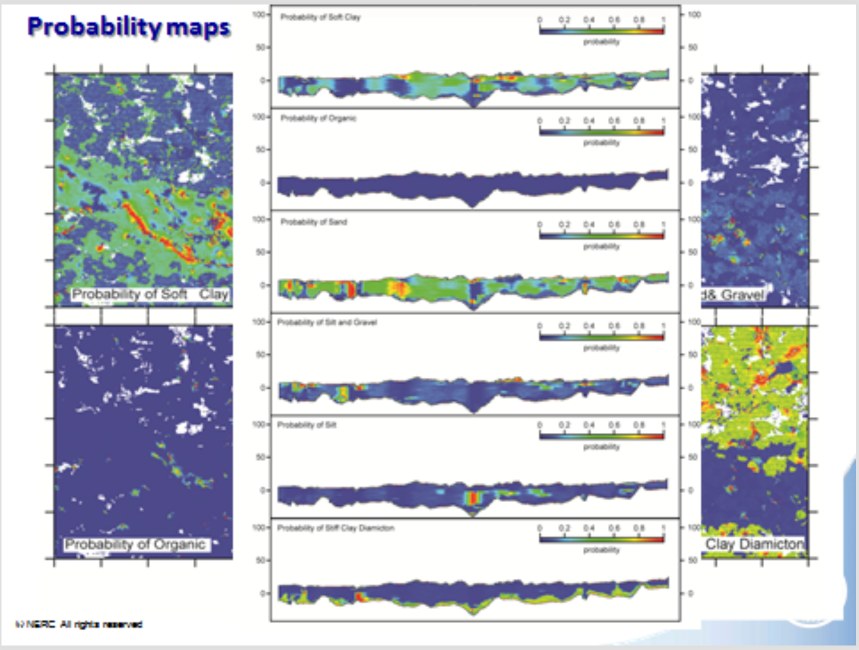
Probability maps
Probability of Soft Clay
Probability of Organic
Probability of Sand
Probability of Silt and Gravel
Probability of Silt
Probability of Stiff Clay Diamicton
probability
d& Gravel
Clay Diamicton
© NERC All rights reserved

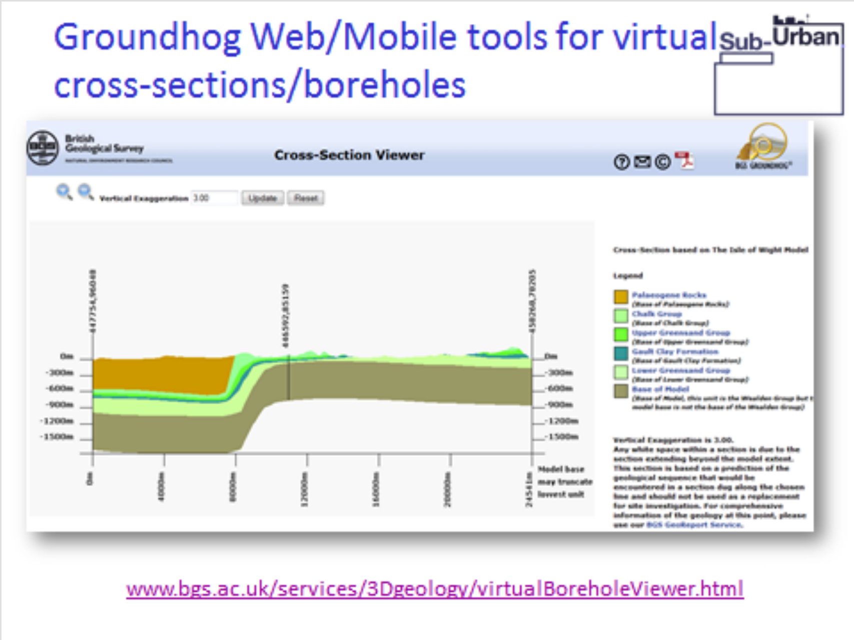
Groundhog Web/Mobile tools for virtual cross-sections/boreholes
Sub-Urban
Cross-Section Viewer
Cross-Section based on The Isle of Wight Model
Legend
www.bgs.ac.uk/services/3Dgeology/virtualBoreholeViewer.html

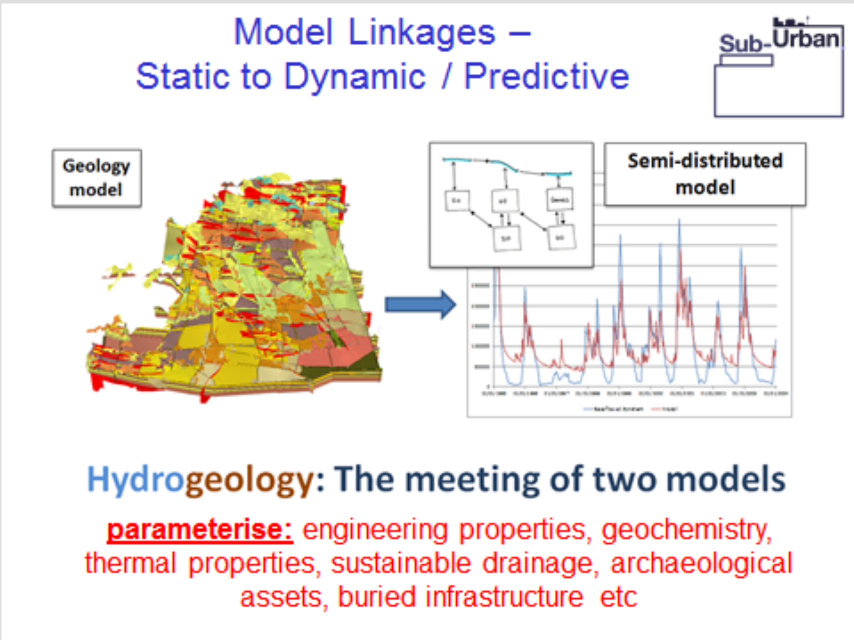
Model Linkages –
Static to Dynamic / Predictive
Sub-Urban
Geology model
Semi-distributed model
Hydrogeology: The meeting of two models
parameterise: engineering properties, geochemistry, thermal properties, sustainable drainage, archaeological assets, buried infrastructure etc

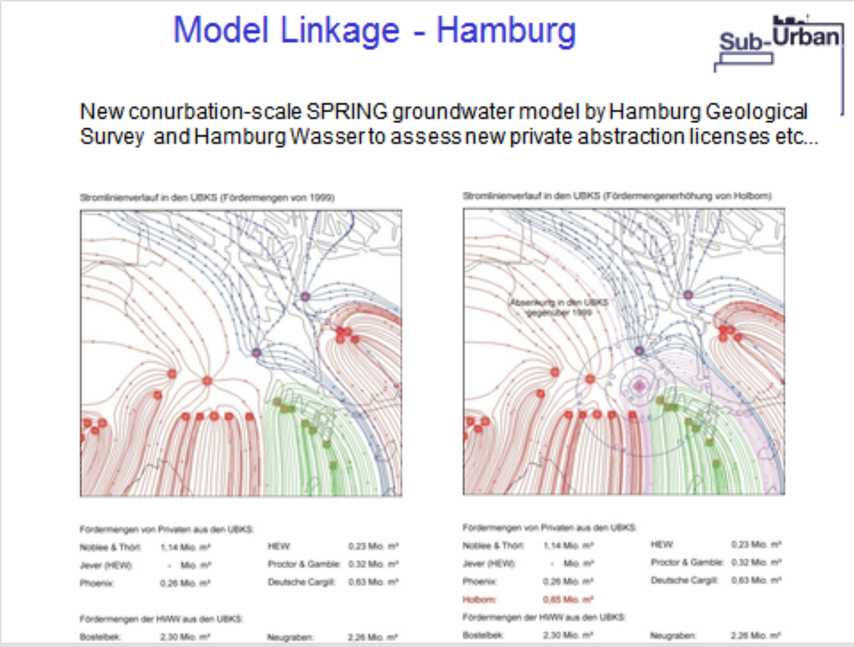
Model Linkage - Hamburg
Sub-Urban
New conurbation-scale SPRING groundwater model by Hamburg Geological Survey and Hamburg Wasser to assess new private abstraction licenses etc...
Stromlinienverlauf in den UBKS (Fördermengen von 1999)
Stromlinienverlauf in den UBKS (Fördermengenerhöhung von Holborn)
Fördermengen von Privaten aus den UBKS:
Noblee & Thörl: 1,14 Mio. m³
Jever (HEW): - Mio. m³
Phoenix: 0,26 Mio. m³
HEW: 0,23 Mio. m³
Proctor & Gamble: 0,32 Mio. m³
Deutsche Cargill: 0,63 Mio. m³
Holborn: 0,65 Mio. m³
Fördermengen der HWW aus den UBKS:
Bostelbek: 2,30 Mio. m³
Neugraben: 2,26 Mio. m³

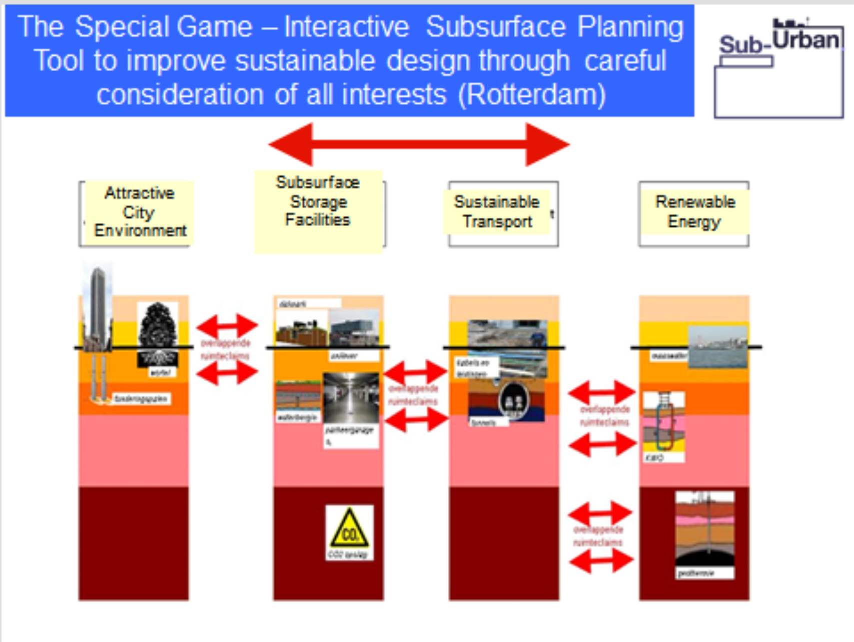
The Special Game – Interactive Subsurface Planning Tool to improve sustainable design through careful consideration of all interests (Rotterdam)
Sub-Urban
Attractive City Environment
Subsurface Storage Facilities
Sustainable Transport
Renewable Energy

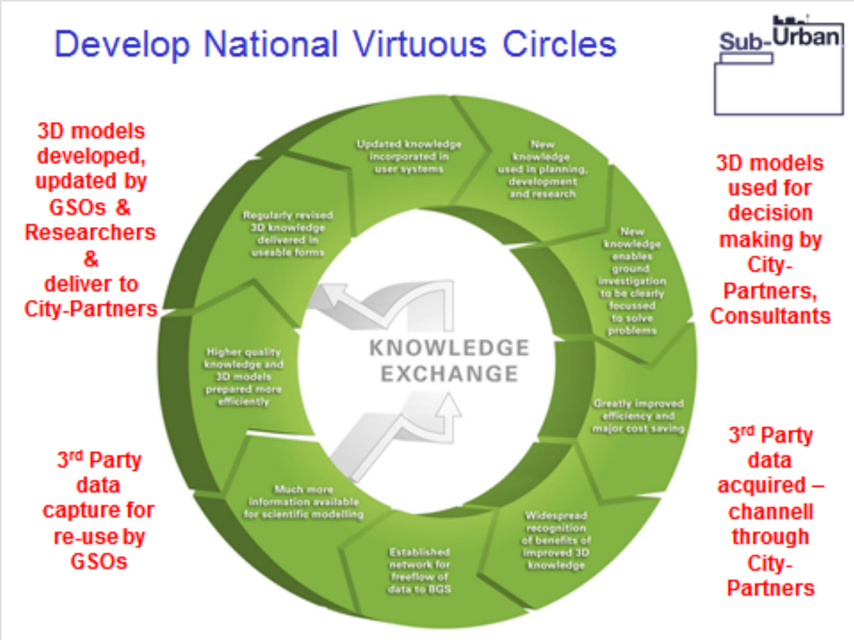
Develop National Virtuous Circles
Sub-Urban
3D models developed, updated by GSOs & Researchers & deliver to City-Partners
3rd Party data capture for re-use by GSOs
3D models used for decision making by City-Partners, Consultants
3rd Party data acquired – channell through City-Partners
Updated knowledge incorporated in user systems
New knowledge used in planning, development and research
New knowledge enables ground investigation to be clearly focussed to solve problems
Greatly improved efficiency and major cost saving
Widespread recognition of benefits of improved 3D knowledge
Established network for freeflow of data to BGS
Much more information available for scientific modelling
Higher quality knowledge and 3D models prepared more efficiently
Regularly revised 3D knowledge delivered in useable forms
KNOWLEDGE EXCHANGE

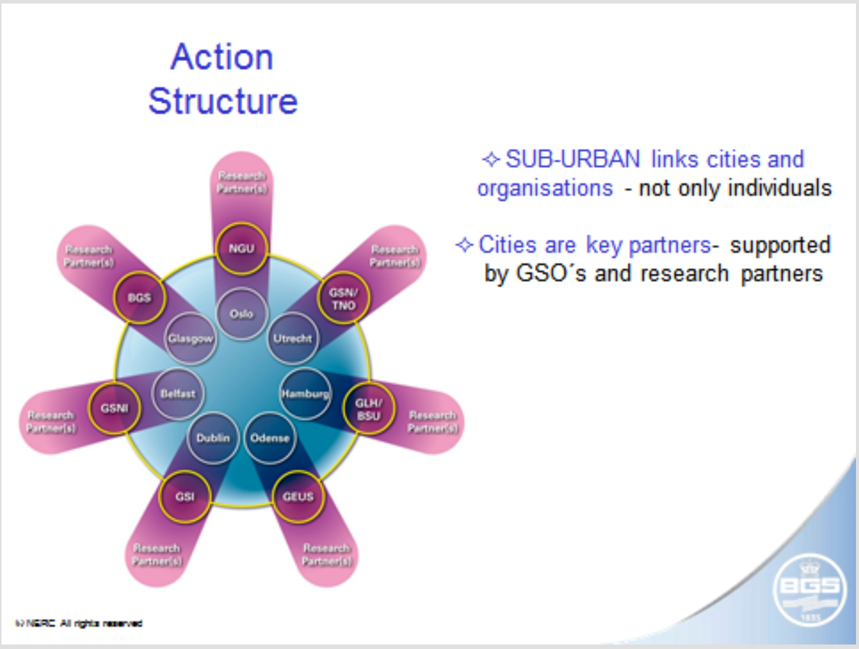
Action Structure
✧SUB-URBAN links cities and organisations - not only individuals
✧Cities are key partners- supported by GSO´s and research partners
Research Partner(s)
NGU
BGS
GSN/ TNO
GSNI
GLH/ BSU
GSI
GEUS
Oslo
Glasgow
Utrecht
Belfast
Hamburg
Dublin
Odense
© NERC All rights reserved
BGS

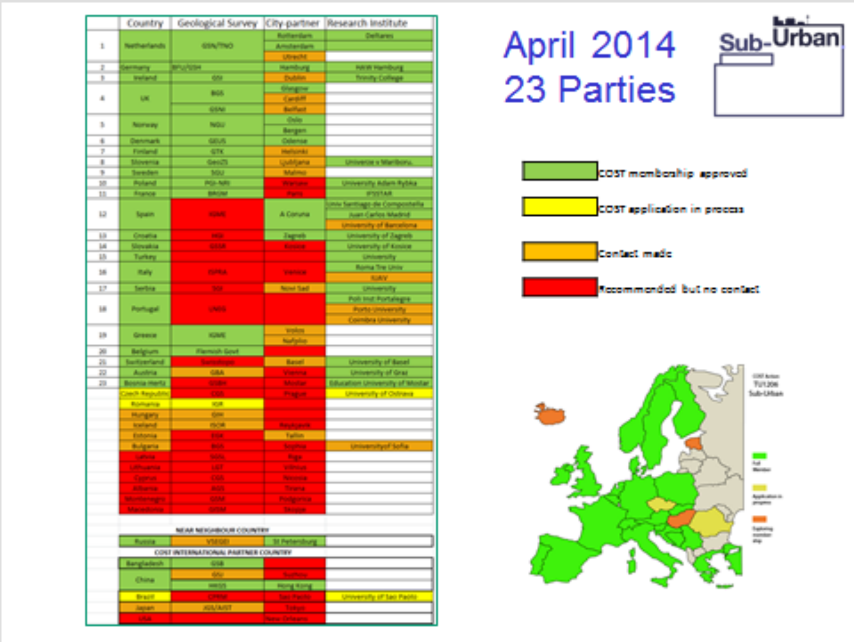

Strong City-partner Growth

Potential outcomes

Sub-Urban

Significant Progress towards:

- Transform relationships between National Geological Survey Organisations (GSOs) / researchers - and City-partners / practitioners – raise profile of the urban subsurface
- Europe-wide and International roll-out of Good Practice Guidance (basis for future standards) to develop critical mass of users trained in developing subsurface knowledge (GSOs / researchers), and its improved understanding and use (City-partners and Practitioners in policy, planning and construction project delivery)

EUROPEAN COOPERATION IN SCIENCE AND TECHNOLOGY

Potential outcomes – Scientific Impacts

Sub-Urban

Improve 3D/4D modelling practice (static and dynamic)…

- Integration of deterministic and stochastic modelling and express model uncertainty
- Model linkage for improved predictive/dynamic models (groundwater, thermal etc.)
- Integration of urban subsurface and above ground 3D/4D modelling, including anthropogenic deposits
- National and European exemplars of urban 3D/4D subsurface modelling, and a critical mass of providers

EUROPEAN COOPERATION IN SCIENCE AND TECHNOLOGY

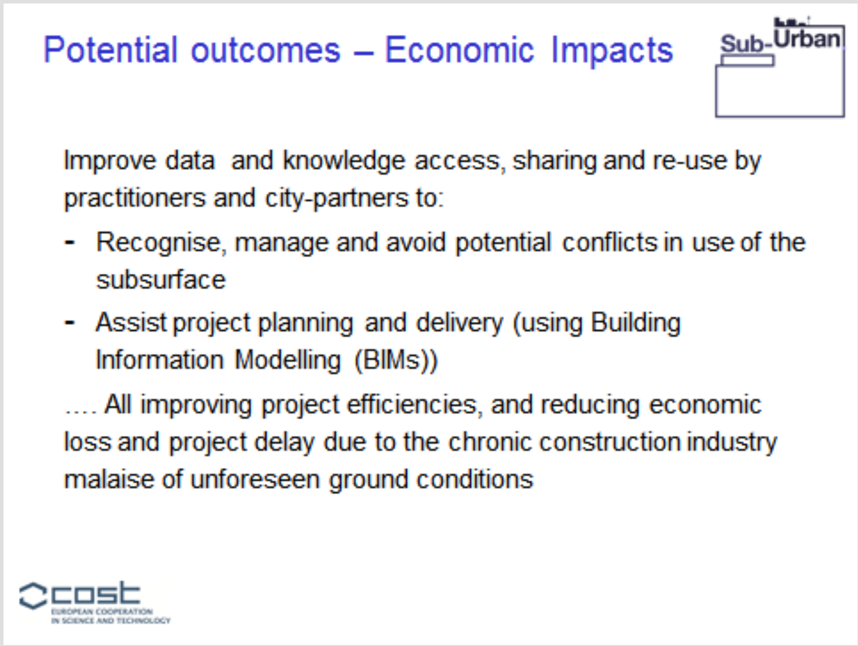
Potential outcomes – Economic Impacts
Sub-Urban
Improve data and knowledge access, sharing and re-use by practitioners and city-partners to:
- Recognise, manage and avoid potential conflicts in use of the subsurface
- Assist project planning and delivery (using Building Information Modelling (BIMs))
…. All improving project efficiencies, and reducing economic loss and project delay due to the chronic construction industry malaise of unforeseen ground conditions
cost
EUROPEAN COOPERATION IN SCIENCE AND TECHNOLOGY

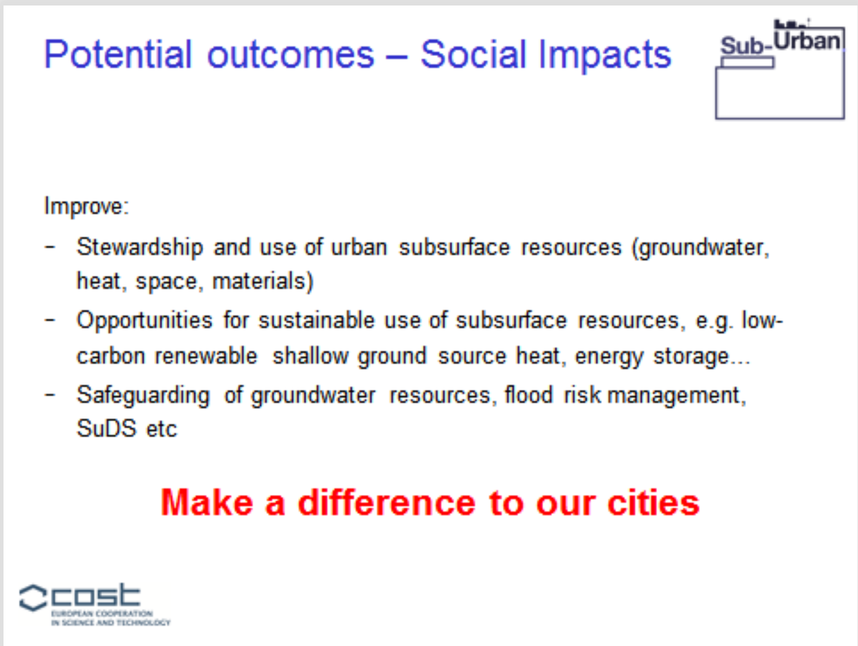
Potential outcomes – Social Impacts
Sub-Urban
Improve:
- Stewardship and use of urban subsurface resources (groundwater, heat, space, materials)
- Opportunities for sustainable use of subsurface resources, e.g. low-carbon renewable shallow ground source heat, energy storage…
- Safeguarding of groundwater resources, flood risk management, SuDS etc
Make a difference to our cities
cost
EUROPEAN COOPERATION IN SCIENCE AND TECHNOLOGY

"Showing GPR possibilities to elementary-school children and citizens in Estonia"

Hannes Tõnisson (EE), Kaarel Orviku (EE)
Hannes.tonisson@tlu.ee

Abstract

Ground Penetrating Radar (GPR) profiling is not very commonly used non-destructive (NDT) geophysical technology in Estonia. It is mostly used by the university researchers in the fields of geology, archaeology, ecology, etc. There are at least two GPR systems in Estonia, and both of them are owned by research groups at the universities. However, both groups have recently been involved in several projects ordered by private enterprises or public authorities. Therefore, an increasing interest in the use of GPR in private and public sectors has recently been arisen. Such phenomenon is most probably the result of an active educational and promotional work carried out by the researchers from the Institute of Ecology at Tallinn University. A number of lectures in secondary schools, practical workshops in the city centre during the Researchers Night, lectures in summer schools and short lectures on TV have all increased public awareness on the possibilities of GPR.

1. Introduction

This paper introduces educational and promotional activities carried out by the researchers from the Institute of Ecology, Tallinn University.

A senior member of the coastal research group started to use GPR already over 20 years ago. The older GPR devices were rather heavy (had to be carried by car), limiting the use of them. A lightweight GPR system, SIR-3000 manufactured by GSSI, was bought in 2011. Small size, light weight and long-lasting batteries allowed us to use it practically everywhere. The workload of the new GPR system in our coastal research group was not that high, and it was reasonable to use the machinery for other purposes as well. We discovered several geology-related works carried out by public or private companies that were often done using destructive methods. It was obvious that most of the geological investigations (digging, drilling, etc.) could have been done using GPR as

a non-destructive method. We witnessed several cases of unnecessary spending. Therefore, we hoped to increase the efficiency of the Estonian economy by educating various age and interest groups.

The following Sections present some descriptions and principles of our educational work among different age and interest groups in Estonia. These activities also helped us to obtain more experience in various geological conditions and to promote our services.

2. GPR Lessons in secondary schools

The first steps were relatively easy. Tallinn University is one of the leaders in the field of teacher education and training in Estonia. Many young teachers of geography, biology and natural sciences in schools have recently graduated from our university. We offered them an opportunity to take GPR lessons for the pupils of their schools. The interest in the lessons was enormous. We had to select a few schools from different regions of Estonia and plan the routes of the lectures, combining them with our fieldworks after or before the lessons (most of the lectures were delivered in the vicinity of our study areas). The lectures were free of charge and we just asked the schools to organize accommodation for us if needed (for the more remote places). We were finally able to visit 10 schools in different regions of Estonia. We mostly expected the pupils from grades 6 to 9. However, even some high schoolers attended the lessons. The groups usually consisted of 10 and 20 pupils.

Our lesson was simple. The first 15 minutes was a lecture where we described the main principles of the GPR system and demonstrated a few examples of GPR pictures (pipes, cables, caves, buried treasures/artificial objects, etc.). The short theoretical lecture helped the pupils to understand the GPR images better. The following 30 minutes were used for practical work. We walked around the school territory and searched for buried artificial objects using GPR. The locations of heating pipes, power cables and many other objects were marked on the ground using wooden sticks on the grass or chalk on the asphalt. Finally, the pupils could draw the basic schemes of the utilities located on the territories of their schools. Moreover, in one school we found the ruins

of the old school house (nearly 100 years old). The most interesting finding was a cave described in an old legend. We were the first ones who found it and may confirm that the old legend is actually a true story (Figure 1a, b).

It came out during our lessons that the younger the pupils were the more enthusiastically they took part in the GPR activities. Therefore, we decided to give one lesson also for the pupils of grades 1 and 2. We decided to skip the lecture part and carry out the entire lesson on the beach. We buried a few "treasures" in the sand to make the study more attractive. Moreover, several simple skills were needed to reach the final "treasure (initial finding was just the first clue to the real treasure)," including the use of compass, reading the distance from the measuring tape, etc (Figure 2a, b, c, d). Finally, we may conclude that the lesson for such young pupils was a huge success. They were really enthusiastic and proud to find the "treasure (candies, some lemonade and a book for the school library)," and to hand over the book to the school library. The lesson needed a little more preparatory work but the final outcome was worth it. We also discovered (from the feedback) that the parents of the pupils were very well informed (by their children after the lesson) on what GPR is and how it could be used in different tasks.

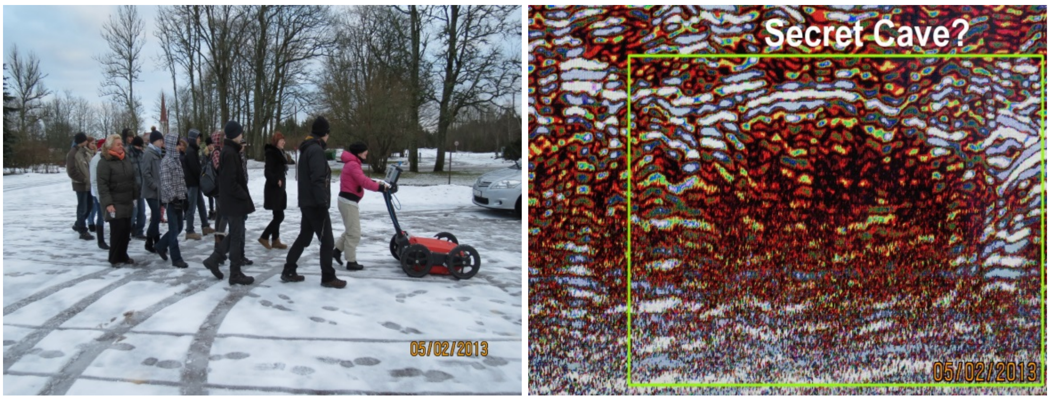

FIG. 1 – GPR lessons at schools. The pupils were intensively working in the school's parking lot (left); An old legend describing secret caves from the local church to manor was confirmed (right)!?

FIG. 2 – Second grade pupils in Tallinn. Reading their research task (top left), searching the "treasure" from the beach sand (top right), using some additional tools (lower left) and finally, the treasure was found (lower right).

3. INVESTIGATIONS DURING THE RESEARCHERS NIGHT

We were discovered by several interest groups as a result of our lessons in schools, and we were invited to present our equipment in the frames of the Estonian Researchers Night held in the city centre of Tallinn. Several researchers were demonstrating their studies, new equipment and the most recent research findings. Hundreds of people came by and got their first impressions on what GPR was and how it could be used.

Luckily, the event took place on the Freedom Square of Tallinn. This square was established on top of the ruins of the old medieval city wall. Our working group was involved in the mapping procedure of the ruins. That gave us the opportunity to demonstrate how these old walls looked like on the GPR screen (Figure 3a, b). The audience was rather diverse – from kids to retired citizens.

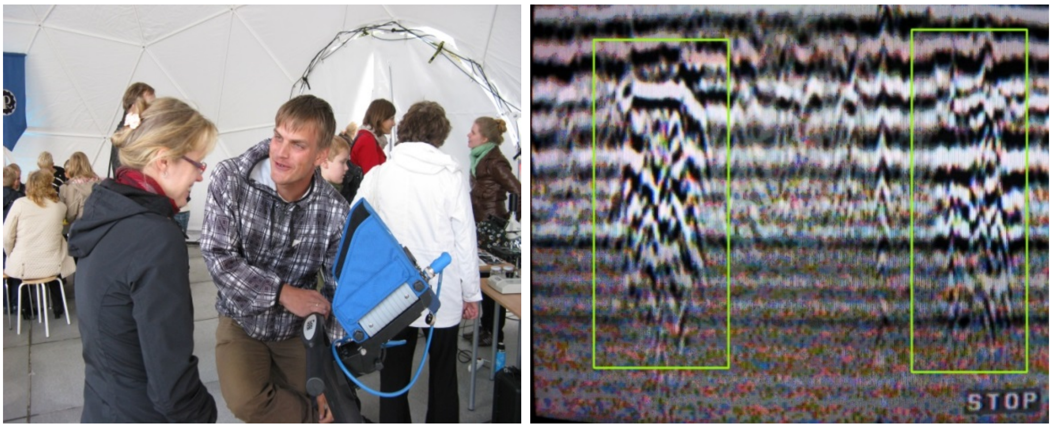

FIG. 3 – Researchers Night was organized in the city centre of Tallinn. GPR was demonstrated and tested among other activities (left); C) the ruins of the buried medieval city walls were demonstrated (right).

4. JOINT FIELDWORKS WITH ARCHAEOLOGISTS AND TV CREW

The previous educational work has brought us in contact with a lot of different interest groups and several job offers. However, we are a research institution and our first aim is to contribute to scientific activities. Therefore, we contacted the archaeologists from our own university. They had preliminary information about a buried Viking ship near Salme village on Saaremaa Island. The site was investigated using an older version of GPR and the Viking ship was found (Figure 4 a, b, c, d). It appeared that a pile of stones placed on top of the buried ship gave the strongest signal and helped us to locate this object. The whole investigation process was filmed by the archaeology students (Figure 4a).

The final movie was meant for educational purpose for the (archaeology) students, which was another educational outcome of our activities.

FIG. 4 – Searching for ancient Viking ship on Saaremaa Island. A special movie was designed for educational purposes (top left), search is in progress (top right), ship was found (lower left) and archaeologists expose the ship remains (lower right).

5. 1-MINUTE LECTURES ON NATIONAL TV CHANNEL

Our final and maybe the most notable educational and also a little bit promotional product is one minute lecture of GPR. Tallinn University is involved in the project called "one minute lectures." These are short, easy to understand and high-quality lectures introducing scientific

problems or new scientific methods/equipment. The lecture is on air on the biggest national TV channel and the lecture with longer introduction remains visible on the webpage of our national TV channel - Estonian TV. Finally, it helps us to reach every Estonian's home. Our lecture will be (currently in Estonian only) available with English subtitles as well (http://teadus.err.ee/v/uhe_minuti_loeng/46de5675-c067-4552-b36d-4912a821887a).

6. CONCLUSIONS

We were facing a situation where only very few people in Estonia knew what GPR was and how it could be used in different fields of activity. It was just a few years ago. Fortunately, we were able to spread the knowledge to a significant number of people without the need of additional GPR-related projects or funding. We hope that our promotional work has raised awareness of the Estonian companies about the possibilities of using GPR in more efficient business activity. Moreover, GPR profiling is an environment-friendly non-destructive method of investigation.

ACKNOWLEDGEMENT

The authors acknowledge the COST Action TU1208 "Civil Engineering Applications of Ground Penetrating Radar" supporting this work. The presented results were possible thanks to the financial support of the ESF grant 8549.

"A Two-day GPR Training Course in the University of Greenwich, United Kingdom"

Amir Alani (UK), Kevin Banks (UK)
amir.alani@uwl.ac.uk

Abstract

To provide specialist and focused training in supporting GPR users (with different capabilities and backgrounds), in partnership with industry (Blue Hat Training), the University of Greenwich has developed a tailor-made GPR training programme in the form of a two day course consisting of presentation, discussion, coaching and practical outdoor tuition, using the university's own GPR equipment. The focus of this training is to underpin and enhance the understanding of attendees of the applications of GPR in the identification of utilities and associated fields.

1. Introduction

Since the release of the Mala Easy Locator in 2002, GPR (Ground Penetrating Radar) has been introduced to the mass market as an affordable and easy to use device. This market has continued to grow significantly year on year as other manufacturers have released their own variations of the entry level and easy to use GPR system.

The Easy Locator is a single channel GPR which allows the user to detect and identify features on-site. In 2007 the entry level radar took another step forward when IDS launched the Detector Duo, the world's first dual channel, easy use GPR, which expanded the capability of on-site detection equipment to a new level.

Now, most manufacturers have released or are in the development of a dual frequency, on site detection GPR system.

The ease of use of the entry level GPR has resulted in a dramatic decline in the average level of education of the operator of the equipment. In the past the user would have had to be a geotechnical or geophysical engineer, having completed a university degree, but now the user could be any person with a basic education.

Over recent years, the most significant growth application for GPR has been for the purpose of utility detection. This has been driven by the availability of affordable and easy to use equipment, and the fact that

the shape of a utility when it is depicted on the GPR display is relatively easy for most users to learn to recognise. GPR solves a problem which currently cannot be solved in any other way: the detection of nonmetallic utilities such as gas pipes.

Despite this, a GPR operator requires training and experience to get the best out of their equipment and many operators lack this.

Now, there is a significant and growing number of GPR users who are not highly educated in radar principles or signal processing, but who are utilising GPR on a regular basis for the purpose of utility detection. In many cases they have received little training and may be skeptical of the capabilities of their equipment. Some operators only use GPR at its minimum capability, simply to comply with regulations or as a result of a lack of knowledge and understanding of the extent of GPR applications. This in turn often results in inadequate outcomes.

In order to address this shortfall, in partnership with industry (Blue Hat Training), the University of Greenwich is offering GPR training in the form of a two day course consisting of presentation, discussion, coaching and practical outdoor tuition, using the university's available facilities and infrastructure.

2. Course Content

The formal aspect of training (lectures) explains the principles of a GPR system, outlining the system's operation, control and referencing as well as data processing (basic and intermediate). For example, the material presented explains why a hyperbola looks the way it does, elaborating upon factors affecting GPR reflections and why and how these influence the results (outcome). This new knowledge and understanding is then applied in the discussion and coaching part of the course.

The course then moves from formal presentation to discussion about the capabilities and limitations of a GPR system, covering what can and cannot be identified in terms of targets as well as characteristics of different targets and their configurations within the processed data.

The discussions then lead into the coaching sessions, using the university's GPR system and facilities. This provides ample opportunity to trainees to underpin the principles of what they have been taught in class with reality. This involves the location and identification of several targets around the university campus. As a former naval base, the University of Greenwich Medway Campus is ideal for this purpose,

having a diverse spread of utilities and ground conditions dispersed around the site.

After successfully coaching the operators to locate and identify targets, the final part of the course is outdoor tuition: how to perform and operate GPR in application to the utility survey in accordance with TSA (The Survey Association in the UK) guidelines, level 4. Utilising the standard grid system and soft chalk for an on-site mark out survey, the trainees will comprehensively scan the ground to map all the utilities in a given location.

In order to ensure that all participants get sufficient time with the equipment, course numbers are limited to eight trainees and approximately one day of the course is spent outdoors.

In the latter part of the training, trainees are examined and graded; certificates and performance reports are subsequently issued to their employers.

The idea for GPR training was first conceived in September 2013 and it has taken over six months of course and facility preparation including multiple visits and meetings with Blue Hat and mapping the underground features of all of the training areas in the university to prepare the coaching routes and survey sites.

The main feature of this training can be summarised as a unique and hands-on opportunity for GPR users to enhance their understanding of the system's operations and applications. This has led to a well balanced and highly appreciated course by trainees in terms of the emphasis on practical experience and understanding gained.

The course covers a variety of content including recognising different targets such as the examples in Figures 1 and 2. In Table I, the approximate GPR penetration depth is reported, for different materials. In Figure 4, the course flyer is shown.

The first GPR training course was successfully completed in April 2014 for a number of trainees, with excellent feedback from participants. Bookings are already in place for repeat courses in May, June and July.

ACKNOWLEDGEMENT

The authors acknowledge the COST Action TU1208 "Civil Engineering Applications of Ground Penetrating Radar", supporting this work.

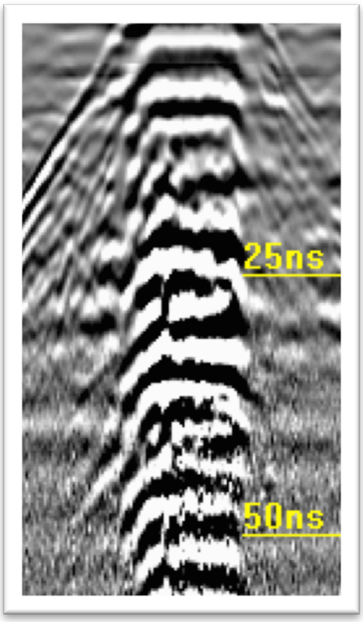

FIG. 1 - Manhole Cover

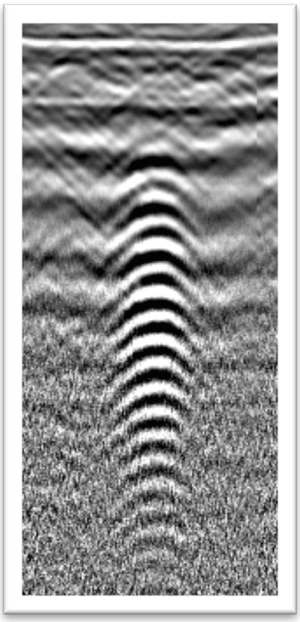

FIG. 2 - Electricity Cable

Material	Relative Permittivity	Approx. Max Penetration
Granite	5	3.5 m
Asphalt	6	3 m
Sand	7	3 m
Soil	9	2.5 m
Concrete	12	2 m
Clay	20	1 m

TAB. I - Approximate Penetration Depth by Material

FIG. 4 - Training course Advertising Flyer

"COST INITIATIVES FOR EARLY-STAGE RESEARCHERS: SHORT-TERM SCIENTIFIC MISSIONS, TRAINING SCHOOLS, CONFERENCE GRANTS, AND TARGETED NETWORK TN1301 (SCI-GENERATION)"

Marian Marciniak (PL), Lara Pajewski (IT)
lara.pajewski@uniroma3.it, m.marciniak@itl.waw.pl

Abstract

Supporting Early-Stage Researchers (ESRs) to develop independent careers and to establish their first research group under their own responsibility is a strategic priority for COST [1].
For COST, the definition of ESR is based on the time that elapses between the date of the PhD (or equivalent experience) and the date of involvement in a COST Action. If this time span is less than 8 years, a person fits the definition; of course, periods of career's leave have to be added to the mentioned time span.
In this work, four COST instruments, particularly interesting for ESRs, are presented: Short-Term Scientific Missions (STSMs), Training Schools (TS), Conference Grants, and the Targeted Network TN1301. ESRs willing to receive more information are strongly encouraged to take contact with the Action Chair and the Action STSM Manager.

1. SHORT-TERM SCIENTIFIC MISSIONS

Short Term Scientific Missions (STSM) are aimed at supporting individual mobility, strengthening networks and fostering collaborations. They allow scientists to visit an institution or laboratory in another COST Country participating to the Action, or in an approved Near Neighbour Country (NNC) institution, or else in an approved IPC institution. A STSM should specifically contribute to the scientific objectives of the Action offering the grant, while at the same time allowing applicants to learn new techniques or gain access to specific instruments and/or methods not available in their own institutions.
The evaluation of STSM applications is performed by the Management Committee (MC) of the Action providing the grant; the MC of the COST Action TU1208 formally delegated the evaluation of STSM applications to the Action Chair and the STSM Manager. The selection of applicants is based on the scientific scope of the STSM application, that must be in line with the Action objectives, and on the applicant CV. Geographical and gender balance issues are taken into consideration as well.

STSM applicants must be engaged in a research programme as a postgraduate student or postdoctoral fellow, or be employed by or officially affiliated to an institution or legal entity. This institution is considered as the Home institution. Institutions may be public or private entities.
Standard STSMs need to take place according to the following rules:
1. Be a minimum duration of 5 days;
2. Be a maximum duration of 90 days;
3. Carried out in their entirety within a single grant period and within the Action's lifetime.

ESRs may extend the duration of the STSM beyond the 90 days (the maximum allowed duration is 180 days), in well justified cases. The justifications are to be documented in the approval of the STSM.
A STSM grant is a fixed contribution, based on the budget requested by the applicant and on the evaluation of the application by the MC Chair and STSM Manager. The aim of the grant is to support the costs associated with the exchange visit. It will not necessarily cover all expenses and has to be intended as a contribution to the travel and subsistence costs of the participant. A maximum of EUR 2500,00 in total can be afforded to the grantee, in case of a standard STSM. For an ESR STSM lasting more than 91 days, instead, the maximum grant is EUR 3500,00.
More detailled information on STSMs can be found in [2], Section 6.

During Year 1 of the Action TU1208, 4 STSMs were funded and successfully carried out; 100% of the granted scientists were ESRs or PhD Students and perfect gender balance was achieved.

A. Granted ESR: Dr. Lara Pajewski, IT - Host: Dr. Antonis Giannopoulos, UK
STSM Title: *Electromagnetic modelling of Ground Penetrating Radar responses to complex targets*
Dates: from 21 October 2013 to 20 December 2013 - Location: University of Edinburgh, School of Engineering, Edinburgh, United Kingdom

B. Granted PhD Student: Philippe De Smedt, BE - Host: Dr. Wolfgang Neubauer, AT
STSM Title: *Reconstructing prehistoric environments at Stonehenge with multiple electromagnetic survey methods*

Dates: from 1 February 2014 to 31 March 2014 - Location: Ludwig Boltzmann Institute for Archaeological Prospection and Virtual Archaeology, Vienna, Austria

C. Granted ESR: Dr. Sonia Santos Assunçao, ES - Host: Klisthenis Dimitriadis, EL
STSM Title: *The preservation of the Tholos Tomb of Acharnon*
Dates: from 15 January 2014 to 15 February 2014 - Location: GEOSERVICE, Athens, Greece

D. Granted PhD Student: Iraklis Giannakis, UK – Host: Dr. Lara Pajewski, IT
STSM Title: *Numerical modelling of Ground-Penetrating Radar antennas*
Dates: from 15 January 2014 to 21 March 2014 - Location: Roma Tre University, Rome, Italy.

Carrying out a STSM is a very positive and fruitful experience, both from the personal and the professional point of view. ESRs participating to the COST Action TU1208 are strongly encouraged to apply for a STSM grant!

2. Training Schools

Training Schools (TSs) aim at widening, broadening and sharing knowledge relevant to the Action's objectives, through the delivery of intensive training on a new and emerging subject. They can offer familiarisation with unique equipment or expertise that are typically to the benefit of ESR, although not exclusively. They are not intended to provide general training or education.
COST support covers the organisation costs of TSs, as well as the participation of trainees (by assigning grants) and trainers (by reimbursing travel, accommodation and meal expenses).
More detailled information on TSs can be found in [2], Section 7.
During Year 1 of the Action TU1208, 2 TSs were organized; 100% of the granted scientists were ESRs or PhD Students, with a perfect gender balance among them.
A. The first TS focused on "Microwave Imaging and Diagnostics: Theory, Techniques, Applications." It was held in Madonna di Campiglio, Italy, on March 24-28, 2014. It was co-organised by the Action TU1208, the Action TD1301 "Development of a European-based Collaborative Network to Accelerate Technological, Clinical and Commercialisation Progress in the Area of Medical Microwave Imaging," and the European School of Antennas (ESoA).

B. The second TS covered the state of the art and new trends on radar technologies: "Future Radar Systems: Radar2020." It was held in the Karlsruhe Institute of Technology, in Karlsruhe, Germany, on May 5-9, 2014. This school was co-organised by the Action TU1208, the ESoA, and the European Microwave Association (EuMA).
The next planned TU1208 schools will be:
C. A TS on "Civil Engineering Applications of Ground Penetrating Radar," to be held in the School of Engineering of the Univerity of Pisa and in IDS Ingegneria dei Sistemi, on September 22-25, 2014. This school will be fully organised by the Action TU1208.
D. A TS on "Ultra Wide-Band Antennas, Technologies and Applications," to be held in Karlsruhe on April 20-24, 2015. This school will be co-organised by the Action TU1208, the ESoA and the European Association on Antennas and Propagation (EurAAP).
Note that scientists can attend a TS (and possibly receive a grant) even if they aren't involved in the Action organising it. ESRs participating to the Action TU1208 are strongly encouraged to participate to the TU1208 schools as well as to check the websites of the other running Actions, in order to find out whether schools of their interest are going to be organised in the next future.

3. Conference Grants

Each COST Scientific Domain offers to ESRs 3 supporting grants per year (max. 3000 € each), to participate in an international conference outside of the COST Action activities.
In order to be eligible for this grant, an accepted oral contribution is required. The grant can be used to cover travel and subsistence costs, conference fees, and the costs of conference workshops. A written application has to be submitted through the Action Chair to the COST Office. The application must contain the personal data and curriculum vitae of the applicant, a short description of the involvement in the COST Action, information on the conference to which the applicant wishes to participate, a copy of the abstract/paper submitted to the conference and a proof of acceptance of this contribution by the conference, and finally the amount of the support needed.
There is a call for Conference Grants three times per year. Each time a grant per Scientific Domain is assigned.
More information on COST Conference Grant can be found in [3].
The ESRs participating to the COST Action TU1208 are strongly encouraged to apply.

4. Targeted Network TN1301

COST Targeted Networks are CSO (Committee of Senior Officials)-driven Actions, aiming to strengthen the role that COST plays in a given policy domain (inclusiveness, early-stage researchers' involvement, gender balance, international cooperation), stimulate the strategic development of future-oriented societal challenges, and contribute to EU2020 policy goals [4].

There are currently three COST Targeted Networks, running since 2012:

- TN1201 – genderSTE (Gender, Science, Technology and Environment), started in November 2012 and ending in November 2016;
- TN1301 – Sci-GENERATION (Next Generation of Young Scientist: Towards a Contemporary Spirit of R&I), started in November 2013 and ending in November 2017;
- TN1302 – BESTPRAC (The Voice of Research Administrators - Building a Network of Administrative Excellence), started in October 2013 and ending in October 2017.

Anyone interested in joining a Targeted Network is invited to contact the Action Chair and, subsequently, the COST National Coordinator.

In this paper, we wish to focus on the TN1301, exclusively dedicated to excellent next-generation scientists in order to help them dealing with the limitation and obstacles they run across on a daily basis, as they strive towards an outstanding research career.

The Targeted Network Sci-GENERATION aims at elaborating contemporary scientific thought and thereby disseminating a new spirit of research and innovation in Europe, at enhancing career perspectives for young researchers in public research centres and universities (particularly from less research-intensive countries), at promoting new and emergent research topics as well as research methods and organization, and at improving synergy and avoid duplication of efforts between organisations, universities and other EU platforms.

The network is structured in 4 Working Groups (WGs). WG1 aims to propose measures for countries with fewer opportunities for next generation researchers to increase the visibility, inclusivity and success of their excellent young European researchers and research teams. WG2 fosters continuity in funding opportunities and career perspectives, as a result of combined national and European funding schemes. WG3 deals with promoting new and emergent research topics, as well as research methods and organisation. Finally, WG4 is concerned with producing a mapping of EU Science policies, initiatives and associations.

The ESRs participating to the COST Action TU1208 are strongly encouraged to read more about the TN1301 on www.scigeneration.eu.

4. Conclusions

Excellent young researchers in many European countries lack the visibility and administrative or organisational support crucial for developing their scientific career. This applies particularly to certain countries within Southern and Eastern Europe, where working conditions or a hierarchical mentality have often motivated qualified young researchers to emigrate to Northern-Western Europe or overseas. For COST, supporting ESRs to develop independent careers, to establish their first research group under their own responsibility, and to network with colleagues in different countries, is a strategic priority, which is effectively and concretely pursued.
The COST Targeted Network Sci-GENERATION, together with interesting COST networking tools as Short-Term Scientific Missions, Training Schools and Conference Grants were presented in this paper.

Ackwnoledgement

The authors are grateful to COST, for funding the Action TU1208 "Civil Engineering Applications of Ground Penetrating Radar."

References

[1] COST Strategy towards increased support of early stage researchers, COST 295/09, Brussels, 4 December 2009 (www.cost.eu).
[2] COST Vademecum – Part 1: COST Action (www.cost.eu).
[3] COST Vademecum – Part 2: Other COST Activities (www.cost.eu).
[4] COST Plan for the Strategic Activities 2012-2014, COST 4111/13, Brussels, 29 May 2013 (www.cost.eu).

WORKING GROUP 1

Novel GPR instrumentation

KEYNOTE TALK 1 - "NETTUN AND ORFEUS PROJECTS"

Guido Manacorda (IT) - *g.manacorda@idscorporation.com*

The NeTTUN (Leading the Way in New Technology for the Tunnelling Industry) project has received funding from the European Union's Seventh Framework Programme for research, technological development and demonstration, under grant agreement no. 280712 – www.nettun.org (September 2012 – March 2017). The ORFEUS (Optimised Radar to Find Every Utility in the Street) project has received funding from the European Union's Seventh Framework Programme for research, technological development and demonstration, under grant agreement no. 308356 – www.orfeus.org (October 2012 – March 2015)

NeTTUN addresses tunnelling works, ORFEUS the installation of pipes with horisontal directional drilling (HDD). Both applications rely upon data collected from the surface, the scenarios are different but danger is the same: "blind" digging is anyway a risk! GPR has been experimented in both these applications, but not concurrently with digging. When used from the surface, the GPR detection range is limited. Both NeTTUN and ORFEUS address the installation of GPR on the cutting head in a very harsh environment. Automatic detection is also required.

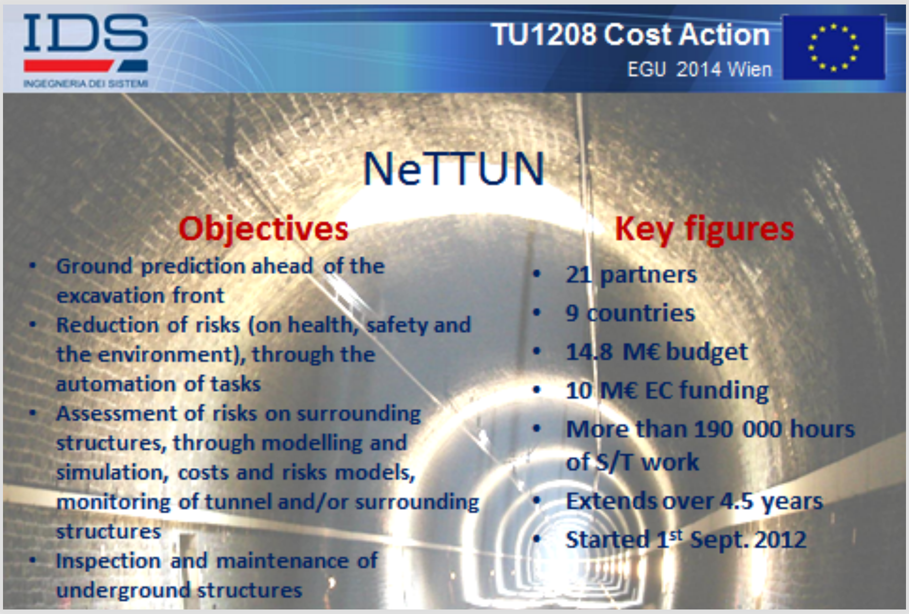

Ground prediction ahead the Tunnel Boring Machine (TBM):

- No existing system capable of reasonable performance in soft ground TBMs → e.g. seismic systems not applicable through segmental lining.

- Data acquisition mainly implemented during maintenance periods, e.g. on a weekly basis → very long penetration range required, currently not achievable.

- Systems require expert knowledge for data/image interpretation → a slow process, providing results many hours after collecting the data.

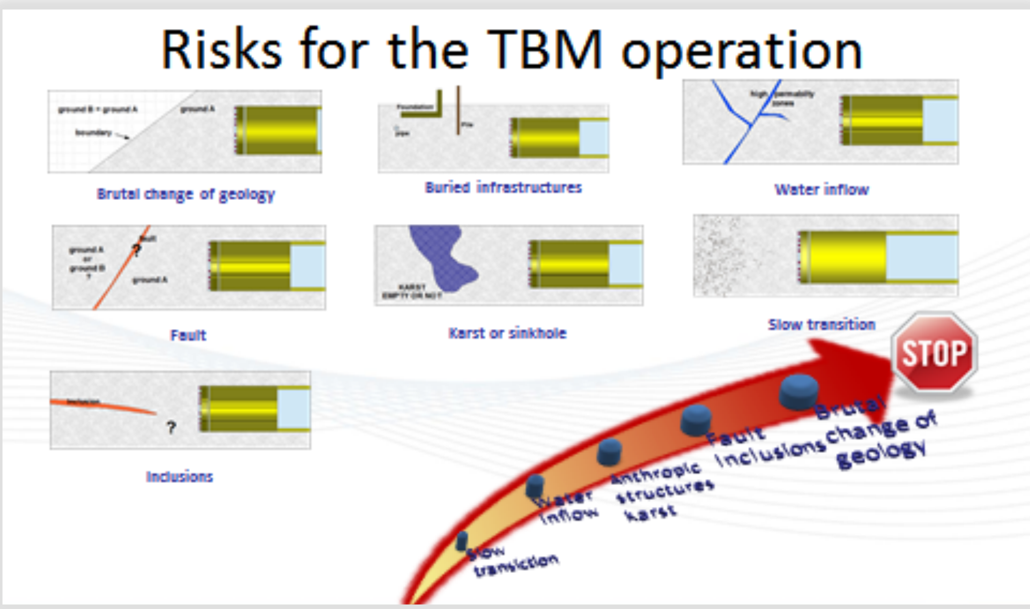

The NeTTUN approach:

- Advanced multi-sensor configuration (based on different and complementary methods).
- Integrated inside the TBM (for a fast, frequent and effective look ahead during boring).
- Modular (can be expanded).
- Four partners involved in the development of the GPR to be installed on the cutting head of a TBM and capable of providing an accurate and detailled image of the ground in front of the TBM.

- The system will be equipped with two set of antennas, combining long range and high resolution (multi-frequency approach).
- Data will be delivered to the data fusion system and merged to those provided by seismic, to produce an easy-to-interpret output.

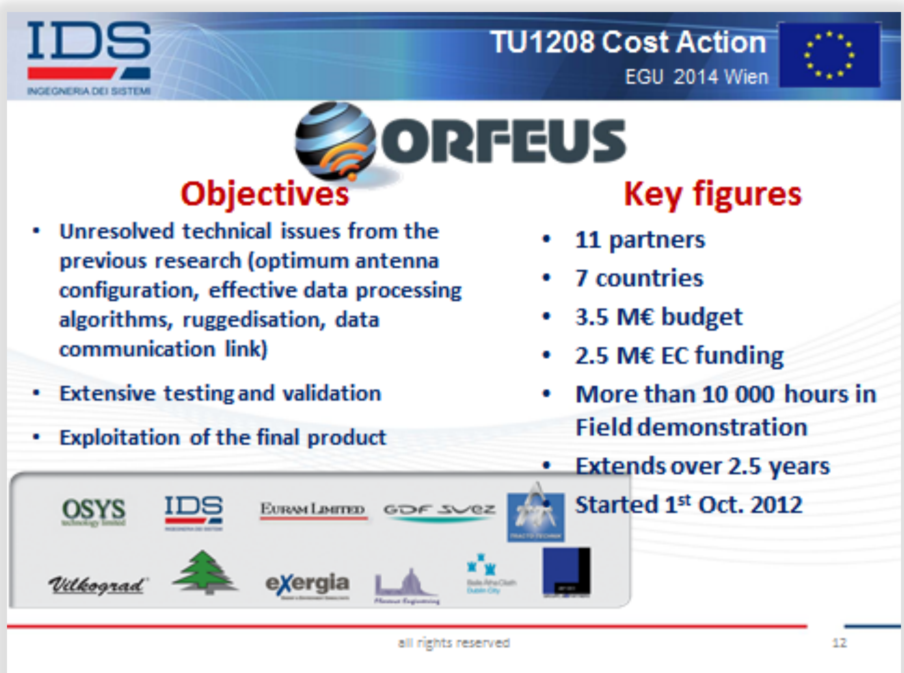

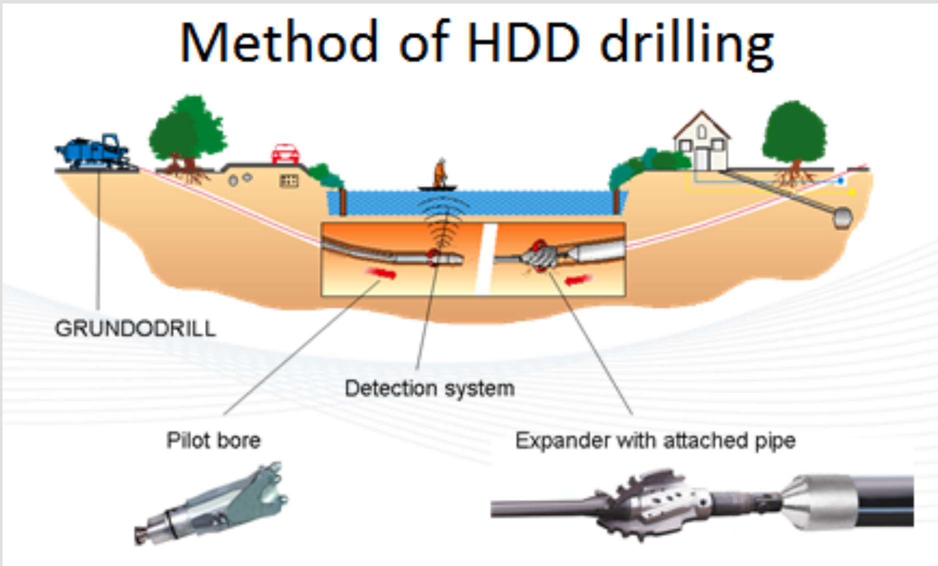
Method of HDD drilling
GRUNDODRILL
Detection system
Pilot bore
Expander with attached pipe

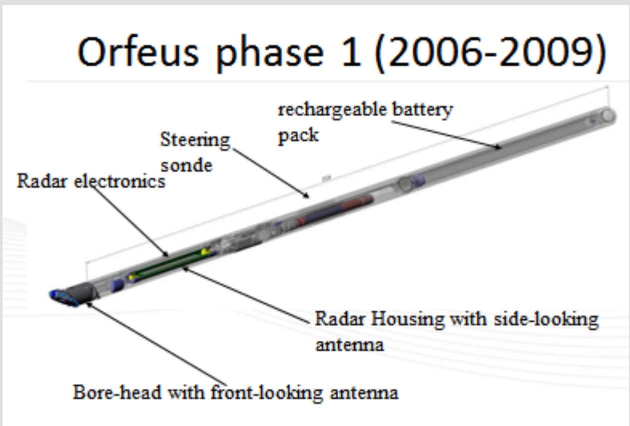
Orfeus phase 1 (2006-2009)
rechargeable battery pack
Steering sonde
Radar electronics
Radar Housing with side-looking antenna
Bore-head with front-looking antenna


Orfeus 2
Critical choices
number of antennas
ruggedisation strategy
suitable radome material
elimination of battery PSU
design for drill rod connectors
power strategy to minimise corrosion

System flow diagram:

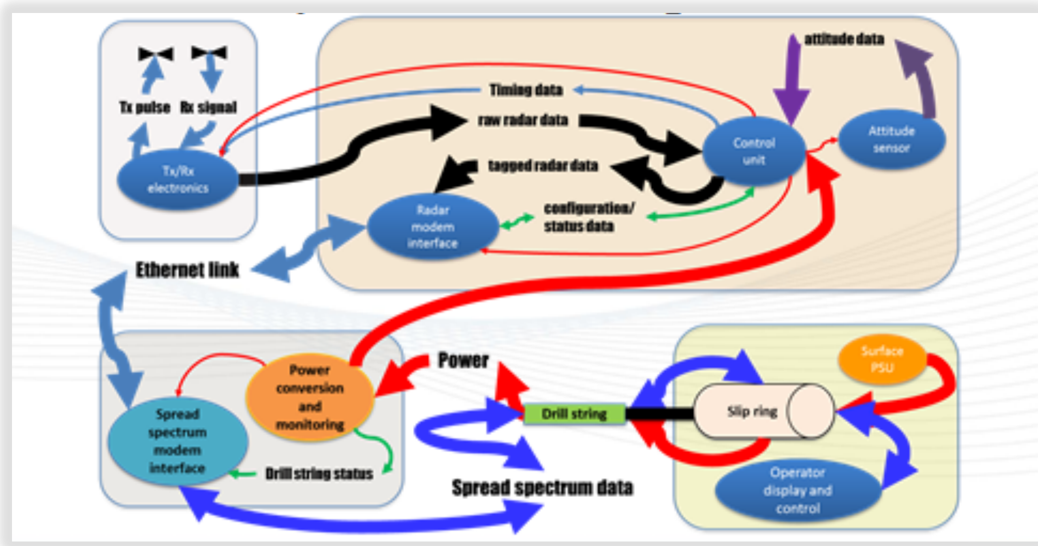

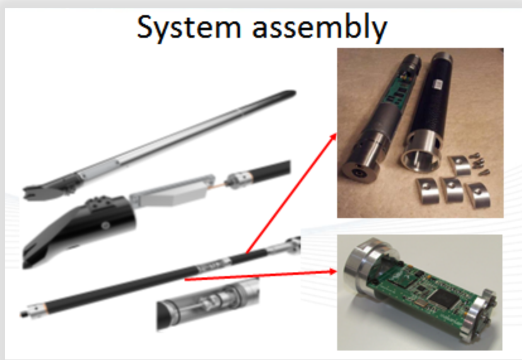

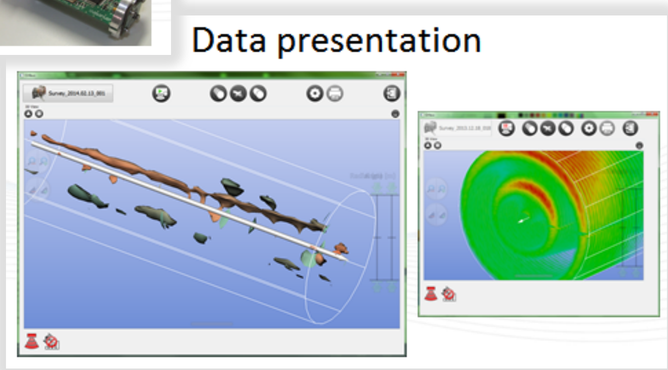

Acknowledgement - The author acknowledges the COST Action TU1208 "Civil Engineering Applications of GPR".

"A GPR SYSTEM FOR THE HIGH-RESOLUTION INSPECTION OF WALLS AND STRUCTURES" (CONTRIBUTION TO PROJECT 1.1)

Guido Manacorda (IT), Alessandro Simi (IT), Giorgio Barsacchi (IT)
g.manacorda@idscorporation.com

The abstract is published in *Geophysical Research Abstracts*, Vol. 16, EGU2014-16422, 2014 and is available on *www.egu2014.eu*

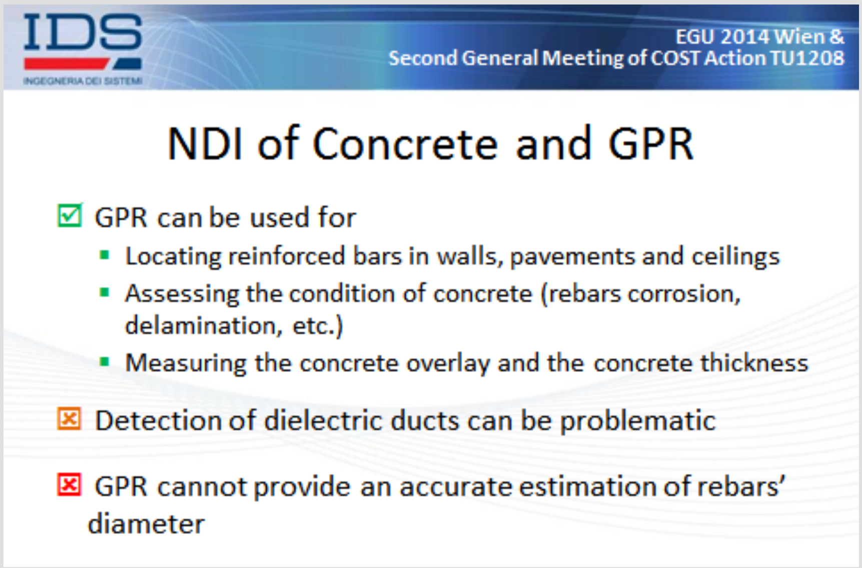

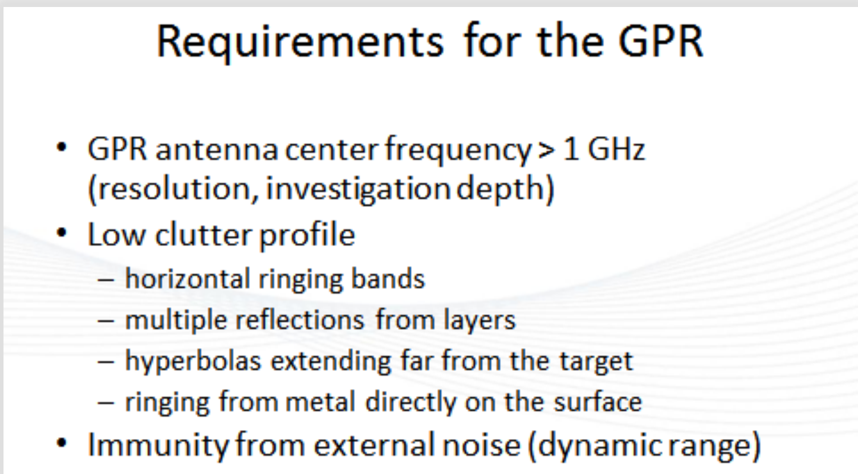

New Design Requirements

- Center frequency > 2 GHz (t_{pulse}<500 psec)
- Bandwidth > 2 GHz
- Dynamic range > 70dB (penetration range > 30 cm)
- High Resolution

Antenna feeding pulse

- The step recovery diode generates a very fast transient pulse moving from conduction to interdiction state
- As lower the diode V_{br} as shorter the T_{rise} of the generated pulse

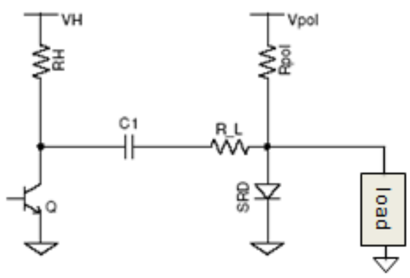

Antenna radiated pulse

- The radiating dipole is not a pure resistive load over the whole transmission band

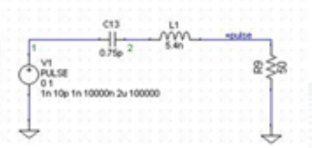

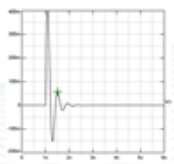

- The correct matching between the radiating dipole and the Tx is a key task during the design

The receiver

The receiver holds a voltage from a high frequency waveform long enough for an ADC sample to be done.

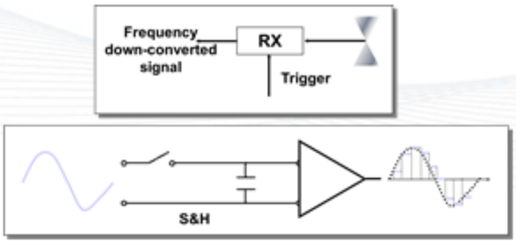

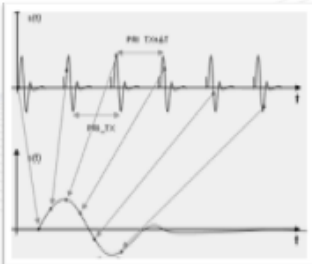

The receiver generates noise
1) Folding of interferences having an instantaneous bandwidth greater than PRF (+38dB higher than N_{rms}= $KT*B_{RF}$)
2) Non-ideal sampling

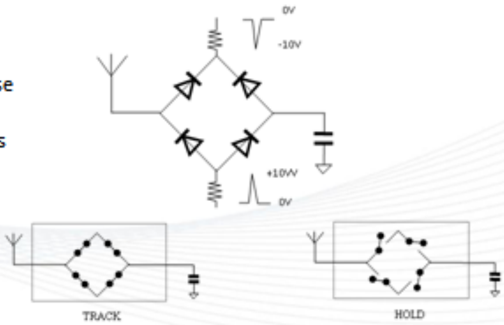

Receiver bandwidth and dynamic range are the key tasks in the design

Main achievements

- Increased transmitter performance reducing pulsewidth (~0.3 ns)
- Improvement of receiver bandwidth extending it up to 5 GHz
- Main benefit: **higher frequency = higher resolution**
- **In range resolution: < 1 cm** (resolution of TRHF ~ 1.6 cm)

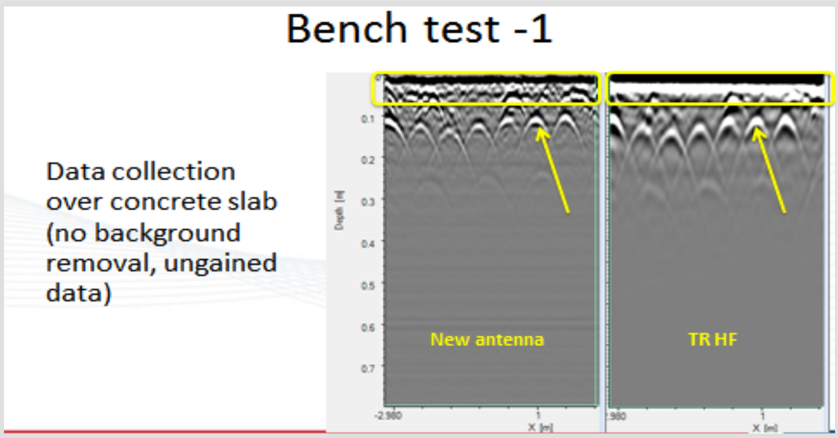

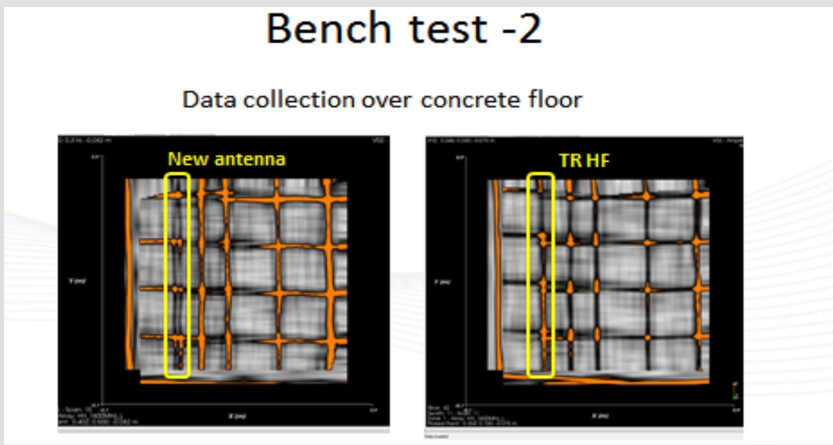

- The novel GPR antenna has been found capable of providing a very clear image of the concrete internal structure
  - Higher resolution
  - Reduced blind area
  - Enlarged dynamic range
- This was achieved by a proper design of the transmitter and receiver electronics and solving several issues

ACKNOWLEDGEMENT - The authors acknowledge the COST Action TU1208 “Civil Engineering Applications of GPR”.

“The neglected exactness”
Exact positioning of mobile GPR applications

Jörg Endom (DE)
Joerg.Endom@dmt.de

The abstract is published in *Geophysical Research Abstracts*, Vol. 16, EGU2014-4350, 2014 and is available on *www.egu2014.eu*

Common Geophysical Survey

Measuring Tape, Rope, Ranging Pole


GPR combined with GPS

High precision GPS = DGPS
- mobile rover unit
- correction signal from fixed base unit
  or correction service

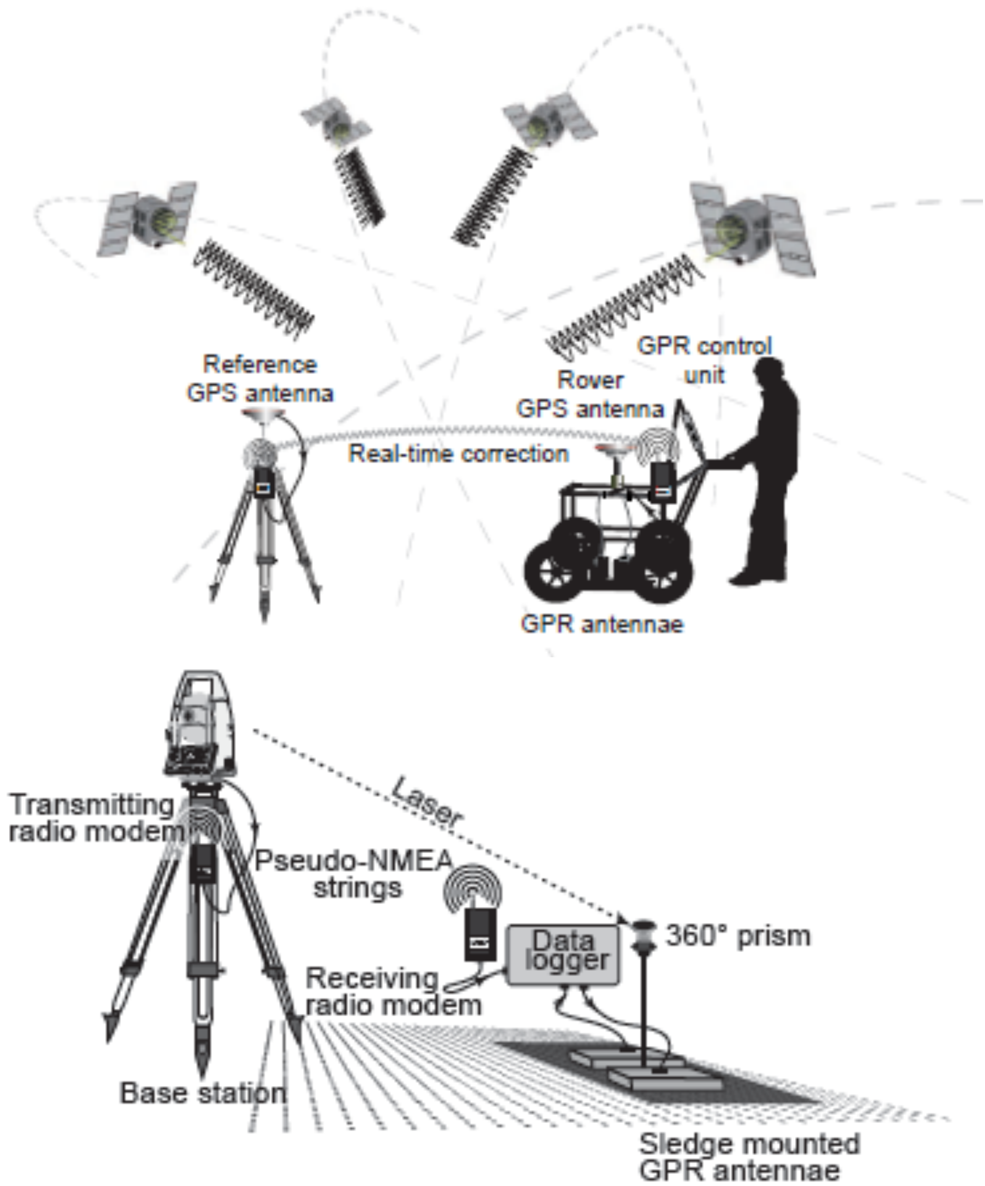

(from Börner, U., PHD thesis, 2010)

Observed Errors:

- GPS quality changes during survey ⇒ loss of precision.
- GPS latency is significant even at walking speed, and variable. It depends on hardware, firmware and settings, and produces errors ranging from 0.5 m (walking) to 30 m (high speed).
- GPS post-processing is not time consistent (trimble).

The GPS problems:

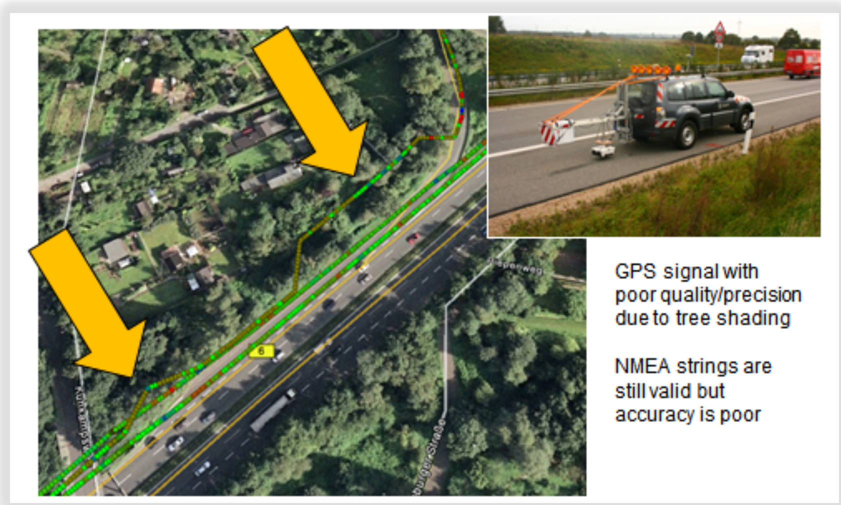

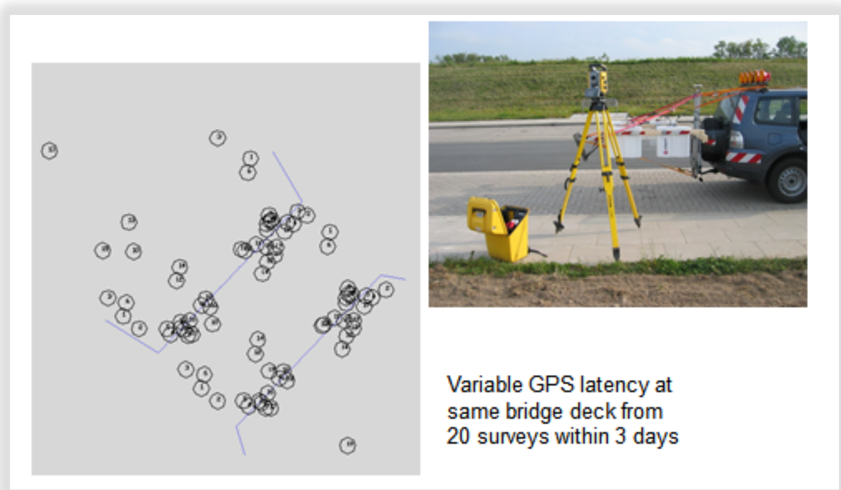

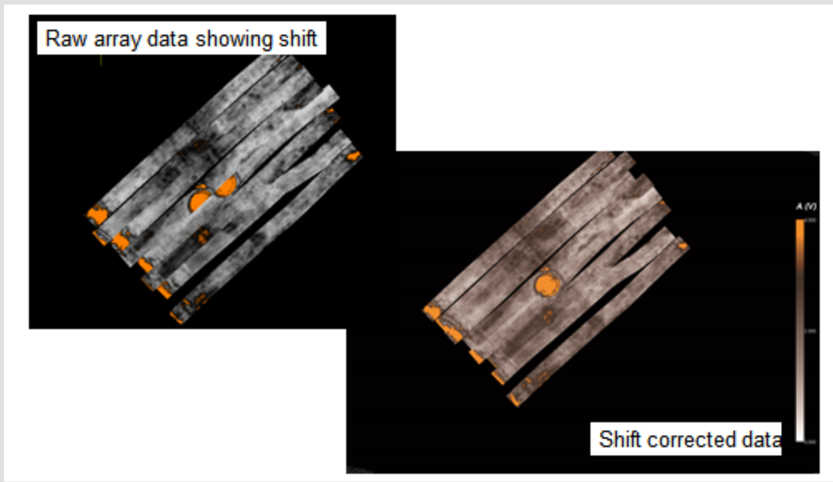

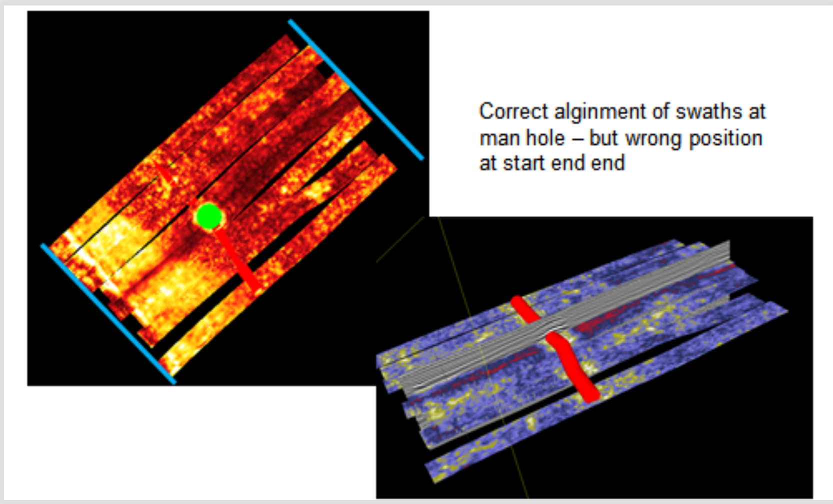

DGPS survey with local base and post-processing produces a time lag of 1 s (trimble hardware and software).

There is no sufficient QC during the survey, without a GPS handheld attached.

The total station problems:

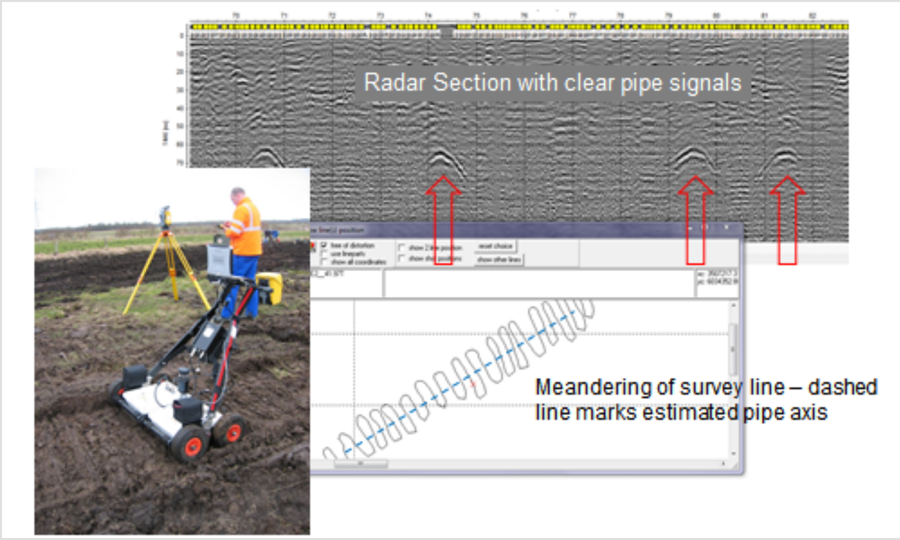

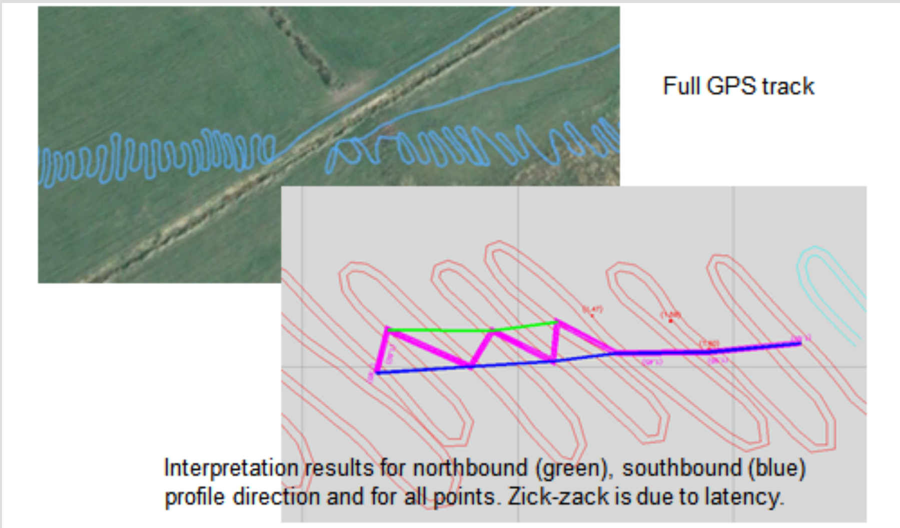

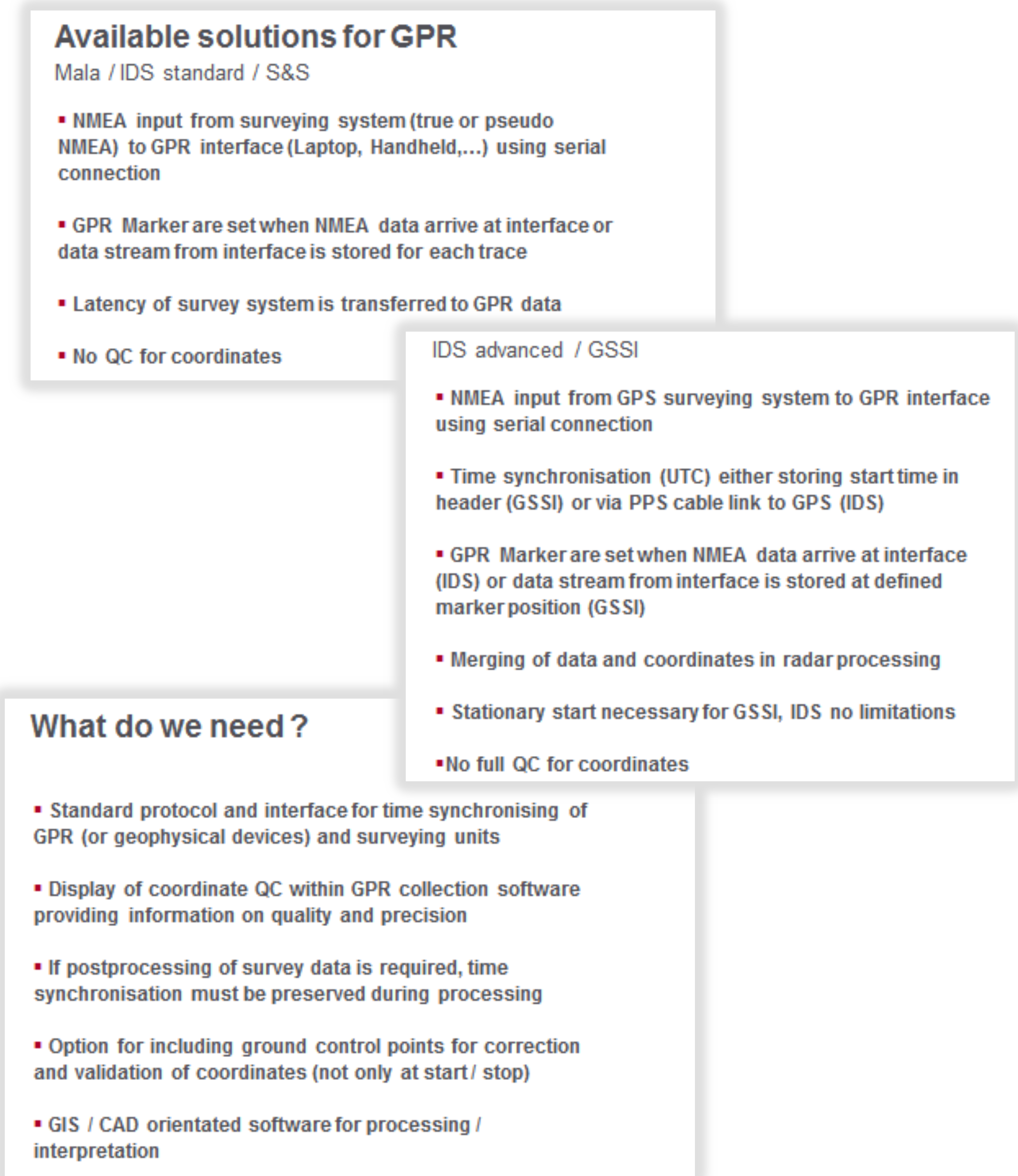

ACKNOWLEDGEMENT

The author acknowledges the COST Action TU1208 “Civil Engineering Applications of Ground Penetrating Radar”, supporting this work.

"IMPROVEMENT OF THE ENERGETIC PROPERTIES OF THE GPR"
(CONTRIBUTION TO PROJECT 1.1)

Gennadiy P. Pochanin (UA), Vadim P. Ruban (UA), Pavlo V. Kholod (UA), Alexander A. Shuba (UA), Alexander G. Pochanin (UA), Alexander A. Orlenko (UA) - *gpp_15@ukr.net*

The abstract is published in *Geophysical Research Abstracts*, Vol. 16, EGU2014-16928, 2014 and is available on *www.egu2014.eu.*

"COMPARISON OF PULSE AND SFCW GPR
IN TIME, FREQUENCY AND WAVELET DOMAIN"
(CONTRIBUTION TO PROJECT 1.1)

Jan De Pue (BE), Ellen Van De Vijver (BE), Wim Cornelis (BE), Marc Van Meirvenne (BE) - *jan.depue@ugent.be*

The abstract is published in *Geophysical Research Abstracts*, Vol. 16, EGU2014-16072, 2014 and is available on *www.egu2014.eu.*

These contributions were presented as posters.

"Electromagnetic exposure of GPR operators and interference issues" (contribution to Project 1.2)

Simone Chicarella (1), Vincenzo Ferrara (1), Paolo D'Atanasio (2), Fabrizio Frezza (1), Lara Pajewski (3), Settimio Pavoncello (4), Santo Prontera (1), Nicola Tedeschi (1), and Alessandro Zambotti (2)

(1) Dept. of Information Engineering, Electronics and Telecommunications, Sapienza University of Rome, Rome, IT (ferrara@diet.uniroma1.it), (2) ENEA - Casaccia Research Centre, Rome, IT (3) "Roma Tre" University, Engineering Department, Rome, IT (4) "ARPA Lazio" Regional Environmental Protection Agency, Rome, IT

The abstract is published in *Geophysical Research Abstracts*, Vol. 16, EGU2014-5387, 2014 and is available on *www.egu2014.eu.*

Abstract

This paper aims at investigating two aspects: first, the evaluation of electromagnetic radiation intensity to which humans operating with ground penetrating radar are exposed; the second topic is to investigate effects of electromagnetic interferences of specific devices, such as cellular phones, and transceivers built on the IEEE 802.15.4 MAC/PHY layers.

1. Introduction

GPR systems operate from 10 MHz up to 5 GHz, with about a decade of bandwidth within that range, so placing themselves into the most extreme class of ultra-wideband (UWB) radars. In order to evaluate the electromagnetic emissions, comparing them to the limits that now exist in a number of jurisdictions, recent studies have focused on the basic steps needed to translate UWB GPR's results into regulatory parameters [1]. When analyzing a GPR we need to distinguish two functional aspects: operation as intentional radiator, and Electromagnetic Compatibility (EMC) requirements which equipment must satisfy. As deliberate radio frequency radiator, it can be assimilated to a Short Range Device (SRD), such as movement detectors and metal detectors, covered by the R&TTE Directive of European Commission [2]. Regarding EMC issues, emission requirements of equipment are defined by "Comité international spécial des perturbations radioélectriques" (CISPR) [3], and

those of immunity by the International Electrotechnical Commission (IEC) committees. European Telecommunications Standards Institute (ETSI) published standards on compatibility, and ground- and wall-probing radar applications, approved by the European National Standards Organizations in form of European Norm (EN). Specifically, ETSI Standard EN-302066-1 V1.2.1 [4] defines technical characteristics, and test methods, whereas ETSI Standard EN-302066-2 V1.2.1 [5] harmonizes requirements of an article of R&TTE Directive.

This work presents experimental test implementations for verifying how mobile phones and other common sources of possible interference can contaminate GPR data, and how to post-process the data in order to filter such interference effects. Among the interfering devices, XBee transceivers, based on *IEEE 802.15.4 standard,* are considered, since participants of Project 4.2 intend to combine them with a GPR, mounted on Unmanned Aerial Vehicle (UAV), for wireless communication of the detection and localisation of people buried under avalanche.

Considering that GPR systems:

- are not operated for extended duration and their mean radiated power is very low;
- are often used in areas where the density of population is low;
- are designed to radiate energy into the ground, where it is quickly absorbed (Fig. 1);
- are often equipped with a shut-off switch that automatically stops the radiation when the radar is lifted from the ground surface, or is not operated in the proper position;

interference is very rare and the human health protection issue is ignored. Nevertheless, when GPR application is exactly the people detection, this issue cannot be overlooked. Therefore, another focus of the work is to quantify the exposure of GPR operators to electromagnetic waves emitted by the radar, for human health protection.

Fig. 1: GPR radiates energy into the ground normally with reduced back-propagation toward operator.

2. EM Exposure of GPR Operators

Figure 2 shows the devices under test: the SIR2000, a GPR model by Geophysical Survey Systems, Inc. (GSSI), and the SUB-ECHO HBD 300 antenna by Radarteam Sweden AB factory.

SIR2000 is a single channel general-purpose system requiring a 12 V DC power input at 3 A. It can be used with antennas from 16 MHz to 2000 MHz providing penetration depths ranging from tens of m to a few cm.

The SUB-ECHO HBD 300 antenna operates at 300 MHz as central frequency. Its frequency boundaries of 3-dB bandwidth are 120-780 MHz. Front to back ratio stated around -14.5 dB. It weighs 4 kg and its dimension is (L x W x H) 720x360x160 mm.

(a) (b)

Fig. 2: Devices under test: (a) GPR GSSI SIR2000, (b) Radarteam SUB-ECHO HBD 300 antenna.

For our test, we used the following equipment:

- Lecroy Wavemaster 8500A oscilloscope that allows measures up to 6 GHz;
- FSP30 spectrum analyzer by Rohde Schwarz operating in the range 9 kHz ÷ 30 GHz;
- E4440 spectrum analyzer by Agilent which works from 3 Hz to 26.5 GHz.

The measurement setup has been completed with:

- preamplifier HP8447F (9 kHz ÷1300 MHz);
- Shuner Sukoflex 100 microwave cables 104 & 106;

- Precision Conical Dipole (PCD) 8250 by Seibersdorf factory, like receiving antenna used in the frequency range 80 MHz ÷ 3 GHz, with a sensitivity that rises from 0.8 to 1.1 mV/m in the same frequency range.

We carried out measures inside an anechoic chamber of large dimension: 9x6x5.4 m. This chamber allows measurements in the frequency range 300 kHz÷18 GHz. Table 1 specifies its electric and magnetic shielding efficiency in different frequency ranges, and picture in Fig. 3 shows setup of measure. A sketch of the same experimental setup is reported in Fig. 4.

Frequency range	Electric shielding efficiency (dB)
300 kHz ÷ 30 MHz	120
30 MHz ÷ 400 MHz	105
400 MHz ÷ 18 GHz	100

Frequency	Magnetic shielding efficiency (dB)
10 kHz	60
100 kHz	90

Table 1: Electric and magnetic shielding efficiency of the anechoic chamber.

Fig. 3: Anechoic chamber.

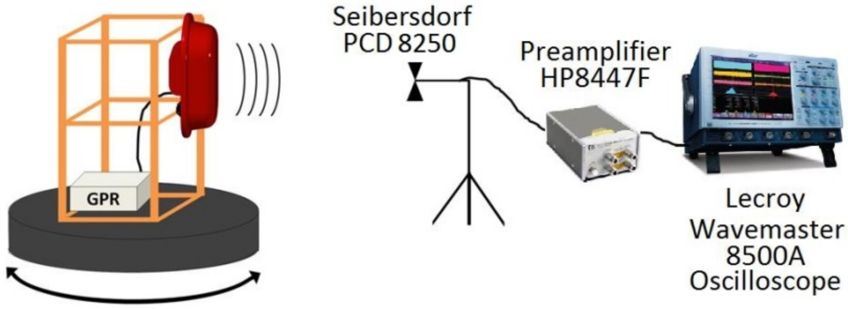

Fig. 4: Sketch of the experimental setup.

Normally, a GPR operator is exposed to the back lobe of the transmitting antenna, as well as to the signal reflected from soil under investigation. We considered the worst case, evaluating the electric field transmitted from the GPR directly to a receiving antenna, located about at 2 m of distance.

The measured radiation pattern of the GPR antenna is shown in Fig. 5.

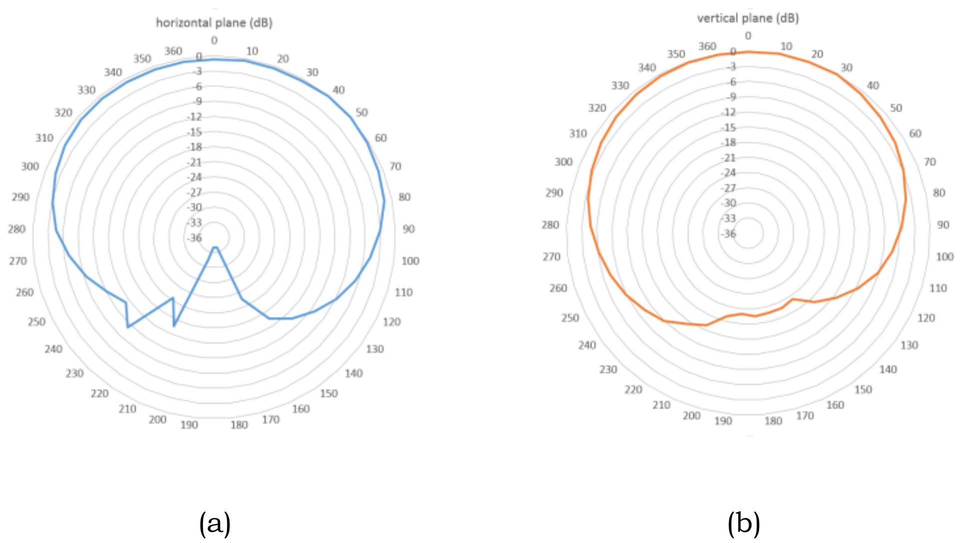

Fig. 5: Radiation patterns of the GPR antenna measured in dB units: (a) horizontal and (b) vertical.

Results were collected by supposing that all radiated energy reaches the operator, along a direct line of maximum electromagnetic radiation, disregarding the back lobe transmission.

The intensity of the electric field E is evaluated by means of the following equation (1):

$$E = ACF \cdot V_a = ACF \cdot Att_{Cable} \cdot V_r \qquad (1)$$

where: V_a is the voltage value across output of receiving antenna, Att_{Cable} defines the cable attenuation, V_r is the voltage intensity measured by the receiver, and *ACF* represents the antenna calibration factor.
By using a spectrum analyser (SA), we could measure the signal spectrum, identify its portion generated by the radar, and evaluate the peak and average voltage intensity. Furthermore, by exploiting a suitable setting of the Resolution Bandwidth (RBW) of our SA, we could put in evidence the actual radar pulses. In Figure 6, typical pulses generated by the GPR are shown, in time and frequency domains. The SIR2000 GPR generates single pulses that have a time duration of about 2.7 ns and a variable Pulse Repetition Time (PRT = T). Measures carried out in the controlled room confirm the presence of spectral traces separated among them by a constant PRF = 1/T (Pulse Repetition Frequency), as shown in Figure 7.

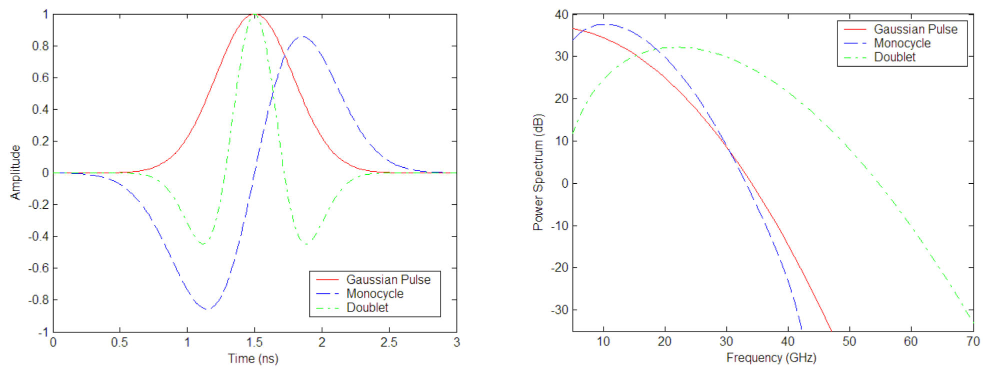

(a) (b)

Fig. 6: Pulse generated by the GPR, in time (a) and spectral (b) domains.

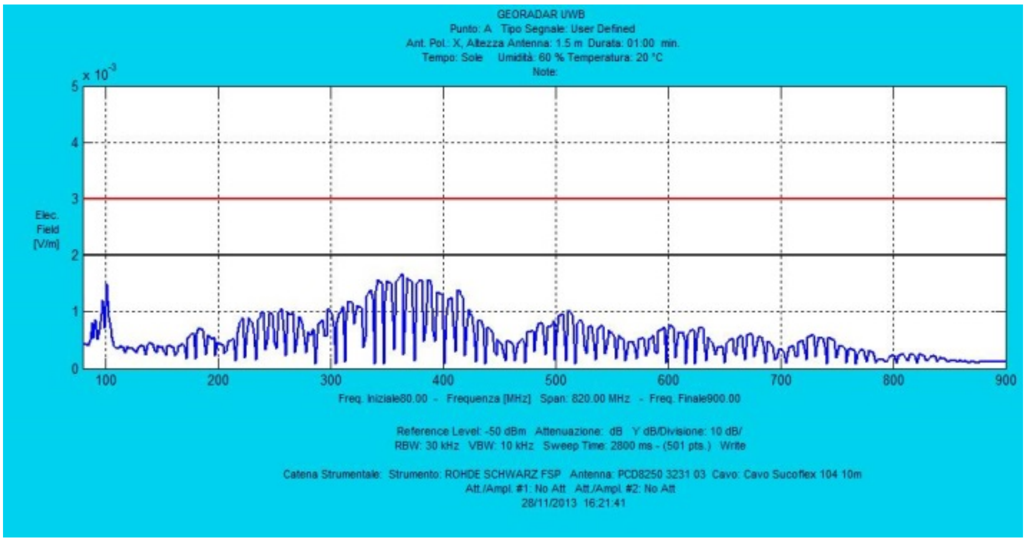

Fig. 7: Measured spectrum.

Two SA modes are possible, depending on the ratio between bandwidth at 3 dB of IF filter (RBW), and frequency distance between contiguous spectral rows, as shown in Fig. 8. These two procedures are named: line spectrum mode and pulse spectrum mode.

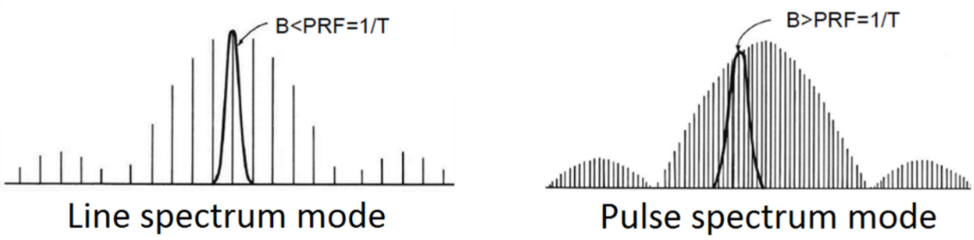

Fig. 8: Spectral traces permitted.

When we operate by using the line spectrum mode, the analyzer resolution allows us to display each single spectral component. In this case, the norm CEI 211-7B regulates how to measure the electric field peak: is the dB value, estimated by means of analyzer at carrier frequency, corrected by adding the de-sensitivity factor α_L:

$$\alpha_L\left[dB\right] = -20 \cdot \log_{10}\left(\frac{\tau}{T}\right) \qquad (2)$$

where τ is the peak duration time.

DPCM (Decree of the President of the Council of Ministers of the Italian Republic) July 8, 2003 is the Italian rule regarding exposure of people to the electromagnetic fields. Nevertheless, it regulates only the cases of telecommunication fixed services (art. 1). However, in the case of pulsed signal, the same decree at subsection no. 4 recommends to adopt the European Recommendation (July 12, 1999). This rule, conformable to the ICNIRP (International Commission on Non-Ionizing Radiation Protection), evaluates maximum power density (S) as the average power density multiplied by factor 1000. This is equivalent to multiply the average electric field by the factor 32 for obtaining maximum electric field, at identical frequency obviously. Similarly, D. Lgs (Legislative Decree) 81-2008, conformable to the rule CE 2004/40, regulates worker exposure. Specifically, in the frequency range 10 MHz÷300 GHz, peak values are evaluated by multiplying the rms values by factors 32 and 1000, respectively for electric field and power density of the equivalent plane wave.

When the voltage receiver is expressed in dBm, we can use the equation:

$$E(dBV/m) = ACF(dB) + Att_{Cable}(dB) + V_r(dBm) - 13 \qquad (3)$$

In our experimental results, the value of electrical field peak has been measured equal to E_{peak} = 1.7 mV.
GPR's setup can be changed. In the case of setup as 900TAS, 300S, 2500HHS, we measured a PRT of 12 μs, different from that shown when setup is 500DPH (PRT=23.3 μs).

Consequently, the rms values of electrical field are:

$$E_{RMS} = E_{peak}\sqrt{\frac{\tau}{T}} = \begin{cases} 0.025 \ \dfrac{V}{m} & \text{, for setup: 900TAS, 300S, 2500HHS.} \\ 0.018 \ \dfrac{V}{m} & \text{, for setup: 500DPH} \end{cases}$$

In any case, these measured values are very little, lower than limits imposed by rule. The following Fig. 9 exemplifies the rules, by evaluating limits imposed respectively for average and for peak values of electric field.

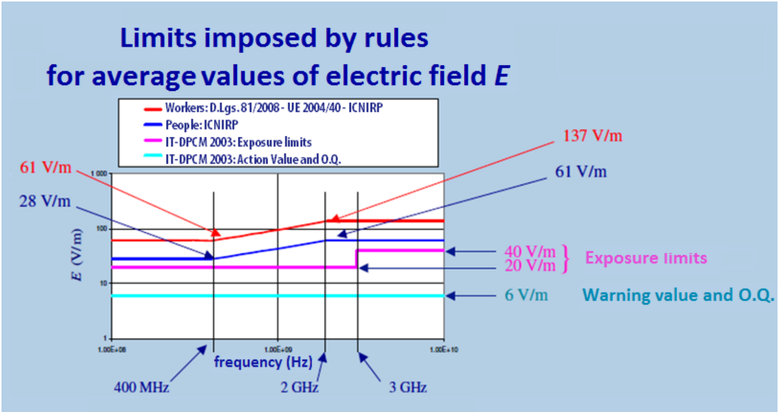

(a)

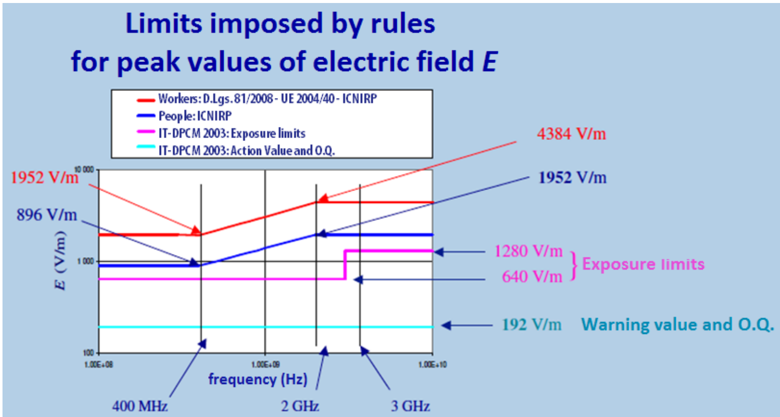

(b)

Fig. 9: Limits imposed by rules, respectively for average (a) and peak (b) values of electric field.

3. Interference Testing Analysis to Develop a GPR Application: Detection of People Under Avalanches

The detection and precise localization of people buried or trapped under avalanche or debris is an emerging field of application of GPR [6÷11]. In the last years, processing approaches and technological solutions have been developed to improve detection accuracy, speed up localization, and reduce false alarms. In case of emergency scenario for avalanche, improvement of these three aspects is fundamental for increasing probability of survivals. Indeed, the survival time is very short, since the

relative probability decreases to 90, 40 and 30 per cent, if the victim is removed from the snow within 15, 30 and 60 minutes, respectively. So, radar at direct contact with the snow surface is not a viable option. In fact, moving radar systems on a mountain slope run over by avalanche is particularly complicated, due to the presence of bulky slabs of ice mixed with snow. Therefore, placing the radar just on the snow is not fast enough for using it during emergency.
In order to solve this problem, since 2005 researchers have considered a GPR system mounted on an airborne platform [12÷14], e.g. helicopter shown in Fig. 10, or UAV in the future. Especially for the last case, there is need to add electronic devices to the basic GPR system. These subsystems allow wireless communication between GPR and operating unit, located on the snowy surface or inside a control room.
In order to evaluate interferences generated by transmitters located near the GPR antenna, we organized two different measurements, in the presence of a cellular phone and of a XBee transceiver.
The first test concerned an UMTS cellular phone. The distance between the GPR antenna and the phone was 1.4 m. Fig. 11 shows radargram output (3849 scans), in absence (a) and in presence (b) of the cellular transmission. Fig. 12 shows the oscilloscope representation, allowing us to put in evidence a very limited spread of traces.

Fig. 10: GPR system mounted on an airborne platform (from the Radarteam Sweden AB web-site).

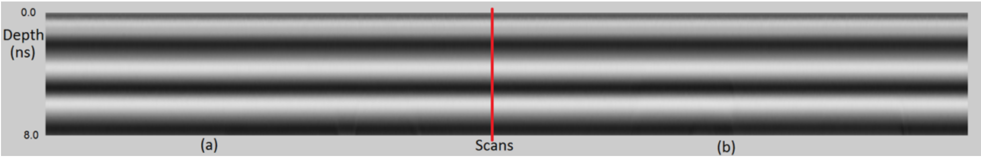

Fig. 11: Radargram in absence (a) and in presence (b) of the cellular transmission.

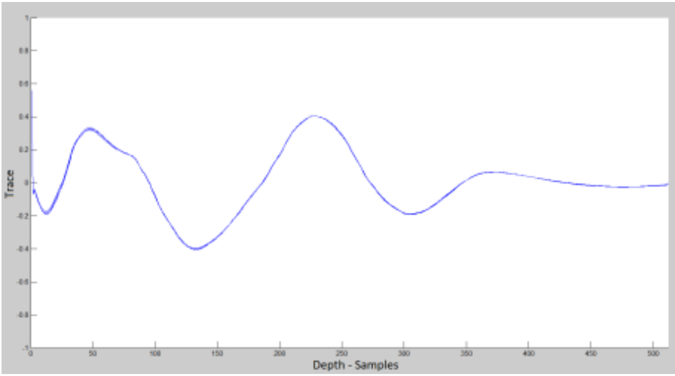

Fig. 12: Oscilloscope representation.

For the second test, a transceiver XBee PRO-S2 (international variant by Digi International), is arranged on the top at direct contact with GPR's antenna, as shown in Fig. 13. Specifications of the RF module are: transmitting power output 10 mW, outdoor RF LOS range 1500 m, operating frequency band ISM 2.4 GHz, RF data rate 250 kbps, 14 direct sequence channels.
The radargram of Fig. 14 shows a first interval of data acquisition with the XBee in off state, and a following interval characterized by the XBee continuously transmitting.
Both tests demonstrate a very low interference generated by the devices, due to the fact that their operating frequency bands are different from the GPR bandwidth. Therefore, the design for adding wireless communication devices to the GPR is justified.

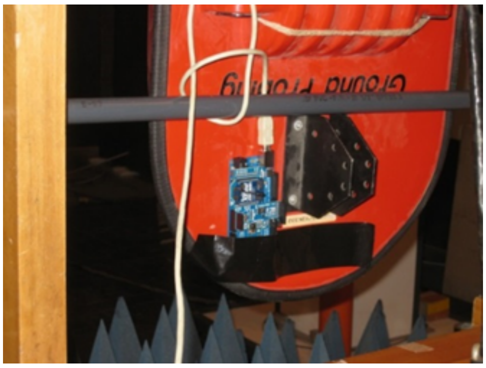

Fig. 13: XBee transceiver on the top of the antenna.

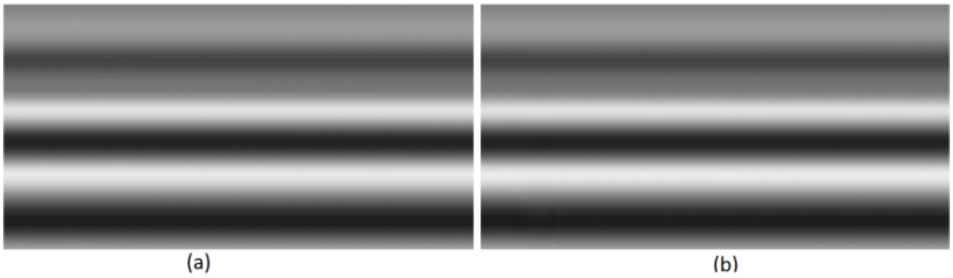

Fig. 14: Radargram in presence (a) and in absence (b) of an operating XBee transceiver.

Acknowledgement

The authors thank COST for funding the COST Action TU1208 "Civil Engineering Applications of GPR."

References

[1] A.P. Annan, N. Diamanti, and J.D. Redman, "GPR Emissions and Regulatory Limits," 15th International Conference on Ground Penetrating Radar - GPR 2014, Brussels, Belgium, pp. 714-718, 2014.

[2] European Commission's Directorate-General for Enterprise and Industry, "Guide to the R&TTE Directive 1999/5/EC - Version of 20 April 2009".

[3] CISPR 16-1: "Specifications for radio disturbance and immunity measuring apparatus and methods- Part I: Radio disturbance and immunity measuring apparatus".

[4] ETSI Standard EN-302066-1 V1.2.l "Electromagnetic compatibility and Radio spectrum Matters (ERM); Ground- and Wall- Probing Radar applications (GPR/WPR) imaging systems; Part I: Technical characteristics and test methods".
[5] ETSI Standard EN-302066-2 V1.2.l: "Electromagnetic compatibility and Radio spectrum Matters (ERM); Ground- and Wall- Probing Radar applications (GPR/WPR) imaging systems; Part 2: Harmonized EN covering essential requirements of article 3.2 of the R&TTE Directive".
[6] C. Jaedicke, "Snow mass quantification and avalanche victim search by ground penetrating radar," Survey in Geophysics, vol. 24, no. 5/6, 2003, pp. 431-445.
[7] A. Instanes, I. Lonne, and K. Sandaker, "Location of avalanche victims with ground penetrating radar," Cold regions Sci. Technol., vol. 38, no. 1, 2004, pp. 55-61.
[8] J. Modroo and G. Olhoeft, "Avalanche rescue using ground penetrating radar," in Proc. 10th Int. Conf. Ground Penetrating Radar, Delft, The Netherlands, 2004, pp. 785-789.
[9] E. Zaikov and J. Sachs, "UWB radar for detection and localization of trapped people," Ultra Wideband, Boris Lembrikov (Ed.), ISBN: 978-953-307-139-8, InTech, 2010.
[10] J. Sachs, M. Helbig, R. Herrmann, M. Kmec, K. Schilling, E. Zaikov, and P. Rauschenbach, "Trapped victim detection by pseudo-noise radar," in Proc. ACWR '11, 1st International Conference on Wireless Technologies for Humanitarian Relief, 2011, pp. 265-272.
[11] M. Loschonsky, C. Feige, O. Rogall, S. Fisun, and L. M. Reindl, "Detection technology for trapped and buried people," IEEE MTT-S International Microwave Workshop on Wireless Sensing, Local Positioning, and RFID (IMWS 2009 - Croatia), 2009, pp. 1-6.
[12] M. Haltmeier, R. Kowar, and O. Scherzer, "Computer aided location of avalanche victims with ground penetrating radar mounted on a helicopter," in Proc. 30th Workshop OAGM/AAPR Digital Imaging Pattern Recog., Obergurgl, Austria, 2005, pp. 19-28.
[13] A. Heilig, M. Schneebeli, and W Fellin, "Feasibility study of a system for airborne detection of avalanche victims with ground penetrating radar and a possible automatic location algorithm," Cold Regions Sci. Technol., vol. 51, no. 2/3, 2008, pp. 178-190.
[14] F. Fruehauf, A. Heilig, M. Schneebeli, W. Fellin, and O. Scherzer, "Experiments and algorithms to detect snow avalanche victims using airborne ground-penetrating radar, "IEEE Trans. On Geoscience and Remote Sensing, vol. 47, no. 7, 2009, pp. 2240-2251.

"Characterisation and Optimisation of Ground Penetrating Radar Antennas" (contribution to project 1.3)

Craig Warren (UK), Antonios Giannopoulos (UK) - *craig.warren@ed.ac.uk*

The abstract is published in *Geophysical Research Abstracts*, Vol. 16, EGU2014-12971, 2014 and is available on *www.egu2014.eu.*

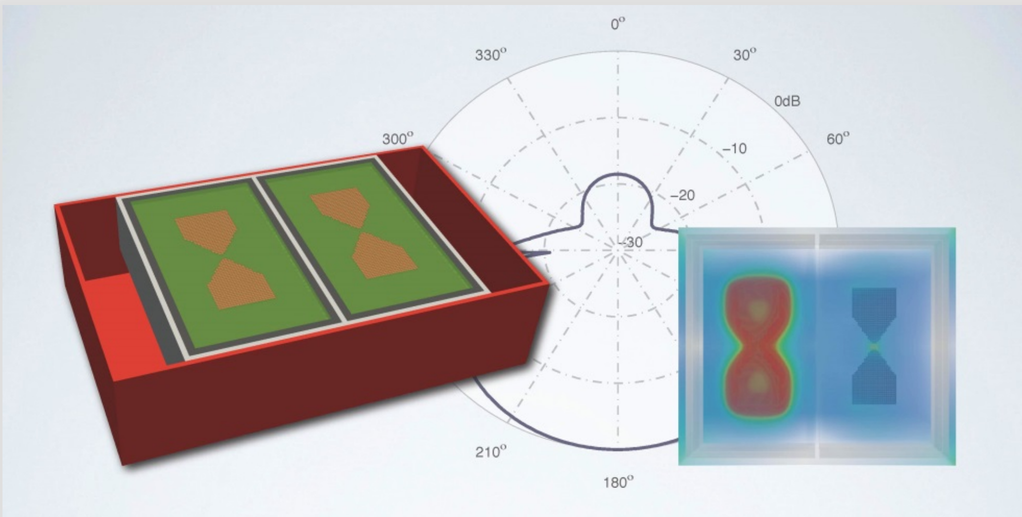

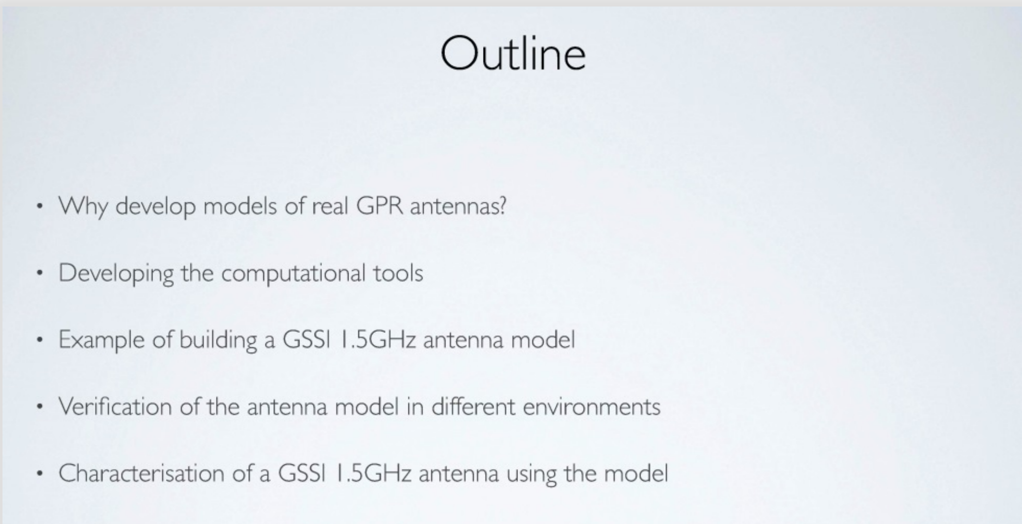

Motivation

Why model real GPR antennas?

"To enable GPR simulations to replicate real GPR responses with accurate amplitude and phase information"

- To improve understanding and aid interpretation of complex responses and data sets
  - Critical to obtain *quantitative* information from near-surface targets
- To develop and optimise antenna designs
- Increased computing power makes 3D modelling more accessible and usable

If we do not attempt to model real transducers…

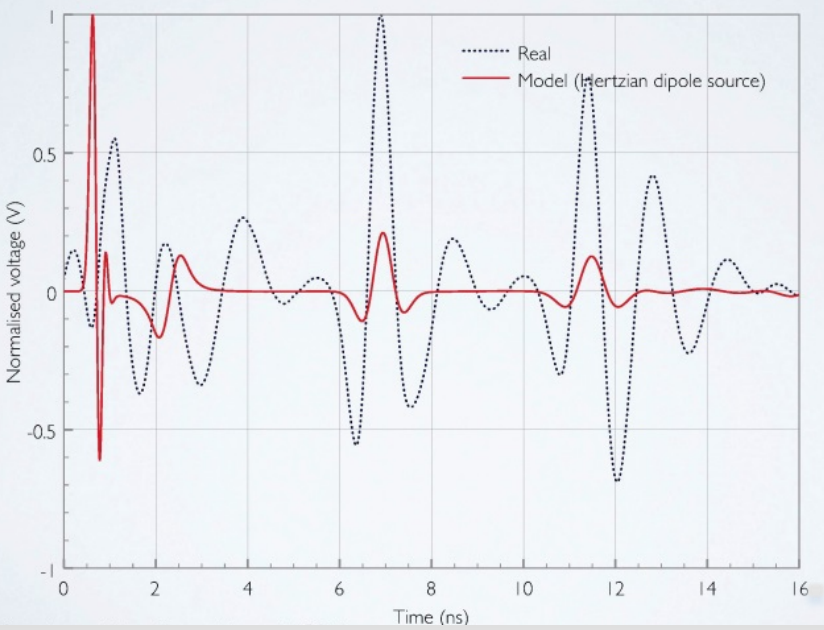

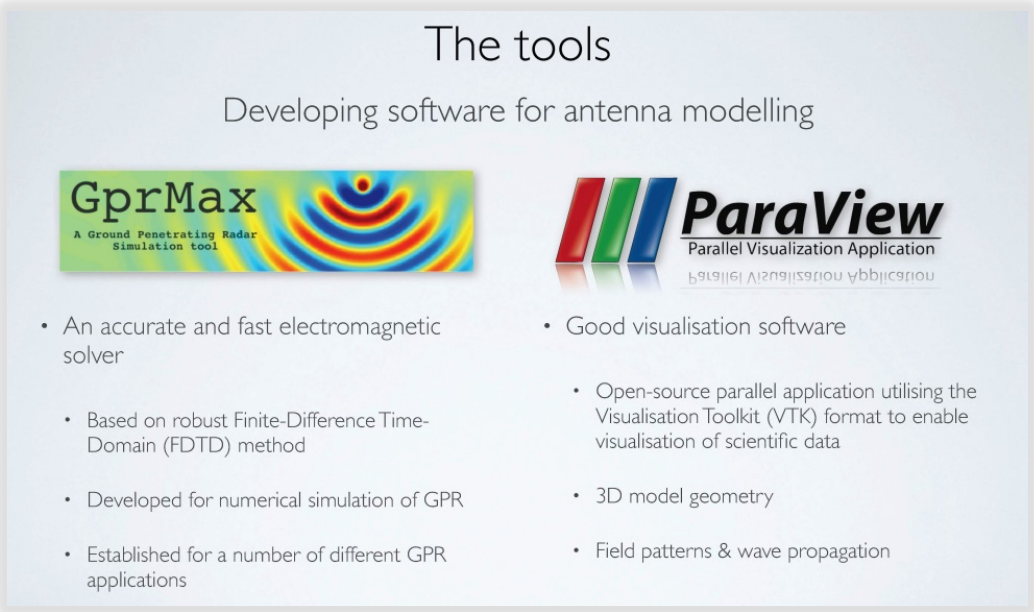
The tools
Developing software for antenna modelling
GprMax
A Ground Penetrating Radar Simulation tool
ParaView
Parallel Visualization Application
• An accurate and fast electromagnetic solver
• Based on robust Finite-Difference Time-Domain (FDTD) method
• Developed for numerical simulation of GPR
• Established for a number of different GPR applications
• Good visualisation software
• Open-source parallel application utilising the Visualisation Toolkit (VTK) format to enable visualisation of scientific data
• 3D model geometry
• Field patterns & wave propagation

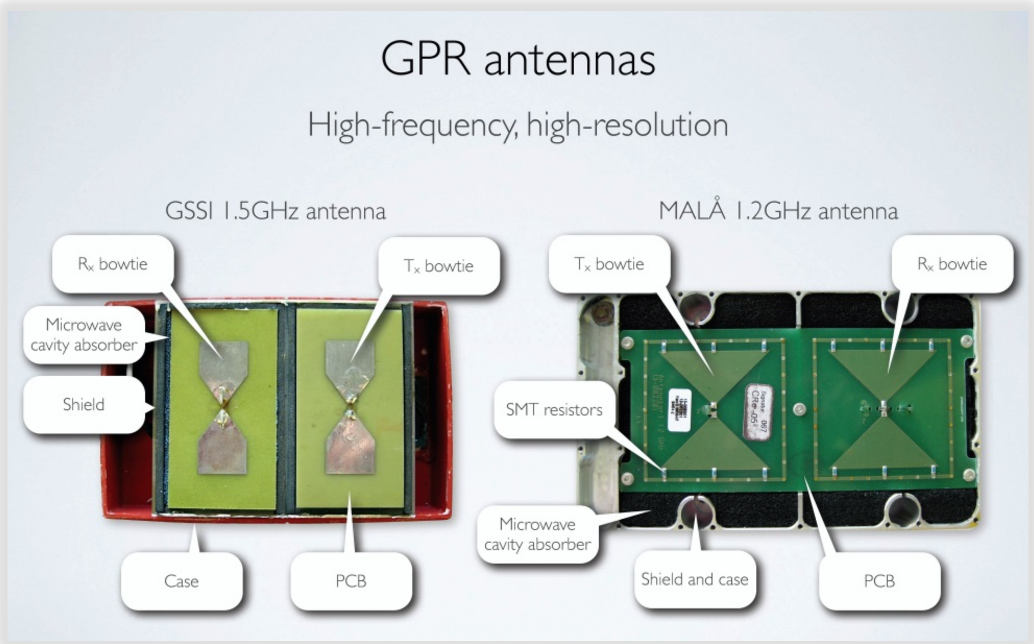
GPR antennas
High-frequency, high-resolution
GSSI 1.5GHz antenna
Rx bowtie
Tx bowtie
Microwave cavity absorber
Shield
Case
PCB
MALÅ 1.2GHz antenna
Tx bowtie
Rx bowtie
SMT resistors
Microwave cavity absorber
Shield and case
PCB

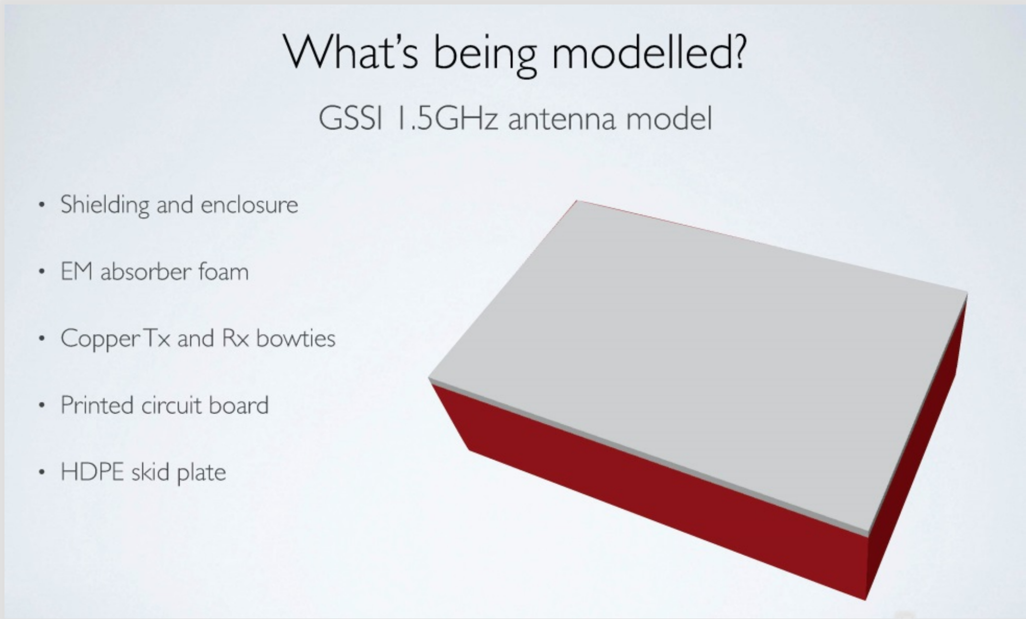
What's being modelled?
GSSI 1.5GHz antenna model
• Shielding and enclosure
• EM absorber foam
• Copper Tx and Rx bowties
• Printed circuit board
• HDPE skid plate

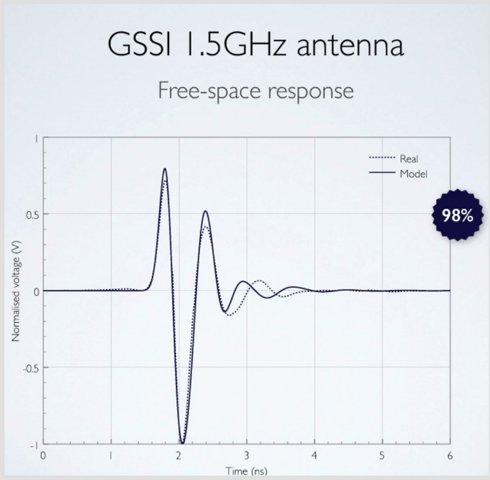
GSSI 1.5GHz antenna
Free-space response
Real
Model
98%
Normalised voltage (V)
Time (ns)

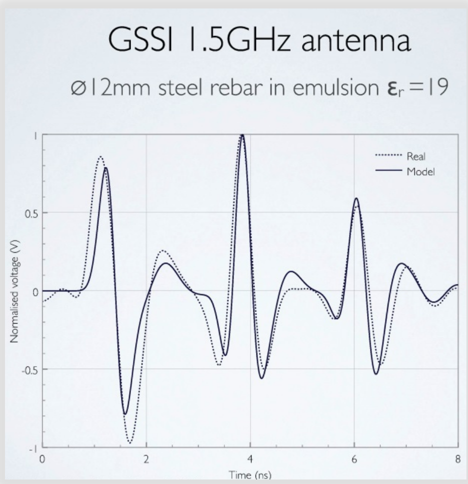
GSSI 1.5GHz antenna
Ø12mm steel rebar in emulsion εr =19
Real
Model
Normalised voltage (V)
Time (ns)

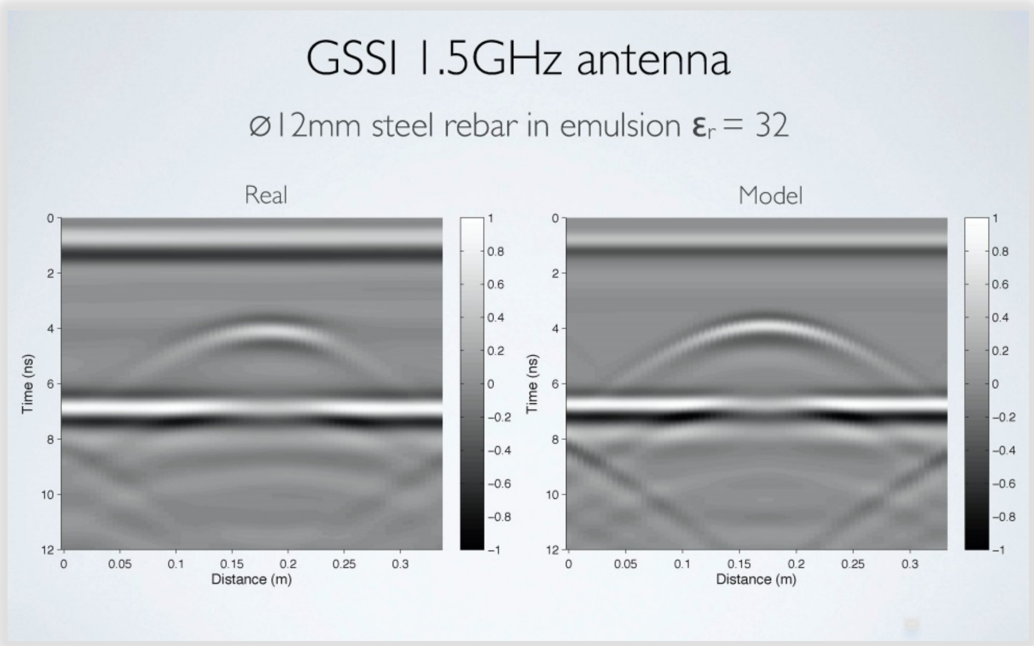
GSSI 1.5GHz antenna
Ø12mm steel rebar in emulsion εr = 32
Real
Model
Time (ns)
Distance (m)

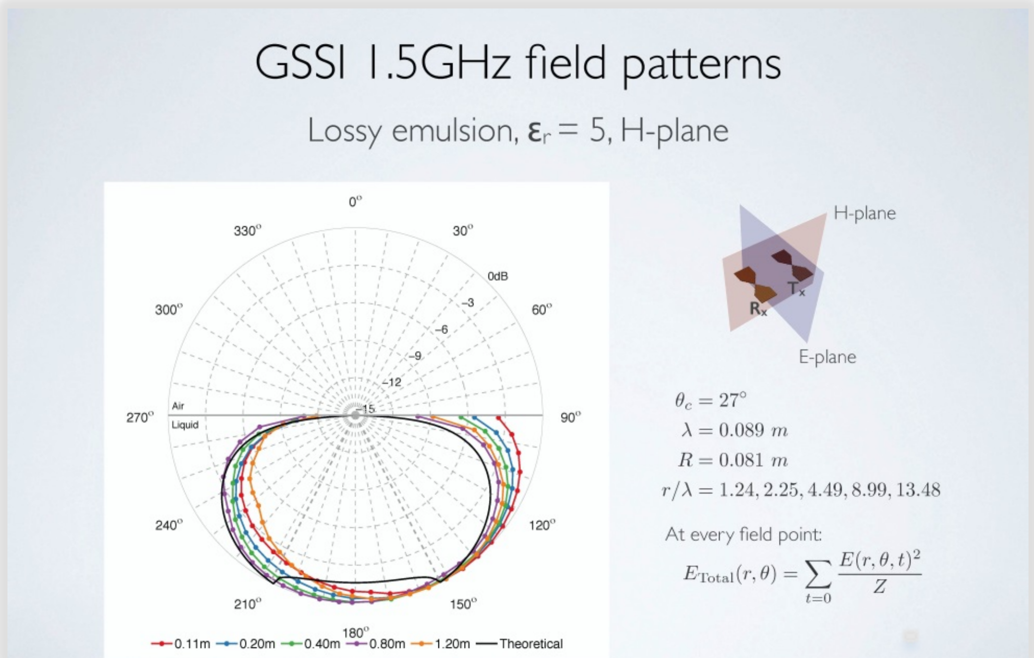
GSSI 1.5GHz field patterns
Lossy emulsion, εr = 5, H-plane
Air
Liquid
0.11m
0.20m
0.40m
0.80m
1.20m
Theoretical
H-plane
E-plane
Rx
Tx
$\theta_c = 27°$
$\lambda = 0.089\ m$
$R = 0.081\ m$
$r/\lambda = 1.24, 2.25, 4.49, 8.99, 13.48$
At every field point:
$E_{\text{Total}}(r,\theta) = \sum_{t=0} \frac{E(r,\theta,t)^2}{Z}$

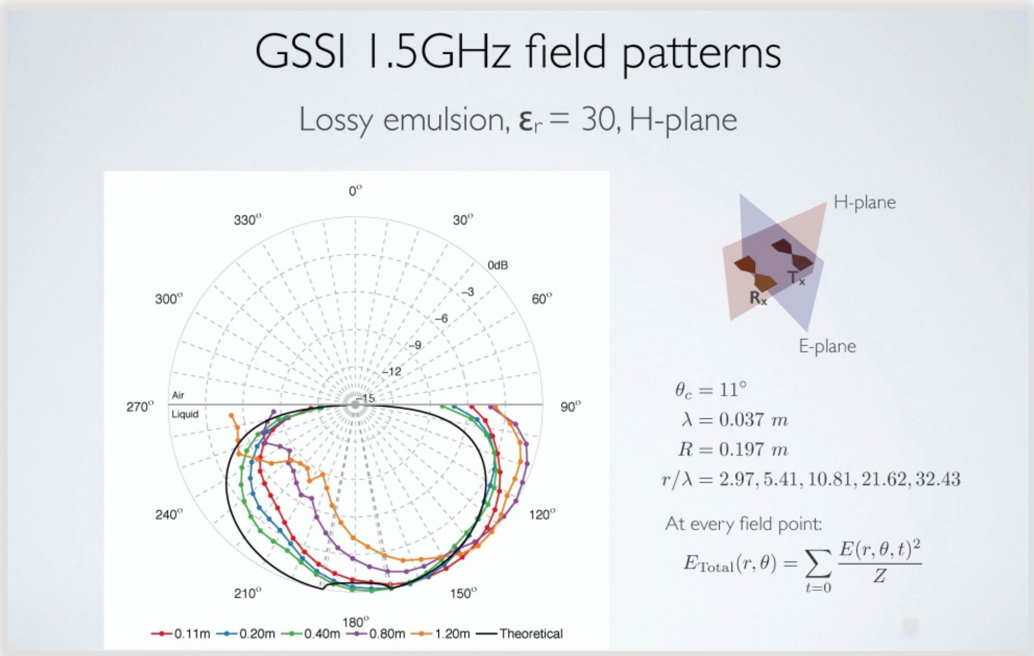
GSSI 1.5GHz field patterns
Lossy emulsion, εr = 30, H-plane
0°
330°
30°
300°
60°
270°
90°
240°
120°
210°
150°
180°
0dB
−3
−6
−9
−12
−15
Air
Liquid
0.11m
0.20m
0.40m
0.80m
1.20m
Theoretical
H-plane
E-plane
Rx
Tx
$\theta_c = 11°$
$\lambda = 0.037\ m$
$R = 0.197\ m$
$r/\lambda = 2.97, 5.41, 10.81, 21.62, 32.43$
At every field point:
$E_{\mathrm{Total}}(r,\theta) = \sum_{t=0} \frac{E(r,\theta,t)^2}{Z}$

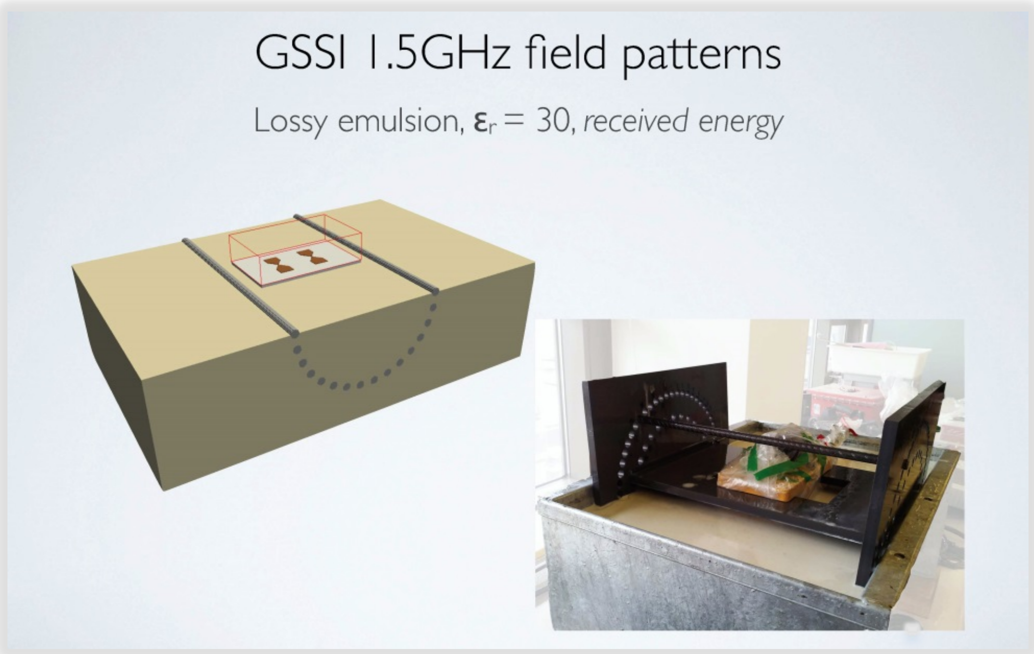
GSSI 1.5GHz field patterns
Lossy emulsion, εr = 30, received energy

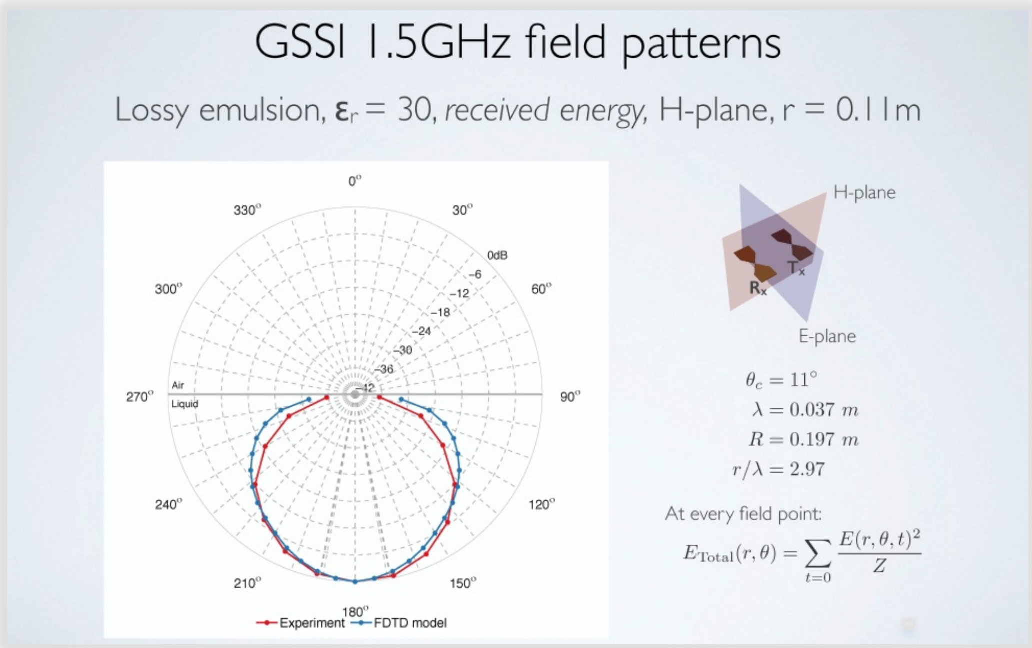

Conclusions

- There is a need to model real GPR antennas:
  - Quantitative information from targets (especially near-surface)
  - Design and optimisation of antennas
- Characterisation of antenna from transmitted field and received energy H-plane patterns
  - No pronounced cusps/nulls in real patterns (as expected)
  - In low permittivities main lobe remains broad for usable range of antenna
  - In higher permittivities and for ranges >10-20 wavelengths, main lobe narrows and skews

Acknowledgement - The authors acknowledge the COST Action TU1208 "Civil Engineering Applications of GPR".

"ELECTROMAGNETIC MODELLING OF GPR HORN ANTENNAS" (CONTRIBUTION TO PROJECT 1.3)

Iraklis Giannakis (UK), Antonios Giannopoulos (UK), Lara Pajewski (IT) - *i.giannakis@ed.ac.uk*

The abstract is published in *Geophysical Research Abstracts*, Vol. 16, EGU2014-1553, 2014 and is available on *www.egu2014.eu.*

The main focus of this work was the accurate and realistic implementation of GPR antennas into a FDTD model. During the Second General Meeting, this work was presented as a poster.

The main challenges in electromagnetic modelling of GPR for civil-engineering applications are A) the implementation of the dielectric properties of the media (soils, concrete, etc.) in a realistic way; B) the implementation of the geometry of the media (soils inhomogeneities, rough surface, vegetation, concrete features like fractures and rock fragments, etc.); and, C) the detailed modelling of the antenna units.

Accurate models based on general characteristics of the commercial antennas GSSI 1.5 GHz and MALA 1.2 GHz have been already incorporated in GprMax, a free software which solves Maxwell's equation using a second order in space and time FDTD algorithm [1-3].

The present work was concerned with the implementation of horn antennas with different geometrical parameters, as well as ridged horn antennas, into the FDTD model. Realistic models of soils and concrete were used to test and compare different horn-antenna units. In particular, stochastic methods were used in order to realistically simulate the geometrical characteristics of the medium. Regarding the dielectric properties, Debye approximations were adopted in order to simulate the frequency-dispersive properties of the medium within the frequency range of interest.

ACKNOWLEDGEMENT

The authors thank COST for funding the Action TU1208 "Civil Engineering Applications of Ground Penetrating Radar," supporting this work through a Short-Term Scientific Mission grant.

References

[1] A. Giannopoulos, "Modelling ground penetrating radar by GprMax," Constr Build Mater, vol. 19, pp. 755-762, 2005.
[2] C. Warren, A. Giannopoulos, "Creating FDTD models of commercial GPR antennas using Taguchi's optimisation method," Geophysics, vol. 76, no. 37, 2011.
[3] C. Warren, A. Giannopoulos, "Investigation of the directivity of a commercial Ground-Penetrating Radar antenna using a Finite-Difference Time-Domain antenna model," 13th International Conference on Ground Penetrating Radar (GPR), pp.226-231, 4-8 Jun. 2012.

WORKING GROUP 2

GPR surveying of pavements, bridges, tunnels and buildings; underground utility and void sensing

Progress Report of Project 2.1

"Innovative inspection procedures for effective GPR surveying of critical transport infrastructures (pavements, bridges and tunnels)"

Josef Stryk (CZ)
josef.stryk@cdv.cz

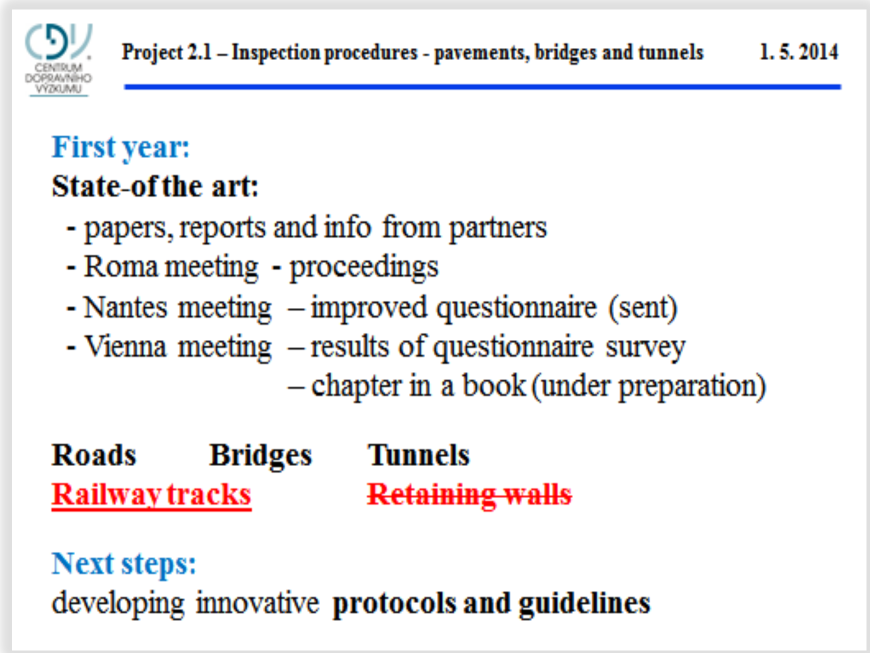

Roma Meeting:	**Nantes Meeting:**
36 Participants	46 Participants
15 Countries	18 Countries

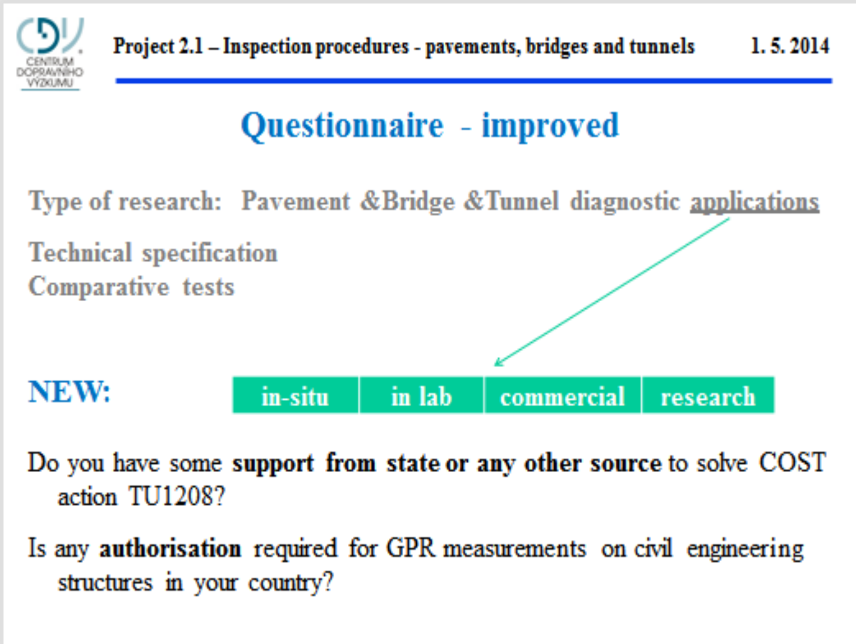
Project 2.1 – Inspection procedures - pavements, bridges and tunnels
1. 5. 2014
Questionnaire - improved
Type of research: Pavement &Bridge &Tunnel diagnostic applications
Technical specification
Comparative tests
NEW:
in-situ
in lab
commercial
research
Do you have some support from state or any other source to solve COST action TU1208?
Is any authorisation required for GPR measurements on civil engineering structures in your country?

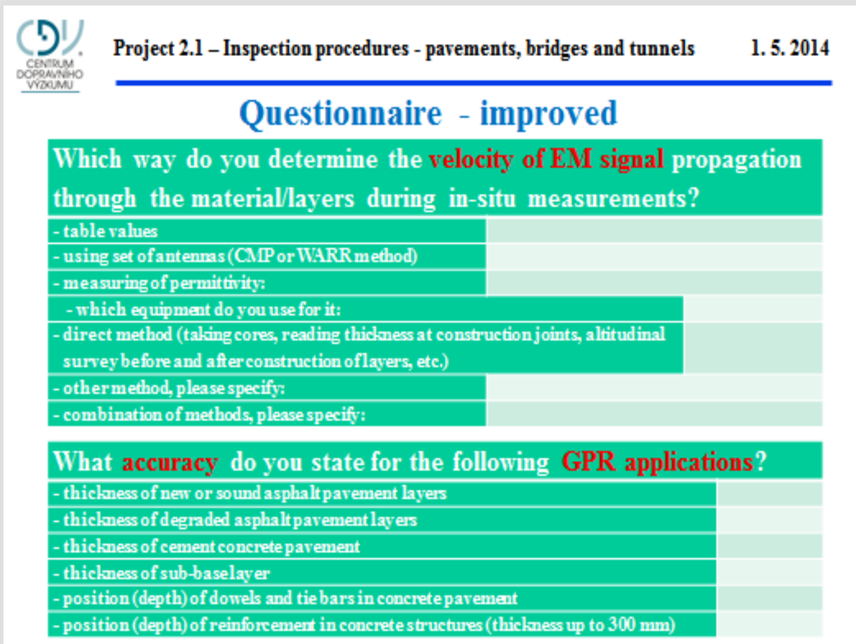
Project 2.1 – Inspection procedures - pavements, bridges and tunnels
1. 5. 2014
Questionnaire - improved
Which way do you determine the velocity of EM signal propagation through the material/layers during in-situ measurements?
- table values
- using set of antennas (CMP or WARR method)
- measuring of permittivity:
- which equipment do you use for it:
- direct method (taking cores, reading thickness at construction joints, altitudinal survey before and after construction of layers, etc.)
- other method, please specify:
- combination of methods, please specify:
What accuracy do you state for the following GPR applications?
- thickness of new or sound asphalt pavement layers
- thickness of degraded asphalt pavement layers
- thickness of cement concrete pavement
- thickness of sub-base layer
- position (depth) of dowels and tie bars in concrete pavement
- position (depth) of reinforcement in concrete structures (thickness up to 300 mm)

CENTRUM DOPRAVNÍHO VÝZKUMU

Project 2.1 – Inspection procedures - pavements, bridges and tunnels 1. 5. 2014

Countries (12) , answers (16):

- Belgium	- BRRC
- Croatia	- University of Zagreb
- Czech Republic	- CDV
- Finland	- Geological survey of Finland
- Germany (2)	- DMT , Technische Universitaet Ilmenau
- Greece	- NTUA: Laboratory of Pavement Engineering
- Italy (2)	- Roma Tre University, University of Trento
- Poland	- IBDiM: Road and Bridge Research Institute
- Portugal (2)	- LNEC: National Laboratory for Civil Engineering
	- University of Minho
- Spain	- University of Vigo
- Turkey	- Suleyman Demirel University
- UK	- Univertsity of Greenwich

CENTRUM DOPRAVNÍHO VÝZKUMU

Project 2.1 – Inspection procedures - pavements, bridges and tunnels 1. 5. 2014

Support from state or any other source to solve COST action?

- Belgium (BRRC) - R&D project
- Czech Republic (CDV) - national project
- Spain (University of Vigo) - national project
- Turkey (Suleyman Demirel University) - national project

Type of your GPR activities:

Commercial measurements		9/16
Research:	- GPR hardware	2/16 – Germany
	- GPR software	3/16 – Italy, Poland, Spain
	- application of GPR	16/16

Applications:

Project 2.1 – Inspection procedures - pavements, bridges and tunnels 1. 5. 2014

Pavement diagnostics:

	In-situ	In-lab.	Commer.	Research
- thickness of **asphalt** layers	12	8	9	10
- thickness of **concrete** layers	10	7	9	9
- thickness of **bound** sub-base layers	9	5	9	8
- thickness of **unbound** sub-base layers	9	8	9	8
- position of **reinforcement** in concrete pavement	7	7	7	7
- **de-bonding** and delamination of pavement layers	4	6	4	5
- identification of **caverns**	5	3	5	4
- identification of **frost heaves**	1-Fin	1-Germ	2	1
- depth of surface **cracks**	7	7	3	9
- localisation of bottom-surface initiated **cracks**	4	3	2	7
- condition of **reinforcement** in concrete pavement	1-UK	1	1	1
- **moisture** content	7	7	2	9
- **air voids** content	3	4	1-Ger	5
- **compaction**	4	7	1-Ger	8

Project 2.1 – Inspection procedures - pavements, bridges and tunnels 1. 5. 2014

Bridge diagnostics:

	In-situ	In-lab.	Commer.	Research
- concrete cover of reinforcement in bridge deck	5	3	5	4
- position of reinforcement in bridge deck	5	3	5	3
- thickness of bridge deck	4	2	4	3
- position of pre-stressed or post-tensioned tendons or tendon ducts	4	3	4	3
- de-bonding and delamination of pavement layer	2	1-Ger	2	2
- bridge deck deterioration (cracks, caverns, etc.)	2	1-Ger	2	2
- bridge girder diagnostics	3	3	3	3
- diameter of reinforcement in-build in concrete	1-UK	0	1	1
- condition of reinforcement in bridge deck	1-UK	0	1	1
- evaluation of sealing course on bridge deck	1-UK	1	2	1
- moisture content	3	1-Ger	2	3
- abutment (pillars) scanning	1-Pol	1	1	1

mainly UK, Poland, Portugal, (Germany) and CZ

Project 2.1 – Inspection procedures - pavements, bridges and tunnels 1. 5. 2014

Tunnel diagnostics:

	In-situ	In-lab.	Commer.	Research
- position of reinforcement in tunnel wall	2	2	2	3
- thickness of tunnel wall	2	1-Ger	2	2
- homogeneity of tunnel wall	1- UK	1	2	1
- hollow spaces between concrete and rock	1-UK	2	2	2
- diameter of reinforcement in-build in concrete	1-UK	1	1	2
- condition of reinforcement in tunnel wall	1-UK	0	1	1
- moisture content	0	0	0	0

mainly UK, Italy and (Germany)

Project 2.1 – Inspection procedures - pavements, bridges and tunnels 1. 5. 2014

Railway track diagnostics:

	In-situ	In-lab.	Commer.	Research
- weathered basement	1-Fin	0	1	1
- frost sensibility	1-Fin	0	1	1
- ballast thickness	1-Port	1	0	1
- sub-ballast thickness	1-Port	1	0	1
- ballast fouling	1-Port	1	0	1
- moisture content	0	1-Port	0	1
- evaluation of trackbed	1-Gre	0	1	1

Retaining wall diagnostics:

	In-situ	In-lab.	Commer.	Research
- basement wall moisture	1-Fin	0	0	1
- wooden walls floors	1-UK	0	1	1

Project 2.1 – Inspection procedures - pavements, bridges and tunnels 1. 5. 2014

Technical specification/guide/manual for pavement/ bridge/ tunnel/… diagnostics with GPR:

- CZ – TP233 Pavements and bridge pavements (2011)
- BASt – Guideline Nr. S31 (2003)
- UK – DMRB 7.3.2
- BRRC – own (home produced) procedure for Highway, Bridge and Tunnel surveys

Comparative tests for GPR diagnostics organised:

- CZ – pavement (first one in 2013 – asphalt layers)
- Turkey – roads and railway tracks

Authorisation required for GPR measurements on civil engineering structures :

no

Project 2.1 – Inspection procedures - pavements, bridges and tunnels 1. 5. 2014

How many channels do you use with your GPR system during the measurement?

- Roads – 1, 1 or 2, -6 Germany, -15 Poland, muti-channel UK
- Bridges – 1, 1or 2, -16 Germany, -5 Poland, muti-channel UK
- Tunnel – 1 , 2
- Railway tracks – 1, 1 or 2, -3 Portugal

Which way do you determine the speed of EM signal propagation through the material/layers during in-situ measurements?

- table values	6
- using set of antennas (CMP or WARR method)	6
- measuring of permittivity:	3
- direct method (taking cores, reading thickness at construction joints, altitudinal survey before and after construction of layers, etc.)	13
- other method, please specify:	Metal plate calibration, Capacimetry (Poland)

Project 2.1 – Inspection procedures - pavements, bridges and tunnels 1. 5. 2014

What accuracy [% or mm] do you state for the following GPR applications?

- thickness of **new or sound asphalt** pavement layers	3-10 %, 5%, 5-10 %, 3 to 5% +10mm
- thickness of **degraded asphalt** pavement layers	5-10 %, < 10 %, 10% +20mm
- thickness of cement **concrete** pavement	10 %, 10% +30mm
- thickness of **sub-base** layer	10-15 %, 15%, 10-25 %, 20% +50mm
- position (depth) of **dowels and tie bars** in concrete pavement	+/- 10 mm, 3-7 %, <10%, 10% +30mm
- position (depth) of **reinforcement** in concrete structures (thickness up to 300 mm)	5-10 %, +/- 20 (25) mm, <10%, 10% +30mm

Comments:
Accuracy will strongly depend on available number of calibrations
It depends on antenna type and velocity calibration method
This depends on the accuracy required

Project 2.1 – Inspection procedures - pavements, bridges and tunnels 1. 5. 2014

Next steps – inspection procedures (guidelines)

1) Detailed analysis of current texts:

- In Europe, there is no equivalent to **standards** ASTM D4748-10 (Determining the Thickness of Bound Pavement Layers) and ASTM D6087-08 (Evaluating Asphalt-Covered Concrete Bridge Decks), which deals with the application of GPR for roads and bridges
- only in some European countries, there are **technical specifications**, e.g. DMRB 7.3.2 (Design Manual for Roads and Bridges, Data for pavement assessment - annex 6 HD 29/2008: Ground-Penetrating Radar) in UK and B 10 Merkblatt (Radarverfahren zur Zerstörungsfreien Prüfung im Bauwesen) in Germany
- **Guidelines:**
  - Mara Nord – 5 recommendations for guidelines (R &B)
  - Euro GPR association works on new g. (R)

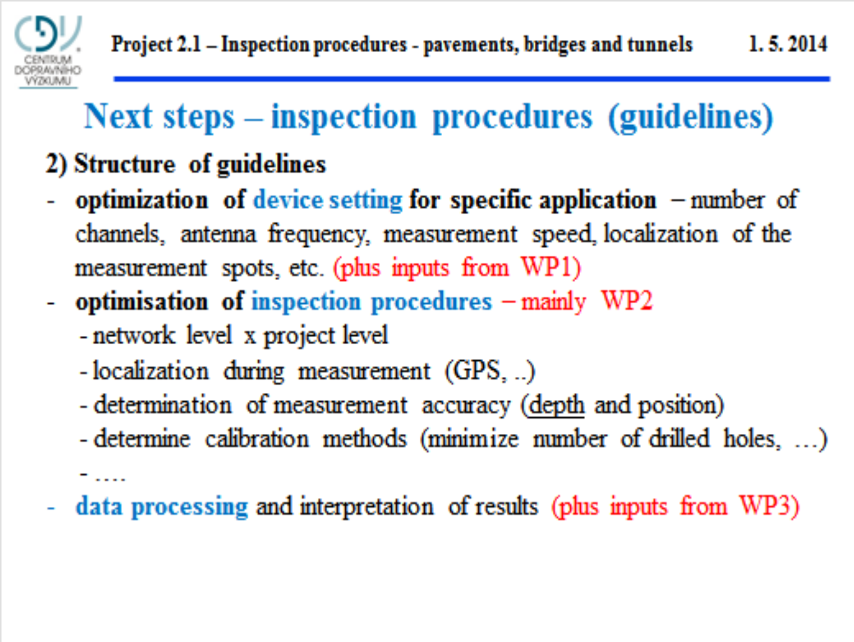

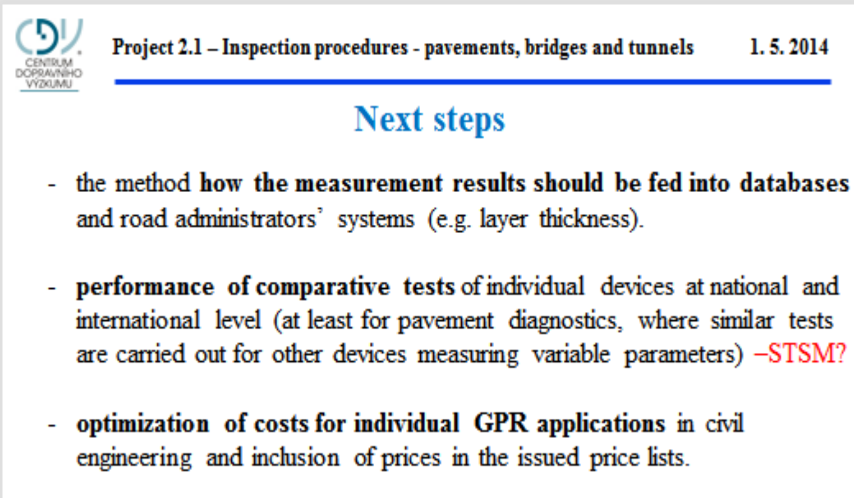

ACKNOWLEDGEMENT

The Author thanks COST for funding the Action TU1208 "Civil Engineering Applications of Ground Penetrating Radar".

"ASSESSMENT OF ASPHALT MIXTURES CHARACTERISTICS THROUGH GPR TESTING" (CONTRIBUTION TO PROJECT 2.1)

Jorge Pais (PT), Francisco Fernandes (PT)
jpais@civil.uminho.pt

The abstract is published in *Geophysical Research Abstracts*, Vol. 16, EGU2014-13087, 2014 and is available on *www.egu2014.eu*

1. SOME GROUND PENETRATING RADAR THEORY

The GPR system transmits and receives pulses of electromagnetic energy. The signal reflected from interfaces in the pavement gives information about subsurface conditions.

Typical GPR reflections from a pavement are sketched below:

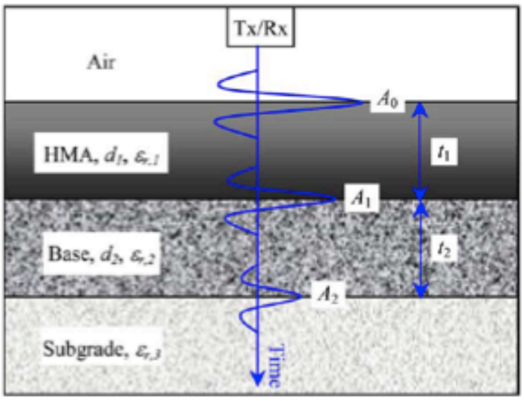

$$d_i = \frac{ct_i}{2\sqrt{\varepsilon_{r,i}}} \qquad v = \frac{c}{\sqrt{\varepsilon_r}}$$

d_i = thickness of the ith layer
t_i = EM wave two-way travel time through the ith layer
c = speed of light in free space (c = 10^8 m/s)
$\varepsilon_{r,i}$ = the dielectric constant of the ith layer

A_0 can be used to calculate the dielectric constant of the surface layer and Δt_1 to calculate the layer thickness. Similarly, A_1 and Δt_1 can be used to calculate the dielectric constant and thickness of the second layer. Finally, A_1 can provide the dielectric constant of the third layer.
Changes in pavement condition have effects on the radar signal, as resumed in Table I.

Table I – Effects on changes in pavement condition on radar signal.

Maintenance Condition	Effect on Radar Signal				
	A_0	A_1	A_2	Δt_1	Δt_2
Increase in base moisture	-	↑	↓	-	↑
Increase in subgrade moisture	-	-	↑	-	-
Increase in moisture below slab joint	-	↑	↓	-	-
Moisture in surface layer					
a. Layer completely wet	↑	↓	↓	↑	-
b. Large wet area	-	↑	↓	↓	↓
Buried low-density stripped layer	Negative peak between A_0 and A_1				
Air voids or loss of support	Distortion of peak A_1				
Overlay delamination	Multiple small peaks between A_0 and A_1				

For moisture assessment, in the case of granular layers, the complex refractive index model can be employed:

$$\sqrt{e_b} = \theta_s\sqrt{e_s} + \theta_w\sqrt{e_w} + \theta_a\sqrt{e_a} \qquad \sqrt{\epsilon_b} = \theta_s\sqrt{\epsilon_s} + 9\theta_w + \theta_a$$

e_b = dielectric constant of the base calculated from field measurements
$\theta_s, \theta_w, \theta_a$ = volumetric concentrations of solid, water, and air, respectively, in the base course
e_s, e_w, e_a = dielectric constants of the solids (typically 4 to 8), water (81), and air (1), respectively

$$V_w = \frac{\left(\sqrt{\epsilon_b} - 1\right) - \frac{W_s}{\gamma_s}\left(\sqrt{\epsilon_s} - 1\right)}{8}$$

For the estimation of the effective dielectric constant of the asphalt mixtures, the following formula can be used:

$$e_{ac} = e_s V_s + e_{as} V_{as} + e_a V_a$$

e_{ac} = Dielectric constant of the asphalt mixture
e_s, e_{as}, e_a = Dielectric constants of the aggregate, asphalt, and air, respectively
V_s, V_{as}, V_a = Volumetric ratios of aggregate, asphalt, and air, respectively

❑ Complex Refractive Index Model

$$(\epsilon_{\mathrm{HMA}})^{1/\alpha} = V_a(\epsilon_a)^{1/\alpha} + V_{\mathrm{sb}}(\epsilon_s)^{1/\alpha} + V_b(\epsilon_b)^{1/\alpha}$$

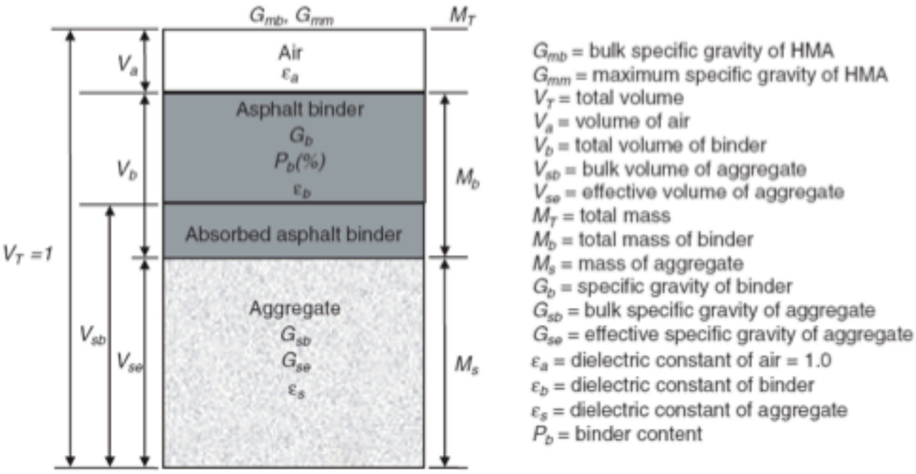

$$V_a = 1 - \frac{G_{\mathrm{mb}}}{G_{\mathrm{mm}}} \qquad V_b = \frac{M_b}{G_b} = \frac{G_{\mathrm{mb}}P_b}{G_b} \qquad V_{\mathrm{sb}} = \frac{M_s}{G_{\mathrm{sb}}} = \frac{G_{\mathrm{mb}}(1-P_b)}{G_{\mathrm{sb}}}$$

Density of the asphalt mixture

$$G_{\mathrm{mb}} = \frac{\sqrt{\epsilon_{\mathrm{HMA}}} - 1}{\frac{P_b}{G_b}\sqrt{\epsilon_b} + \frac{(1-P_b)}{G_{\mathrm{sb}}}\sqrt{\epsilon_s} - \frac{1}{G_{\mathrm{mm}}}}$$

❑ Rayleigh Mixing Model (Al-Qadi et al., 2010)

$$\frac{\epsilon_{\mathrm{eff}} - \epsilon_b}{\epsilon_{\mathrm{eff}} + 2\epsilon_b} = \sum_{i=1}^{N} \frac{n_i\alpha_i}{3\epsilon_b}$$

n_i = the number of inclusions
α_i = polarizability factor of material *i*

Density of the asphalt mixture

$$G_{\mathrm{mb}} = \frac{\frac{\epsilon_{\mathrm{HMA}} - \epsilon_b}{\epsilon_{\mathrm{HMA}} + 2\epsilon_b} - \frac{1-\epsilon_b}{1+2\epsilon_b}}{\left(\frac{\epsilon_s - \epsilon_b}{\epsilon_s + 2\epsilon_b}\right)\left(\frac{1-P_b}{G_{\mathrm{sb}}}\right) - \left(\frac{1-\epsilon_b}{1+2\epsilon_b}\right)\left(\frac{1}{G_{\mathrm{mm}}}\right)}$$

- **Böttcher Mixing Model (Al-Qadi et al., 2010)**

$$\frac{\epsilon_{\mathrm{HMA}} - \epsilon_b}{3\epsilon_{\mathrm{HMA}}} = V_{sb}\frac{\epsilon_s - \epsilon_b}{\epsilon_s + 2\epsilon_{\mathrm{HMA}}} + V_a\frac{\epsilon_a - \epsilon_b}{\epsilon_a + 2\epsilon_{\mathrm{HMA}}}$$

Density of the asphalt mixture

$$G_{mb} = \frac{\dfrac{\epsilon_{\mathrm{HMA}} - \epsilon_b}{3\epsilon_{\mathrm{HMA}}} - \dfrac{1-\epsilon_b}{1+2\epsilon_{\mathrm{HMA}}}}{\left(\dfrac{\epsilon_s - \epsilon_b}{\epsilon_s + 2\epsilon_{\mathrm{HMA}}}\right)\left(\dfrac{1-P_b}{G_{sb}}\right) - \left(\dfrac{1-\epsilon_b}{1+2\epsilon_{\mathrm{HMA}}}\right)\left(\dfrac{1}{G_{mm}}\right)}$$

Comparison between different models – density of the asphalt mixture:

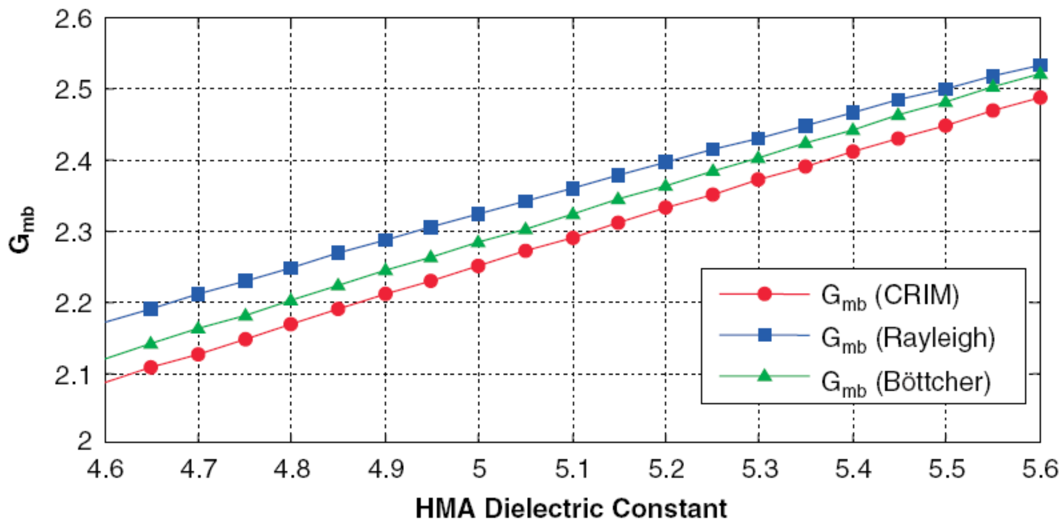

Comparison between different models – air void %:

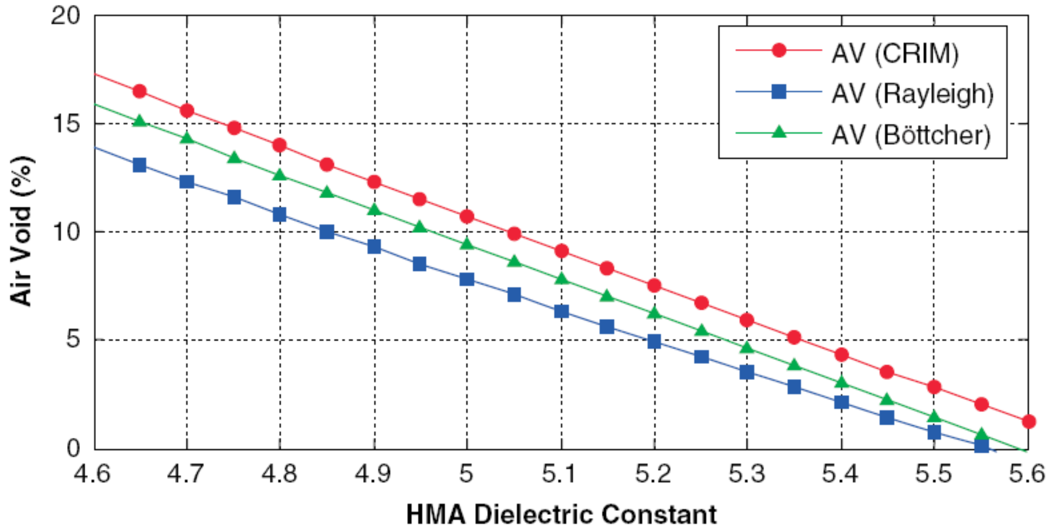

2. Testing Programme

- **1 asphalt mixture type (more 3 types asphalt mixtures in progress)**
  - Used in wearing course layers
- **2 densities**
  - 2.37 and 2.1 g/cm^3 (representative of low and high void content)
- **3 asphalt contents**
  - 4%, 5% and 6%
- **Evaluation**
  - EM wave velocity
  - Dielectric constant

Physical characteristics of the slabs

Asphalt mixture: AC14 (14 mm max aggregate size)

Slab	Max density (g/cm^3)	Bitumen (%)	Density (g/cm^3)	Void content (%)
1	2.50	5	2.37	5.0
2	2.52	4	2.37	6.0
3	2.46	6	2.37	3.7
4	2.50	5	2.1	15.9
5	2.53	4	2.1	16.9
6	2.46	6	2.1	14.6

Quantity of water sprayed over each slab (g)

Slab	1st phase (5%)	2^{nd} phase (10%)	3^{rd} phase (20%)	4^{th} phase (40%)
1	65	65	130	260
2	77	77	154	308
3	48	48	96	192
4	205	205	410	820
5	218	218	436	871
6	187	187	375	749

Slabs (70 cm x 50 cm x 8 cm), produced in laboratory:

Steel roller compactor:

3. Testing equipment

MALA RAMAC/GPR system with a 1,6GHz ground-coupled antenna

Operating parameters: Time window of 4ns and sampling frequency around 30GHz; Trace interval of 2mm (small length slabs).

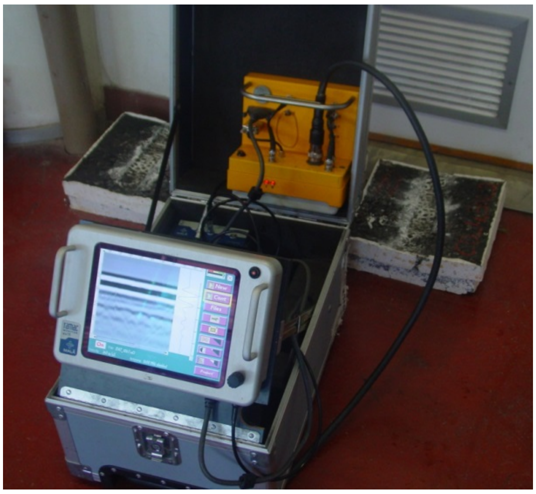

4. Results – dry slabs

Slab	BMT (g/cm³)	% Bitumen	Density (g/cm3)	Porosity (%)	Velocity (cm/ns)	ε
1	2.5	5	2.37	5.2	16.211	3.425
2	2.52	4	2.37	6	16.278	3.396
3	2.46	6	2.37	3.7	16.104	3.470
4	2.5	5	2.1	16	16.408	3.343
5	2.53	4	2.1	17	16.355	3.365
6	2.46	6	2.1	14.6	16.292	3.391

Dielectric constant as function of density and binder content:

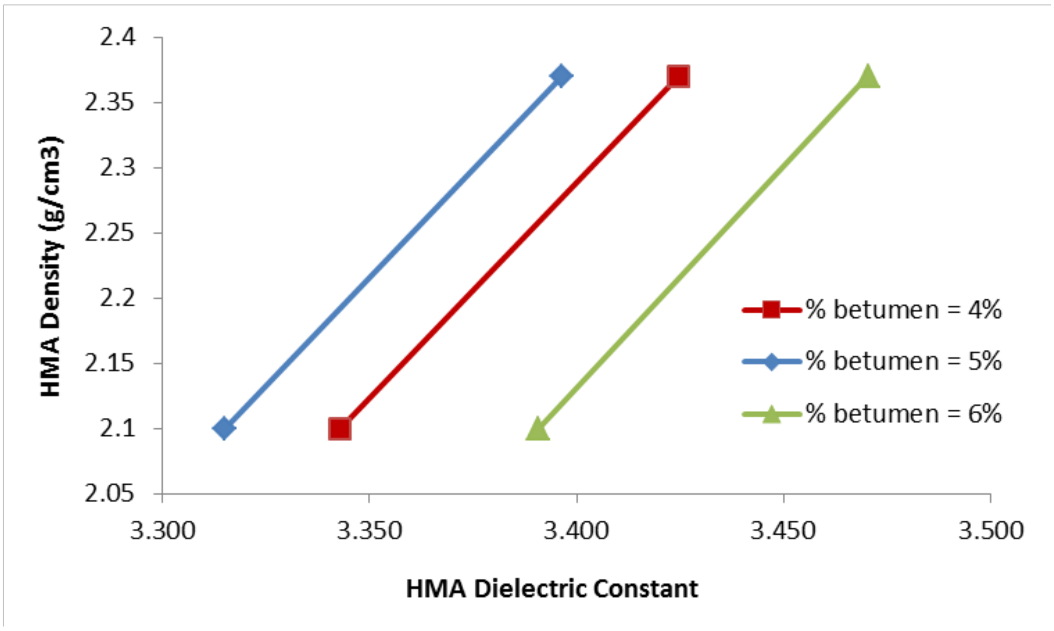

Dielectric constant as function of the binder content:

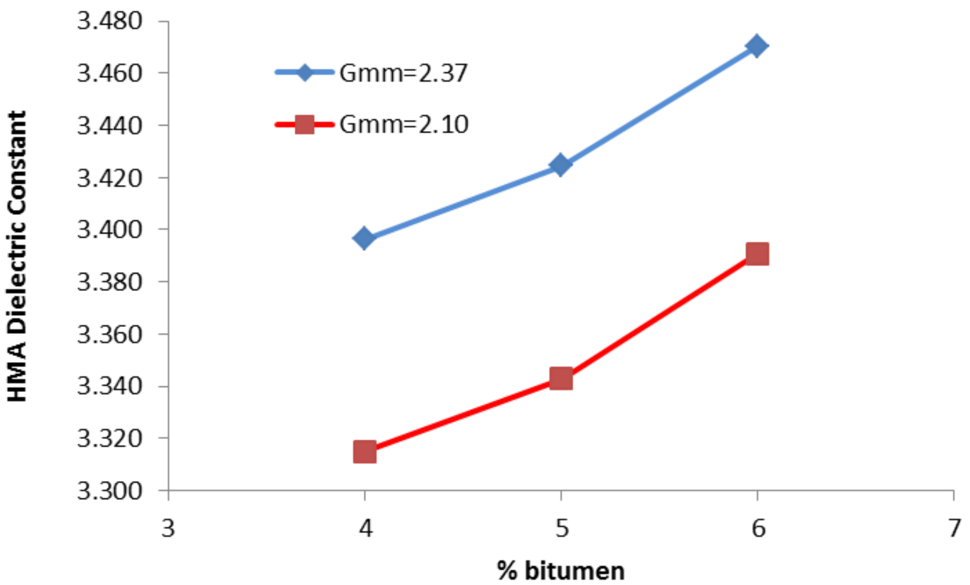

Prediction of density as a function of the HMA dielectric constant:

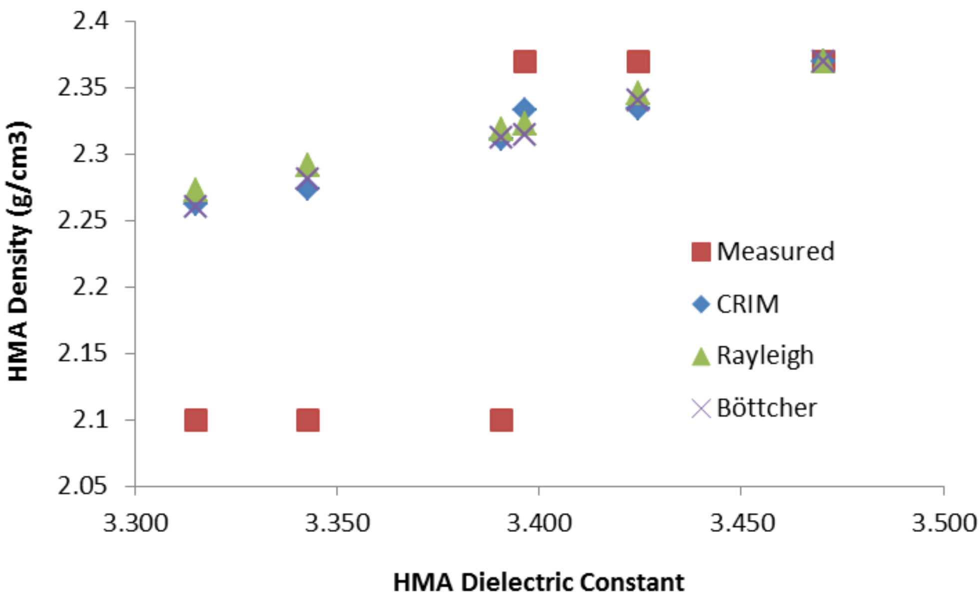

Prediction of density – numerical values:

	ε_s	ε_b	G_b	G_{sb}
CRIM	3.77	1.94	1.025	2.650
Rayleigh	3.93	1.98	1.025	2.650
Böttcher	3.88	2.00	1.025	2.650

5. RESULTS – WET SLABS

The following histograms resume the experimental results obtained for the propagation velocity (cm/ns) in the six slabs.

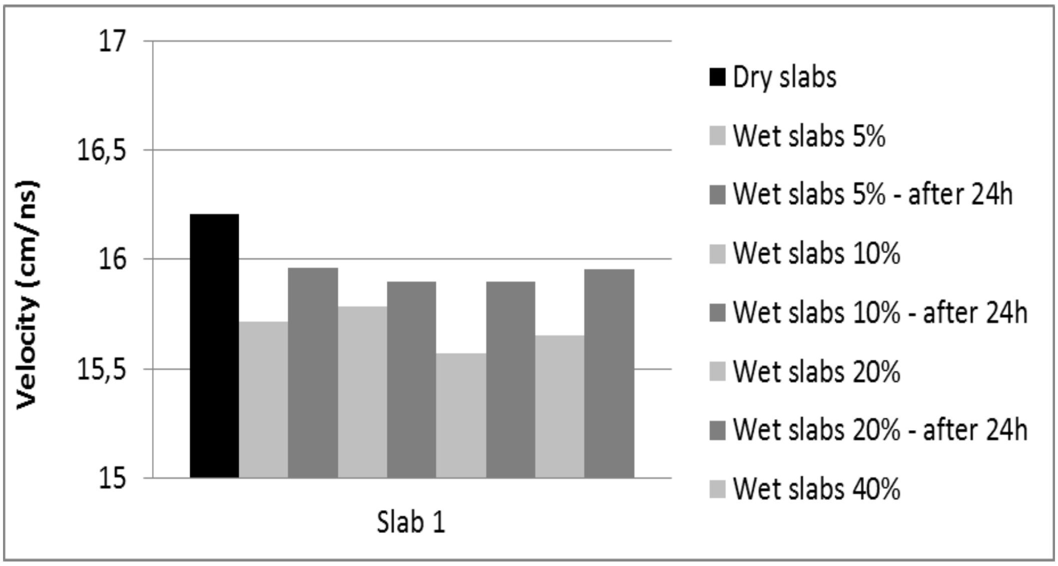

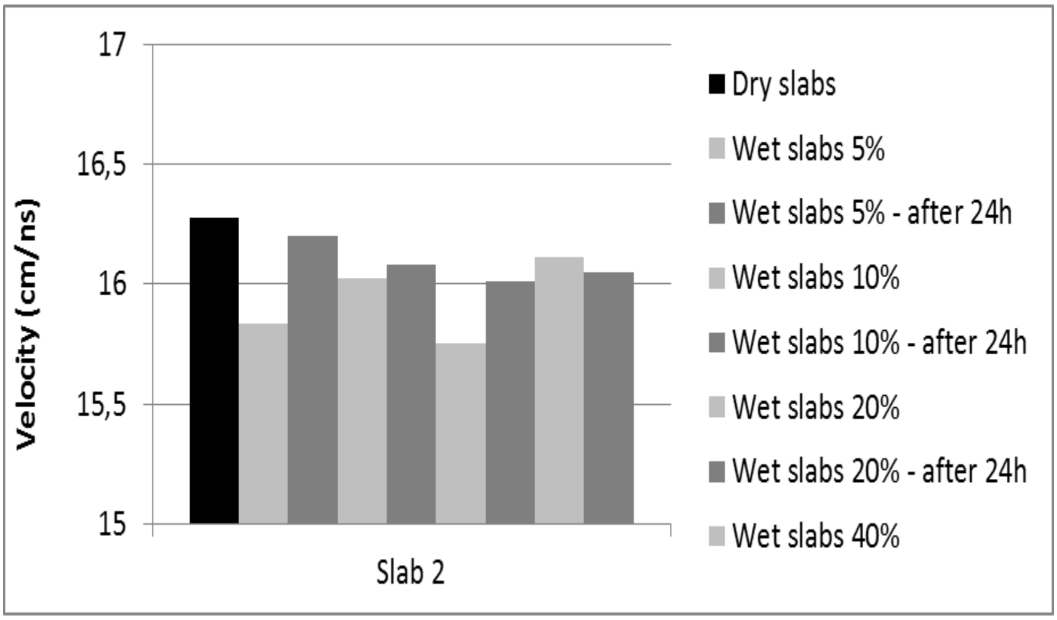

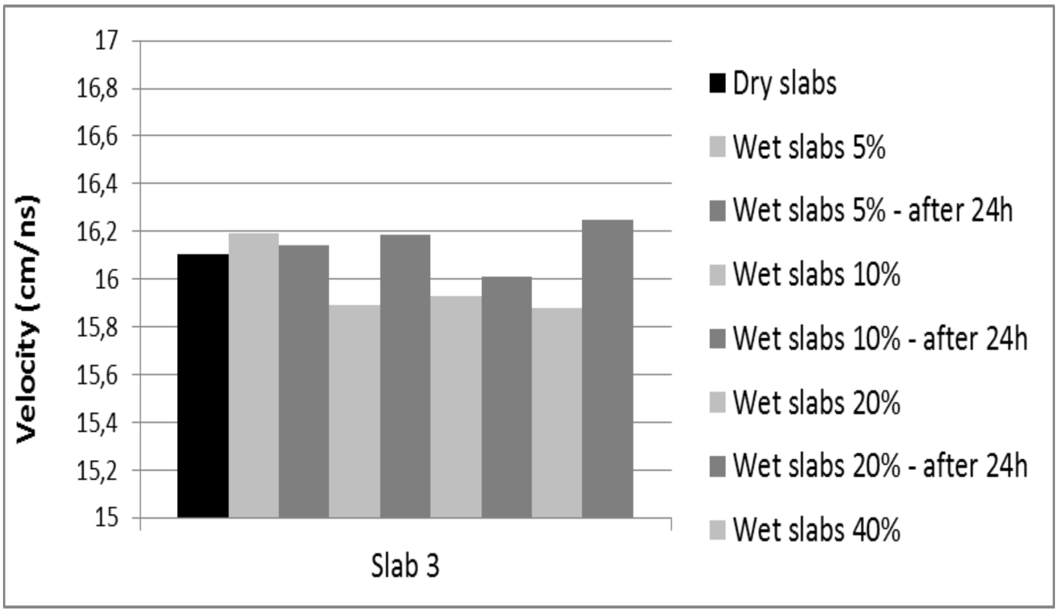
17
16,8
16,6
16,4
16,2
16
15,8
15,6
15,4
15,2
15
Velocity (cm/ns)
Slab 3
Dry slabs
Wet slabs 5%
Wet slabs 5% - after 24h
Wet slabs 10%
Wet slabs 10% - after 24h
Wet slabs 20%
Wet slabs 20% - after 24h
Wet slabs 40%

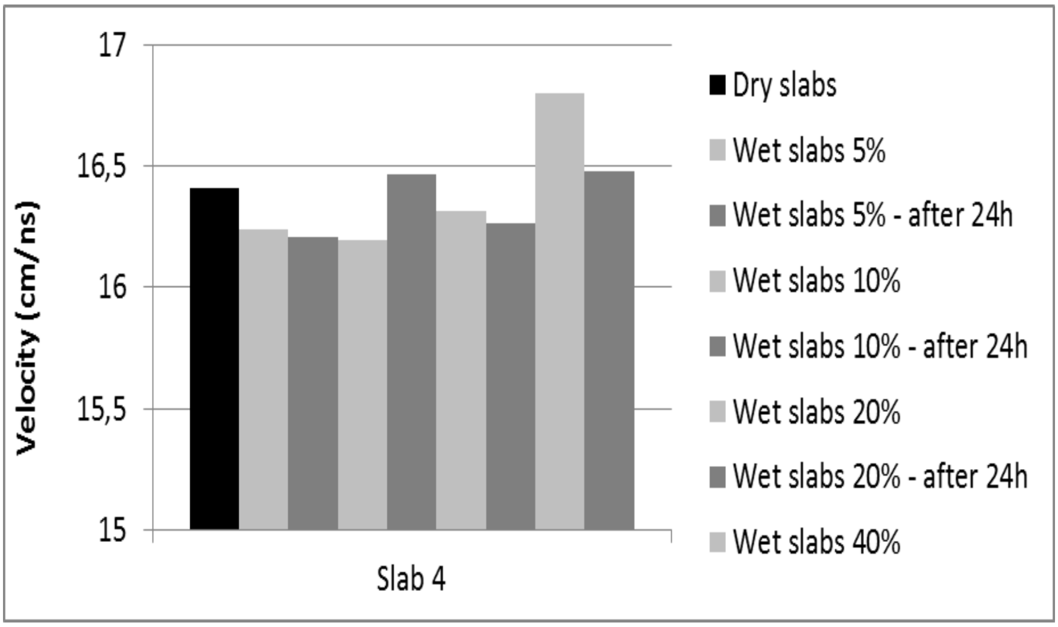
17
16,5
16
15,5
15
Velocity (cm/ns)
Slab 4
Dry slabs
Wet slabs 5%
Wet slabs 5% - after 24h
Wet slabs 10%
Wet slabs 10% - after 24h
Wet slabs 20%
Wet slabs 20% - after 24h
Wet slabs 40%

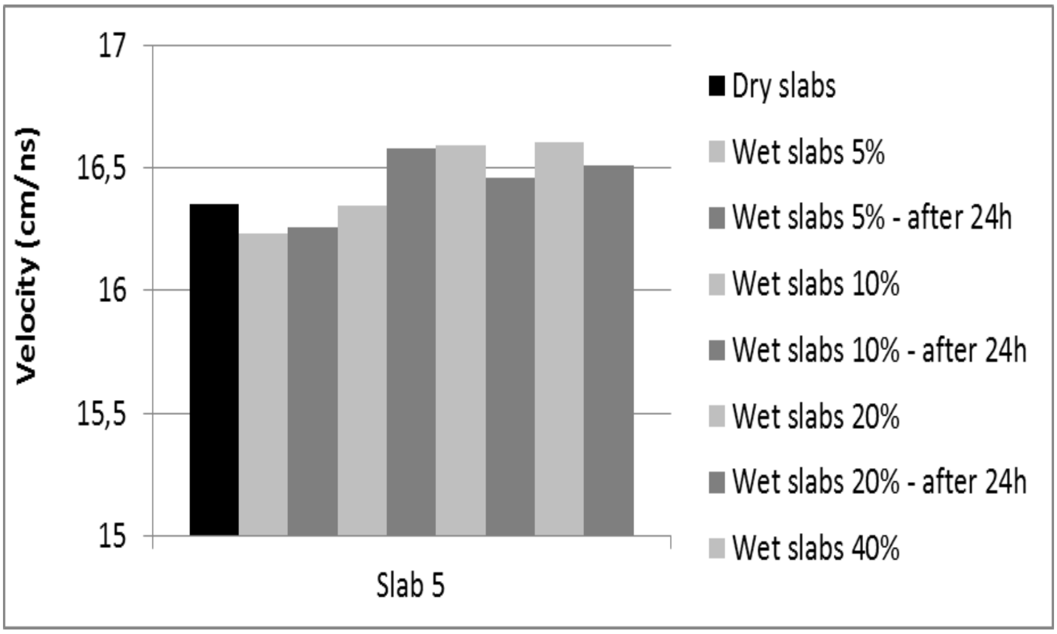
17
16,5
16
15,5
15
Velocity (cm/ns)
Slab 5
Dry slabs
Wet slabs 5%
Wet slabs 5% - after 24h
Wet slabs 10%
Wet slabs 10% - after 24h
Wet slabs 20%
Wet slabs 20% - after 24h
Wet slabs 40%

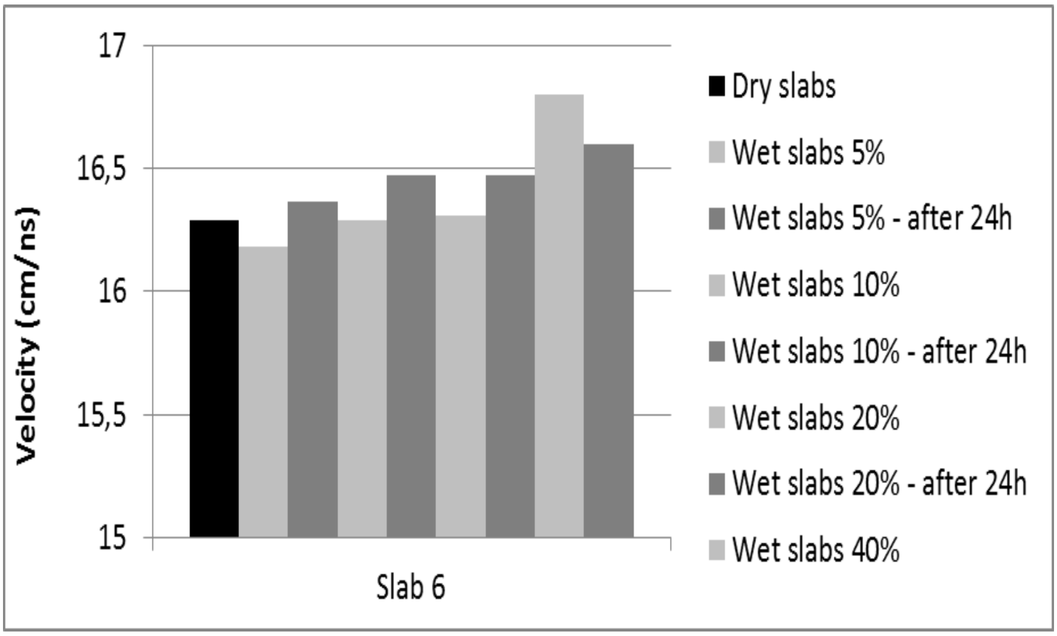
17
16,5
16
15,5
15
Velocity (cm/ns)
Slab 6
Dry slabs
Wet slabs 5%
Wet slabs 5% - after 24h
Wet slabs 10%
Wet slabs 10% - after 24h
Wet slabs 20%
Wet slabs 20% - after 24h
Wet slabs 40%

6. Conclusions and future work

Asphalt mixtures physical characteristics can be assessed by GPR.

The application of the existing models to predict dielectric constant presented some problems in the cases studied. The presence of water in the asphalt mixtures was observed.

Future developments of this study include:

- Development of models for voids and moisture
- Validation of the models
- Assessment of stiffness and fatigue resistance of asphalt mixture
- Development a model for mechanical properties
- Identification of cracking in asphalt pavements

Acknowledgement

The authors acknowledge the COST Action TU1208 "Civil Engineering Applications of Ground Penetrating Radar".

"INFLUENCE OF FOULING ON THE DIELECTRIC CONSTANT OF RAILWAY BALLAST" (CONTRIBUTION TO PROJECT 2.1)

Simona Fontul (PT), Francesca de Chiara (IT),
Eduardo Fortunato (PT), Burrinha Rui (PT)
simona@lnec.pt

The abstract is published in *Geophysical Research Abstracts*, Vol. 16, EGU2014-1334, 2014 and is available on *www.egu2014.eu*

Objectives: To better characterise the dielectric constant of railway materials used in Portugal & to study the influence of material condition and ballast fouling on the GPR measurements.
Methodology: Laboratory tests, with several antennas and for different material conditions; in situ tests for validation of results. Materials studied: ballast, soils and fouled ballast

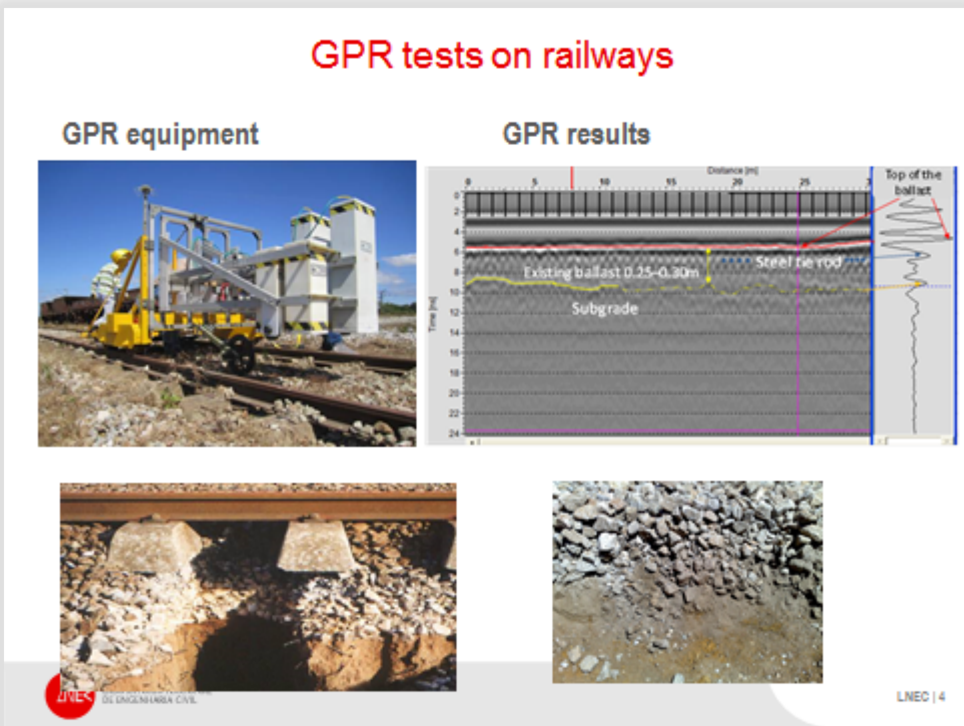

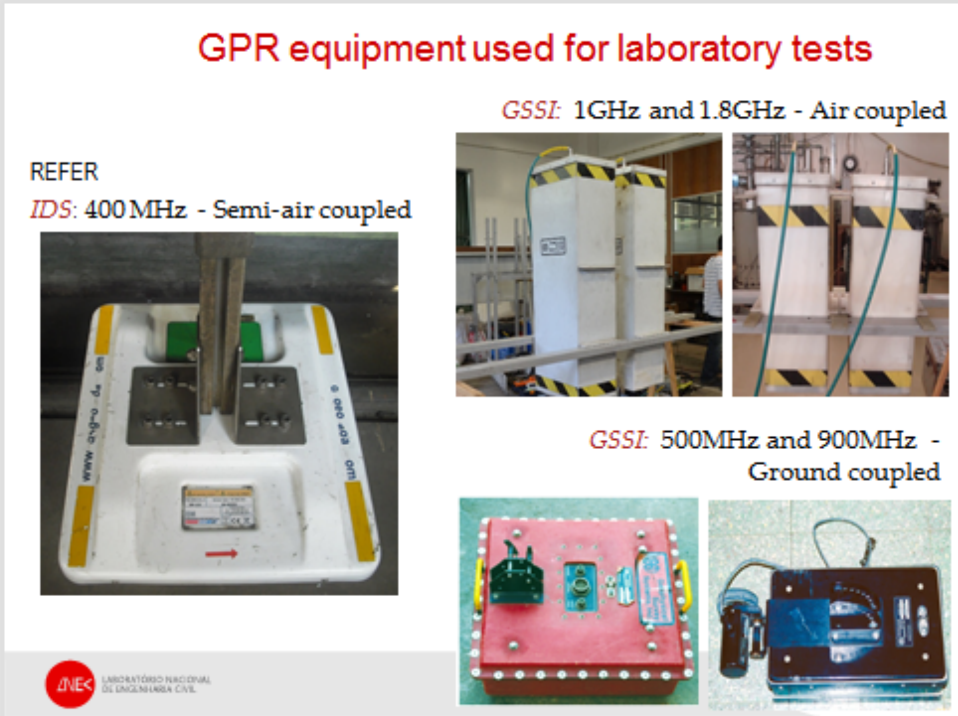
GPR equipment used for laboratory tests
GSSI: 1GHz and 1.8GHz - Air coupled
REFER
IDS: 400 MHz - Semi-air coupled
GSSI: 500MHz and 900MHz - Ground coupled
LNEC
LABORATÓRIO NACIONAL DE ENGENHARIA CIVIL


Acquisition systems:
GSSI SIR-10H
GSSI SIR-20
System IDS
Software:
• RADAN 6.5
• IDS – Railwaydoctor


GPR equipment *in situ* railway survey
Existing Railway
During construction

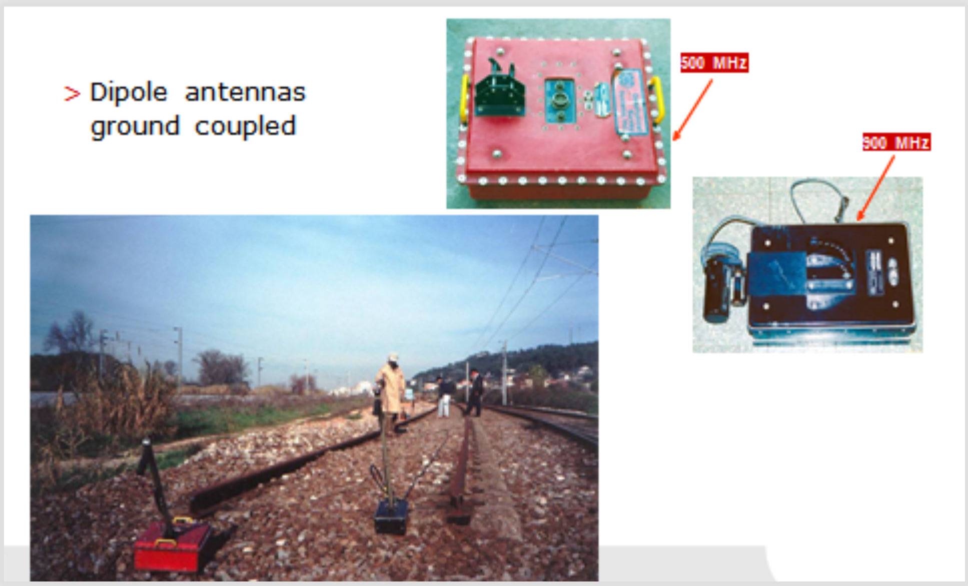
> Dipole antennas ground coupled
500 MHz
900 MHz


> Dipole antennas ground coupled
500 and 900 MHz
v ≈ 20 km/h
suspended at 0.2 m
5 scans/m
> Horn Antennas

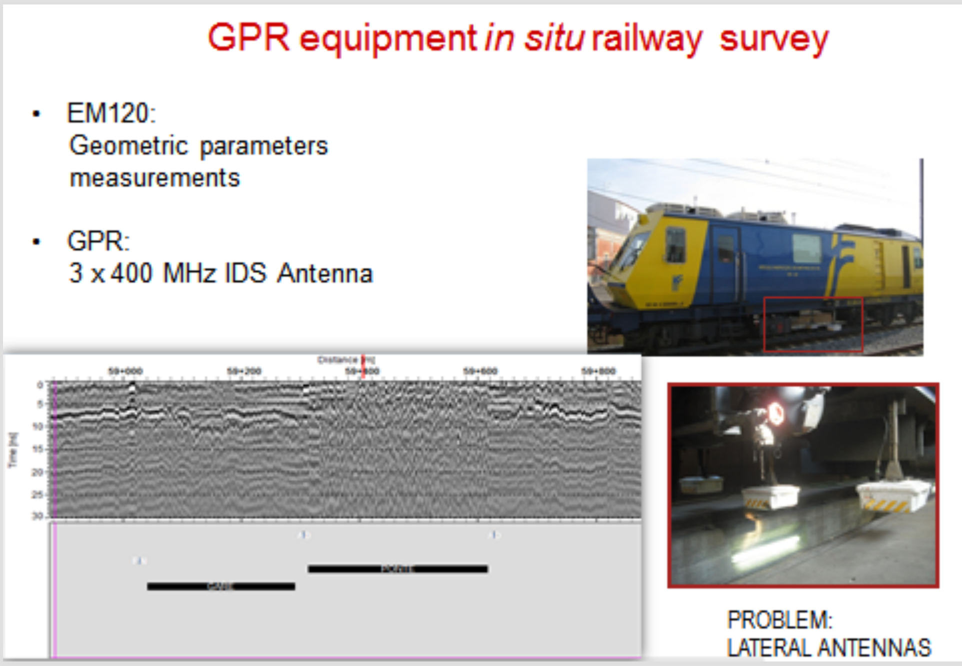
GPR equipment *in situ* railway survey
EM120:
Geometric parameters measurements
GPR:
3 x 400 MHz IDS Antenna
PROBLEM:
LATERAL ANTENNAS

Laboratory tests – Testing setup

Case studies		Fouling Index	Water content w(%)
1 Clean ballast		-	7 levels (dry, wet, saturated and dried in time)
2 Soil		-	6%, 8%, 10% e 12%
3 Fouled Ballast	3.1	1	8,4%
	3.2	6	6%, 8%, 10% e 12%
	3.3	15	6%, 8%, 10% e 12%
	3.4	35	6%, 8%, 10% e 12%
	3.5	55	6%, 8%, 10% e 12%

Case study 1: granite clean ballast

Dielectric constants for dry, wet and saturated conditions

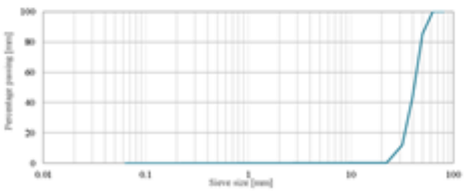

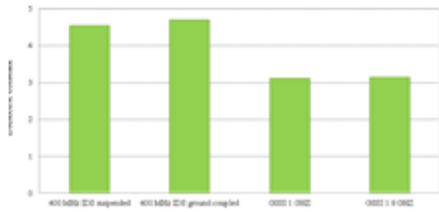

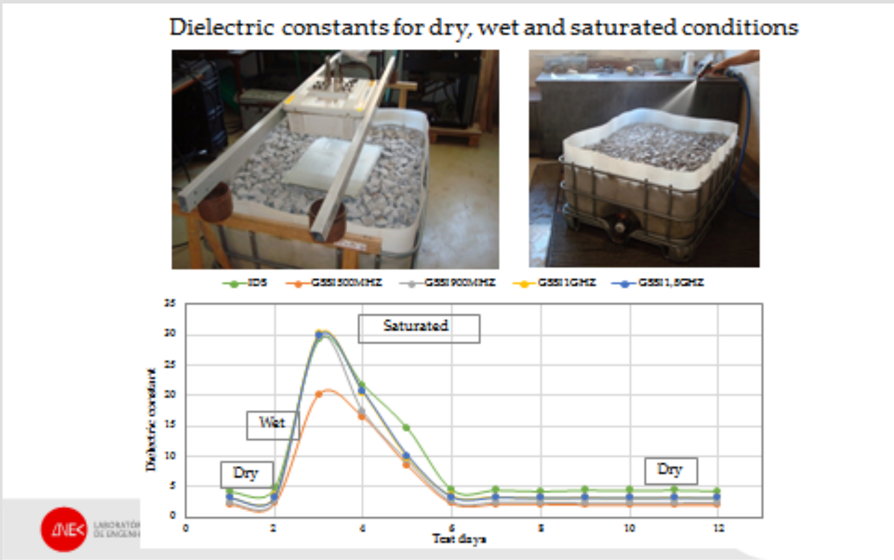
Dielectric constants for dry, wet and saturated conditions
IDS
GSSI 500MHZ
GSSI 900MHZ
GSSI 1GHZ
GSSI 1,8GHZ
Saturated
Wet
Dry
Dry
Dielectric constant
Test days

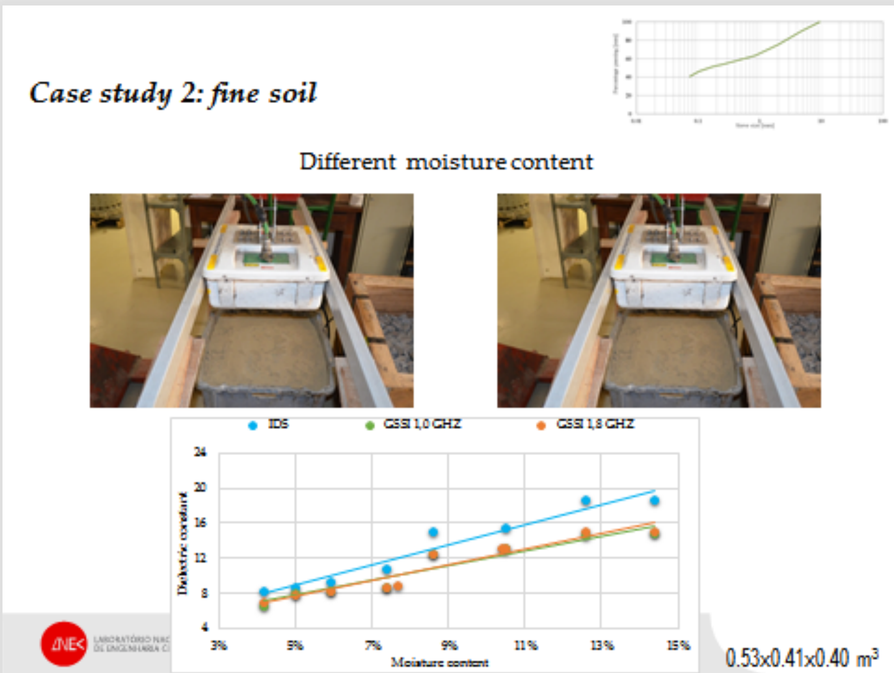
Case study 2: fine soil
Different moisture content
IDS
GSSI 1,0 GHZ
GSSI 1,8 GHZ
Dielectric constant
Moisture content
0.53x0.41x0.40 m3

Case study 3: fouled ballast model construction

Relative ballast fouling ratio (%)

$$R_{b-f} = \frac{M_f\left(\frac{G_{s-b}}{G_{s-f}}\right)}{M_b}$$

- M_f and M_b represent the dry mass of fouling and ballast material;
- G_{s-b} and G_{s-f} are the specific gravities (density) of fouling and ballast material.

9.5 mm

$0.50 \times 0.75 \times 0.52$ m^3

LABORATÓRIO NACIONAL DE ENGENHARIA CIVIL

Category	Rbf (%)	Laboratory (%)
Moderately clean	2 to 9.5	6
Moderately fouled	9.5 to 17.5	15
Fouled	17.5 to 34	35
Highly fouled	≥ 34	55

Water content
6 %
8 %
10 %
12 %

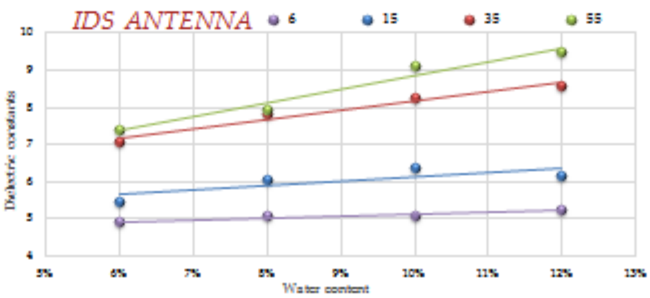

LABORATÓRIO NACIONAL DE ENGENHARIA CIVIL

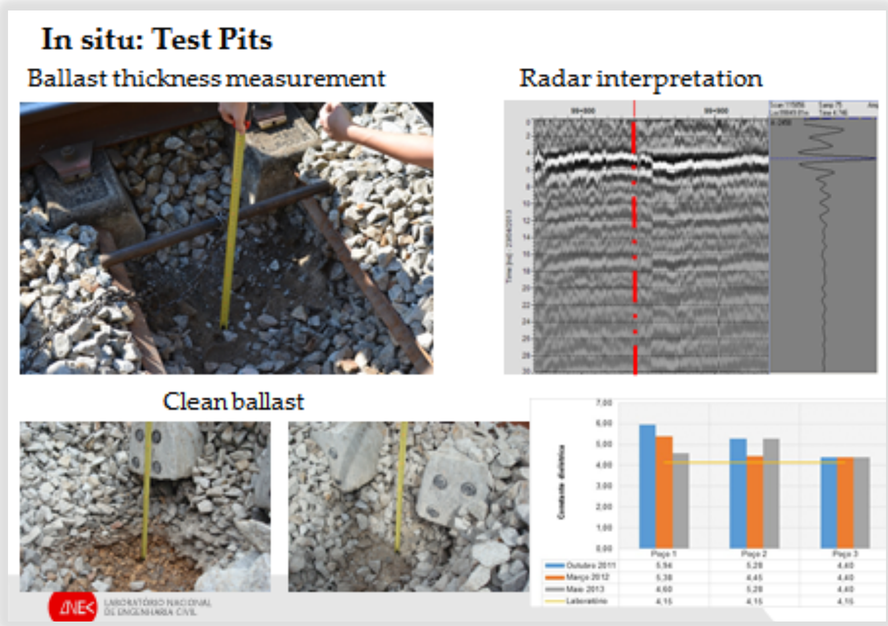

Conclusions

The higher is the frequency, the higher are the observed dielectric constant values, both for the IDS antenna and the GSSI air-coupled antenna. A great variation of dielectric constant values was obtained for saturated and partially saturated conditions. For fine soil, the collected values show a linear increment of the dielectric constant as the water content increases, for all the used GPR systems. For fouled ballast, results show a linear increment for both the fouling levels and the water content variation, in different proportion: dielectric constant is more affected by fouling variation than by water content.

For in situ validation, the dielectric constant of clean ballast is consistent with the values obtained in laboratory. The main problem for fouling layers evaluation is the presence of other materials, such as old limestone ballast that increased the dielectric constant of the material.

Acknowledgement

The authors acknowledge the COST Action TU1208 "Civil Engineering Applications of Ground Penetrating Radar".

"A SEMI-EMPIRICAL APPROACH FOR INVESTIGATING MECHANICAL PROPERTIES OF PAVEMENT THROUGH GPR" (CONTRIBUTION TO PROJECT 2.1)

Andrea Benedetto (IT), Fabio Tosti (IT), Fabrizio D'Amico (IT),
Luca Bianchini Ciampoli (IT)
andrea.benedetto@uniroma3.it

Abstract

The wide-ranging flexibility of ground-penetrating radar (GPR), makes it one of the most effective and efficient tools in several fields of application, including pavement engineering. In such increasingly established framework, the evaluation of mechanical properties of road pavements directly from electromagnetic surveys could represent a real breakthrough toward a more efficient management of the road asset. According to the above, a pulsed GPR system with ground-coupled antennas, 600 MHz and 1600 MHz center frequencies of investigation, was employed over a 4m×30m flexible pavement test site, composed of an 836-nodes grid. Elastic moduli were measured at each node using a light falling weight deflectometer (LFWD), as ground-truth data for both model calibration and validation. Data processing has foreseen to construct a 3-D matrix of the scanned area, wherein a number of C-scans was extracted up to a maximum depth z = 200 mm, according to the influence domain of the LFWD. From the calibration procedure, a number of signal amplitude values was picked and related to a consistent amount of grid points randomly selected within each sampled C-scan. Similarly, amplitude values from other randomly selected nodes, in the same number than the calibration step, were also picked in order to validate such semi-empirical model. The comparison between observed and predicted elastic moduli shows a relatively good matching. Future developments of the research could lead to a system calibration in laboratory, under known conditions, and to the use of different center frequencies of investigation.

INTRODUCTION

A strong relationship between the frequency of road accidents and the presence of pavement surface damages has been widely investigated over time [20]. Several causes involve the loss of strength and deformation properties of pavements, ranging from environmental conditions, such as precipitations or freezing, to traffic loads [13, 18].

Strength and deformation properties of pavements are traditionally evaluated through destructive techniques, although they have demonstrated a low efficiency in terms of costs and time, as well as of results reliability. In such a scenario, the use of a non-destructive technique such as falling weight deflectomer (FWD) has significantly increased over the past few decades [4]. Basically, the functioning of this tool, included its portable version named light falling weight deflectometer (LFWD) [2], is based on the application of a load through a circular plate coupled to the ground, and on the sensing of the relevant echoes coming from the surface by means of ground-coupled geophones. The structural conditions of the pavement and any weaknesses of its layers are therefore assessed through the deflection bowl retrieved from these echoes. In this regard, Benedetto et al. [10] analyzed the influence domain of deflections related to LFWD tests on several subgrade soils. Such instrument has also demonstrated to be really promising in the field of ruts prediction in unpaved natural soils [6].
Amongst the several non-destructive testing (NDT) methods, ground-penetrating radar (GPR) is increasingly established in evaluating the physical properties of the subsurface. This electromagnetic tool basically relies on the transmission and reception of electromagnetic waves in a fixed frequency-band [12, 22]. Applications of GPR can range from agriculture to archaeology, up to many fields of engineering and beyond [15]. In pavement engineering, it is possible to count several GPR applications, spanning from the assessment of deterioration in HMA layers [5, 19] or deeper layers [9], up to the evaluation of the health state of concrete structures [7, 14]. In addition, recent investigations have focused on the assessment of those properties causing structural damages in pavements, such as moisture and clay [1, 11, 17, 21].
In this framework, new challenging frontiers could be more deeply explored in the field of relating dielectric and mechanical properties of materials [16]. Basically, this issue has herein been tackled relying on the undeniable dependence between mechanical characteristics of soils and friction between soil particles, and on the assumption that the dielectric behavior is related to the bulk density of soils [16].

OBJECTIVES AND METHODOLOGY

In this work, GPR data were collected in a test site of 4m×30m, with a flexible pavement structure, in order to retrieve the Young's modulus values of the pavement. For this purpose, EM data were related to the observed values of E by LFWD, for both calibration and validation

procedures. A semi-empirical prediction model is then described and results are discussed.

EXPERIMENTAL FRAMEWORK

The test site consists of a 4m×30m flexible pavement structure, that can be broadly described as follows:

- General information: the test site is located at the Department of Engineering of Roma Tre University, Rome. The elevation above the sea level is 11.5 m.
- Vertically (in-depth structure): the cross-section consists of an 80 mm of hot mix asphalt (HMA) layer, 100 mm of bitumen-bound base and 100 mm of unbound sub-base [8] (Figure 1). The absence of metallic targets below the surface was ensured by former surveys.
- Horizontally (surface structure): a square mesh grid of 76×11 nodes was realized, with a step of 0.4 m each other, for overall 836 nodes. The longitudinal slope can be considered as broadly flat. Former visual inspections of the pavement revealed general good conditions, with a 62 m^2 of repaved zone, at the last 12m of the test site.
-

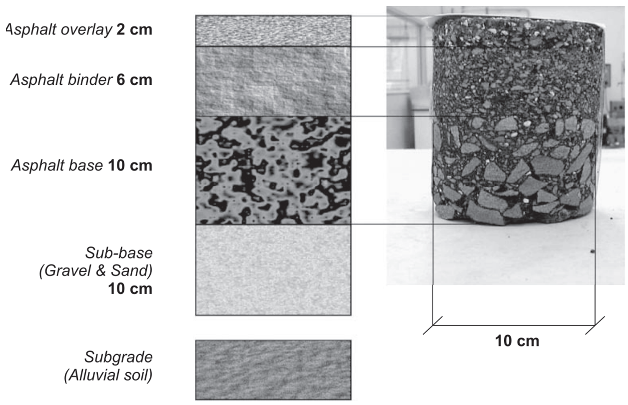

FIG. 1 – Core drilling showing the typical cross-section structure of the experimental test site.

The EM surveys were developed using a pulsed GPR system with two ground-coupled antennas, 600 MHz and 1600 MHz center frequencies of investigation (RIS 99-MF system realized by IDS S.p.A., Italy). Data were collected with two mono-static and two bi-static channels, in the time domain, providing a 40.076 ns time-window. The time step for data acquisition was dt = 7.8273×10^{-2} ns, with the horizontal resolution of

data sampling set as 2.4×10^{-2} m. Data collected with the 1600 MHz antenna were used for cross-checking, while data from the 600 MHz antenna were post-processed, according to the LFWD domain of influence. Overall, 11 longitudinal and 76 transversal tracks were surveyed, for a total amount of 26415 radar traces.

In addition, mechanical surveys were carried out using a Prima 100 LFWD, manufactured by Carl Bro Pavement Consultants Kolding, Denmark. The instrument is made of a metal plate (diameter 100 mm*)* loaded by a 10kg hammer, and geophone sensors enabling to measure deflections δ_c. The elastic Young's modulus E is calculated by using the Boussinesq solution, as follows:

$$E = \frac{k(1-\nu^2)\sigma R}{\delta_c} \tag{1}$$

where k equals 2 or $\pi/2$ for flexible and rigid pavements, respectively; δ_c being the deflection at the center of the plate [μm], σ being the load stress [MPa], and R being the plate radius [mm]. LFWD tests were developed during five days, in the same period of GPR measurements. Basically, a number of six LFWD measurements was performed on each grid node, to retrieve more stable and reliable mechanical data by statistical analyses [3].

PREDICTION MODEL

In order to perform a proper calibration of the model, LFWD and GPR data have been formerly processed with the aim of minimizing the instability of results and increasing the compatibility of both mechanical and EM data.

Concerning the LFWD measurements, the reliability of the observed values of Young's modulus E_{OBS} node in the grid was increased by applying a 10% trimmed mean to the above six measurements, node by node.

On other hand and with regards to the EM data, a depth zero filtering was applied to each trace, which was in turn averaged amongst the neighborhood traces collected alongside the longitudinal and transverse direction of acquisition, with spatial lengths of +0.20 m and -0.20 m from each sensing point. Under the hypothesis of an average standard value of wave propagation velocity equals to 10 cm/ns, it was possible to build a 3D matrix of the signal. The comparison between such 3D amplitudes matrix and the E_{OBS} matrix can be considered as the base of the modeling process. The generic value of predicted elastic modulus $E_{x,y}$

related to a certain general position $[x, y]$ on the grid is defined by the following equation:

$$E_{x,y} = \left[\rho\left(\tau \int_0^{z_{max}} A_{x,y,z_{[0,1]}} \varphi_z dz\right) + \sigma\right]^{-1} \quad (2)$$

with $A_{x,y,z_{[0,1]}}$ being the generic value of signal amplitude, normalized in the range [0,1]. φ_z is a coefficient depending on the depth, that takes into account the interaction between the attenuation of the signal and the contribution of the material, at a generic depth, to the pavement elastic response. z_{max} is defined as 0.2 m, according to the domain of influence of LFDW. τ is a scale coefficient allowing to retrieve the absolute $E_{x,y}$ value, from the normalized one, while ρ and σ are amplification coefficients whose values are calibrated by minimizing errors between E_{OBS} and $E_{x,y}$ through an empirically-based reciprocal regression process.

Calibration and validation of the model

With the aim of both minimizing computational efforts and properly describing the relationship between GPR and LFWD results, four C-scans from the 3D amplitudes matrix were sampled at fixed depths, namely, the interfaces between air and pavement surface, HMA and base layers, base and sub-base layers, sub-base and subgrade. The calibration of the model according to Equation (2) was performed by randomly selecting 24 points within the 836 nodes of the grid and by running the reciprocal regression process. The model was then validated by randomly selecting 24 further nodes amongst the measured data.
A good estimate of elastic moduli by the EM data was observed, both for high and low values of E_{OBS}. Comparison between observed and predicted values of elastic modulus is shown in Figure 2. The determination coefficient R^2 between observed and predicted values amounts to 0.87, as shown in Figure 3.

Main results

An observed elastic modulus map was realized by interpolating the LFWD measurements (Figure 4a). Overall, the maximum and minimum values observed of the population are below and above 3200 MPa and 350 MPa, respectively, with an average value and a standard deviation of around 1020 MPa and 390 MPa. Four main areas characterized by highest values of strength can be identified, namely, $[x, y]$=[4.8m, 2.0m], $[x, y]$=[21.6m÷22.8m,0.8m÷1.6m], $[x, y]$=[24.4m, 4.0m], $[x, y]$=[26.4m÷29.6m, 0.8m÷2.0m]. Moreover, the middle area of the test site

(2.4m < x < 17.6m) shows average E values ranging from 1300 MPa to 1900 MPa. Analogous values can be observed for the area defined by 18.4 m < x < 22.8 m and y> 1.2 m. Lowest values of E can be identified alongside the longitudinal upper and lower edges, from x = 0.0 m to x = 20.0 m, and from x = 23.6 m to x = 30.0 m.

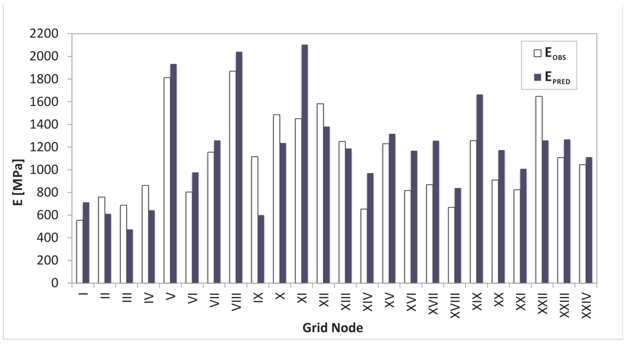

FIG. 2 – Comparison between observed and predicted Young's moduli for the validation process.

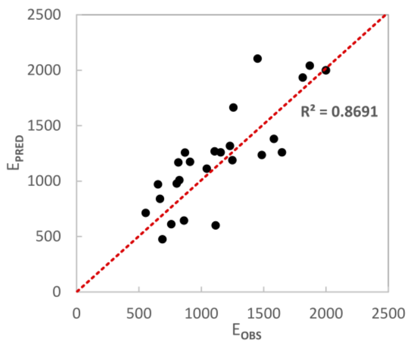

FIG. 3 – Determination coefficient between observed and predicted values of Young's modulus.

On other hand, by interpolating the prediction model results it was possible to build up a map of predicted elastic moduli (Figure 4b). The predicted population shows maximum, minimum and average values of ≈3000 MPa, ≈340 MPa and ≈1230 MPa, respectively, with a standard deviation □$_{\overline{E_{OBS}}}$ ≈435 MPa, thereby confirming a good reliability of predictions. Comparing these two maps, a good match can be identified in the area edged by 1.2 m < y < 2.0 m and 27.6 m < x < 29.6 m with E >

2600 MPa. Such an area corresponds to that one interested by past repaving works, as identified by former visual inspections. Analogously, another good match can be observed alongside the longitudinal centerline of the test site, bounded by 2.4 m < x < 22.4 m. Here, medium-high values of elastic modulus (1300÷1900 MPa) can be reasonably related to compaction procedures carried out under construction, that perform traditionally better in the longitudinal direction as well as in the center of the pavement cross section, due to the absence of edge effects from the compactors. In addition, good correspondences can be identified alongside the upper and lower edges of the test site.

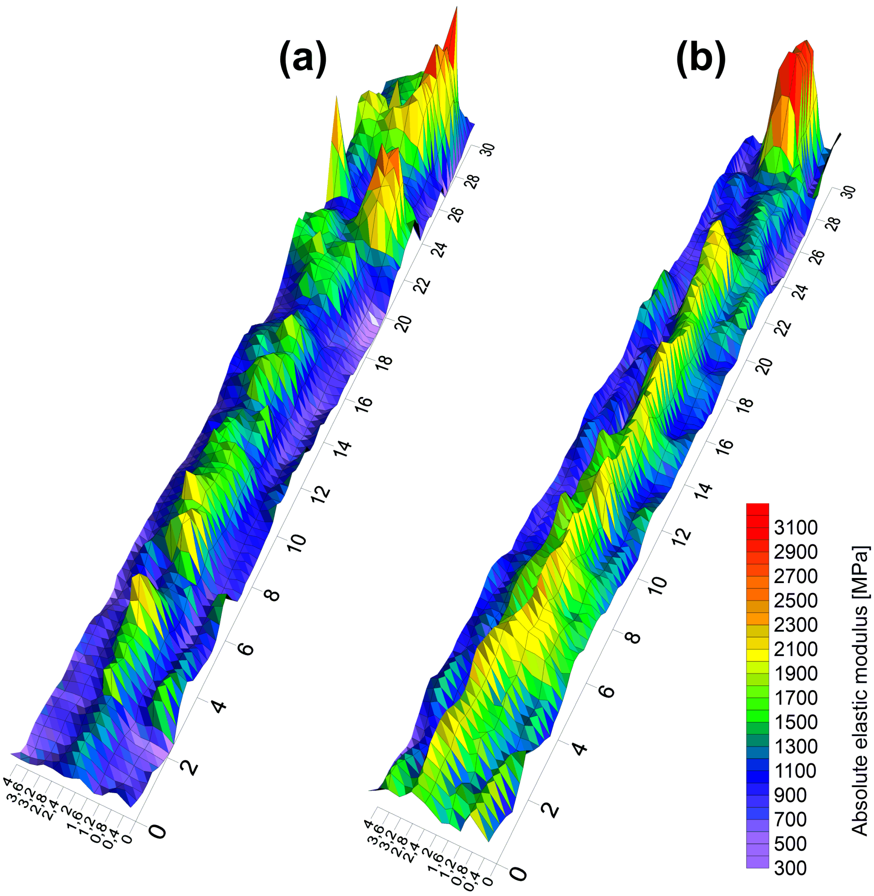

FIG. 4 – Observed (a) and predicted (b) elastic modulus maps from LFWD and GPR measurements, respectively.

CONCLUSIONS

In this work, a semi-empirical predictive model for evaluating mechanical properties of pavement by non-destructive GPR surveys is presented [9, 16]. For this purpose, a flexible pavement test site with dimensions 4m×30m was investigated, by surveying an 836 nodes square mesh grid, being 0.40 m the spacing between each scan.
The calibration of the model was performed by relating the LFWD measurements, collected on 24 randomly sampled nodes, and the signal amplitudes from GPR data, within the depth of influence of the LFWD.
The validation of the model was obtained by randomly selecting 24 further nodes and by minimizing the errors between observed and predicted values. A determination coefficient R^2 = 0.87 along with a general good matching of both high and low E values were shown. In addition, the comparison between the two elastic modulus maps has proved to be really promising.
Although some mismatches are identified and need to be further refined, the model shows good perspectives in order to achieve large-scale evaluations of pavement mechanical properties through GPR inspections. Further studies can be devoted on considering non-constant propagation velocity values of the electromagnetic signal through the material, i.e., in multi-layered configurations of pavements.

ACKNOWLEDGMENTS

Authors sincerely acknowledge Mr. Spartaco Cera, from Roma Tre University, for his precious help during fieldwork.

REFERENCES

[1] I. L. Al-Qadi, S. Lahouar, A. Loulizi, M. A. Elseifi and J.A. Wilkes, "Effective approach to improve pavement drainage layers", *Journal of Transportation Engineering*, vol. 130(5), pp. 658-664, 2004.

[2] K. A. Alshibli, M. A. Farsakh and E. Seyman, "Laboratory evaluation of the geogauge and light falling weight deflectometer as construction control tools", *Journal of Materials in Civil Engineering*, vol 17(5), pp. 560–569, 2005.

[3] American Society for Testing and Materials (ASTM). Standard test method for measuring deflections with a Light Weight Deflectometer (LWD). Annual Book of ASTM Standards 2007.

[4] R. Belt, T. Morrison and E. Weaver, "Long-term pavement performance program falling weight deflectometer maintenance manual," Rep. n. FHWA-HRT-05-153, 2006.

[5] A. Benedetto, "A three dimensional approach for tracking cracks in bridges using GPR", *Journal of Applied Geophysics*, vol. 1(97), pp. 37–44, 2013.

[6] A. Benedetto, F. D'Amico and F. Tosti, "Improving safety of runway overrun through the correct numerical evaluation of rutting in Cleared and Graded Areas", *Safety Science*, vol. 1(62), pp. 326–338, 2014.

[7] A. Benedetto, G. Manacorda, A. Simi and F. Tosti, "Novel perspectives in bridges inspection using GPR," *Nondestructive Testing Evaluation*, vol. 27 (3), pp. 239-251, 2012.

[8] A. Benedetto and S. Pensa, "Indirect diagnosis of pavement structural damages using surface GPR reflection techniques", *Journal of Applied Geophysics*, vol. 62, pp. 107-123, 2007.

[9] A. Benedetto and F. Tosti, "Inferring bearing ratio of unbound materials from dielectric properties using GPR: the case of Runaway Safety Areas", *Proceedings of the 2013 Airfield and Highway Pavement Conference*, Los Angeles, CA (USA), Jun. 2013, pp. 1336-1347

[10] A. Benedetto, F. Tosti and L. Di Domenico, "Elliptic model for prediction of deflections induced by a Light Falling Weight Deflectometer," *Journal of Terramechanics*, vol. 49(1), pp. 1–12, 2012.

[11] A. Benedetto, F. Tosti, B. Ortuani, M. Giudici and M. Mele, "Soil moisture mapping using GPR for pavement applications," *Proceedings of the 7th International Workshop on Advanced Ground Penetrating Radar*, Nantes, France, July 2013, pp. 243-248.

[12] D. J. Daniels, "Ground Penetrating Radar", The Institution of Electrical Engineers, 2004.

[13] R. Haas, W. R. Hudson and J. Zaniewski, "Modern pavement management", FL: Krieger Publishing Company, 1994.

[14] D. R. Huston, J. Hu, K. Maser, W. Weedon and C. Adam "Ground penetrating radar for concrete bridge health monitoring applications", *Proceedings of SPIE*, pp. 170-179, 1999.

[15] J. Minet, P. Bogaert, M. Vanclooster and S. Lambot, "Validation of ground penetrating radar full-waveform inversion for field scale soil moisture mapping", *Journal of Hydrology*, vol. 424, pp. 112–113, 2012.

[16] J. K. Mitchell, "Fundamentals of Soil Behaviour", Second Edition. New York, NY: John Wiley & Sons, 1993.

[17] C. Patriarca, F. Tosti, C. Velds, A. Benedetto, S. Lambot and E.C. Slob, "Frequency dependent electric properties of homogeneous multi-phase lossy media in the ground-penetrating radar frequency range", *Journal of Applied Geophysics*, vol. 1(97), pp. 81-88, 2013.

[18] M. Samson and L. Fréchette, "Seasonal variation of pavement strength based on Benkelman Beam rebounds", Canadian Strategic Highway Research Program (C-SHRP), 1995.

[19] T. Scullion, C. L. Lau and Y. Chen, "Pavement evaluations using ground penetrating radar", In Proc. of the 5th International Conference on Ground Penetrating Radar, Kitchener, Ontario, Canada 1994, pp. 449-463.

[20] S. Tighe, N. Li, L.C. Falls and R. Haas, "Incorporating road safety into pavement management", *Transportation Research Record*, vol. 1699, pp. 1-10, 2000.

[21] F. Tosti, C. Patriarca, E.C. Slob, A. Benedetto and S. Lambot, "Clay content evaluation in soils through GPR signal processing," *Journal of Applied Geophysics*, vol. 1(97), pp. 69-80, 2013.

[22] J. van der Kruk and E.C. Slob, "Reduction of reflections from above surface objects in GPR data", *Journal of Applied Geophysics*, vol. 55, pp. 271–278, 2004.

"INVESTIGATION OF HMA COMPACTABILITY USING GPR TECHNIQUE" (CONTRIBUTION TO PROJECT 2.1)

Christina Plati (GR), Panos Georgiou (GR), Andreas Loizos (GR)
cplati@central.ntua.gr

The abstract is published in *Geophysical Research Abstracts*, Vol. 16, EGU2014-1949, 2014 and is available on *www.egu2014.eu*

This contribution was presented as a poster.

"POTENTIAL OF AN AIR-LAUNCHED GPR SYSTEM FOR DETECTING PAVEMENT DAMAGES EVOLUTION: A CASE STUDY" (CONTRIBUTION TO PROJECT 2.1)

Fabio Tosti (IT), Fabrizio D'Amico (IT), Alessandro Calvi (IT),
Luca Bianchini Ciampoli (IT), Andrea Benedetto (IT)
fabio.tosti@uniroma3.it

Abstract

Among the effects of the Global Economic Crisis, it is possible to count a growth of the demand for Non-Destructive Technologies (NDTs). This is mainly due to their high performances, whereby they allow to collect many data over large distances, such as in case of road pavement inspections, in a really shortened time range and with relatively low financial efforts. In this research work, ground-penetrating radar (GPR) data collected on a rural road network were analysed. Analyses were carried out twice, with a seven-month time span each other, with the main goals to i) detect critical sections for road unsafety conditions occurrence; ii) monitor the evolution of existing damages and evaluate early-stage deep failures, even though not visible at the ground level; iii) interpret the impact of human factors in accident occurrence instead of environmental factors. An instrumented van supporting a 1GHz GPR air-launched horn antenna was employed to collect data at traffic speed. The reliability of results was enhanced by cross-checking multiple data from different support technologies (e.g. GPS, odometer, HD video camera). Lastly, GPR data were processed and pavement layers identified. Results show promising perspectives in predicting pavement damages evolution, paving the way to further implementation of prediction models for assessing residual life-cycle of pavements.

INTRODUCTION

As a result of an overall decrease of economic resources for infrastructural asset maintenance, public administrations are progressively reshaping their investment strategies towards the application of more time- and cost-efficient technologies, focused at optimizing both maintenance and rehabilitation processes.
With regard to pavement engineering purposes, the need for effective and efficient management and maintenance operations involves more crucial issues, which can be mainly related to social costs due to deaths and injuries from car accidents. Poor conditions of pavement surface have been identified as among the main causes of driving unsafety [22].

In line with this, cracks, potholes and surface deformations with related water ponding, usually cause a lowering of friction between vehicle tires and pavement surface due to vertical accelerations, thereby contributing to increase poor safety conditions of driving. In this scenario, it seems quite evident how proper pavement management actions could lead to both effective uses of resources and significant reductions of car accidents by preventing the causes of damages. Accordingly, NTD*s* are nowadays the most widespread techniques employed in road rehabilitations. Amongst them, it is worth citing the light falling weight deflectometer (LFWD) as a useful tool for evaluating the mechanical properties of subsurface [3, 8], while many applications on moisture content rely on the use of time domain reflectometry (TDR) [19]. Despite a relatively high reliability of results achieved through the above systems, GPR-based surveys broadly enable a huge gathering of data in relatively low time periods, directly on site. [6, 20]. Several GPR applications are carried out in the field of pavement engineering. Amongst them, we can cite the detection of subsurface voids [16], the investigation of layer thicknesses [1] and delamination in concrete structures [10, 14], the detection of rebars [12, 13], the positioning of underground utilities [4], asphalt stripping evaluation [21] and bridges monitoring [7]. The assessment of volumetric water content in pavement structures [2], load-bearing layers and subgrade soils [5, 9, 11, 15, 23] are further important issues that have been tackled by using GPR techniques, as well as the evaluation of clay content in soils, that causes unwanted plasticity effects [17, 23]. In addition, several studies have dealt with the potential of off-ground GPR configurations, which enable large-scale efficient road surveys [18, 20].

METHODOLOGY AND OBJECTIVES

In this work, the reliability and efficiency of an off-ground GPR radar system have been tested at the large-scale of investigation. Radar surveys have involved about 320 km of roads, with the aim to infer information about layers arrangement, along with the main causes and the evolution of visible and hidden damages. In order to investigate this latter, surveys were performed twice, 320 km and 160 km length, respectively, at a time distance of about seven months.

TOOLS AND EQUIPMENT

Radar data were collected using the RIS Hi-Pave HR1 1000 GPR system, manufactured by IDS S.p.A., Italy, working with one mono-static off-

ground antenna, 1GHz center frequency of investigation. The antenna array was fixed behind an instrumented van, hosting the control unit.
GPS logging of the van trajectories, has ensured the exact positioning of the GPR data gathered. In addition, the use of an odometer and an HD video recorder has enabled, respectively, to measure the covered distance and to provide data processing with visual feedbacks of surface conditions. Post-processing of the raw data was carried out by using the GRED 3D software by IDS S.p.A.

SYSTEM CALIBRATION

In order to calibrate the GPR system, preliminary surveys were performed both in laboratory environment and real-life roads, in order to ensure a good reliability of the data collected by isolating and filtering out unwanted signal noise factors. Basically, the calibration parameters have included *i)* the radar positioning on the van (i.e., the height of the antenna array above the ground and its distance from the back of the van); *ii)* the acquisition parameters (time window, samples per scan, etc..); *iii)* the post-processing procedure (sequence of applied signal filters); *iv)* optimal scan length to streamline heavy computational loads. Table 1 synthesizes the optimal configuration retrieved for each of the aforementioned parameters during system calibration.

TABLE 1 – OUTCOMES FROM THE CALIBRATION OF THE GPR SYSTEM

Category	Parameter	S.I.	Optimal Configuration
Radar positioning	Height from the ground	mm	400
	Distance from the van body	mm	1200
Data acquisition	Time window	ns	25
	Samples per scan	No.	512
	Horizontal resolution	mm	50
Post-processing	Soil Sample	ns	≈5
	Vertical Pass Band	GHz	0.5÷2.0
	Linear Gain		Standard
Computation process	Scan length	m	10,000

Domain of investigation

Inspections were carried out on a rural road network in the District of Rieti, about 100 km north from Rome, in Italy. The surveyed topography is mostly characterized by a hilly and mountainous environment. According to both the center frequency of investigation and the investigated type of structure, the maximum signal penetration depth is around 900 mm, which is consistent with the deepest layer interfaces.
Overall, around 320 km were investigated at traffic speed in both travel directions, on the following routes:

- SR 4 bis – "del Terminillo": 16 km + 900 m;
- SR 79 – "Ternana": 17 km + 300 m;
- SR 313 – "Passo Corese": 45 km + 000 m;
- SR 471 – "di Leonessa": 32 km + 500 m;
- SR 578 – "Salto Cicolana": 46 km + 450 m;

All across the considered road network, the road section is mostly composed by two lanes, 3.5 m wide each, with both left and right shoulders 0.5 m wide. A typical pavement cross-section consists, on the average, of a 65mm thick HMA layer, a 100mm thick base layer and a 300mm thick sub-base layer.

Approach for data analysis

According to the digital filters listed in Table 1, raw data have been processed firstly in the time domain, in order to remove reflections from antenna coupling and the air layer separating the source of the signal and the ground surface, and band pass filters have been subsequently applied in the frequency domain to reduce the noise. Lastly, signal amplitudes and their attenuation in depth have been re-modulated through a standard amplification function.
To develop a proper data analysis, GPR traces were divided into homogenous sections, due to the combination of the following parameters:

- considered route;
- cross-section type;
- pavement distress;
- regularity of layer thicknesses kept along considerable distances;
- marked loss of regularity in layers arrangement;

- widespread overlays and repairs;
- widespread subsurface water presence in the neighborhood of streams or rivers;
- widespread frost action effects within the pavement structure.

MAIN RESULTS

Since around 320 km have been broadly investigated in two days during the first set of surveys, and about 160 km during the second one, it is worth to cite how this off-ground GPR system has shown a very high productivity of approximately 160 km/day, at the average speed of 40 km/h. In addition, the results from the second set of surveys have shown a high consistency with those collected during the first one. As expected, minor changes have been observed in those sections interested by lower traffic loads, while major evolutions of pavement distresses were detected very close to water bodies, such as rivers or streams, in work zones as well as in those sections already damaged in the past. In this work, GPR surveys related to Routes S.R. 313 and S.R. 578 are presented as case studies. Concerning Route S.R. 313, Figures 1 and 2 show the GPR scans and relevant photographic reports carried out in different time periods, on the way to "Terni". Such two figures relate to the homogeneous section developing from km 13+400 to km 13+500, for an overall length of 100 m. Both the radar scans highlight widespread failures at the subsurface level (i.e., subgrade). The length of this type of damage is about 50 m. By cross-checking GPR data, HD video camera and GPS logger, it was easy to verify that such distress is revealed by surface cracking and potholes over the pavement surface. By means of figures comparison, it is worthwhile noting that this damage has suffered a relevant evolution during the 7months interlude. Concerning Route S.R. 578, the homogeneous section developing between km 40+700 and km 40+800, "Torano" direction, was taken into account. In contrast to the previous case study of Figure 1, a good matching between the two radar scans can be found in this case. Pavement faults are mostly concentrated in load-bearing layers. Although the local topography suggests possible relevant freeze-thaw cycles affecting the pavement, GPR and video camera data do not observe relevant subsurface considerable changes during survey time periods.

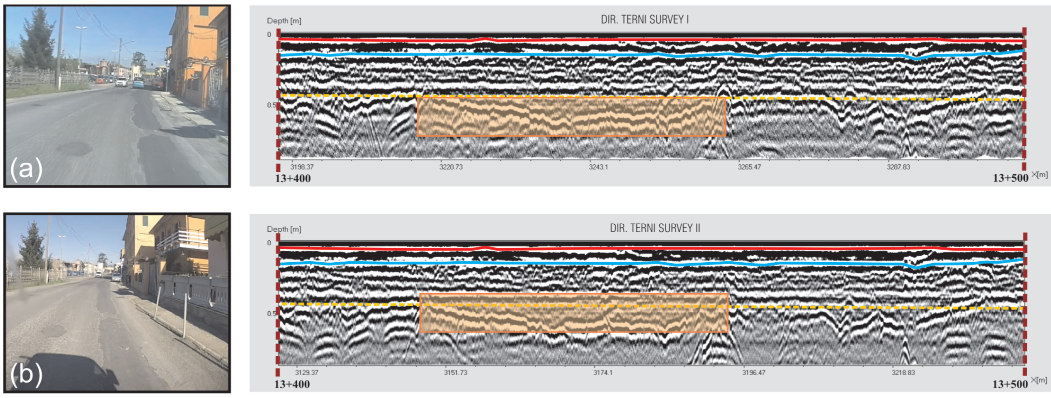

FIG. 1 – GPR scans and relevant photographic reports of one homogenous section located between km 13+400 and km 13+500 of Route S.R. 313 in the first set of surveys (a) and after seven months (b).

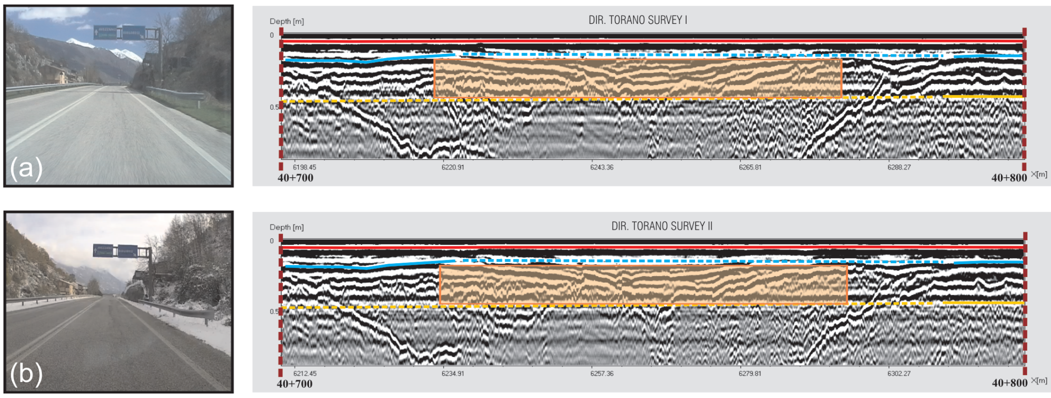

FIG. 2 – GPR scans and relevant photographic report of one homogenous section located between km 40+700 and km 40+800 of Route S.R. 578 in the first set of surveys (a) and after seven months (b).

CONCLUSIONS

The effectiveness and efficiency of an air-launched GPR system in a large-scale road network domain of investigation are analyzed in this work. Two set of surveys, 320 km and 160 km of length, respectively, were performed at an average speed of 40 km/h. The GPR system was calibrated through laboratory and real-life roads tests. Two case studies are herein presented, concerning two out of five investigated routes of the rural road network.

The efficiency and effectiveness of such a GPR system have been proved by both the high productivity of this technology (around 160 km/day) and the possibility to avoid any traffic flow interruptions. Furthermore, considerable results were achieved in correctly identifying the positioning of mismatches in layers arrangement. In line with this, the comparison between radar scans at different time periods and data collected through other tools, have confirmed the crucial role of GPR in identifying the causes of damages, regardless from surface evidences. Lastly, the repetition of surveys after a significant time period could pave the way for future GPR-based approaches capable to predict how specific pavement damages may develop over time, such that the most effective maintenance actions can be timely implemented.

Acknowledgements

The authors would like to sincerely acknowledge the precious help provided by Mr. Spartaco Cera, Roma Tre University, in both laboratory and field operations. This work also benefited from the network activities carried out within the EU funded COST Action TU1208 "Civil Engineering Applications of Ground Penetrating Radar".

References

[1] I. L. Al-Qadi and S. Lahouar, "Use of GPR for thickness measurement and quality control of flexible pavements", *Journal of the Association of Asphalt Paving Technologists*, vol. 73, pp. 501-528, 2004.

[2] I. L. Al-Qadi, S. Lahouar, A. Loulizi, M. A. Elseifi and J. A. Wilkes, "Effective approach to improve pavement drainage layers", *Journal of Transportation Engineering*, vol. 130(5), pp. 658-664, 2004.

[3] K. A. Alshibli, M. A. Farsakh and E. Seyman, "Laboratory evaluation of the geogauge and light falling weight deflectometer as construction control tools", *Journal of Materials in Civil Engineering*, vol. 17(5), pp. 560-569, 2005.

[4] D. Ayala-Cabrera, M. Herrera, J. Izquierdo and R. Pérez-Garcia, "Location of buried plastic pipes using multi-agent support based on GPR images", *Journal of Applied Geophysics*, vol. 75, pp. 679-686, 2011.

[5] A. Benedetto, "Water content evaluation in unsaturated soil using GPR signal analysis in the frequency domain", *Journal of Applied Geophysics*, vol. 75, pp. 679-686, 2010.

[6] A. Benedetto, F. Benedetto and F. Tosti "GPR applications for geotechnical stability of transportation infrastructures", *Nondestructive Testing and Evaluation*, vol. 27(3), pp. 253-262, 2012.

[7] A. Benedetto, G. Manacorda, A. Simi and F. Tosti, "Novel perspectives in bridges inspection using GPR", *Nondestructive Testing and Evaluation*, vol. 27 (3), pp. 239-251, 2012.

[8] A. Benedetto, F. Tosti and L. Di Domenico. "Elliptic model for prediction of deflections induced by a Light Falling Weight Deflectometer", *Journal of Terramechanics*, vol. 49 (1), pp. 1-12, 2012.

[9] A. Benedetto, F. Tosti, B. Ortuani, M. Giudici and M. Mele, "Soil Moisture Mapping using GPR for Pavement Applications. International Workshop on Advanced Ground Penetrating Radar. *Proceedings of 7th International Workshop*, Nantes, 2-5 July 2013, pp. 243-248, 2013.

[10] X. Dérobert, G. Villain, R. Cortas and J. L. Chazelas, "EM characterization of hydraulic concretes in the GPR frequency-band using a quadratic experimental design", NDT-CE, *Proceedings of 7th International Symposium*, Nantes, 2009.

[11] K. Grote, S. S. Hubbard and Y. Rubin, "Field-scale estimation of volumetric water content using GPR ground wave techniques". *Water Resources Research*, vol. 39(11), pp. 1321-2003.

[12] J. Hugenschmidt and R. Loser, "Detection of chlorides and moisture in concrete structures with ground penetrating radar", *Materials and Structures*, vol. 41, pp. 785-179, 2008.

[13] D. R. Huston, J. Hu, K. Maser, W. Weedon and C. Adam, "Ground penetrating radar for concrete bridge health monitoring applications", International Society for optics and Photonics, *Proceedings of SPIE 1355*, pp. 170-179, 1999.

[14] A. Kalogeropoulos, A. van der Kruk, J. Hugenschmidt, J. Bikowski and E. Brühwiler, "Full-waveform GPR inversion to assess chloride gradients in concrete", *NDT&E International*, vol. 57, pp. 74,84, 2013

[15] S. Lambot, E. C. Slob, I. van den Bosch, B. Stockbroeckx and M. Vanclooster, "Modeling of ground-penetrating radar for accurate characterization of subsurface electric properties", *IEEE Transactions on Geoscience and Remote Sensing*, vol. 42, pp. 2555-2568, 2004.

[16] C. L. Lau, T. Scullion and P. Chan, "Modeling of ground-penetrating radar wave propagation in pavement systems", *Transportation Research Record*, vol. 1355, pp. 99-107, 1992.

[17] C. Patriarca, F. Tosti, C. Velds, A. Benedetto, E. C. Slob and S. Lambot, "Frequency dependent electric properties of homogeneous multi-phase lossy media in the ground-penetrating radar frequency range", *Journal of Applied Geophysics*, vol. 97, pp. 81-88, 2013.

[18] J. Redman, J. Davis, L. Galagedara and G. Parkin, "Field studies of GPR air launched surface reflectivity measurements of soil water content" *International Conference on Ground Penetrating Radar; Proceedings of the 9th International Conference*, 29 April-02 May 2002. S. Koppenjan and K. Lee, Eds. 4758: 156-161.

[19] D.A. Robinson, S.B. Jones, J.M. Wraith, D. Or and S.P. Friedman, "A review of advances in dielectric and electrical conductivity measurement in soils using time domain reflectometry", *Vadose Zone Journal*, vol. 2(4), pp. 444-475, 2003.

[20] T. Saarenketo and T. Scullion, "Road evaluation with ground penetrating radar", *Journal of Applied Geophysics*, vol. 43(2), pp. 119-138, 2000.

[21] T. Scullion, C. L. Lau and Y. Chen, "Pavement evaluations using ground penetrating radar", *International Conference on Ground Penetrating Radar, Proceedings of the 5th International Conference*, Kitchener, pp. 449-463, 1994.

[22] S. Tighe, N. Li, L.C. Falls and R. Haas, "Incorporating road safety into pavement management", *Transportation Research Record*, vol. 1699, pp. 1-10, 2000.

[23] F. Tosti, "Determination, by using GPR, of the volumetric water content in structures, substructures, foundations and soil. State of the art and open issues", Civil Engineering Applications of Ground Penetrating Radar. *Proceedings of the 1st COST Action General Meeting TU1208*, Roma, 22-24 July 2013. pp. 99-105, 2013.

Progress Report of project 2.2

"Innovative inspection procedures for effective GPR surveying of buildings"

V. Pérez Gracia (ES), Mercedes Solla (ES)
vega.perez@upc.edu

I. Project Participants

In July 2013, 11 Members from 7 Countries were participating to this project. We now have 22 Members from 9 Countries: Belgium, Croatia, France, Germany, Greece, Italy, Norway, Portugal and Spain.

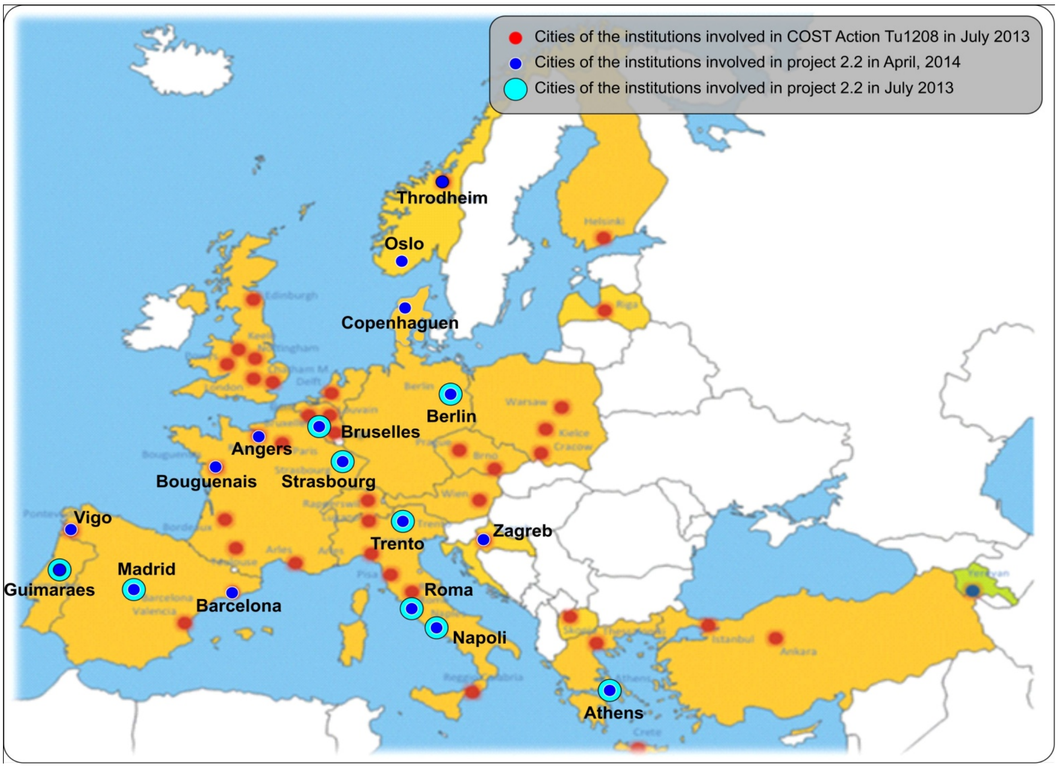

II. Report of activities

In February 2014, a state-of-the-art report on the topics of Project 2.2 was presented and open issues were identified. The report is included in the "Proceedings of the 2014 Working Group Progress Meeting - Nantes, France, February 2014," COST Action TU1208, Aracne, L. Pajewski and X. Derobert, Eds., Rome, Italy, May 2014, ISBN 978-88-548-7223-3 (available online at www.GPRadar.eu).
Before the Second General Meeting, Members of Project 2.2 were asked to report about their current activities on the topics of Project 2.2 (or of possible interest for this Project). Their answers are resumed below.

Portugal

In the University of Guimaraes, a PhD thesis recently started, focusing on GPR surveying of historical buildings and different typologies of masonries (supervised by Dr. Francisco Fernandes).

Italy

In Eledia Research Centre, inverse scattering techniques for the GPR data processing are being developed and integrated with multi-scaling methods. The integration of stochastic and deterministic inversion algorithms with multi-focusing strategies, in order to produce high-resolution images with high computational efficiency, is a topic under study. Inversion techniques based on Bayesian Compressive Sampling are being developed, suitable to recover sparse objects such as rebar, cracks and voids inside reinforced concrete, pillars and walls. Further techniques are being developed, based on the Learning-by-Examples (LBE) paradigm, for real-time detection, localization and classification of defects, voids and cracks inside lossy dielectric mediums.

[1] M. Salucci, G. Oliveri, A. Randazzo, M. Pastorino, and A. Massa, "Electromagnetic subsurface prospecting by a multi-focusing inexact Newton method within the second-order Born approximation," Journal of Optical Society of America A (Accepted).
[2] M. Salucci, L. Tenuti, C. Nardin, M. Carlin, F. Viani, G. Oliveri and A. Massa, "Gpr survey through a multiresolution deterministic approach," IEEE AP-S International Symposium, Memphis, Tennessee, USA, July 6-12, 2014 (Accepted).
[3] M. Salucci, L. Tenuti, C. Nardin, G. Oliveri, F. Viani, P. Rocca, and A. Massa, "Civil engineering applications of ground penetrating radar:

recent advances @ the ELEDIA Research Center," European Geosciences Union General Assembly (EGU2014), Vienna, Austria, April 27 - May 2, 2014 (Accepted).
[4] M. Salucci, G. Oliveri, A. Randazzo, M. Pastorino, and A. Massa, "Multi-Focusing Procedure based on the Inexact-Newton Method for Electromagnetic Subsurface Prospecting," EGU2014, Vienna, Austria, April 27 - May 2, 2014 (Accepted).
[5] M. Salucci, D. Sartori, N. Anselmi, A. Randazzo, G. Oliveri, and A. Massa, "Imaging Buried Objects within the Second-Order Born Approximation through a Multiresolution Regularized Inexact-Newton Method", 2013 International Symposium on Electromagnetic Theory (EMTS), (Hiroshima, Japan), May 20-24 2013 (invited).
[6] M. Salucci, P. Rocca, G. Oliveri, and A. Massa, "An innovative frequency hopping multi-zoom inversion strategy for GPR subsurface imaging," 15th International Conference on Ground Penetrating Radar (GPR2014), Brussels, Belgium, June 30 - July 04, 2014 (Submitted).

In Roma Tre University, laboratory tests on loose materials for the construction of load-bearing layers are being made, as well as workfield addressed to the characterization of pavement structures and typical subgrade soils (water content detection, clay content analysis, ...).

[7] Tosti, F., Patriarca, C., Slob, E.C., Benedetto, A., Lambot, S., Clay content evaluation in soils through GPR signal processing, Journal of Applied Geophysics 97, 69–80, 2013
[8] Benedetto, F., Tosti, F., GPR spectral analysis for clay content evaluation by the frequency shift method, Journal of Applied Geophysics 1(97), 89–96, 2013
[9] Patriarca, C., Tosti, F., Velds, C., Benedetto, A., Lambot, S., Slob, E.C., Frequency dependent electric properties of homogeneous multi-phase lossy media in the ground-penetrating radar frequency range, Journal of Applied Geophysics1 (97), 81–88, 2013
[10] Ortuani, B., Benedetto, A., Giudici, M., Mele, M., and Tosti, F., A non-invasive approach to monitor variability of soil water content with electromagnetic methods. Proc. International conf. on: Four Decades of Progress in Monitoring and Modeling of Processes in the Soil-Plant-Atmosphere System: Applications and Challenges, Naples, Italy, 19-20 June 2013. Procedia Environmental Sciences, Vol. 19, pp. 446-455
[12] Benedetto, A., Tosti, F., Ortuani, B., Giudici, M., and Mele, M. Soil moisture mapping using GPR for pavement applications. Proceedings of the 7th International Workshop on Advanced Ground Penetrating Radar

2013, Nantes, France, 02-05 July 2013, pp. 243-248. IEEE Digital Object Identifier: 10.1109/IWAGPR.2013.6601550, pp. 1-5.

SPAIN

In the University of Vigo, research activities are based on the application of GPR to different kind of structures, usually combined with topographic and photogrammetric studies. Recently, evaluation of soils in buildings was performed, combining termography and GPR in the inspection of radiant floors.

[13] S. Lagüela, M. Solla, L.Díaz-Vilariño, J. Armesto, "Integral inspection of radiant heating floor applying nondestructive testing techniques", Construction and building materials (submitted).

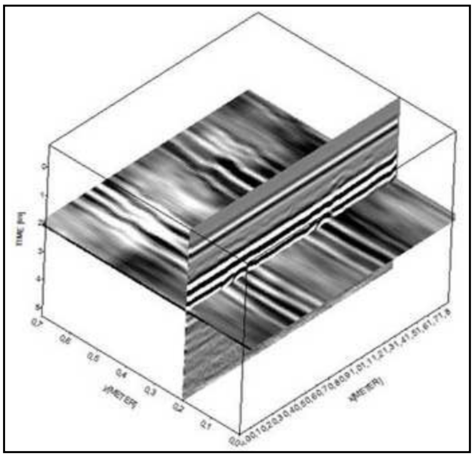

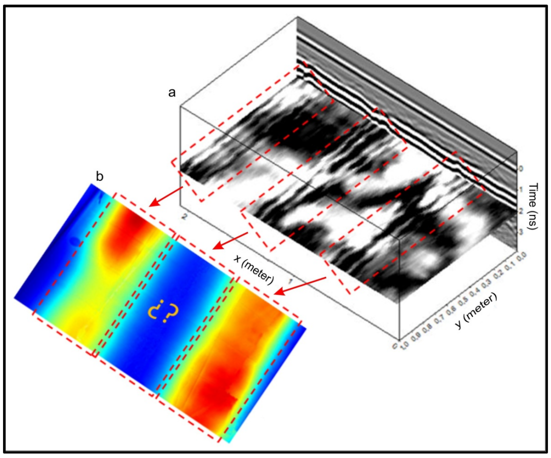

In the Technical University of Catalonia, Barcelona, the GPR is applied to different types of structures, being in most cases cultural heritage buildings. Building and soils are investigated, in order to define accurate seismic risks maps. GPR is often combined with other methodologies. Two PhD theses are being developed, on topics of interest for Project 2.2. Further ongoing work is based on the construction of a catalogue showing different constructive structures of buildings in Barcelona, and their radar images.

[14] V. Pérez-Gracia, J.O. Caselles, J. Clapés, G. Martinez, R. Osorio, "Non-destructive analysis in cultural heritage buildings: Evaluating the Mallorca cathedral supporting structures", NDT&E International 59 (2013) 40–47

[15] V. Salinas, J.O. Caselles, V. Pérez-Gracia, S. Santos-Assunçao, J. Clapes, L.G. Pujades, R. González-Drigo, J.A. Canas, J. Martinez-Sanchez, "Nanozonation in Dense Cities: Testing a Combined Methodology in Barcelona City (Spain)", Journal of Earthquake Engineering 18:1 (2014) 90-112
[16] V. Pérez-Gracia, S. Santos-Asssunçao, O. Caselles, J. Clapés, V. Salinas, R. González, "Geophysical exploration of columns in historical heritage buildings", GPR2014, Brussels, Belgium, June 30 - July 04, 2014 (Accepted).
[17] V. Pérez-Gracia, S. Santos-Assunçao, O. Caselles, J. Clapés, J.A. Canas, "Study of wood beams in buildings with ground penetrating radar", GPR2014, Brussels, Belgium, June 30 - July 04, 2014 (Accepted).
[18] S. Santos-Assunçao, V. Pérez-Gracia, V. Salinas, O. Caselles, J. Clapés, L.G. Pujades, R. González, N. Lantada, "Geological structures evaluated by means of scattering noise in Ground penetrating radar images", 15th International Conference on Ground Penetrating Radar (GPR2014), Brussels, Belgium, June 30 - July 04, 2014 (Accepted).
[19] V. Pérez-Gracia, H. Lorenzo, S. Santos-Assunçao, M. Solla, "GPR applications in Civil Engineering in Spain – state-of-the-art", EGU2014, Vienna, Austria, April 27 - May 2, 2014.
]20] S. Santos-Assunção, K. Dimitriadis, Y. Konstantakis, V. Perez-Garcia, E. Anagnostopoulou, M. Solla, H. Lorenzo, "Non-destructive assessment of the Ancient "Tholos Acharnon" Tomb building geometry", EGU2014, Vienna, Austria, April 27 - May 2, 2014.

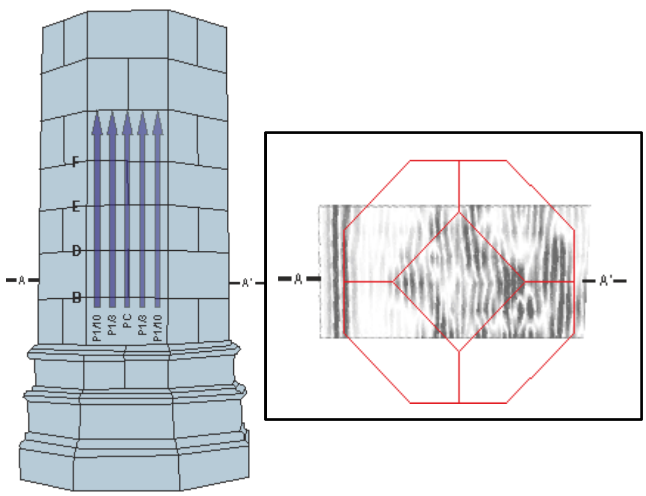

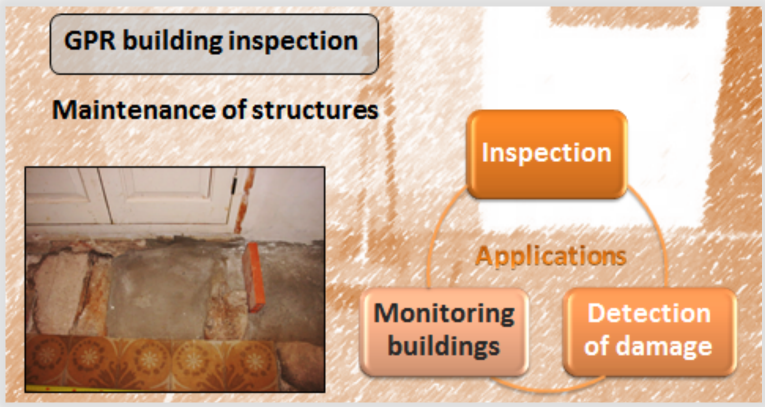
GPR building inspection
Maintenance of structures
Inspection
Applications
Monitoring buildings
Detection of damage

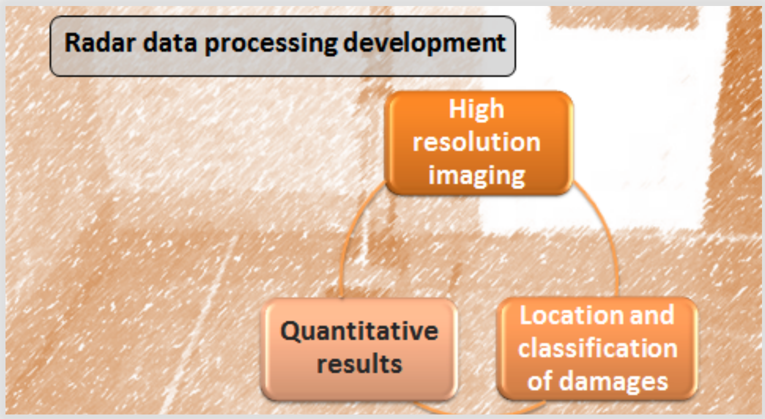
Radar data processing development
High resolution imaging
Quantitative results
Location and classification of damages

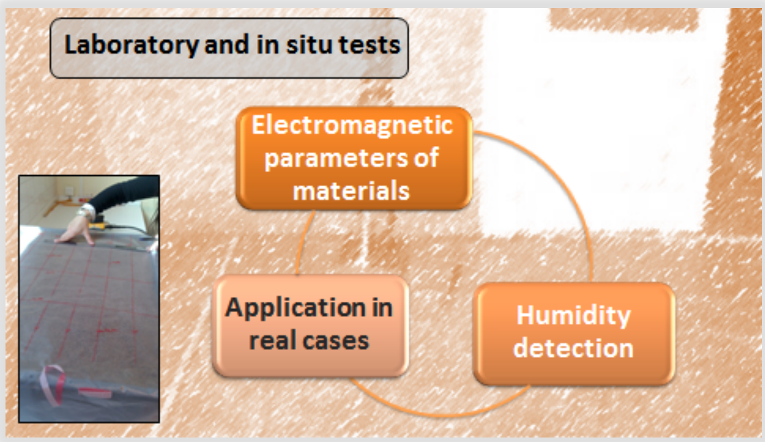
Laboratory and in situ tests
Electromagnetic parameters of materials
Application in real cases
Humidity detection

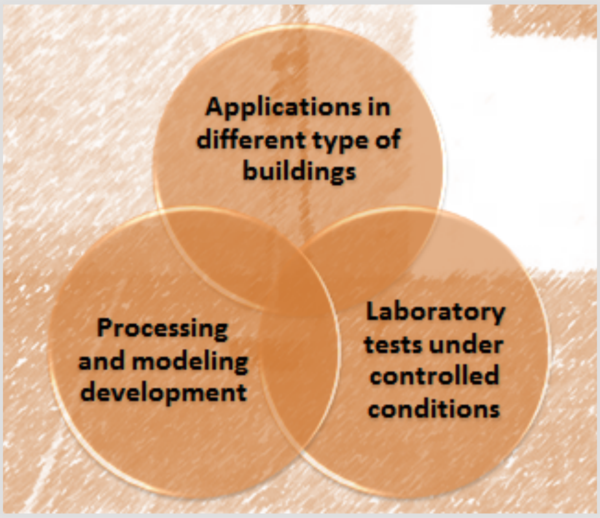

Activities of the Project Members

III. Future work

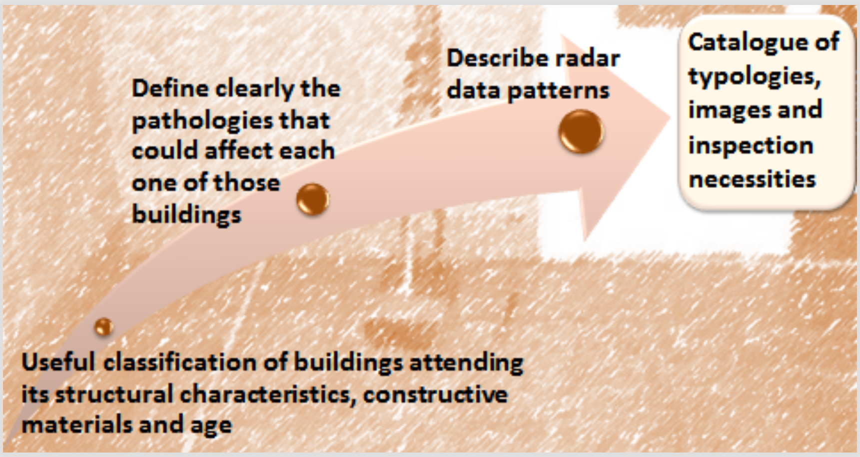

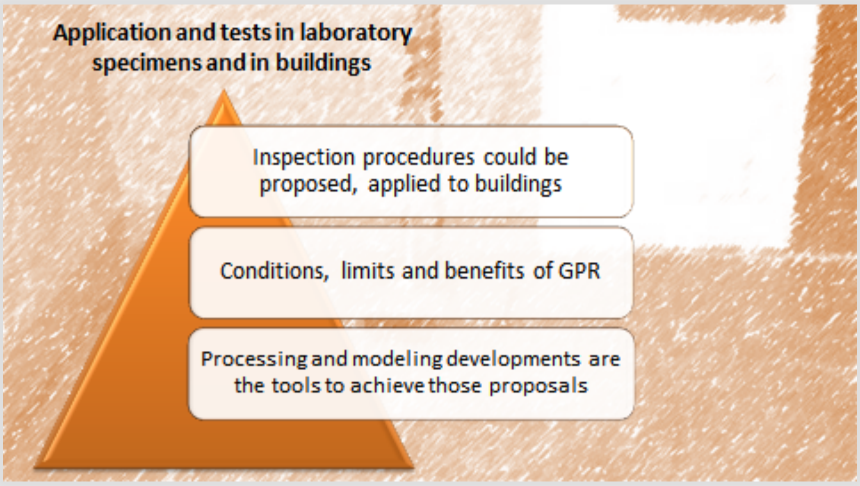

Acknowledgement

This work is a contribution to COST Action TU1208 "Civil Engineering Applications of Ground Penetrating Radar."

"2D and 3D GPR imaging of structural ceilings in historic and existing constructions" (contribution to Project 2.2)

Camilla Colla (IT)
camilla.colla@unibo.it

The abstract is published in *Geophysical Research Abstracts*, Vol. 16, EGU2014-16923, 2014 and is available on *www.egu2014.eu.*

PROGRESS REPORT OF PROJECT 2.3

"INNOVATIVE INSPECTION PROCEDURES FOR EFFECTIVE GPR SENSING AND MAPPING OF UNDERGROUND UTILITIES AND VOIDS, WITH A FOCUS TO URBAN AREAS"

Christina Plati (GR), Xavier Deròbert (FR)
xavier.derobert@ifsttar.fr

During the first year of COST action TU1208, the project devoted to underground utilities and voids detection has been part of a more general approach followed by the WG2 "GPR surveying of pavements, bridges, tunnels and buildings, undergrounds utilities and void sensing". The work of P2.3, once the applications of utilities and voids dissociated, has been composed of the following steps:

- state-of-the-art
- test sites
- survey procedures

For the particular case of voids detection, another section has been added dedicated to case studies.

The state-of-art related to the utilities detection and mapping has been mainly focused on some references, listed in Plati and Dérobert [1], some methodologies [2-5] and national standards or common practices [6-9]. the objective herein is to gather such information and compare the practices from one state to another one.

Another important action, initiated by WG2, has been to design some questionnaires. The first one being related to the kind of research and application studied by the actors of COST TU1208. This information has been gathered by the WP2.1 leader J. Stryk. The second questionnaire corresponds to a sheet to be filled describing test sites of benchmarks, used by the partners and that can be at disposal to this action.

One important geophysical test site that can be mentioned is located at Ifsttar [10]. This site is constituted essentially by a pit length of 30 m and 5 m in width in bottom with sides sloping to 2/1. Useful depth varies from 3.30 to 4.70 m. This pit is filled with various materials arranged in horizontal compacted slices separated by a vertical interface and water-tighted in surface, such as silt, limestone sand and gravel

gneiss. The embedded objects are mainly pipes elements, buried at three depths and polystyren hollows representing some voids.

Some GPR profiles, done at various central frequencies on this test site, should be available soon on the Website of this COST action. The objective herein is to propose as well as some typical and controlled GPR signatures and some examples to be modeled through the WG3.

The second part is devoted to voids created by pipes leaks or breaks, or by dislocated joints, while draining fine particles of base and sub-base road structures. The corresponding action follows the same steps than for the pipes. But as the shape of this kind of voids beneath roadways can present a wide range of variations (from discompacted materials to large cavities), the GPR responses vary in the same range order.

Then, the working group provides to design a sheet formular to be proposed and filled by the COST partners, who have performed such case studies in real situation. The objective herein is to create a catalog available to the COST partners.

The survey procedures will be designed in a last step, once the different actions will be performed and evaluated, including the hardware and signal or imaging processing, on controlled sites.

Acknowledgement

The authors acknowledge the COST Action TU1208 "Civil Engineering Applications of Ground Penetrating Radar", supporting this work.

References

[1] C. Plati, X. Dérobert, "Project 2.3 – Innovative inspection procedures for effective GPR sensing and mapping of underground utilities and voids, with a focus to urban areas – State of the art and open issues", Cost Action TU1208, 1srt action's General Meeting Proceedings, pp.79-98, 22-24 July 2013, Rome, Italy.
[2] A. P. Annan, "Ground Penentrating Radar principles, procedures & applications", Sensors and Software incorporated, 2003.
[3] J. Nissen, B. Johansson, M. J. Wolf and L. Skoog, "Ground Penetrating Radar - a ground investigation method applied to utility

locating in no-dig technologies", Mala Geoscience Raycon, Stockholm, 2001, pp. 1-6.
[4] J. D. A. Grivas, "Applications of Ground Penetrating Radar for highway pavements", NYSERDA TIRC Project C-04-04, New York State Department of Transportation, December 2006.
[5] NCHRP , "Ground Penetrating Radar for evaluating subsurface conditions for transportation facilities", National Cooperative Highway Research Program, Synthesis of Highway practice 255, Transportation Research Board, Washington D.C., 1998.
[6] French Standard NF S70-003-2 (2012), "Travaux à proximité des réseaux. Partie 2 : Techniques de détection sans fouille" / "Works in the neighborhood of utilities. Part2: Trenchless techniques of detection".
[7] ITU-T, recommendation L39 (2000), "Investigation of the soil before using trenchless techniques".
[8] Italian Standard CEI-C883 (2004), "Regulations for performing preliminary surveys with ground probing radar for before laying underground utilities and infrastructures".
[9] ASTM Designation D 6432-11, "Standard Guide for Using the Surface Ground Penetrating Radar Method for Subsurface Investigation".
[10] J.L. Chazelas (1998), "Création d'un site-test pour les méthodes géophysiques appliquées aux travaux sans tranchée – Projet National Microtunnels", Ifsttar Final report, 53 p.
[11] Holt, F.B., Eales, J.W., 1997. Nondestructive Evaluation of Pavements, Concrete Int., 9, 41-45.
[12] Morey, R.M., 1998. Ground Penetrating Radar for Evaluating Subsurface Conditions for Transportation Facilities, Synth. of Highway Practice 255, NCHRP, National Academy Press, Washington, D.C.
[13] TxDOT, "Using Ground-Penetrating Radar (GPR) techniques to detect concealed subsurface voids", Texas Department of Transportation, September 2010.

PROGRESS REPORT OF PROJECT 2.4

"INNOVATIVE PROCEDURES FOR EFFECTIVE GPR INSPECTION OF CONSTRUCTION MATERIALS AND STRUCTURES"

Lech Krysinski (PL)
lkrysinski@ibdim.edu.pl

Abstract

This report resumes the current efforts in Project 2.4. The basic information about participants was collected and a preliminary review of the methodologies being used by the project participants was provided. Several interesting laboratories for experimental studies on large samples are available, for joint activities.

BASIC INFORMATION

The Project 2.4 (WG2) currently has 30 participants from 11 Countries (Belgium 3, Croatia 3, Denmark 2, Finland 1, France 5, Germany 3, Greece 5, Italy 4, Poland 2, Portugal 1, Spain 1).

SCOPE OF THE PROJECT

The project deals with a wide area of problems related to material properties determination in GPR inspection practice. The quality/damage characteristics (like cracks and delaminations) are treated as material characteristics within the project interests. The structural studies of constructions belong also to the area of interest of this project, due to their close connections with the determination of the electromagnetic properties of the materials. The field and laboratory large scale constructions dedicated to experimental studies of the GPR response signals are of particular interest for the project.

A special questionnaire dedicated to the topics of the project was prepared. Based on the answers given by the participants, the preliminary review of methods being practiced is presented below.

MAIN CONSTRUCTION MATERIAL TYPES, THEIR CHARACTERISTICS AND PATHOLOGIES BEING ESTIMATED BY GPR

Among the most common construction materials, the following categories are being reported: concretes, masonry, bituminous mixtures, cobblestones, loose or improved materials like aggregates or sands

(unbound or reworked), railway ballast, isolation, geotextiles, soils and reworked soils, frost, rocks, karstic background of constructions like tunnels or roads, wood. For every category some typical properties, defects and characteristic problems were identified.

Typical inspection tasks are focused usually on structural aspects like the determination of layer thickness (depths 0 to 2m), finding out the position of reinforcement elements and infrastructure, the detection and localization of defects, construction changes and anomalies. The typical referred equipment uses time-domain antennas (200MHz to 2.2GHz) or frequency-domain antennas (Vivaldi and horn antennas, 3DR).

The typical structures being studied by the use of GPR by the project participants, belong to the following classes:

- **Pavements** (roads, squares and airport): bituminous pavement, concrete pavement, unbound aggregate pavement, sub-structures (covered or not covered), water supply systems.
- **Bridges, tunnels, railway infrastructure**: concrete and masonry bridges, retaining walls, tunnels, railway tracks.
- **Grounds**: soils, frost.
- **Buildings**: walls, floors and ceilings, columns, balconies, wood buildings and other constructions.

LABORATORY EQUIPMENT, METHODS AND SYSTEMS BEING USED FOR ELECTROMAGNETIC PROPERTIES ASSESSMENT

The laboratory methods for the estimation of the electromagnetic properties of the materials belong to two formal categories: GPR based methods, and auxiliary electromagnetic sensors. Some solutions (like TDR) have intermediate character.

GPR based methods (reflectometry, refractometry, transition systems, WARR, CMP methods):

- GPR Frequency-domain and time-domain, full inversion method.
- Large-sample measurements to analyse reflection amplitude, wave velocity, direct wave amplitude and shape.
- Estimation of backscattering efficiency in granular media.
- Medium-size test boxes for loose materials.

- Scattering impulse reflectometry on cylindrical samples (core 10 cm diameter).
- Ellipsometry (small, thin homogeneous layers of well determined thickness of several mm).

Transmission lines and tubes etc.:

- Cylindrical coaxial cell with a vectorial network analyser from 0.05 to 1.6 GHz (material cores of 75 mm in diameter and 70 mm in height).
- TEM co-axial line for measurements of the complex permittivity of hardened concrete in the frequency band 300 MHz - 900 MHz. Samples have a diameter of 8 cm and a height of 10 cm.

Electromagnetic probes (capacimetry, TDR, methods based on resistivity or induction):

- Percometer (permittivity, conductivity)
- Campbell probes CS615, CS616, CS650, HydraProbe (water content, conductivity)
- GTK probe (conductivity)
- EC CS547(Campbell), CS615 compared to water (permittivity, liquids)
- Ferroscan (induction)

METHODS FOR NEAR-SURFACE ELECTROMAGNETIC PROPERTIES DETERMINATION BY GPR (FIELD MEASUREMENTS)

The field methods of structural interpretations and assessment of material properties apply the whole range of seismic data processing and analysis. The main techniques for the determination of near-surface permittivity and attenuation, are:

- Surface reflection amplitude in air-coupled systems.
- Velocity analysis using inter-layer reflections.
- Full-wave inversion for stratified media.
- Velocity analysis using CMP.
- Velocity analysis using WARR multi-offset configurations.
- Assessment of damping (CMP, scattering objects).
- Calculation of dispersion curves (either phase velocity or permittivity vs. frequency).
- Normalised amplitude of direct wave and direct wave analysis in ground-coupled systems.

- Velocity of direct and reflected waves.
- Attenuation assessment using deeper reflections or scattering.

To estimate the wave velocity, some auxiliary (calibration) methods are being used:

- Drilling cores, trenches and outcrops.
- Local measurements carried out before and after laying the layers.
- Geodetic tests.

OTHER METHODS FOR ELECTROMAGNETIC PROPERTIES ESTIMATION BY GPR STUDIES (REAL CONSTRUCTIONS)

The methods described above are usually focused on the interpretation of plenty of relatively easy available data and the expected precision is large. Among the methods being used in real scenarios, the following techniques can be mentioned:

- Forward or inverse modelling of intricate structure and permittivity distribution.
- Hyperbola fitting (e.g. for positioning of reinforcement estimation, sometimes with verification of electromagnetic signal velocity by another methods), velocity analysis using numerous hyperbolic anomalies, numerical hyperbola fitting (in development).
- Migration (especially when the depth of reinforcement is accurately known).
- Backscattering; estimation of backscattering efficiency in granular media and forward modelling of backscattering in granular media.
- Attenuation characterization by interpretation of the frequency spectrum peaks shifting, (moisture content).

LABORATORIES & TEST SITES FOR MEASUREMENTS ON LARGE SAMPLES

The participants described in details some very interesting and inspiriting solutions dedicated to experimental studies of methodologies focused on material properties determination and on structural problems (fig. 1).

- Collections of concrete slabs: 60x60x12cm of 6 different concrete samples without reinforcement, walls containing reinforcement, different thicknesses, slabs 70x90x13cm made of different concrete mix with reinforcement or not, imbibed in pipe water or in sea water, containing THR sensors at different depth.

- Field sites: pavement test sections with different pavement structures (cement concrete, dense asphalt, porous asphalt, cobblestone) and laboratory geotechnical testing field for experiments with soils and different subbase layers (full scale tests) – the structure depends on current experiment.
- Laboratory position for modelling of backscattering in granular media: boxes containing materials to be compared with field tests using GPR, seismic and resistivity methods.

RECENT RESEARCH EFFORTS CONNECTED WITH THE PROJECT TOPICS.

The review paper [1] expressing area of the project interests is being prepared. Research activity carried out in recent months concerned:

- Numerical modelling of the GPR response for different types of damage structures, which is an important tool in echogram interpretation practice [2].
- Attempts of finding relation between bearing capacity of asphalt pavement and its GPR characteristics in field measurements [3].
- Investigations of raw construction materials permittivity for the purposes of GPR diagnostics [4].
- Detailed studies of 3D imaging abilities in investigations of the cracking process in asphalt pavements [5].
- Effectiveness of the use of surface permittivity estimation in the asphalt package thickness determination [6].

ACKNOWLEDGEMENT

The author acknowledges the participants of the project for their significant response and the COST Action TU1208 "Civil Engineering Applications of Ground Penetrating Radar", supporting this work.

REFERENCES

[1] L. Krysinski, J. Hugenschmidt, "Effective GPR Inspection Procedures for Construction Materials and Structures," Springer book on "Civil Engineering Applications of Ground Penetrating Radar," A. Benedetto & L. Pajewski, Eds., 2015.

[2] A. Benedetto, F. Tosti, L. Pajewski, F. D'Amico, W. Kusayanagi, "FDTD Simulation of the GPR Signal for Effective Inspection of Pavement Damages", Proceedings of the GPR 2014 Conference.

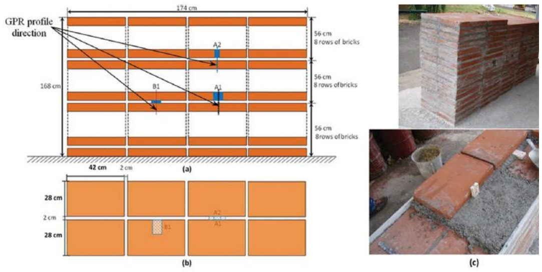

Brick masonry wall with jointing defects inside (LMDC Université de Toulouse, France)

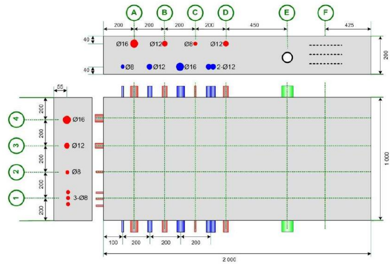

Concrete slab with embeded reinforcement, voids, delamination (LMDC Université de Toulouse, France)

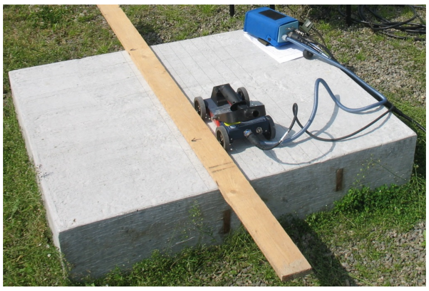

Concrete slab with 3 inbuild dowels in exact positions (CDV – Transport Research Centre, Czech Republic)

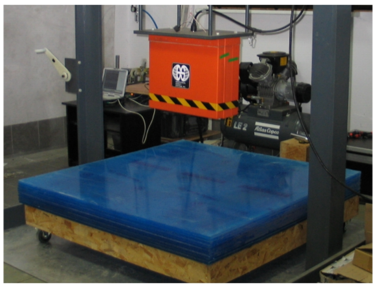

Test position for simulation GPR response of layered systems and small scale structures (Road and Bridge Research Institute, Poland)

“Sand box” for simulation of GPR response of different structures (ULB), automated scanning in three directions.

FIG. 1 - Laboratories and test sites for measurements on large samples.

[3] F. Tosti, S. Adabi, L. Pajewski, G. Schettini, A. Benedetto, “Large-scale analysis of dielectric and mechanical properties of pavement using GPR and LFWD”, Proceedings of the GPR 2014 Conference.
[4] L. Krysinski, “Permittivity Investigations of the Road Construction Raw Materials for Purposes of GPR Data Interpretations”, *Geophysical*

Research Abstracts, vol. 16, 2014 EGU General Assembly 2014, 27 April - 02 May 2014, Wien, Austria, 1pp.
[5] L. Krysinski, J. Sudyka, "Efficiency of 3D imaging in GPR diagnostics of joints and vertical construction contacts", Proceedings of the GPR 2014 Conference.
[6] M. Graczyk, L. Krysinski, J. Sudyka, "Application of ground penetrating radar in the diagnosis of the state of pavement design," *Logistyka* 2/2014.

"Permittivity Investigations of the Road Construction Raw Materials for Purposes of GPR Data Interpretations" (Contribution to Project 2.4)

Lech Krysinski (PL)
lkrysinski@ibdim.edu.pl

The abstract is published in *Geophysical Research Abstracts*, Vol. 16, EGU2014-2227, 2014 and is available on *www.egu2014.eu*

This contribution was presented as a poster.

Progress Report of Project 2.5

"Determination, by using GPR, of the volumetric water content in structures, substructures, foundations and soil"

Fabio Tosti (IT)
fabio.tosti@uniroma3.it

I. Outline of the Report

Overall Information

- Number of Participants
- Countries Involved

Project Purposes and Methods

- Definition of the Main Purposes of Working Project 2.5
  - Overall Purpose
  - Specific Purposes: Main Issues & Methods
    - Issue A
    - Issue B
    - Issue C
    - Issue D

Achieved Results

- Issue A
- Issue B
- Issue C
- Issue D

Conclusions

II. Overall Information

- Statistics on Project 2.5 Participants: number of Participants & countries involved

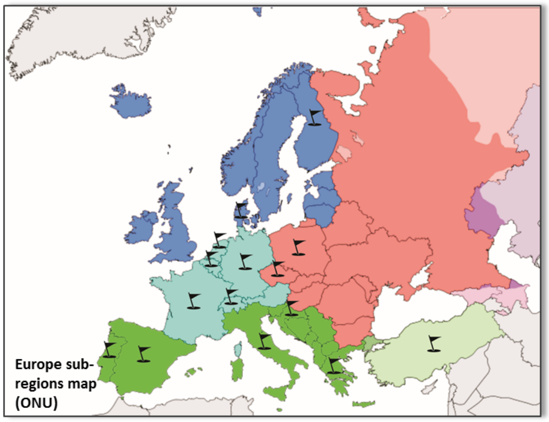

43 Participants

25 Institutions

14 Countries

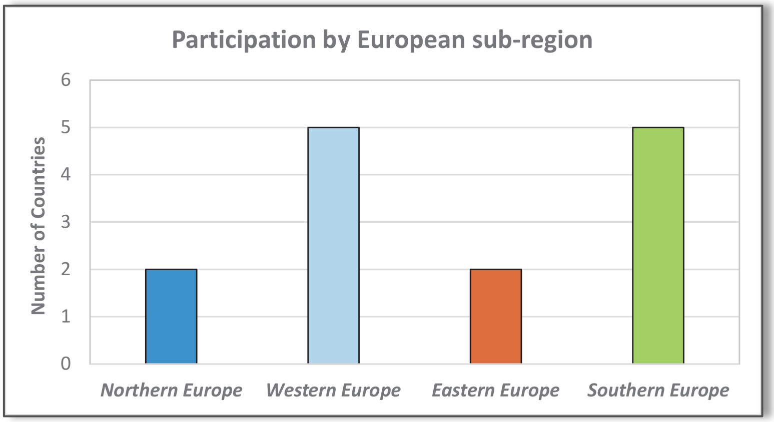

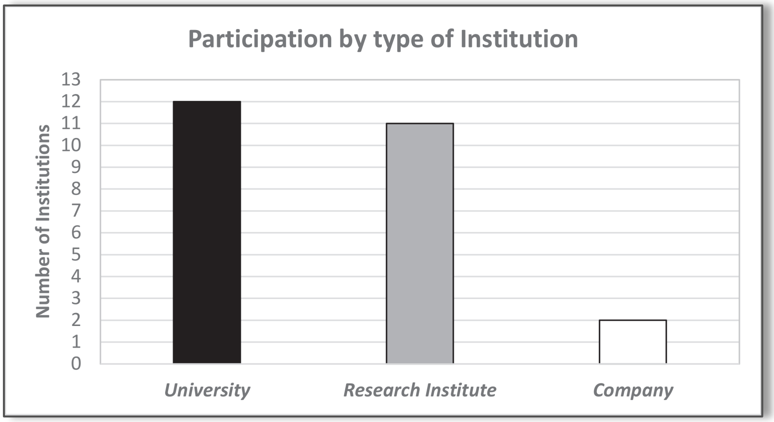

III. Project Purposes and Methods

- **Definition of the Main Purposes of Working Project 2.5**

- Overall Purpose

GPR-based evaluation of volumetric water content (VWC) in structures, substructures , foundations, and soils

- Specific Purposes: Main issues & Methods

GPR-based evaluation of volumetric water content (VWC) in structures, substructures , foundations, and soils

A. ISSUE A

Broad-ranging topic covering the main disciplines of civil engineering, differently demanding

- *Maritime engineering*

- *Structural engineering*

- *Geotechnical engineering*

- Geotechnical engineering

ACTION NEEDED

<u>Provide a comprehensive state of the art on the topic</u>

B. ISSUE B

Risk of overlapping amongst topics of the other Working Projects

- ***Project 2.1*** *– Innovative inspection procedures for effective GPR surveying of critical transport infrastructures (pavements, bridges and tunnels)*
- ***Project 2.4*** *– Innovative procedures for effective GPR inspection of construction materials and structures*

ACTION NEEDED

Discussions among WG Chairs and other WP Leaders to define independent and complementary topics

C. ISSUE C

"Heterogeneous" scenario about Project Participants

- ***Experience, Purposes, Fields of Application, Equipment, Facilities, Investigation Scale, Survey techniques***

ACTION NEEDED

Outline of such wide scenario by gathering comprehensive synthetic information from Project Participants

D. ISSUE D

Avoid that research gets stucked

- *No spreading of research results, then lower possibilities to grow the scientific quality on VWC determination using GPR*
- *Few possibilities for future partnerships and collaborations*

ACTION NEEDED

Ensure continuous updating of the latest results achieved by GPR Participants in VWC determination by GPR

IV. ACHIEVED RESULTS

A. ISSUE A

Broad-ranging topic covering the main disciplines of civil engineering, differently demanding

ACTION NEEDED

Provide a comprehensive state of the art on the topic

ACHIEVED RESULTS

Two main publications:

- *Tosti, F., Determination, by using GPR, of the volumetric water content in structures, substructures, foundations and soil. State of the art and open issues. Proceedings of the 1st COST Action General Meeting TU1208, Rome, Italy, 22-24 July 2013, pp. 99-105. ISBN: 978-88-548-6190-9.*
- *Tosti, F., Slob, E.C., Determination, by using GPR, of the volumetric water content in structures, substructures, foundations and soil. In. "Civil Engineering applications of Ground Penetrating Radar", Springer ed. (submitted).*

PROJECT 2.5
"DETERMINATION, BY USING GPR, OF THE VOLUMETRIC WATER CONTENT IN STRUCTURES, SUBSTRUCTURES, FOUNDATIONS AND SOIL"
STATE OF THE ART AND OPEN ISSUES

F. Tosti

Department of Engineering, University of "Roma Tre"
Via Vito Volterra 62, 00146 Rome, Italy
fabio.tosti@uniroma3.it

Abstract

Volumetric water content assessment in structures, substructures, soils, and subsurface in general is a crucial issue in a wide range of applications. The main disadvantages of subsurface moisture sensing techniques are usually related both to the lack of cost-effectiveness of the measurements, and to unsuitable support scales with respect to the extension of the surfaces to be covered and to the dimensions of the target to detect. In this regard, ground-penetrating radar (GPR) is an increasingly used non-destructive tool specifically suited for characterization and imaging. Several GPR techniques have been developed for different applications. In the case of moisture evaluation in concrete, the detection is important for the diagnosis of concrete structures at early stages of deterioration: water penetrating into the concrete pore networks contributes to the transfer of degrading and corrosive agents such as chloride. Concerning the particular case of identifying soil surface water content, two GPR approaches are commonly used, namely the ground-wave method and the reflection method; further, a different approach to shallow soil water content estimation is based on the analyses of the surface reflections of an off-ground system. This can be performed by using traditional off-ground methods or by using inverse modeling of an off-ground monostatic GPR system.

I. INTRODUCTION

Volumetric water content (VWC) dynamics in structures, substructures, soils, and subsurface in general is a key component in many fields of application such as agriculture, construction, geotechnical stability analyses, hydrological, and other environmental studies. Usually, water content measurements techniques at the field scale are invasive as well as time-consuming methods, e.g., gravimetric sampling or time-domain reflectometry (TDR) [1].

In that respect, ground-penetrating radar (GPR) is an increasingly used near-surface remote sensing tool specifically suited for characterization and imaging. Many efforts have been devoted to the

1

Determination, by Using GPR, of the Volumetric Water Content in Structures, Substructures, Foundations and Soil

Fabio Tosti (1), Evert Slob (2)

(1) Department of Engineering, Roma Tre University, Via Vito Volterra 62, 00146 Rome, Italy, fabio.tosti@uniroma3.it

(2) Delft University of Technology, Faculty of Civil Engineering and Geosciences, Section of Applied Geophysics and Petrophysics Department of Geoscience & Engineering, Stevinweg 1, Delft 2628 CN, The Netherlands, e.c.slob@tudelft.nl

Abstract Volumetric water content evaluation in structures, substructures, soils, and subsurface in general is a crucial issue in a wide range of applications. The main weaknesses of subsurface moisture sensing techniques are usually related both to the lack of cost-effectiveness of measurements, and to unsuitable support scales with respect to the extension of the surface to be investigated. In this regard, ground-penetrating radar (GPR) is an increasingly used non-destructive tool specifically suited for characterization and imaging. Several GPR techniques have been developed for different application purposes. Moisture evaluation in concrete is important for diagnosing structures at early stages of deterioration, as water contributes to the transfer of degrading and corrosive agents e.g., chloride. Traditionally, research efforts have been focused on the processing of GPR signal in time domain, although more recent studies are being increasingly addressed towards frequency domain analysis, providing additional information on moisture content in concrete. Concerning the evaluation of soil surface water content, different models ranging from empirical to theoretical are used for converting permittivity values into moisture. In that respect, two main GPR approaches are commonly employed for permittivity evaluation in time-domain measurements, namely the ground-wave method and the reflection method. Furthermore, the use of borehole transmission measurements, traditional off-ground methods, and of an inverse modeling approach allowing for a full waveform inversion of radar signals have been developed in the past decade. More recently, a self-consistent approach based on the Rayleigh scattering theory has allowed the direct evaluation of moisture content from frequency spectra analysis.

B. ISSUE B

Risk of overlapping amongst topics of the other Working Projects

ACTION NEEDED

Discussions among WG Chairs and other WP Leaders to define independent and complementary topics

ACHIEVED RESULTS

Discussions among WG Chairs and other WP Leaders to define independent and complementary topics:

- *WG Meeting of Rome - 1st COST Action General Meeting TU1208, Rome, Italy, 22-24 July 2013*
- *Discussions and exchange of views via e-mail among WG2 Chair and Co-Chair and WP2 Leaders*
- *Debate and suggestions by WP 2.5 Participants*

List of Topics: WP 2.5 Questionnaire

- *List of* ***typical targets*** *(e.g., structures, substructures, foundations, soils) to which research efforts on VWC determination are mainly devoted*
- *List of* ***main constituent materials*** *of the above targets, within VWC determination purposes (e.g., concrete, reinforced concrete, HMA layers, rail ballast, organic soils, clayey soils)*
- ***Scale of investigation*** *s related to GPR-based VWC measurement (s ≤ 0.01 m²; 0.01 m² < s < 100 m²; s ≥ 100 m²)*
- ***Preparation protocols*** *of test specimens/field site prior to the implementation of the GPR measures (e.g., packaging protocols of samples in laboratory environment; sweeping of the surface vegetation before large-scale inspections in field tests; etc.)*
- *List of* ***main protocol procedures for controlling boundary conditions during testing*** *(monitoring conditions of pressure, humidity and temperature environment; real-time monitoring of VWC using alternative techniques for direct/indirect assessment e.g., TDR, capacitance probe, core drilling; bulk density monitoring; etc.)*

Questionnaire for Project P2.5 (COST Action TU1208)

"Determination, by using GPR, of the volumetric water content in structures, sub-structures, foundations and soil"

1. List of typical targets (e.g., structures, substructures, foundations, soils) to which your research efforts on VWC determination are mainly devoted
   - ....
   - ....
   - ....
2. List of the main constituent materials of the above targets, within VWC determination purposes (e.g., concrete, reinforced concrete, HMA layers, rail ballast, organic soils, clayey soils)
   - ....
   - ....
   - ....
3. Scale of investigation s related to your GPR-based VWC measurements ($s \leq 0.01$ m^3; 0.01 m$^3 < s < 100$ m^3; $s \geq 100$ m^3)
   - ....
   - ....
   - ....
4. Preparation protocols of test specimens/field site prior to the implementation of the GPR measures (e.g., packaging protocols of samples in laboratory environment; sweeping of the surface vegetation before large-scale inspections in field tests; etc.)
   - ....
   - ....
   - ....
5. List of the main protocol procedures for controlling boundary conditions during testing (monitoring the conditions of pressure, humidity and temperature environment; real-time monitoring of VWC using alternative techniques for direct/indirect assessment e.g., TDR, capacitance probe, core drilling; bulk density monitoring; etc.)
   - ....
   - ....
   - ....
6. List of radar system and survey configurations used for VWC assessment (e.g., ground-coupled and/or air-coupled in zero-offset configuration; multi-offset configuration; SFCW radar systems; etc.)
   - ....
   - ....
   - ....
7. List of GPR signal processing techniques for VWC determination (pre-processing and processing after data collection – reflection methods, ground-wave measurements, borehole transmission measurements, surface reflection methods; frequency-based analysis of the radar signal; etc.)
   - ....
   - ....
   - ....
8. List of procedures carried out for ensuring the intrinsic stability of GPR measurements (e.g. repetition of measures, variability statistics)

- *List of **radar system and survey configurations** used for VWC assessment (e.g., ground-coupled and/or air-coupled in zero-offset configuration; multi-offset configuration; SFCW radar systems; etc.)*

- *List of **GPR signal processing techniques** for VWC determination (pre-processing and processing after data collection – reflection methods, ground-wave measurements, borehole transmission measurements, surface reflection methods; frequency-based analysis of the radar signal; etc.)*

- *List of procedures for ensuring **stability of GPR measurements** (e.g. repetition of measures, variability statistics)*

Identification of test scenarios for advanced comparison of inspection procedures WP 2.5 test site template

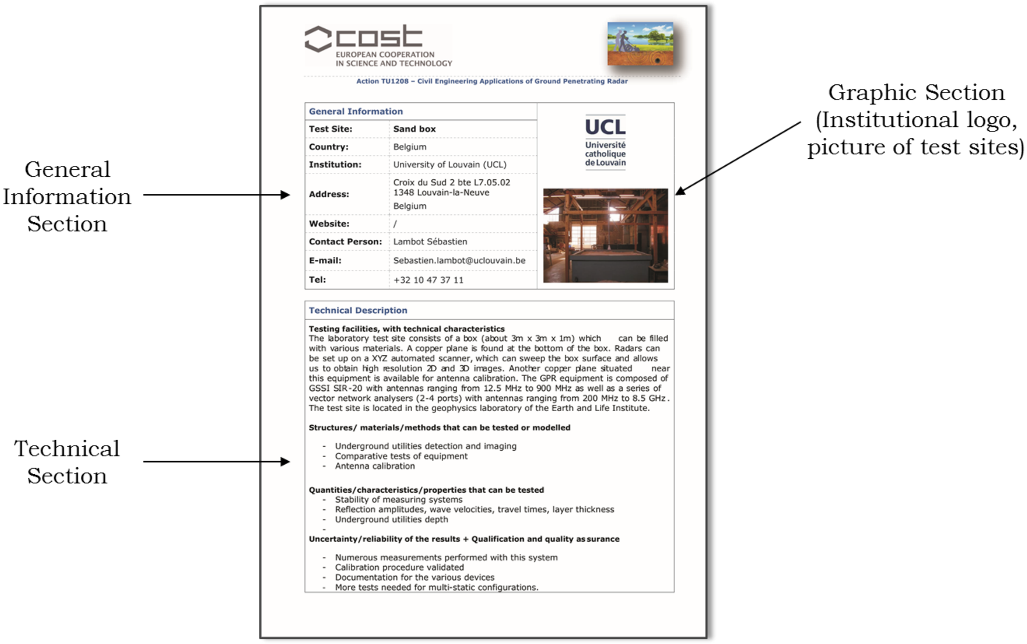

General Information	
Test Site:	**Sand box**
Country:	Belgium
Institution:	University of Louvain (UCL)
Address:	Croix du Sud 2 bte L7.05.02 1348 Louvain-la-Neuve Belgium
Website:	/
Contact Person:	Lambot Sébastien
E-mail:	Sebastien.lambot@uclouvain.be
Tel:	+32 10 47 37 11

Technical Description

Testing facilities, with technical characteristics
The laboratory test site consists of a box (about 3m x 3m x 1m) which can be filled with various materials. A copper plane is found at the bottom of the box. Radars can be set up on a XYZ automated scanner, which can sweep the box surface and allows us to obtain high resolution 2D and 3D images. Another copper plane situated near this equipment is available for antenna calibration. The GPR equipment is composed of GSSI SIR-20 with antennas ranging from 12.5 MHz to 900 MHz as well as a series of vector network analysers (2-4 ports) with antennas ranging from 200 MHz to 8.5 GHz. The test site is located in the geophysics laboratory of the Earth and Life Institute.

Structures/ materials/methods that can be tested or modelled

- Underground utilities detection and imaging
- Comparative tests of equipment
- Antenna calibration

Quantities/characteristics/properties that can be tested
- Stability of measuring systems
- Reflection amplitudes, wave velocities, travel times, layer thickness
- Underground utilities depth
-

Uncertainty/reliability of the results + Qualification and quality assurance

- Numerous measurements performed with this system
- Calibration procedure validated
- Documentation for the various devices
- More tests needed for multi-static configurations.

C. ISSUE C

"Heterogeneous" scenario about Project Participants

ACTION NEEDED

Outline of such wide scenario by gathering comprehensive synthetic information from Project Participants

ACHIEVED RESULTS

<u>Outline of the "heterogeneous" scenario about Project Participants by gathering comprehensive synthetic information from Project Participants</u>

- ***Database***

Questionnaire	Test Site availability
Belgian Road Research Centre	/
IFSTTAR	O
Geological Survey of Finland	O
Hochschule Rapperswil	/
National Technical University of Athens	/
Ruhr-Universität Bochum	O
Transport Research Centre	O
Université Catholique de Louvain	O
University of Ghent	O
University of Minho	/
University of Roma Tre	O
University Suleyman Demirel	O
University of Toulouse	/
13 / 25	**8**

- *Database including information about 13 Institutions out of 25 available*

- *Within the surveyed Institutions, 8 of them own a test site for VWC determination by GPR*

- ***Main outcomes***

Typical Targets

- *Structures* *5%*
- *Roads* *53%*
- *Soils* *21%*
- *Concrete* *11%*
- *Wood* *5%*
- *Snow* *5%*

Constituent Materials

- *Reinforced and pre-stressed structures* *11%*
- *Asphalt* *39%*
- *Compacted loose material* *22%*
- *Organic soils* *22%*
- *Wood* *6%*

Scale of Investigation

- *$s \leq 0.01$ m²* *13%*
- *0.01 m² $< s < 100$ m²* *40%*
- *$s \geq 100$ m²* *47%*

D. ISSUE D

Avoid that research gets blocked

ACTION NEEDED

Ensure continuous updating of the latest results achieved by GPR Participants in VWC determination by GPR

ACHIEVED RESULTS

<u>Updating of the latest results achieved by GPR Participants in VWC determination by GPR</u>

Submitted works to Journals or Conferences

Hochschule Rapperswil

- ❖ Hugenschmidt J., Wenk F. and Brühwiler E. GPR chloride inspection of a RC bridge deck slab followed by an examination of the results, GPR 2014, Brussels, BE.

Université Catholique de Louvain - Belgium

- ❖ De Coster A., Tran A.P. and Lambot S. Information content in frequency-dependent, multi-offset GPR data for layered media reconstruction using full-wave inversion, EGU Conference, 2014, Vienna, AT.
- ❖ Mourmeaux N., Meunier F., Tran A.P. and Lambot S. High-resolution monitoring of root water uptake dynamics in laboratory conditions using full-wave inversion of near-field radar data, EGU Conference, 2014, Vienna, AT.
- ❖ De Coster A., Tran A.P. and Lambot S. Impact of the antenna offset and the number of frequencies on layered media reconstruction using full-wave inversion in near-field conditions, GPR 2014, Brussels, BE.
- ❖ Mourmeaux N., Tran A.P. and Lambot S. Soil permittivity and conductivity characterization by full-wave inversion of near-field GPR data, GPR 2014, Brussels, BE.

University of Ghent – Belgium

- ❖ De Pue J., Van Meirvenne M. and Cornelis W. Simultaneous measurement of surface and subsoil water content with air-coupled GPR, GPR 2014, Brussels, BE.

University of Minho

- ❖ Fernandes J.M. and Pais J. Assessment of moisture in road pavements, GPR 2014, Brussels, BE.

V. CONCLUSIONS

There is a wide interest in volumetric water content determination by using GPR. VWC assessment in pavement has proved to be the most widespread application. Within pavement applications, major efforts are devoted to the investigation of water content in asphalt layers. Intermediate scale and large-scale VWC inspections are the most common GPR inspection scales. From the available database, it is expected to have at least one test site for half of the institution involved in project 2.5 (13 out of 25).

ACKNOWLEDGEMENT - The author acknowledges the COST Action TU1208 "Civil Engineering Applications of GPR," supporting this work.

WORKING GROUP 3

Electromagnetic methods for near-field scattering problems by buried structures; data-processing techniques

KEYNOTE TALK 2
"FDTD MODELLING OF THE GPR SIGNAL BASED ON DATA OBTAINED FROM OTHER NDT METHODS: AN APPROACH FOR MORE EXHAUSTIVE INTERPRETATION OF FIELD DATA"

Mercedes Solla (ES), Xavier Núñez-Nieto (ES)
merchisolla@uvigo.es

Abstract

GPR is a non-destructive (NDT) geophysical technology that shows many applications in different fields, such as civil engineering, geology, forensics, etc., where its implementation is becoming very important. In some cases, the diffraction events produced by scattering make difficult the interpretation of interesting reflectors. In this work, the FDTD modelling was used to analyse the complex pattern of reflection obtained in order to assist and to improve the interpretation of field GPR data for different applications. More realistic models were built based on the data provided by other NDT techniques, and the results have demonstrated its capabilities to achieve more understanding of the radar wave propagation phenomena and exhaustive interpretation.

1. INTRODUCTION

The analysis and interpretation of GPR data can be complicated since many factors can adversely affect radar waves, including ringing noise, diffraction events and reflection multiples. Numerical modelling has become an interpretational tool that can be used to compare field GPR data to synthetic data to understand the radar wave propagation phenomena and to facilitate GPR data interpretation [1]. Many numerical modelling methods are available for simulating the propagation of the GPR waves in different media. However, when more sophisticated interpretations are required, the finite-difference time-domain (FDTD) technique has evolved into one of the most popular advanced modelling tools [2]. This modelling method allows for the extraction of subtle information from the field real data, such as diffraction patterns and the presence of reflection multiples [3].

This work presents different study cases in which the capabilities of the technique are demonstrated. Moreover, the approach here presented includes the use of data provided by other NDT methods as inputs to create large scale and more realistic models.

2. Approach for FDTD Modelling

The method uses cubic cells (Yee cell) to create the computational domain. Therefore, when structures of fine geometry need to be modelled, the spatial resolution has to be very small in order to make a reasonable staircase approximation of the curved interfaces [3]. This approach results in excessive computer memory requirements and subsequent increase in execution time. The latest GprMax version uses a mixed model of parallelisation based on a hybrid MPI and OpenMP programming, which allowed to assign the computation of different traces to different nodes of a cluster.

A. Synthetic Models

In the study cases here presented, the input to elaborate on the FDTD modelling, was the data provided by complementary NDT methods, such as the precise geometry (2D orthoimages) provided by laser scanning or photogrammetric techniques. The purpose was to design realistic, large-scale, synthetic GPR models to assist in the interpretation of the processed field data. However, simulating large-scale and realistic models requires high-performance computing to obtain results in a reasonable time. Thus, the synthetic models were created using a parallelized version of GprMax, which is an electromagnetic wave simulator for GPR using the FDTD method [3]. The FDTD algorithm was previously developed using the MATLAB programming language. The synthetic models are built from the contour of the elements defined by the orthoimages. For that purpose, the images had to be reprocessed before they were introduced into the algorithm for FDTD modelling. This operation consisted of classifying the materials presented in the image according to the different hypotheses of simulation. As a result, an image was obtained that was formed by different objects (defined by pure colours). This approach encompasses the geometry of the model in fine detail.

B. Simulations

The synthetic models were built with a small spatial step (grid cell size in the x- and y-directions), and the excitation was a Gaussian pulse of the same centre frequencies used in field acquisition to get the best approximation compared with the field data. The trace distance interval and the total time were also defined in accordance with the real data. After simulation, the synthetic data were exported and provided by

GprMax to ReflexW, and then filtered using a similar processing sequence to that used for the field data.

For simulations, the electromagnetic properties to characterize the propagation media were determined from the acquired field GPR data or assumed from the typical values published in the literature.

3. Study Cases: Results & Discussion

This section presents different study cases in the application of the GPR signal simulation, based on the use additional NDT techniques (such as Photogrammetric or Laser scanning geometric techniques and Thermography) for different field applications: heterogeneous masonry structures, volcanic environments, as well as forensic and crime scene investigations. The synthetic GPR data generated is compared with the field GPR data acquired in order to improve the interpretation.

A. Simulations for Masonry Bridge Inspections

Masonry bridges are built using heterogeneous filling that often complicates the interpretation and analysis of field GPR data. FDTD modelling of the GPR signal is therefore typically used as additional interpretational tool. Some studies have included the use of photogrammetry or laser scanning methods as a tool in the geometric characterization of the structures for the elaboration of the simulated models.

As shown in Fig. 1, the precise external geometry of the bridge (orthoimage) provided by laser scanning (Fig. 1A) was used to create the synthetic model (Fig. 1B). What is more, a heterogeneous medium was simulated. This approach replicates the structure in fine detail and allows reproducing the exact geometry. Apart from the reflections generated from the arch-air interfaces (Fig. 1C:R1), subtle information was interpreted such as the presence of reflection multiples produced from the arch and because of the proximity between arches (Fig. 1C:R2 and R3, respectively). These reflection multiples were also observed in the field GPR data (Fig. 1D:R2). All these complex reflections, if unrecognized, can hinder the detection of other interesting reflectors. In this frame, it was possible to identify, from the real data, the corner reflections (Fig. 1D:R4) from the perpendicular interfaces between the top of the vault and the water level (Fig. 1D:R3).

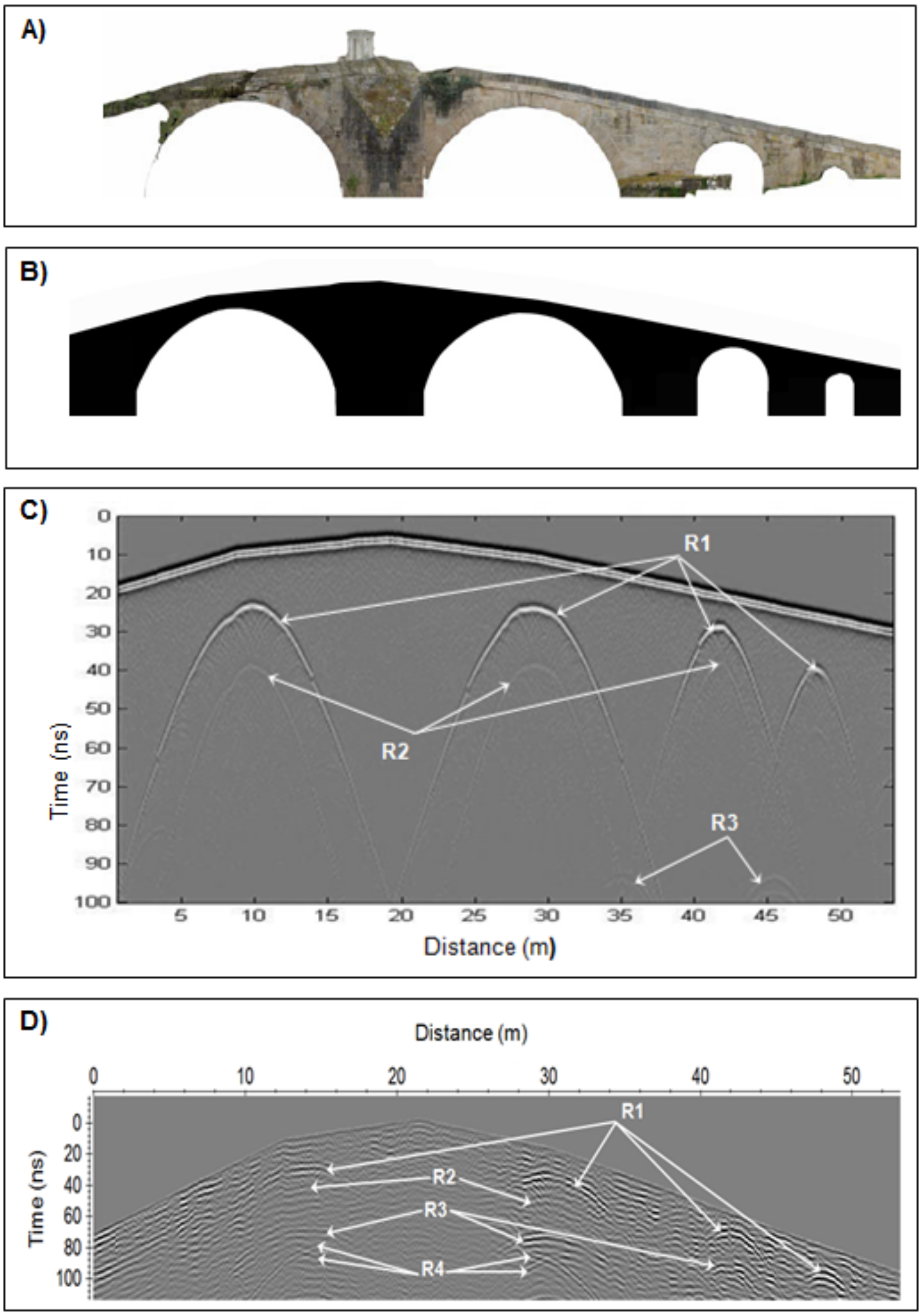
A)
B)
C)
Time (ns)
0
10
20
30
40
50
60
70
80
90
100
R1
R2
R3
5
10
15
20
25
30
35
40
45
50
Distance (m)
D)
Distance (m)
0
10
20
30
40
50
Time (ns)
0
20
40
60
80
100
R1
R2
R3
R4

FIG. 1 – (Previous Page) – The Carracedo Bridge (Galicia, Spain): A) 2D orthoimage of the bridge provided by laser scanning data, B) synthetic model, C) synthetic GPR data showing the reflections produced by the arch-air interfaces (R1), reflection multiples from the arch (R2) as well as the ones due to the proximity between arches (R3), and D) field GPR data showing additional reflections such as the water level (R3) and the corner reflections (R4). (*Data available from [4]).*

Other interesting application of simulation in masonry bridges is the most appropriate recognition of the complex pattern of reflections produced by the arch-stone interface caused by the irregular shape of the ring stones. Fig. 2 presents a synthetic model (Fig. 2A) constructed from the contour of the arch ring defined by the orthoimages generated from laser scanning data. Additionally, arch ring separation was considered in the model in a portion of the arch at the right hand. This simulation allows for the detection of inner structural damage such as delamination and ring stone separation. In Fig. 2B, it is possible to distinguish the hyperbolic reflection generated from the cavity simulated, which could be directly compared to the field GPR data.

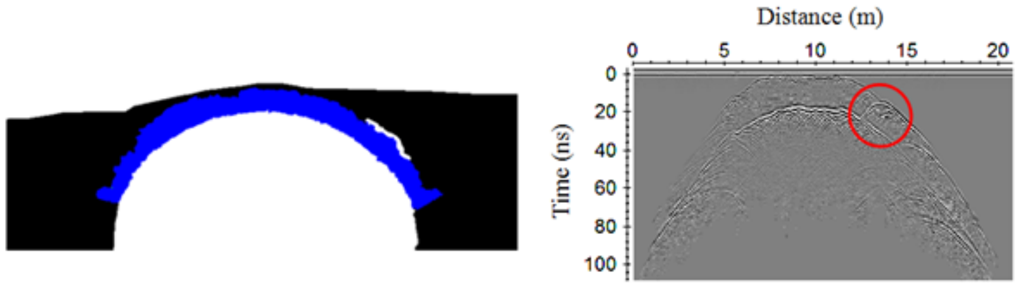

FIG. 2 – The Monforte Bridge (Galicia, Spain): FDTD modelling to analyze how arch-ring separation is identified by GPR. Left: synthetic model built from an orthoimage provided by laser scanning, and right: synthetic data obtained showing the reflection (circle area) produced by the cavity simulated. (*Data available from [5]).*

The final study case in masonry is to evaluate the potential of the GPR to detect and analyse moisture content. A masonry bridge was inspected by combining the techniques of GPR and infrared thermography. To assist the GPR field data interpretation, FDTD was used. The model was

created from the orthothermograms (images obtained through the orthogonal projection of each wall to a parallel plane, with no distortions or perspective effect and with geometric information that enables them to function as two-dimensional (2D) maps with thermographic texture) provided by both photogrammetry and thermography (Fig. 3A). This way, after an image pre-processing using MATLAB programming language and considering a heterogeneous medium, a more accurate and complete vision of the structure was obtained (Fig. 3B), and the detection and analysis of moisture areas provide noteworthy information for planning subsequent conservation actions. Observing the field data, although the thermography (Fig. 3A) detected lower temperature over the first arch (from 2 to 6 m) and the synthetic data (Fig. 3D) showed attenuation at this portion of the bridge, the field GPR data did not reveal attenuation of the signal at that position (Fig. 3C). The different pattern of reflections that occurs over the first arch could be therefore an indication of the existence of building materials different to the original ones. Historical references were found, which inform a reconstruction of this vault because of a great flood of water in 1984.

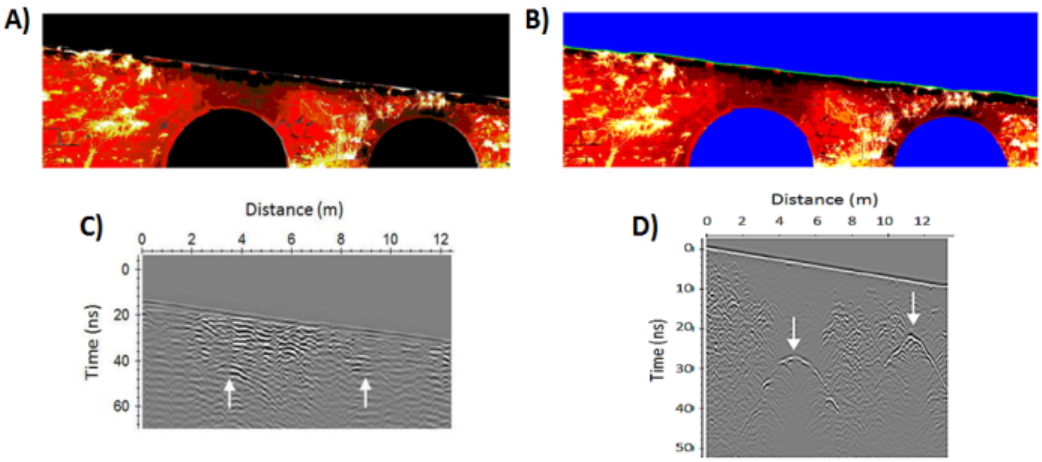

FIG. 3 – The Lubians Bridge (Galicia, Spain): FDTD modelling to analyze moisture content. A) Orthothermogram (the colour goes from dark red (6°C) to white (12°C), B) Synthetic model created, C) 500 MHz field GPR data, and D) Synthetic data obtained. (*Data available from [6] and [7]).*

B. Simulations for Volcanic Environments

To prevent collapse hazards in volcanic areas, exhaustive interpretation of the GPR data, by using FDTD modelling, have demonstrated its capabilities to detect lava tubes in the Timanfaya National Park (Spain).

The input geometry for synthetic models corresponded to the results obtained from microgravity. (Fig. 4A) shows the gravity model created using the field GPR data (Fig. 4B). Observing the synthetic GPR data generated (Fig. 4C), several strong reflections are visible corresponding to the roof, bottom and edges of the different lava tubes. Good correlation, in location and geometry, was observed for lava tubes A, B and C.

Nevertheless, the tube D did not show good correspondence neither in location nor geometry.

A possible explanation could be that the observed reflections are due to heterogeneities in the internal structure of the lava flow and not really to the small cavity deduced from the gravity model. Moreover, the identification of a vertical dyke in the gravity data occurs at the same position of the GPR reflections detected.

C. Simulations for Forensic and Crime Scene Investigations

Reference [8] presents the use of FDTD modelling and GPR signal characterization in forensics. Experimental scenes that mimic the most frequent real forensic cases were built by considering several buried objects: bone remains, clothes, active and inactive mobile phones, drug caches, guns and bullet shells, etc. Additionally, the geometric characterization of the scenes was made using photogrammetric methods. The 3D models of the experimental grids were provided, and the 2D sections obtained from these models were used as inputs in creating the synthetic models. Both synthetic and field data were compared to assist in the interpretation. As example, Fig. 5 shows the experimental scene (2D orthoimage) (Fig. 5A) as well as the synthetic and field data produced (Fig. 5 B and C, respectively) for the case of the scene containing bone remains at 0.5 m depth. Although the field data showed more complex reflections produced by the heterogeneous backfill (Fig. 5C), the interpreted reflection patter produced by the bone remains is very similar to that modelled in the synthetic radargram (Fig. 5B).

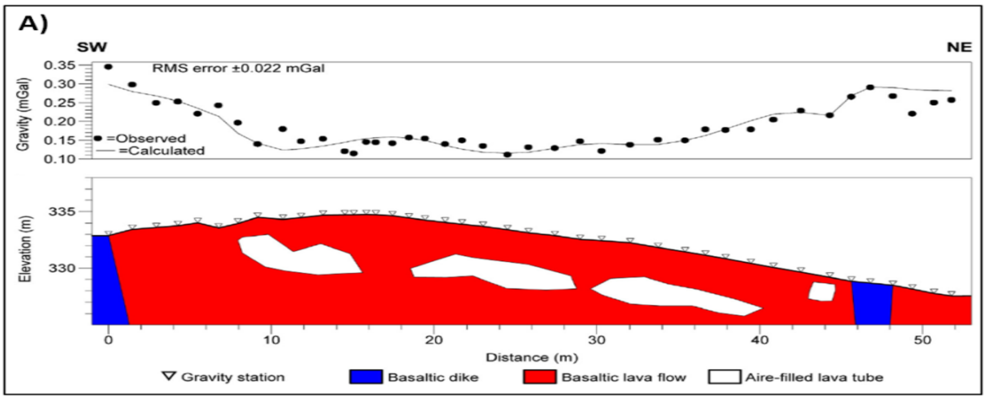
A)
SW
NE
RMS error ±0.022 mGal
Gravity (mGal)
=Observed
=Calculated
Elevation (m)
Distance (m)
Gravity station
Basaltic dike
Basaltic lava flow
Aire-filled lava tube

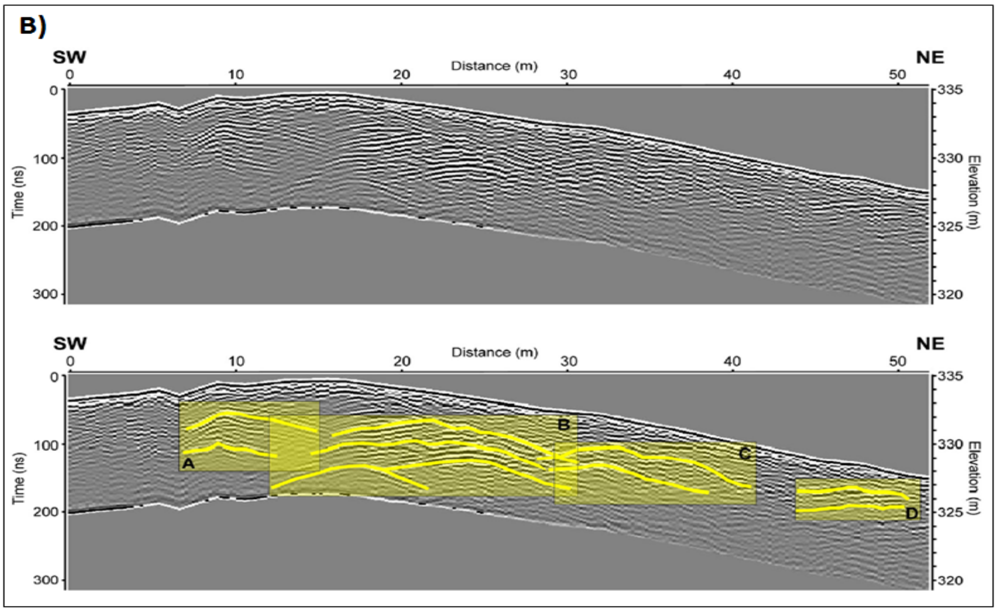
B)
SW
NE
Distance (m)
Time (ns)
Elevation (m)
A
B
C
D

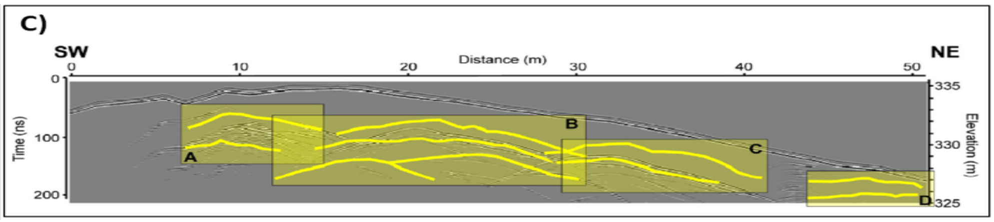
C)
SW
NE
Distance (m)
Time (ns)
Elevation (m)
A
B
C
D

FIG. 4 (previous page) – A) Microgravity data and 2.5D density model with 4 air-filled lava tubes with different size and shape, and two vertical basaltic dykes at the edges of the profile. B) Field GPR data and interpretation of 4 probable lava tube, C) Synthetic data using the gravity model as input.

4. CONCLUSIONS

Realistic FDTD models can provide subtle information that can help with field data interpretation. The data generated from other NDT allowed the simulation of more realistic modelling scenarios using a mixed model of parallelization. This approach encompasses the overall structures or geometries in fine detail in a reasonable amount of time. In complex scenarios, it can be difficult to obtain an accurate interpretation without a comparison of the field data with the models.

ACKNOWLEDGEMENT

The authors acknowledge the COST Action TU1208 "Civil Engineering Applications of Ground Penetrating Radar", supporting this work. The results presented in this work were possible thanks to the financial support of the Spanish Ministry of Science and Innovation (BIA2009-08012 and INCITE09 304 262 PR), The Spanish Ministry of the Environment and Rural and Marine Affairs (320/2011), the Spanish Centre for Technological and Industrial Development (IDI- 201001770), and the facilities made available by the HPC-EUROPA2 project with the support of the EU Commission – Capacities Area – Research Infrastructures.

REFERENCES

[1] S.G. Millard, M.R. Shaw, A. Giannopoulos, M.N. Soutsos, "Modeling of subsurface pulsed radar for nondestructive testing of structures," ASCE J Mater Civil Eng., vol. 10, pp. 188-196, 1998.

[2] H.M. Jol, "Ground penetrating radar: theory and applications," Amsterdam: Elsevier Science, 2009.

[3] A. Giannopoulos, "Modelling ground penetrating radar by GprMax," Constr Build Mater, vol. 19, pp. 755-762, 2005.

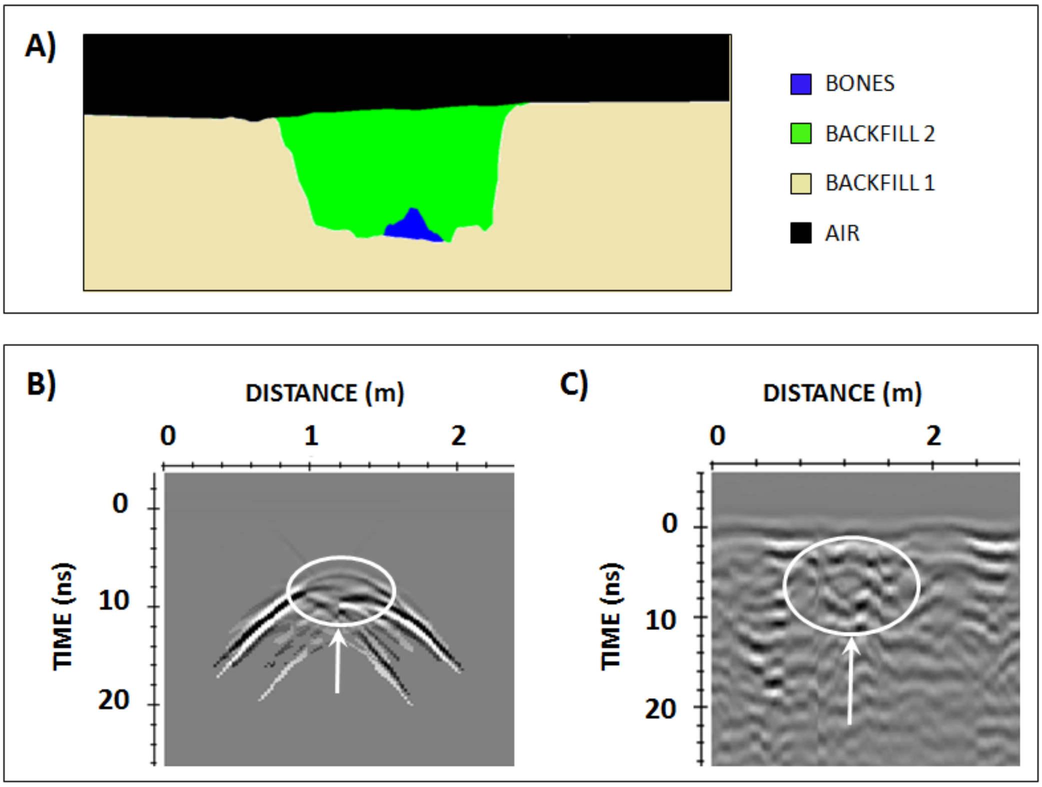

FIG. 5 – Experimental scene: bone remains at 0.5 m depth. A) Synthetic model built from the longitudinal section provided by photogrammetric methods, B) synthetic data generated from FDTD modelling, and C) 500 MHz field data collected. (*Data available from [8]*).

[4] M. Solla, H. Lorenzo, F.I. Rial, A. Novo, "Ground-penetrating radar for the structural evaluation of masonry bridges: Results and interpretational tools," Construction and Building Materials, vol. 29, pp. 458-465, 2012.

[5] M. Solla, B. Riveiro, H. Lorenzo, J. Armesto, "Ancient Stone bridge surveying by ground-penetrating radar and numerical modeling methods", Journal of Bridge Engineering, vol. 19, pp. 110-119, 2014.

[6] M. Solla, S. Lagüela, B. Riveiro, H. Lorenzo, "Non-destructive testing for the analysis of moisture in the masonry arch bridge of Lubians (Spain)," Struct. Control Health Monit., vol. 20, pp. 1366-1376, 2013.

[7] X. Núñez-Nieto, M. Solla, R. Asorey-Cacheda, B. Riveiro, "Documentation of moisture content in masonry by means of GPR," 8ª Asamblea Hispano-Portuguesa de Geodesia y Geofísica, Évora (Portugal), 29-31 January, pp. 233-238, 2014.

[8] M. Solla, B. Riveiro, M.X. Álvarez, P. Arias, "Experimental forensic scenes for the characterization of ground-penetrating radar wave response," Forensic Science International, vol. 220, 50-58, 2012.

KEYNOTE TALK 3
"OVERVIEW OF CROSSHOLE GPR FULL-WAVEFORM INVERSION TO CHARACTERIZE AQUIFERS"

Jan van der Kruk (DE), A. Klotzsche (DE), J. van der Kruk(DE),
N. Güting (DE), X. Yang (DE), and H. Vereecken (DE)
j.van.der.kruk@fz-juelich.de

Mapping shallow subsurface electrical properties:

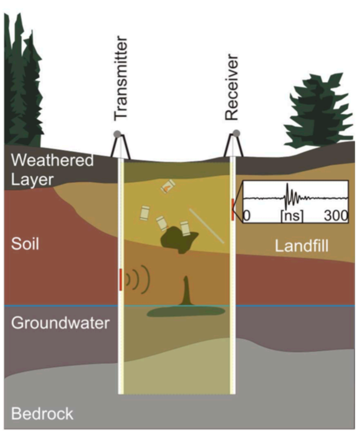

GPR is able to minimal-invasively investigate distributions of

- dielectric permittivity ε:
  ⇨ soil water content, porosity
- electrical conductivity σ
  ⇨ clay/silt content, salinity (chloride)

⇨ improved characterization compared to other methods

Ray-based methods

Input data:

- First arrival times
- First cycle amplitudes

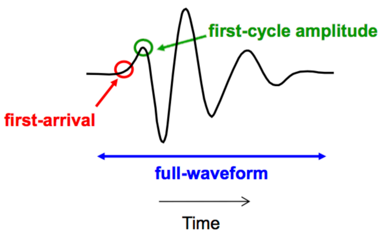

⇨ inexpensive, coarse structures

Waveform methods*

Input data:

- Significant parts of wavefields
- Inversion based on Maxwell's Eq.

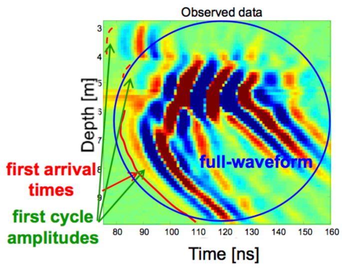

⇨ detailed sub-wavelength structures, expensive

* Ernst et al. (2007a, b); Meles et al. (2010); Klotzsche et al. (2010)

Important steps of the Full-waveform inversion

- Preprocessing:
  - Ray-based inversion for starting model
  - 3D to 2D conversion
- Source wavelet estimation
- Full-waveform inversion (Super Computer)
  - Calculation of the gradients (update direction) & step lengths
  - Update of the permittivity and conductive models
  - Steps repeated until a good fit between obs. & mod. data is obtained (RMS changes less than 1%).
  - Remaining gradient is a measure for quality of mod. data

3D Case study: Thur River

- Test side established by RECORD project & investigated by e. g. Doetsch et al. (2010), Klotzsche et al. (2010), Diem et al. (2010) & Cosia et al. (2011), Klotzsche et al. (2012).

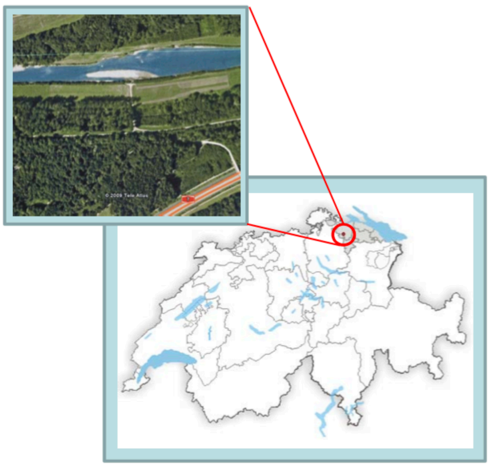

Klotzsche et al. GJI 2013

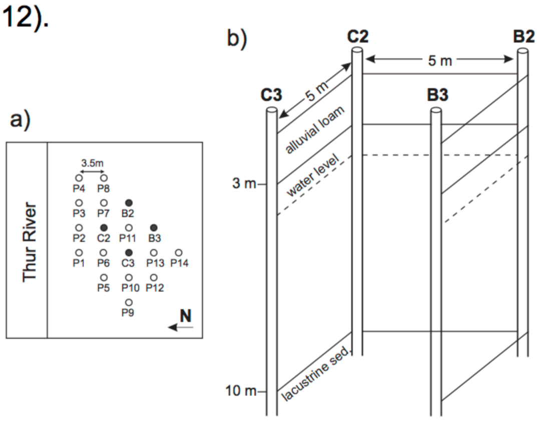

Antenna:
- 250 MHz
- 100 MHz (B3-C2)

Ray-based starting model

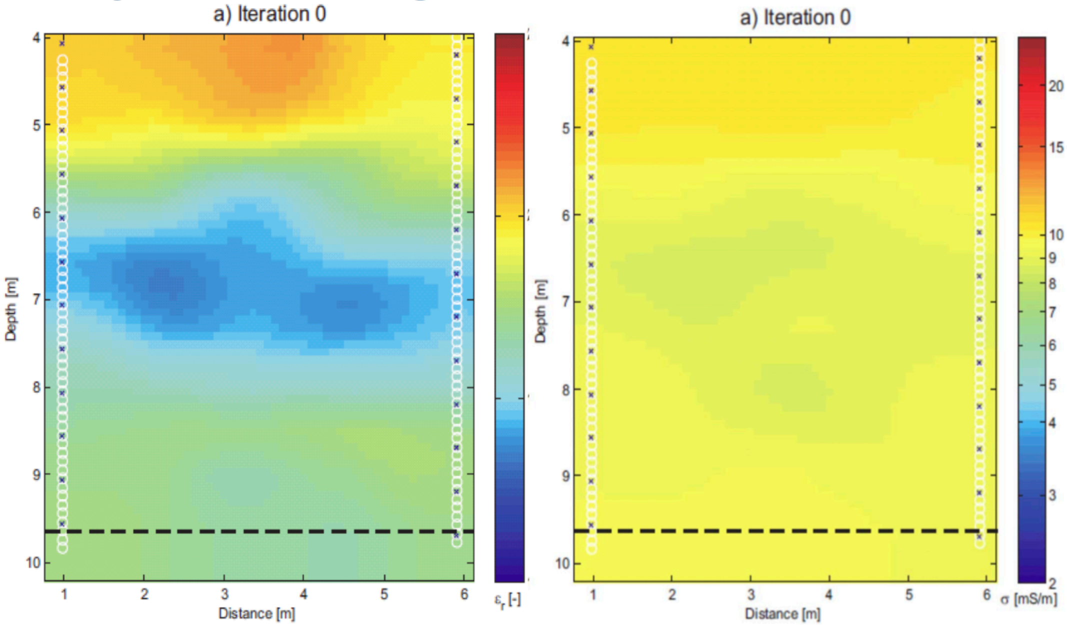

Full-waveform inversion results

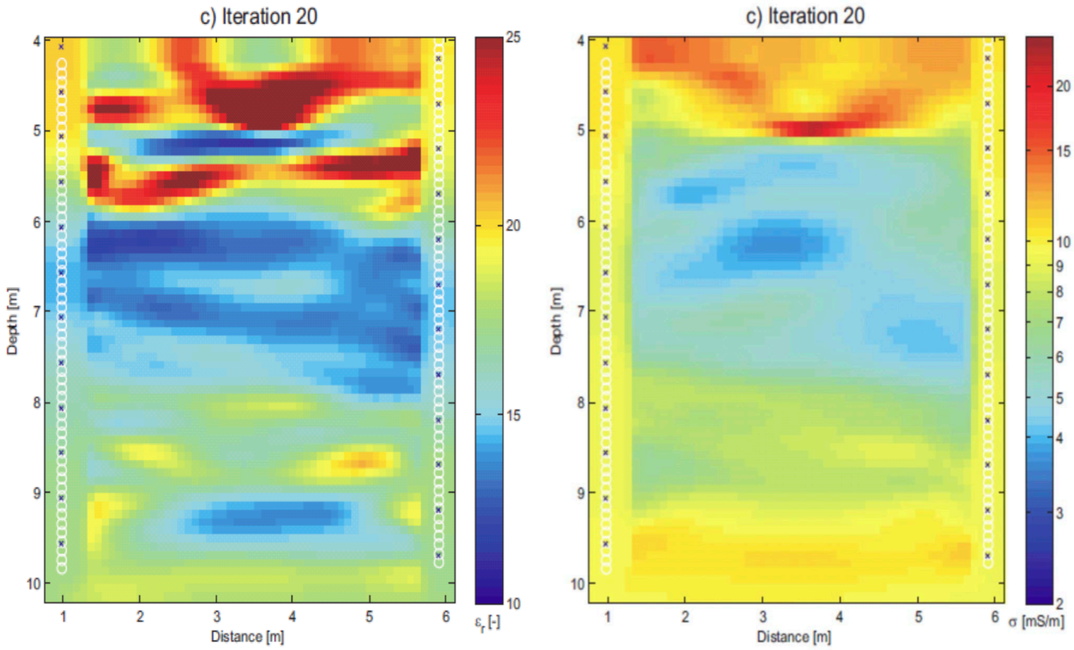

Remaining Gradients

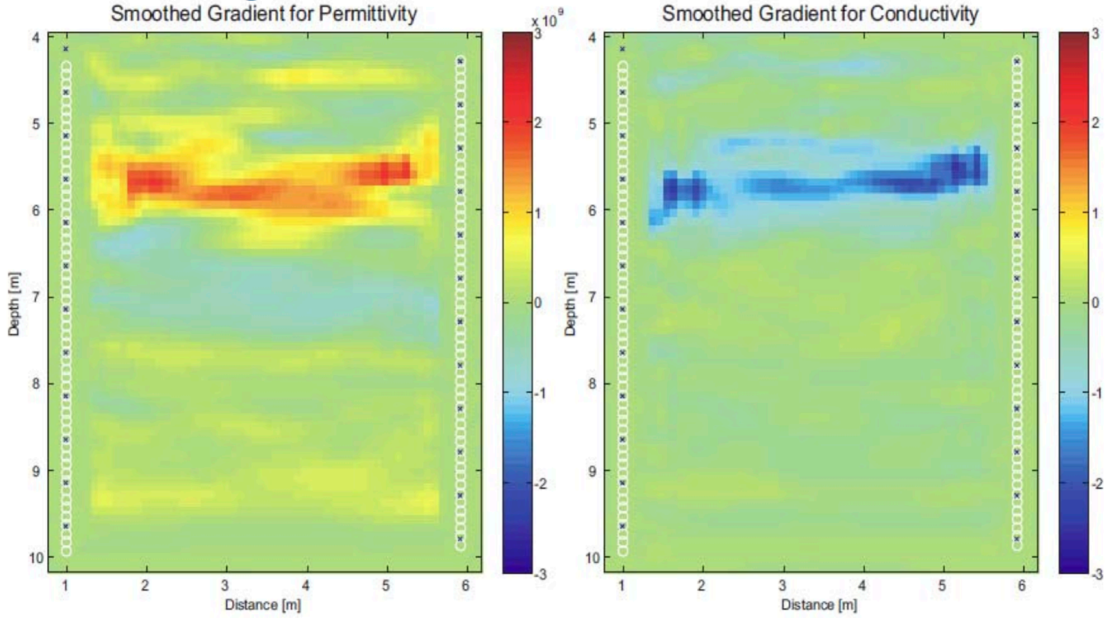

Updated starting model

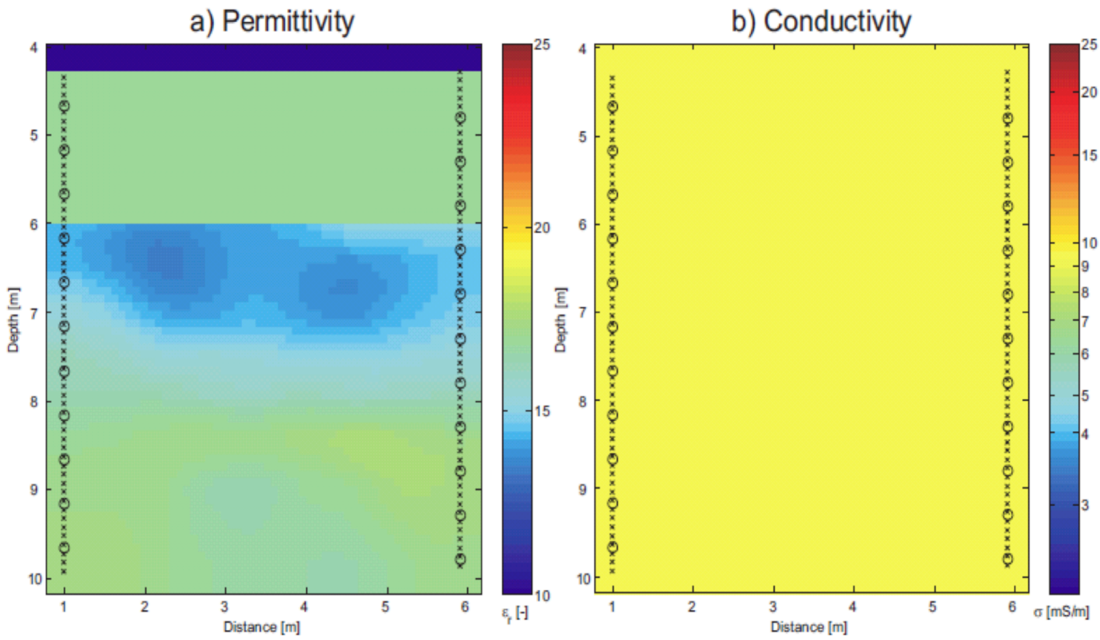

Full-waveform inversion results

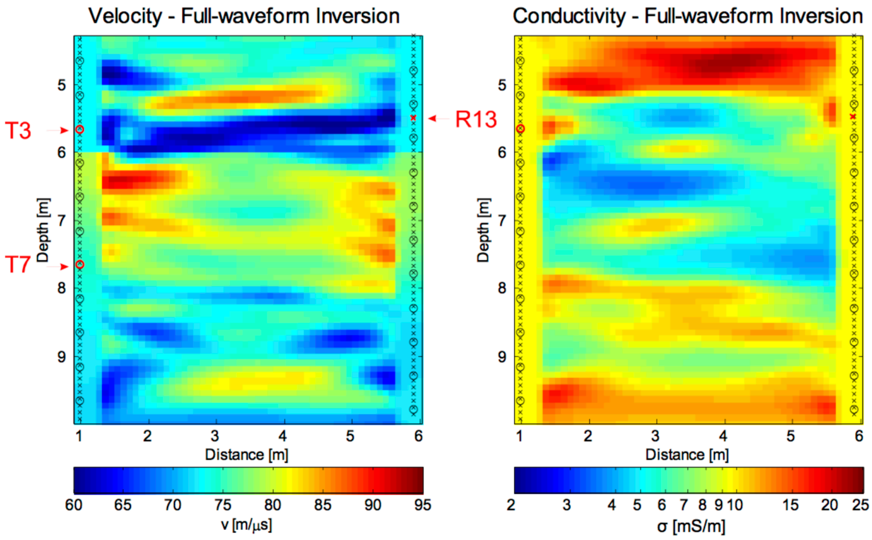

Comparison of measured & modeled data B3-C3

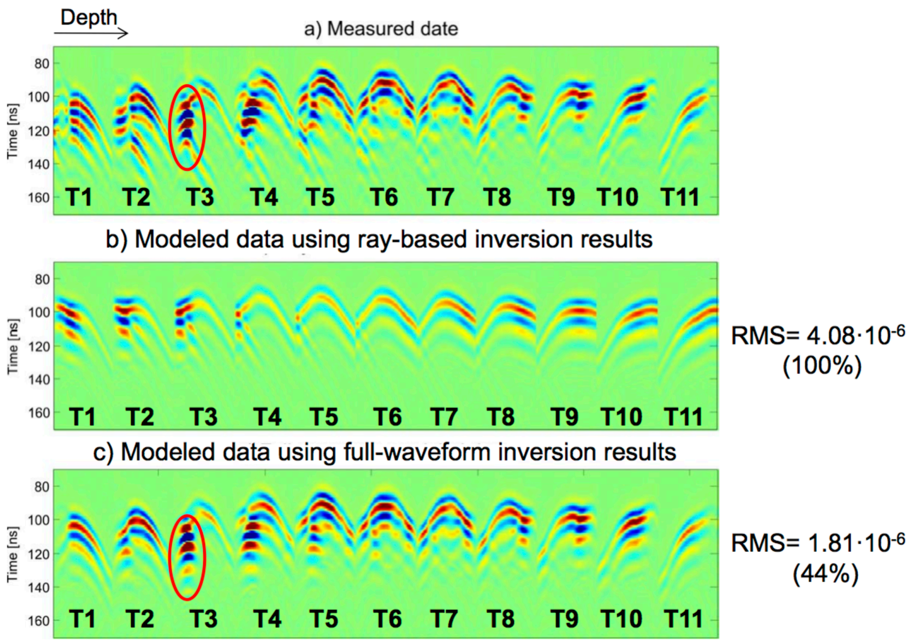

Propagation of the E_z-field – Transmitter 3

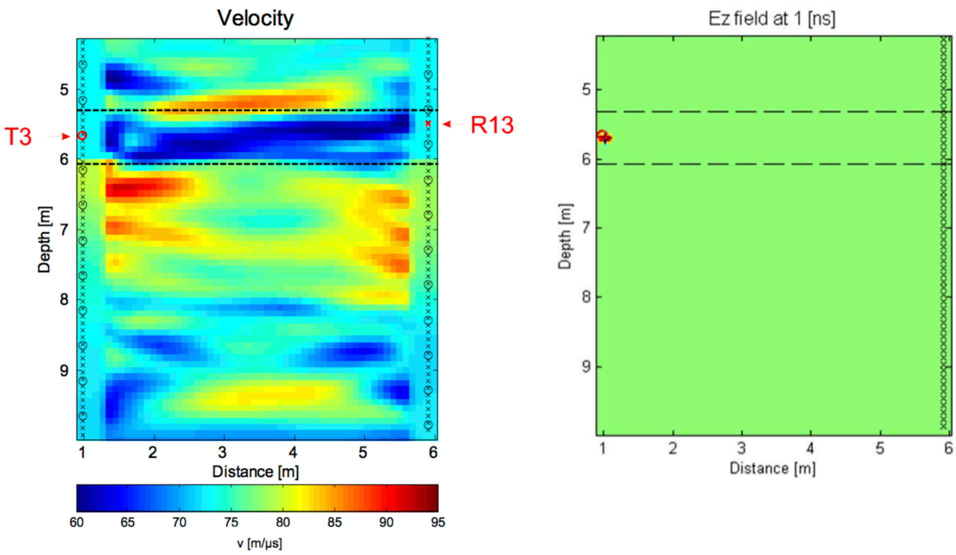

Propagation of the E_z-field – Transmitter 7

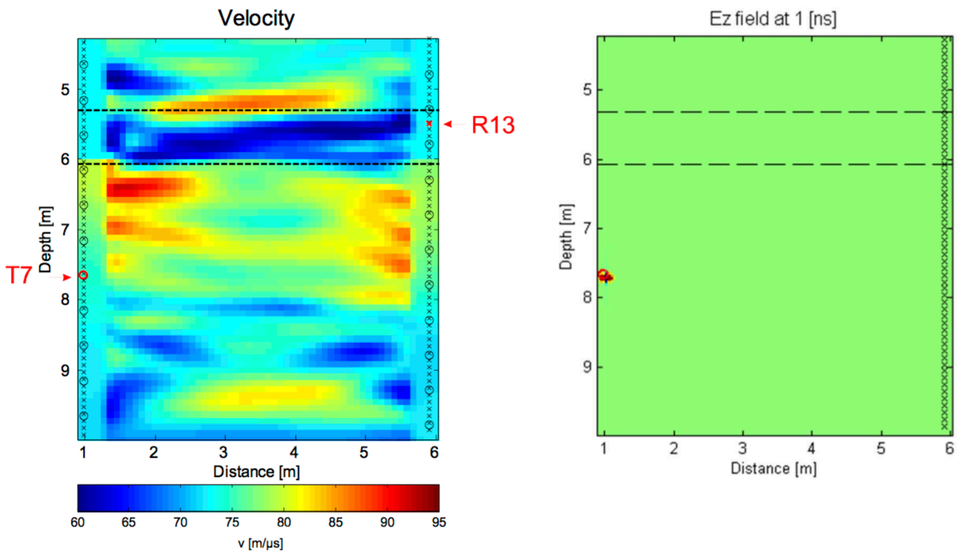

Snapshots at t = 64 ns

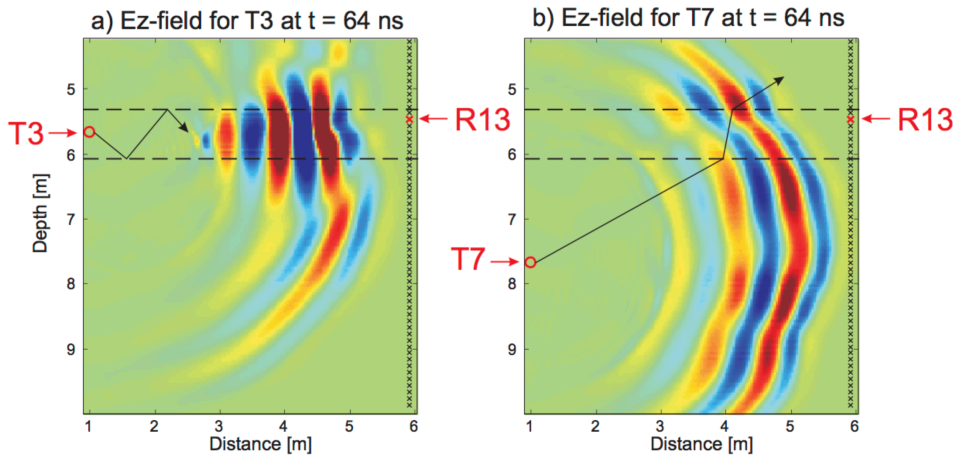

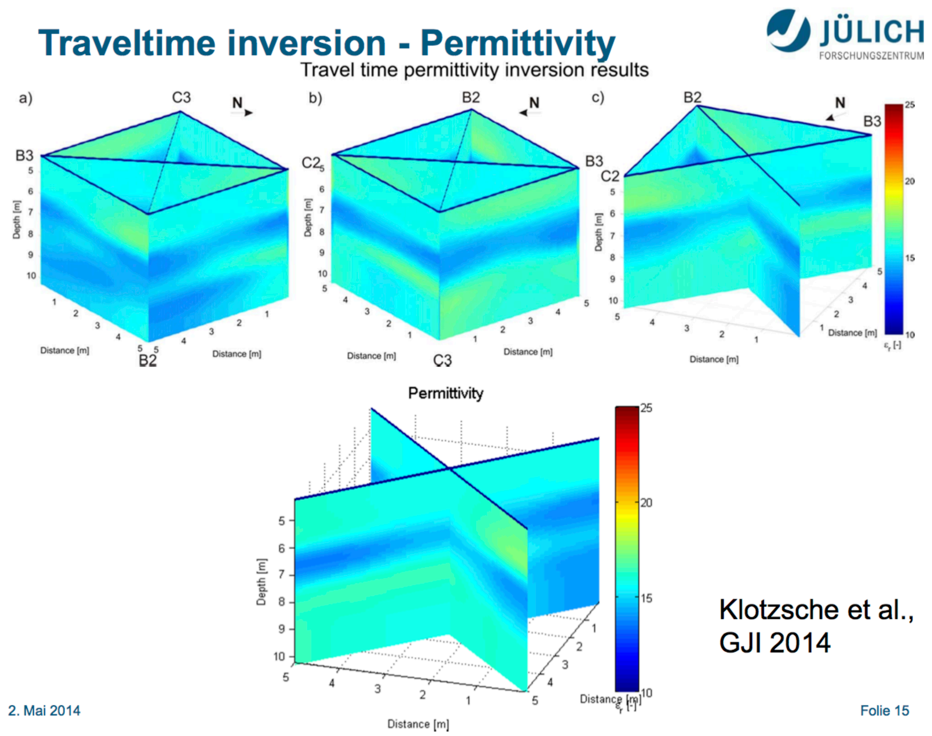

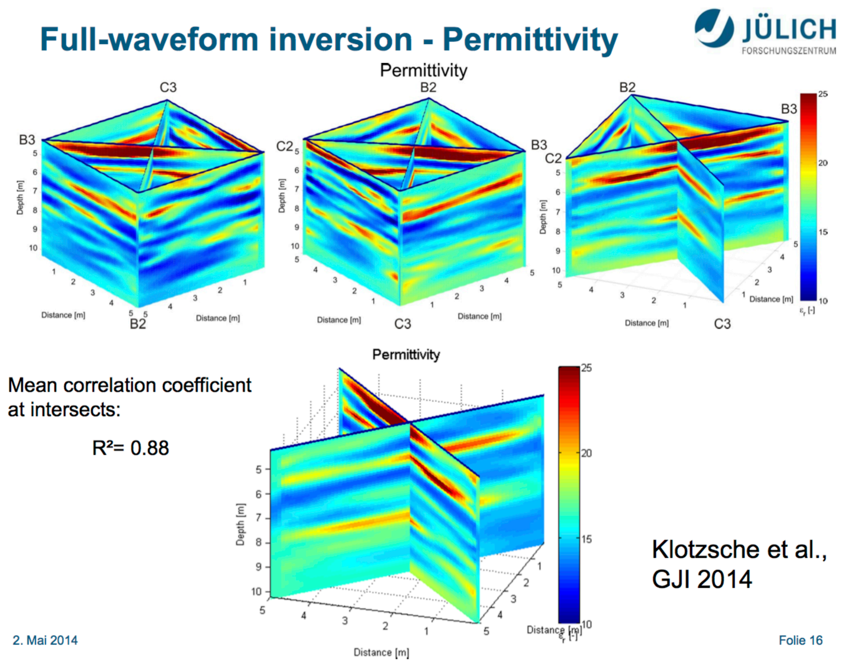
Full-waveform inversion - Permittivity
JÜLICH
FORSCHUNGSZENTRUM
Permittivity
Mean correlation coefficient at intersects:
R²= 0.88
Permittivity
Klotzsche et al., GJI 2014
2. Mai 2014
Folie 16

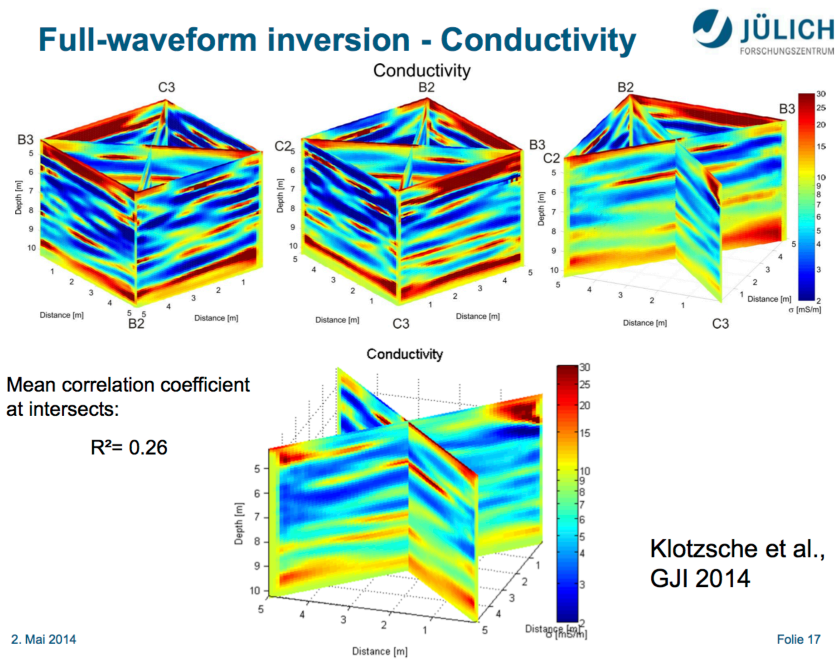
Full-waveform inversion - Conductivity
JÜLICH
FORSCHUNGSZENTRUM
Conductivity
Mean correlation coefficient at intersects:
R²= 0.26
Conductivity
Klotzsche et al., GJI 2014
2. Mai 2014
Folie 17

Porosity and hydraulic permeability

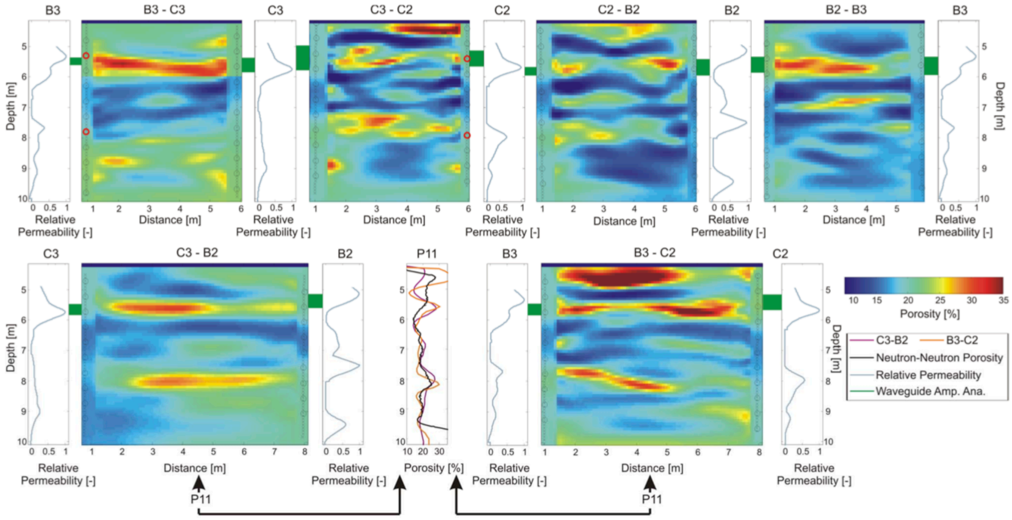

Klotzsche et al., GJI 2014

2D Case study: Boise Hydrogeophysical Research Site

- established by the University of Boise (Idaho/USA)

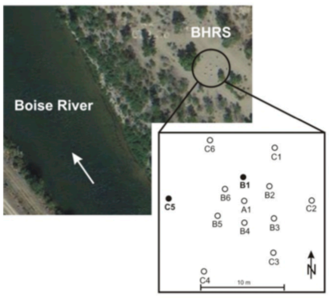

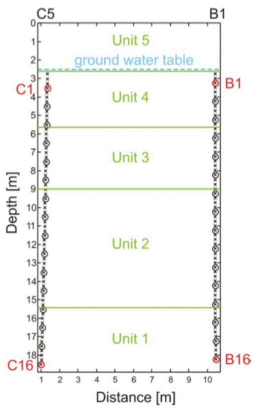

 Klotzsche et al., WRR, 2014

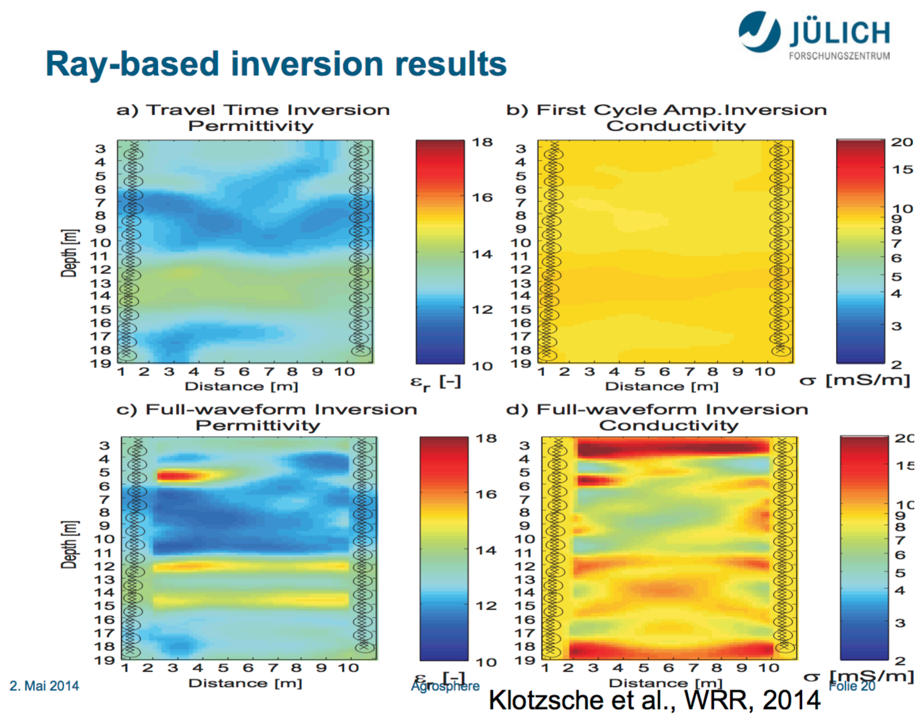
JÜLICH
FORSCHUNGSZENTRUM
Ray-based inversion results
a) Travel Time Inversion Permittivity
b) First Cycle Amp.Inversion Conductivity
c) Full-waveform Inversion Permittivity
d) Full-waveform Inversion Conductivity
Depth [m]
Distance [m]
ε_r [-]
σ [mS/m]
2. Mai 2014
Agrosphere
Klotzsche et al., WRR, 2014
Folie 20

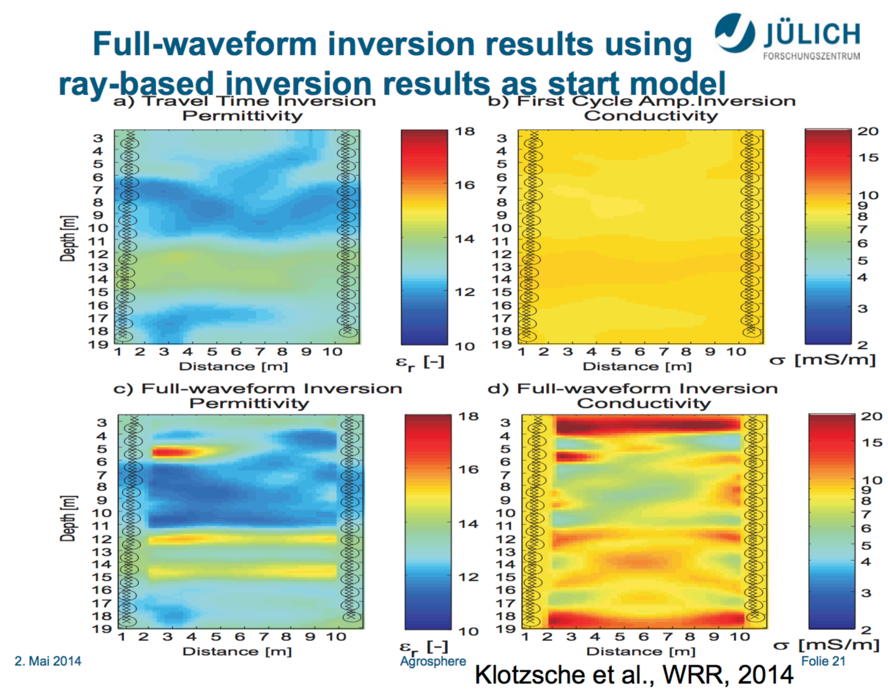
JÜLICH
FORSCHUNGSZENTRUM
Full-waveform inversion results using ray-based inversion results as start model
a) Travel Time Inversion Permittivity
b) First Cycle Amp.Inversion Conductivity
c) Full-waveform Inversion Permittivity
d) Full-waveform Inversion Conductivity
Depth [m]
Distance [m]
ε_r [-]
σ [mS/m]
2. Mai 2014
Agrosphere
Klotzsche et al., WRR, 2014
Folie 21

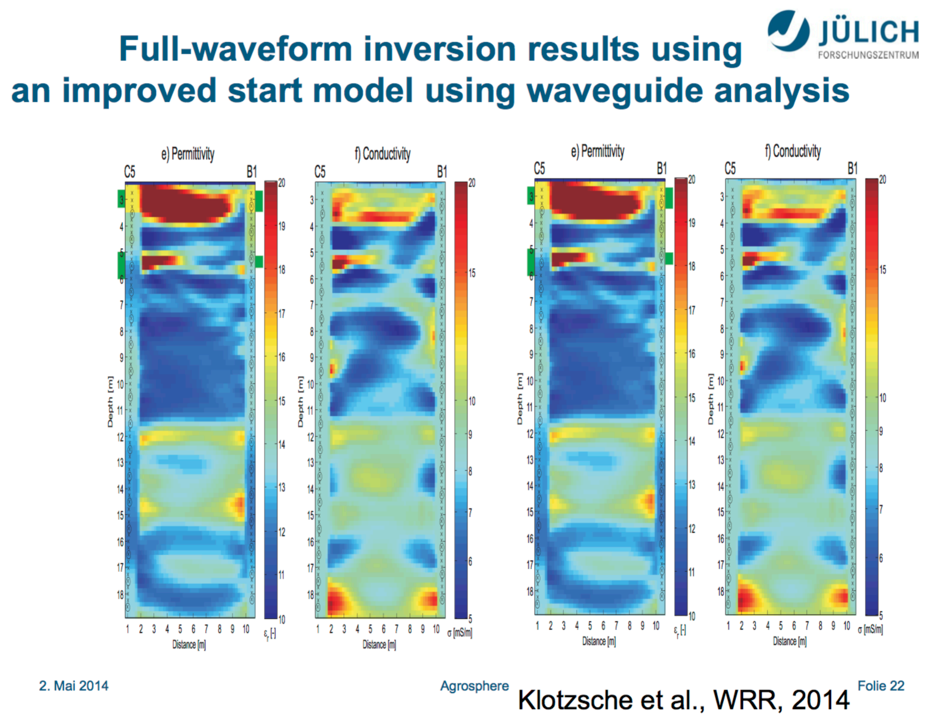
Full-waveform inversion results using
an improved start model using waveguide analysis
JÜLICH
FORSCHUNGSZENTRUM
e) Permittivity
f) Conductivity
e) Permittivity
f) Conductivity
C5
B1
Depth [m]
Distance [m]
2. Mai 2014
Agrosphere
Klotzsche et al., WRR, 2014
Folie 22

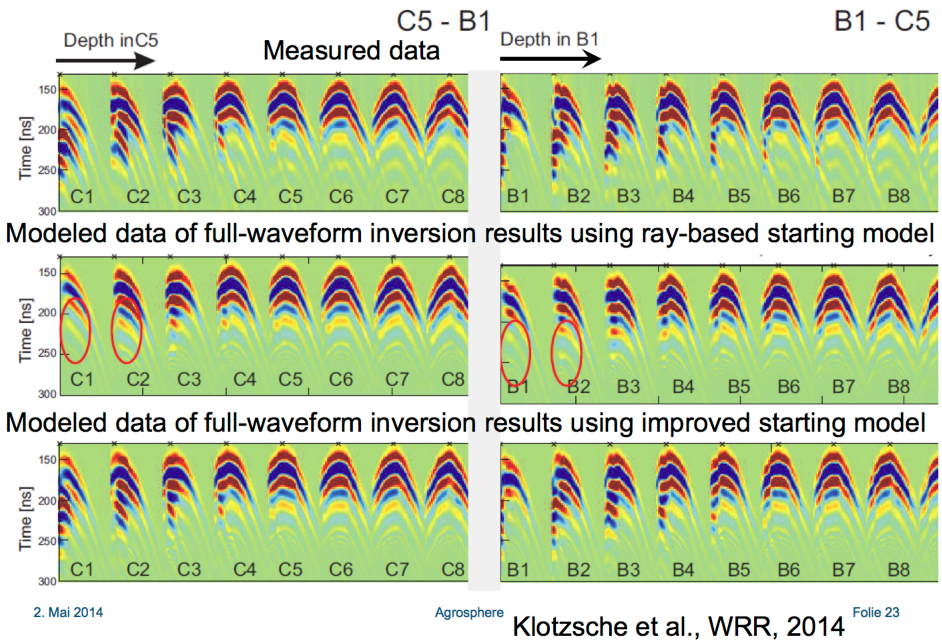
C5 - B1
B1 - C5
Depth inC5
Depth in B1
Measured data
Time [ns]
C1 C2 C3 C4 C5 C6 C7 C8
B1 B2 B3 B4 B5 B6 B7 B8
Modeled data of full-waveform inversion results using ray-based starting model
Modeled data of full-waveform inversion results using improved starting model
2. Mai 2014
Agrosphere
Klotzsche et al., WRR, 2014
Folie 23

Neutron-Neutron measurements -> Porosity

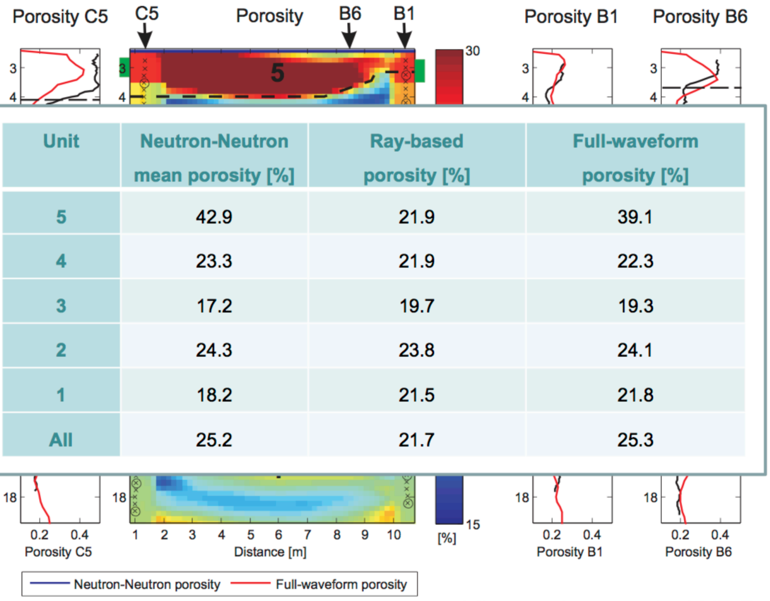

Unit	Neutron-Neutron mean porosity [%]	Ray-based porosity [%]	Full-waveform porosity [%]
5	42.9	21.9	39.1
4	23.3	21.9	22.3
3	17.2	19.7	19.3
2	24.3	23.8	24.1
1	18.2	21.5	21.8
All	25.2	21.7	25.3

Klotzsche et al., WRR, 2014

Conclusions

- Full-waveform inversion returns decimeter-scale high resolution images of permittivity and conductivity with consistent structures where acquisition planes intersect.
- Full-waveform inversion and amplitude analysis are able to detect and characterize electromagnetic low-velocity waveguides, that can be related to zones of preferential flow (high porosity) or clay lenses.
- Good correspondence between measured and modeled traces in shape and amplitude, including high-amplitude late-time waveguide arrivals ⇨ reliable inversion results.
- Comparison of the full-waveform porosities and logging data showed a good agreement and confirmed high porosity zones and zones of preferential flow.

PROGRESS REPORT OF PROJECT 3.1

"DEVELOPMENT OF NEW METHODS FOR THE SOLUTION OF FORWARD ELECTROMAGNETIC SCATTERING PROBLEMS BY BURIED STRUCTURES"

Nicolas Pinel (IT), Cristina Ponti (IT)
nicolas.pinel@alyotec.com

New Countries & Institutions

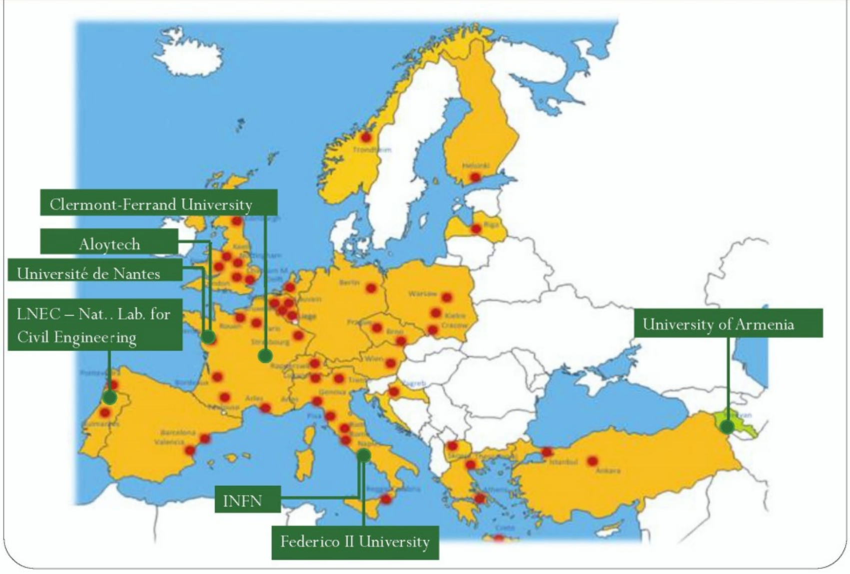

Motivations

❑ **The forward electromagnetic scattering by buried objects**

Civil Engineering	✓ Roads ✓ Buildings ✓ Bridges
Archeology	✓ Tunnels ✓ Utilities and voids ✓ Archaeological sites
Geophysics	✓ Geological formations ✓ Mines
Forensic Investigations	✓ Ordnances ✓ Corpses
GPR instrumentation	✓ Antenna
Data processing	✓ Testing of new data processing techniques

✓ *Need of an advanced modeling*

A multi-disciplinary topic!

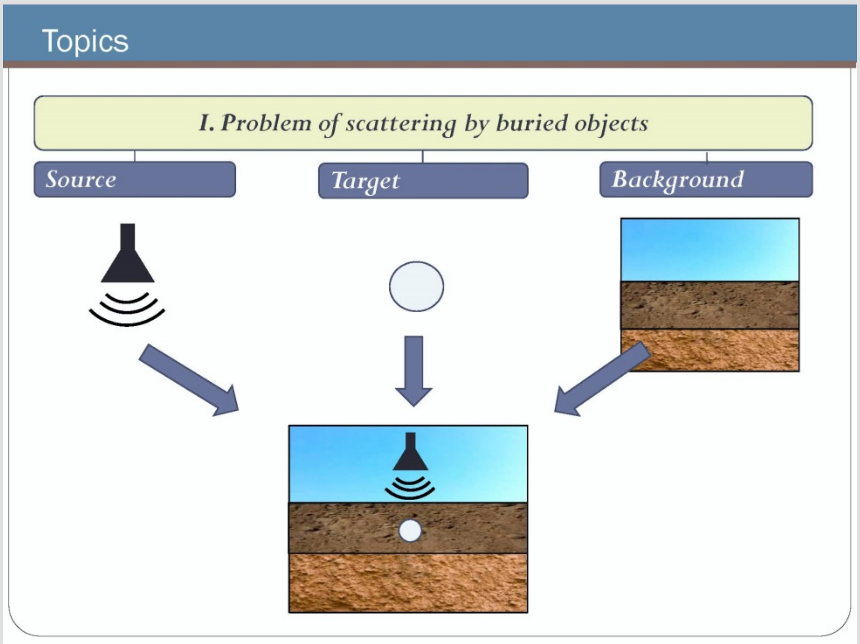
Topics
I. Problem of scattering by buried objects
Source
Target
Background

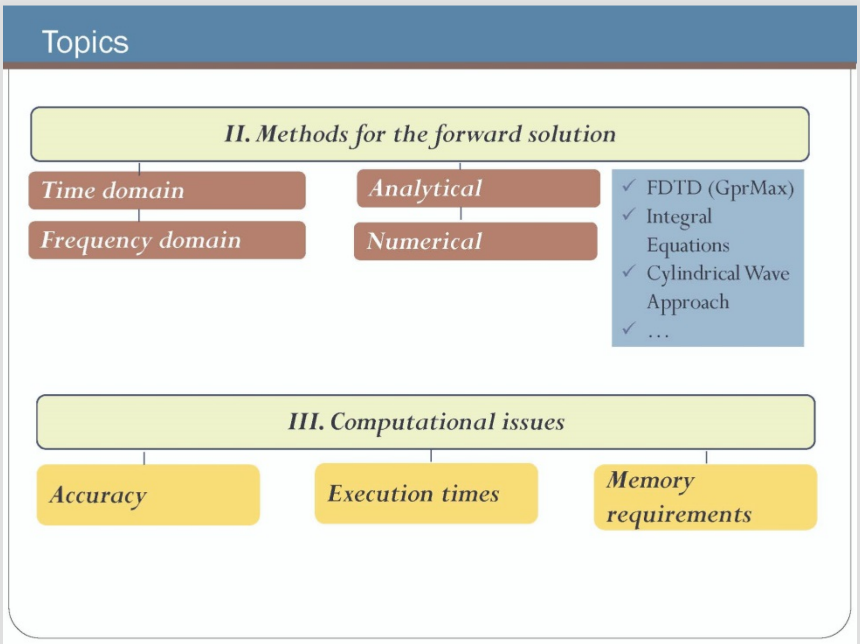
Topics
II. Methods for the forward solution
Time domain
Frequency domain
Analytical
Numerical
FDTD (GprMax)
Integral Equations
Cylindrical Wave Approach
…
III. Computational issues
Accuracy
Execution times
Memory requirements

Integral equations and Method of Moments

Institution

Université de Nantes

Alyotech

- **Integral Equations Approach and Method of Moments (MoM)**

- **Scattering by objects of canonical shape**
  - Cylinder
  - Plate
- **Scattering by a random rough surface**
- **Scattering by an object below or above a rough surface**

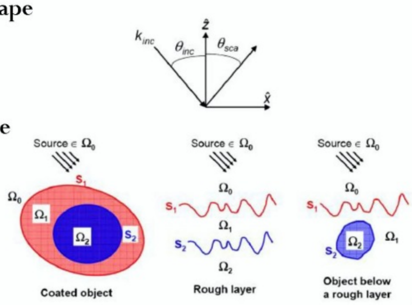

Integral equations and Method of Moments

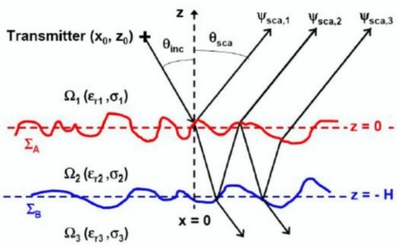

- **MoM and PILE (Propagation Inside Layer Expansion Method) applied to GPR**
- **+ SKA (Scalar Kirchhoff-tangent plane Approximation)**

- **Frequency domain**
- **Ricker pulse (IFFT)**
- **Near or/and far-field**
- **Non-destructive pavement survey**
- **Time delay estimation**
- **Surface roughness estimation**

Integral equations and Method of Moments

Journal

M. Sun, C. Le Bastard, N. Pinel, Y. Wang, "Time delay and interlayer roughness estimations by GPR for pavement survey", submitted in Near Surface Geophysics, 20 pages, Nov. 2013.

Conference contributions

M. Sun, N. Pinel, C. Le Bastard, V. Baltazart, A. Ihamouten, Y. Wang, "Time delay and surface roughness estimation by subspace algorithms for pavement survey by radar", IWAGPR (Nantes, France), 2013.

C. Bourlier, C. Le Bastard, and N. Pinel, "Full wave PILE method for the electromagnetic scattering from random rough layers," accepted at *GPR2014 Conference*, 2014.

N. Pinel, C. Bourlier, and C. Le Bastard, "Rigorous and asymptotic models of coherent scattering from random rough layers with applications to roadways and geoscience," accepted at *EGU2014* Conference, 2014.

M. Sun, C. Le Bastard, N. Pinel, Y. Wang, "Estimation of time delay and roughness parameters by GPR using ESPRIT method", submitted in *IEEE International Geoscience and Remote Sensing Symposium* (Québec, Canada), July 2014.

Book

C. Bourlier, N. Pinel, and G. Kubické, Method of moments for 2D scattering problems. Basic concepts and applications. London, UK: FOCUS SERIES in WAVES, Ed. WILEY-ISTE, 2013.

Cylindrical Wave Approach

Institutions

Roma Tre University

Sapienza University

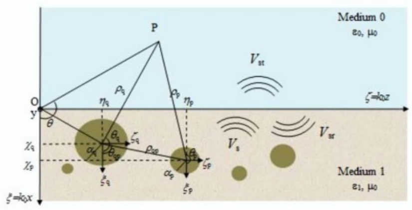

- **Frequency domain analysis with the Cylindrical Wave Approach (CWA)**
  - **Excitation by a two-dimensional source**

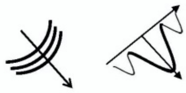

  - **Through-wall scattering model**

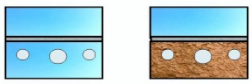

  - **Scattering by a cylinder buried under a rough surface**

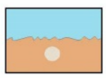

Cylindrical Wave Approach

Journals

F. Frezza, L. Pajewski, C. Ponti, G. Schettini e N. Tedeschi, "On some numerical aspects of the scattering problem by buried cylinders", *COMPEL*, Vol. 32, n. 6, pp. 1809-1820 , 2013.

F. Frezza, L. Pajewski, C. Ponti, G. Schettini, and N. Tedeschi "Cylindrical-Wave Approach for electromagnetic scattering by subsurface metallic targets in a lossy medium," *Journal of Applied Geophysics*, Vol. 97, pp. 55-59, 2013.

F. Frezza, L. Pajewski, C. Ponti, and G. Schettini, "Through-wall electromagnetic scattering by N conducting cylinders," *J. Opt. Soc. Am. A*, Vol. 30, pp. 1632-1639, 2013.

M. A. Fiaz, F. Frezza, C. Ponti, and G. Schettini, "Electromagnetic scattering by a circular cylinder buried below a slightly rough Gaussian surface," *J. Opt. Soc. Am. A*, Vol. 31, pp. 26-34, 2014.

Conference contributions

C. Ponti, F. Frezza, L. Pajewski, and G. Schettini, "Scattering by Buried PEC Cylinders from an Arbitrary 2D Illumination," *Proc. of URSI-EMTS 2013*, Hiroshima, Japan, May 19-24, 2013.

F. Frezza, L. Pajewski, C. Ponti, and G. Schettini, "Cylindrical-wave approach for line-source electromagnetic scattering by buried dielectric cylinders ," *Proc. of IWAGPR 2013*, 2013.

M. A. Fiaz, C. Ponti, and G. Schettini, "'On the scattering by a cylindrical object below a rough surface with the CWA," accepted at *NEMO 2014 Conf.*, 2014.

C. Ponti, L. Pajewski, and G. Schettini, "Simulation of scattering by cylindrical targets hidden behind a layer," accepted at *GPR 2014 Conf.*, 2014.

Time domain analysis

Institution

University of Split

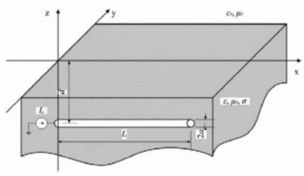

Design and modeling of Grounding and Lighting Protection Systems

- Horizontal grounding electrode
- Transient response

- ❑ **Pocklington integro-differential equation**
- ❑ **Simplified reflection coefficient from the Modified Image Theory**

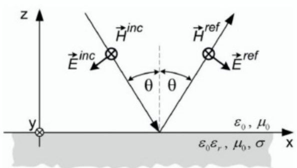

Time domain analysis

Journals

S. Šesnić and D. Poljak, " Antenna model of the horizontal grounding electrode for transient impedance calculation: Analytical versus Boundary Element Method," *Engineering analysis with boundary elements*, Vol. 37, pp. 909-913, 2013.

D. Cavka and D. Poljak, "On the Evaluation of Input Impedance and Transient Impedance for Grounding Electrodes Using Antenna Theory," *COMPEL: The International Journal for Computation and Mathematics in Electrical and Electronic Engineering*, Vol. 32, pp. 2045-2062, 2013.

S. Šesnić, D. Poljak, and S. V. Tkachenko, " Analytical Modeling of a Transient Current Flowing Along the Horizontal Grounding Electrode" *IEEE Transactions on electromagnetic compatibility*, Vol., 55; pp. 1132-1139, 2013.

S. Antonijevic and D. Poljak, "A Novel Time-Domain Reflection Coefficient Function: TM Case," *IEEE Transactions on electromagnetic compatibility*, Vol. 55; pp. 1147-1153, 2013.

Conference contributions

D. Poljak, D. Cavka, B. Nekhoul, D. Sekki, K. Drissi, K. Kerroum, "Transient Voltage Induced along the Grounding System using the Antenna Theory Approach," *Proc. ICECOM 2013.*, Dubrovnik, 4-16 Oct. 2013.

D. Poljak, S. Sesnic, K. Drissi, K. Kerroum, "Transient Response of a Buried Wire," *Proc. ICECOM 2013.*, Dubrovnik, 4-16 Oct. 2013.

D. Cavka, N. Mora, Nicolas, F. Rachidi, D.Poljak, "Transient Voltage Induced along the Grounding System using the Antenna Theory Approach," *Proc. of the EMC Symp. 2013*, Aug. 5-9 2013, Denver, pp. 777-781.

1. Concrete

L. Pajewski, and A. Giannopoulos, "Electromagnetic modelling of Ground Penetrating Radar responses to complex targets," *Geophysical Research Abstracts* Vol. 16, EGU2014-16421, 2014 EGU General Assembly 2014.

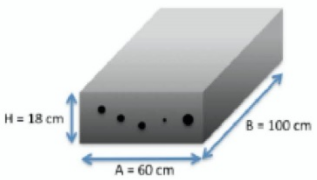

- 2D: cell size A × H
- 3D: cell size A × B × H

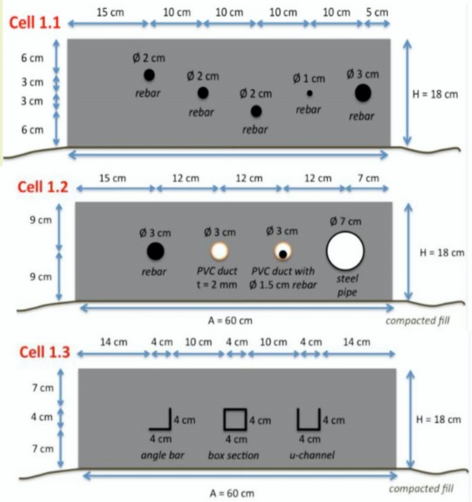

1. Concrete

Transmitter

✓Central frequency: 1.5 GHz
✓Pulse shape: Ricker
✓2D source: line current
✓3D source:
• Hertzian dipole //B or //A
•Bow-tie antenna //B or //A
•GSSI
✓Rx and Tx at 2 cm from concrete-air interface
✓The distance between Tx and Rx is d = 10 cm

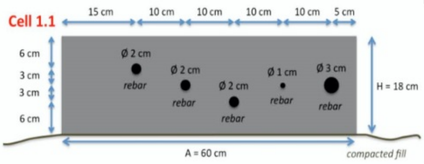

Output

✓B-scan with step 5 mm
✓A-scan above the center of each scatterer
✓Total field and backscattered field
✓Time window: 5 ns

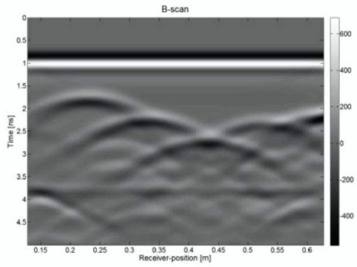

2. Bridge

Sant'Antón bridge

M. Solla, H. Lorenzo, A. Novo, and F.I. Rial, Ground-Penetrating Radar Assessment of the Medieval Arch Bridge of San Antón, Galicia, Spain, *Archaeol. Prospect.* 17, 223-232 (2010).

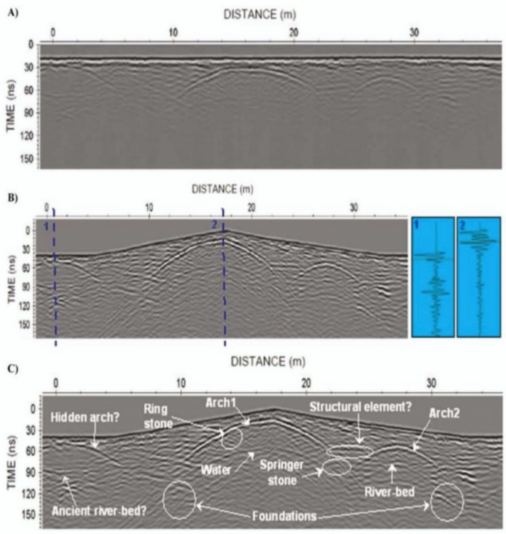

2. Bridge

Sant'Antón bridge

- Overall length: 45 m
- Primary arch: 10.2 m × 5.1 m
- Secondary arch: 4.0 m × 2.0 m
- Hidden arch: 4.0 m × 2.0 m

- Antenna height from the surface: 0.1 m
- Central frequency: 200 MHz
- Time-window: 100 ns
- 430 GPR scans with horizontal resolution 0.1 m
- Offset between Tx and Rx: 0.6 mm

Material	Relative permittivity (ε_r)	Conductivity [S/m] (σ)	Relative permeability (μ_r)
Water	80	0.5	1.0
Granite	7	0.0001	1.0
Filling	8	0.0001	1.0
River-bed	20	0.0005	1.0
Masonry	5	0.0001	1.0
Free space	1.0	0.0	1.0

2. Bridge

Sant'Antón bridge

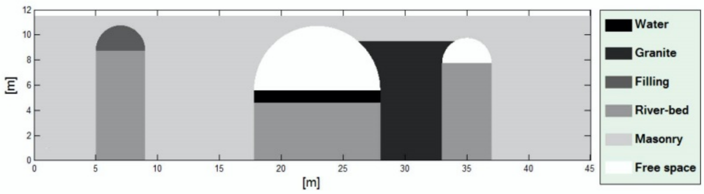

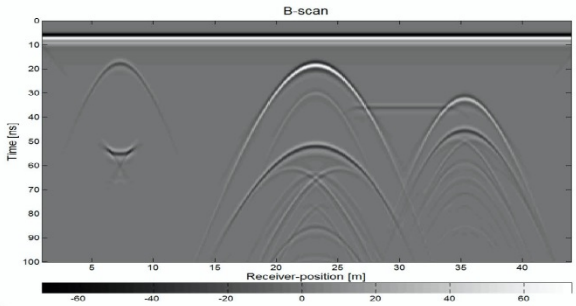

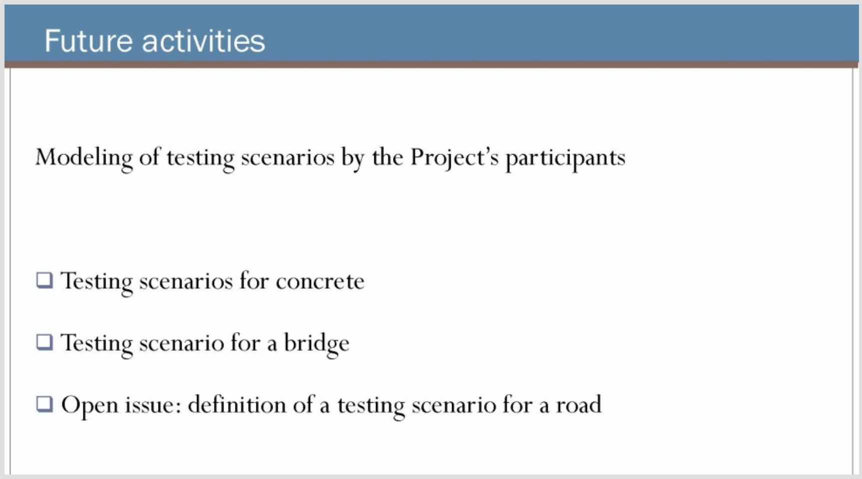

ACKNOWLEDGEMENT

The author acknowledges the COST Action TU1208 “Civil Engineering Applications of Ground Penetrating Radar”, supporting this work.

"Electromagnetic modelling of GPR responses to complex scenarios" (contribution to project 3.1)

Lara Pajewski(IT), Antonios Giannopoulos (UK)
lara.pajewski@uniroma3.it

The abstract is published in *Geophysical Research Abstracts*, Vol. 16, EGU2014-16421, 2014 and is available on *www.egu2014.eu*

This work was presented as a poster and concerned the electromagnetic modelling of concrete structures, for Ground Penetrating Radar (GPR) applications.

A set of scenarios was proposed by the authors, involving concrete cells with various embedded objects. A detailed description of the cells and the obtained FDTD [1] results are available for the Members of the COST Action TU1208. The simplest cell includes circular-section bars of different diameters, placed in concrete at increasing depths. Other cells contain polyvinyl chloride ducts, steel objects commonly used in civil engineering (as a pipe, an angle bar, a box section, and an u-channel), voids and honeycombing defects. For each structure, a subset of models with growing complexity is defined, starting from a simple representation of the cell and ending with a more realistic one. In particular, the model's complexity increases from the geometrical point of view, as well as in terms of how the constitutive parameters of the involved media and GPR antennas are described.

The idea beyond this work is to start designing a new database that will contain both numerical and experimental GPR responses from natural and manmade structures. Researchers working on the development of electromagnetic forward- and inverse-scattering techniques, imaging methods and data-processing algorithms will thus have a further opportunity of testing and validating, against reliable data, their approaches.

The motivation to start this project came out during previous TU1208 meetings and takes inspiration by successful past initiatives carried out in different areas, as the Ipswich [2-5] and Fresnel [6-9] databases in the field of free-space electromagnetic scattering (collections of experimental data measured on metallic and dielectric scatterers, in anechoic chamber), and the Musumeci [24] database in seismic science (a dataset

of 151 events, leading the July 17th – August 9th, 2001 lateral eruption at Mt. Etna volcano, in Italy).

ACKNOWLEDGEMENT

The authors are grateful to COST for funding the Action TU1208 "Civil Engineering Applications of Ground Penetrating Radar", supporting the Second General Meeting and this work.

REFERENCES

[1] Giannopoulos, A. Modelling ground penetrating radar by GprMax. *Construction and Building Materials* 2005, *19*, pp. 755-762.
[2] McGahan, R.V.; Kleinman, R.E. Special session on image reconstruction using real data. IEEE Antennas and Propagations Magazine 1996, 38(3), pp. 39-59.
[3] McGahan, R.V; Kleinman, R.E. Second annual special session on image reconstruction using real data. IEEE Antennas and Propagations Magazine 1997, 39(2), pp. 7-32.
[4] McGahan, R.V.; Kleinman, R.E. Third annual special session on image reconstruction using real data: part 1. IEEE Antennas and Propagations Magazine 1999, 41(1), pp. 34-51.
[5] McGahan, R.V.; Kleinman, R.E. Third annual special session on image reconstruction using real data: part 2. IEEE Antennas and Propagations Magazine 1999, 41(2), pp. 20-40.
[6] Belkebir, K.; Saillard, M. Special section on testing inversion algorithms against experimental data. Inverse Problems 2001, 17, pp. 1565-1571.
[7] Belkebir, K.; Saillard, M. Special section on testing inversion algorithms against experimental data: Inhomogeneous targets. Inverse Problems 2005, 21, pp. S1-S3.
[8] Geffrin, J.-M.; Sabouroux, P.; Eyraud, C. Free space experimental scattering database continuation: experimental set-up and measurement precision. Inverse Problems 2005, 21, pp. S117-S130.
[9] Geffrin, J.-M.; Sabouroux, P. Continuing with the Fresnel database: experimental setup and improvements in 3D scattering measurements. Inverse Problems 2009, 25, 024001.
[10] Musumeci, C.; Cocina, O.; De Gori, P.; Patanè, D. Seismological evidence of stress induced by dike injection during the 2001 Mt. Etna eruption. Geophysical Research Letters 2004, 31(7), L07617.

"On the Analysis Methods for the Time Domain and Frequency Domain Response of a Buried Objects" (contribution to project 3.1)

Dragan Poljak (HR), Silvestar Šesnic (HR), Mario Cvetkovic (HR)
dpoljak@fesb.hr

The abstract is published in *Geophysical Research Abstracts*, Vol. 16, EGU2014-5274, 2014 and is available on *www.egu2014.eu*

1. Introduction

A continuous interest in the analysis of GPR systems and related applications in civil engineering is observed. A deeper insight of scattering phenomena in a lossy half-space, plus development of sophisticated numerical methods based on FDTD method, FEM, BEM, MoM and various hybrid methods, is required.

Generally, transient analysis of buried objects can be carried out in either frequency domain (FD), or time domain (TD). The present work deals with certain TD and FD analysis techniques for buried conducting and dielectric objects. Both TD and FD approaches discussed throughout this work and demonstrated on canonical geometries could be useful for benchmark purpose.

TD analysis is related to the transient response of a horizontal thin wire buried in a lossy half-space using a rigorous antenna theory (AT) approach. The AT approach is based on the space-time integral equation of the Pocklington type. The influence of the earth-air interface is taken into account via the simplified reflection coefficient arising from the Modified Image Theory (MIT).

Transient current induced along the wire due to the transmitted plane wave excitation is compared in this work to the numerical results calculated via TL approach and the AT approach based on the FD variant of the Pocklington IDE. FD-IDE is numerically solved via the Galerkin-Bubnov variant of the Indirect Boundary Element Method (GB-IBEM) and the transient response is calculated via IFFT.

FD analysis is used to determine FD response of dielectric sphere using the full wave model based on the set of coupled electric field integral

equations (EFIEs) for surfaces. Numerical solution is carried out by means of an improved variant of the Method of Moments (MoM) providing numerically stable and efficient procedure for the extraction of singularities arising in integral expressions.

2. TIME-DOMAIN MODELLING: PREVIOUS WORK

Full wave model – radiation of overhead wires

Formulation – Set of TD Hallen integral equations

Numerical solution (Galerkin-Bubnov Indirect Boundary Element Method; GB-IBEM)

Transient response of M parallel wires above a real ground is governed by the set of the coupled Hallen integral equations:

$$\sum_{s=1}^{M}\int_{0}^{L_s}\frac{I_s(x',t-\frac{R_{vs}}{c})}{4\pi R_{vs}}dx'-\sum_{s=1}^{M}\int_{-\infty}^{t}\int_{0}^{L_s}r_{vs}(\theta,\tau)\frac{I_s(x',t-\frac{R_{vs}^*}{c}-\tau)}{4\pi R_{vs}^*}dx'd\tau$$
$$=F_{0v}(t-\frac{x-x_{0v}}{c})+F_{Lv}(t-\frac{x_{Lv}-x}{c})+\frac{1}{2Z_0}\int_{0}^{L_s}E_{xv}^{exc}(x',t-\frac{|x-x'|}{c})dx'$$

Unknown time signals $F_{0v}(t)$ and $F_L(t)$ related to the multiple reflections of transient currents at the wires free ends are given by:

$$F_{0v}(t)=\sum_{n=0}^{\infty}K_{0v}(t-\frac{2nL_v}{c})-\sum_{n=0}^{\infty}K_{Lv}(t-\frac{(2n+1)L_v}{c})$$

$$F_{Lv}(t)=\sum_{n=0}^{\infty}K_{Lv}(t-\frac{2nL_v}{c})-\sum_{n=0}^{\infty}K_{0v}(t-\frac{(2n+1)L_v}{c})$$

The auxilliary functions K are defined as follows:

$$K_{0v}(t)=\sum_{s=1}^{M}\int_{0}^{L_s}\frac{I_s(x',t-\frac{R_{vs}^{(0)}}{c})}{4\pi R_{vs}^{(0)}}dx'-\sum_{s=1}^{M}\int_{-\infty}^{t}\int_{0}^{L_s}r_{vs}(\theta,\tau)\frac{I_s(x',t-\frac{R_{vs}^{*(0)}}{c}-\tau)}{4\pi R_{vs}^{*(0)}}dx'd\tau-\frac{1}{2Z_0}\int_{0}^{L_s}E_x^{exc}(x',t-\frac{|x-x'|}{c})dx'$$

$$K_{Lv}(t) = \sum_{s=1}^{M} \int_0^{L_s} \frac{I_s\left(x', t - \frac{R_{vs}^{(L)}}{c}\right)}{4\pi R_{vs}^{(L)}} dx' - \sum_{s=1}^{M} \int_{-\infty}^{t} \int_0^{L_s} r_{vs}(\theta, \tau) \frac{I_s\left(x', t - \frac{R_{vs}^{*(L)}}{c} - \tau\right)}{4\pi R_{vs}^{*(L)}} dx' d\tau - \frac{1}{2Z_0} \int_0^{L_s} E_x^{exc}\left(x', t - \frac{|x - x'|}{c}\right) dx'$$

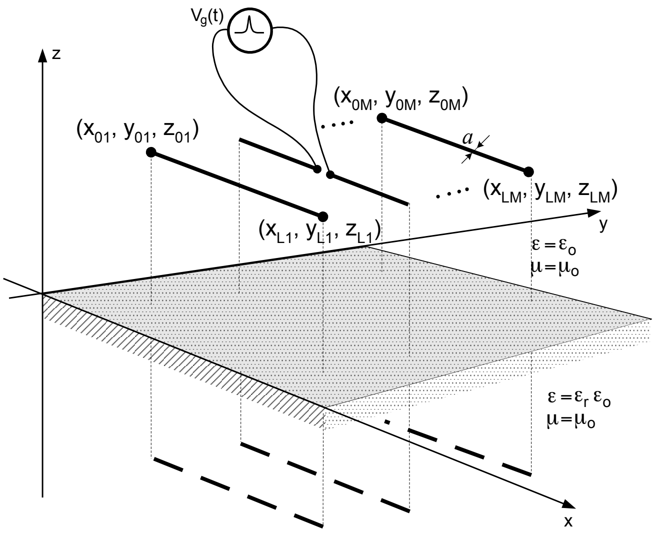

Geometry of the problem.

The following matrix equation can be obtained:

$$\sum_{s=1}^{M} [A_{vs}]\{I_s\}\Big|_{t - \frac{R_{vs}}{c}} - \sum_{s=1}^{M} [A_{vs}^*]\{I_s\}\Big|_{t - \frac{R_{vs}^*}{c}} =$$

$$= [B_v]\{E_v\}\Big|_{t - \frac{|x - x'|}{c}} + \sum_{s=1}^{M} [C_{vs}]\left\{\sum_{n=0}^{\infty} I_s^n\right\}\Bigg|_{t - \frac{x - x_{0v}}{c} - \frac{2n}{c}L_v - \frac{R_{vs}^{(0)}}{c}} - \sum_{s=1}^{M} [C_{vs}^*]\left\{\sum_{n=0}^{\infty} I_s^n\right\}\Bigg|_{t - \frac{x - x_{0v}}{c} - \frac{2n}{c}L_v - \frac{R_{vs}^{*(0)}}{c}} - [D_v]\left\{\sum_{n=0}^{\infty} E_v^n\right\}\Bigg|_{t - \frac{x - x_{0v}}{c} - \frac{2n}{c}L_v - \frac{|x' - x_{0v}|}{c}} -$$

$$- \sum_{s=1}^{M} [E_{vs}]\left\{\sum_{n=0}^{\infty} I_s^n\right\}\Bigg|_{t - \frac{x - x_{0v}}{c} - \frac{2n+1}{c}L_v - \frac{R_{vs}^{(L)}}{c}} + \sum_{s=1}^{M} [E_{vs}^*]\left\{\sum_{n=0}^{\infty} I_s^n\right\}\Bigg|_{t - \frac{x - x_{0v}}{c} - \frac{2n+1}{c}L_v - \frac{R_{vs}^{*(L)}}{c}} + [D_v]\left\{\sum_{n=0}^{\infty} E_v^n\right\}\Bigg|_{t - \frac{x - x_{0v}}{c} - \frac{2n+1}{c}L_v - \frac{|x_{Lv} - x'|}{c}} + \sum_{s=1}^{M} [E_{vs}]\left\{\sum_{n=0}^{\infty} I_s^n\right\}\Bigg|_{t - \frac{x_{Lv} - x}{c} - \frac{2n}{c}L_v - \frac{R_{vs}^{(L)}}{c}} -$$

$$- \sum_{s=1}^{M} [E_{vs}^*]\left\{\sum_{n=0}^{\infty} I_s^n\right\}\Bigg|_{t - \frac{x_{Lv} - x}{c} - \frac{2n}{c}L_v - \frac{R_{vs}^{*(L)}}{c}} - [D_v]\left\{\sum_{n=0}^{\infty} E_v^n\right\}\Bigg|_{t - \frac{x_{Lv} - x}{c} - \frac{2n}{c}L_v - \frac{|x_{Lv} - x'|}{c}} - \sum_{s=1}^{M} [C_{vs}]\left\{\sum_{n=0}^{\infty} I_s^n\right\}\Bigg|_{t - \frac{x_{Lv} - x}{c} - \frac{2n+1}{c}L_v - \frac{R_{vs}^{(0)}}{c}} + \sum_{s=1}^{M} [C_{os}^*]\left\{\sum_{n=0}^{\infty} I_s^n\right\}\Bigg|_{t - \frac{x_{Lo} - x}{c} - \frac{2n+1}{c}L_o - \frac{R_{os}^{*(0)}}{c}} +$$

$$+ [D_o]\left\{\sum_{n=0}^{\infty} E_o^n\right\}\Bigg|_{t - \frac{x_{Lo} - x}{c} - \frac{2n+1}{c}L_o - \frac{|x' - x_{0o}|}{c}}$$

where the space dependent matrices are:

$$\left[A_{vs}\right]=\int_{\Delta l_j}\int_{\Delta l_i}\frac{1}{4\pi R_{vs}}\{f\}_j\{f\}_i^T\,dx'dx;\quad \left[A_{vs}^*\right]=\int_{\Delta l_j}\int_{\Delta l_i}\frac{r_{vs}(\theta)}{4\pi R_{vs}^*}\{f\}_j\{f\}_i^T\,dx'dx$$

$$\left[B_v\right]=\frac{1}{2Z_0}\int_{\Delta l_j}\int_{\Delta l_i}\{f\}_j\{f\}_i^T\,dx'dx\quad ,\left[C_{vs}\right]=\int_{\Delta l_j}\int_{\Delta l_i}\frac{1}{4\pi R_{vs}^{(0)}}\{f\}_j\{f\}_i^T\,dx'dx$$

$$\left[C_{vs}^*\right]=\int_{\Delta l_j}\int_{\Delta l_i}\frac{r_{vs}(\theta)}{4\pi R_{vs}^{*(0)}}\{f\}_j\{f\}_i^T\,dx'dx\quad \left[D_v\right]=\frac{1}{2Z_0}\int_{\Delta l_j}\int_{\Delta l_i}\{f\}_j\{f\}_i^T\,dx'dx$$

$$\left[E_{vs}\right]=\int_{\Delta l_j}\int_{\Delta l_i}\frac{1}{4\pi R_{vs}^{(L)}}\{f\}_j\{f\}_i^T\,dx'dx\;,\left[E_{vs}^*\right]=\int_{\Delta l_j}\int_{\Delta l_i}\frac{r_{vs}(\theta)}{4\pi R_{vs}^{*(L)}}\{f\}_j\{f\}_i^T\,dx'dx$$

The weighted residual approach in the time domain gives:

$$\int_{t_k}^{t_k+\Delta t}\left(\left[A\ \right]\{I\}\Big|_{t-\frac{R_{vs}}{c}}-\left[A^*\right]\{I\}\Big|_{t-\frac{R_{vs}^*}{c}}-\{g\}\theta_k\right)dt=0;\ k=1,2,\ldots,N_t$$

and the recurrence formula for the transient current at j-th space node and k-th time node is:

$$I_j\Big|_{t_k}=\frac{-\sum_{i=1}^{N}\left(\overline{A_{ji}}\,I_i\Big|_{t_k-\frac{R_{vs}}{c}}+A_{ji}^*\,I_i\Big|_{t_k-\frac{R_{vs}^*}{c}}\right)+g_j\Big|_{all\ previous\ discrete\ instants}}{A_{jj}}$$

Some computational examples are now presented.

Wire arrays, with a two- or three-wire antenna array horizontally located, are considered.

The excitation is a time-dependent Gaussian pulse voltage source. The parameters of the Gaussian pulse are: V_0=1V, g=2*10^{9}s^{-1} and t_0=2ns, the entire length of the wires is L=1 m, while the radius of all wires is a=2mm. The array is located above half-space (ε_r =10).

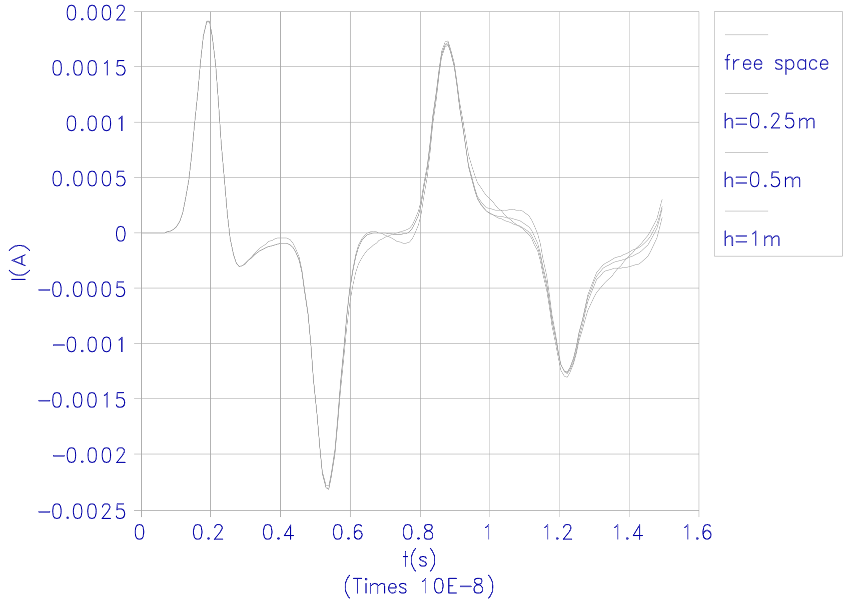

Current at the centre of the wire *A* (active wire) versus time with height *h* over interface as parameter (*L*=1m, *a*=2mm, ε_r=9, *h*=0.25m)

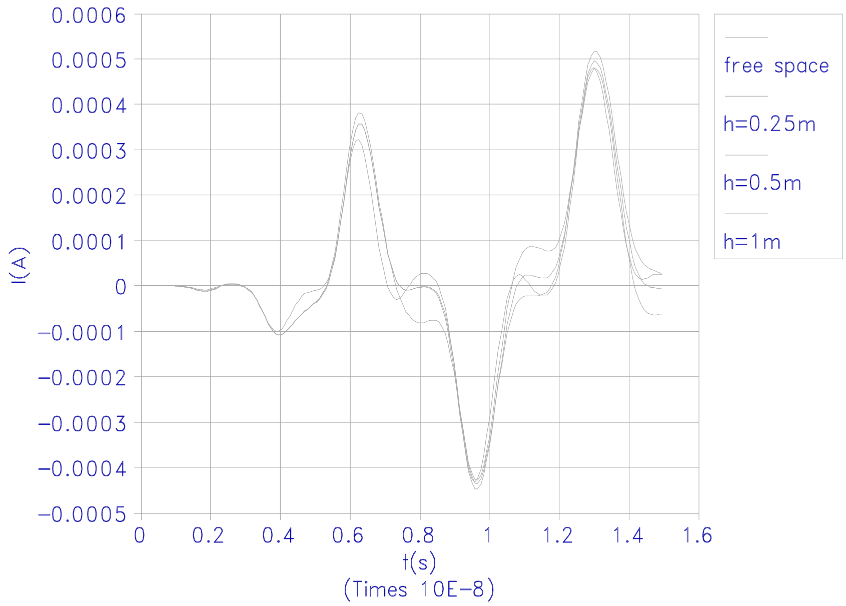

Current at the centre of wired *B* (passive wire) versus time with height *h* over interface as parameter (*L*=1m, *a*=2mm, ε_r=9, *h*=0.25m).

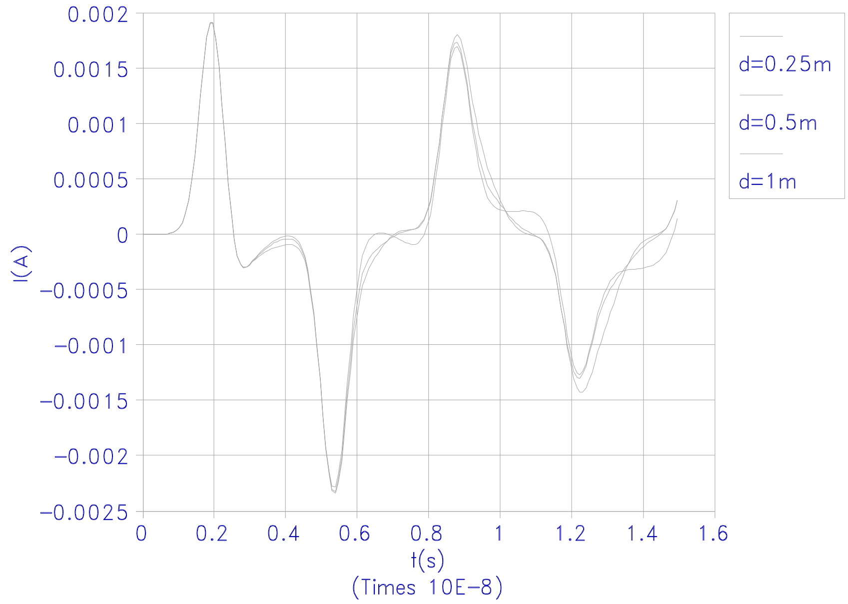

Current at the centre of wire A (active wire) versus time with distance *d* between the wires as a parameter (*L*=1m, *a*=2mm, ε_r=9, *d*=0.5m)

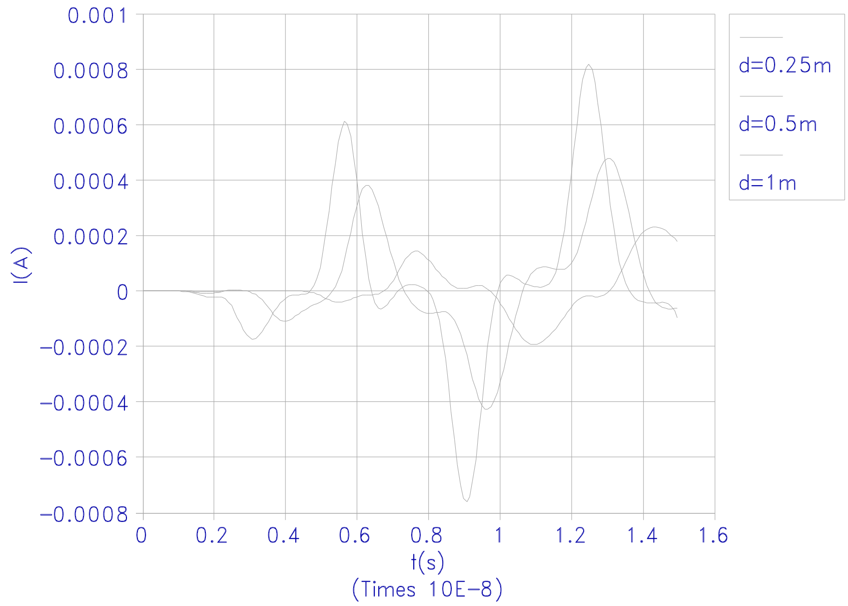

Current at the centre of wire *B* (passive wire) versus time with distance *d* between the wires as a parameter (*L*=1m, *a*=2mm, ε_r=9, *d*=0.5m)

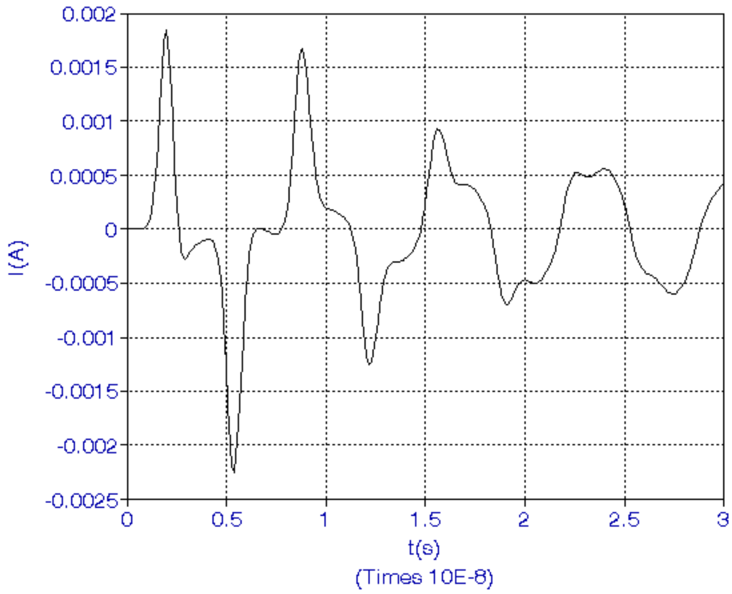

Transient current induced at the center of the active wire

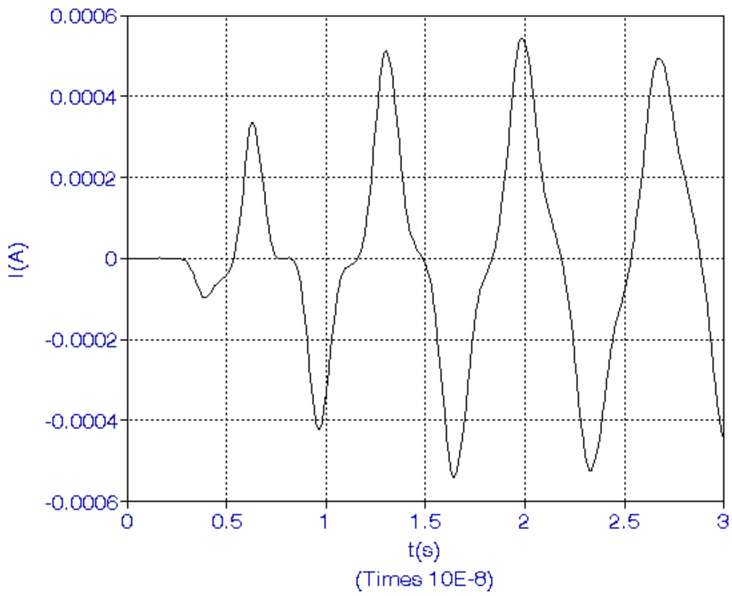

Transient current induced at the center of the passive wires

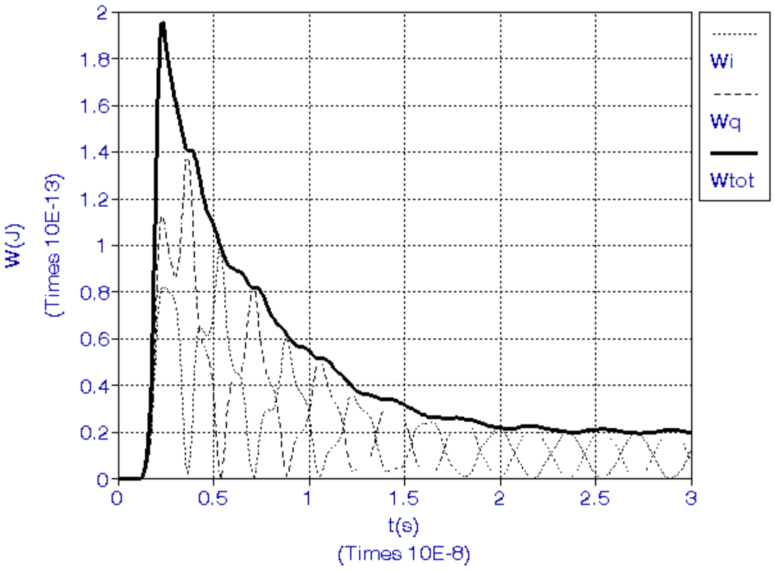

The H-field (W_I) E-field (W_q) and total energy (W_{tot}) energy measures as a function of time for the active wire

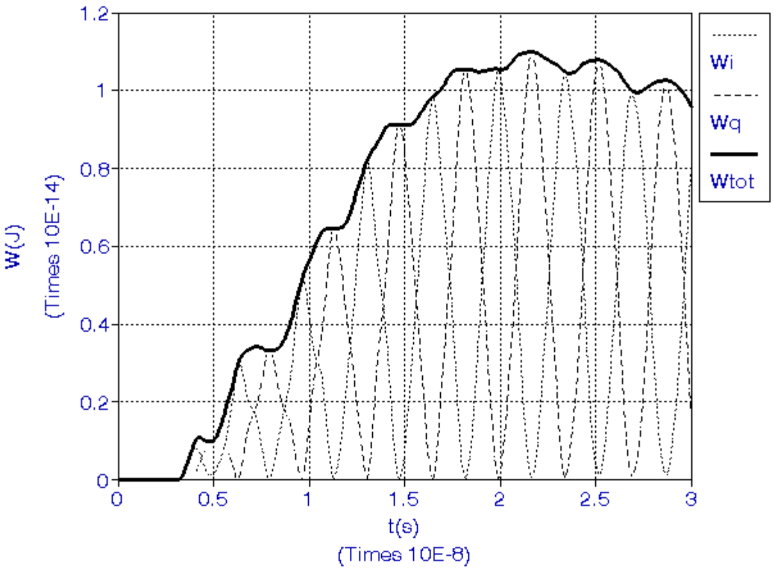

The H-field (W_I) E-field (W_q) and total energy (W_{tot}) energy measures as a function of time for the passive wire

3. TIME-DOMAIN MODELLING: ONGOING WORK

The full wave model – the most rigorous approach to analyze the EM field coupling to arbitrary configurations of wires

The formulation - TD Pocklington integro-differential equation

Analytical/numerical solution (Galerkin-Bubnov Indirect Boundary Element Method; GB-IBEM)

Formulation of the method:

A horizontal thin wire buried in a lossy half-space is considered.

TD-IDE of Pocklington type for a single wire buried in a lossy ground can be derived by enforcing the continuity conditions for the tangential components of the electric field along the PEC wire surface and can be written in the form:

$$\left(\mu\varepsilon\frac{\partial}{\partial t}+\mu\sigma\right)E_x^{tr}(t)=-\left(\frac{\partial^2}{\partial x^2}-\mu\sigma\frac{\partial}{\partial t}-\mu\varepsilon\frac{\partial^2}{\partial t^2}\right)$$

$$\cdot\left[\frac{\mu}{4\pi}\int_0^L I\left(x',t-\frac{R}{v}\right)\frac{e^{-\frac{1}{\tau_g}\frac{R}{v}}}{R}dx'-\frac{\mu}{4\pi}\int_0^t\int_0^L\Gamma_{ref}^{MIT}(\tau)I\left(x',t-\frac{R^*}{v}-\tau\right)\frac{e^{-\frac{1}{\tau_g}\frac{R^*}{v}}}{R^*}dx'd\tau\right]$$

where the time constants, propagation velocity and reflection coefficient are:

$$\tau_g=\frac{2\varepsilon}{\sigma}\qquad \tau_1=\frac{\varepsilon_0(\varepsilon_r-1)}{\sigma}\qquad \tau_2=\frac{\varepsilon_0(\varepsilon_r+1)}{\sigma}\qquad v=\frac{1}{\sqrt{\mu\varepsilon}}$$

$$\Gamma_{ref}^{MIT}(t)=-\left[\frac{\tau_1}{\tau_2}\delta(t)+\frac{1}{\tau_2}\left(1-\frac{\tau_1}{\tau_2}\right)e^{-\frac{t}{\tau_2}}\right]$$

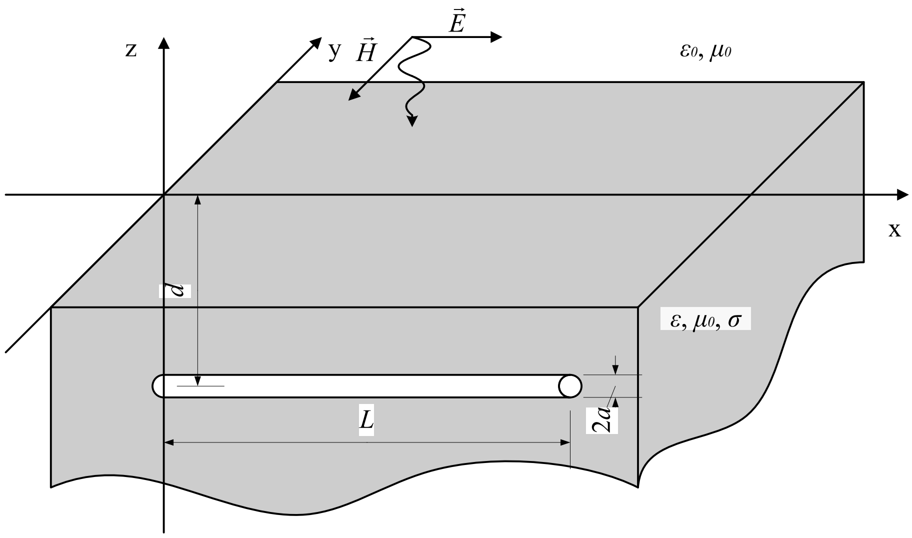

Geometry of the problem.

Solving TD-IDE analytically for the case of impulse excitation yields the impulse response of the form:

$$I(x,t) = \frac{4\pi}{\mu}\left\{ \begin{aligned} & R(s_\Psi)\left[1 - \frac{\cosh\left(\gamma_\Psi\left(\frac{L}{2} - x\right)\right)}{\cosh\left(\gamma_\Psi \frac{L}{2}\right)}\right] e^{\left(t+\frac{a}{v}\right)s_\Psi} \\ & - \frac{\pi}{\mu\varepsilon L^2}\sum_{n=1}^{\infty}\frac{2n-1}{\pm\sqrt{b^2 - 4c_n s_{1,2n}}\,\Psi\left(s_{1,2n}\right)}\sin\frac{(2n-1)\pi x}{L}\, e^{\left(t+\frac{a}{v}\right)s_{1,2n}} \end{aligned} \right\}$$

where:

$$R(s_\Psi) = \frac{1}{2\ln\frac{L}{2d}\,\frac{s_\Psi}{s_\Psi\tau_2 + 1}\left(\tau_1 - \tau_2\frac{s_\Psi\tau_1 + 1}{s_\Psi\tau_2 + 1}\right)} \qquad s_\Psi = -\frac{\ln\frac{L}{a} + \ln\frac{L}{2d}}{\tau_1\ln\frac{L}{a} + \tau_2\ln\frac{L}{2d}}$$

$$s_{1,2n} = \frac{1}{2}\left(-b \pm \sqrt{b^2 - 4c_n}\right) \qquad \gamma_\Psi = \sqrt{\mu\varepsilon\left(s_\Psi^2 + bs_\Psi\right)}$$

$$b = \frac{\sigma}{\varepsilon} \qquad c_n = \frac{(2n-1)^2\pi^2}{\mu\varepsilon L^2},\ n = 1,2,3,\ldots$$

Transmitted E-field (normal incidence) exciting the buried wire in the Laplace domain is:

$$E_x^{tr}(s) = \Gamma_{tr}(s)E_x(s)e^{-\gamma d}$$

Incident field and Fresnel transmission coefficient are given by:

$$E_x(t) = E_0\left(e^{-\alpha t} - e^{-\beta t}\right) \qquad E_x(s) = E_0\left(\frac{1}{s+\alpha} - \frac{1}{s+\beta}\right) \qquad \Gamma_{tr}(s) = \frac{2\sqrt{s\varepsilon_0}}{\sqrt{s\varepsilon + \sigma} + \sqrt{s\varepsilon_0}}$$

TD waveform of the E-field excitation is obtained by undertaking discrete (normal) convolution. The FD-AT approach is based on the FD-IDE of Pocklington type:

$$E_x^{tr}(x) = j\omega\frac{\mu}{4\pi}\int_0^L I(x')g(x,x')dx' - \frac{1}{j4\pi\omega\varepsilon_{eff}}\frac{\partial}{\partial x}\int_o^L \frac{\partial I(x')}{\partial x'}g(x,x')dx'$$

where the Green's function and reflection coefficients are given by:

$$g(x,x') = g_0(x,x') - \Gamma_{ref}g_i(x,x') \qquad \Gamma_{ref}^{MIT} = -\frac{\varepsilon_{eff} - \varepsilon_0}{\varepsilon_{eff} + \varepsilon_0}$$

$$\Gamma_{ref}^{Fr} = \frac{\frac{1}{\underline{n}}\cos\theta - \sqrt{\frac{1}{\underline{n}} - \sin^2\theta}}{\frac{1}{\underline{n}}\cos\theta + \sqrt{\frac{1}{\underline{n}} - \sin^2\theta}},\quad \underline{n} = \frac{\varepsilon_{eff}}{\varepsilon_0};\ \theta = \arctan\frac{|x-x'|}{2d}$$

and the complex permittivity and propagation constant are:

$$\varepsilon_{eff} = \varepsilon_r\varepsilon_0 - j\frac{\sigma}{\omega} \qquad \gamma = \sqrt{j\omega\mu\sigma - \omega^2\mu\varepsilon}$$

FD-IDE is handled numerically via GB-IBEM. The matrix equation is:

$$\sum_{j=1}^{M}\left[Z\right]_{ji}\left\{I\right\}_{i}=\left\{V\right\}_{j}$$

where the mutual impedance matrix and voltage vector are:

$$\left[Z\right]_{ji}=-\frac{1}{j4\omega\pi\varepsilon_{eff}}\left[\int_{\Delta l_j}\left\{D\right\}_j\int_{\Delta l_i}\left\{D'\right\}_i^T g\left(x,x'\right)dx'dx+\gamma^2\int_{\Delta l_j}\left\{f\right\}_j\int_{\Delta l_i}\left\{f'\right\}_i^T g\left(x,x'\right)dx'dx\right]$$

$$\left\{V\right\}_j=-j4\pi\omega\varepsilon_0\int_{\Delta l_j}E_x^{inc}(x)\left\{f\right\}_j dx$$

Transient excitation of horizontal buried wire in a lossy medium is governed by TL equations:

TD-TL equations are:

$$\frac{\partial v(x,t)}{\partial x}+Ri(x,t)+L\frac{\partial i(x,t)}{\partial t}=E_x^{tr}(x,t)$$

$$\frac{\partial i(x,t)}{\partial x}+Gv(x,t)+C\frac{\partial v(x,t)}{\partial t}=0$$

and the FD-TL equations are:

$$\frac{\partial U\left(x,\omega\right)}{\partial x}+ZI\left(x,\omega\right)=E_x^{tr}\left(x,\omega\right)$$

$$\frac{\partial I\left(x,\omega\right)}{\partial x}+YU\left(x,\omega\right)=0$$

The solution of FD-TL equations for a horizontal buried wire excited by an external fields is given by:

$$I(x,\omega) = A(\omega)e^{-\Gamma x} + B(\omega)e^{\Gamma x} + \frac{E_x^{tr}(\omega)}{Z(\omega)}$$

where the coefficients, per-unit lenght, are:

$$A(\omega) = \frac{E_x^{tr}(\omega)}{Z(\omega)} \frac{\left(1-e^{\Gamma L}\right)}{\left(e^{\Gamma L} - e^{-\Gamma L}\right)} \qquad B(\omega) = -\frac{E_x^{tr}(\omega)}{Z(\omega)} \frac{\left(1-e^{-\Gamma L}\right)}{\left(e^{\Gamma L} - e^{-\Gamma L}\right)}$$

$$Z(\Gamma(\omega)) \cdot Y(\Gamma(\omega)) = (\Gamma(\omega))^2$$

$$Z(\Gamma) = \frac{j\omega\mu_0}{2\pi}\left[K_0(\gamma_1 a) - K_0(\gamma_1(2d-a)) + I_1(\Gamma)\right]$$

$$Y(\Gamma) = \frac{j2\pi\omega\varepsilon_{eff}}{K_0(\gamma_1 a) - K_0(\gamma_1(2d-a)) + k_1^2 I_2(\Gamma)}$$

$$I_1(\Gamma) = \int_{-\infty}^{+\infty} \frac{\exp(-2u_1 d)}{u_1 + u_2} d\lambda \qquad I_2(\Gamma) = \int_{-\infty}^{+\infty} \frac{\exp(-2u_1 d)}{k_2^2 u_1 + k_1^2 u_2} d\lambda$$

$$u_1 = \left(\lambda^2 - \Gamma^2 - k_1^2\right)^{\frac{1}{2}} = \left(\lambda^2 + \gamma_1^2\right)^{\frac{1}{2}} \qquad u_2 = \left(\lambda^2 - \Gamma^2 - k_2^2\right)^{\frac{1}{2}} = \left(\lambda^2 + \gamma_2^2\right)^{\frac{1}{2}}$$

Some examples for the transient response of a buried wire excited via transient plane wave are now presented.

Wire data:
- Depth d=0.3, 1, 15 m
- Radius a=5 mm
- Length L=1, 20 m

Medium properties:
- Relative permittivity ε_r=10
- Conductivity σ=1, 10, 100 mS/m

Excitation parameters:
- "Bell laboratory" waveform E_0=1 V/m, α=4·106 s^{-1}, β=4.78·108 s^{-1}

Distribution of RMS value of the transient current:

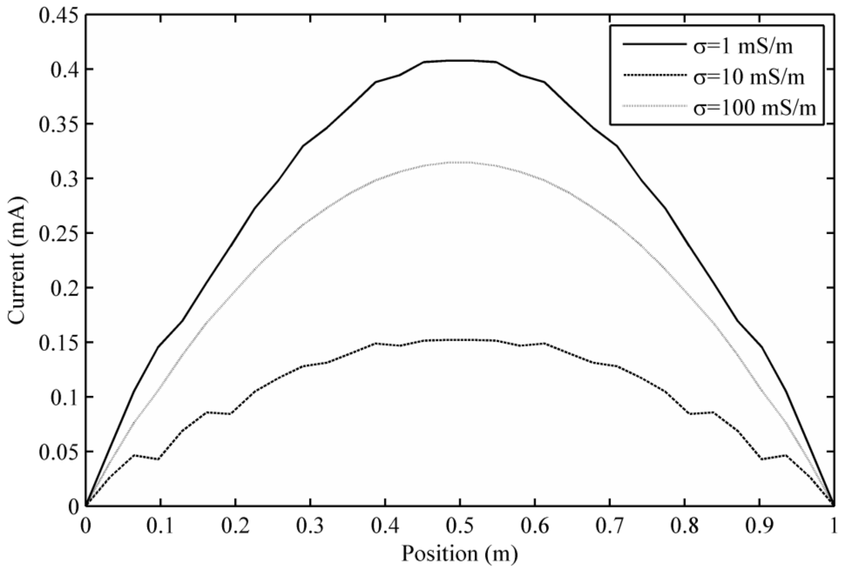

L=20 m, σ=1 mS/m

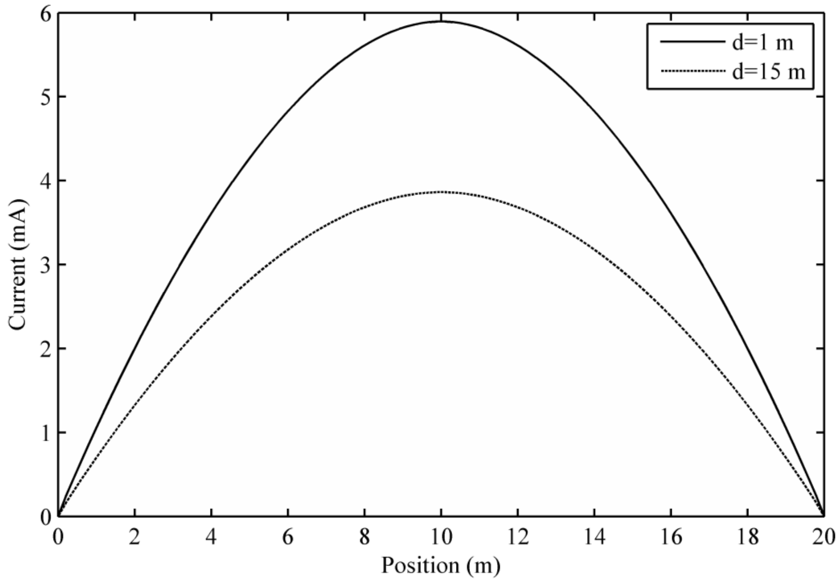

L=1 m, d=30 cm

Transient current at the center of the buried wire, for different values of the conductivity

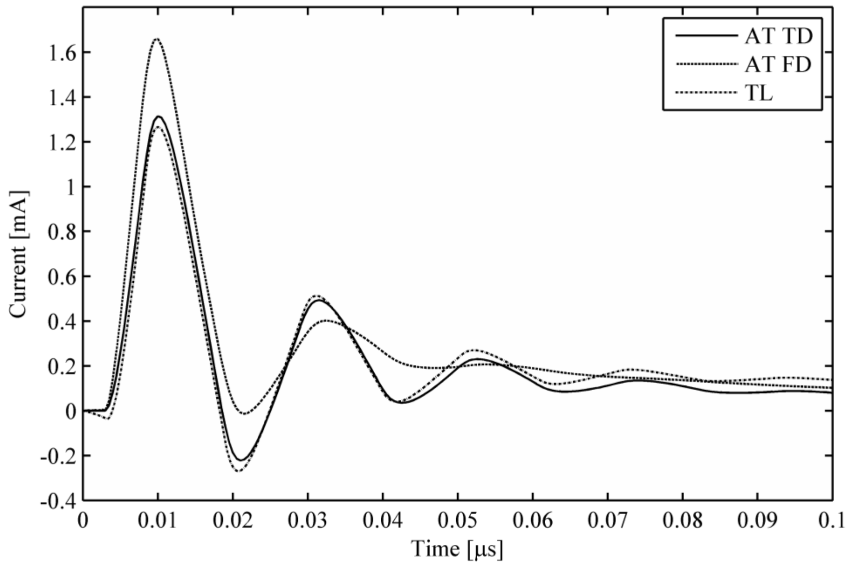

L=1 m, d=30 cm, σ=10 mS/m

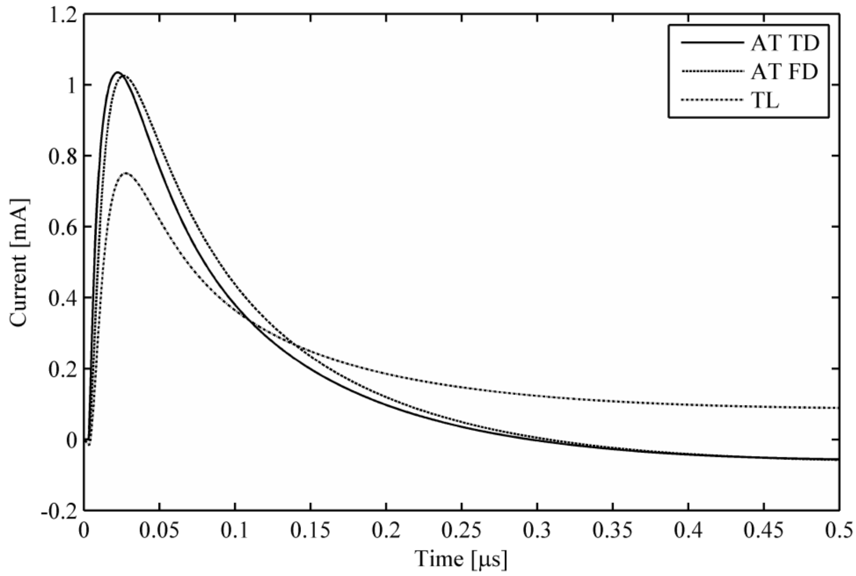

L=1 m, d=30 cm, σ=100 mS/m

Transient current at the center of the straight buried wire, for different values of the burial depth:

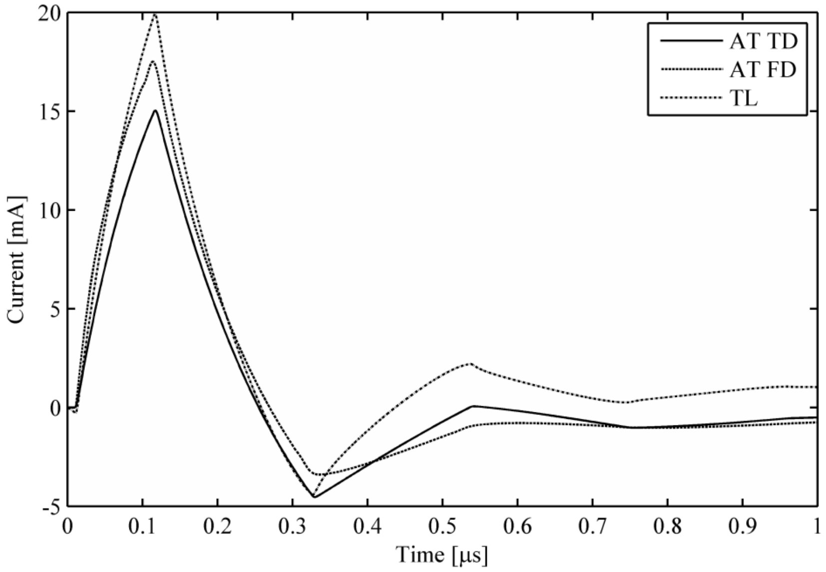

L=20 m, *d*=1 m, *σ*=1 mS/m

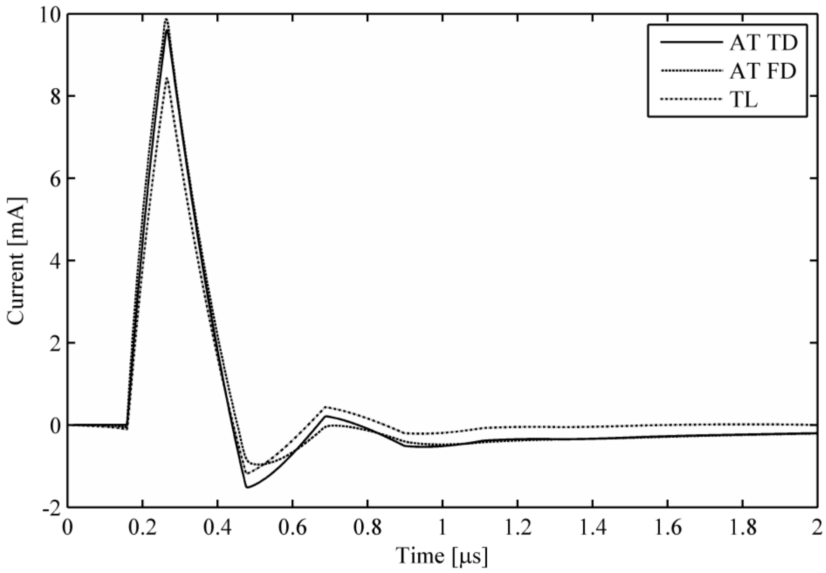

L=20 m, *d*=15 m, *σ*=1 mS/m

Transient current at the center of the wire buried at different depths:

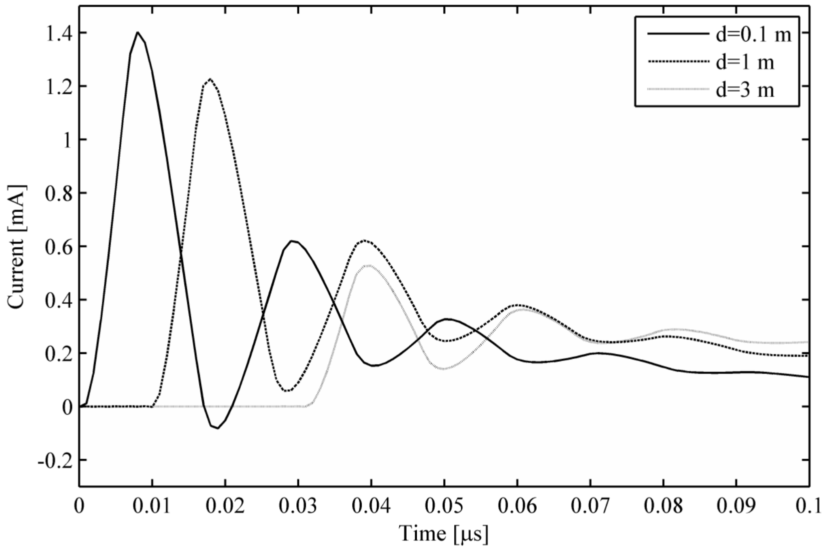

L=1 m, σ=10 mS/m

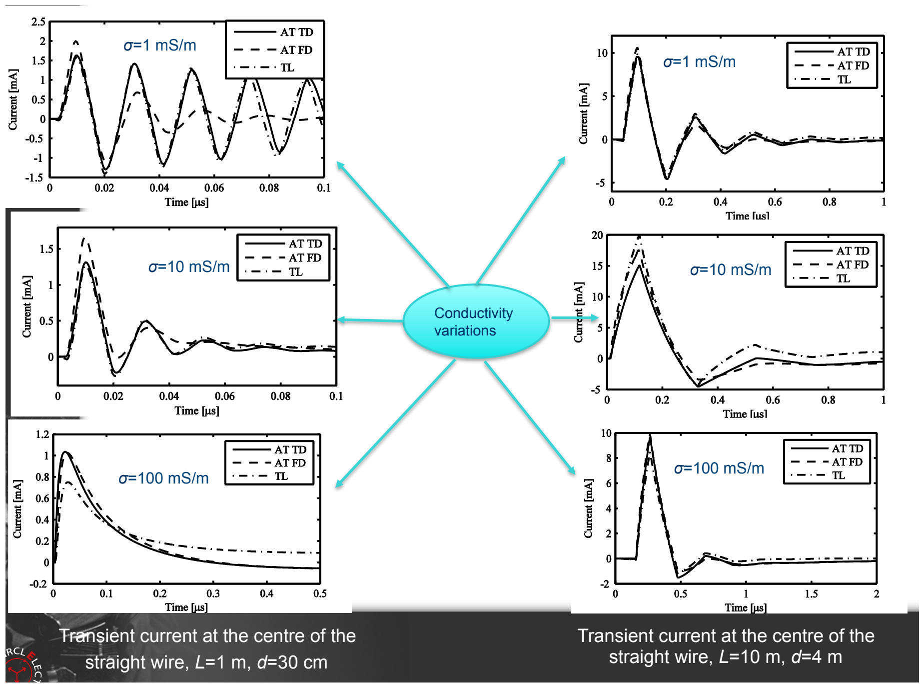

4. Frequency-domain modelling: previous work

Full wave model – the most rigorous approach to analyze the EM field coupling to realistic 3D objects

Formulation - set of the FD Electric Field Integral Equations (EFIEs)

Numerical solution: an efficient Method of Moments (MoM) scheme featuring the use of RWG base functions

The method was applied to the modeling of the human brain exposed to EM radiation, and o study transcranial magnetic stimulation.

5. Frequency-domain modelling: ongoing work

Full wave model – the most rigorous approach to analyze the EM field coupling to buried 3D objects

Formulation - set of the FD Surface Integral Equations (SIEs)

Numerical solution: an efficient Method of Moments (MoM) scheme featuring the use of RWG base functions

FD-SIE formulation:

Equivalence theorem + boundary conditions for *E*-field on the object surface give:

$$-\hat{n} \times \vec{E}_i^{sca}(\vec{J}, \vec{M}) = \begin{cases} \hat{n} \times \vec{E}^{inc}, & i = 1 \\ 0, & i = 2 \end{cases}$$

where:

$$\vec{E}_i^{sca}(\vec{J}, \vec{M}) = -j\omega \vec{A}_i - \nabla \varphi_i - \frac{1}{\varepsilon_i} \nabla \times \vec{F}_i$$

$$\vec{A}_i(\vec{r}) = \mu_i \iint_S \vec{J}(\vec{r}\,')G_i(\vec{r},\vec{r}\,')\,\mathrm{d}S'$$

$$\vec{F}_i(\vec{r}) = \varepsilon_i \iint_S \vec{M}(\vec{r}\,')G_i(\vec{r},\vec{r}\,')\,\mathrm{d}S'$$

$$\varphi_i(\vec{r}) = \frac{1}{\varepsilon_i} \iint_S \rho(\vec{r}\,')G_n(\vec{r},\vec{r}\,')\,\mathrm{d}S'$$

$$G_i(\vec{r},\vec{r}\,') = \frac{e^{-jk_iR}}{4\pi R}; \quad R = |\vec{r}-\vec{r}\,'|. \qquad k_i = \omega\sqrt{\mu_i\varepsilon_i}$$

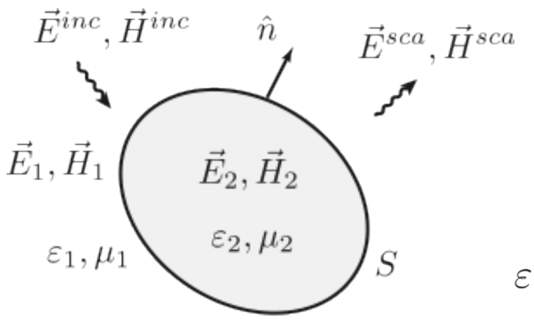

$$\varepsilon_2 = \varepsilon_0\varepsilon_r - j\frac{\sigma}{\omega}$$

Geometry of a dielectric object.

The formulation is based on a set of coupled Surface Integral Equations (SIE) in terms of fictitious unknown surface current densities **J** and **M**

$$j\omega\mu_i \iint_S \vec{J}(\vec{r}\,')G_i(\vec{r},\vec{r}\,')\,\mathrm{d}S' - \frac{j}{\omega\varepsilon_i}\nabla \iint_S \nabla'_S \cdot \vec{J}(\vec{r}\,')G_i(\vec{r},\vec{r}\,')\,\mathrm{d}S' + \\ + \nabla\times \iint_S \vec{M}(\vec{r}\,')G_i(\vec{r},\vec{r}\,')\,\mathrm{d}S' = \begin{cases} \vec{E}^{inc}, & i=1 \\ 0, & i=2. \end{cases}$$

Numerical solution is carried out via an efficient scheme of Method of Moments. Surface currents are expanded in terms of basis functions f_n and g_n. Then, multiplying SIE by set of test functions f_m, and integrating over surface S, a system of linear equations is obtained.

$$\vec{f}_n^{\pm}(\vec{r}) = \begin{cases} \dfrac{l_n}{2A_n^{\pm}}\vec{\rho}_n^{\pm} & ,\vec{r} \in T_n^{\pm} \\ 0 & ,\vec{r} \notin T_n^{\pm} \end{cases} \qquad \vec{g}_n = \hat{n} \times \vec{f}_n$$

$$\begin{aligned}
& j\omega\mu_i \sum_{n=1}^{N} J_n \iint_S \vec{f}_m(\vec{r}) \cdot \iint_{S'} \vec{f}_n(\vec{r}\,')G_i \, dS' \, dS+ \\
& +\frac{j}{\omega\varepsilon_i} \sum_{n=1}^{N} J_n \iint_S \nabla_S \cdot \vec{f}_m(\vec{r}) \iint_{S'} \nabla'_S \cdot \vec{f}_n(\vec{r}\,')G_i \, dS' \, dS+ \\
& \quad \pm \sum_{n=1}^{N} M_n \iint_S \vec{f}_m(\vec{r}) \cdot [\hat{n} \times \vec{g}_n(\vec{r}\,')] \, dS+ \\
& \quad + \sum_{n=1}^{N} M_n \iint_S \vec{f}_m(\vec{r}) \cdot \iint_{S'} \vec{g}_n(\vec{r}') \times \nabla' G_i \, dS' \, dS = \\
& \qquad\qquad = \begin{cases} \displaystyle\iint_S \vec{f}_m(\vec{r}) \cdot \vec{E}^{inc} \, dS & ,i = 1 \\ 0 & ,i = 2 \end{cases}
\end{aligned}$$

The system of linear equations can be rewritten as follows:

$$\begin{aligned}
& \sum_{n=1}^{N} \left(j\omega\mu_i A_{mn,i} + \frac{j}{\omega\varepsilon_i} B_{mn,i} \right) J_n + \\
& \qquad + \sum_{n=1}^{N} \left(C_{mn,i} + D_{mn,i} \right) M_n = \begin{cases} V_m & ,i = 1 \\ 0 & ,i = 2. \end{cases}
\end{aligned}$$

The integrals A_{mn}, B_{mn}, C_{mn}, D_{mn} are efficiently solved by numerical, analytical and combined approach.

The following computational example is related to electric field scattered by a buried dielectric sphere. The calculated results were compared to the results obtained by using some commercial software packages. A satisfactory agreement has been achieved.

Sphere : $r = 3$ cm , $\varepsilon_{r2} = 2$, $\sigma = 0$
Ground (dry soil) : $\varepsilon_{r1} = 4$, $\sigma = 5$ mS/m
Incident field : $E_0 = 1$ V/m, $f = 2.45$ GHz, $k = -\hat{e_z}$, $E_{pol} = \hat{e_y}$

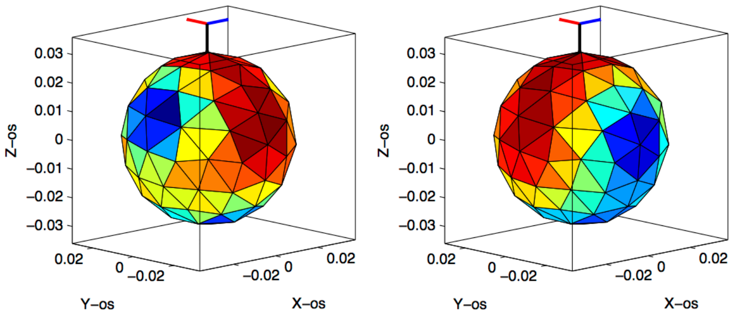

Calculated equivalent surface currents **J** and **M**

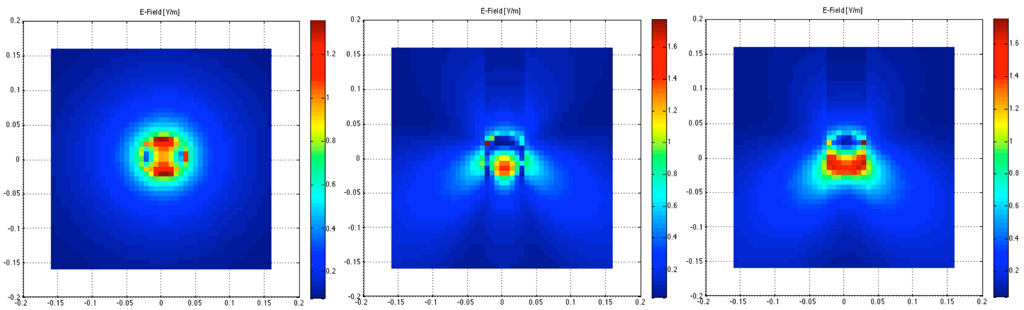

Electric field distribution in *X-Y*, *X-Z*, *Y-Z* plane, respectively

Conclusions

TD and FD methods for the analysis of scattering from buried objects were presented. Transient response of a horizontal straight thin wire buried in a lossy half-space was analysed using TD-AT approach, featuring the approximate analytical solution. Analytical results obtained via TD-AT approach were compared to the numerical results obtained via the FD-AT and FD-TL models, with good agreement. An efficient FD-SIE apprach to the analysis of scattering from buried lossy dielectric object was presented. Using an efficient MoM scheme we solved the corresponding SIE set. Some numerical results for the scattering from a lossy dielectric sphere were presented. Future work will deal with the direct TD analysis of wire antenna configurations for GPR.

Acknowledgement - The authors acknowledge the COST Action TU1208 "Civil Engineering Applications of Ground Penetrating Radar".

"Wire-grid electromagnetic modelling of 2D metallic objects with arbitrary cross-section" (contribution to Project 3.1)

Lara Pajewski (IT), Saba Adabi (IT)
lara.pajewski@uniroma3.it

The abstract is published in *Geophysical Research Abstracts*, Vol. 16, EGU2014-13992, 2014 and is available on *www.egu2014.eu*

This work dealt with the wire-grid modelling of metallic cylindrical objects, with a particular focus to GPR applications, and it was presented as a poster.

Two-dimensional cylinders, with arbitrary section, were simulated through a suitable set of perfectly-conducting wires; results were obtained by using the Finite-Difference Time-Domain technique [1].

Wire-grid modelling of conducting objects was introduced by Richmond in 1966 [2] and, since then, the method has been extensively used over the years to simulate arbitrarily-shaped objects and compute radiation patterns of antennas, as well as the electromagnetic field scattered by targets. For any wire- grid model, a better accuracy can be achieved with a larger number of wires; moreover, a fundamental question is the choice of the optimum wire radius and grid spacing. The most widely used criterion to fix the wire size is the so-called equal-area rule (EAR) [3, 4]: the total surface area of the wires has to be equal to the surface area of the object being modelled. This rule comes from empirical observation and few authors have investigated its reliability for 2D objects through the years [5, 6].

We analysed the reliability of the EAR, showing that it yields affordable results but is quite far from being the optimum: higher accuracy can be achieved by using a wire radius 12-15% shorter than what is suggested by the rule. We considered circular- and square-section scatterers embedded in a half-space, as well as objects partially buried in different media of a multilayered structure or soil; the electromagnetic source was always a line of current emitting an ultra-wide band pulse. Our results are in good agreement with [5], where the wire-grid modelling of a circular-section cylinder, buried in a half-space and illuminated by a monochromatic plane wave, was studied.

We investigated as well the possibility to apply the wire-grid approach to the simulation of buried slotted objects. In case of small slots, the wire-grid results follow quite well the main reflections of the exact results, but with some delay. More accurate results can be obtained for larger slots. To model thick objects with large slots, it is recommended to use two concentric arrays of wires, simulating both the inner and outer sections of the scatterer.

The wire-grid approach can significantly enhance the versatility of those electromagnetic methods which can deal only with scatterers having a canonical shape of the cross-section, embedded in a homogeneous material (e.g., the Cylindrical Wave Approach [7]). Outside from the Ground Penetrating Radar field, our study may be useful for shielding applications [8], and in the measurement of electromagnetic properties of materials through the use of coaxial cages [9].

The wire-grid modelling of slotted objects, at the best of our knowledge, hasn't been studied by other authors and we plan to explore it more in depth. Finally, we look forward to analysing the reliability of the same-volume rule [10], for the modelling of dielectric two-dimensional objects by small dielectric circular-section cylinders.

ACKNOWLEDGEMENT

The authors are grateful to COST for funding the Action TU1208 "Civil Engineering Applications of Ground Penetrating Radar", supporting the Second General Meeting and this work.

REFERENCES

[1] A. Giannopoulos, "Modelling ground penetrating radar by GprMax," *Construction and Building Materials*, vol. 19, 2005, pp. 755–762.
[2] J. H. Richmond, "A wire-grid model for scattering by conducting bodies," *IEEE Trans. Antennas Propagat.,* vol. 14, 1966, pp. 782–786.
[3] A.C. Ludwig, "Wire grid modeling of surfaces," *IEEE Trans. Antennas Propagat.,* vol. 35, 1987, pp.1045–1048.
[4] R.J. Paknys, "The near field of a wire grid model," *IEEE Trans. Antennas Propagat.*, vol. 39, 1991, pp. 994–999.
[5] F. Frezza, L. Pajewski, C. Ponti, G. Schettini, "Accurate wire-grid modelling of buried conducting cylindrical scatterers," *Nondestructive Testing and Evaluation*, vol. 27, 2012, pp. 199–207.

[6] P. A. Martin, "On acoustic and electric Faraday cages," *Proc. Royal Society*, vol. 470, 2014, 20140344.
[7] M. Di Vico, F. Frezza, L. Pajewski, G. Schettini, "Scattering by a finite set of perfectly conducting cylinders buried in a dielectric half-space: a spectral-domain solution," *IEEE Trans. Antennas Propagat.*, vol.53, 2005, pp. 719–727.

[8] Celozzi, R. Araneo, G. Lovat, "Electromagnetic shielding," *Wiley-IEEE Press*, 2008.
[9] E. Mattei, S. E. Lauro, E. Pettinelli, G. Vannaroni, "Coaxial-Cage Transmission Line for Electromagnetic Parameters Estimation," *IEEE Transactions on Instrumentation and Measurements,* vol. 62, 2013, pp. 2938-2942.
[10] A. Z. Elsherbeni, A. A. Kishk "Modeling of cylindrical objects by circular dielectric and conducting cylinders," *IEEE Transactions on Antennas and Propagation*, 40, 96–99, 1992.

"DETECTION OF LIMESTONE SETTLING IN A WATER TUBE EMBEDDED IN A CEMENT" (CONTRIBUTION TO PROJECT 3.1)

Fabrizio Frezza (IT), Fabio Mangini (IT), Carlo Santini (IT), Endri Stoja (IT), Nicola Tedeschi(IT) - *fabio.mangini@diet.uniroma1.it*

Abstract

The electromagnetic scattered field by a buried pipeline is calculated by means of frequency-domain numerical simulations and by making use of the scattered-field formulation. The pipeline, supposed to be used for water conveyance, is modeled as a cylindrical shell made of poly-vinyl chloride (PVC) material buried in a wall or pavement composed of cement with very low losses and filled with water. In order to make the model simpler, the pipeline is supposed running parallel to the air-cement interface. To excite the model, a linearly-polarized plane wave impinging normally on the above-mentioned interface is adopted. We consider two different polarizations in order to determine the most useful in terms of scattered-field sensitivity. Moreover, a preliminary frequency sweep allows us to choose the most suitable operating frequency depending on the dimensions of the pipeline cross-section. All the three components of the scattered field are monitored along a line just above the interface.

The electromagnetic properties of the materials employed in this study are present in the literature and, since a frequency-domain technique is adopted, no further approximation is needed. Once the ideal problem has been studied, we further complicate the model by introducing two fouling scenarios due to limestone formation on the pipeline walls. In the first case, the fouling is deposited at the bottom of the pipeline when the water pressure is low enough and the second one considers the fouling to deposit on the entire internal perimeter of the pipeline's cross-section by forming an additional limestone cylindrical layer. The results obtained in these cases are compared with those of the initial problem with the goal of determining the scattered field dependency on the fouling geometrical characteristics. One of the practical applications in the field of Civil Engineering of this study may be the use of ground penetrating radar (GPR) techniques to monitor the fouling conditions of water pipelines without the need to intervene destructively in the structure.

See also *Geophysical Research Abstracts*,
Vol. 16, EGU2014-13008, 2014 available on *www.egu2014.eu*

1. THEORETICAL ANALYSIS

The first structure under consideration is a buried cylinder, with a cover in PVC (PolyVinyl Chloride), filled by freshwater, with a layer, between the water and the PVC cover, of limestone, see Fig. 1. From an electromagnetic point of view, the problem can be studied as a multilayer cylinder buried in a half-space.

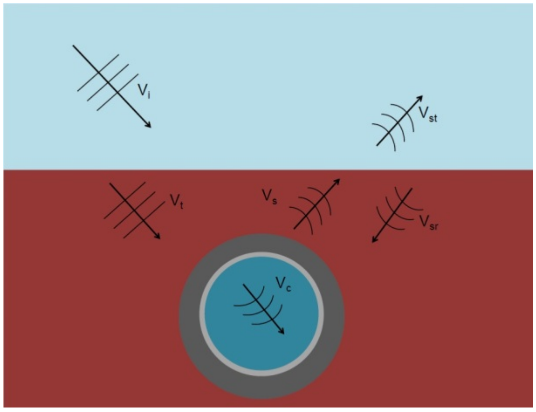

Figure 1: Geometry of the problem with concentric cylinders.

We consider an electromagnetic plane wave, coming from air, impinging on the interface with a cement, having a relative permittivity ε_C = 5.24. Inside the cement, at a distance h = 250.0 mm, is a cylinder of radius a = 125.0 mm, composed of three layers. The external layer, of thickness a_{PVC} = 14.8 mm, is filled by PVC, with electromagnetic relative permittivity ε_{PVC} = 3.10. The second layer, of thickness a_L, is filled by limestone, with electromagnetic relative permittivity ε_L = 8.01 and electric conductivity σ_L = 0.10 S/m. We consider different thickness of the limestone, between 0.0 mm, and 36.8 mm, in order to understand the behavior of the electromagnetic interaction as a function of this parameter. Finally, the last layer, i.e., the core of the cylinder, is filled by freshwater, with electromagnetic relative permittivity ε_W = 81.00 and electric conductivity σ_W = 0.01 S/m. The frequency range under consideration is f = 10.0 ÷120.0 MHz. We suppose that the relative permittivity and the electric conductivity do not change in the frequency range, i.e., we consider non dispersive materials. It is important to note

that, while the conductivity of the media does not change with the frequency, the wave attenuation does. In fact, as it is well known, the attenuation is related to the conductivity, but it is also proportional to the frequency.

The principal aim of this investigation is to understand how the electromagnetic scattering by this cylinder is affected by the presence of the limestone layer, in order to find some indications on the crucial parameters to take into account for the detection of the limestone residues in a water tube. To implement this analysis, we consider a decomposition of the electromagnetic field. Each field will be taken into account as the superposition of two different polarizations, in order to consider the general case of circular polarization. We refer to each polarization with a scalar function V, that would represents the electric or the magnetic field parallel to the cylinder's axis, depending on the polarization. We consider an electromagnetic plane wave, coming from the air, V_i, this field is transmitted in the cement half-space, where we find a second plane wave V_t, obtained from the incident one by the multiplication times the Fresnel coefficient of the relevant polarization. This field interacts with the cylinder, generating the scattered field V_s, and penetrating inside the cylinder, generating the field V_c. The scattered field interacts with the interface, generating other two fields: the scattered-reflected field and the scattered-transmitted field, V_{sr} and V_{st}, respectively [1-5]. Moreover, the internal field to the cylinder, can be decomposed in three different fields, one in the PVC, one in the limestone and the final one in the freshwater. To solve the electromagnetic scattering problem, we have to expand all the fields in cylindrical harmonics, in order to impose the boundary conditions on each layer of the cylinder. This procedure bring us to define a linear system which solution gives all the unknown coefficients of the cylindrical harmonic expansions. At this point we are able to calculate the scattered-transmitted field, which is the field that a receiver measures outside the cement layer.

After the analysis of the multilayer cylinder, we study another interesting case. We consider a PVC cylinder filled by water, where the limestone stratification is only on the bottom part of the pipeline, see Fig. 2. This case of study is to represent that the limestone usually settling only in the bottom part of the pipeline. From an electromagnetic point of view, we can consider the limestone deposition as an eccentric cylinder, with the center at a small distance below the center of the principal cylinder.

The problem of the scattering by two or more eccentric cylinders has been widely discussed in the literature, and it can be faced by mean of different numerical techniques [6-8]. The field decomposition outside the external cylinder is the same of the previous case. Inside the cylinders, the fields in the PVC layers and in the water core must be decomposed in cylindrical harmonics centered in the reference frame of the eccentric limestone cylinder, in order to apply the boundary conditions on its surface. In the same way, the field in the limestone layer must be decomposed in cylindrical harmonics centered in the reference frame of the external cylinder, in order to apply the boundary conditions on the external surface.

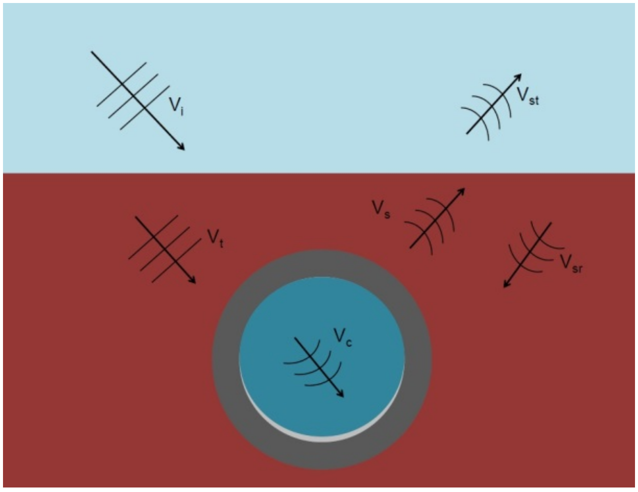

Figure 2: Geometry of the problem with eccentric cylinders.

2. Numerical Results

The first result that we show is related to the case of the PVC pipeline with a freshwater core and without the limestone layer. This case can be taken into account by considering a_L = 0.0 mm. We consider the plane wave at normal incidence, along the x-axis. Therefore, the x-component of the electric field will be zero for both the polarizations. The cylinder axis coincides with the z-axis. In Fig. 3, the amplitude of the scattered-

transmitted field on the interface, for both the polarizations, is shown, in the whole frequency range. It can be seen that the E-polarization backscattering grows in frequency, while the H-polarization is almost constant and start to grow in the last part of the frequency range. The most interesting frequency is around f = 100.0 MHz, where, the E-polarization presents a maximum, and the H-polarization presents a minimum.

At this point, we consider this value of the frequency and analyze the scattering by the cylinder for different thickness of the limestone layer, in the hypothesis of concentric cylinders. In Fig. 4, we can see the amplitude of the electric field, for both the polarizations. The two polarizations respond in two opposite ways to the growing of the limestone thickness. The backscattering in E-polarization decrease by increasing a_L, while the backscattering in H-polarization increase by increasing the limestone thickness.

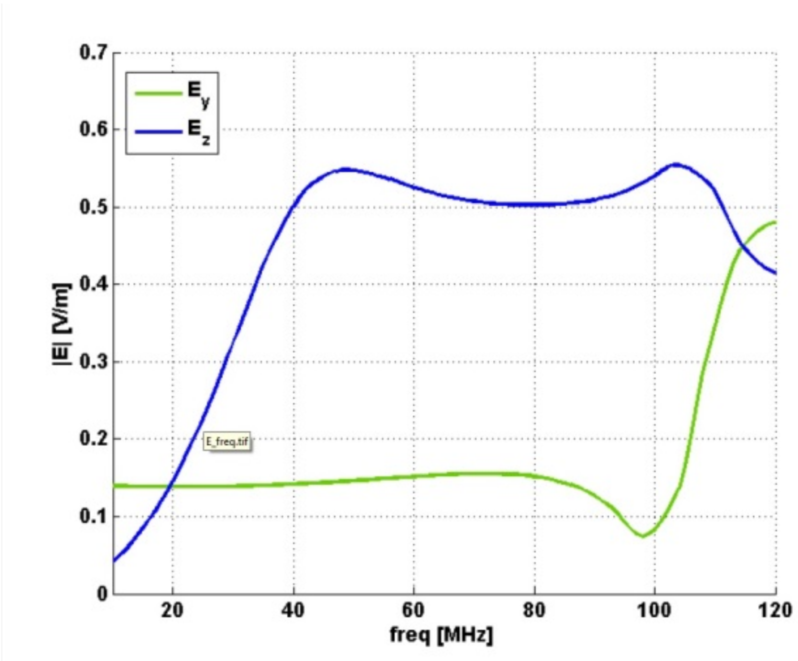

Figure 3: Amplitude of the electric field components in the two polarizations in the whole frequency range.

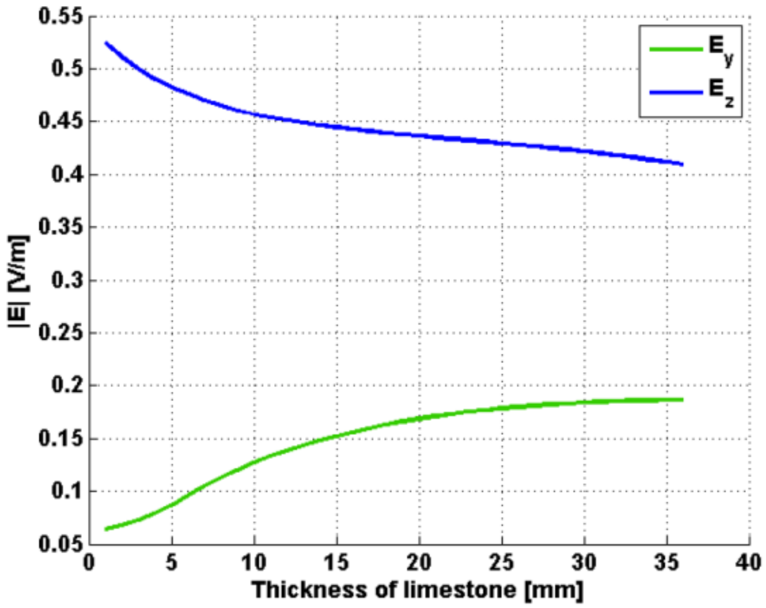

Figure 4: Amplitude of the electric field components as a function of the limestone thickness, in the hypothesis of concentric layers.

We can find a simple physical explanation to these two opposite behaviors. In E-polarization, the electric field, being parallel to the cylinder axis, is principally affected by the freshwater content, due to the high permittivity of the water. When the limestone layer grows in thickness, the quantity of the water decrease, and as a consequence also the backscattering for this polarization decreases. On the other hand, in H-polarization, the electric field is on the plane of the cylinder section. Therefore, the backscattering is driven by the capacitance effects. The effective capacitance of the cylinder section grows by increasing the limestone thickness and, as a consequence, also the backscattering increases.

In Fig. 5, we consider the case of a limestone settling. We can see that the electric fields response is approximately the same of Fig. 4. Therefore, the hypothesis of a uniform deposition is a good approximation of the case of the deposition in the bottom part of the pipeline.

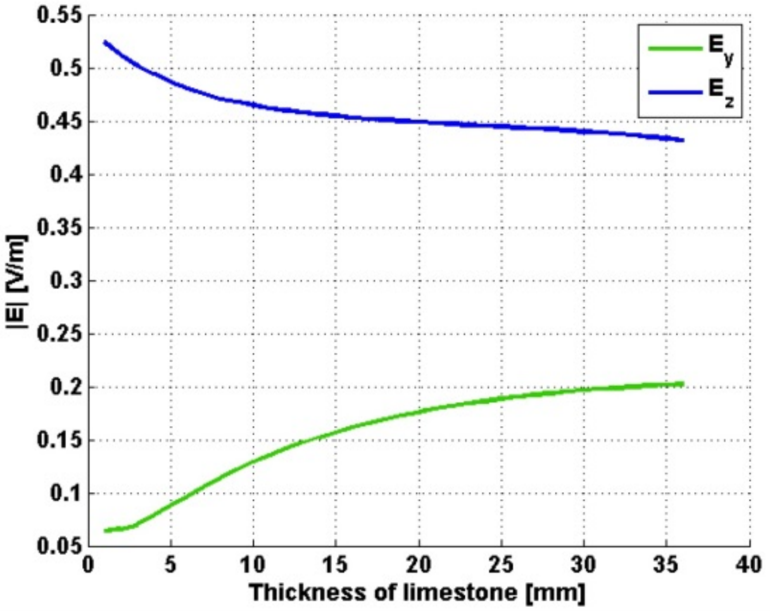

Figure 5: Amplitude of the electric field components as a function of the limestone thickness, in the hypothesis of eccentric layers.

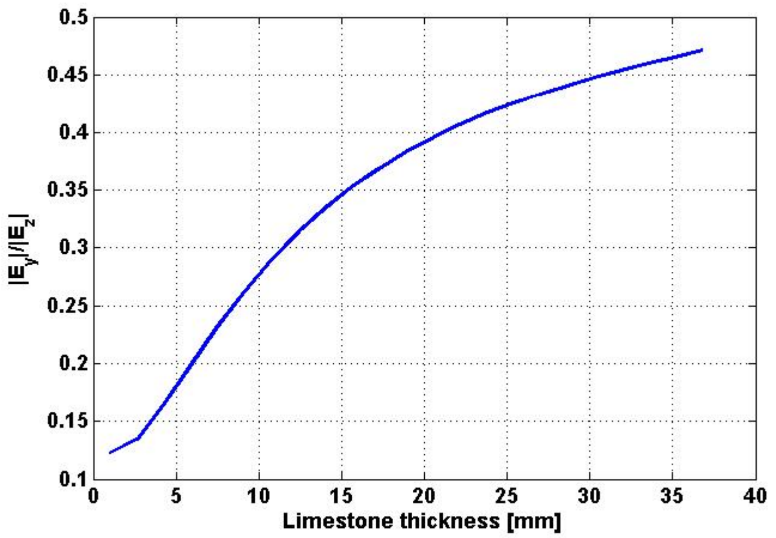

Figure 6: Ratio between the magnitudes of the backscattering electric field in the two polarizations for cylinder relevant to Fig. 4.

This behavior of the two polarizations suggests to consider as an index of the limestone thickness, the ratio between the backscattered field magnitudes in the two polarizations: $e = |E_y|/|E_z|$. This parameter grows with the limestone thickness in both the case of a homogeneous deposition of the limestone around the inner surface of the PVC cover, see Fig. 6, and in the case of a deposition of the limestone on the bottom part of the pipeline, see Fig. 7. By knowing the tube transverse dimension and its orientation, it is possible to derive the standard value of the e coefficient. Measuring the backscattering field in both polarizations, it is possible to compare the value of the parameter e in order to obtain an estimation of the limestone thickness. This result is important because we are considering a thickness many times smaller than the wavelength.

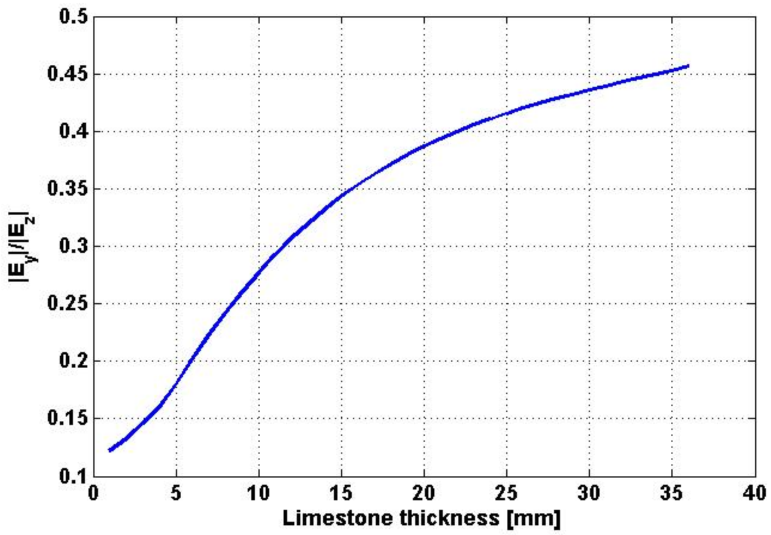

Figure 7: Ratio between the amplitudes of the backscattering electric field in the two polarizations for cylinder relevant to Fig. 5.

3. Conclusions

In the present paper, we analyzed the scattering of a plane wave by a buried circular pipeline made by a PVC cover and a freshwater core. In this study, we considered the presence of a limestone layer between the

water and the PVC. We performed a frequency sweep in order to find the frequency for which the ratio between the responses to the two different polarizations was maximum. At this particular frequency, we considered the backscattering magnitudes as functions of the limestone thickness in two cases: a homogeneous layer of limestone all around the inner surface of the PVC cover, and a settling of the limestone on the bottom of the pipeline. In both cases, we found an opposite behavior of the responses of the two polarizations: when the electric field is parallel to the cylinder axis, the backscattering decreases with the limestone thickness, while, when the magnetic field is parallel to the cylinder axis, the backscattering increases with such thickness. From these results, we proposed the ratio between the magnitudes of the backscattering in the two polarizations as an index to obtain the limestone thickness in the pipeline. Future works will consider an investigation on the index behavior at different frequencies and its validation for other kinds of materials.

REFERENCES

[1] M. Di Vico, F. Frezza, L. Pajewski, and G. Schettini, "Scattering by buried cylindrical structures," Radio Sci., Vol. 40, RS6S18, (11 pp.), 2005.
[2] S.C. Lee, "Scattering by closely spaced parallel nonhomogeneous cylinders in an absorbing medium," J. Opt. Soc. Am. A, Vol. 28, No. 9, pp. 1812-1819, 2011.
[3] F. Frezza, L. Pajewski, C. Ponti, G. Schettini, and N. Tedeschi, "Cylindrical-Wave Approach for electromagnetic scattering by subsurface metallic targets in a lossy medium," J. Appl. Geophys., Vol. 97, pp. 55-59, 2013.
[4] F. Frezza, F. Mangini, M. Muzi, C. Santini , E. Stoja, and N. Tedeschi, "Sphygmic stress diagnosis in arterial blood vessels by electromagnetic radiation scattering," Proceedings of the 2013 World Congress on Advances in Nano, Biomechanics, Robotics, and Energy Research (ANBRE13), Seoul, South Korea, 25-28 August 2013.
[5] F. Frezza, F. Mangini, E. Stoja, and N. Tedeschi, "Effects on the Electromagnetic Scattering of a Plane Wave due to the Surface Roughness of a Buried Perfectly Conducting Pipeline," Geophysical Research Abstracts, Vol. 15, EGU2013, Vienna, Austria, April 2013.
[6] J.A. Roumeliotis, J.G. Fikioris, and G.P. Gounaris, "Electromagnetic scattering from an eccentrically coated infinite metallic cylinder," Appl. Phys., Vol. 51, No. 8, pp. 4488- 4494, 1980.

[7] A.A. Kishk, R.P. Parrikar, and A.Z. Elsherbeni, "Electromagnetic scattering from an eccentric multilayered circular cylinder," IEEE Trans. Antennas Propag., Vol. 40, No. 3, pp. 295-303, 1992.
[8] A.J. Yuffa, P.A. Martin, and J.A. Scales, "Scattering from a large cylinder with eccentrically embedded core: An orders-of-scattering approximation," J. Quant. Spectrosc. Radiat. Transfer, Vol. 133, No. 1, pp. 520-525, 2014.

ACKNOWLEDGEMENT

The authors acknowledge the COST Action TU1208 "Civil Engineering Applications of Ground Penetrating Radar", supporting this work.

"Rigorous and asymptotic models of coherent scattering from random rough layers with applications to roadways and geoscience" (Contribution to Project 3.1)

Nicolas Pinel (FR), Christophe Bourlier (FR), Cédric Le Bastard (FR)
nicolas.pinel@alyotech.fr

The abstract is published in *Geophysical Research Abstracts*, Vol. 16, EGU2014-12342, 2014 and is available on *www.egu2014.eu*

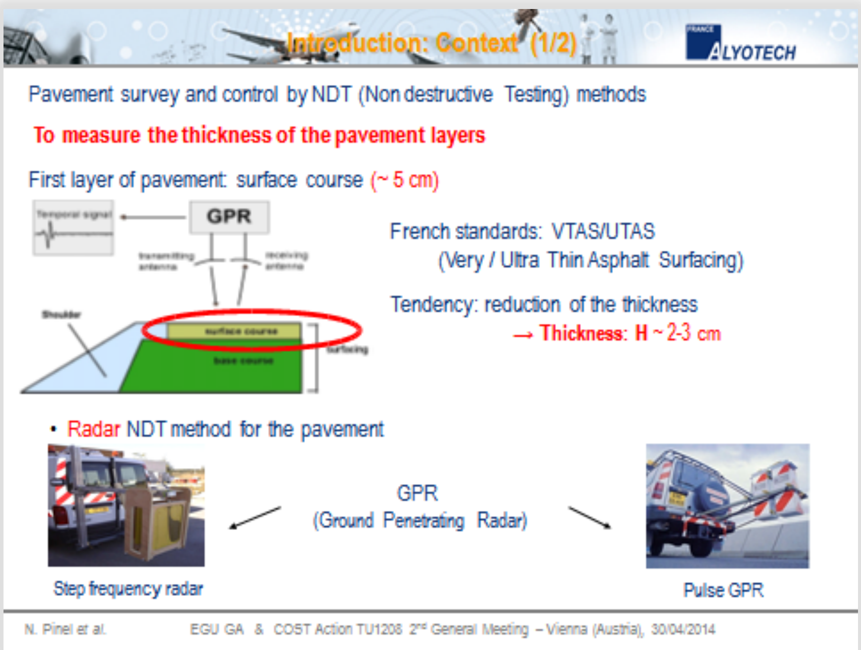

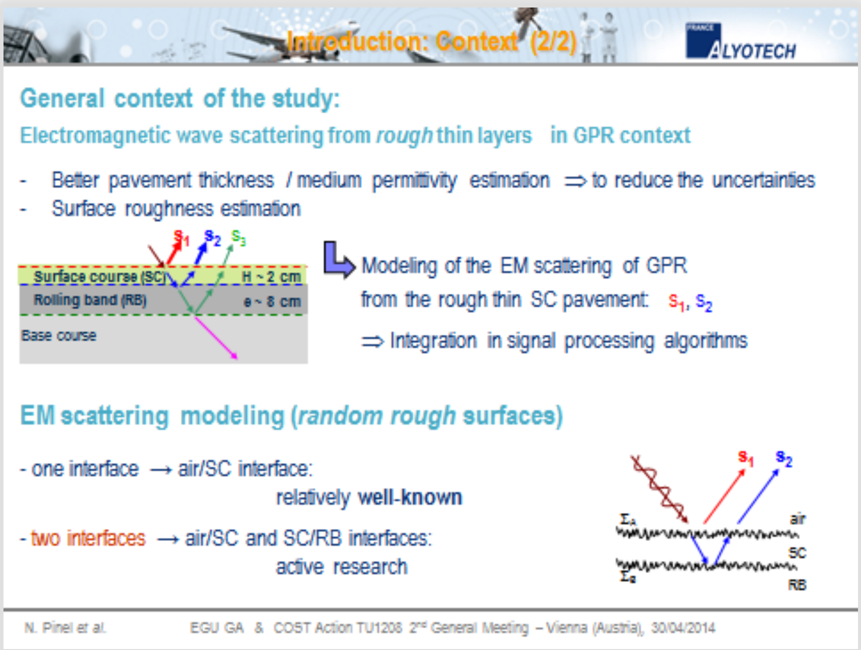
Introduction: Context (2/2)
ALYOTECH
General context of the study:
Electromagnetic wave scattering from *rough* thin layers in GPR context
- Better pavement thickness / medium permittivity estimation ⇒ to reduce the uncertainties
- Surface roughness estimation
Surface course (SC)
H ~ 2 cm
Rolling band (RB)
e ~ 8 cm
Base course
Modeling of the EM scattering of GPR
from the rough thin SC pavement: s_1, s_2
⇒ Integration in signal processing algorithms
EM scattering modeling (*random rough* surfaces)
- one interface → air/SC interface:
relatively **well-known**
- two interfaces → air/SC and SC/RB interfaces:
active research
air
SC
RB
N. Pinel et al.
EGU GA & COST Action TU1208 2nd General Meeting – Vienna (Austria), 30/04/2014

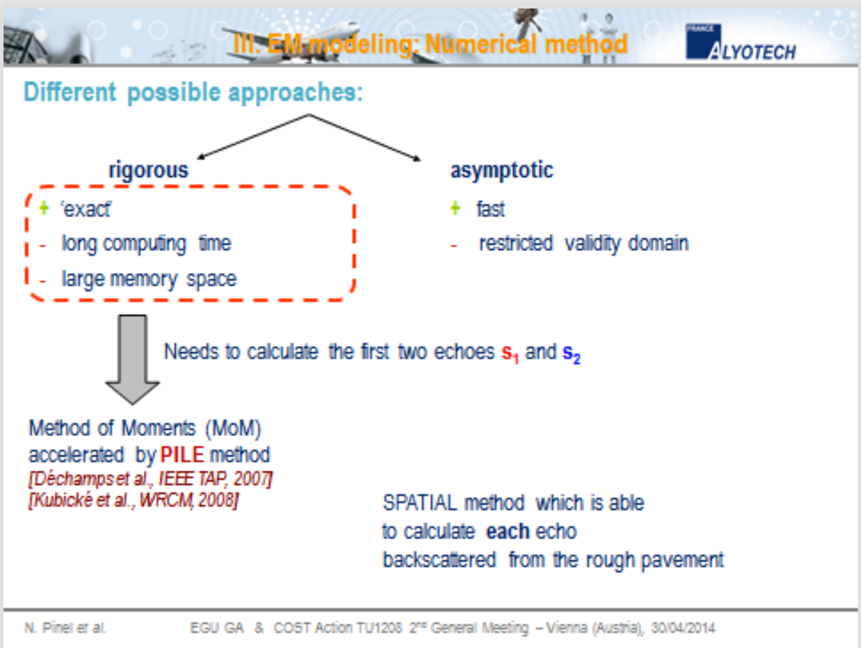
III. EM modeling: Numerical method
ALYOTECH
Different possible approaches:
rigorous
+ 'exact'
- long computing time
- large memory space
asymptotic
+ fast
- restricted validity domain
Needs to calculate the first two echoes s_1 and s_2
Method of Moments (MoM)
accelerated by PILE method
[Déchamps et al., IEEE TAP, 2007]
[Kubické et al., WRCM, 2008]
SPATIAL method which is able
to calculate **each** echo
backscattered from the rough pavement
N. Pinel et al.
EGU GA & COST Action TU1208 2nd General Meeting – Vienna (Austria), 30/04/2014

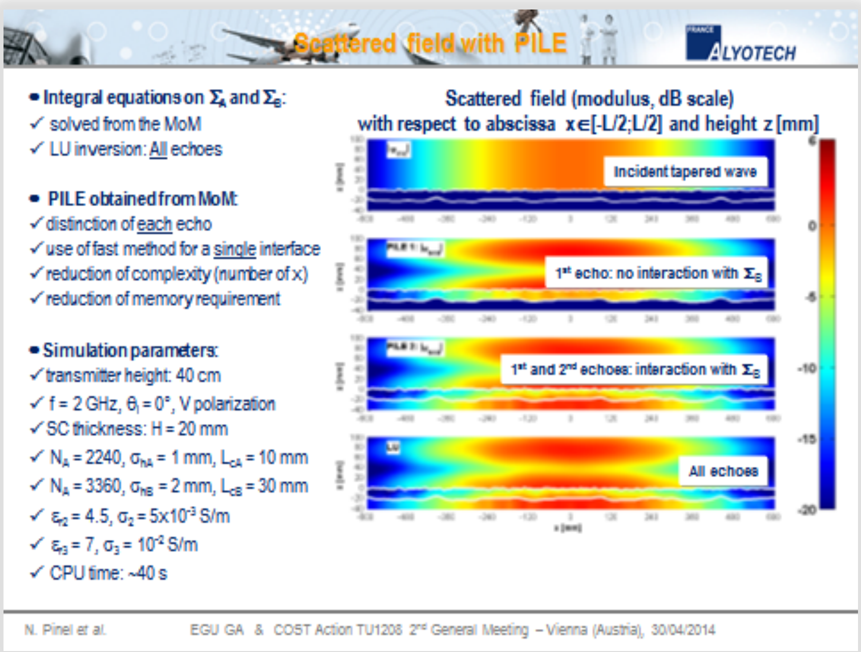
Scattered field with PILE
ALYOTECH
• Integral equations on Σ_A and Σ_B:
✓ solved from the MoM
✓ LU inversion: All echoes
• PILE obtained from MoM:
✓ distinction of each echo
✓ use of fast method for a single interface
✓ reduction of complexity (number of x)
✓ reduction of memory requirement
• Simulation parameters:
✓ transmitter height: 40 cm
✓ f = 2 GHz, $\theta_i = 0°$, V polarization
✓ SC thickness: H = 20 mm
✓ $N_A = 2240$, $\sigma_{hA} = 1$ mm, $L_{cA} = 10$ mm
✓ $N_A = 3360$, $\sigma_{hB} = 2$ mm, $L_{cB} = 30$ mm
✓ $\varepsilon_{r2} = 4.5$, $\sigma_2 = 5\times10^{-3}$ S/m
✓ $\varepsilon_{r3} = 7$, $\sigma_3 = 10^{-2}$ S/m
✓ CPU time: ~40 s
Scattered field (modulus, dB scale)
with respect to abscissa $x \in [-L/2; L/2]$ and height z [mm]
Incident tapered wave
1st echo: no interaction with Σ_B
1st and 2nd echoes: interaction with Σ_B
All echoes
N. Pinel et al.
EGU GA & COST Action TU1208 2nd General Meeting – Vienna (Austria), 30/04/2014

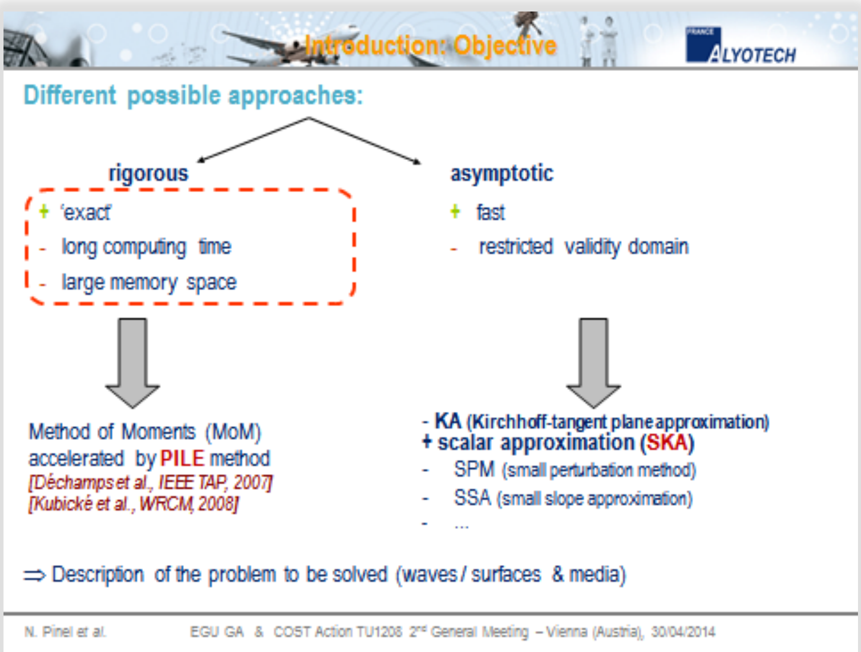
Introduction: Objective
ALYOTECH
Different possible approaches:
rigorous
+ 'exact'
- long computing time
- large memory space
asymptotic
+ fast
- restricted validity domain
Method of Moments (MoM)
accelerated by PILE method
[Déchamps et al., IEEE TAP, 2007]
[Kubické et al., WRCM, 2008]
- KA (Kirchhoff-tangent plane approximation)
+ scalar approximation (SKA)
- SPM (small perturbation method)
- SSA (small slope approximation)
- ...
⇒ Description of the problem to be solved (waves / surfaces & media)
N. Pinel et al.
EGU GA & COST Action TU1208 2nd General Meeting – Vienna (Austria), 30/04/2014

Configuration of the study

ALYOTECH

Configuration of the study (2D problems → copolarisations)

- Monostatic configuration, Normal incidence ($\theta_i = 0$), Far-field assumption
- Plane incident wave → Gaussian beam: Illumination width: ~ 100 mm ↔ $L_{cA} \approx$ 5-10 mm
  ⇒ *Variability of the backscattered echoes*
- Frequency study (large frequency band: $B \approx 10$ GHz)

- Homogeneous media (OK at $\theta_i = 0$ for this frequency range *[Gentili and Spagnolini, TGRS, 2000]*)
- Statistical description of the rough surfaces ⇒ Realistic simulations:
- Height distribution $p_h(\zeta)$ (≈Gaussian)
  → RMS height σ_h: $\sigma_{hA} \approx 1$ mm, $\sigma_{hB} \approx 2$ mm
- Height autocorrelation function $W(x_d)$ (≈exponential)
  → correlation length L_c: $L_{cA} \approx$ 5-10 mm, $L_{cB} \approx$ 10-20 mm

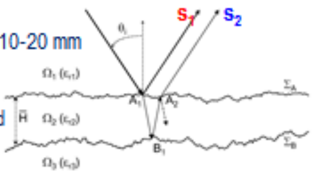

Representation of air/SC and SC/RB surface heights

N. Pinel et al. EGU GA & COST Action TU1208 2nd General Meeting – Vienna (Austria), 30/04/2014

EM modeling: Simulation parameters

ALYOTECH

Simulation parameters:

Media permittivities ϵ_r and conductivities σ:

$$\begin{cases} \epsilon_2 = 4.5 \ - \ \sigma_2 = 5\times10^{-3} \text{ S/m} \\ \epsilon_3 = 7.0 \ - \ \sigma_3 = 1\times10^{-2} \text{ S/m} \end{cases}$$

Rough surfaces Σ_A and Σ_B characteristic values (σ_h and L_c):

1. $\sigma_{hA} = \mathbf{0.5}$ mm - $L_{cA} = 6.4$ mm ; $\sigma_{hB} = \mathbf{1.0}$ mm - $L_{cB} = 15.0$ mm
2. $\sigma_{hA} = \mathbf{0.5}$ mm - $L_{cA} = 6.4$ mm ; $\sigma_{hB} = \mathbf{2.0}$ mm - $L_{cB} = 15.0$ mm
3. $\sigma_{hA} = \mathbf{1.0}$ mm - $L_{cA} = 6.4$ mm ; $\sigma_{hB} = \mathbf{2.0}$ mm - $L_{cB} = 15.0$ mm

Mean layer thickness H:
H = 20 mm

Radar central frequency f_0 and bandwidth B:
f_0 = 5.8 GHz - B = 10 GHz

Incidence angle θ_i and polarization:
θ_i = 0 deg. - V polarization

Monte-Carlo process: N = 1000 realizations
Sampling step $\Delta x = \lambda_2/8$

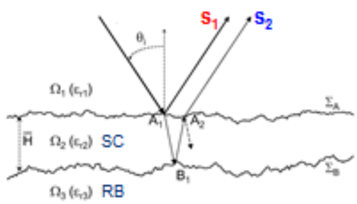

N. Pinel et al. EGU GA & COST Action TU1208 2nd General Meeting – Vienna (Austria), 30/04/2014

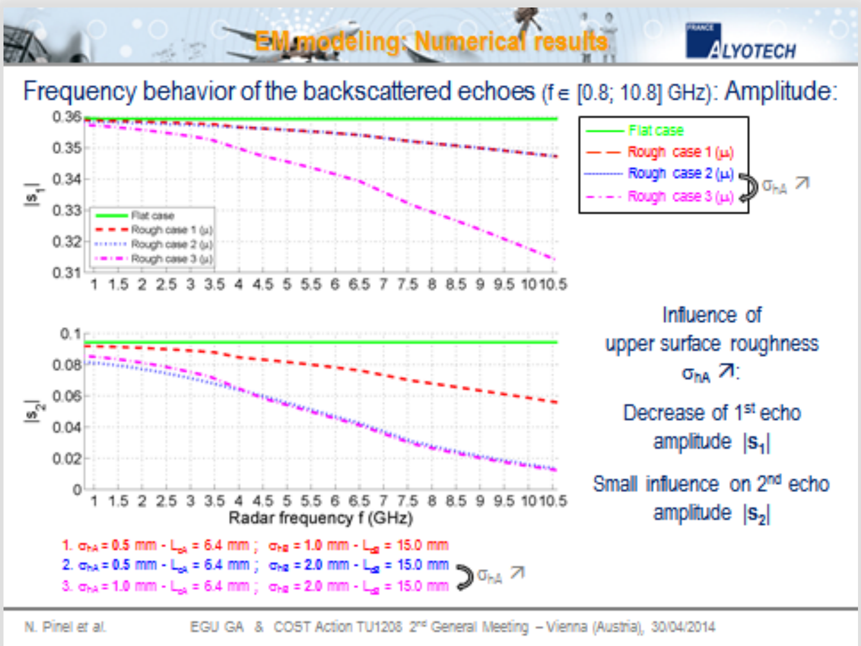
EM modeling: Numerical results
ALYOTECH
Frequency behavior of the backscattered echoes (f ∈ [0.8; 10.8] GHz): Amplitude:
|s1|
|s2|
Flat case
Rough case 1 (μ)
Rough case 2 (μ)
Rough case 3 (μ)
σhA ↗
Radar frequency f (GHz)
Influence of upper surface roughness σhA ↗:
Decrease of 1st echo amplitude |s1|
Small influence on 2nd echo amplitude |s2|
1. σhA = 0.5 mm - LcA = 6.4 mm ; σhB = 1.0 mm - LcB = 15.0 mm
2. σhA = 0.5 mm - LcA = 6.4 mm ; σhB = 2.0 mm - LcB = 15.0 mm
3. σhA = 1.0 mm - LcA = 6.4 mm ; σhB = 2.0 mm - LcB = 15.0 mm
N. Pinel et al.
EGU GA & COST Action TU1208 2nd General Meeting – Vienna (Austria), 30/04/2014

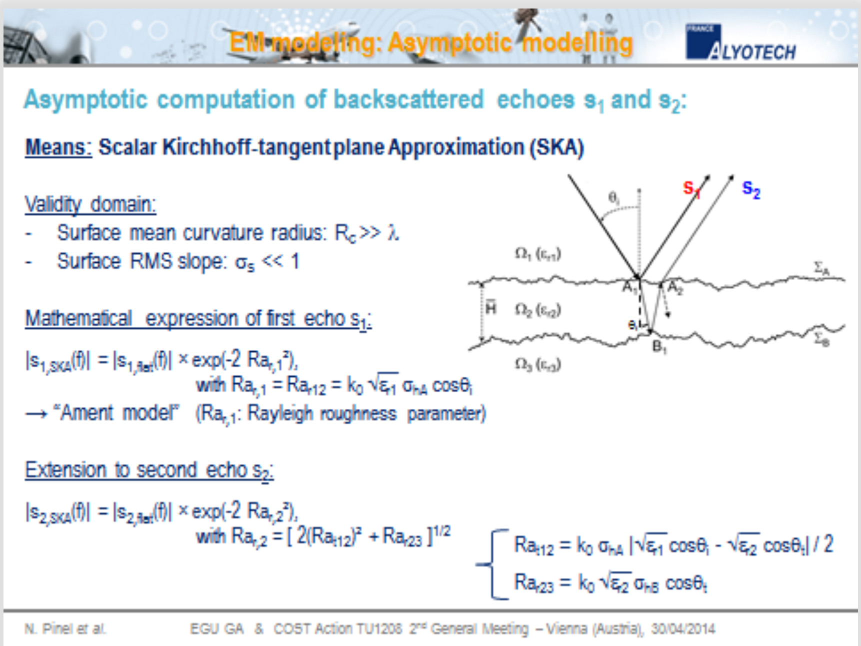
EM modelling: Asymptotic modelling
ALYOTECH
Asymptotic computation of backscattered echoes s1 and s2:
Means: Scalar Kirchhoff-tangent plane Approximation (SKA)
Validity domain:
- Surface mean curvature radius: Rc >> λ
- Surface RMS slope: σs << 1
Mathematical expression of first echo s1:
|s1,SKA(f)| = |s1,flat(f)| × exp(-2 Rar,1²),
with Rar,1 = Rai12 = k0 √εr1 σhA cosθi
→ "Ament model" (Rar,1: Rayleigh roughness parameter)
Extension to second echo s2:
|s2,SKA(f)| = |s2,flat(f)| × exp(-2 Rar,2²),
with Rar,2 = [2(Rai12)² + Rai23]1/2
Rai12 = k0 σhA |√εr1 cosθi - √εr2 cosθt| / 2
Rai23 = k0 √εr2 σhB cosθt
s1
s2
θi
Ω1 (εr1)
Ω2 (εr2)
Ω3 (εr3)
ΣA
ΣB
A1
A2
B1
H
N. Pinel et al.
EGU GA & COST Action TU1208 2nd General Meeting – Vienna (Austria), 30/04/2014

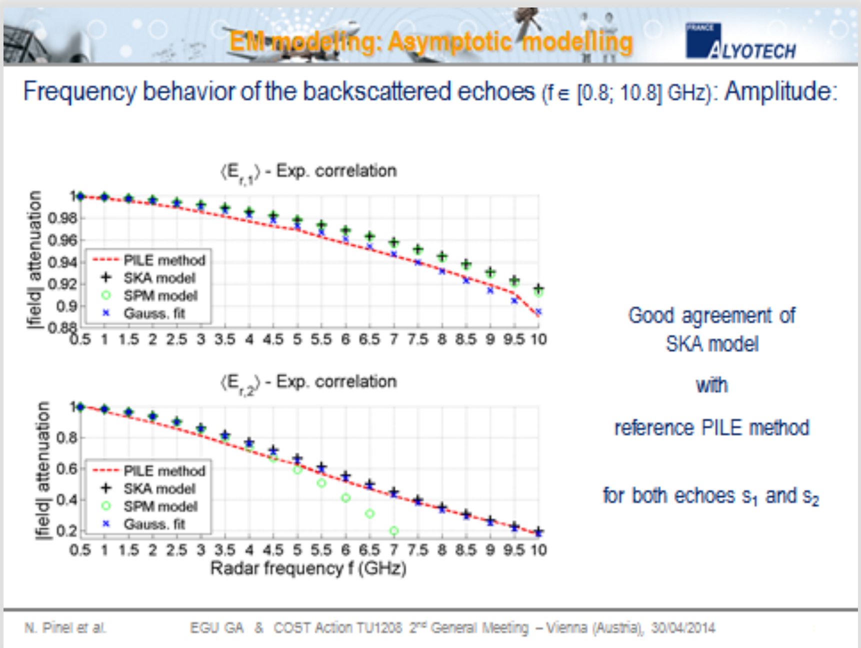
EM modelling: Asymptotic modelling
ALYOTECH
Frequency behavior of the backscattered echoes (f ∈ [0.8; 10.8] GHz): Amplitude:
⟨E_{r,1}⟩ - Exp. correlation
|field| attenuation
PILE method
SKA model
SPM model
Gauss. fit
⟨E_{r,2}⟩ - Exp. correlation
Radar frequency f (GHz)
Good agreement of SKA model
with
reference PILE method
for both echoes s1 and s2
N. Pinel et al.
EGU GA & COST Action TU1208 2nd General Meeting – Vienna (Austria), 30/04/2014

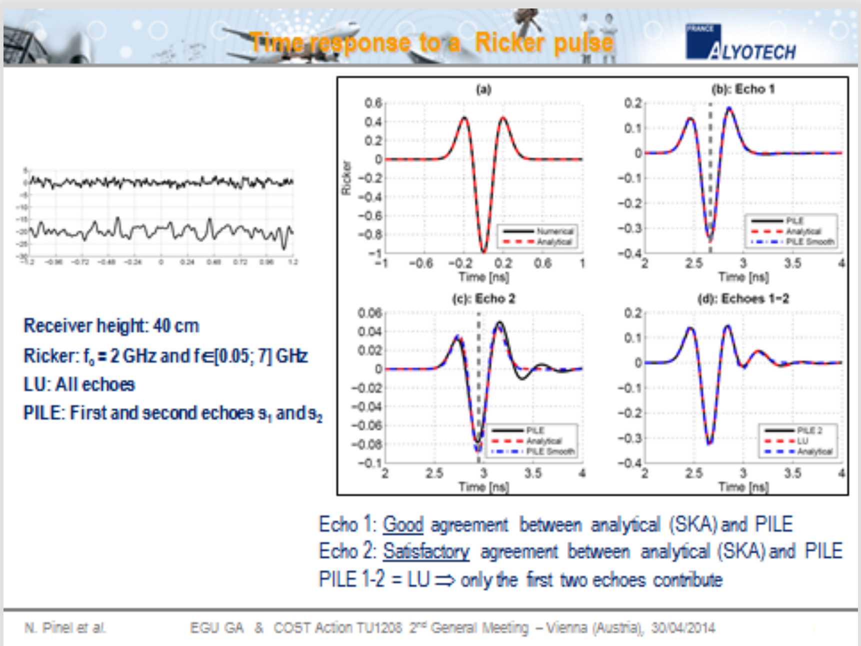
Time response to a Ricker pulse
ALYOTECH
Receiver height: 40 cm
Ricker: f0 = 2 GHz and f∈[0.05; 7] GHz
LU: All echoes
PILE: First and second echoes s1 and s2
(a)
(b): Echo 1
(c): Echo 2
(d): Echoes 1-2
Time [ns]
Echo 1: Good agreement between analytical (SKA) and PILE
Echo 2: Satisfactory agreement between analytical (SKA) and PILE
PILE 1-2 = LU ⇒ only the first two echoes contribute
N. Pinel et al.
EGU GA & COST Action TU1208 2nd General Meeting – Vienna (Austria), 30/04/2014

Acknowledgement

The Authors thank COST for funding the Action TU1208 "Civil Engineering Applications of Ground Penetrating Radar".

Progress Report of Projects 3.2 and 3.4

"Development of new methods for the solution of inverse electromagnetic scattering problems by buried structures"

Andrea Randazzo (IT), Raffaele Solimene (IT)
andrea.randazzo@unige.it

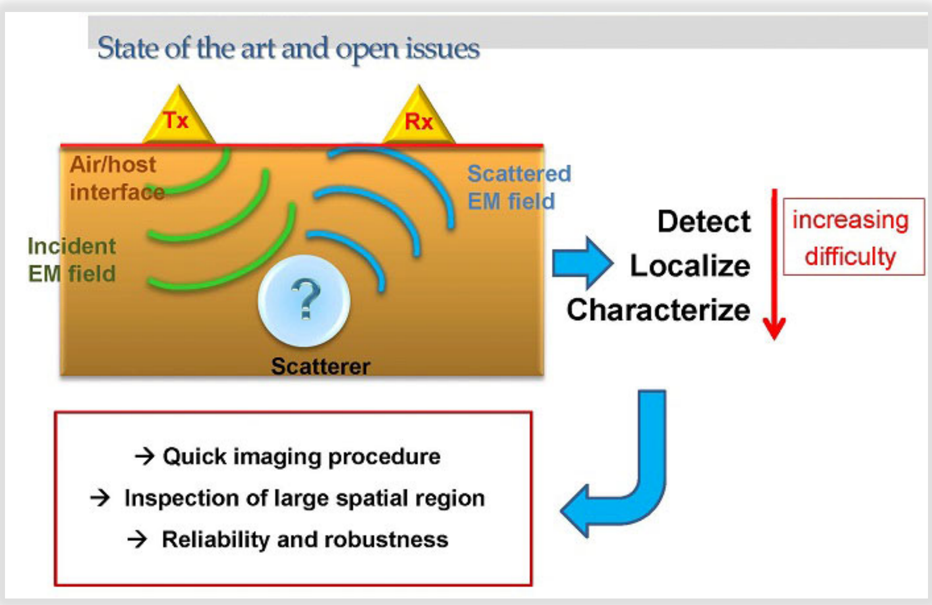

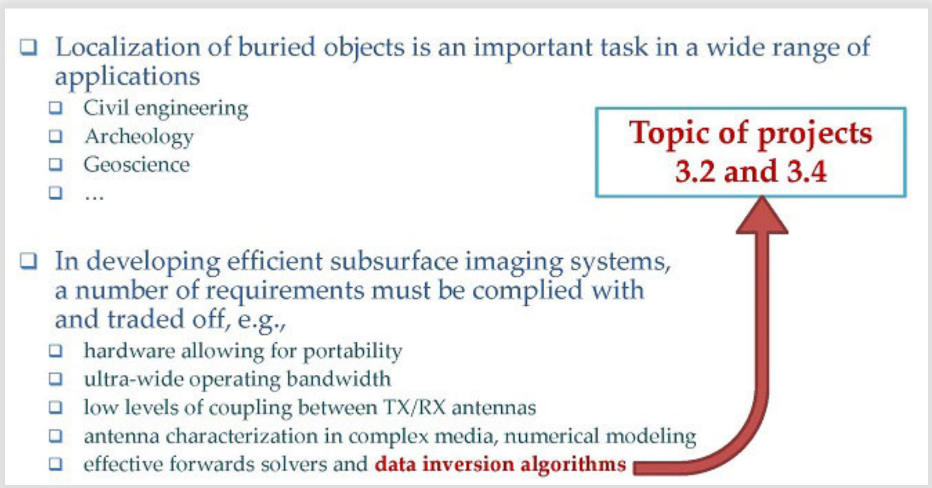

From a mathematical point of view, the imaging procedures require to solve an inverse problem.

Proposed solving approaches:

- Quantitative inversion methods
  - Linear schemes
  - Non-linear schemes (stochastic and deterministic)
- Qualitative inversion methods
  - Migration/beamforming
  - Linear qualitative inversion
  - Sampling methods
  - Machine-learning based approaches
- Hybrid approaches
  - Integration of quantitative and qualitative schemes
  - Use of specific inversion strategies

Projects 3.2 and 3.4

Linear inverse scattering

- Advantages
  - Computationally effective
  - No local minima problems
  - Easier regularization
- Drawbacks
  - Based on model approximations
  - Only detection localization and "geometrical" features

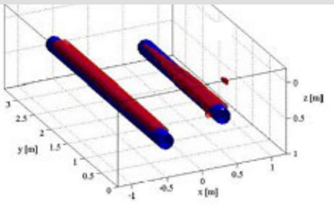

Reconstruction of two buried pipes by linear inversion[1]

Non-linear inverse scattering (deterministic and stochastic)

- Advantages
  - Able to retrieve the full distribution of the dielectric properties
  - Quantitative information about the investigated area
- Drawbacks
  - Computational complexity
  - Local minima problem

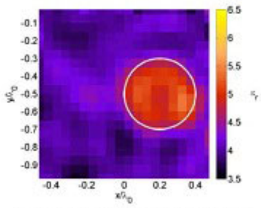

Quantitative reconstruction of a buried cylinder[2]

Sampling methods (MUSIC, LSM, …)

- Advantages
  - Do not require simplified models of the scattering phenomenon
  - Directly provide the scatterer support
- Drawbacks
  - Provide only information about localization and "geometrical" features
  - Performances are reduced when aspect-limited configurations are adopted

Hybrid approaches

- Advantages
  - Combine the advantages of qualitative and quantitative approaches
- Drawbacks
  - More complex strategies

- Although several advancements have been done in developing inversion methods, several issues must still be faced, e.g.,
  - Development of ever more efficient direct solvers
  - Reduction of computational complexity of algorithms
  - Ability of inspecting large regions
  - Reduction of field samples needed to perform the inversion
  - Identification/classification of targets inside reconstructed images
  - Development of efficient clutter suppression procedures
  - Medium estimation (e.g., for focusing-based algorithms)
  - Antenna modeling (with particular reference to the interaction with the air-ground interface) and deconvolution

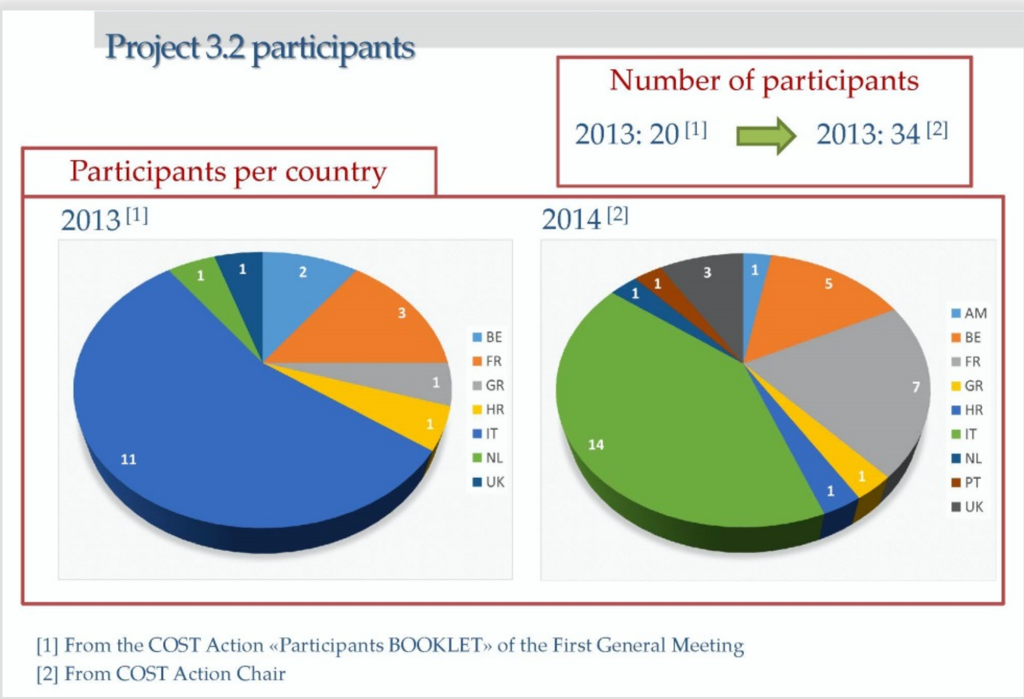
Project 3.2 participants
Number of participants
2013: 20 [1]
2013: 34 [2]
Participants per country
2013 [1]
BE
FR
GR
HR
IT
NL
UK
2014 [2]
AM
BE
FR
GR
HR
IT
NL
PT
UK
[1] From the COST Action «Participants BOOKLET» of the First General Meeting
[2] From COST Action Chair

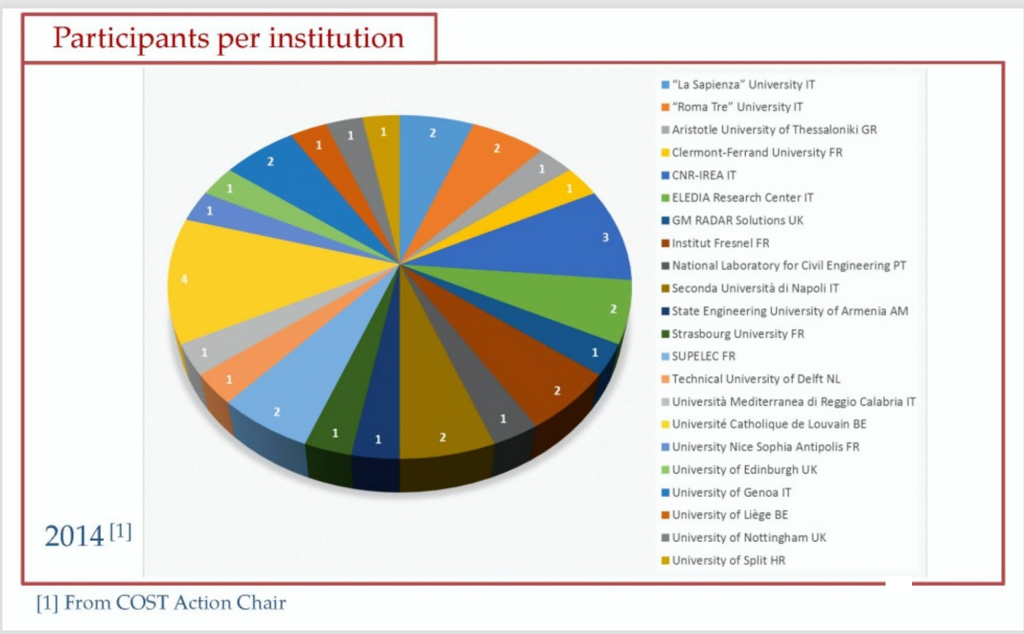
Participants per institution
"La Sapienza" University IT
"Roma Tre" University IT
Aristotle University of Thessaloniki GR
Clermont-Ferrand University FR
CNR-IREA IT
ELEDIA Research Center IT
GM RADAR Solutions UK
Institut Fresnel FR
National Laboratory for Civil Engineering PT
Seconda Università di Napoli IT
State Engineering University of Armenia AM
Strasbourg University FR
SUPELEC FR
Technical University of Delft NL
Università Mediterranea di Reggio Calabria IT
Université Catholique de Louvain BE
University Nice Sophia Antipolis FR
University of Edinburgh UK
University of Genoa IT
University of Liège BE
University of Nottingham UK
University of Split HR
2014 [1]
[1] From COST Action Chair

Participants' activities

Development of novel inverse-scattering schemes

- Localization technique for buried metallic and dielectric objects based on Sub-Array Processing
  - Some related publications ("Roma Tre" University, Italy)
    - S. Meschino, L. Pajewski, and G. Schettini, "A SAP-DoA Method for the Localization of Two Buried Objects," Int. J. Antennas Propag., vol. 2013, pp. 1–10, 2013.
    - S. Meschino, L. Pajewski, M. Pastorino, A. Randazzo, and G. Schettini, "Detection of Subsurface Metallic Utilities by Means of a SAP Technique: Comparing MUSIC- and SVM-Based Approaches," J. Appl. Geophys,, vol. 97, pp. 60-68, Oct. 2013.

- Inverse scattering techniques for GPR prospecting based on sampling methods
  - Some related publications (Applied Electromagnetics Research Group, Second University of Naples, Italy)
    - R. Solimene, A. Dell'Aversano and G. Leone, "MUSIC algorithms for rebar detection," J. Geophys. Eng., vol. 10, pp. 1-8, 2013.
    - R. Solimene, I. catapano, G. Gennarelli, A Dell'Aversano, A. Cuccaro, F. Soldovieri, "SAR imaging algorithms and some unconventional applications: a unified mathematical overview," in print on IEEE Signal Processing Magazine.
    - R. Solimene, A. Dell'Aversano, G. Leone, "Detecting a subsurface cylinder by a Time Reversal MUSIC like method," European Geosciences Union General Assembly (EGU2014), Vienna, Austria, April 27 - May 2, 2014 (Accepted).
    - R. Solimene, A. Dell'Aversano, G. Leone, "Detection of Heterogeneous Small Inclusions by a Multi-Step MUSIC Method," European Geosciences Union General Assembly (EGU2014), Vienna, Austria, April 27 - May 2, 2014 (Accepted).
    - R. Solimene, A. Dell'Aversano, G. Leone, "Rebar Detection: Comparing MUSIC and COMPRESSED Approaches," GPR2014 (accepted).

Some examples

D^III SUN
Dipartimento di Ingegneria Industriale e dell'Informazione

A two-step TR-MUSIC algorithm for rebar and duct detection

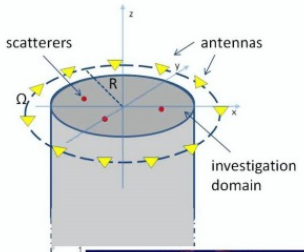

Procedure

1) First TR-MUSIC run: returns location of strong inhomogeneoties
2) Compute corresponding scattering coefficients and up-date data and Green's fucntion
3) Second TR-MUSIC run: detects duct

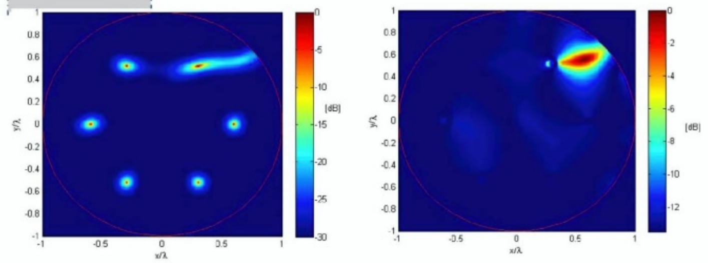

Left: One-stage MUSIC. Duct is not detected.
Right: Second-stage MUSIC. Duct is detected.

Participants' activities

- Development of non-linear inverse scattering approaches (stochastic and deterministic) for subsurface prospecting
- Exploitation of novel regularization paradigms (e.g., regularization in Banach spaces)
- Application of machine-learning paradigms to target localization
- Retrieval of dielectric and velocity profiles of elliptical pipelines.

- Some related publications (Applied Electromagnetics Group, University of Genoa, Italy.)

- C. Estatico, M. Pastorino, and A. Randazzo, "Buried Object Detection by Means of a L^p Banach-Space Inversion Procedure," Proc. 2013 URSI EMTS, Hiroshima, Japan, 2013, pp. 131-134.
- M. Salucci, G. Oliveri, A. Massa, A. Randazzo, and M. Pastorino, «Multi-Focusing Procedure based on the Inexact-Newton Method for Electromagnetic Subsurface Prospecting," 2014 EGU General Assembly, Vienna, Austria, 2014.
- S. Meschino, L. Pajewski, M. Pastorino, A. Randazzo,and G. Schettini, "Detection of Subsurface Metallic Utilities by Means of a SAP Technique: Comparing MUSIC- and SVM-Based Approaches," J. Appl. Geophys,, vol. 97, pp. 60-68, Oct. 2013.
- M. Salucci, G. Oliveri, A. Randazzo, M. Pastorino, and A. Massa, "Electromagnetic subsurface prospecting by a multi-focusing inexact Newton method within the second-order Born approximation," Journal of Optical Society of America A. In print.
- M. Pastorino, M. Raffetto, and A. Randazzo, "Reconstruction of dielectric and velocity profiles in pipelines through an electromagnetic inverse scattering technique," in Proc. 2013 IEEE Int. Conf. Imag. Syst. Tech., Beijing, China, 2013, pp. 85–90.

Some examples

Regularization of inverse problems in Banach spaces

Outer/inner approach based on an inexact-Newton scheme exploiting the properties of Banach spaces.

Benefits: Thanks to the geometrical properties of Banach spaces, they usually provide solutions endowed with low over-smoothness (resulting in a better localization and reconstruction), especially when dealing with "small" localized objects.

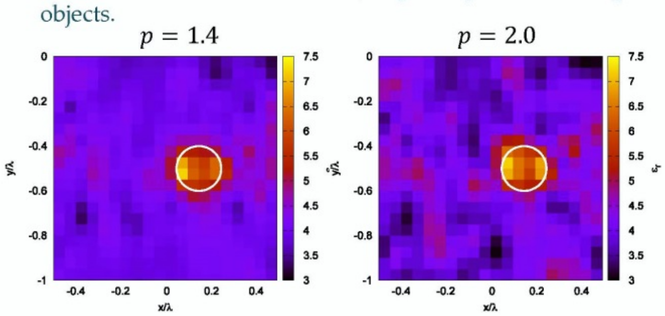

Example of the advantage in using regularization in Banach spaces [1]

C. Estatico, M. Pastorino, and A. Randazzo, "Buried Object Detection by Means of a L^p Banach-Space Inversion Procedure," *Proc. EMTS2013*, Hiroshima, 2013.

17

Participants' activities

- Exploitation of advanced inverse scattering techniques and integration with multi-scaling methods for the processing of GPR data
- Development of inversion strategies that can profitably exploit the frequency diversity of GPR measurements, in order to improve the quality of the retrieved dielectric profiles, both qualitatively and quantitatively
- Extension of innovative imaging approaches based on Bayesian Compressive Sensing (BCS) and Interval Analysis (IA) to the problem of subsurface prospecting
- Exploitation of Learning-By-Example (LBE) algorithms for enabling real-time detection and classification of buried objects

- Some related publications (ELEDIA Research Center, University of Trento, Italy)

- M. Salucci, L. Tenuti, C. Nardin, M. Carlin, F. Viani, G. Oliveri, and A. Massa, "Gpr survey through a multiresolution deterministic approach," IEEE AP-S International Symposium, Memphis, Tennessee, USA, July 6- 12, 2014 (Accepted).
- M. Salucci, L. Tenuti, C. Nardin, G. Oliveri, F. Viani, P. Rocca, and A. Massa , "Civil engineering applications of ground penetrating radar: recent advances @ the ELEDIA Research Center," European Geosciences Union General Assembly (EGU2014), Vienna, Austria, April 27 - May 2, 2014 (Accepted).
- A. Benedetto, F. Frezza, G. Manacorda, A. Massa, and L. Pajewski, "GPR technologies and methodologies in Italy: a review," European Geosciences Union General Assembly (EGU2014), Vienna, Austria, April 27 - May 2, 2014 (Accepted).

Some examples

Cross-borehole setup

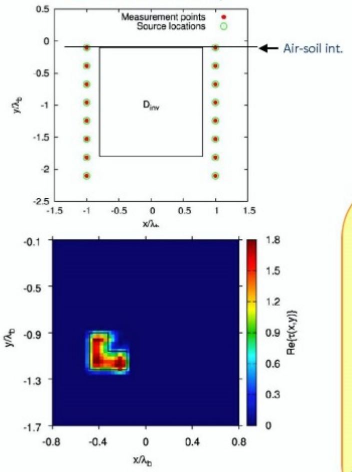

Example of reconstructed dielectric profile

- Integrated electromagnetic inverse scattering strategy exploiting
  - an iterative multi-scaling approach for focusing the reconstruction only on limited subdomains of the original investigation region
  - an efficient inexact-Newton method within the second-order Born approximation for the regularization of the inverse problem

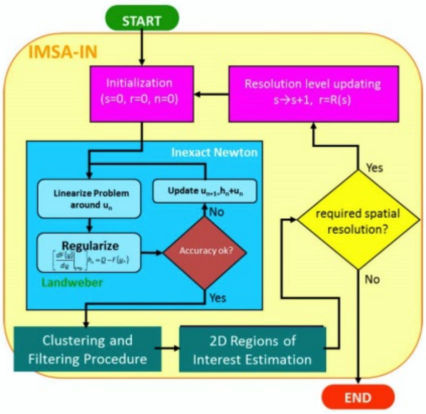

Participants' activities

- Full 3D microwave tomographic inversion procedures
- Imaging of buried targets from airborne gathered scattered field data

  - Some related publications (IREA-CNR, Italy)
  - I. Catapano, A. Affinito, G. Gennarelli, F. Maio, A. Loperte, and F. Soldovieri, "Full three-dimensional imaging via ground penetrating radar: assessment in controlled conditions and on field for archaeological prospecting," Appl. Phys. A, Nov. 2013.
  - G. Gennarelli, I. Catapano, R. Persico, and F. Soldovieri, "A comparison between two measurement configurations for full 3D GPR imaging," in Proc. 8th Europ. Conf. Antennas Propag., The Hague, The Netherlands, 2014.
  - I. Catapano, L. Crocco, Y. Krellmann, G. Triltzsch, and F. Soldovieri, "Tomographic airborne ground penetrating radar imaging: Achievable spatial resolution and on-field assessment," ISPRS J. Photogramm. Remote Sens., vol. 92, pp. 69–78, Jun. 2014.
  - I. Catapano, F. Soldovieri, and M. A. González-Huici, "Performance Assessment of a Microwave Tomographic Approach for the Forward Looking Radar Configuration," Sensing and Imaging, vol. 15, no. 1, Nov. 2014.

Some examples

Full 3D GPR inversion with TSVD

A 3D microwave vectorial model accounting the interactions occurring between electromagnetic waves and probed materials is used

$$E_{sx}(r_m) = -j\omega\mu k_b^2 \int_{\Omega} \underline{\mathbf{G}}(r_m, r_p)\chi(r_p)[\underline{\mathbf{G}}(r_p, r_m)\cdot\hat{x}]\, dr_p \cdot \hat{x}$$

TSVD

$$\hat{\chi}(r_p) = \sum_{n=1}^{N_T} \frac{1}{s_n}\langle E_{sx}, u_n\rangle v_n(r_p).$$

The approach has also been tested in a real environment @ Grotte dell'Angelo, Pertosa, (SA)

Reconstruction of a dielectric sphere ($\epsilon_{r_b} = 4.5$, $\sigma_b = 0.001\ S/m$, $f \in [1.1, 1.8]\ GHz$)

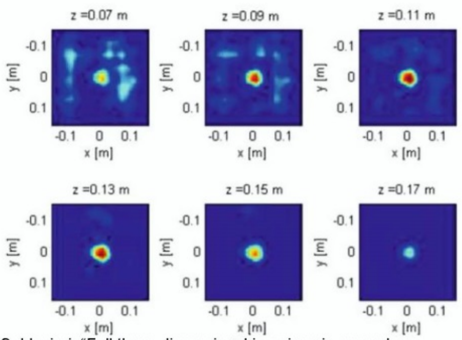

I. Catapano, A. Affinito, G. Gennarelli, F. Maio, A. Loperte, and F. Soldovieri, "Full three-dimensional imaging via ground penetrating radar: assessment in controlled conditions and on field for archaeological prospecting," Appl. Phys. A, Nov. 2013.

21

Participants' activities

Background removal and clutter rejection

- Some related publications (Department of Industrial and Information Engineering, Second University of Naples, Italy)
- R. Solimene, A. Cuccaro, A. Dell'Aversano, I. Catapano, F. Soldovieri, "Background Removal Methods in GPR Prospecting," in European Radar Conference (EuRAD) 2013, Nuremberg, 9-11 October, 2013.
- R. Solimene, I. Catapano, A. Cuccaro, A. Dell'Aversano, and F. Soldovieri, "Ground clutter removal in GPR surveys," IEEE Journal Of Selected Topics In Applied Earth Observations And Remote Sensing, vol. 7, NO. 3, pp. 792 - 798, 2014.

Some examples

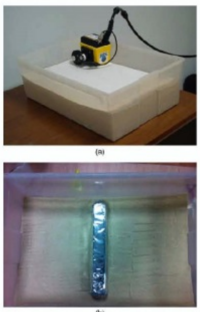

Experimental setup:
(a) sand box view; (b) metal target

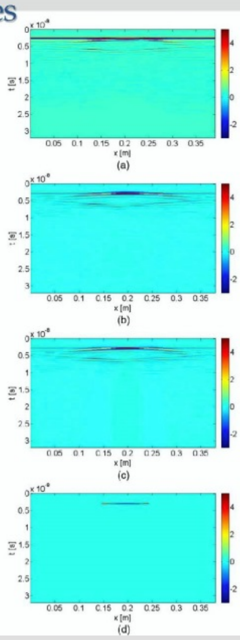

Metallic cylinder radargram:
(a) raw-data; (b) average trace subtraction;
(c) subspace projection method;
(d) entropy based time-gating.

Time-gating entropy based surface clutter rejection

Procedure

Build the normalized A-scan as

$$\tilde{e}_n(t) = |e_n(t)|^2 / \sum_{m=1}^{M} |e_m(t)|^2$$

Compute the entropy for each t (M is the number of A-scan)

$$\varepsilon_S(t) = -\sum_{m=1}^{M} \tilde{e}_m(t) \log[\tilde{e}_m(t)]$$

Define the time-gating window as

$$W(t) = \begin{cases} 0 & \text{if } \varepsilon_S(t) > \alpha \log M \\ 1 & \text{elsewhere} \end{cases}$$

D$^{\text{III}}$ SUN
Dipartimento di Ingegneria Industriale e dell'Informazione

23

Participants' activities

Development of soil models and efficient approaches for solving the forward scattering problem by buried structures

- Analytical and semi-analytical solution algorithms
  - Some related publications ("Roma Tre" University, Italy)
  - F. Frezza, L. Pajewski, C. Ponti, G. Schettini, and N. Tedeschi, "Cylindrical-Wave Approach for electromagnetic scattering by subsurface metallic targets in a lossy medium," J. Appl. Geophys., vol. 97, pp. 55–59, Oct. 2013.
- Characterization of the response of multi-layer structures
  - Some related publications (SUPELEC, France)
  - Y. Zhong, M. Lambert, D. Lesselier, and X. Chen, "Electromagnetic Response of Anisotropic Laminates to Distributed Sources," IEEE Transactions on Antennas and Propagation, vol. 62, no. 1, pp. 247–256, Jan. 2014.

- Development of analytical models (e.g., for soil response)
  - Some related publications (University of Split, Croatia)
  - S. Antonijevic, and D. Poljak, "A Novel Time-Domain Reflection Coefficient Function: TM Case," IEEE Trans Electromagn. Compat., vol. 99, pp. 1-7, 2013.
  - D. Cavka, N. Mora, F. Rachidi, and D. Poljak, "On the Application of Frequency Dependent Soil Models to the Transient Analysis of Grounding Electrodes," Proc. 2013 Int. Symp. Electromagn. Compat. (EMC Europe 2013), Brugge, 2013, pp. 777-781.
  - S. Šesnić, and D. Poljak, "Antenna model of the horizontal grounding electrode for transient impedance calculation: Analytical versus Boundary Element Method," Engineering analysis with boundary elements, vol. 37, pp. 909-913, 2013.
  - S. Šesnić, D. Poljak, and S. V. Tkachenko, "Analytical Modeling of a Transient Current Flowing Along the Horizontal Grounding Electrode, "IEEE Transactions on electromagnetic compatibility, pp. 1-8, 2013.

Some examples

Developmnet of new soil and forward models

A new time domain reflection coefficient for TM polarization has been developed. The RC function is derived using Gaver-Stehfest algorithm for numerical Inverse Lapalce Transform.

This simple and efficient formulation could be used within time do main integral equation approaches to analyze wire structures in the presence of a lossy half-space.

$$r(\theta,t)=\frac{1-\beta}{1+\beta}\delta(t)+\frac{2\ln 2}{t}\frac{\beta}{1+\beta}\sum_{n=1}^{N}V_n\frac{\sqrt{1+(K/n)t}-1}{\sqrt{1+(K/n)t}+\beta}.$$

$$E^{\mathrm{ref}}(t)=\int_0^t r(\theta,\tau)E^{\mathrm{inc}}(t-\tau)d\tau$$

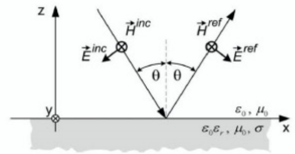

Fig. 1. TM space wave incident on an interface.

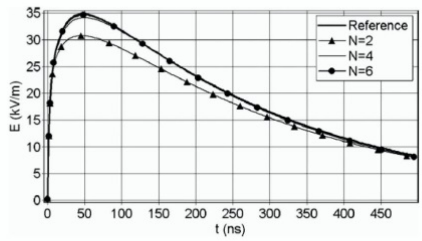

Fig. 3. Reflected electric field for different values of N compared with referent waveform obtained via FFT.

S. Antonijevic, and D. Poljak, "A Novel Time-Domain Reflection Coefficient Function: TM Case," IEEE Trans Electromagn. Compat., vol. 99, pp. 1-7, 2013.

26

Development of medium estimation procedures

- Estimation of time delays, permittivities, and roughness parameters by GPR, especially with subspace methods (MUSIC, ESPRIT, etc)
- Detection of debonding within pavement structures by GPR with machine learning methods
  - Some related publications (Cerema, France)
  - C. Le Bastard, Y. Wang, V. Baltazart and X. Dérobert, "Time Delay and Permittivity Estimation by Ground Penetrating Radar with Support Vector Regression", IEEE Geosci. Remote Sens. Lett., vol. 11, no. 4, pp. 873-877, April 2014.
  - M. Sun, N. Pinel, C. Le Bastard, V. Baltazart, A. Ihamouten and Y. Wang, "Time delay and surface roughness estimation by subspace algorithms for pavement survey by radar", 7th Int. Workshop Adv. Ground Penetrating Radar, Nantes, July, 2013.

Some examples

Estimation of time delays, permittivities and roughness parameters by GPR

Use of machine learning algorithms for time delay and dielectric constant estimation from backscattered field data

Offline phase: Train the SVMs by using known examples of received data (properly preprocessed) and time delays/permittivities

Online phase: used the trained SVMs to estimate the unknown time delays/permittivities

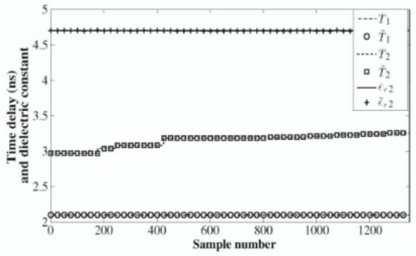

Fig. 2. Nonoverlapped echoes: True and estimated time delays and true and estimated dielectric constants, with $B = [0.5; 2.5]$ GHz and SNR = 20 dB.

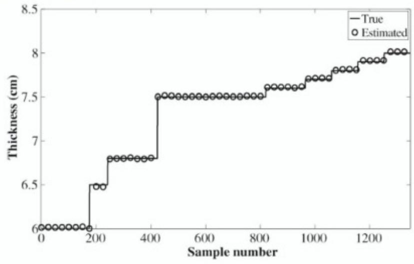

Fig. 3. Nonoverlapped echoes: True and estimated layer thicknesses obtained from Fig. 2, with $B = [0.5; 2.5]$ GHz and SNR = 20 dB.

C. Le Bastard, Y. Wang, V. Baltazart and X. Dérobert, "Time Delay and Permittivity Estimation by Ground Penetrating Radar with Support Vector Regression", IEEE Geosci. Remote Sens. Lett., vol. 11, no. 4, pp. 873-877, April 2014.

28

- Soil composition (e.g., moisture and clay) evaluation
  - Some related publications
  - A. P. Tran, F. Andre, and S. Lambot, "Validation of Near-Field Ground-Penetrating Radar Modeling Using Full-Wave Inversion for Soil Moisture Estimation," IEEE Transactions on Geoscience and Remote Sensing, vol. 52, no. 9, pp. 5483–5497, Sep. 2014.
  - A. Di Matteo, E. Pettinelli, and E. Slob, "Early-Time GPR Signal Attributes to Estimate Soil Dielectric Permittivity: A Theoretical Study," IEEE Transactions on Geoscience and Remote Sensing, vol. 51, no. 3, pp. 1643–1654, Mar. 2013.
  - F. Tosti, C. Patriarca, E. Slob, A. Benedetto, and S. Lambot, "Clay content evaluation in soils through GPR signal processing," Journal of Applied Geophysics, vol. 97, pp. 69–80, Oct. 2013.
  - C. Patriarca, F. Tosti, C. Velds, A. Benedetto, S. Lambot, and E. Slob, "Frequency dependent electric properties of homogeneous multi-phase lossy media in the ground-penetrating radar frequency range," Journal of Applied Geophysics, vol. 97, pp. 81–88, Oct. 2013.

Development of measurement systems

- Some related publications (University Nice Sophia Antipolis, France)
- A. Zeitler, C. Migliaccio, A. Moynot, I. Aliferis, L. Brochier, J.-Y. Dauvignac, and C. Pichot, "Amplitude and Phase Measurements of Scattered Fields for Quantitative Imaging in the W-band," IEEE Transactions on Antennas and Propagation, vol. 61, no. 7, pp. 3927–3931, Jul. 2013.

GPR antenna modeling and deconvolution techniques

- Antenna deconvolution techniques for soil permittivity estimation
  - Some related publications
    - R. Solimene, A. D'Alterio, G. Gennarelli and F. Soldovieri, "Estimation of Soil Permittivity in Presence of Antenna-Soil Interactions, IEEE Journal Of Selected Topics In Applied Earth Observations And Remote Sensing, vol.7, NO.3, pp. 805-812, 2014.
    - L. Mertens, A. P. Tran, and S. Lambot, "Towards physically-based filtering of the soil surface, antenna and coupling effects from near-field GPR data for improved subsurface imaging," 7th Int. Workshop Adv. Ground Penetrating Radar, 2013, pp. 1–5.
- Antenna near-field modeling
  - Some related publications
    - N. Diamanti and A. P. Annan, "Characterizing the energy distribution around GPR antennas," Journal of Applied Geophysics, vol. 99, pp. 83–90, Dec. 2013.
    - A. P. Tran, C. Warren, F. André, A. Giannopoulos, and S. Lambot, "Numerical evaluation of a full-wave antenna model for near-field applications," Near Surface Geophysics, vol. 11, no. 2, pp. 155–165, Apr. 2013.
    - S. Lambot and F. Andre, "Full-Wave Modeling of Near-Field Radar Data for Planar Layered Media Reconstruction," IEEE Transactions on Geoscience and Remote Sensing, vol. 52, no. 5, pp. 2295–2303, May 2014.

Conclusions

- The development of efficient imaging algorithms, able to face the complexity of the underlying electromagnetic inverse scattering problem, is highly important for enhancing modern GPR systems.
- Several activities concerning such topic have been started in the framework of project 3.2.
- Very good results have been obtained by the participants.
- However, there are still some open issues that must be faced and that should drive future developments.
- Moreover, it would be useful to have a set of benchmark simulated and measured testbed to test the developed approaches.

- Main difficulties:
  - The field inside the scatterers depends upon the unknown dielectric contrast between the target and the host medium

    ⇩

    The relationship between the contrast function and the scattered field is nonlinear
  - The inverse problem is ill posed problem

    ⇩

    Regularization algorithms are needed

"Full-waveform inversion of GPR data for civil engineering applications"

(Contribution to Project 3.2)

Jan van der Kruk (DE), Alexis Kalogeropoulos (CH),
Johannes Hugenschmidt (CH), Anja Klotzsche (DE),
Sebastian Busch (DE), Harry Vereecken (DE)
j.van.der.kruk@fz-juelich.de

The abstract is published in *Geophysical Research Abstracts*, Vol. 16, EGU2014-16051, 2014 and is available on *www.egu2014.eu*

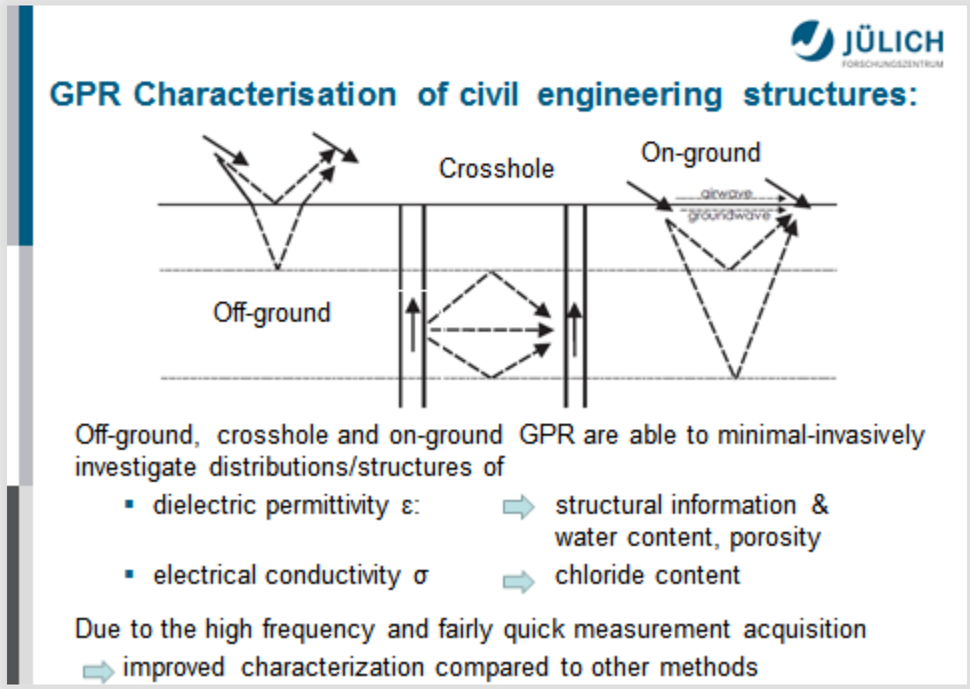

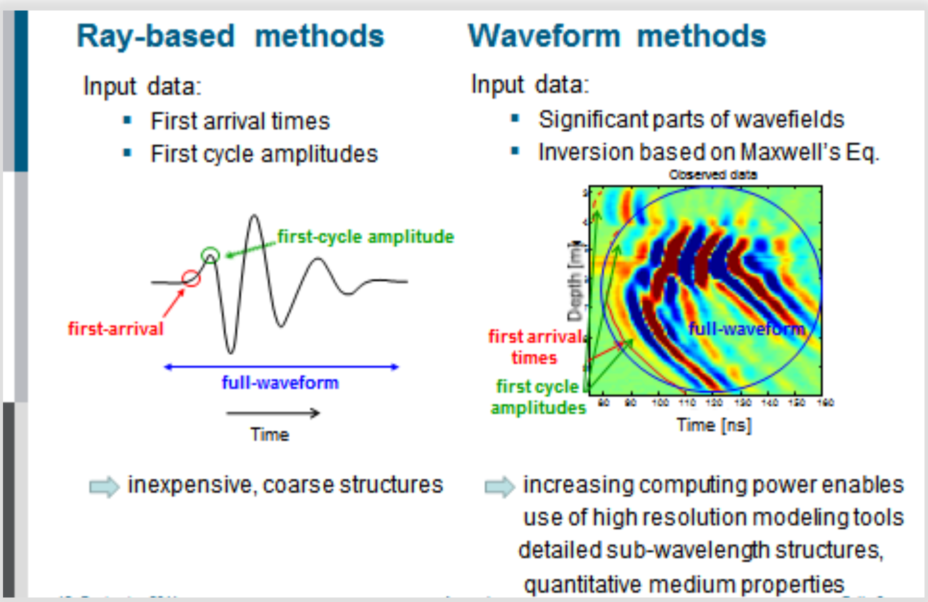
Ray-based methods
Input data:
First arrival times
First cycle amplitudes
first-cycle amplitude
first-arrival
full-waveform
Time
inexpensive, coarse structures
Waveform methods
Input data:
Significant parts of wavefields
Inversion based on Maxwell's Eq.
Observed data
Depth [m]
first arrival times
first cycle amplitudes
full-waveform
Time [ns]
increasing computing power enables use of high resolution modeling tools
detailed sub-wavelength structures,
quantitative medium properties

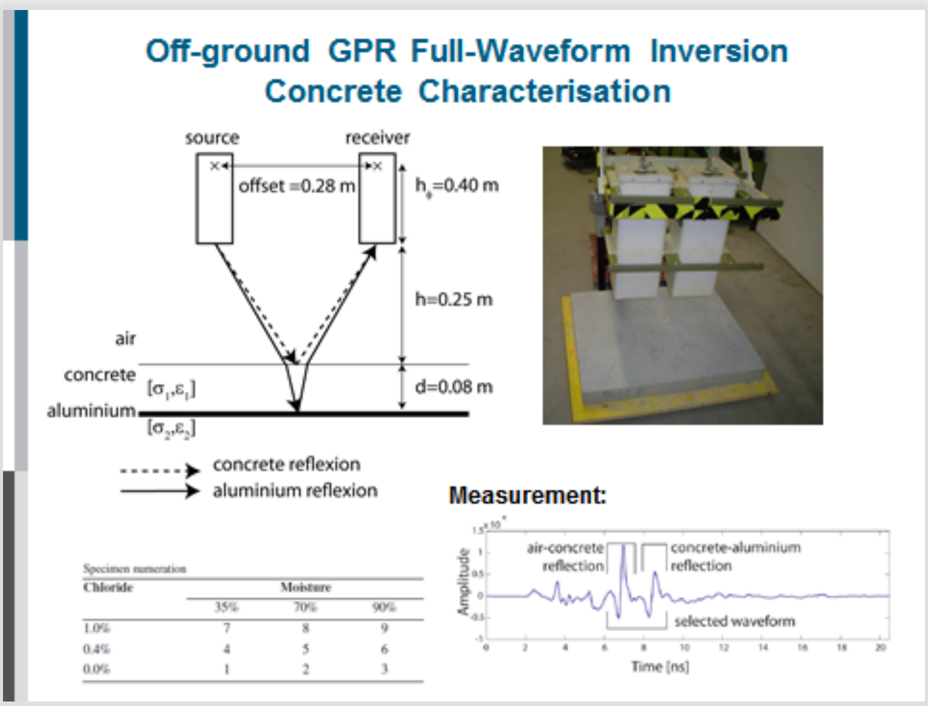
Off-ground GPR Full-Waveform Inversion
Concrete Characterisation
source
receiver
offset =0.28 m
h_0=0.40 m
h=0.25 m
d=0.08 m
air
concrete
aluminium
$[\sigma_1,\varepsilon_1]$
$[\sigma_2,\varepsilon_2]$
concrete reflexion
aluminium reflexion
Specimen numeration
Chloride
Moisture
35% 70% 90%
1.0% 7 8 9
0.4% 4 5 6
0.0% 1 2 3
Measurement:
Amplitude
air-concrete reflection
concrete-aluminium reflection
selected waveform
Time [ns]

GPR calibration

Measurement over stainless steel plate for different heights to determine:

Phase center Estimation:

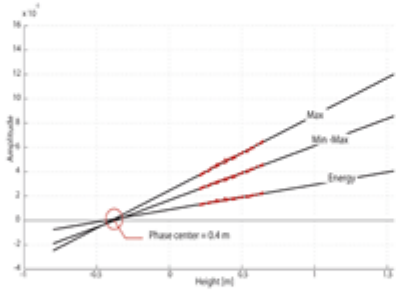

Effective wavelet Estimation:

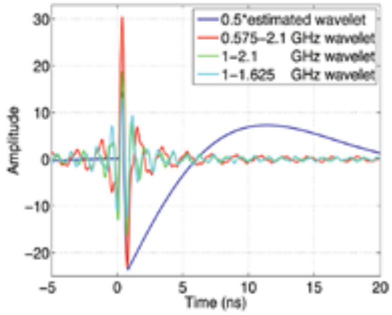

A. Kalogeropoulos, J. van der Kruk, J. Hugenschmidt, S. Busch and K. Merz (2011), Chlorides and moisture assessment in concrete by GPR full waveform inversion *Near Surface Geophysics, 2011*, **9**, doi:10.3997/1873-0604.2010064

Off-ground GPR Full-waveform Inversion

Using the accurate forward model the measured data is fitted with the modeled data using the phase and amplitude using a combined global and local inversion scheme

Inversion for
Relative permittivity ε
Conductivity: σ and Δ σ

Specimen numeration

Chloride	Moisture 35%	Moisture 70%	Moisture 90%
1.0%	7	8	9
0.4%	4	5	6
0.0%	1	2	3

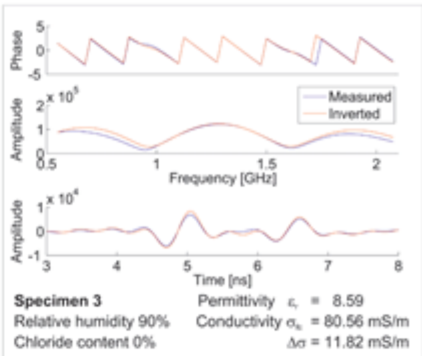

A. Kalogeropoulos, J. van der Kruk, J. Hugenschmidt, S. Busch and K. Merz (2011), Chlorides and moisture assessment in concrete by GPR full waveform inversion *Near Surface Geophysics, 2011*, **9**, doi:10.3997/1873-0604.2010064

Homogeneous Slab Inversion Results: Permittivity and Conductivity

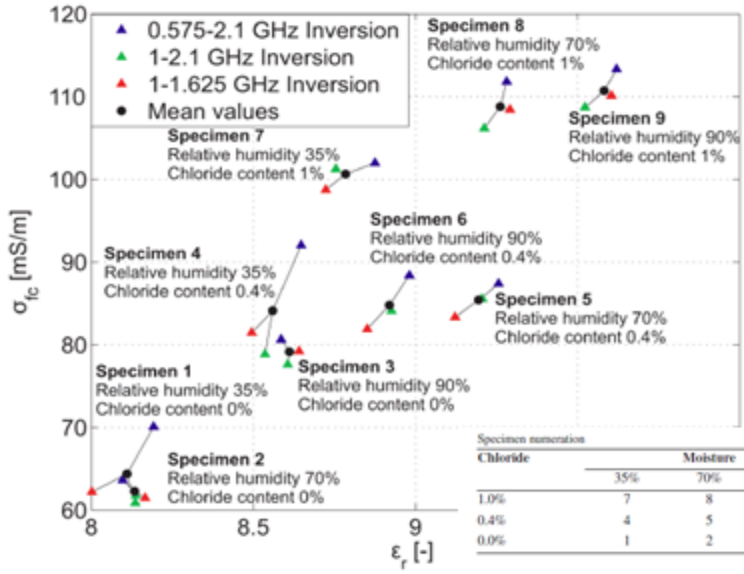

Specimen numeration

Chloride	Moisture 35%	70%	90%
1.0%	7	8	9
0.4%	4	5	6
0.0%	1	2	3

Generation of Chloride Gradients in Concrete

- Three Concrete Specimen were made
- Different Saline Solutions were put on the specimen's open surface with different exposure length to generate chloride gradients

	Specimen A	Specimen B	Specimen C
Saline Solution (g/l)	165	165	247.5
Exposure in Days	56	157	36

- Repeated off-ground GPR measurements were made
- Weighing measurements indicate water evaporation
- Presence of gradients was confirmed by destructive testing

Synthetic models for different gradients

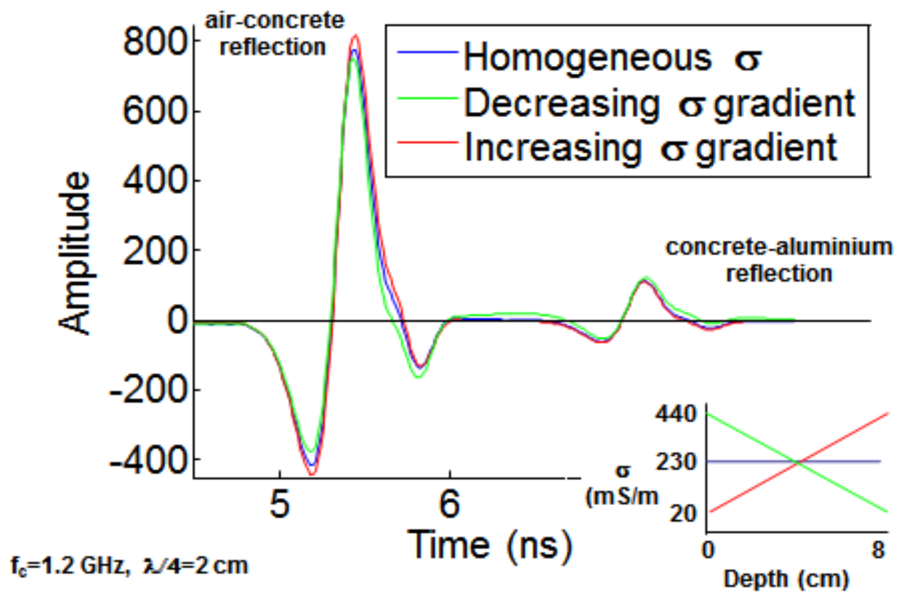

Full-waveform inversion approach to determine Chloride Gradient Determination in Concrete

- Use ray-based far-field approximations to determine start parameters (ε, σ) for full-waveform inversion
- ε, σ full-waveform inversion using air-concrete reflection
  ⇒ indicative for upper concrete properties
- ε, σ full-waveform inversion using concrete-metal reflection
  ⇒ indicative for average concrete properties
- Full-waveform inversion for conductivity gradient
  - using both air-concrete and concrete-metal reflection
  - using former results as start values
  - constant permittivity assumption

Inversion results of experimental data

	Specimen A		Specimen B		Specimen C	
	Days	Cl^- (g/l)	Days	Cl^- (g/l)	Days	Cl^- (g/l)
	56	165	157	165	36	247.5
Inversion:	ε (-)	σ (mS/m)	ε (-)	σ (mS/m)	ε (-)	σ (mS/m)
Ray-based	10.2	$\bar{\sigma}$ = 230	9.5	$\bar{\sigma}$ = 200	10.7	$\bar{\sigma}$ = 240
Full-waveform Air-concrete reflection	11.5	250 ⇒	13.0	230 ⇒	12.9	340 ⇒
Full-waveform Concrete-metal reflection	9.8	$\bar{\sigma}$ = 180	9.1	$\bar{\sigma}$ = 160	10.3	$\bar{\sigma}$ = 180
Full-waveform Air-concrete & Concrete-metal reflection	9.9	270 ⇒ 150	9.3	250 ⇒ 120	10.2	320 ⇒ 120

Full-waveform inversion results for increasing chloride content using both reflections: (Specimen A)

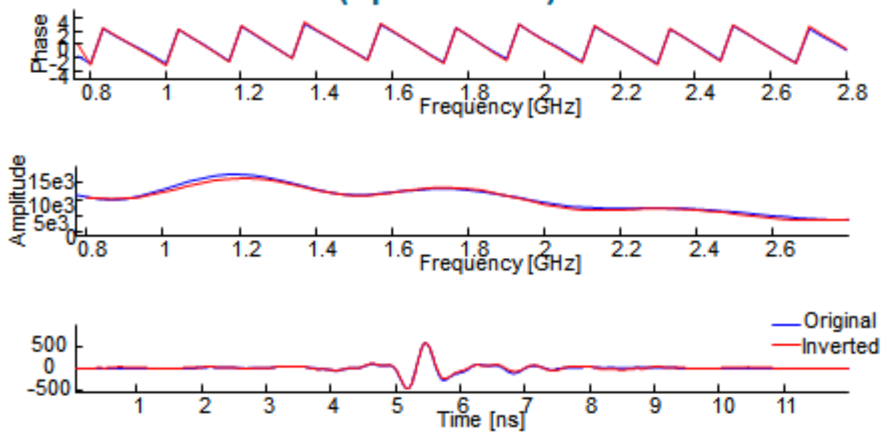

A. Kalogeropoulos, J. van der Kruk, J. Hugenschmidt, J. Bikowski, E. Bruhwiler, 2013, Full-waveform GPR inversion to assess chloride gradients in concrete, NDT&E International, 57, 74-84, DOI:10.1016/j.ndteint.2013.03.003

	Spec. A	Spec. B	Spec. C
Cl^- (g/l), days	165 (56 days)	165 (157 days)	247.5 (36 days)
Full-waveform Inversion	σ (mS/m): 0.27⇒0.15	σ (mS/m): 0.25⇒0.12	σ (mS/m): 0.32⇒0.12
Destructive test.: Free Cl^- (%)	1.75%	1.60%	2.05%

Comparison with destructive measurements

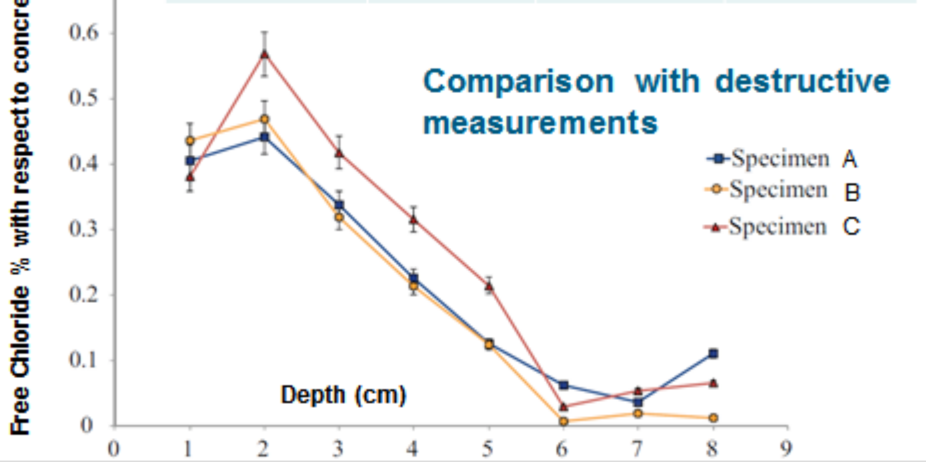

Off-ground GPR FWI Conclusions

- Full-waveform inversion returns quantitative values of relative permittivity and conductivity for homogeneous concrete slabs
- Chloride concentration dominates the diffusion through the concrete, whereas exposure time is of minor importance
- Full-waveform inversion can identify chloride gradients which are consistent with destructive data
- Further research is needed to obtain improved quantitative conductivity gradient values for more complicated scenarios

A. Kalogeropoulos, J. van der Kruk, J. Hugenschmidt, S. Busch and K. Merz (2011), Chlorides and moisture assessment in concrete by GPR full waveform inversion *Near Surface Geophysics, 2011*, **9**, doi:10.3997/1873-0604.2010064
A. Kalogeropoulos, J. van der Kruk, J. Hugenschmidt, J. Bikowski, E. Bruhwiler, 2013, Full-waveform GPR inversion to assess chloride gradients in concrete, NDT&E International, 57, 74-84, DOI:10.1016/j.ndteint.2013.03.003

"Multi-Focusing Procedure based on the Inexact-Newton Method for Electromagnetic Subsurface Prospecting" (contribution to projects 3.2 and 3.4)

Marco Salucci (IT), Giacomo Oliveri (IT), Andrea Massa (IT), Andrea Randazzo (IT), Matteo Pastorino (IT) – *andrea.randazzo@unige.it*

The abstract is published in *Geophysical Research Abstracts*, Vol. 16, EGU2014-11040, 2014 and is available on *www.egu2014.eu*

1. Introduction

Ground penetrating radars (GPRs) are key instruments for subsurface monitoring and imaging. Further research is however needed for facing the complexity of the underlying inverse scattering imaging problem (non-linearity and ill-posedness). A novel integrated electromagnetic inverse scattering strategy is proposed, using an iterative multi-scaling approach for focusing the reconstruction only on limited subdomains of the original investigation region, and using an efficient inexact-Newton method within the second-order Born approximation for the regularization of the inverse problem. The approach is validated by means of numerical simulations.

2. Buried Inverse Scattering Problem

Objective: starting form measures of the electric field collected in a given observation domain, find an approximation of some model parameters describing the electromagnetic properties of the investigated area (e.g., the contrast function $\tau=\epsilon/\epsilon_b - 1$)

Hypthesis

- cylindrical configuration

$\tau=\epsilon(x,y)/\epsilon_b - 1$

- TM polarized time-harmonic incident field

$\mathbf{E}_{inc}(\mathbf{r})=\Psi_{inc}(x,y)\mathbf{z}$

Two-dimensional scalar problem

$\mathbf{E}_{scatt}(\mathbf{r})=\Psi_{scatt}(x,y)\mathbf{z}$

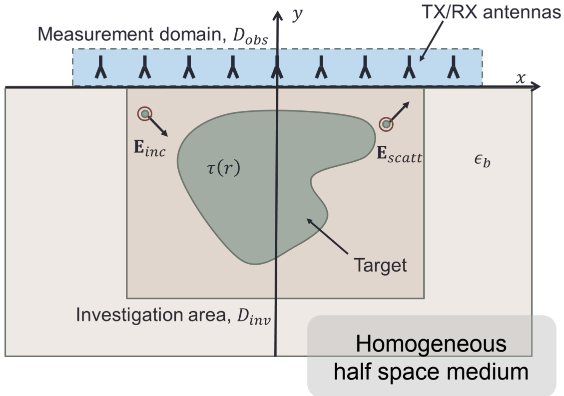

Data equation

Green's function for the half space [1]

$$\Psi^p_{scat}(\mathbf{x}) = \Psi^p_{tot}(\mathbf{x}) - \Psi^p_{inc}(\mathbf{x}) = -k_b^2 \int_{D_{inv}} \tau(\mathbf{y})\Psi^p_{tot}(\mathbf{x}) G_{hs}(\mathbf{x}/\mathbf{y}) d\mathbf{y} \qquad \mathbf{x} \in D_{obs}$$

HP: Second Order Born Approximation (SOBA) [2]:

$$\Psi^p_{scat}(\mathbf{x}) \cong F^p_{B1}\tau(\mathbf{x}) - k_b^2 \int_{D_{inv}} \tau(\mathbf{y}) F^p_{B1}\tau(\mathbf{y}) G_{hs}(\mathbf{x}/\mathbf{y}) d\mathbf{y} = F^p_{B2}(\tau)(\mathbf{x})$$

first order Born operator

$$F^p_{B1}\tau(\mathbf{x}) = -k_b^2 \int_{D_{inv}} \tau(\mathbf{y}) \Psi^p_{inc}(\mathbf{y}) G_{hs}(\mathbf{x}/\mathbf{y}) d\mathbf{y}$$

[1] D.C. Stinson, Intermediate mathematics of electromagnetics. Englewood Cliffs, N.J.: Prentice-Hall, 1976.
[2] C. Estatico, M. Pastorino, and A. Randazzo, "An Inexact-Newton Method for Short-Range Microwave Imaging Within the Second-Order Born Approximation," ***IEEE Trans. Geosci. Remote Sens.***, vol. 43, no. 11, pp. 2593–2605, Nov. 2005.

Set of equations to solve:

$$F_{B2}(\tau) = \begin{bmatrix} F^1_{B2}(\tau) \\ \dots \\ F^P_{B2}(\tau) \end{bmatrix} = \begin{bmatrix} \Psi^1_{scat} \\ \dots \\ \Psi^P_{scat} \end{bmatrix} = \Psi_{scat}$$

Unknowns:

$$\boxed{\tau(\mathbf{x}) = \frac{1}{\varepsilon_b}[\varepsilon(\mathbf{x}) - \varepsilon_b], \mathbf{x} = (x, y) \in D_{inv}}$$

Discretization: *N* square cells

$$\Psi^p_{scat}(\mathbf{x}) \cong F^p_{B1}\tau(\mathbf{x}) - k_b^2 \int_{D_{inv}} \tau(\mathbf{y}) F^p_{B1}\tau(\mathbf{y}) G_{hs}(\mathbf{x}/\mathbf{y}) d\mathbf{y} = F^p_{B2}(\tau)(\mathbf{x})$$

- In compact form

$$\boxed{F\{\underline{u}\} = \underline{d}}$$

where

$\underline{d} \equiv \{\Psi^p_{scat}(\mathbf{x}), p = 1, \dots, P\}$

$F\{\underline{u}\} = F_{B2}(\tau)$

$\underline{u} = \{\tau\}$ contains the unknown object function

Theoretical Difficulties

a) ill-posedness/ill-conditioning
b) local minima issues

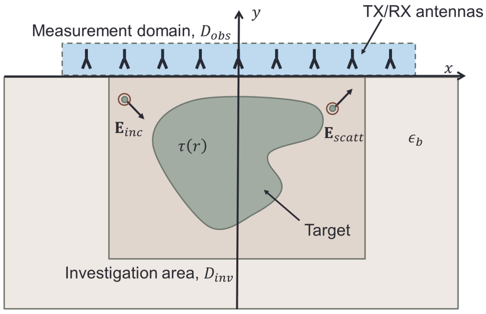

Countermeasures

(a) Regularization techniques

Indirect approaches (applied to deterministic [1] and stochastic [2] algorithms)

Direct Regularization Techniques:
Inexact Newton Method

(b) Reduction of local minima

Global Optimization Techniques [2]
Iterative Multi-Scaling Approaches

IMSA-Inexact Newton Integrated Approaches

[1] P. M. van den Berg and A. Abubakar, "Contrast source inversion method: State of the art," *Prog. Electromagn. Res.*, 2001.
[2] M. Pastorino, "Stochastic Optimization Methods Applied to Microwave Imaging: A Review," IEEE Trans. Antennas Propag., Mar. 2007.

Inexact Newton Method

Iterative Solution of $\boxed{F\{\underline{u}\} = \underline{d}}$

- Algorithm:
  1. Choose a starting $\underline{u}$: $\underline{u}_0$
  2. Linerize F around u_n
  3. Solve

  $$F\{u_n\} - d = F'_{u_n} h_n$$

  4. Update $u_{n+1} = u_n + h_n$

Loop n=0,1,...

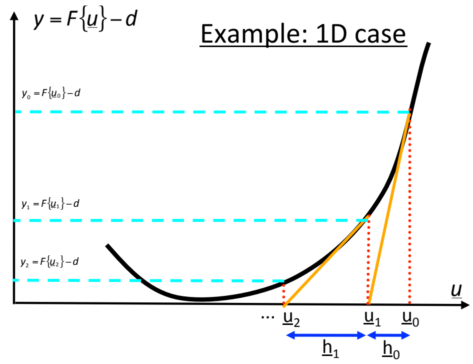

Regularization Capabilities ← **Succession of regularized linear problems**

Local Minima Problem ⇐ **Deterministic Initialization - dependent search**

Local Minima & Resolution

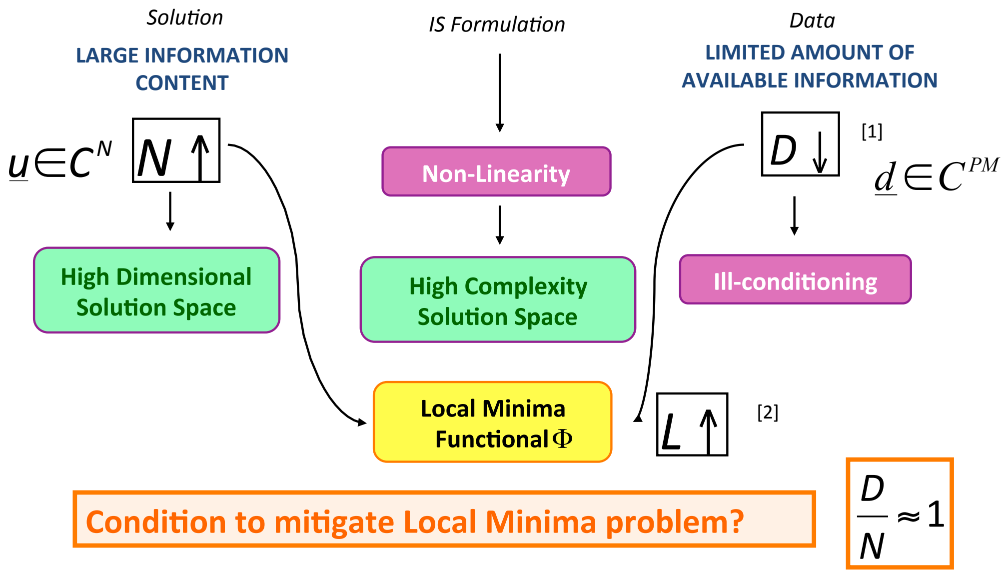

[1] O. M. Bucci and G. Franceschetti, "On the degrees of freedom of scattered field," ***IEEE Trans. Antennas Propag.***, 1989.
[2] T. Isernia, V. Pascazio, and R. Pierri, "On the local minima in tomographic imaging technique," ***IEEE Trans. Geosci. Remote Sens.***, 2001.

Multi-resolution strategy

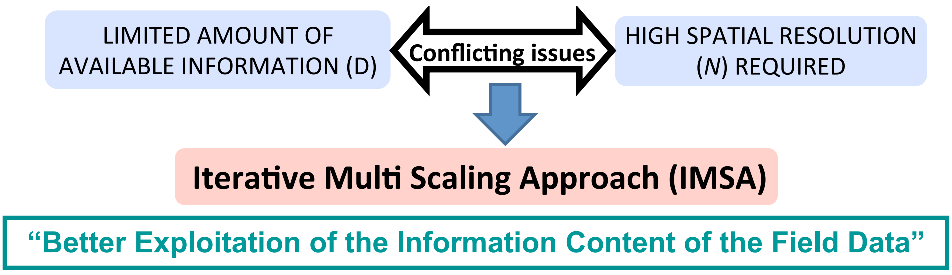

- **Key Issue**

  Smart allocation of the unknowns
  - ✓ Background - Low resolution
  - ✓ RoIs - High resolution

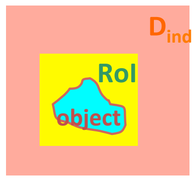

- **IMSA Features**
  - ❖ *Acquired* information - Multi-step process
  - ❖ No *a-priori* hypotheses

SOME MULTI-RESOLUTION STRATEGIES
[1] E. L. Miller. and A. S. Willsky, " A Multiscale, Statistically Based Inversion Scheme for Linearized Inverse Scattering Problems," *IEEE Trans. Geosci. Remote Sens.*, vol. 34, pp. 346-357, 1996.
[2] A. Baussard, E. L. Miller, D. Lesselier, "Adaptive Multiscale Approach for 2D Microwave Tomography", *Proc. URSI2004, Pisa, Italy, May 2004.*
[3] S. Caorsi, M. Donelli, D. Franceschini, and A. Massa, "A new methodology based on an iterative multiscaling for microwave imaging," *IEEE Trans. Microwave theory Tech.*, vol. 51, pp. 1162-1173, Apr. 2003.

The Multi-Scaling Process

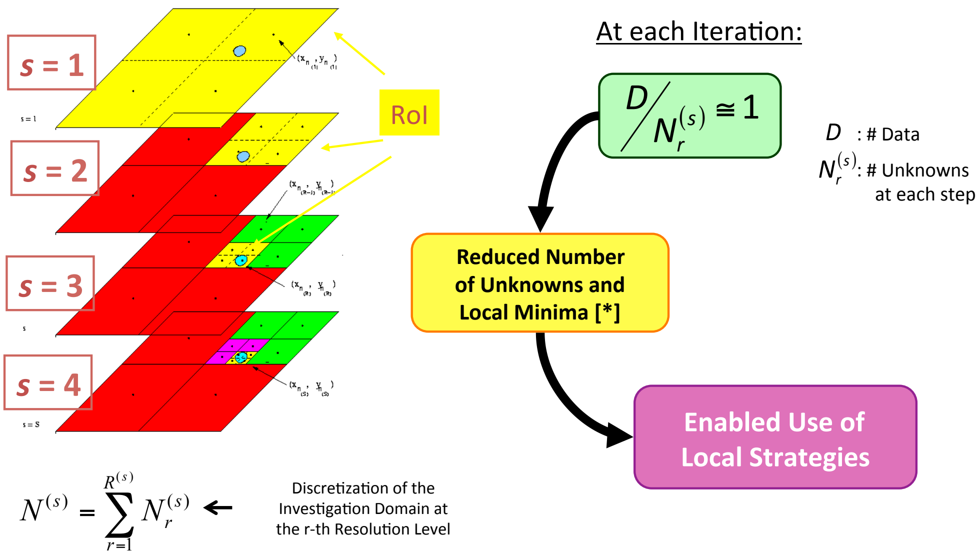

[*] T. Isernia, V. Pascazio, and R. Pierri, “On the local minima in a tomographic imaging technique,” *IEEE Trans. Geosci. Remote Sens.*, vol. 39, pp. 1596-1607, Jul. 2001.

The IMSA-IN Strategy

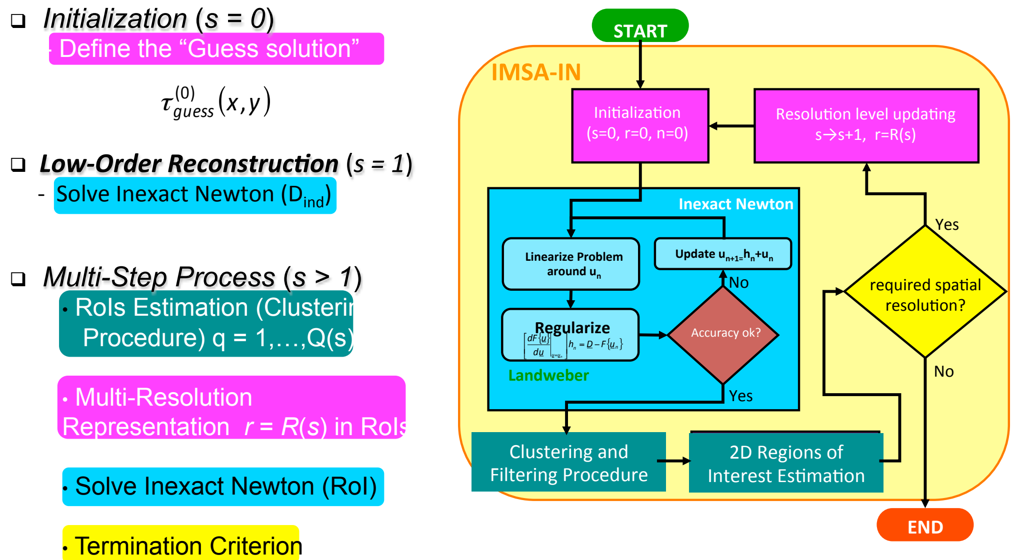

G. Oliveri, A. Randazzo, M. Pastorino, and A. Massa, “Electromagnetic imaging within the contrast source formulation by means of the multiscaling inexact Newton method,” J Opt Soc Am A, 2012.

3. Numerical Results

«L-Shaped» scatteter

Cross-borehole setup

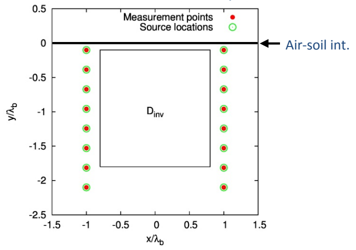

Actual dielectric profile

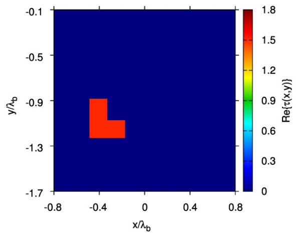

Scattering System Configuration:

- TM illumination: 300 MHz
- setup configuration: cross-borehole
- views: V=16
- measurement points for view: M=15 equally spaced
- D_{inv} dimension: $L_D = 1.6\lambda_b$

Scatterer:

- object function: $\tau = 1.5 + j0.0$

Error Figures:

$$e_{tot} = \frac{1}{N}\sum_{n=1}^{N}\frac{\left|\tau_n^{ric} - \tau_n\right|}{\left|\tau_n + 1\right|} \qquad e_{obj} = \frac{1}{N_{obj}}\sum_{n \in \text{the object}}\frac{\left|\tau_n^{ric} - \tau_n\right|}{\left|\tau_n + 1\right|} \qquad e_{bg} = \frac{1}{N_{bg}}\sum_{n \in \text{the background}}\frac{\left|\tau_n^{ric} - \tau_n\right|}{\left|\tau_n + 1\right|}$$

- Discretization
  - BARE-IN: N = 400
  - IMSA-IN: N = 100

SNR=20 dB

$t_{IMSA-IN}$ = 128 [s]
vs
$t_{BARE-IN}$ = 247 [s]

BARE-IN

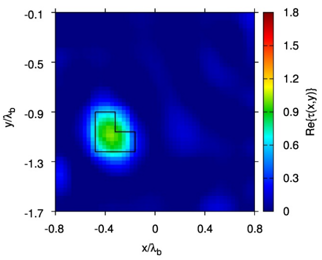

IMSA-IN

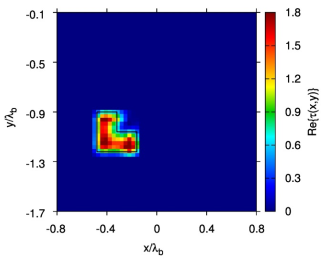

	e_{tot}	e_{obj}	e_{bg}
BARE-IN	8.53 10^{-2}	2.74 10^{-1}	6.19 10^{-2}
↑ IMSA-IN	1.02 10^{-2}	2.24 10^{-1}	1.84 10^{-3}

IN-External It.: 20
IN-Internal It.: 20

- Discretization
  - IMSA-IN: N = 100

$t_{IMSA\text{-}IN}$ = 128 [s]

SNR = 20 [dB]

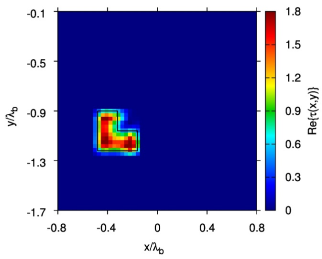

SNR = 10 [dB]

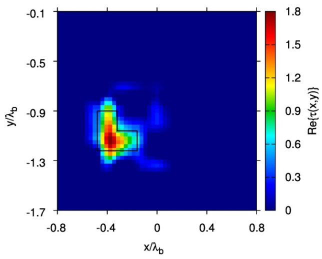

	e_{tot}	e_{obj}	e_{bg}
SNR = 20 [dB]	1.02 10^{-2}	2.24 10^{-1}	1.84 10^{-3}
SNR = 10 [dB]	5.85 10^{-2}	2.32 10^{-1}	4.12 10^{-2}

«O-Shaped» scatteter

Cross-borehole setup

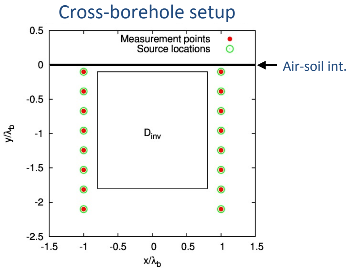

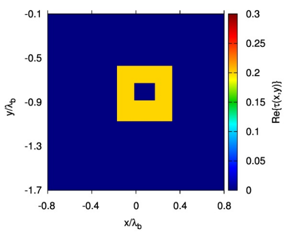

Actual dielectric profile

Scattering System Configuration:

- TM illumination: 300 MHz
- setup configuration: cross-borehole
- views: *V*=16
- measurement points for view: M=15 equally spaced
- D_{inv} dimension: $L_D = 1.6\lambda_b$

Scatterer:

- object function: $\tau = 0.2 + j0.0$
- outer side: $L = \lambda_b / 2$

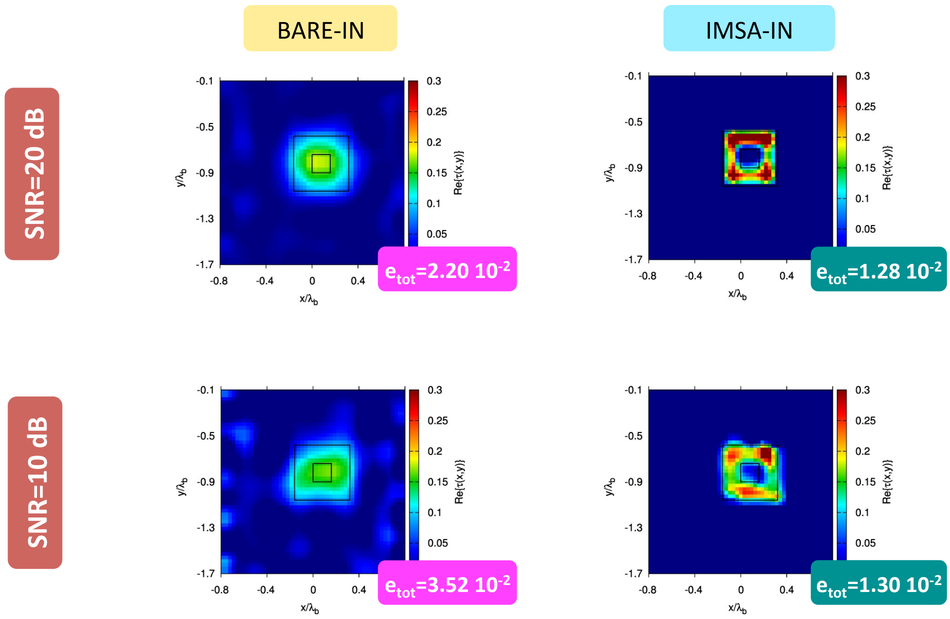
BARE-IN
IMSA-IN
SNR=20 dB
SNR=10 dB
e_{tot}=2.20 10^{-2}
e_{tot}=1.28 10^{-2}
e_{tot}=3.52 10^{-2}
e_{tot}=1.30 10^{-2}
x/λ_b
y/λ_b
Re{τ(x,y)}

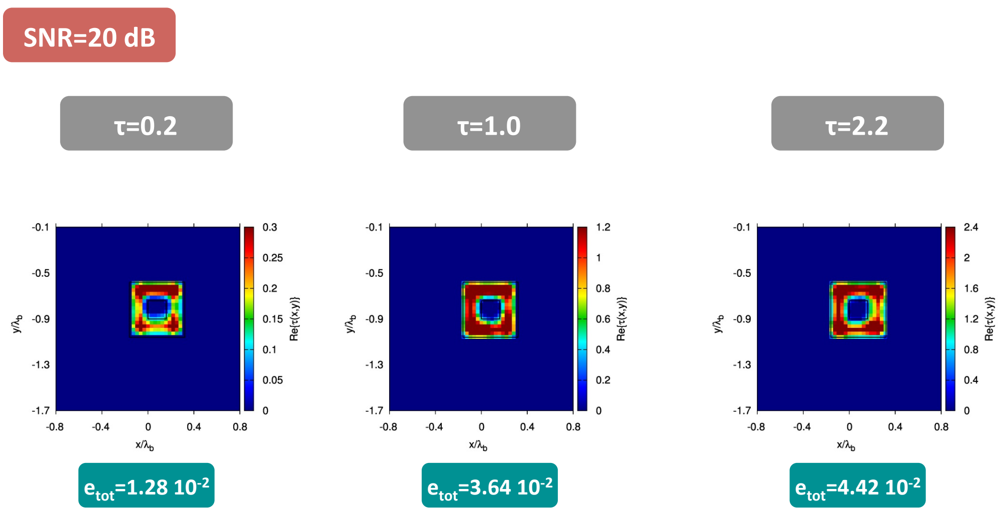
SNR=20 dB
τ=0.2
τ=1.0
τ=2.2
e_{tot}=1.28 10^{-2}
e_{tot}=3.64 10^{-2}
e_{tot}=4.42 10^{-2}
x/λ_b
y/λ_b
Re{τ(x,y)}

Homogeneous scatteter with Small Details

Cross-borehole setup

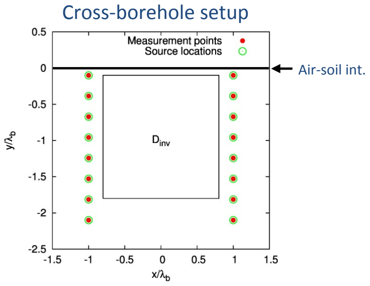

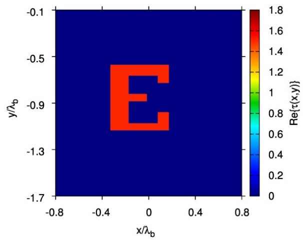

Scattering System Configuration:

- TM illumination: 300 MHz
- setup configuration: cross-borehole
- views: V=16
- measurement points for view: M=15 equally spaced
- D_{inv} dimension: $L_D = 1.6\lambda_b$

Scatterer:

- object function: $\tau = 1.5 + j0.0$

- Discretization
  - BARE-IN: N = 400
  - IMSA-IN: N = 100

SNR=20 dB

Improved Accuracy

BARE-IN

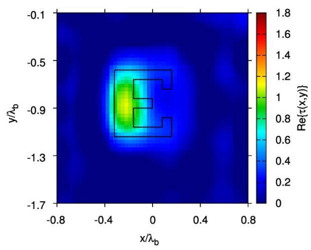

IMSA-IN

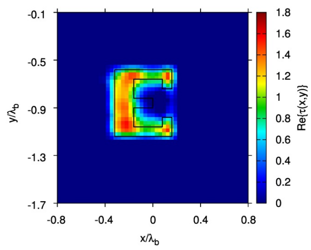

	e_{tot}	e_{obj}	e_{bg}
BARE-IN	1.34 10^{-1}	3.24 10^{-1}	1.04 10^{-1}
↑ IMSA-IN	4.42 10^{-2}	1.88 10^{-1}	3.18 10^{-2}

IN-External It.: 20
IN-Internal It.: 20

4. Conclusions and Future Work

The imaging problem by buried objects was studied, employing a second-order Born approximation. Inexact Newton-based multi-resolution approaches were developed and tested on synthetic data.

Future work will include testing the approach on experimental data and developing a 3D formulation.

Acknowledgement

The Authors thank COST for funding the Action TU1208 "Civil Engineering Applications of Ground Penetrating Radar".

"Detecting a subsurface cylinder by a Time Reversal MUSIC-like method" (contribution to project 3.2 and 3.4)

Raffaele Solimene (IT), Angela Dell'Aversano (IT), Giovanni Leone (IT)
raffaele.solimene@unina2.it

The abstract is published in *Geophysical Research Abstracts*, Vol. 16, EGU2014-10953, 2014 and is available on *www.egu2014.eu*
This contribution was presented as a poster.

"On the exploitation of Ground Penetrating Radar for civil engineering applications @ the ELEDIA Research Center" (contribution to project 3.2 and 3.4)

Marco Salucci (IT), Lorenza Tenuti (IT), Giacomo Oliveri (IT), Federico Viani (IT), Paolo Rocca (IT), and Andrea Massa (IT)
andrea.massa@unitn.it

The imaging of walls, roads, pavements and buildings using Ground Penetrating Radar (GPR) measurements represents a very active topic within the activities of the ELEDIA Research Center (DISI - University of Trento, Italy). More in details, the research activities mainly focus on the exploitation of advanced inverse scattering techniques, both deterministic and stochastic, together with their integration with multi-resolution methods, for the processing of GPR data. The performances of such inversion strategies have been well assessed when dealing with free-space microwave imaging scenarios, while multi-resolution approaches proved to be very effective in mitigating issues such as the non-linearity and ill-posedness of the inverse problem, which turn out to be even more remarkable when dealing with the more complex GPR formulation. In particular, great efforts have been devoted towards the development of a regularized multi-resolution approach based on the Inexact Newton (IN) method, both under the Second Order Born Approximation (SOBA) [1] and exploiting the full non-linear formulation of the GPR microwave imaging problem [2]. Moreover, the use of multi-frequency strategies is currently under investigation. These approaches allow to extract and then exploit the information coming from the intrinsic frequency diversity of the collected GPR data. In this framework, a multi-resolution technique based on a Frequency Hopping (FH) approach has been presented in [3] and [4]. Particular attention is also devoted towards the development of innovative imaging approaches based on Bayesian Compressive Sensing (BCS), which can be profitably exploited for the retrieval of multiple scatterers which are sparse with respect to a properly chosen representation basis [5],[6]. Furthermore, imaging approaches based on the level-set-based optimization technique have been considered, as well, for the qualitative reconstruction of multiple and disconnected homogeneous scatterers [7]. Finally, the real-time detection, localization and classification of defects embedded within inaccessible domains has been investigated by exploiting the so-called Learning-By-Examples (LBE) paradigm [7].

REFERENCES

[1] M. Salucci, G. Oliveri, A. Randazzo, M. Pastorino, and A. Massa, "Electromagnetic subsurface prospecting by a multi-focusing inexact Newton method within the second-order Born approximation," Journal of Optical Society of America A, vol. 31, no. 6, pp. 1167-1179, 2014.
[2] M. Salucci, G. Oliveri, A. Randazzo, M. Pastorino, and A. Massa, "Electromagnetic subsurface prospecting by a fully nonlinear multifocusing inexact Newton method," Journal of Optical Society of America A, vol. 31, no. 12, pp. 2618-2629, 2014.
[3] M. Salucci, P. Rocca, G. Oliveri, and A. Massa, "An innovative frequency hopping multizoom inversion strategy for GPR subsurface imaging," 15th International Conference on Ground Penetrating Radar (GPR 2014), Brussels, Belgium, June 30 - July 04, 2014.
[4] M. Salucci, L. Tenuti, C. Nardin, M. Carlin, F. Viani, G. Oliveri and A. Massa, "Gpr survey through a multi-resolution deterministic approach," IEEE AP-S International Symposium, Memphis, USA, July 6-12, 2014.
[5] L. Poli, G. Oliveri, P. Rocca, and A. Massa, "Bayesian compressive sensing approaches for the reconstruction of two-dimensional sparse scatterers under TE illumination," IEEE Trans. Geosci. Remote Sensing, vol. 51, no. 5, pp. 2920-2936, May. 2013.
[6] L. Poli, G. Oliveri, and A. Massa, "Imaging sparse metallic cylinders through a Local Shape Function Bayesian Compressive Sensing approach," Journal of Optical Society of America A, vol. 30, no. 6, pp. 1261-1272, 2013.
[7] M. Benedetti, D. Lesselier, M. Lambert, and A. Massa, "Multiple shapes reconstruction by means of multiregion level sets," IEEE Trans. Geosci. Remote Sensing, vol. 48, no. 5, pp. 2330-2342, May 2010.
[8] L. Lizzi, F. Viani, P. Rocca, G. Oliveri, M. Benedetti and A. Massa, "Three-dimensional real-time localization of subsurface objects - From theory to experimental validation," 2009 IEEE International Geoscience and Remote Sensing Symposium, vol. 2, pp. II-121-II- 124, 12-17 July 2009.

ACKNOWLEDGEMENT

This work is partially supported by the COST Action TU1208 "Civil Engineering Applications of Ground Penetrating Radar".

Progress Report of Project 3.3

"Development of intrinsic models for describing near-field antenna effects, including antenna-medium coupling, for improved radar data processing using full-wave inversion"

Albéric De Coster (BE), Sébastien Lambot (BE)
alberic.decoster@uclouvain.be

25 participants, 17 institutions and 1 company

8 countries : Italy, France, United Kingdoms, Belgium, Greece, Portugal, Croatia and The Former Yugoslav Republic of Macedonia

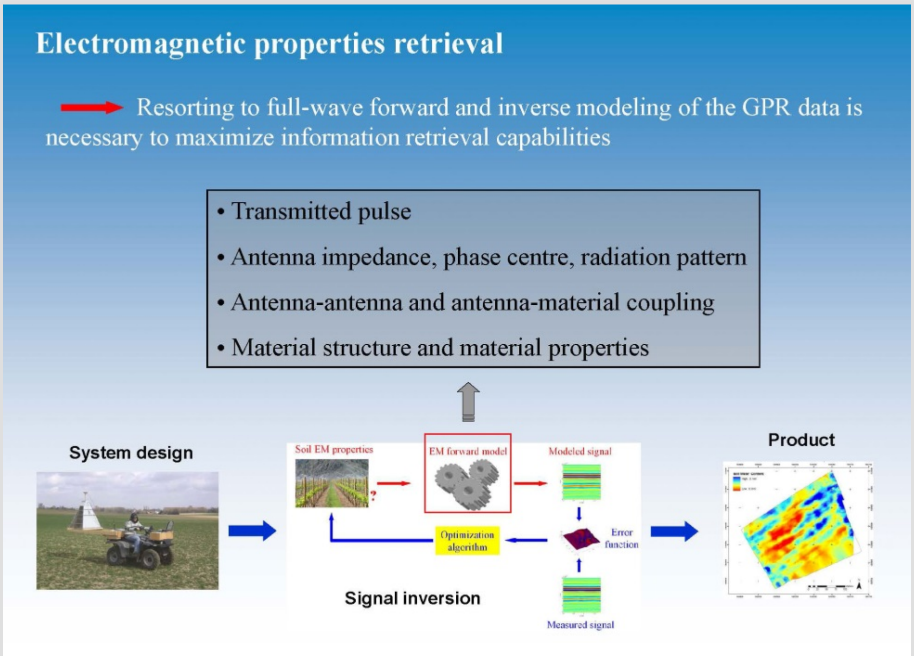

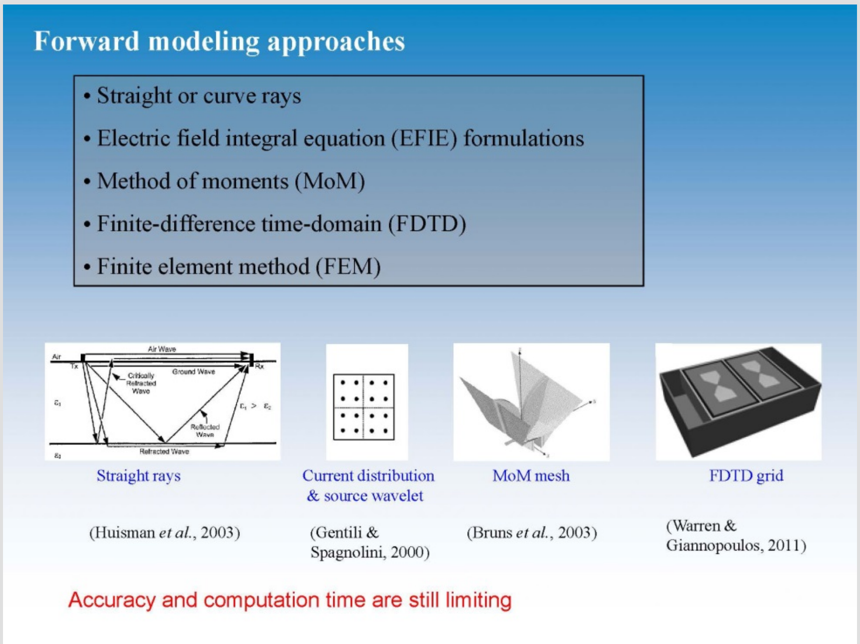
Forward modeling approaches
• Straight or curve rays
• Electric field integral equation (EFIE) formulations
• Method of moments (MoM)
• Finite-difference time-domain (FDTD)
• Finite element method (FEM)
Air Wave
Ground Wave
Critically Refracted Wave
Reflected Wave
Refracted Wave
Straight rays
Current distribution & source wavelet
MoM mesh
FDTD grid
(Huisman et al., 2003)
(Gentili & Spagnolini, 2000)
(Bruns et al., 2003)
(Warren & Giannopoulos, 2011)
Accuracy and computation time are still limiting

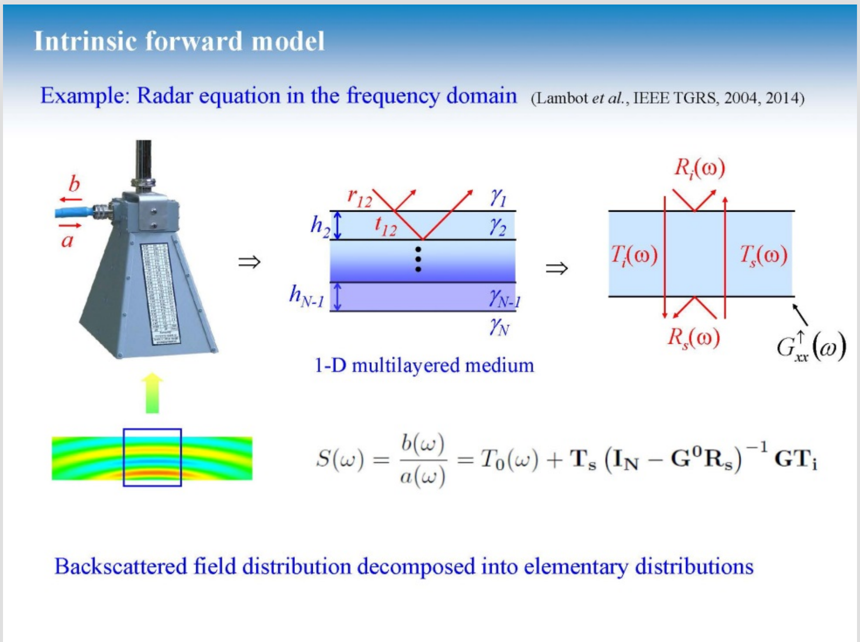
Intrinsic forward model
Example: Radar equation in the frequency domain (Lambot et al., IEEE TGRS, 2004, 2014)
b
a
r_{12}
t_{12}
h_2
h_{N-1}
γ_1
γ_2
γ_{N-1}
γ_N
1-D multilayered medium
$R_i(\omega)$
$T_i(\omega)$
$T_s(\omega)$
$R_s(\omega)$
$G_{xx}^{\uparrow}(\omega)$
$S(\omega) = \frac{b(\omega)}{a(\omega)} = T_0(\omega) + \mathbf{T_s}\left(\mathbf{I_N} - \mathbf{G^0R_s}\right)^{-1}\mathbf{GT_i}$
Backscattered field distribution decomposed into elementary distributions

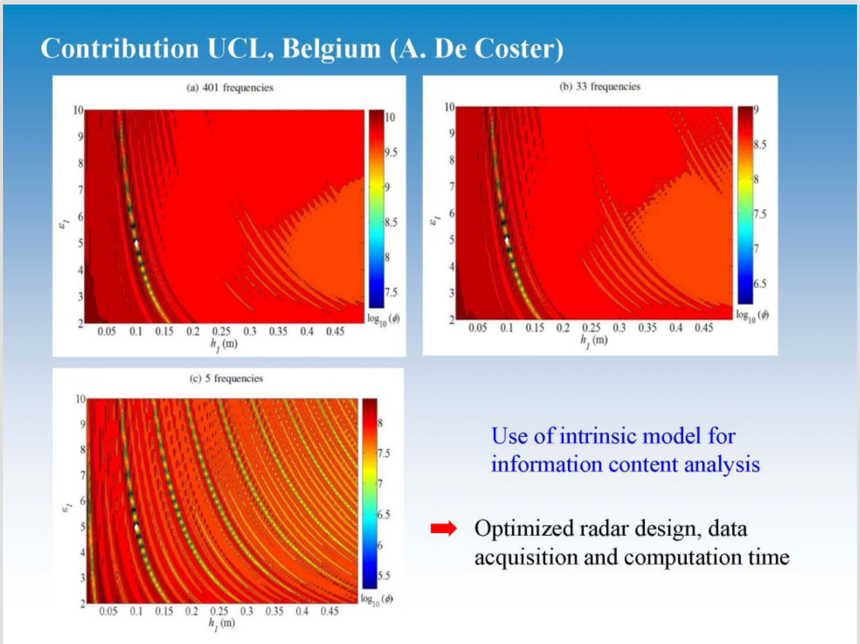
Contribution UCL, Belgium (A. De Coster)
(a) 401 frequencies
(b) 33 frequencies
(c) 5 frequencies
h_1 (m)
ε_1
$\log_{10}(\phi)$
Use of intrinsic model for information content analysis
Optimized radar design, data acquisition and computation time

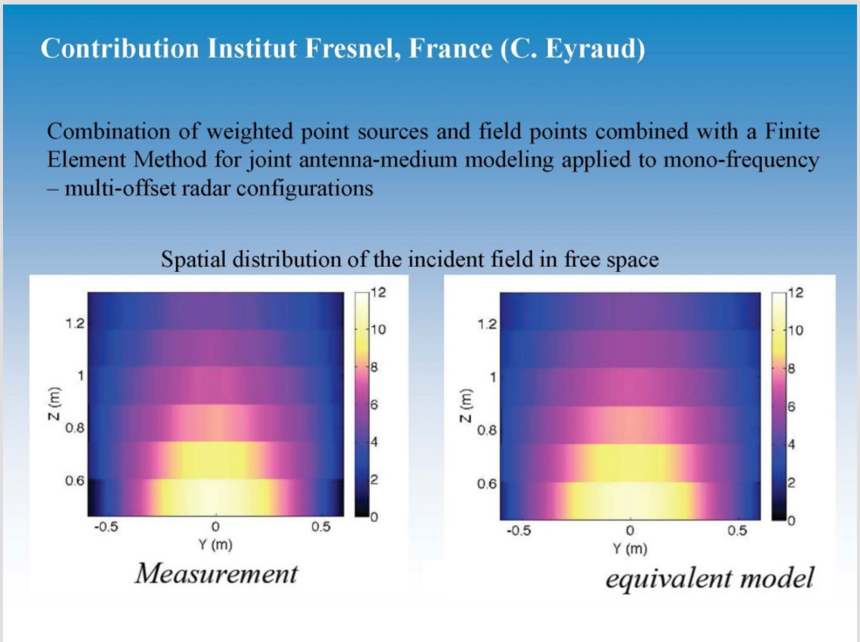
Contribution Institut Fresnel, France (C. Eyraud)
Combination of weighted point sources and field points combined with a Finite Element Method for joint antenna-medium modeling applied to mono-frequency – multi-offset radar configurations
Spatial distribution of the incident field in free space
Z (m)
Y (m)
Measurement
equivalent model

Contribution Alyotech Technologies, France (N. Pinel)

Full wave PILE method for the electromagnetic scattering from random rough layers

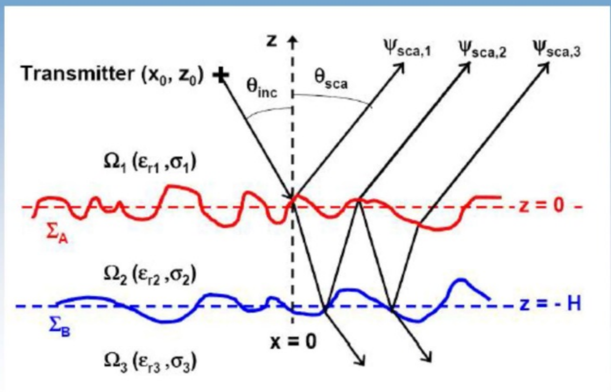

Contribution Split, Croatia (D. Poljak)

Optimization of the Galerkin-Bubnov Integral Boundary Element Method

(Space-time dependant integral equations - no derivatives)

➡ Improvements to fastly model antennas in presence of lossy media

$$\int_0^L \frac{I(x',t-\frac{R}{c})}{4\pi R}dx' - \int_{-\infty}^{t}\int_0^L r(\theta,\tau)\frac{I(x',t-\frac{R^*}{c}-\tau)}{4\pi R^*}dx'd\tau =$$

$$\frac{1}{2Z_0}\int_0^L E_x^{inc}(x',t-\frac{|x-x'|}{c})dx' + F_0(t-\frac{x}{c}) + F_L(t-\frac{L-x}{c})$$

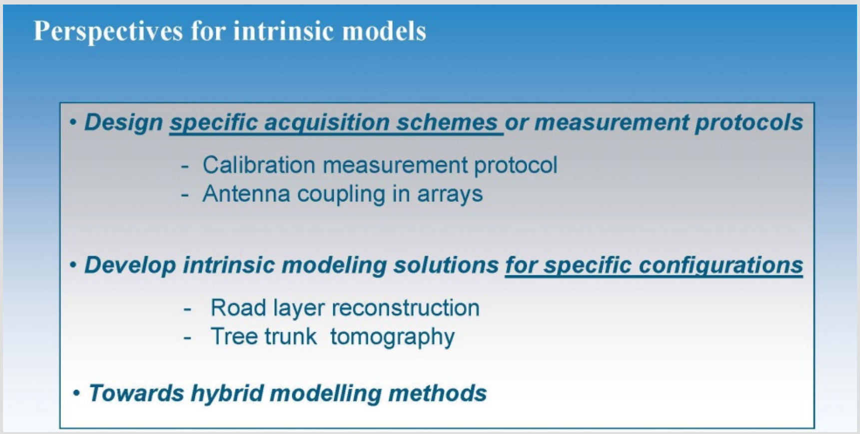

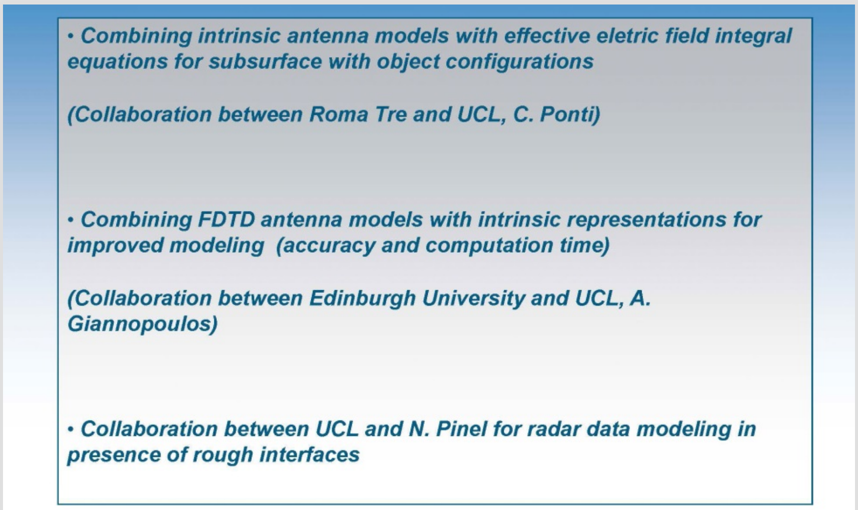

"High-resolution monitoring of root water uptake dynamics in laboratory conditions using full-wave inversion of near-field radar" (contribution to Project 3.3)

Nicolas Mourmeaux (BE), Félicien Meunier (BE), Phuong Anh Tran (BE), Xavier Draye (BE), Sébastien Lambot (BE) - *nicolas.mourmeaux@uclouvain.be*

The abstract is published in *Geophysical Research Abstracts*, Vol. 16, EGU2014-12334, 2014 and is available on *www.egu2014.eu*
This contribution was presented as a poster.

"Information content in frequency-dependent, multi-offset GPR data for layered media reconstruction using full-wave inversion" (Contribution to project 3.3)

Albéric De Coster (BE), Phuong Anh Tran (BE), Sébastien Lambot (BE)
alberic.decoster@uclouvain.be

The abstract is published in *Geophysical Research Abstracts*, Vol. 16, EGU2014-658, 2014 and is available on *www.egu2014.eu*

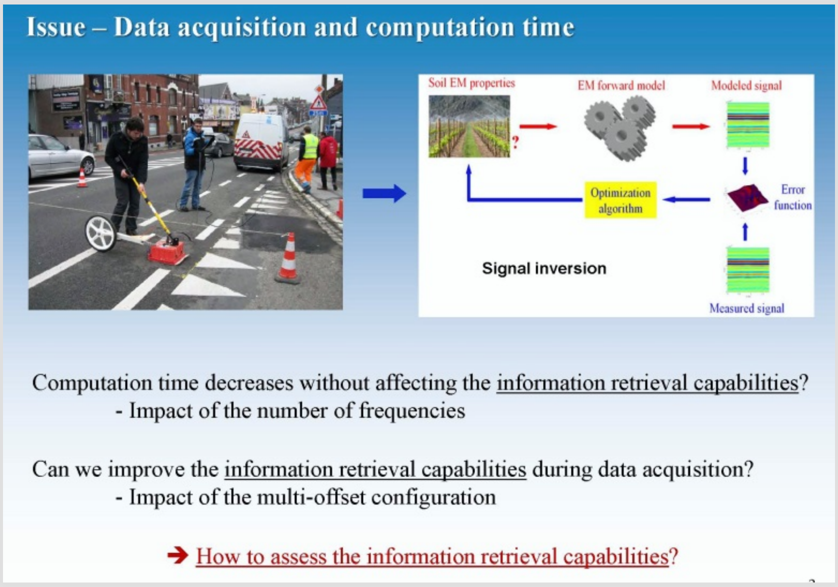

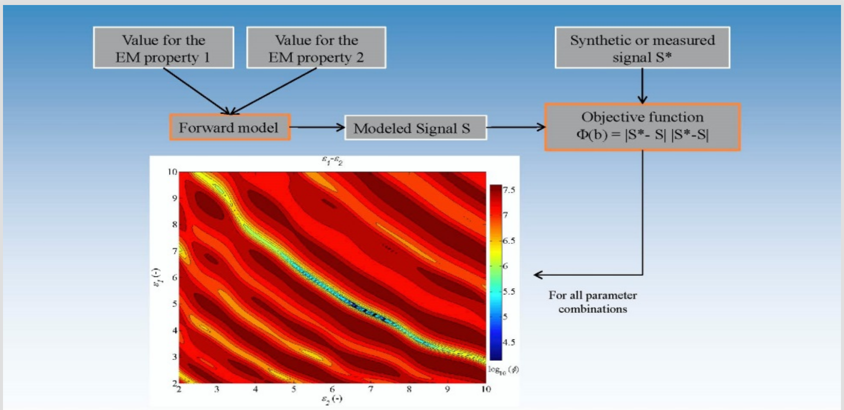

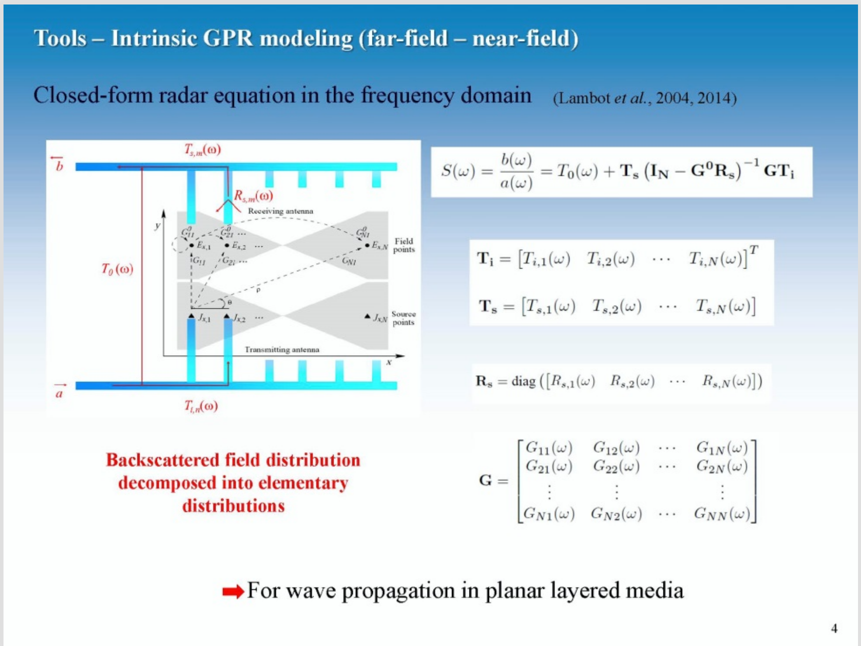
Tools – Intrinsic GPR modeling (far-field – near-field)
Closed-form radar equation in the frequency domain (Lambot *et al.*, 2004, 2014)
$S(\omega) = \frac{b(\omega)}{a(\omega)} = T_0(\omega) + \mathbf{T_s}\left(\mathbf{I_N} - \mathbf{G^0 R_s}\right)^{-1}\mathbf{G T_i}$
$\mathbf{T_i} = [T_{i,1}(\omega) \quad T_{i,2}(\omega) \quad \cdots \quad T_{i,N}(\omega)]^T$
$\mathbf{T_s} = [T_{s,1}(\omega) \quad T_{s,2}(\omega) \quad \cdots \quad T_{s,N}(\omega)]$
$\mathbf{R_s} = \mathrm{diag}\left([R_{s,1}(\omega) \quad R_{s,2}(\omega) \quad \cdots \quad R_{s,N}(\omega)]\right)$
$\mathbf{G} = \begin{bmatrix} G_{11}(\omega) & G_{12}(\omega) & \cdots & G_{1N}(\omega) \\ G_{21}(\omega) & G_{22}(\omega) & \cdots & G_{2N}(\omega) \\ \vdots & \vdots & & \vdots \\ G_{N1}(\omega) & G_{N2}(\omega) & \cdots & G_{NN}(\omega) \end{bmatrix}$
$T_{s,m}(\omega)$
$R_{s,m}(\omega)$
$T_0(\omega)$
$T_{i,n}(\omega)$
Receiving antenna
Field points
Source points
Transmitting antenna
Backscattered field distribution decomposed into elementary distributions
For wave propagation in planar layered media
4

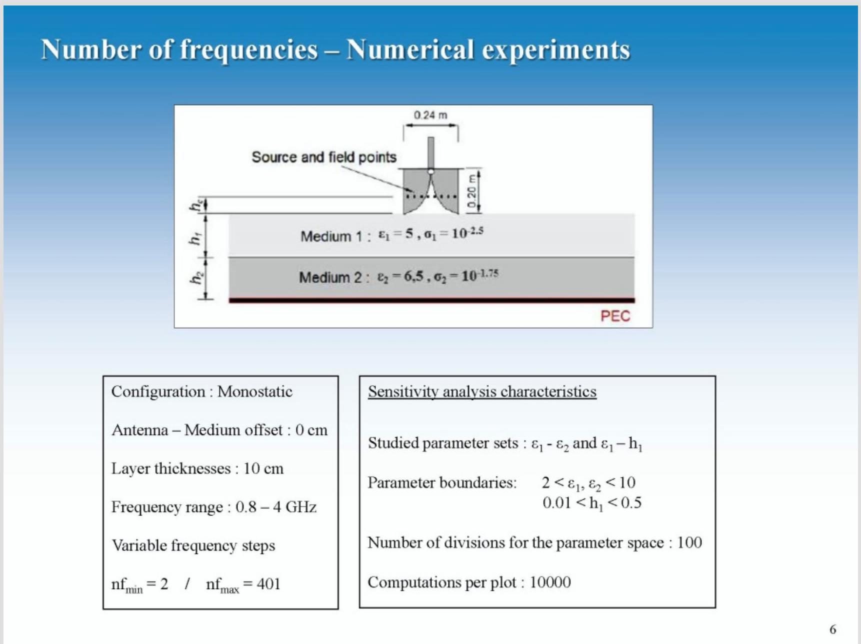
Number of frequencies – Numerical experiments
0.24 m
Source and field points
0.20 m
h_0
h_1
h_2
Medium 1 : $\varepsilon_1 = 5$, $\sigma_1 = 10^{-2.5}$
Medium 2 : $\varepsilon_2 = 6.5$, $\sigma_2 = 10^{-1.75}$
PEC
Configuration : Monostatic
Antenna – Medium offset : 0 cm
Layer thicknesses : 10 cm
Frequency range : 0.8 – 4 GHz
Variable frequency steps
$nf_{min} = 2$ / $nf_{max} = 401$
Sensitivity analysis characteristics
Studied parameter sets : $\varepsilon_1 - \varepsilon_2$ and $\varepsilon_1 - h_1$
Parameter boundaries: $2 < \varepsilon_1, \varepsilon_2 < 10$
$0.01 < h_1 < 0.5$
Number of divisions for the parameter space : 100
Computations per plot : 10000
6

Number of frequencies – Numerical experiments

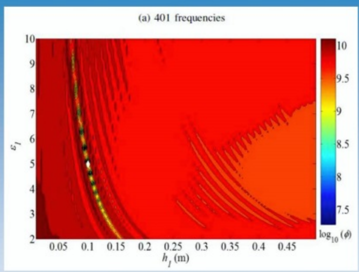

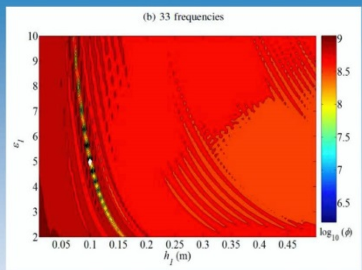

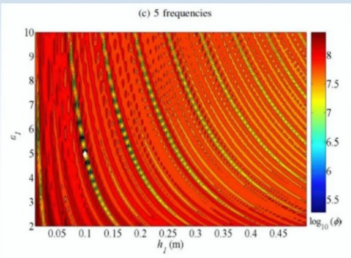

Information content analysis

➡ Optimized radar design, data acquisition and computation time

7

Number of frequencies – Laboratory experiments

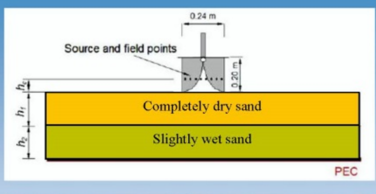

Setup

Layer thicknesses : 10 cm
Slightly wet sand : ~4%

Measurements

Antenna type : Vivaldi
Heights : Various
Frequency range : 0.8 - 4.0 GHz
Frequency step : 2 MHz

Sensitivity analyses

Parameter boundaries: $2 < \varepsilon_1, \varepsilon_2 < 10$
Computations per plot : 10000
Number of frequencies : 1601, 401, 101, 33 & 5

NB : Conductivities previously fixed thanks to an inversion procedure

8

Number of frequencies – Laboratory experiments

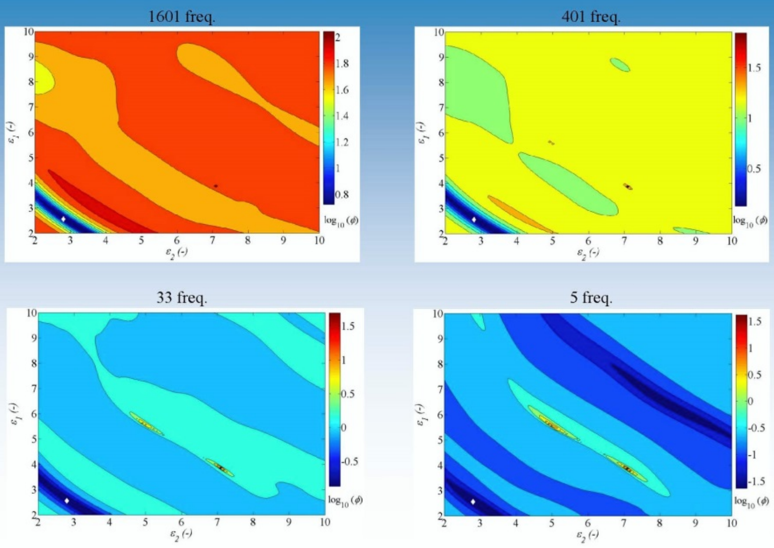

9

Number of frequencies – Laboratory experiments

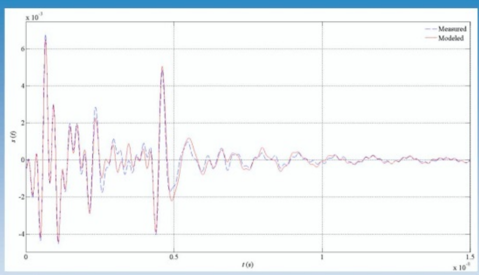

1601 frequencies	
Parameter values	$\varepsilon_1 = 2{,}55$; $\varepsilon_2 = 2{,}80$
Retrieved values	$\varepsilon_1 = 2{,}39$; $\varepsilon_2 = 3{,}04$
Computation time	± 62 minutes

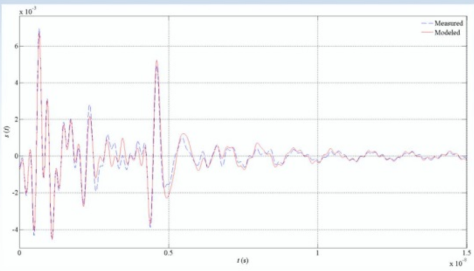

101 frequencies	
Parameter values	$\varepsilon_1 = 2{,}55$; $\varepsilon_2 = 2{,}80$
Retrieved values	$\varepsilon_1 = 2{,}35$; $\varepsilon_2 = 3{,}08$
Computation time	± 9 minutes

10

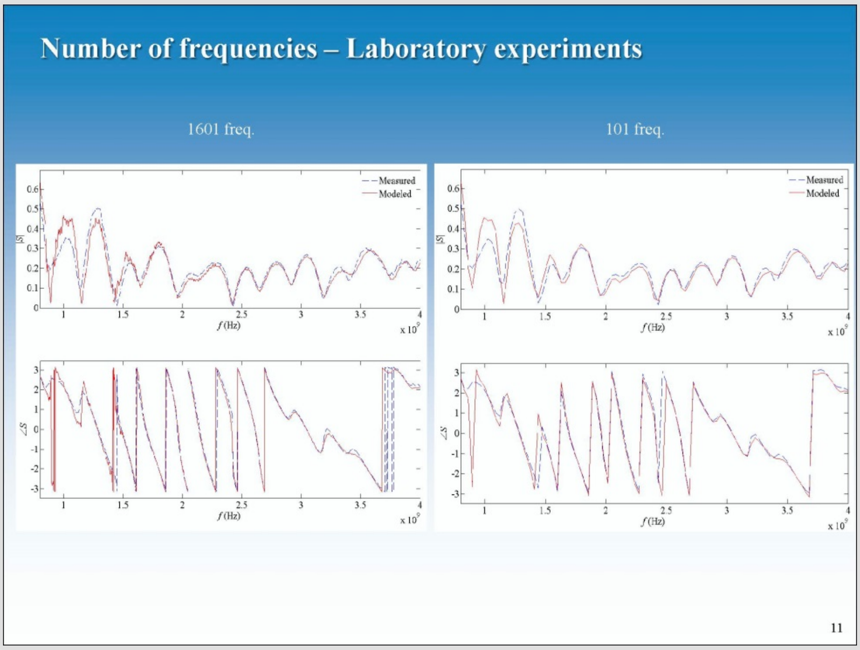

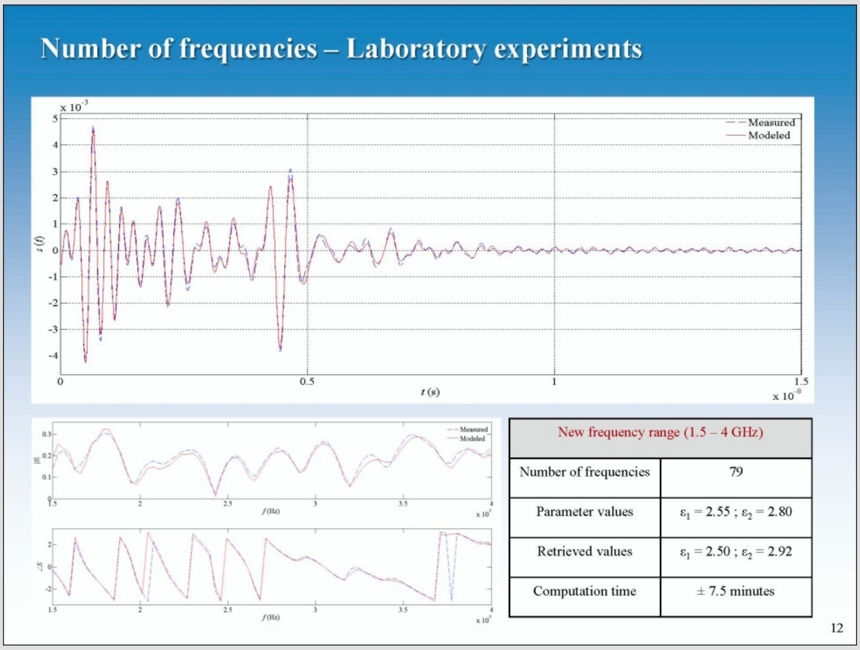

New frequency range (1.5 – 4 GHz)	
Number of frequencies	79
Parameter values	$\varepsilon_1 = 2.55$; $\varepsilon_2 = 2.80$
Retrieved values	$\varepsilon_1 = 2.50$; $\varepsilon_2 = 2.92$
Computation time	± 7.5 minutes

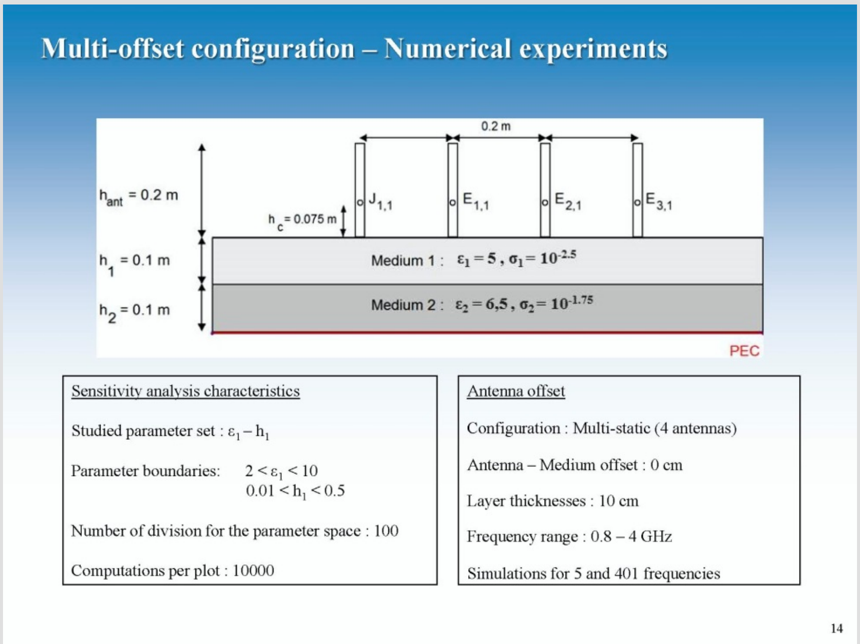

Conclusions

Numerical experiments

- Shrink of the number of frequencies without affecting the objective functions
- Great potential of combining multi-static configurations with the reduction of the number of frequencies

Laboratory experiments

- Information content decreases when less frequencies are taken into account
- The response surface topography remains identical near the minimum

Perspectives

- Laboratory experiments with a multi-static configuration
- Analyze of different methods to combine the multi-static data
- Different number of layers and contrasts
- Full-wave inversion analyses for different heights
- Automatic selection of the relevant frequencies
- Field experiments

Progress Report of Project 3.5

"Development of advanced GPR data processing techniques"

Nikos Economou (GR), Francesco Benedetto (IT)
francesco.benedetto@uniroma3.it

Abstract

Ground penetrating radar (GPR) is a nondestructive geophysical method that uses radar pulses to image the subsurface. Notwithstanding it is particularly promising for soil characteristics interpretation, GPR is characterized by a notoriously difficult automated data analysis. Hence, this contribution reports the works published during the first year of the COST action TU1208, as well as the future directions and the on-going researches in the field of GPR data processing techniques.

1. Introduction

The Project 3.5 of the COST action TU1208 is titled "Development of advanced GPR data processing techniques", and comprises 44 participants (included the 2 co-leaders) originating from 14 different Countries. In particular, participants come from (in alphabetic order): Armenia, Belgium, Croatia, France, Greece, Italy, Latvia, Norway, Portugal, Slovak Republic, Spain, The Netherlands, Turkey, and UK. The focus of Project 3.5 is particularly devoted to the development of GPR data processing techniques, studying and proposing signal processing methods for the enhancement of the GPR signal such as: denoising, deconvolution, migration and attribute analysis as well as visualization of GPR data.

This report is organized as follows. In the next Section, we review the papers published by the 3.5 participants during the first year of the Action. Then, we outline the on-going researches, briefly discussing what more is needed and what is expected during the next years.

2. Related Works

In the field of civil engineering, sounding the pavement layers is classically performed using standard ground penetrating radar, whose vertical resolution is bandwidth dependent. The layer thicknesses are deduced from both the time delays of backscattered echoes and the

permittivity of layers. In contrast with conventional spectral analysis approaches, the work in [1] focuses on one of the machine learning algorithms, namely, the support vector machine, to perform time delay estimation and dielectric constant estimation of the medium from backscattered radar signals. The authors show the super time resolution capability of such technique to resolve overlapping and fully correlated echoes within the context of thin pavement layer testing. Then, in civil engineering, ground penetrating radar is widely used for road pavement surveys. In contrast to the existing literature, in [2] the influence of interface roughness (surface and interlayer roughness of stratified media) is accounted for within the scope of the data processing of radar signals. The rigorous electromagnetic method PILE (propagation inside layer expansion) provides the simulated data. The observed frequency variations of the radar magnitude introduce some shape distortion on the radar wavelet. An adaptation of the root-MUSIC algorithm is proposed on the basis of the work. As a result, it is allowed to jointly estimate the time delay and the interface roughness.
Now let us talk of inverse scattering and imaging by presenting some recent advances in this fields. In [3], the reconstruction of shallow buried object is addressed by an electromagnetic inverse scattering method based on combining different imaging modalities. In particular, the proposed approach integrates the inexact-Newton method with an iterative multi-scaling approach. Moreover, the use of the second-order Born approximation is exploited. A numerical validation is provided concerning the potentialities arising by combining the regularization capabilities of the inexact-Newton method and the effectiveness of the multi-focusing strategy to mitigate the non-linearity and ill-posedness of the inversion problem. Comparisons with the standard "bare" approach in terms of accuracy, robustness, noise levels, and computational efficiency are also included. In addition, in [4], a GPR survey through a multi-resolution deterministic approach is carried out (inverse scattering and imaging). In [5], a novel electromagnetic inverse scattering method is proposed for the reconstruction of shallow buried objects. The inversion procedure is based on the combination of different imaging modalities. In particular, an iterative multi-scaling approach is adopted for focusing the reconstruction only on limited subdomains of the original investigation region. The data inversion is performed by applying an inexact-Newton method (which exhibits very good regularization properties) within the second-order Born approximation. The use of this approximation allows a reduction of the problem unknowns and a mitigation of the nonlinear effects. The proposed approach has been

validated by means of several numerical simulations. In particular, the reconstruction performances have been evaluated in terms of accuracy, robustness, noise levels, and computational efficiency, with particular emphasis on the comparisons with the results obtained by using the standard "bare" approach. Finally, in [6], the inspection of 2-D scatterers buried in a lossy half-space from field measurements is formulated within the framework of the second-order Born approximation (SOBA) of the inverse scattering problem. An iterative multi-scaling approach (IMSA) is combined with a two-step inexact-Newton algorithm to solve the arising problem. A set of preliminary numerical results is presented to assess the features and potentialities of the considered approach also in comparison with state of the art inexact-Newton-SOBA techniques. However, probing the near-subsurface in presence of absorbing media is a very challenging problem. Within that framework, the authors of [7] analyze the capabilities of a mono-frequency/multistatic set-up for detecting shallowly buried targets. As the antennas constitute an important part of the probing device, an accurate method for modelling the antennas behaviour is proposed. This modelling, performed thanks to a correctly balanced set of elementary sources, is then incorporated in the calculation of the scattered field, performed with a home-made Finite Element Method software. The measured multistatic fields serve as input data for the inversion algorithm, an extension of the DORT method to elongated targets [8]. This qualitative and fast imaging procedure allows to obtain imaging results of shallowly buried targets embedded in a highlosses medium [9].Now, let us have a deep look of what has been done in terms of GPR signal processing techinques. In [10], the authors relate the shift of the frequency peak of the Ground Penetrating Radar (GPR) spectrum with the increasing of the moisture content in the soil. The weakness characterizing this approach is represented by the needs of high resolution signals, whereas GPR spectra are affected by low resolution. The novelty introduced by this work is twofold. First, they evidence that clay content information is present in the location where the maximum amplitude of the GPR spectra occurs. Then, they analyze three super resolution methods, namely parabolic, triangular, and sinc-based interpolators, to further refine the location of the frequency peak. In fact, it is really important to be able to find this location quite precisely, to obtain accurate estimates of clay content. They show that the peak location can be found best through sinc-interpolation in the frequency domain of the measured data. Experimental results confirm the effectiveness of the proposed approach to resolve a frequency shift in the GPR spectrum, even for a small amount of clay. Then, the focus of

the work in [11] is to provide the reader with a deep understanding of the state of the art and open issues in the field of GPR data processing techniques as well as of the interesting application of GPR in the field of civil engineering. In particular, the authors present an overview on noise suppression, deconvolution, migration, attribute analysis and classification techniques for GPR data. In [12], the needs for advanced sensing technologies in the field of civil engineering are shown and discussed. In the first part of the work, the authors present an overview of these main needs, fields by fields, from the constructions and inspections of the transportation infrastructures and the hydraulic works, to the geotechnical surveys and environmental monitoring as well as the buildings and bridge structural assessments. In the second part, they discuss the upgrading and evolution of the sensing technologies, oriented to the civil engineering applications. They demonstrate why the Ground Penetrating/Probing Radar is currently considered as one of the most effective and efficient sensing technology and potentially candidate to become the best available remote sensing technology for civil engineering applications. Finally, in [13], an innovative application for mobile platforms (smartphones and tablets) for real-time GPR data processing. This work aims at providing a useful support for engineers and technicians as well, for road and pavement inspection. According to the presented results, this application can play an important role for all the agencies involved in roads and highway management. In particular, it will provide strategic and innovative potentialities, by improving the onsite efficiency and effectiveness of the works.

3. On-going Researches

GPR proves to be very useful in road monitoring applications, pipes, cables, tunnels and other buried objects delineation, railways ballast condition monitoring, concrete structures inspection and bridge deck inspection, buried archaeological ruins mapping, and many other relevant applications which have already been applied or are to come in the future. In [14], an interesting review of the GPR technologies and methodologies used in Italy is carried out. Then, the research centers belonging to the Project 3.5 of the COST Action TU1208 are actually investigating numerous topics in the field of GPR data processing techniques related to the aforementioned applications. For example, currently, subsurface imaging from GPR measurements represents a very active topic within the activities of the ELEDIA Research Center (DISI - University of Trento, Italy) [15]. More in details, the research

activities mainly focus on the exploitation of advanced inverse scattering techniques, whose performances have been well assessed in case of freespace scenarios, and their integration with multi-scaling methods for the processing of GPR data. Moreover, great efforts are devoted to the development of inversion strategies that can profitably exploit the frequency diversity of GPR measurements, in order to improve the quality of the retrieved dielectric profiles, both qualitatively and quantitatively. Particular attention is also devoted to the extension of innovative imaging approaches based on Bayesian Compressive Sensing (BCS) and Interval Analysis (IA) to the problem of subsurface prospecting, as well as to the exploitation of Learning-By-Example (LBE) algorithms for enabling real-time detection and classification of buried objects. The on-going researches of the Université catholique de Louvain linked to the topics of the WP are the following: (*i*) Information content in frequency-dependent and multi-offset GPR data for layered media reconstruction; (*ii*) Image resolution improvement using GPR data fusion; (*iii*) Effective physically- and mathematically-based detection of hyperbola and determination of the dielectric permittivity in complex field radar data; and (*iv*) deconvolution. Other activities related to the COST action carried out at University of Nantes and CEREMA, Les Ponts de Cé, France are: (*i*) Estimation of time delays, permittivities and roughness parameters by GPR, especially with subspace methods (MUSIC, ESPRIT, etc); and (*ii*) Detection of debonding within pavement structures by GPR with machine learning methods. Then, at the Applied Geophysics Lab., School of Mineral Resources Engineering, Technical Univerity of Crete, these are the on-going researches: (*i*) automatic bandpass filtering and deconvolution of GPR data; (*ii*) attenuation analysis of GPR data; and (*iii*) noise suppression of GPR data using the Empirical Mode Decomposition (EMD) method.

4. CONCLUSIONS

This paper has presented a review of what has been done during the first year of the COST action TU1208 in the field of GPR data processing techniques by the WG 3.5 participants. Fundamental topics such as denoising, deconvolution, migration, attribute analysis, inverse scattering and imaging were discussed as well as the on-going studies. Notwithstanding this research area has already been well studied by many researchers as well evidenced by the works presented in the reference's Section, more is needed and even more is expected from automatic GPR data analysis in the next years.

ACKNOWLEDGEMENT

The authors acknowledge the COST Action TU1208 "Civil Engineering Applications of Ground Penetrating Radar", supporting this work.

REFERENCES

[1] C. Le Bastard, Y. Wang, V. Baltazart and X. Dérobert, "Time Delay and Permittivity Estimation by Ground Penetrating Radar with Support Vector Regression", IEEE Geoscience and Remote Sensing Letters, Vol. 11, No. 4, pp. 873-877, April 2014.
[2] M. Sun, N. Pinel, C. Le Bastard, V. Baltazart, A. Ihamouten and Y. Wang, "Time delay and surface roughness estimation by subspace algorithms for pavement survey by radar", 7th International Workshop on Advanced Ground Penetrating Radar, Nantes, July, 2013.
[3] M. Salucci, G. Oliveri, A. Randazzo, M. Pastorino, and A. Massa, "Electromagnetic subsurface prospecting by a multi-focusing inexact Newton method within the second-order Born approximation," Journal of Optical Society of America A (in press), 2014.
[4] M. Salucci, L. Tenuti, C. Nardin, M. Carlin, F. Viani, G. Oliveri and A. Massa, "GPR survey through a multiresolution deterministic approach," IEEE AP-S International Symposium, Memphis, Tennessee, USA, July 6-12, 2014.
[5] M. Salucci, G. Oliveri, A. Randazzo, M. Pastorino, and A. Massa, "Multi-Focusing Procedure based on the Inexact-Newton Method for Electromagnetic Subsurface Prospecting," European Geosciences Union General Assembly (EGU2014), Vienna, Austria, April 27 - May 2, 2014.
[6] M. Salucci, D. Sartori, N. Anselmi, A. Randazzo, G. Oliveri, and A. Massa, "Imaging Buried Objects within the Second-Order Born Approximation through a Multiresolution Regularized Inexact-Newton Method", 2013 International Symposium on Electromagnetic Theory (EMTS), (Hiroshima, Japan), May 20-24 2013 (invited).
[7] S. Nounouh, C. Eyraud, H. Tortel, A. Litman, Near-subsurface imaging from a multistatic/single frequency scanner, IWAGPR, Nantes, 2013.
[8] X. Zhang, H. Tortel, A. Litman, and J. Geffrin, An extended-DORT method and its application in a cavity configuration, Inverse Problems, vol. 28, p. 115008, 2012.
[9] S. Nounouh, C. Eyraud, A. Litman, H. Tortel, Near-subsurface imaging in an absorbing embedding medium with a multistatic/single frequency scanner, Near Surface Geophysics, submitted.

[10] F. Benedetto , F. Tosti, "GPR Spectral Analysis for Clay Content Evaluation by the Frequency Shift Method", Journal of Applied Geophysics, vol. 97, pp. 87-96, 2013.
[11] N. Economou, A. Vafidis, F. Benedetto, A. M. Alani, "GPR Data Processing Techniques", in "Civil Engineering Applications of Ground Penetrating Radar", Springer, in press Dec. 2014.
[12] A. Benedetto, F. Benedetto - "Application Field Specific Synthesizing of Sensing Technology: Civil Engineering Application of Ground Penetrating Radar Sensing Technology", in "Comprehensive Material Processing Technology", Saleem Hashmi editor, Elsevier Publisher, in press, May 2014.
[13] F. Benedetto, A. Benedetto, A. Tedeschi, "A Mobile Android Application for Road and Pavement Inspection by GPR Data Processing", 5th Int. Conf. on Ground Penetrating Radar (GPR 2014), Brussels, Belgium, 2014.
[14] A. Benedetto, F. Frezza, G. Manacorda, A. Massa, and L. Pajewski, "GPR technologies and methodologies in Italy: a review," European Geosciences Union General Assembly (EGU2014), Vienna, Austria, April 27 - May 2, 2014.
[15] M. Salucci, L. Tenuti, C. Nardin, G. Oliveri, F. Viani, P. Rocca, and A. Massa , "Civil engineering applications of ground penetrating radar: recent advances @ the ELEDIA Research Center," European Geosciences Union General Assembly (EGU2014), Vienna, Austria, April 27 - May 2, 2014.

"GPR IMAGE AND SIGNAL PROCESSING FOR PAVEMENT AND ROAD MONITORING ON ANDROID SMARTPHONES AND TABLETS" (CONTRIBUTION TO PROJECT 3.5)

Francesco Benedetto (IT), Andrea Benedetto (IT), Antonio Tedeschi (IT)
francesco.benedetto@uniroma3.it

The abstract is published in *Geophysical Research Abstracts*, Vol. 16, EGU2014-1732, 2014 and is available on *www.egu2014.eu* .

This contribution was presented as a poster.

"Inverse Scattering and GPR Data Processing: an Introduction"
(contribution to projects 3.2, 3.4, 3.5)

Raffaele Persico (IT)
r.persico@ibam.cnr.it

The abstract is published in *Geophysical Research Abstracts*, Vol. 16, EGU2014-10417, 2014 and is available on *www.egu2014.eu.*

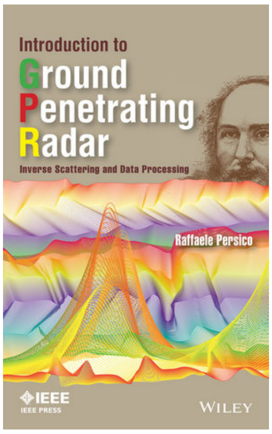

Main Purposes of the Book:

To devote a text to the physics and mathematics related to GPR data processing

To derive the migration formulas for the Maxwell's equations

To discuss the needed data rate and the available resolution on a mathematical basis

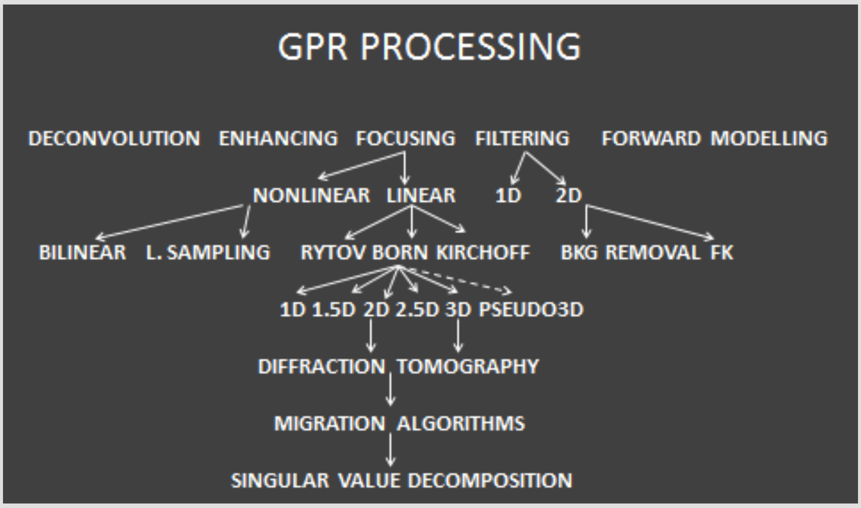

HORIZONTAL RESOLUTION

Reported values

$\lambda_{sc}/2$, $\lambda_{sc}/(2)^{0.5}$, $(d\lambda_{sc}/2)^{0.5}$, $[(d+\lambda_{sc}/4)^2-d^2]^{0.5}$

Proposed value

$\lambda_{sc}/[2\sin(\theta_{max})]$

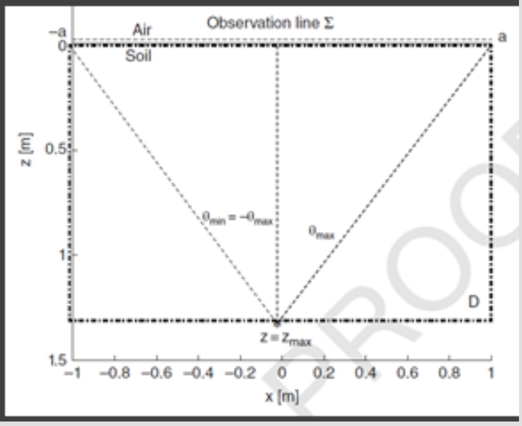

SOME CONSEQUENCES....

The resolution achievable along "short" Bscans is coarser than that achievable along "long" Bscans

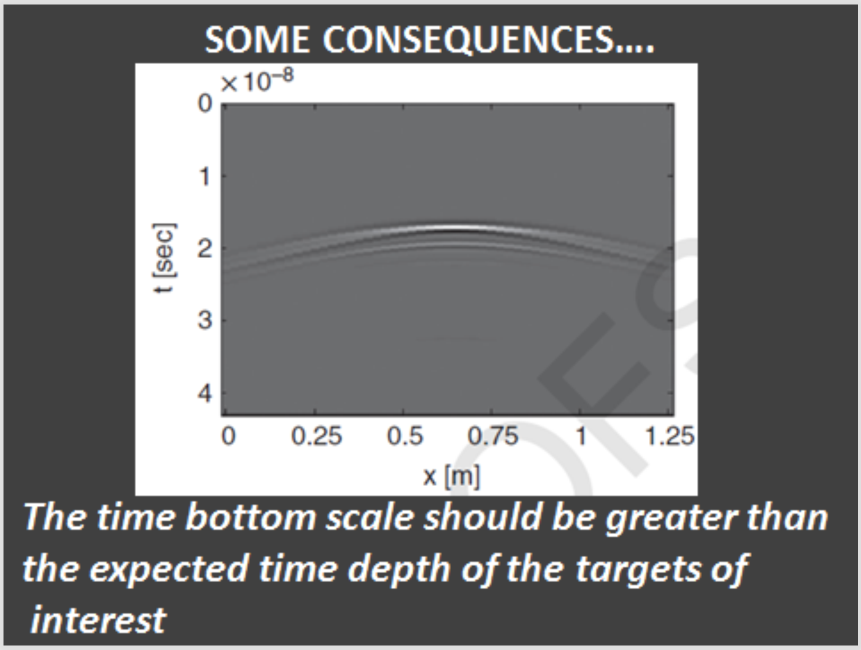
SOME CONSEQUENCES....
×10⁻⁸
0
1
2
3
4
t [sec]
0
0.25
0.5
0.75
1
1.25
x [m]
The time bottom scale should be greater than the expected time depth of the targets of interest

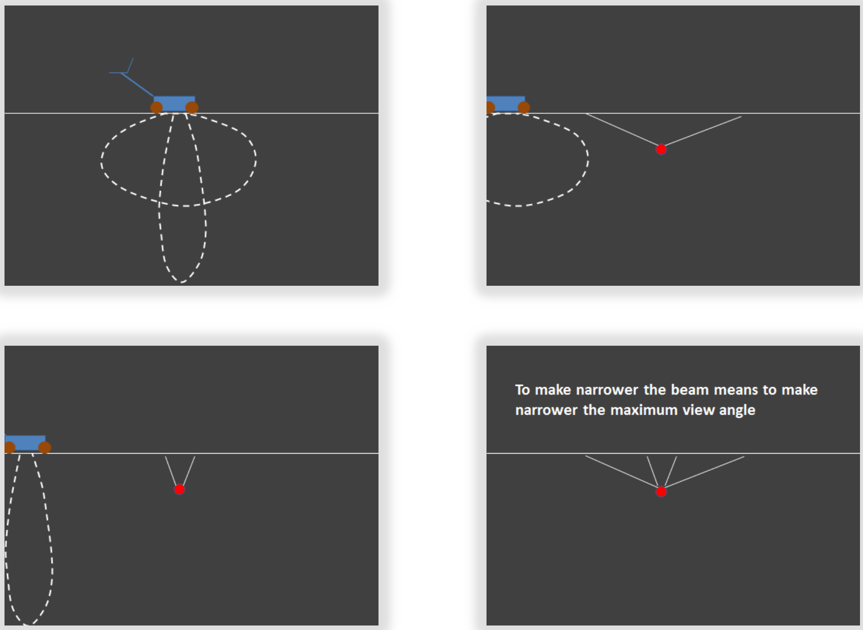
To make narrower the beam means to make narrower the maximum view angle

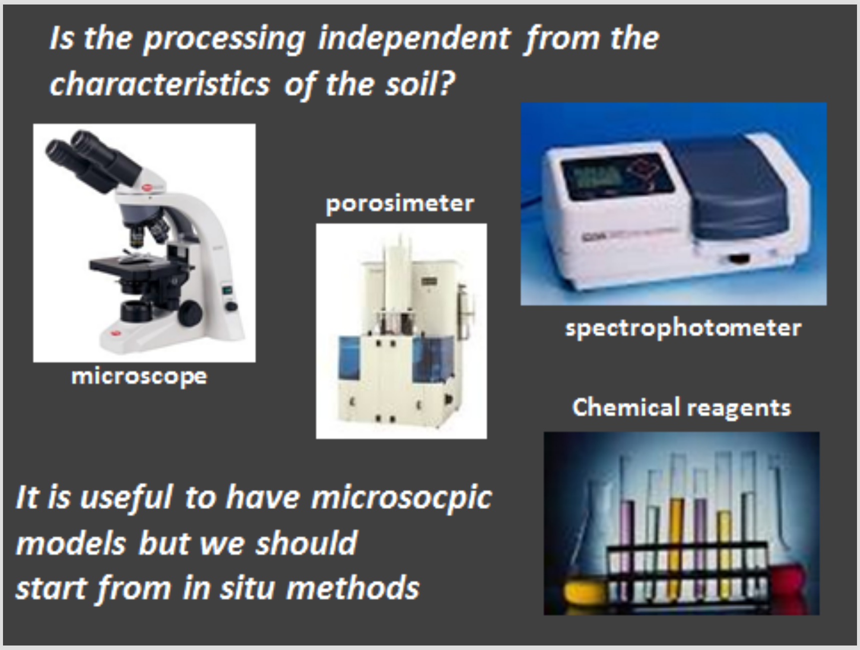
Is the processing independent from the characteristics of the soil?
microscope
porosimeter
spectrophotometer
Chemical reagents
It is useful to have microsocpic models but we should start from in situ methods

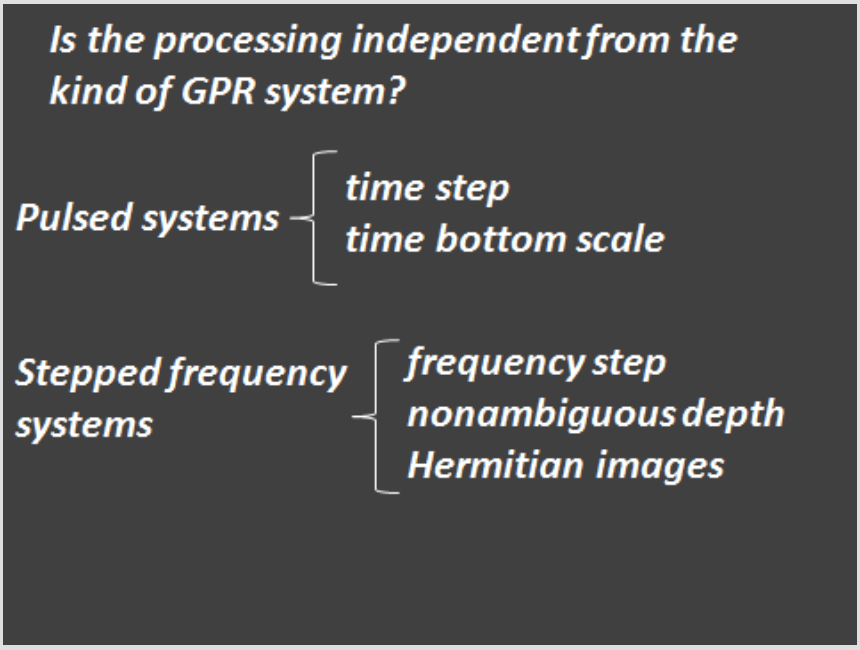
Is the processing independent from the kind of GPR system?
Pulsed systems
time step
time bottom scale
Stepped frequency systems
frequency step
nonambiguous depth
Hermitian images

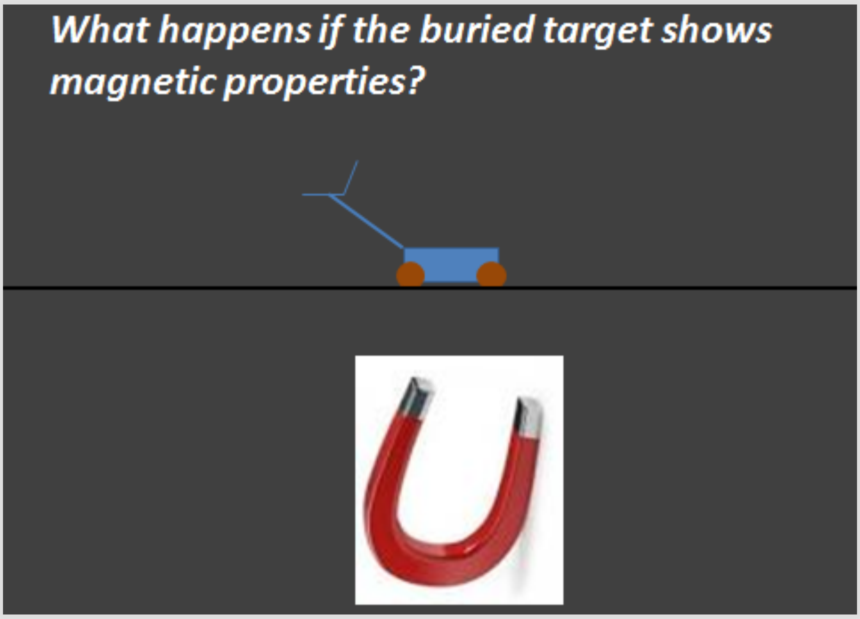

Is the GPR datum the useful datum?

Incident field+scattered field=total field

The incident field in the observation point has to be extracted from the total field

Subtraction
Muting
Differential Configuration
Background removal

Acknowledgement - The author acknowledges the COST Action TU1208 "Civil Engineering Applications of GPR".

WORKING GROUP 4

Different applications of GPR and other NDT techonlogies in Civil Engineering and Archaeology

KEYNOTE TALK 5
"RECENT FRENCH PROJECTS ON THE COMBINATION OF GPR WITH OTHER NDT METHODS FOR THE ASSESSMENT OF CONCRETE PROPERTIES"

JanPaul Balayssac (FR) - *balayssa@insa-toulouse.fr*

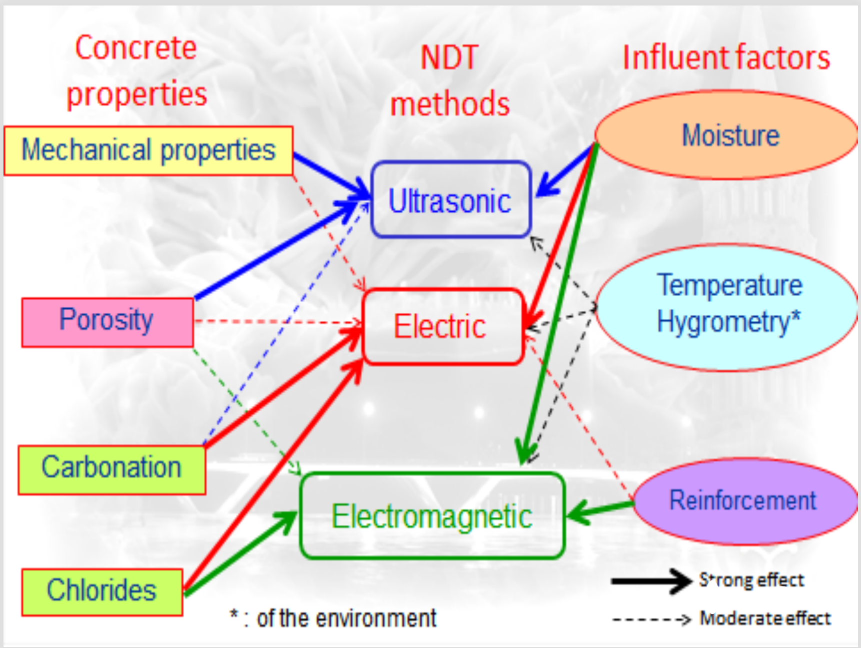

Mechanical properties: E-modulus & compressive strength

Properties connected to material porosity:
volume of porosity, saturation degree, diffusivity

Properties and issues connected to carbonation:
depth of carbonated concrete, corrosion concerns

Properties and issues related to chlorides:
amount of chlorides, corrosion concerns.

- There is almost no method which is affected by only one concrete property
- A specific methodology is necessary for dissociating the conjugated effects of the properties on NDT measurements
- A procedure for merging the results obtained by this combination must also been developed
- The estimation of accuracy of the different techniques versus each property must be quantified → quality and relevance of each NDT method
- The variability of concrete properties is important (particularly on real structures) and must be quantified

⇨ Objectives of french projects

SENSO (2006-2009)
ACDC (2010-2013)
EvaDéOS (2011-2015)

- **Quantitative evaluation of some properties of concrete**
  - porosity
  - E-modulus
  - moisture content
  - carbonation depth
  - chloride content
- **For each property focusing on:**
  - its value on a specific volume (average and variability)
  - the reliability of the evaluation

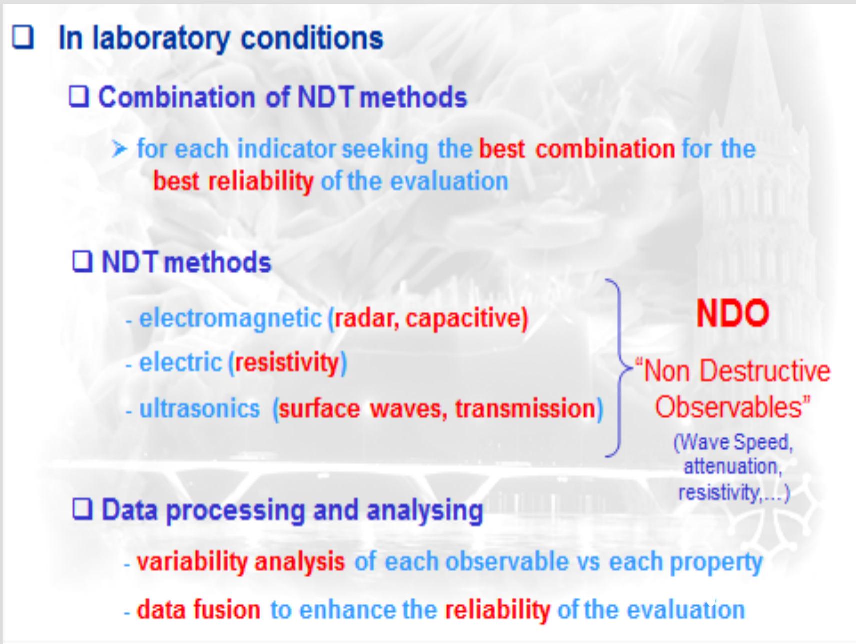
In laboratory conditions
Combination of NDT methods
for each indicator seeking the best combination for the best reliability of the evaluation
NDT methods
- electromagnetic (radar, capacitive)
- electric (resistivity)
- ultrasonics (surface waves, transmission)
NDO
“Non Destructive Observables”
(Wave Speed, attenuation, resistivity,...)
Data processing and analysing
- variability analysis of each observable vs each property
- data fusion to enhance the reliability of the evaluation

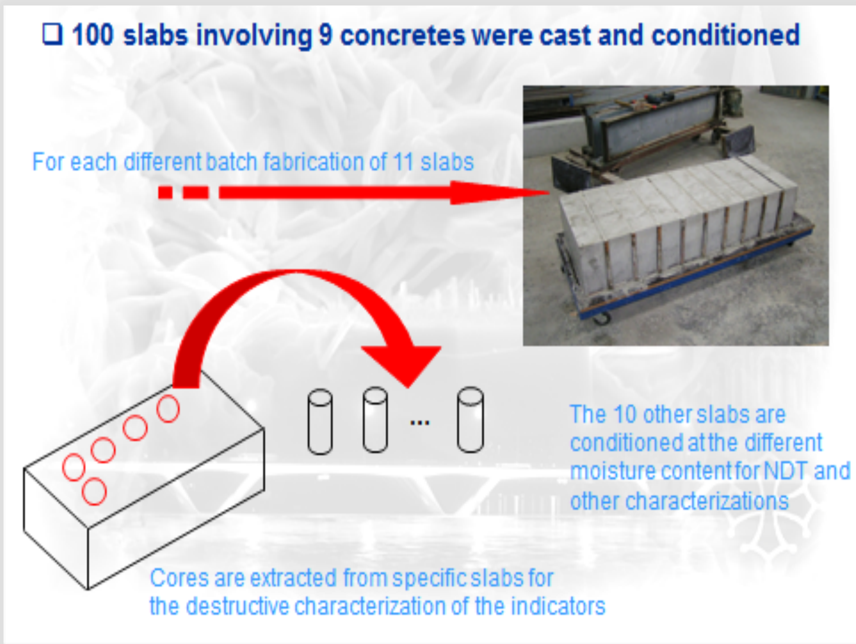
100 slabs involving 9 concretes were cast and conditioned
For each different batch fabrication of 11 slabs
The 10 other slabs are conditioned at the different moisture content for NDT and other characterizations
Cores are extracted from specific slabs for the destructive characterization of the indicators

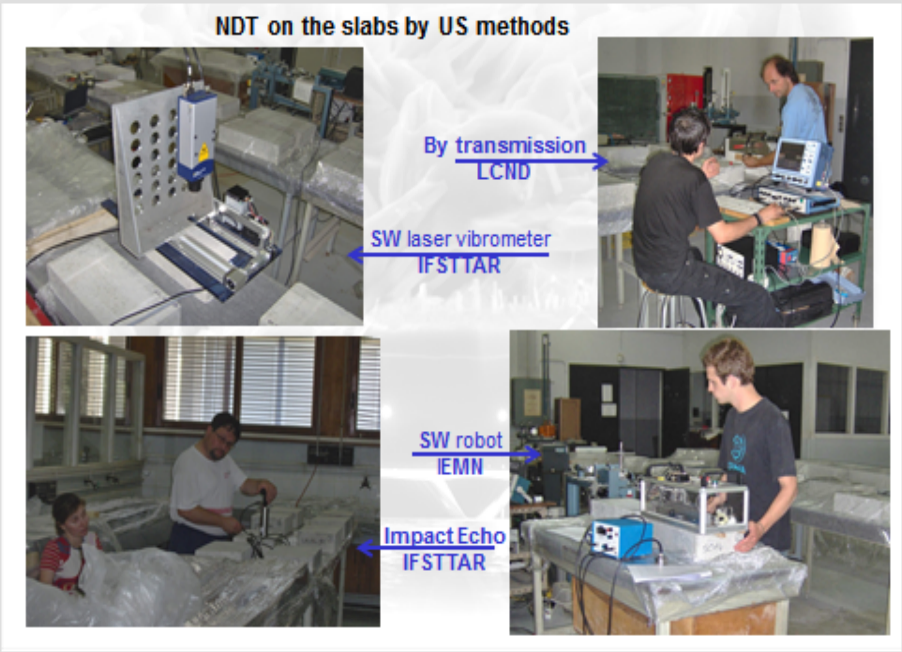
NDT on the slabs by US methods
By transmission
LCND
SW laser vibrometer
IFSTTAR
SW robot
IEMN
Impact Echo
IFSTTAR


NDT by EM, electric and permeability
Capacitive
IFSTTAR
Radar
IFSTTAR, LMDC
Resistivity
I2M
Permeability
IEMN

NDT Results: EM techniques - Results from Xavier Dérobert (IFSTTAR)

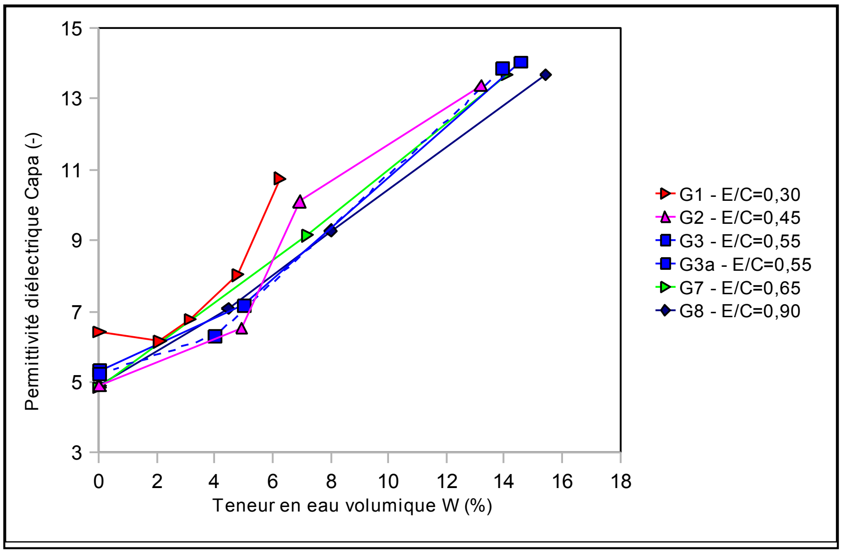

Capacitive technique: Permittivity vs VWC

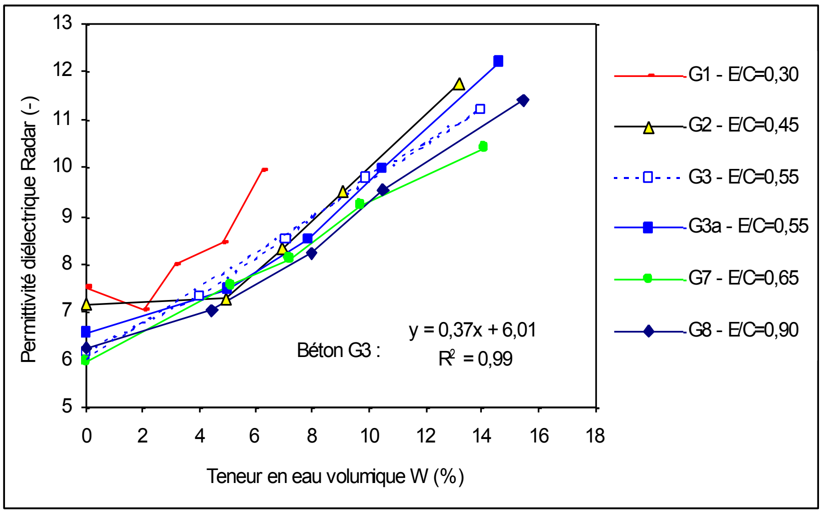

GPR: Permittivity vs VWC

NDT Results: US surface waves - Results from Odile Abraham (IFSTTAR)

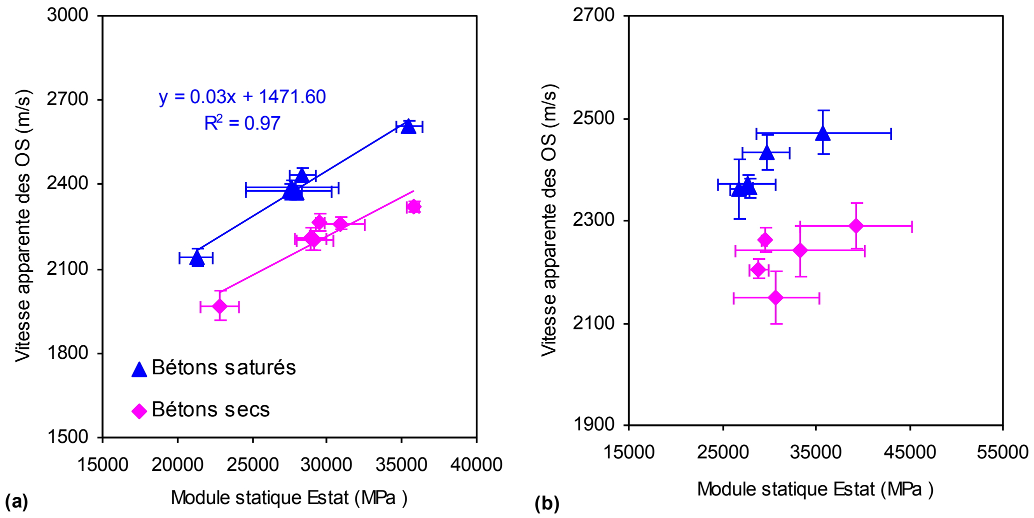

(a) Surface waves velocity vs E-modulus (same aggregates); (b) Surface waves velocity vs E-modulus (different aggregates)

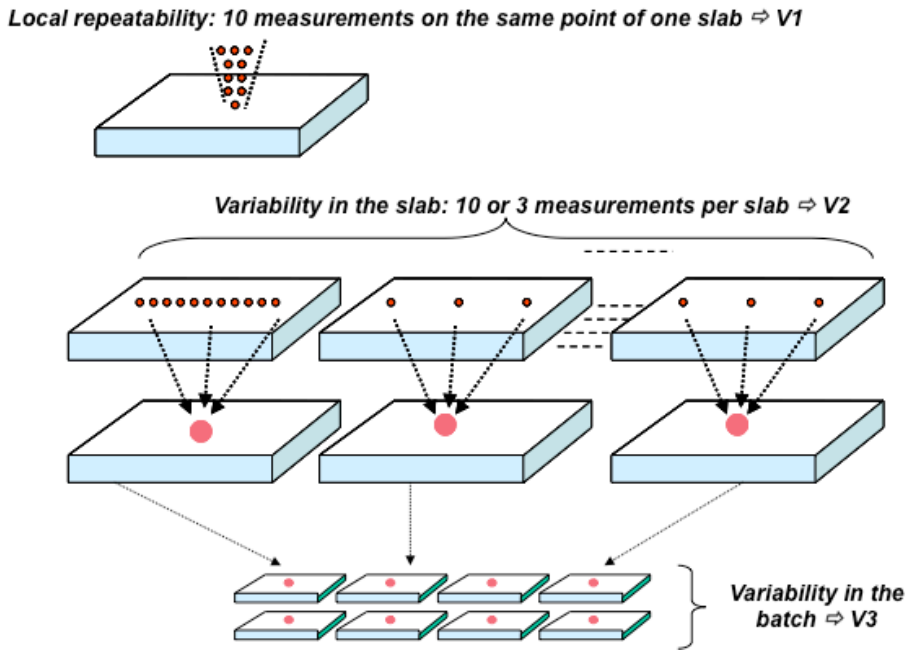

Quantification of the quality of the measurements
IQ = - log (V1/V3) - log (V2/V3)

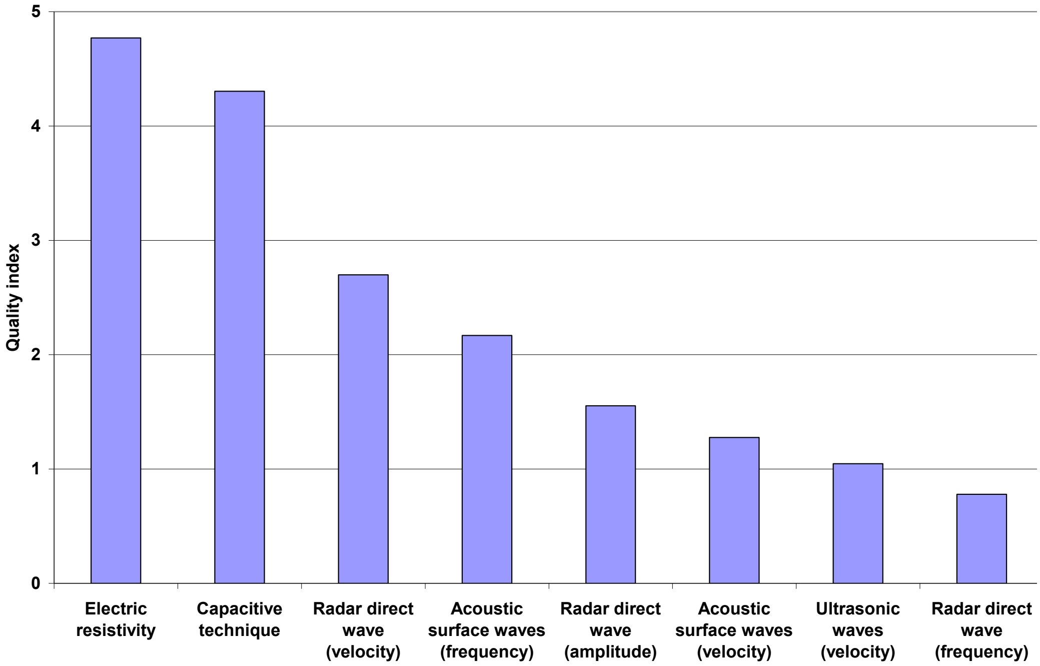

The number of observables was decreased by taking into account the quality index, the relevance index (linked to the correlation quality), as well as some practical considerations (portability of the technique, duration, expertise of the members of the project, feedback from the experience on-site).

18 observables were selected, 6 of which were considered more relevant:

- ultrasonic surface wave velocity
- ultrasonic longitudinal wave velocity
- resistivity quadripole
- resistivity Wenner
- amplitude of radar direct wave
- velocity of radar direct wave

Assessment of two properties: porosity and saturation degree

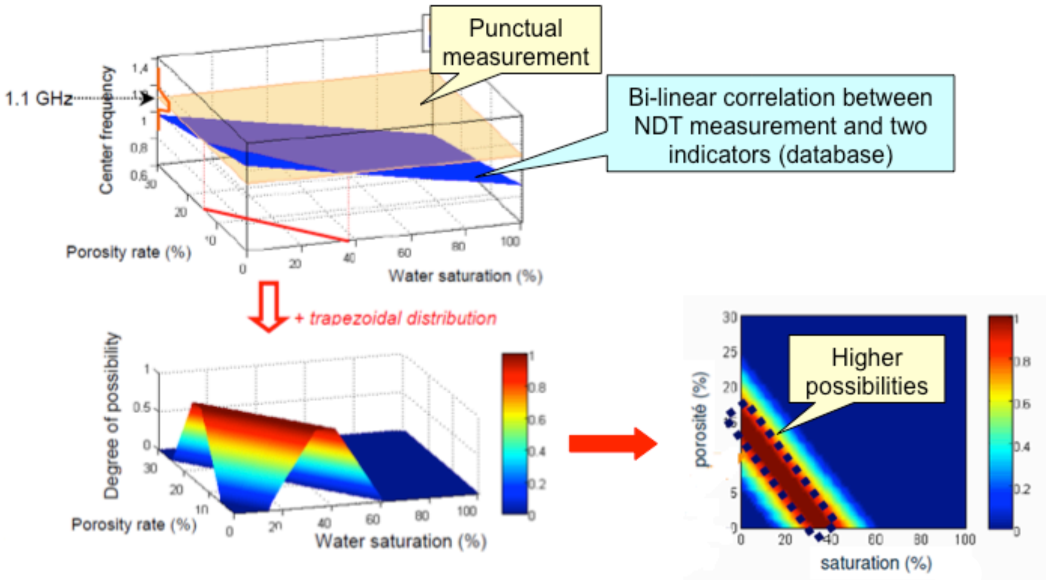

Distribution of possibilities

Fusion of 4 NDT methods:

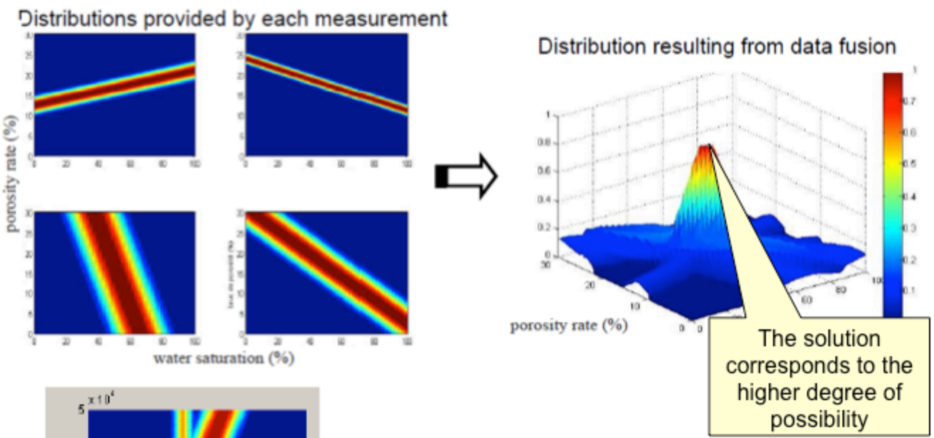

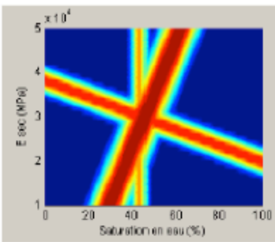

Several distributions can be merged

Of course the better situation is obtained when all the distributions are crossing at the same point

❑ Real Structure application :

Marly Bridge (North of France)

- 3 piles were sounded
- 10 NDT methods were employed
- Destructive testings of the concrete properties were performed to calibrate the fusion procedure

Courtesy of Vincent Garnier (LMA-LCND)

❑ Real Structure application :

Marly Bridge (North of France)

3 combinations are tested to estimate water saturation degree of concrete

Config 1	US, Re & EM	7 (IE Edyn), 12 (Log Re GE) & 16 (Vit Radar)
Config 2	2 US & EM:	5 (US 6), 7 (IE Edyn) & 17 (Offset Radar)
Config 3	US & 2 EM :	7 (IE Edyn), 9 (Capa 1) & 16 (Vitesse Radar)

Config	<δI/δO>	Coût	EQ <0,15	EQ <0,4	EQ>0,5
~~(1)~~	~~0,886~~	~~0,247 avant recal~~ ~~0,125 après recal~~	~~8,70 %~~ ~~4,35 %~~	~~34,8 %~~ ~~13,0 %~~	~~65,2 %~~ ~~87,0 %~~
(2)	0,896	0,109 avant recal 0,103 après recal	0,00 % 0,00 %	14,0 % 8,00 %	84,0 % 88,0 %
(3)	0,953	0,230 avant recal 0,168 après recal	12,0 % 4,00 %	24,0 % 16,0 %	68,0 % 78,0 %

Config 2	Config 3	Real value (DT)
$S = 52{,}2\% \pm 3{,}74\%$	$S = 50{,}4\% \pm 5{,}9\%$	$\boxed{S = 54{,}1\% \pm 5{,}\%}$

Courtesy of Vincent Garnier (LMA-LCND)

CONCLUSIONS

- Combination of techniques is necessary for a reliable evaluation of concrete properties.
- Moisture is a permanent influent factor so electromagnetic methods are fully relevant in this context.
- By analysing the variability of ND measurements we have proposed a possible way for discriminating the most reliable NDT methods regarding each concrete property assessment.
- We proposed to use a procedure of data fusion for enhancing the quality of the combination which must be calibrated by destructive testing.
- The perspectives of current projects are for decreasing the number of cores for destructive evaluation and for optimising their location on the structures.
- Challenges are also for the ND evaluation of new concrete properties.

ACKNOWLEDGEMENT

The author acknowledges: the *Agence Nationale de la Recherche*, the *Ministére de l'Ecologie, du Développement durable, des Transport et du Logement*, the RGC&U. The author thanks COST for funding the COST Action TU1208.

"Non-destructive assessment of the Ancient Tholos Acharnon Tomb" (contribution to project 4.1)

Sonia Santos-Assunçao (ES),Klisthenis Dimitriadis (GR), Yiannis Konstantakis (GR), Vega Pérez-Gracia (ES), Eirini Anagnostopoulou (GR) Mercedes Solla (ES), Henrique Lorenzo (ES)
sonia.assuncao@upc.edu

The abstract is published in *Geophysical Research Abstracts*, Vol. 16, EGU2014-13961, 2014 and is available on *www.egu2014.eu*

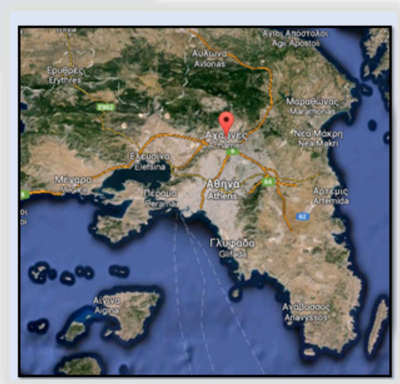

Constructive characteristics

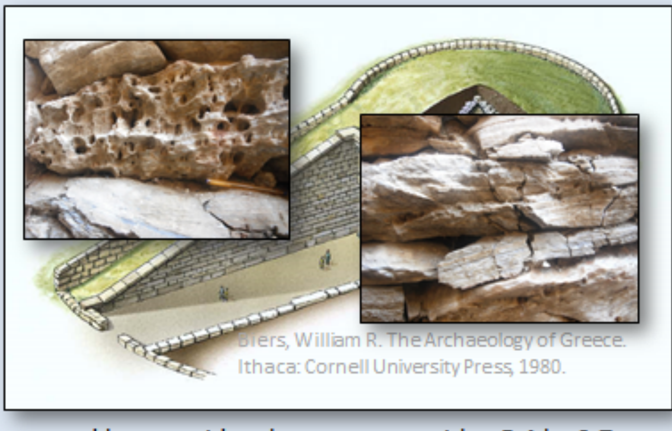

- Composed by a corridor that connects with a 5.4 by 2.7 m entrance.
- The interior part is 8.74 m high with 8.35 m diameter.

Methodology

GPR:
Objective: to define possible inner structure, layers and voids /finding archaeological targets

Microresistivity:
Objective: to define resistivity values and characterize materials

Passive Seismic:
Objective: to measure vibrations that could affect the integrity of the structure

Chemical analysis :
Objective: to determine salinity in material and soil

Endoscopy:
Objective: to obtain direct information about inner targets and structures

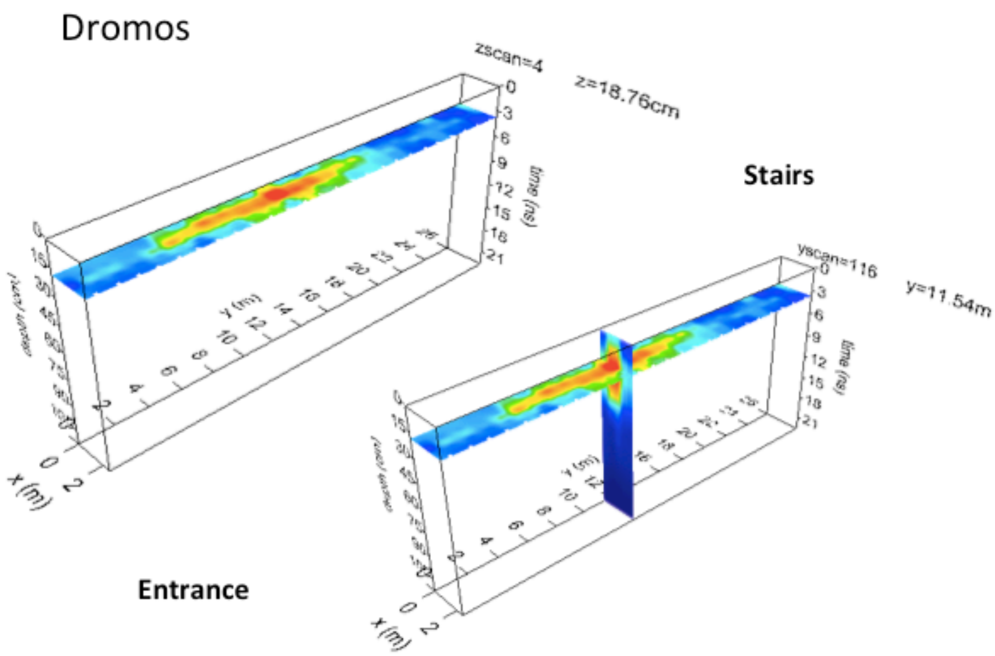
Dromos
zscan=4
z=18.76cm
time (ns)
y (m)
x (m)
Stairs
yscan=116
y=11.54m
time (ns)
y (m)
x (m)
Entrance


Entrance
Stairs

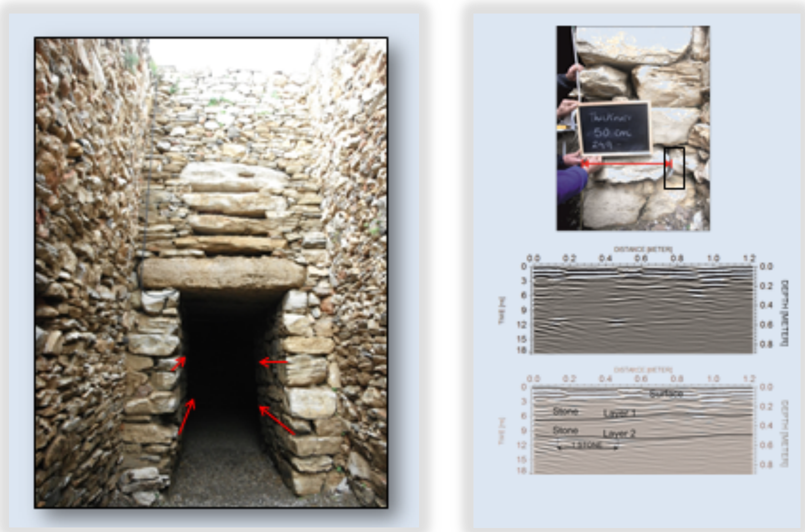

Results collected at the entrance

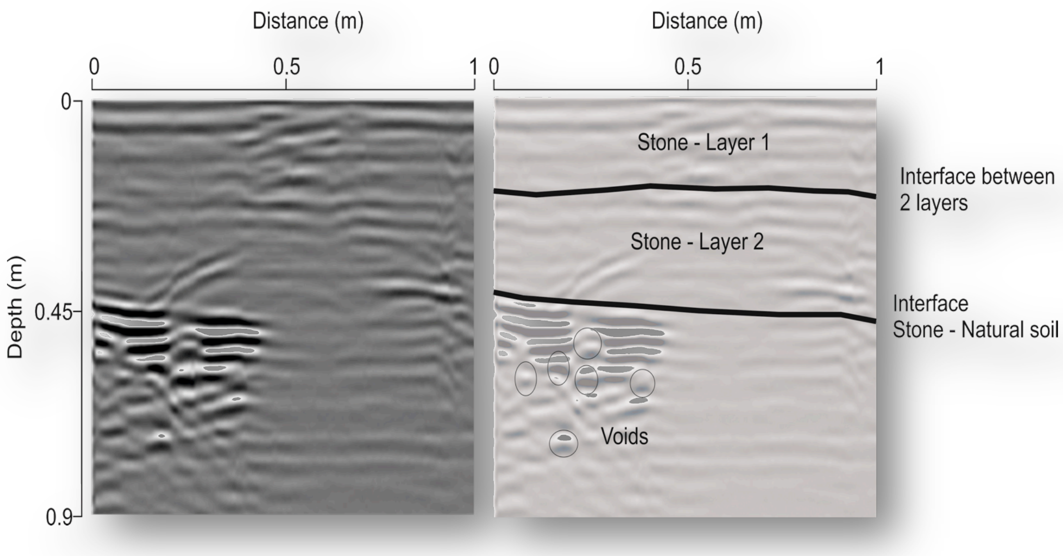

Results collected on the wall

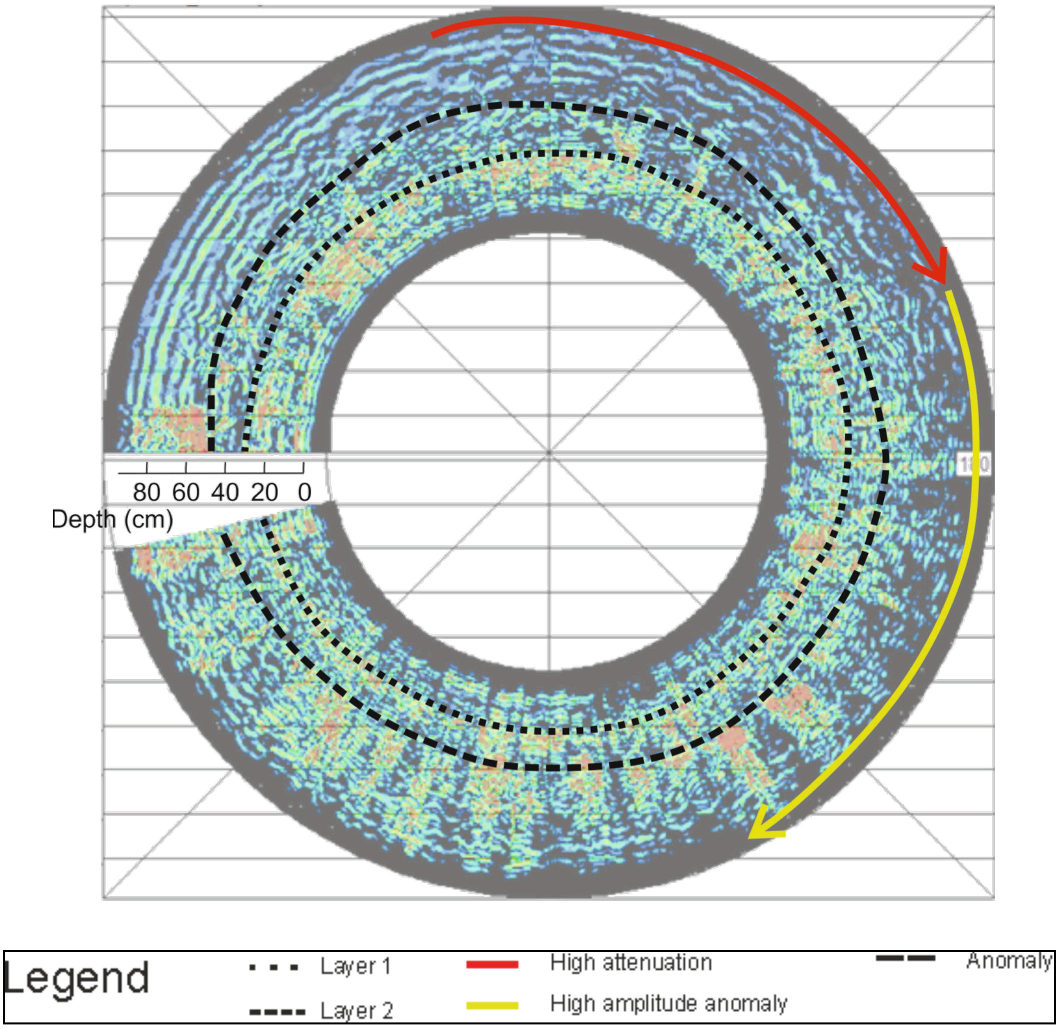

Results collected on the wall – circular radargram

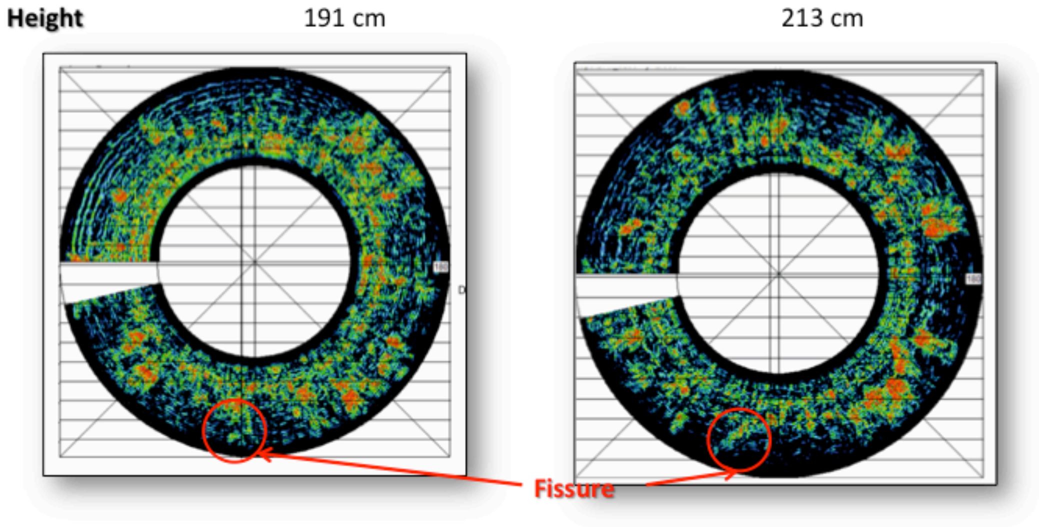
Height
191 cm
213 cm
Fissure

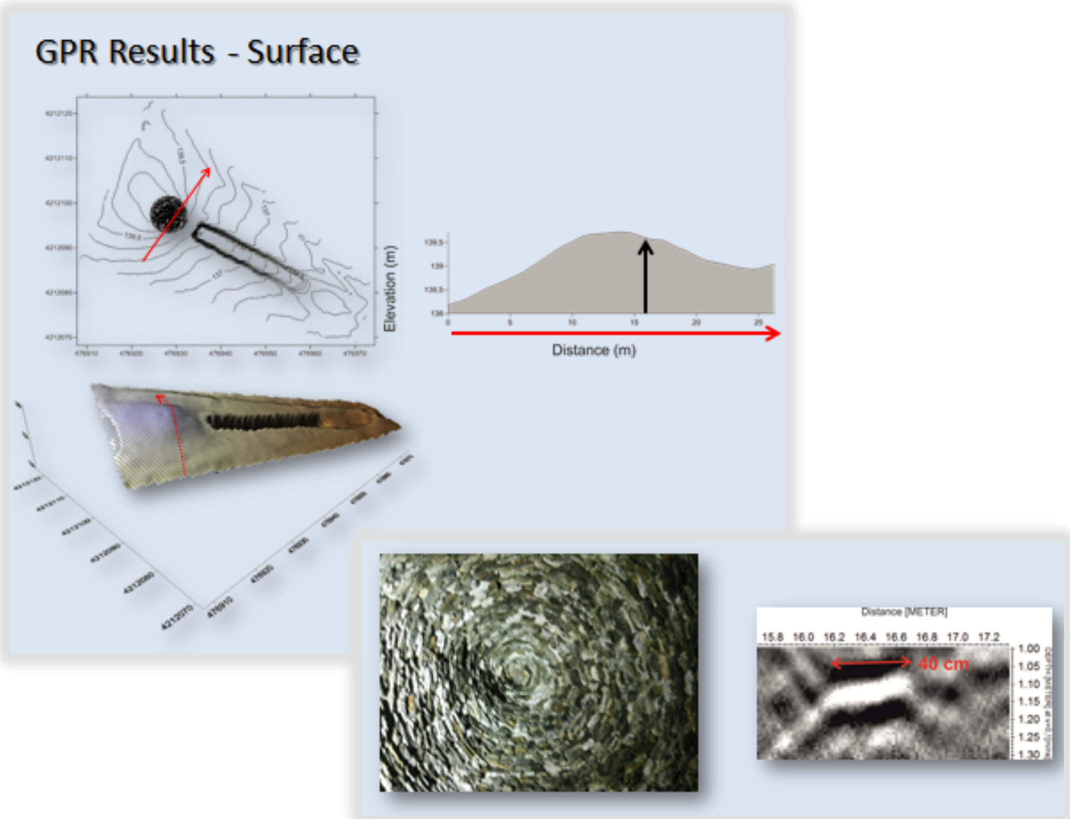
GPR Results - Surface
Elevation (m)
Distance (m)
Distance [METER]
15.8 16.0 16.2 16.4 16.6 16.8 17.0 17.2
1.00 1.05 1.10 1.15 1.20 1.25 1.30
40 cm

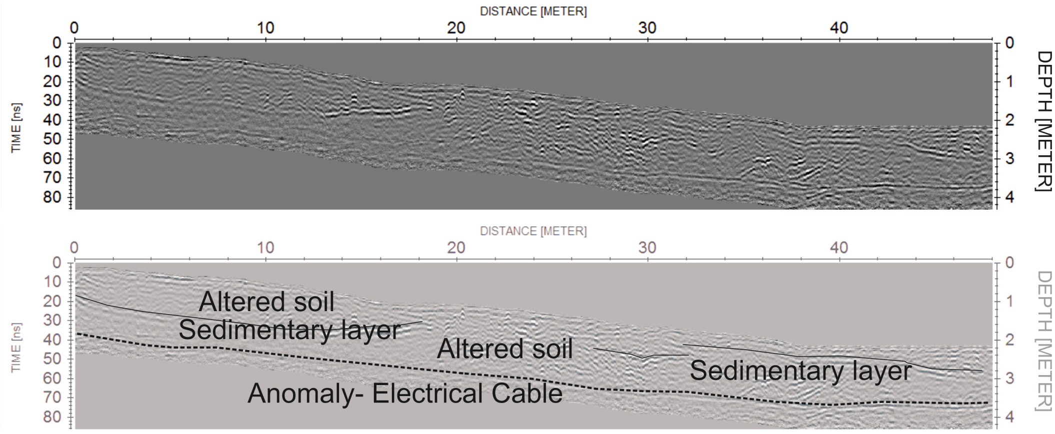

Results collected on the surface

INTEGRATED GEOPHYSICAL METHODS:

- ✓ GPR - Objective: to define possible interior structure , layers and voids /finding archaeological targets
- ✓ Microresistivity - Objective: to define wall thickness, degree of stone deterioration, determine the resistivity values of the Tomb building materials
- ✓ Passive Seismic - Objective: to measure ambient vibrations that could affect the integrity of the structure
- • Geochemical analysis - Objective: to determine the salt content in the Tomb building material and surrounding soils
- ✓ Endoscopy - Objective: to obtain direct information about inner targets and structures

MICRORESISTIVITY SURVEYS

Type of spread:

32 Electrodes in multi electrode configuration.

Schlumberger – Wenner arrangement.

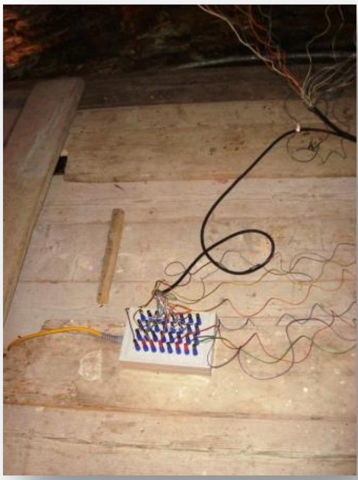

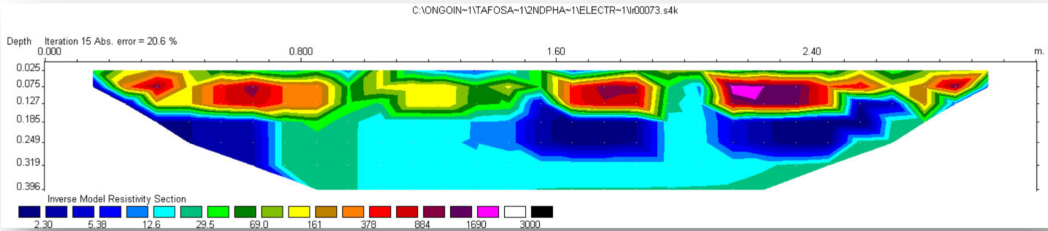

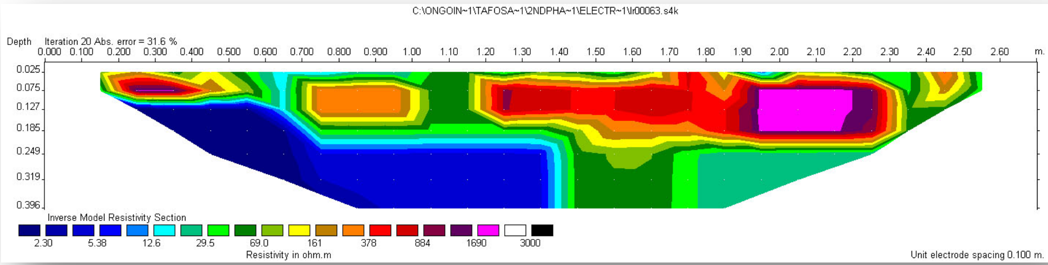

ELECTRICAL RESISTIVITY TOMOGRAPHY (ERT)

Using the composite information such as geometry and resistivity, a view from below gives an idea on the subsurface setup. Yellow and red zones are human constructions „floating“ in one very clayey geological environment.

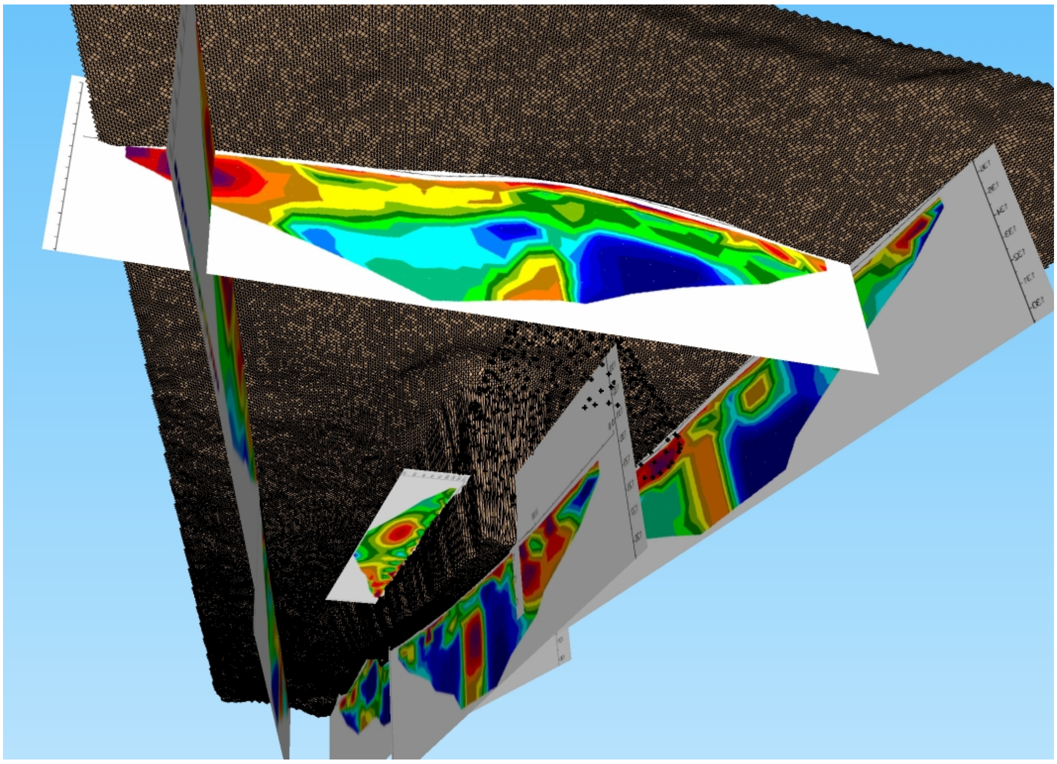

SEISMIC: MASW (MULTICHANNEL ANALYSIS OF SURFACE WAVES)

In an effort to quantify the effect of the vibrations due to the heavy road traffic, one additional geophysical study on earth dynamics was carried out. The first step to this direction was to establish a microzonation study of the subsurface of Tomb is performed. The digital seismograph DAQLINK III of GEOSERVICE was used. As seismic source, the ambient road traffic was used. Passive seismics (MASW) were applied, with 24 geophones in a circular array.

Phase-velocity vs frequency diagram and shear wave velocity (Poisson's ratio) calculation are reported in the following. From the diagrams it is concluded that the average Vs is 270 m/sec for a confidence depth ot 44 m. It is obvious that the Tomb will never suffer from earthquakes!

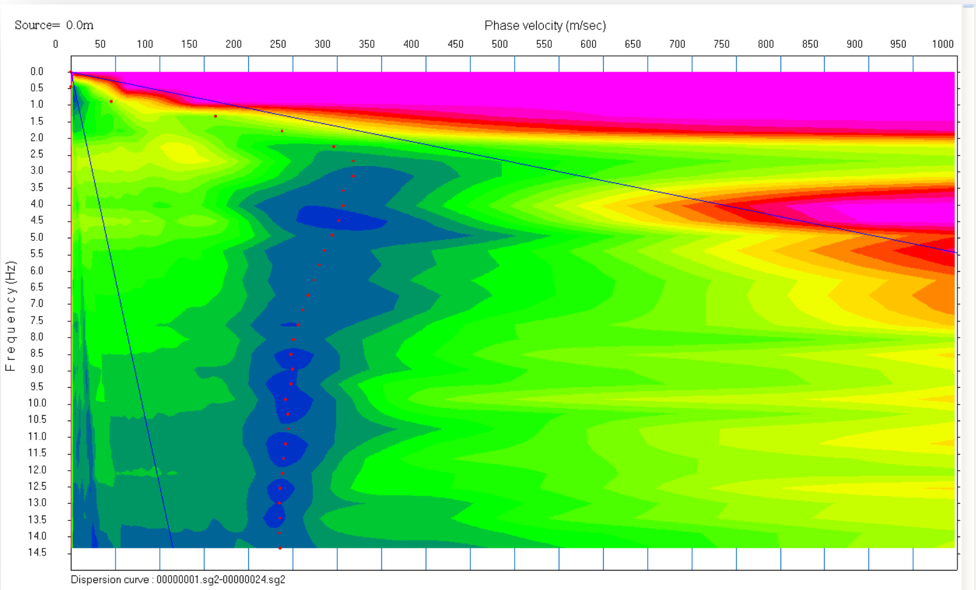

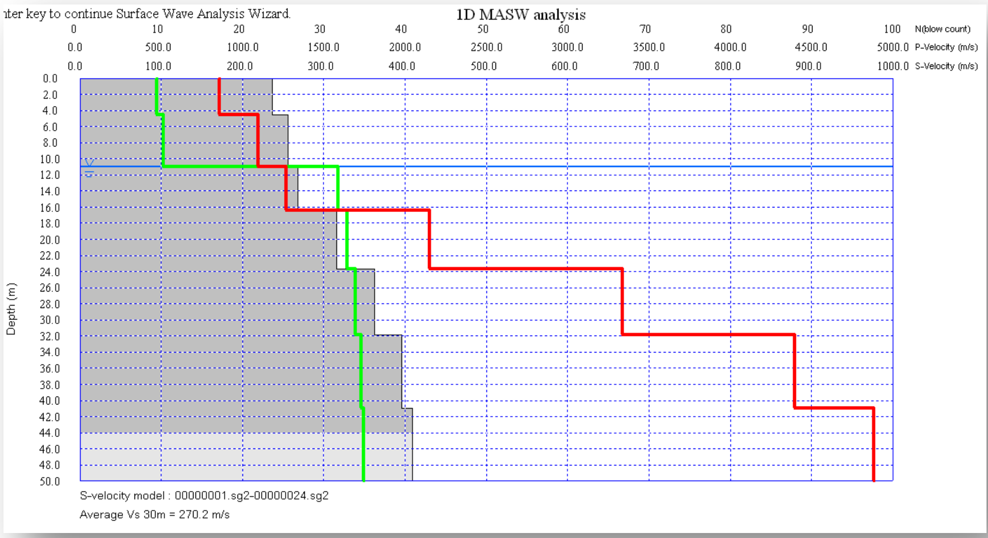

CONCLUSIONS

1) An anomaly was detected at the entrance to the tomb, at 20 cm depth.
2) Two interfaces were detected, at 25 and 50 cm depth (stone-stone and stone-natural soil interfaces).
3) Local fissures were detected, at different levels.
4) High signal attenuation may be associated to high salt content.
5) An anomaly was present in several radargrams and probably indicates the presence of a wall.
6) The apex of the tomb was detected at 1 m depth, according to the Biers model (1980).
7) The integration of GPR and ERT allowed locating voids and confirming high salt content. The passive seismic analysis confirmed the presence of a non-rocky soil.

ACKNOWLEDGEMENT

The authors acknowledge the COST Action TU1208 "Civil Engineering Applications of Ground Penetrating Radar", supporting this work.

"Applications of non-destructive methods (GPR and 3D Laser Scanner) in historic masonry arch bridge assessment" (contribution to project 4.1)

Amir Alani (UK), Kevin Banks (UK) - *amir.alani@uwl.ac.uk*

The abstract is published in *Geophysical Research Abstracts*, Vol. 16, EGU2014-2727, 2014 and is available on *www.egu2014.eu*

Old Bridge – Aylesford, Kent, UK

1. Background

The Old Bridge at Aylesford dates from around 1250. The bridge is made of local "Ragstone". It underwent a major alteration in 1811. The bridge is closed to cars and motorbikes but remains in use for pedestrians, cyclists and horses. There is currently no lighting system on the bridge. Aylesford Parish Council plans to install spotlights flush within the upper layer of the bridge deck.

The bridge is a scheduled ancient monument and listed building and so is firmly under the control of English Heritage. English Heritage would consider a proposal for the installation of a lighting system on the bridge, provided the lights and power cables could be installed within the upper layer of the modern asphalt without any intrusion on to the historic stonework of the bridge.

Objectives

Perform a high frequency GPR survey (2GHz) of the asphalt surface of the Old Bridge, Aylesford to determine the following parameters:

- The thickness of the upper asphalt layer.
- The total depth from the bridge surface to the historic stonework.
- The uniformity of the upper asphalt layer and total depth.

Action

A preliminary reconnaissance visit was made to the bridge in December 2012.

A full high frequency radar survey of the bridge was performed on 15 January 2013, and repeated on 12 September 2013. During the visit on 12 September 2013 the team also acquired a low frequency GPR survey.

On 26 September 2013 the team acquired a full 3D Laser Scanner point cloud image of the bridge.

2. Survey Method 1 – 2 GHz Antenna

The data was acquired using a modified IDS RIS Hi-BrigHT Ground Penetrating Radar (GPR) system consisting of eight horizontally polarised 2GHz channels with 10 cm spacing; this gives each scan or 'swathe' a footprint 80 cm wide.

The bridge deck was surveyed using four scans spaced equally, performed along the length of the bridge providing full coverage with approximately 10 cm spacing.

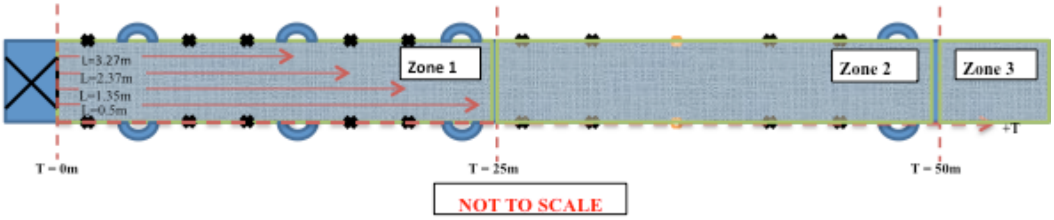

To break the data into more manageable areas, the survey was broken into three 'Zones'.

The following diagram shows the area covered by the four data swathes, each swathe consisting of eight scans.

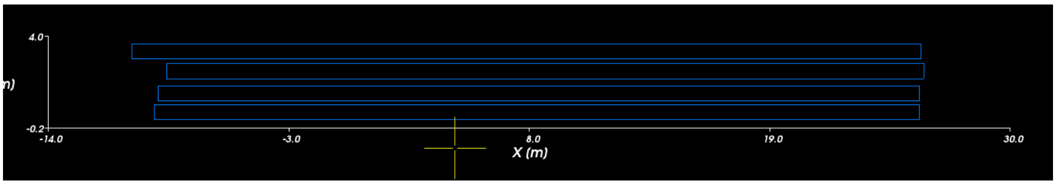

It is possible to represent each channel of the radar data as a 'B-Scan' (a vertical cross-section slice), or to represent the B-Scans side by side and cut them from above in a 'C-Scan' view. The C-Scan is helpful to represent certain features as it gives a plan view of the bridge at a given 'cut' depth.

The following B-Scan view shows two traffic light sensors on the bridge.

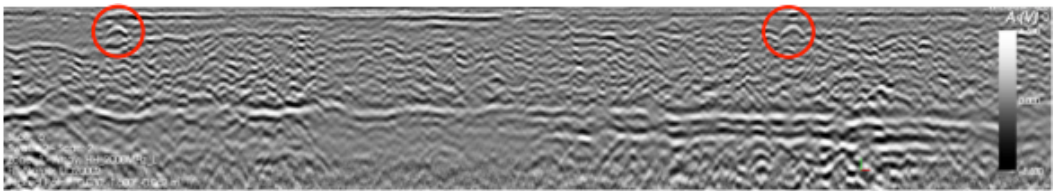

The quantity of data acquired was far greater than was required for identification of bridge deck layers. In the following depictions, layers can be clearly seen on the

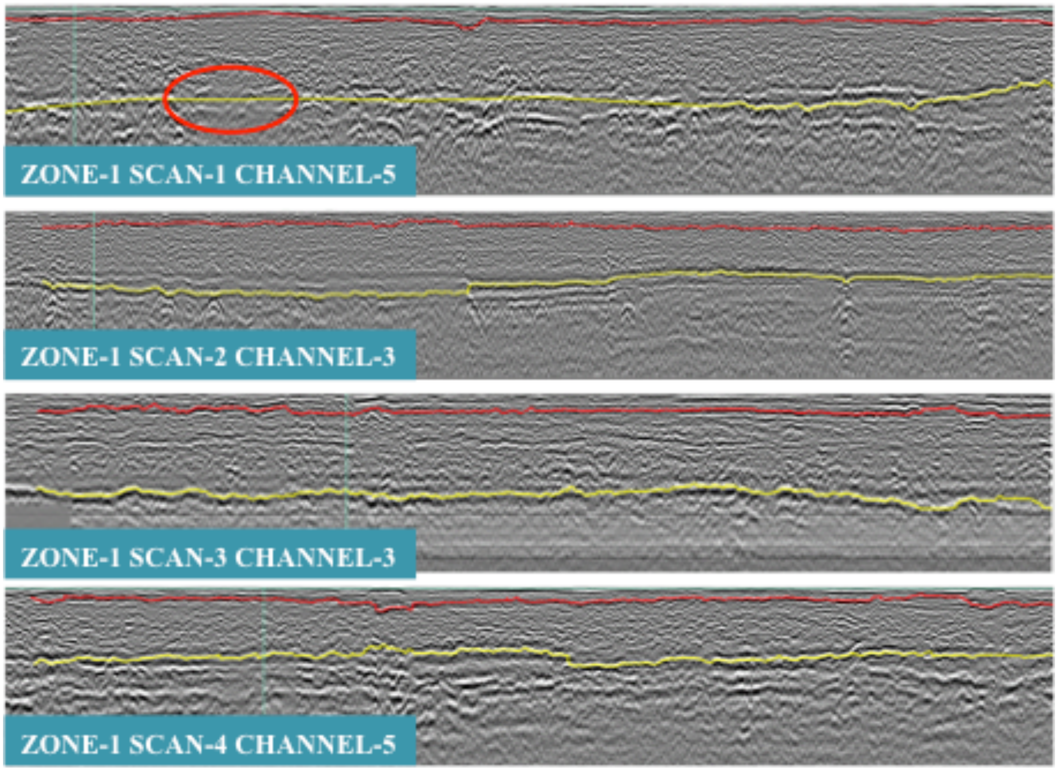

The depth of each layer was exported to Excel in 0.5 m increments, as represented in the table below. Next, the maximum, minimum and average figures (m) for two identified layers for Zone 1 are presented, as well as the distribution of the layers measurements in Zone 1.

	Scan 1 Channel 5		Scan 2 Channel 3		Scan 3 Channel 2		Scan 4 Channel 5	
X [m]	LAYER-2: Depth [m]	LAYER-1: Depth [m]	LAYER-2: Depth [m]	LAYER-1: Depth [m]	LAYER-2: Depth [m]	LAYER-1: Depth [m]	LAYER-2: Depth [m]	LAYER-1: Depth m]
0	0.477	0.072	0.396	0.078	0.418	0.074		
0.5	0.477	0.062	0.408	0.074	0.432	0.07		0.051
1	0.481	0.066	0.402	0.055	0.434	0.053	0.377	0.076
1.5	0.481	0.044	0.428	0.061	0.432	0.059	0.361	0.049
2	0.481	0.044	0.422	0.066	0.404	0.051	0.35	0.051
2.5	0.481	0.046	0.451	0.061	0.416	0.045	0.357	0.055
3	0.477	0.032	0.439	0.059	0.426	0.064	0.359	0.053
3.5	0.477	0.032	0.447	0.057	0.408	0.064	0.35	0.068
4	0.477	0.032	0.439	0.066	0.434	0.062	0.34	0.053
4.5	0.477	0.068	0.449	0.07	0.428	0.059	0.346	0.059
5	0.477	0.068	0.445	0.057	0.451	0.072	0.342	0.061
5.5	0.477	0.076	0.445	0.059	0.436	0.059	0.35	0.055
6	0.485	0.07	0.455	0.061	0.436	0.08	0.336	0.061
6.5	0.485	0.07	0.455	0.057	0.418	0.082	0.33	0.061
7	0.485	0.072	0.459	0.07	0.414	0.084	0.326	0.066
7.5	0.485	0.084	0.449	0.066	0.422	0.09	0.34	0.076
8	0.485	0.089	0.457	0.074	0.441	0.061	0.322	0.061
8.5	0.485	0.117	0.455	0.045	0.443	0.08	0.342	0.08
9	0.469	0.064	0.445	0.045	0.439	0.076	0.289	0.074
9.5	0.469	0.08	0.439	0.049	0.434	0.074	0.299	0.104
10	0.469	0.074	0.441	0.08	0.436	0.076	0.309	0.115
10.5	0.469	0.078	0.396	0.07	0.426	0.072	0.322	0.088
11	0.469	0.084	0.393	0.074	0.426	0.062	0.332	0.076
11.5	0.469	0.091	0.393	0.068	0.426	0.072	0.309	0.072
12	0.503	0.082	0.393	0.07	0.432	0.072	0.314	0.072
12.5	0.503	0.091	0.385	0.074	0.428	0.068	0.309	0.068
13	0.503	0.093	0.385	0.074	0.416	0.07	0.312	0.074
13.5	0.503	0.084	0.385	0.082	0.428	0.068	0.328	0.068
14	0.513	0.08	0.354	0.08	0.428	0.068	0.381	0.074
14.5	0.515	0.084	0.344	0.078	0.414	0.068	0.387	0.074
15	0.509	0.074	0.338	0.086	0.408	0.072	0.391	0.072
15.5	0.515	0.078	0.334	0.09	0.396	0.068	0.377	0.07
16	0.519	0.072	0.34	0.092	0.395	0.068	0.373	0.066
16.5	0.517	0.072	0.326	0.074	0.393	0.066	0.355	0.057
17	0.531	0.078	0.344	0.094	0.406	0.064	0.352	0.055
17.5	0.509	0.07	0.342	0.09	0.418	0.072	0.371	0.066
18	0.501	0.066	0.344	0.086	0.414	0.074	0.365	0.055
18.5	0.493	0.074	0.344	0.092	0.412	0.082	0.359	0.055
19	0.487	0.072	0.355	0.086	0.432	0.076	0.357	0.057
19.5	0.513	0.078	0.363	0.096	0.432	0.084	0.352	0.051
20	0.491	0.087	0.357	0.092	0.438	0.084	0.348	0.059
20.5	0.479	0.068	0.357	0.09	0.453	0.084	0.334	0.061
21	0.475	0.068	0.357	0.104	0.459	0.086	0.334	0.068
21.5	0.453	0.07	0.365	0.102	0.492	0.082	0.328	0.068
22	0.439	0.072	0.365	0.092	0.492	0.062	0.32	0.061
22.5	0.402	0.08	0.365	0.09	0.459	0.074	0.33	0.053
23	0.396	0.082	0.35	0.082	0.457	0.084	0.32	0.045
23.5	0.402	0.097	0.348	0.086	0.438	0.096	0.336	0.049
24	0.39	0.103	0.344	0.092	0.447	0.094	0.338	0.074
24.5	0.374	0.101	0.352	0.086	0.475	0.094	0.336	0.102
25	0.384	0.08					0.338	0.076

Avg	0.4761373	0.0739412	0.39288	0.07564	0.43084	0.07242	0.3414898	0.0663
Min	0.374	0.032	0.326	0.045	0.393	0.045	0.289	0.045
Max	0.531	0.117	0.459	0.104	0.492	0.096	0.391	0.115

Layer 2	**Avg**	0.410	**Layer 1**	**Avg**	0.072
	Min	0.289		**Min**	0.032
	Max	0.531		**Max**	0.117

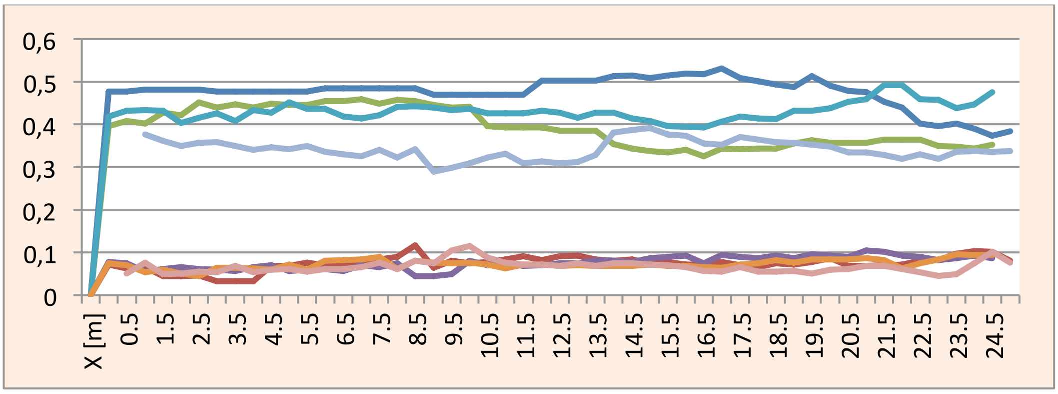

Below, processed data are shown, concerning the identification of layers in Zone 2, Scan 1, Channel 4.

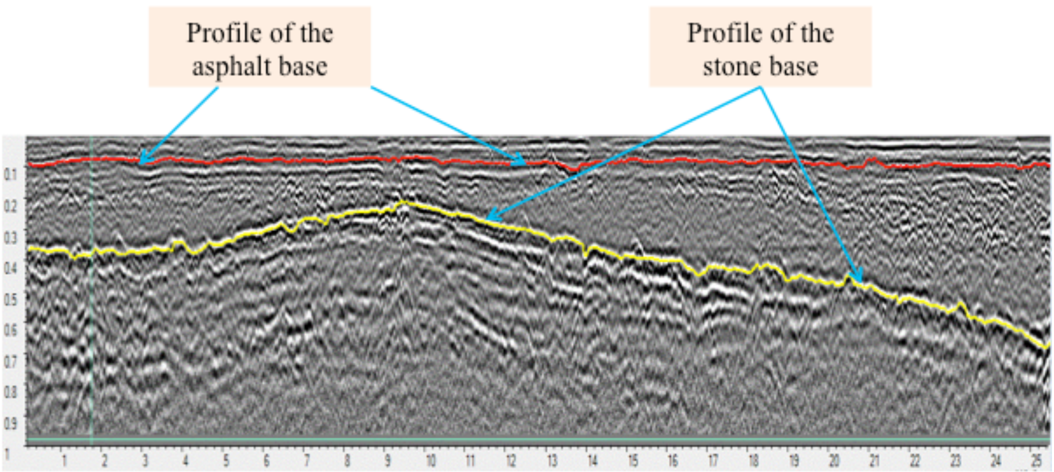

C-Scan and B-Scan showing bridge deck surface damage are presented. By altering the display characteristics of the C-Scan and the depth, different damaged areas are visible.

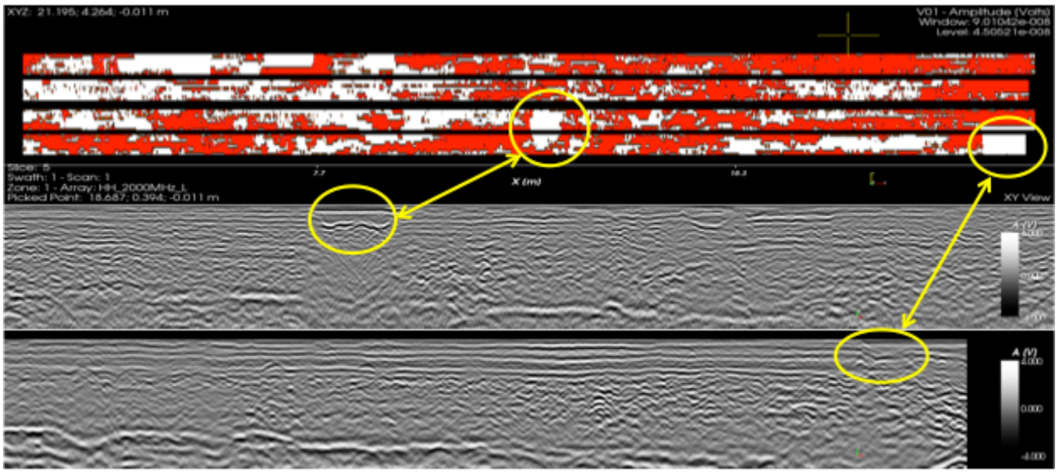

Location of the electricity cable at the centre of the widest section of the bridge (Zone 2), using the combined C-Scan and B-Scan:

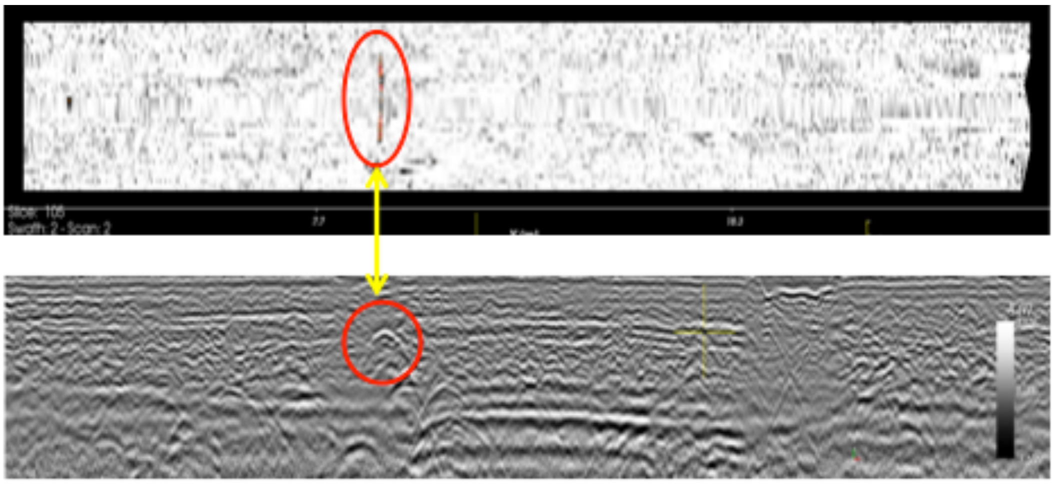

Maximum, minimum and average figures (m) for two identified layers for Zone 2 & Distribution of the two layers' measurements in Zone 2.

	Layer 2	Average	0.3905		Layer 1	Average	0.0670	
		Min	0.203			Min	0.027	
		Max	0.615			Max	0.129	

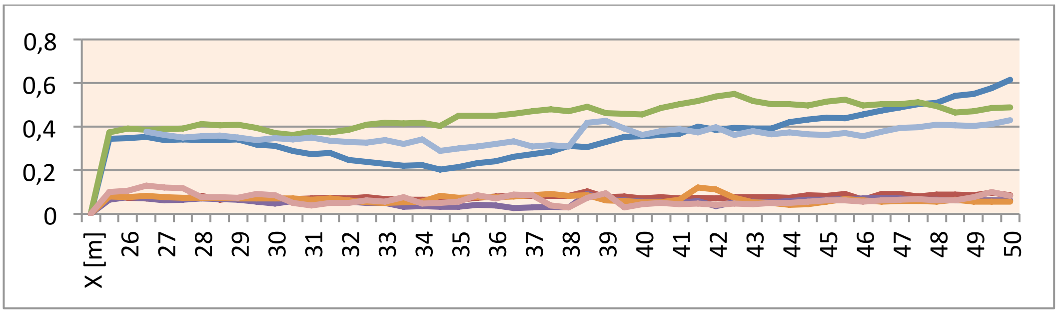

Summary of Results for 2GHz Antenna for all Zones

➤ The thickness of the asphalt / tarmac layer is not uniform and varies across the surface of the bridge:

- Zone 1 – From 3cm to 12cm
- Zone 2 – From 3cm to 13cm
- Zone 3 – From 4cm to 12cm

The average thickness in all three Zones is 7cm

➤ **Total depth from the bridge surface to the historic stonework**

The total depth is variable across the bridge, with the minimum depth being in the centre of the widest arch:

- Zone 1 – From 29cm to 53cm
- Zone 2 – From 20cm to 61cm
- Zone 3 – From 26cm to 73cm

The average thickness across all three Zones is 41cm

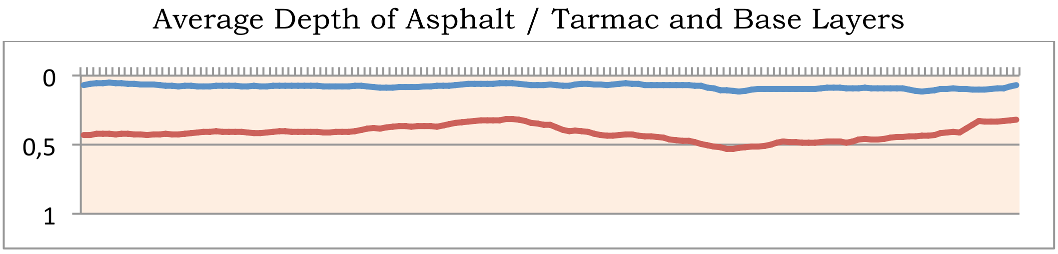

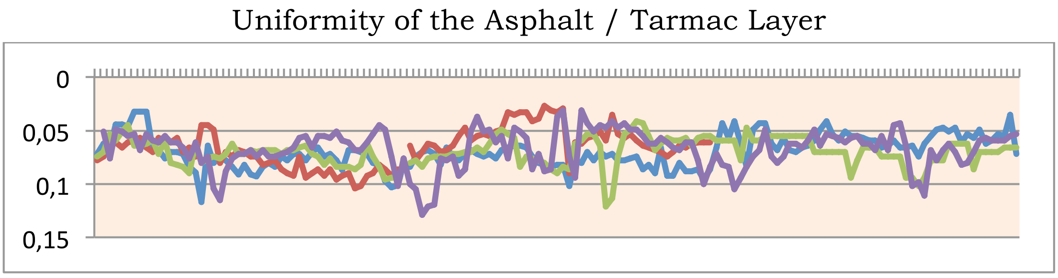

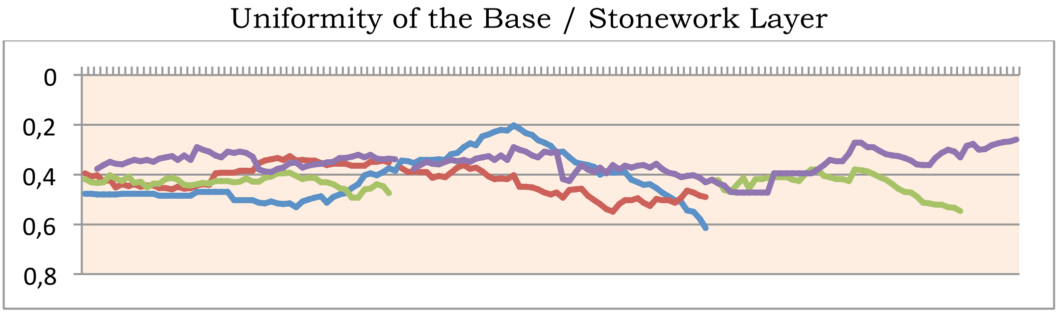

3. Survey Method 2 - Exploring the bridge deck using dual frequency 200MHz and 600MHz Antenna from the RIS Hi Mod

To possibly identify the location of the reinforcement bars / structural ties & To investigate the influence of frequency change on bridge deck structural detail, four scans were performed using the TR Dual-F 200MHz and 600MHz antenna from the RIS Hi Mod. The existing reference points (high frequency survey) were exploited. The above-mentioned antenna box contains an array of two antennas with frequencies optimised for the detection of utilities. In typical ground conditions, the 600MHz antenna should penetrate to approximately 1.5m and the 200MHz to approximately 2.5m, which should be sufficient to identify the reinforcing bars passing through the bridge.

Examples of B-Scans radar data identifying the presence of reinforcing bars, are shown (one example per each frequency).

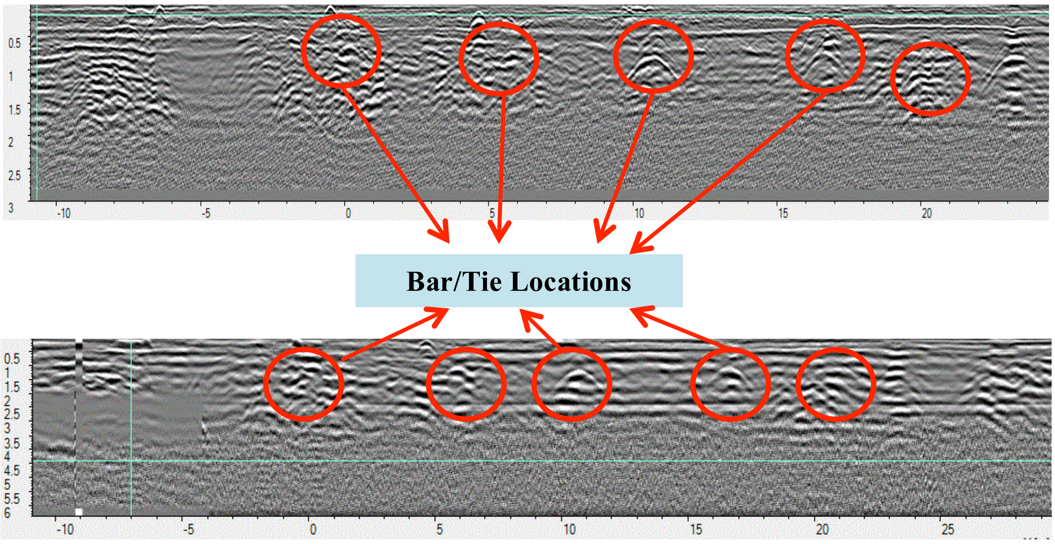

The following C-Scan images show clear targets, which may be the reinforcing bars; they are more visible at the lower frequency

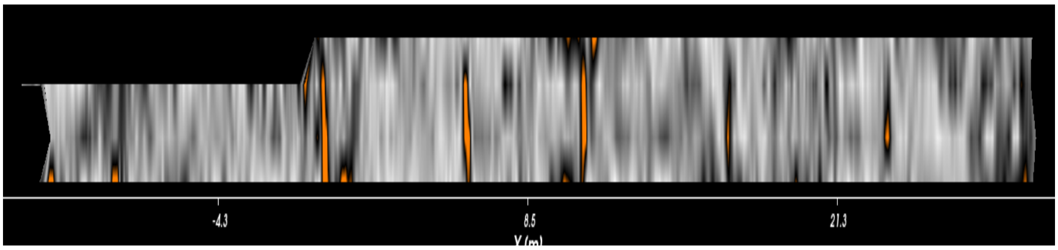

Zone 1, 200 MHz Antenna

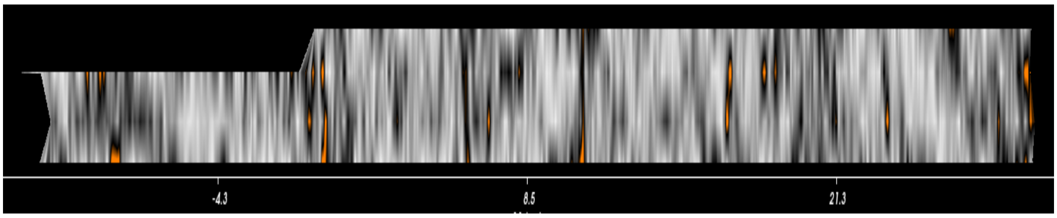

Zone 1, 600 MHz Antenna

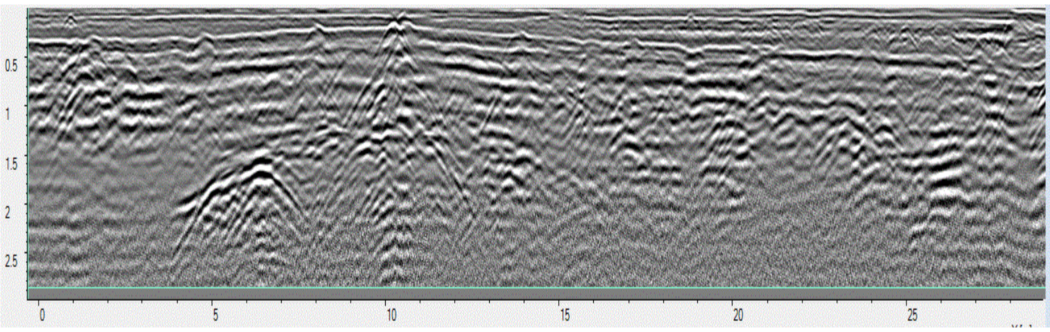

Zone 2, B-Scan, 600 MHz Antenna

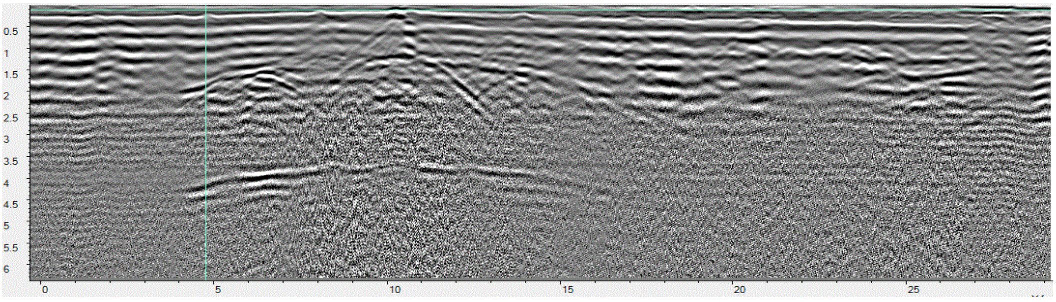

Zone 2, B-Scan, 200 MHz Antenna

4. Survey Method 3 - Production of a 3D Scan of the Bridge using a Leica P20 Laser Scanner

The purpose was that of creating a benchmark for future surveys – detecting possible structural movements and settlements, as well as that of modelling the bridge.

A Google Maps image diagram of the Old Bridge, Aylesford showing the location of each of the scan positions

There is a large amount of unnecessary data included, but "mm" accuracy images of the bridge and surrounding area can be reproduced from any angle.

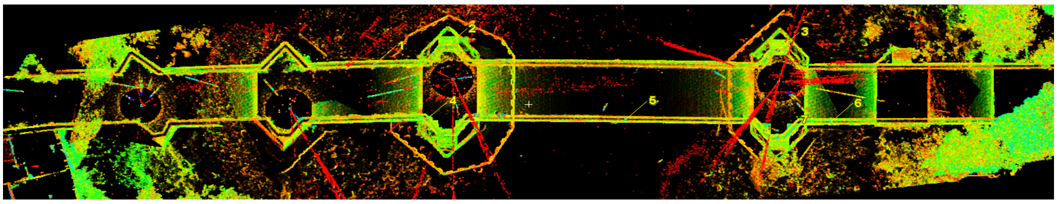

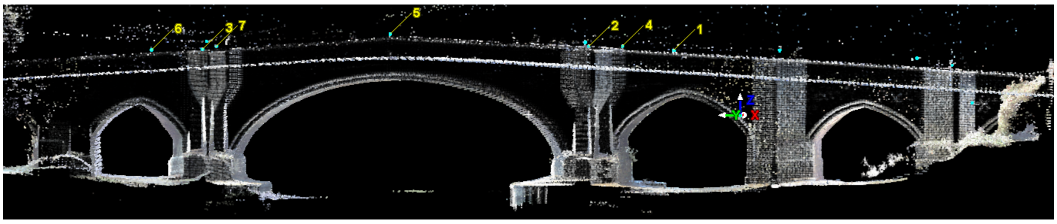

3D laser scan of the bridge:

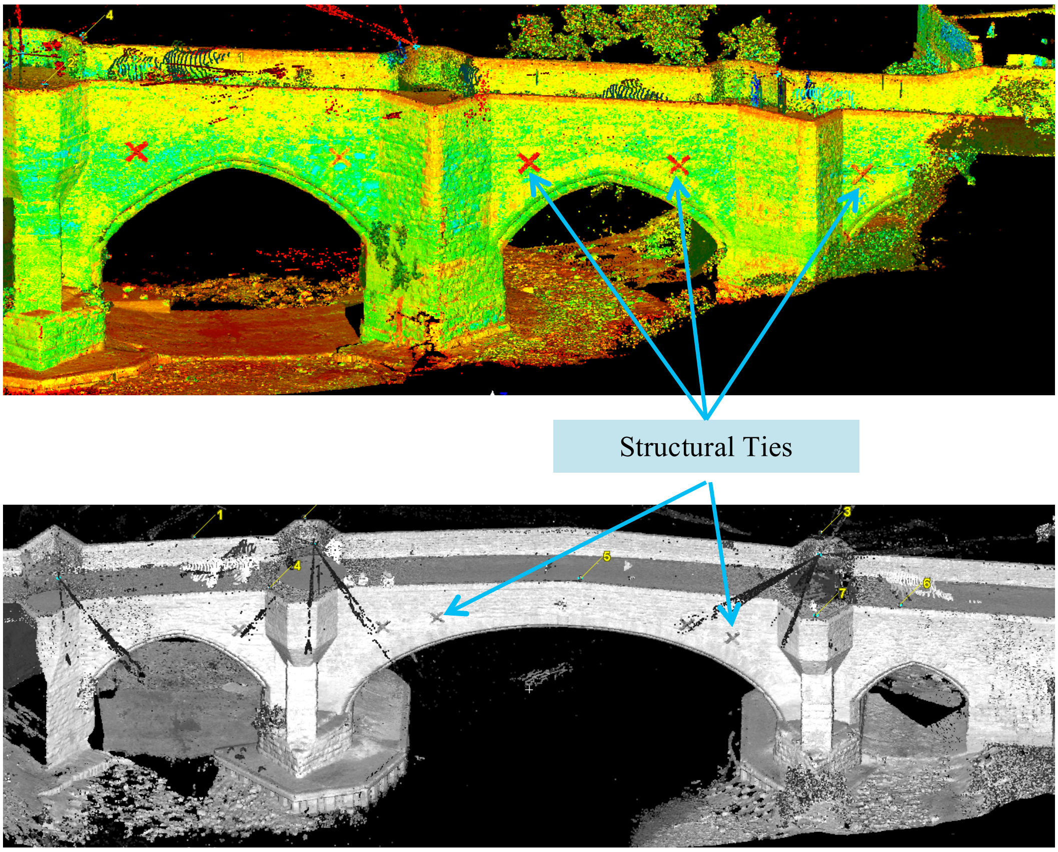

5. Conclusions

"Accurate" profiles of two layers (asphalt and original stone) of the bridge deck were identified and mapped.

Position of structural ties on the bridge were confirmed.

Location of numerous defects and non-structural futures were identified.

3D laser scan of the bridge was obtained (for further analytical and numerical investigation).

EUROPEAN COOPERATION IN SCIENCE AND TECHNOLOGY

UNIVERSITY of GREENWICH

Acknowledgements

The authors would like to acknowledge the support of COST Action TU1208 "Civil Engineering Applications of Ground Penetrating Radar" and The Rochester Bridge Trust in this project and presentation

PROGRESS REPORT OF PROJECT 4.3

"APPLICATIONS OF GPR IN ASSOCIATION WITH OTHER NON-DESTRUCTIVE TESTING METHODS IN SURVEYING OF TRANSPORT INFRASTRUCTURES"

Simona Fontul (PT) - *simona@lnec.pt*

- 57 Participants
- 15 countries

Countries	Participants
Austria	1
Belgium	2
Croatia	6
Czech Republic	2
Denmark	2
Finland	1
France	7
Germany	4
Greece	6
Italy	5
Poland	2
Portugal	3
Spain	12
Turkey	1
United Kingdom	3

Questionnaire

Falling Weight Deflectometer – load tests for structural evaluation

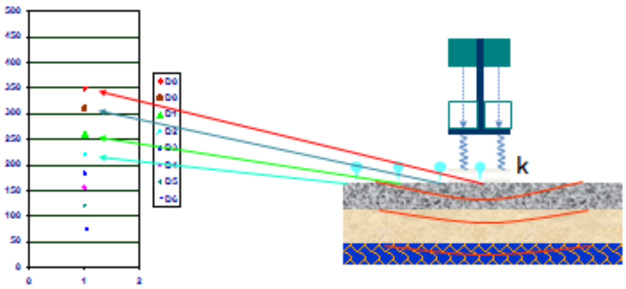

Sum up of presentations on GPR use in different countries at Vienna Meeting

Country	GPR+NDT	NDT	Other Geophysical
Belgium	y	FWD+ Curviameter	
Check republic	y	FWD	
Denmark	y		ERT EM
Estonia	N		
Finland	y	Percometers	FWD
Portugal		FWD, EM120	tomografy
Spain	y		Termografy, tomografy
UK	y	N.S.	
Armenia			R107
Italy	y	NS concrete	
Poland	y		permitivity measurements
Italy	y	LFWD	
Belgum	y		electric conductivity
Germany	y	FWD; HWD	EMI, ERT, electrical

Project 4.3 "Applications of GPR in association with other non-destructive testing methods in surveying of transport infrastructures"

Mercedes Solla	Universidade de Vigo	Spain

3 documents published this last year

- **One paper in journal (NDT&E International)** related to the combination of GPR and Thermography to analyze cracking in asphalt.

- **Two papers for conferences (GPR Conference in Brussels and ISPRS)** regarding the combination of different sensors (GPR+LiDAR+thermography+IRI) mounted on a mobile vehicle, and the software for GPR processing and georeferencing of all the data.

Project 4.3 "Applications of GPR in association with other non-destructive testing methods in surveying of transport infrastructures"

Jean-Paul Balayssac	University of Toulouse	France

- **results of a study performed at the end of 90ths** and the beginning of this century in collaboration with our colleagues from Sherbrooke University (Québec, Canada).
- This method permits to combine **GPR and potential corrosion mapping** for the detection of potentially corroded areas at the surface of **bridge decks**. This method is currently applied in **Québec and in Belgium** (Wallonie)

Laboratoire Matériaux et Durabilité des Constructions

❑ Use of GPR for the detection of zones with high probability of corrosion

- GPR measurements on bridge decks in Québec (Canada)
- Corrosion potential mapping (grid 1m x 1m)
- GPR profiles along the deck (0.5 m between each profile)
- Analysis of the reflection at the interface between the pavement and the concrete structure → index of radar reflection IR²

Laboratoire Matériaux et Durabilité des Constructions

16

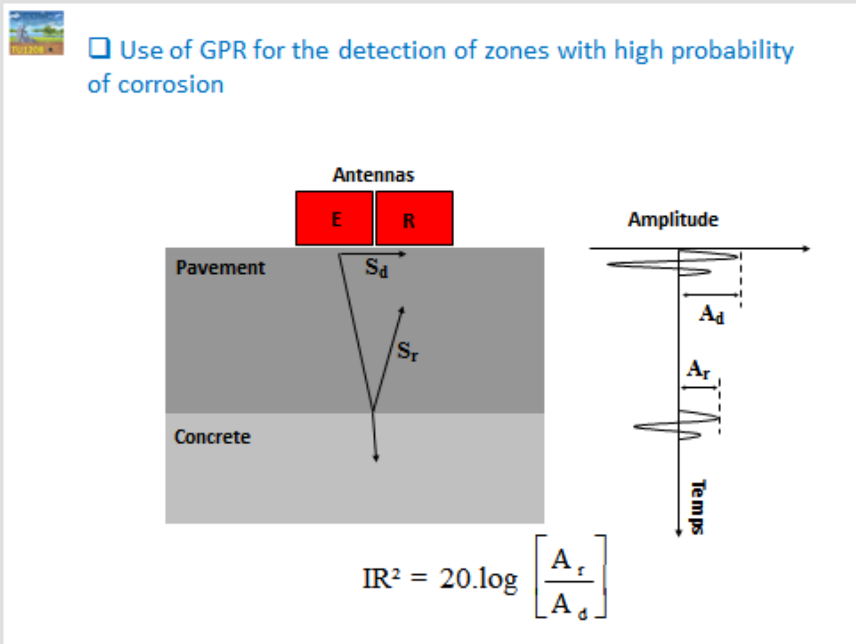
Use of GPR for the detection of zones with high probability of corrosion
Antennas
E
R
Amplitude
Pavement
Concrete
Temps
IR² = 20.log [A r / A d]

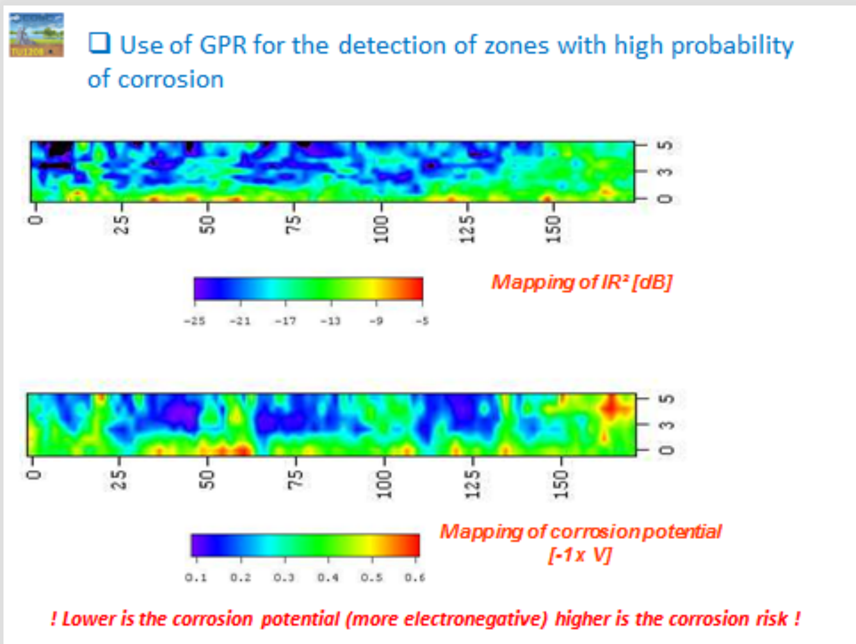
Use of GPR for the detection of zones with high probability of corrosion
Mapping of IR² [dB]
Mapping of corrosion potential [-1x V]
! Lower is the corrosion potential (more electronegative) higher is the corrosion risk !

❑ Use of GPR for the detection of zones with high probability of corrosion

Binary card of IR^2

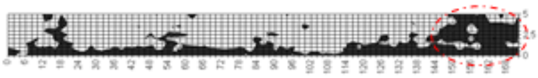

Threshold applied at -17 dB

Deck length (m)

Areas with lower corrosion potential (dark areas < -350 mV) correspond to the zones with high reflectivity (> -17 dB)

Threshold applied at -350 mV

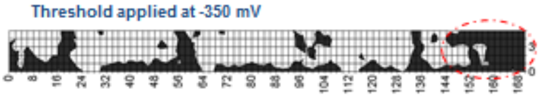

Binary card of corrosion potential

Project 4.3 "Applications of GPR in association with other non-destructive testing methods in surveying of transport infrastructures"

Josipa Domitrović	University of Zagreb	Croatia

1 paper in conference - Application of **GPR with FWD** that was published on 4th International Scientific Conference Road Research and Administration held in Bucharest, 4-5 July 2013.

Carl Van Geem	Belgian Road Research Centre	Belgium

BRRC is working on the preparations for more investigation on the precision and the **optimal procedure for determining layer thicknesses of road layers**.

Layer thickness is important for back-calculation of E-moduli from **deflection measurements.**

BRRC deflection measurements: **Curviameter and FWD.**

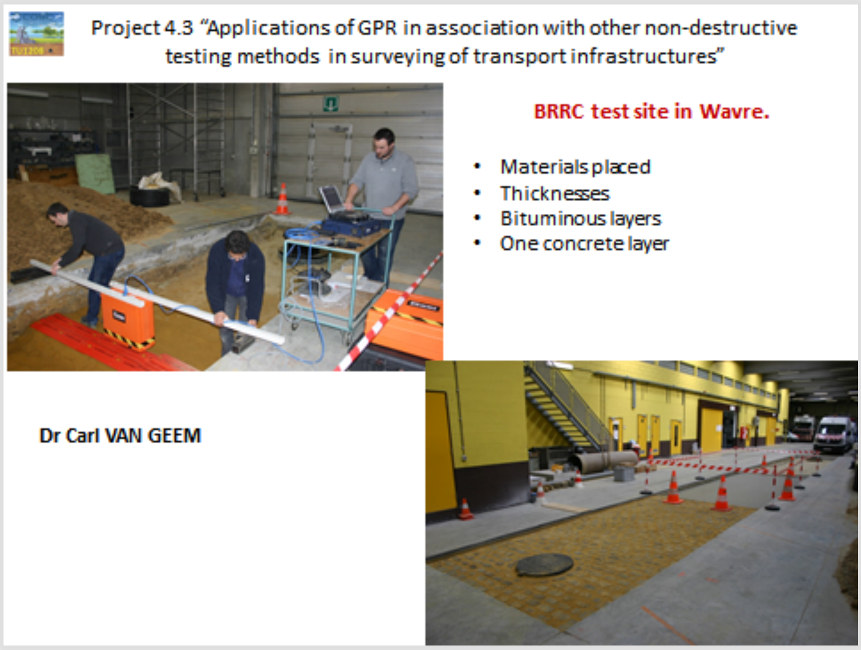

Alex Birtwisle	Atlas Geophysical Limited	United Kingdom

Ground Penetrating Radar (GPR) has traditionally been used to derive pavement layer depth information. Traditional GPR antennas are not normally capable of detecting subsurface cracking. An adapted GPR antenna has been developed and is in current use for the specific application of measuring crack depths in flexible pavement. Traditional methods of assessing the extent of repair work necessary on airfield runways, namely visual inspection and coring, rely on visibility of cracking at the surface and are not capable of **detecting subsurface cracking** although this is an important element of the assessment. The GPR crack detection equipment was used on the runway of a military airfield to locate the joints between the underlying concrete slabs, to identify reflective cracking developing from the joints into the overlying asphalt, or to confirm the integrity of the asphalt. A system of “traffic light” reporting was used to enable the pavement engineers to evaluate the extent of damage to the runway.

Alex Birtwisle | Atlas Geophysical Limited | United Kingdom

Ground Penetrating Radar (GPR) surveys of composite pavement structures are commonly used to derive pavement layer depth information. In order to assess the extent of repair work necessary, it is useful to be able **to evaluate the extent of both vertical cracking and horizontal delamination.** Although the extent of any delamination can be obtained from a traditional GPR survey, vertical subsurface cracking cannot be detected by the same means because traditional GPR antennas are not normally capable of detecting vertical cracks. When subsurface vertical cracks are not visible at the surface traditional methods of assessment based on visual inspection and coring are ineffective. This paper describes how an adapted GPR antenna was used on **the runway of a military airfield to locate the joints between the underlying concrete slabs, and to identify reflective cracking developing from the joints into the overlying asphalt.** The GPR survey successfully identified the location of subsurface cracks and helped paint a 'bigger picture' of crack distribution across the area under investigation. This project demonstrated that crack detection with an adapted GPR antenna could provide a new more comprehensive method of assessing the condition of composite pavements. However, the investigation also highlighted some of the limitations of this type of survey and based on this information the paper proposes a methodology for undertaking this type of investigation and highlights were additional research is needed.

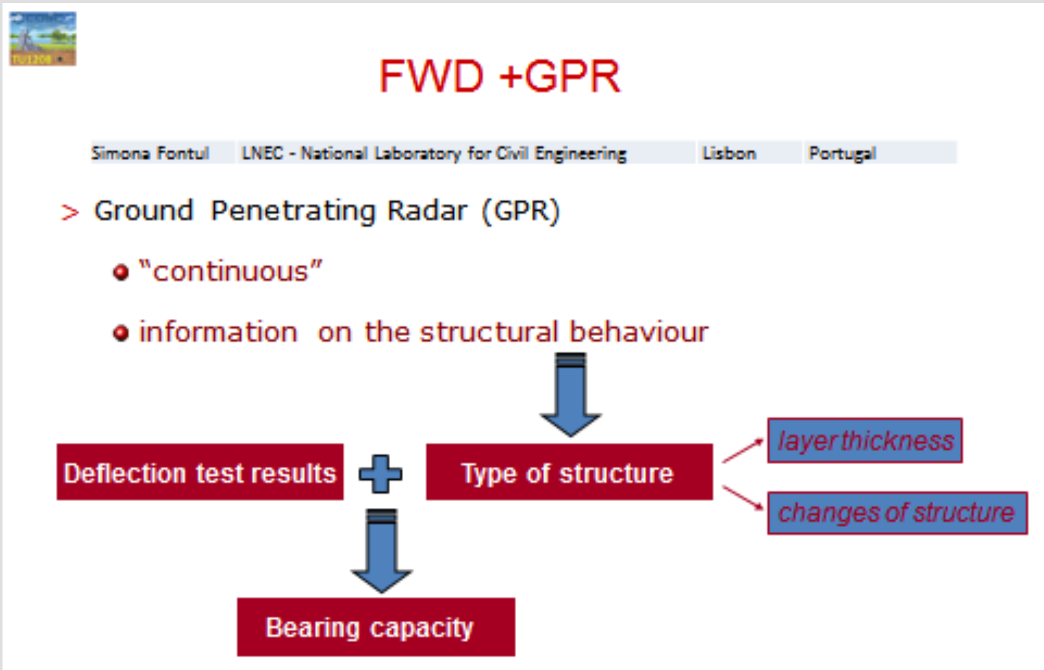

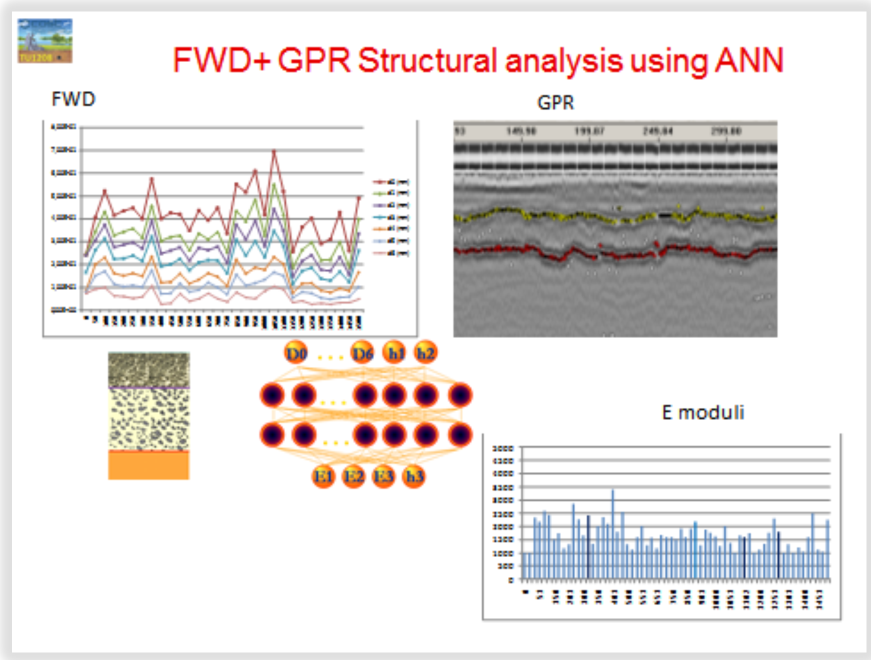
FWD+ GPR Structural analysis using ANN
FWD
GPR
D0
D6
h1
h2
E1
E2
E3
h3
E moduli

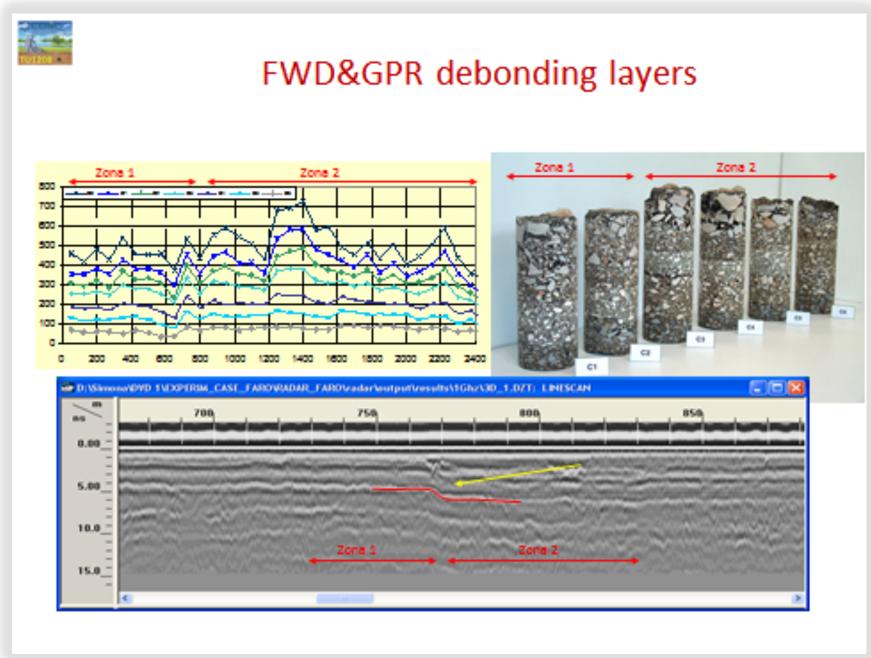
FWD&GPR debonding layers
Zona 1
Zona 2
Zona 1
Zona 2
Zona 1
Zona 2

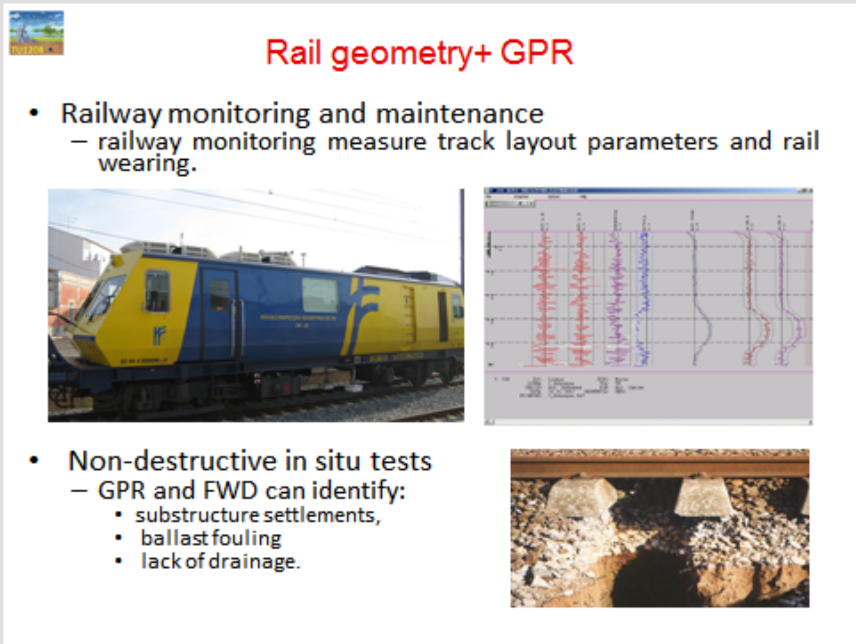
Rail geometry+ GPR
Railway monitoring and maintenance
– railway monitoring measure track layout parameters and rail wearing.
Non-destructive in situ tests
– GPR and FWD can identify:
substructure settlements,
ballast fouling
lack of drainage.

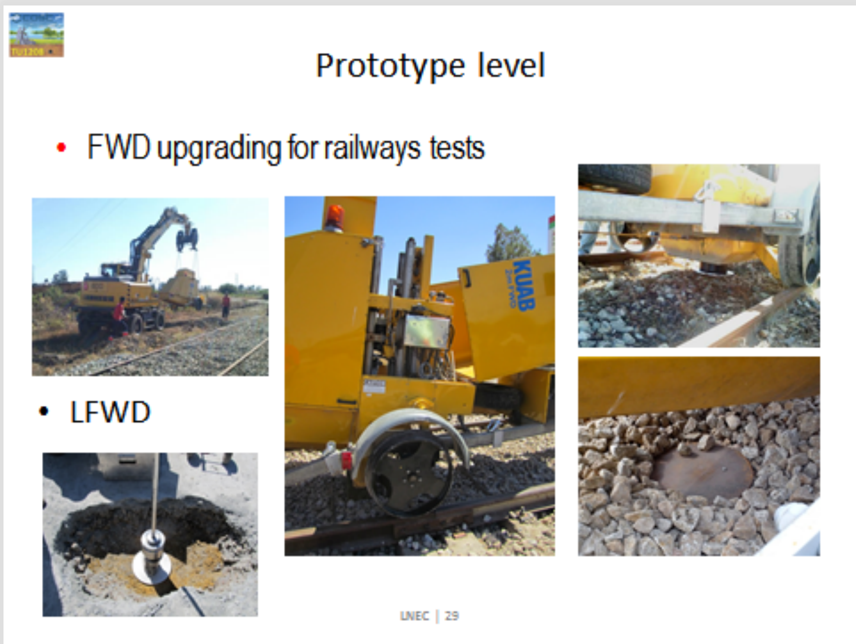
Prototype level
FWD upgrading for railways tests
LFWD
LNEC | 29

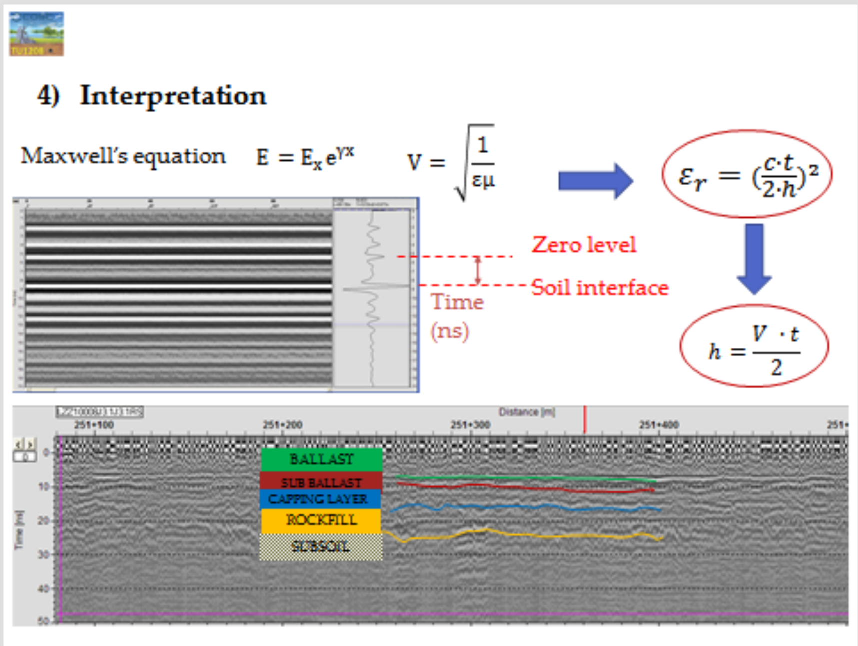
4) Interpretation
Maxwell's equation $E = E_x e^{\gamma x}$ $V = \sqrt{\frac{1}{\varepsilon\mu}}$
$\varepsilon_r = (\frac{c \cdot t}{2 \cdot h})^2$
$h = \frac{V \cdot t}{2}$
Zero level
Soil interface
Time (ns)
BALLAST
SUB BALLAST
CAPPING LAYER
ROCKFILL
SUBSOIL

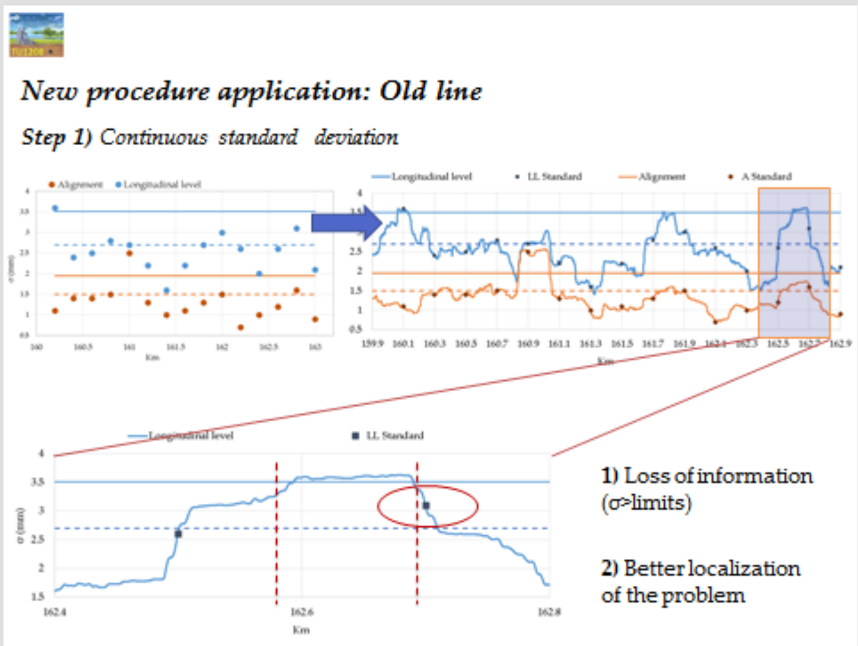
New procedure application: Old line
Step 1) Continuous standard deviation
Longitudinal level
LL Standard
Alignment
A Standard
Km
1) Loss of information (σ>limits)
2) Better localization of the problem

"Applications of GPR in association with other non-destructive testing methods in surveying of **transport infrastructures**".

Brain storm for 4.3

Transport Infrastructures
Roads
Railways
Runways
Bridges ???

- More or less transport infrastructures???
  - Are bridges object of other Project? Should be considered in 4.3?

NDT equipment referred

- Main application:
  - FWD Falling Weight Defletometer / GPR (E moduli)

Loading tests
FWD; LFWD;
High Speed Deflect
vibration tests
Geometric level equipments
Curviameter
SASW

Complementary tests
Digital imaging
3D laser scan
Thermografy

- Shall we distinguish between:
  - loading and other structural tests
  - complementary geophysical tests?

Other geophysical methods
EMI
seismic methods
electric measurements
tomografy

"Applications of GPR in association with other non-destructive testing methods in surveying of **transport infrastructures**".

Transport Infrastructures GPR &NDT	
In situ tests	
Laboratory tests	

- Shall we address both or **only *in situ* tests** as the others are addresseed on

Possible 4.3 objective

- Develop a traffic speed combined evaluation method with GPR&NDT load test ???

Project 4.3 "Applications of GPR in association with other non-destructive testing methods in surveying of transport infrastructures"

- Main issues to be addressed
  - **Location of the tests GPR&NDT**
  - Data Processing
    - Large amount of data
    - Processed toghether to take the best of both GPR&NDT
    - Efficient aproaches like ANN
  - Freeware software FWD/GPR
  - Combined monitoring- improved monitoring methodology
  - Joint interpretation, homogeneous zones, quick interpretation
  - Less NDT load tests, cost and time consuming

"GPR USED IN COMBINATION WITH OTHER NDT METHODS FOR ASSESSING PAVEMENTS IN PPP PROJECTS"
(CONTRIBUTION TO PROJECT 4.3)

Andreas Loizos (GR), Christina Plati (GR)
aloizos@central.ntua.gr

The abstract is published in *Geophysical Research Abstracts*, Vol. 16, EGU2014-1953, 2014 and is available on *www.egu2014.eu*

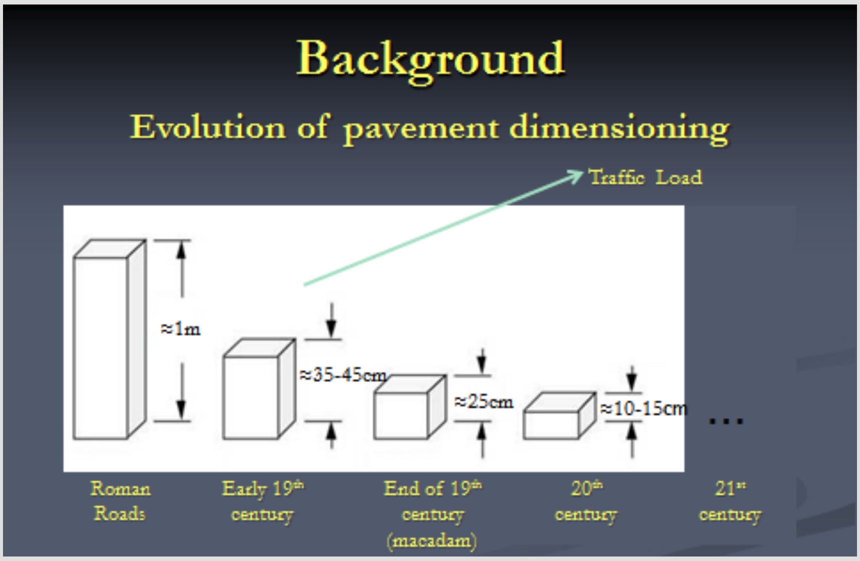


Background
Pavement Types
National Technical University of Athens

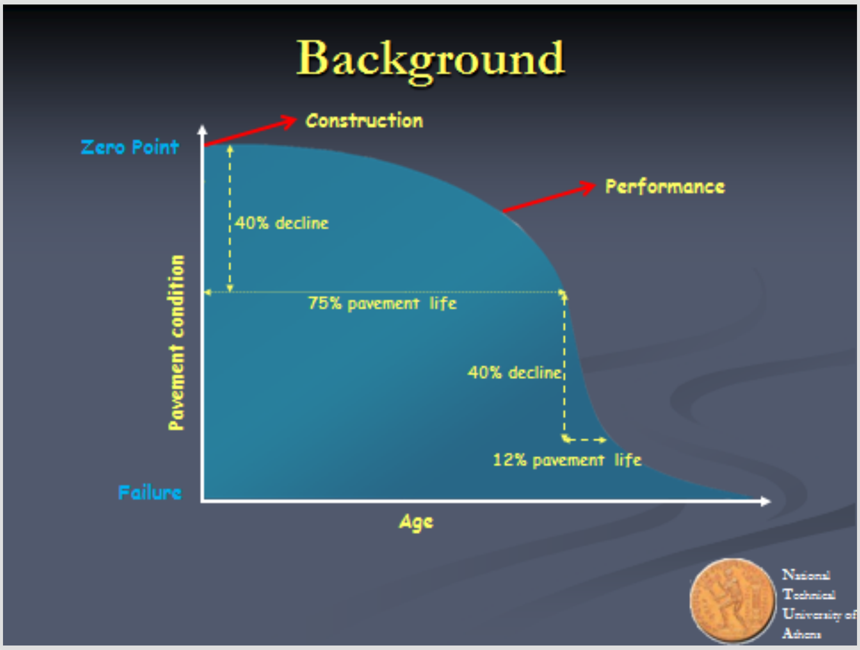
Background
Zero Point
Construction
Performance
40% decline
75% pavement life
40% decline
12% pavement life
Pavement condition
Failure
Age
National Technical University of Athens

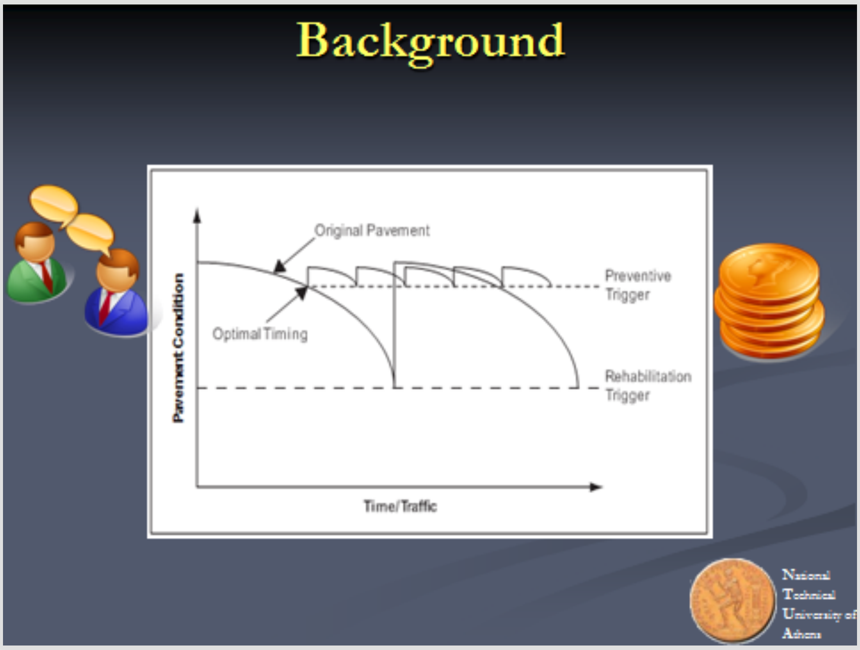
Background
Original Pavement
Preventive Trigger
Optimal Timing
Pavement Condition
Rehabilitation Trigger
Time/Traffic
National Technical University of Athens

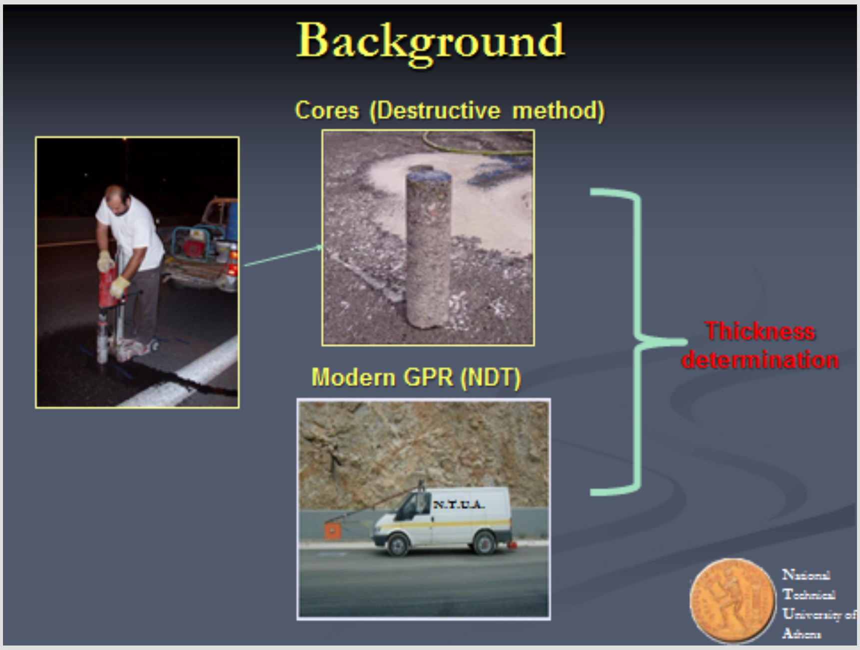
Background
Cores (Destructive method)
Modern GPR (NDT)
N.T.U.A.
Thickness determination
National Technical University of Athens

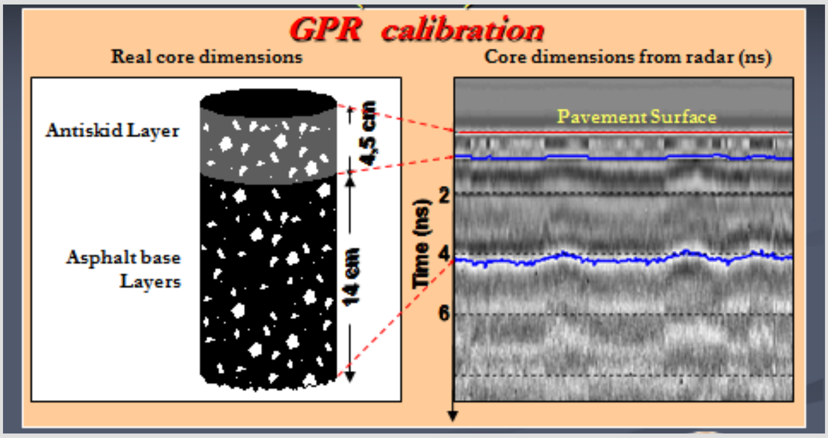
GPR calibration
Real core dimensions
Core dimensions from radar (ns)
Antiskid Layer
Asphalt base Layers
4,5 cm
14 cm
Time (ns)
2
4
6
Pavement Surface

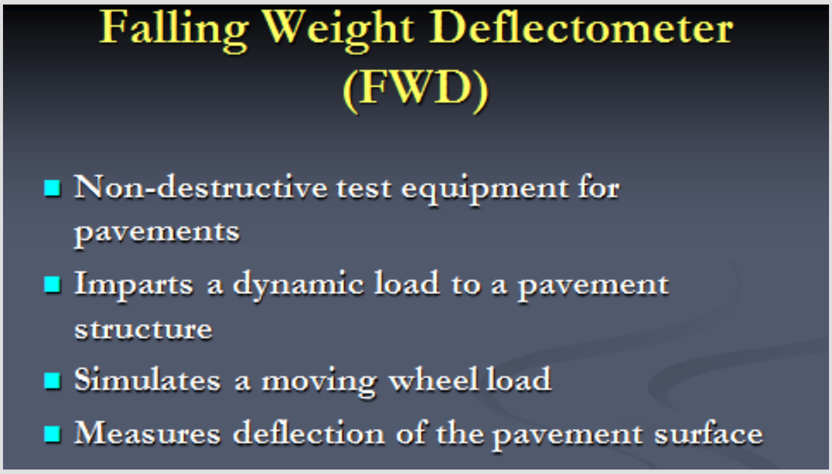
Falling Weight Deflectometer (FWD)
Non-destructive test equipment for pavements
Imparts a dynamic load to a pavement structure
Simulates a moving wheel load
Measures deflection of the pavement surface

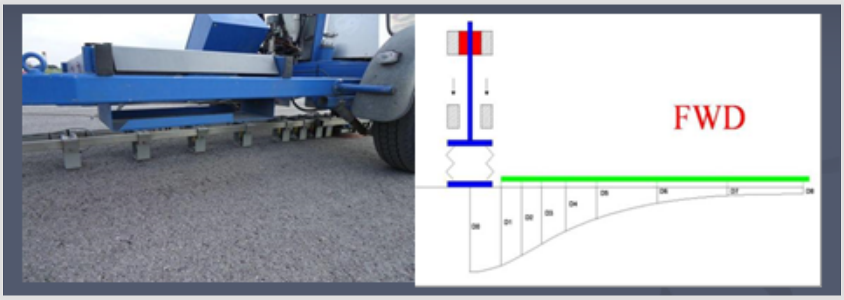
FWD

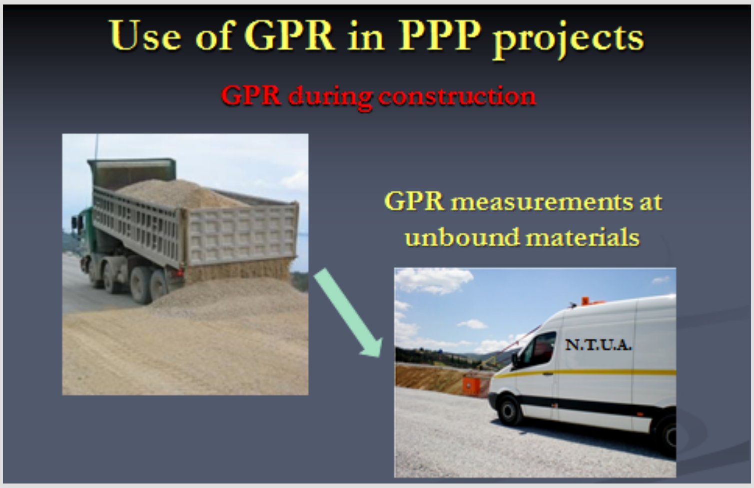
Use of GPR in PPP projects
GPR during construction
GPR measurements at unbound materials
N.T.U.A.

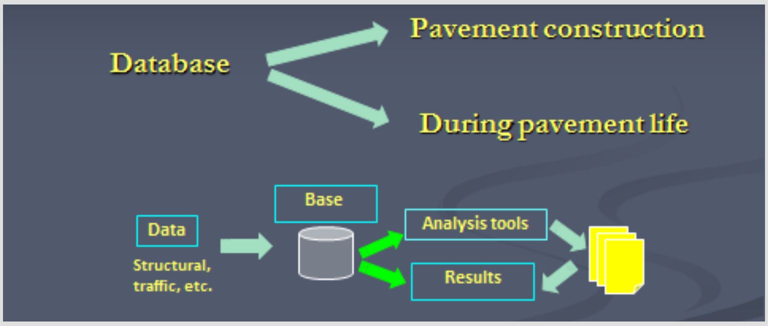
Database
Pavement construction
During pavement life
Data
Structural, traffic, etc.
Base
Analysis tools
Results

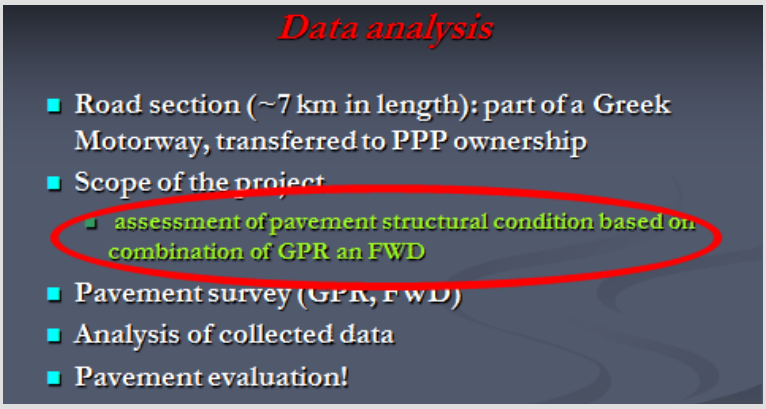
Data analysis
Road section (~7 km in length): part of a Greek Motorway, transferred to PPP ownership
Scope of the project
assessment of pavement structural condition based on combination of GPR an FWD
Pavement survey (GPR, FWD)
Analysis of collected data
Pavement evaluation!

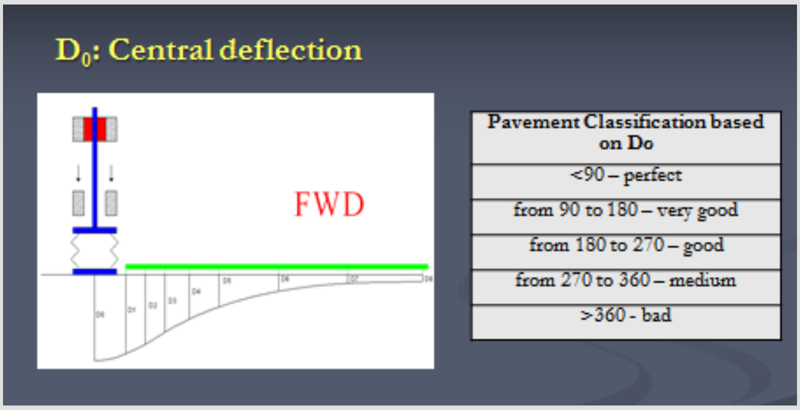
D$_0$: Central deflection
FWD
Pavement Classification based on Do
<90 – perfect
from 90 to 180 – very good
from 180 to 270 – good
from 270 to 360 – medium
>360 - bad

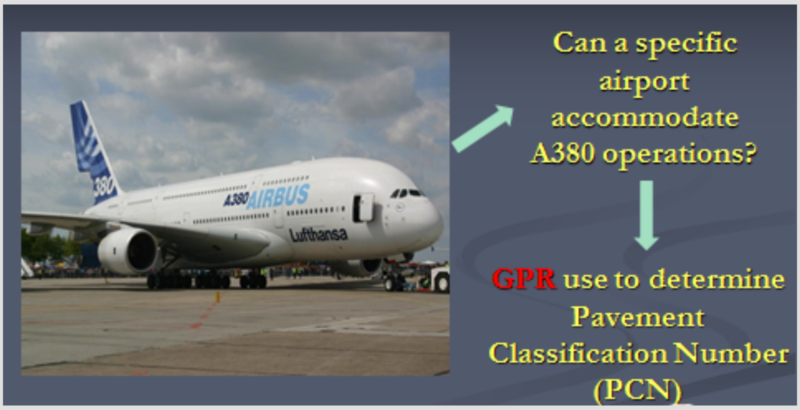
Can a specific airport accommodate A380 operations?
GPR use to determine Pavement Classification Number (PCN)


Road closure
Cannot delay airplane operations

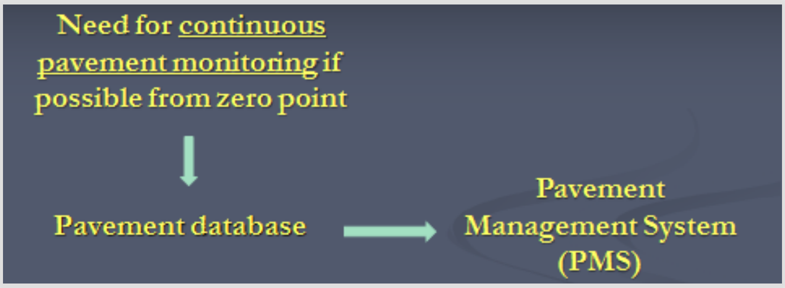
Need for continuous pavement monitoring if possible from zero point
Pavement database
Pavement Management System (PMS)

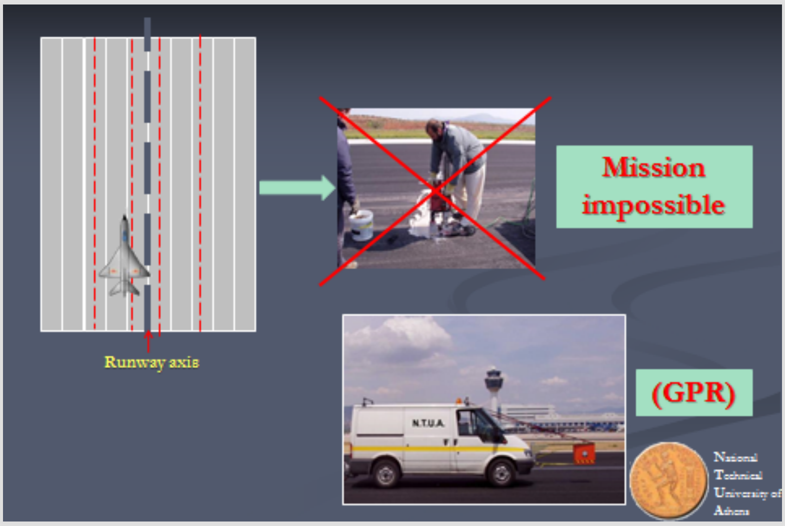
Runway axis
Mission impossible
N.T.U.A.
(GPR)
National Technical University of Athens

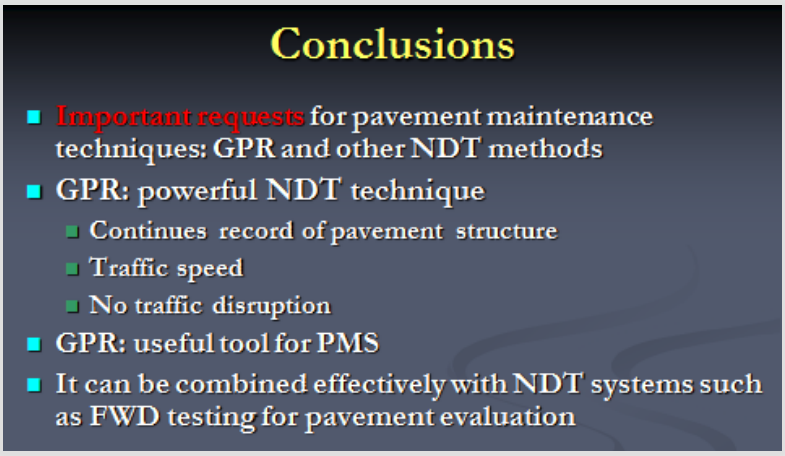
Conclusions
Important requests for pavement maintenance techniques: GPR and other NDT methods
GPR: powerful NDT technique
Continues record of pavement structure
Traffic speed
No traffic disruption
GPR: useful tool for PMS
It can be combined effectively with NDT systems such as FWD testing for pavement evaluation

PROGRESS REPORT OF PROJECT 4.4

"APPLICATIONS OF GPR IN ASSOCIATION WITH OTHER NON-DESTRUCTIVE TESTING METHODS IN BUILDING ASSESSMENT AND IN GEOLOGICAL/GEOTECHNICAL TASKS"

Klisthenis Dimitriadis (GR) - *workst@geoservice.gr*

Project 4.4. participants

- During the last 9 months, after the last meeting of the Action, in Rome, the total number of participants of the project 4.4. increased to 41 members.

Project 4.4. progress

- In the same period, nine new scientific publications have been published, according to the feedback received from the project members.

New ideas, strategies and action plans

- In one effort to initiate discussions between partners of the project 4.4 and take the benefit of the networking capacities of the COST framework, I have asked from the partnership, to provide to the project their recent activities in GPR but also their new ideas and perspectives for the future.

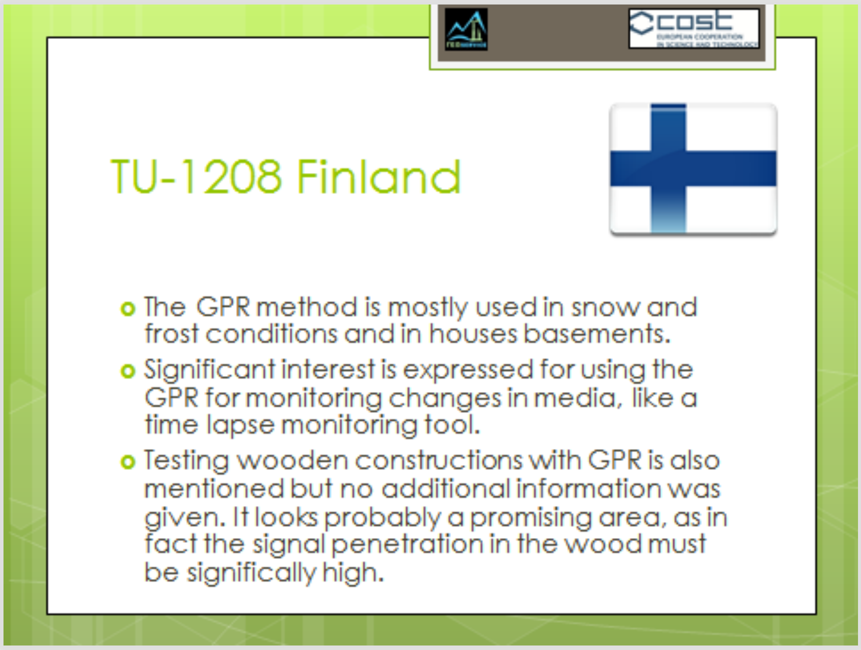
TU-1208 Finland
The GPR method is mostly used in snow and frost conditions and in houses basements.
Significant interest is expressed for using the GPR for monitoring changes in media, like a time lapse monitoring tool.
Testing wooden constructions with GPR is also mentioned but no additional information was given. It looks probably a promising area, as in fact the signal penetration in the wood must be significally high.

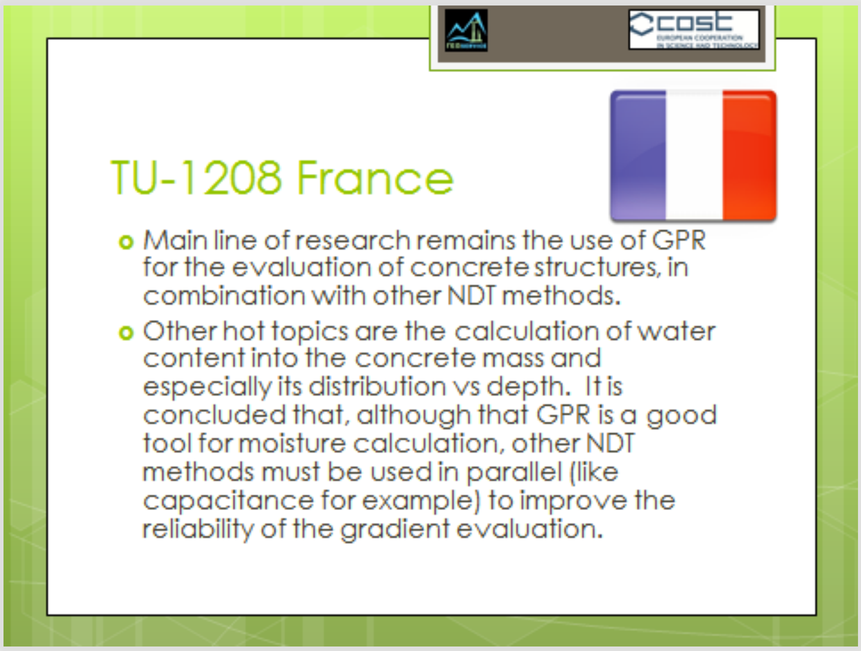
TU-1208 France
Main line of research remains the use of GPR for the evaluation of concrete structures, in combination with other NDT methods.
Other hot topics are the calculation of water content into the concrete mass and especially its distribution vs depth. It is concluded that, although that GPR is a good tool for moisture calculation, other NDT methods must be used in parallel (like capacitance for example) to improve the reliability of the gradient evaluation.


TU-1208 Spain
The activities of partners from Spain, related to GPR are oriented towards archaeology and buildings inspection. GPR is mostly combined with seismics for complementarity in the results and variety in the calculated parameters.


TU-1208 Portugal
In Portugal, GPR method looks expanding in the last period, due to the new orientations of the construction sector. Tendency is in these days to maintain old structures rather than constructing new ones, due to the economic crisis. GPR is one very effective tool in these fields.
In addition, combined approaches are recently adopted like multisprectal imaging and laser scanning.

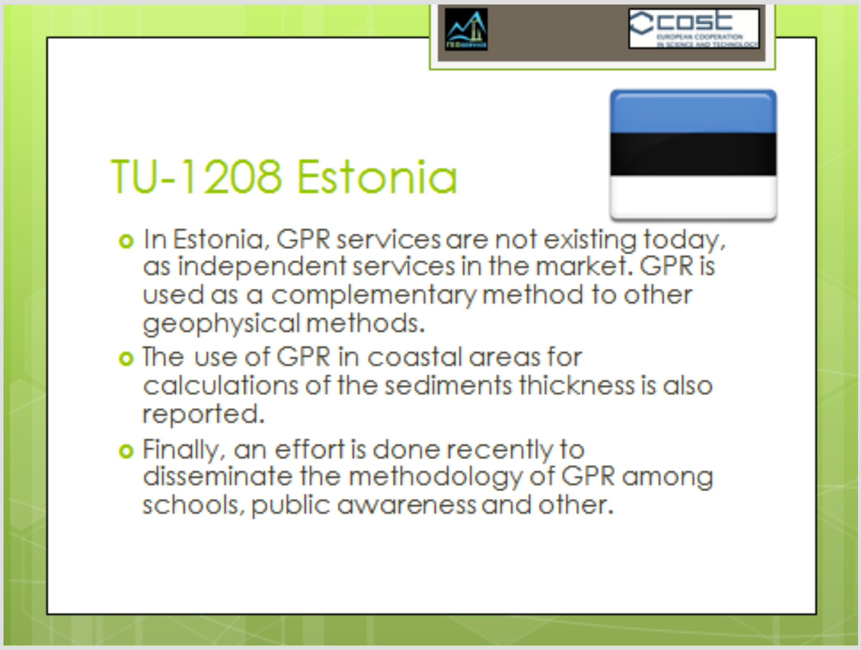
TU-1208 Estonia
In Estonia, GPR services are not existing today, as independent services in the market. GPR is used as a complementary method to other geophysical methods.
The use of GPR in coastal areas for calculations of the sediments thickness is also reported.
Finally, an effort is done recently to disseminate the methodology of GPR among schools, public awareness and other.

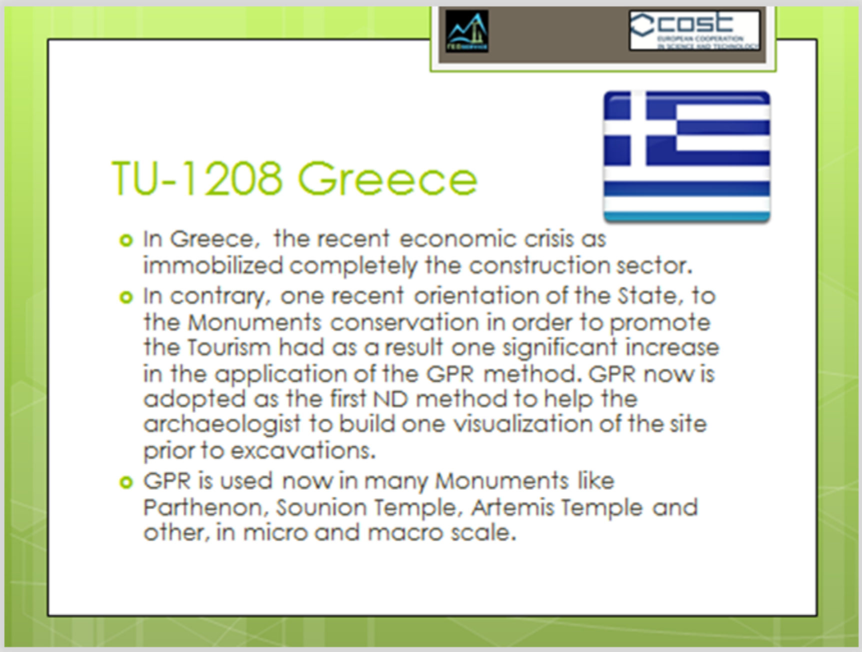
TU-1208 Greece
In Greece, the recent economic crisis as immobilized completely the construction sector.
In contrary, one recent orientation of the State, to the Monuments conservation in order to promote the Tourism had as a result one significant increase in the application of the GPR method. GPR now is adopted as the first ND method to help the archaeologist to build one visualization of the site prior to excavations.
GPR is used now in many Monuments like Parthenon, Sounion Temple, Artemis Temple and other, in micro and macro scale.

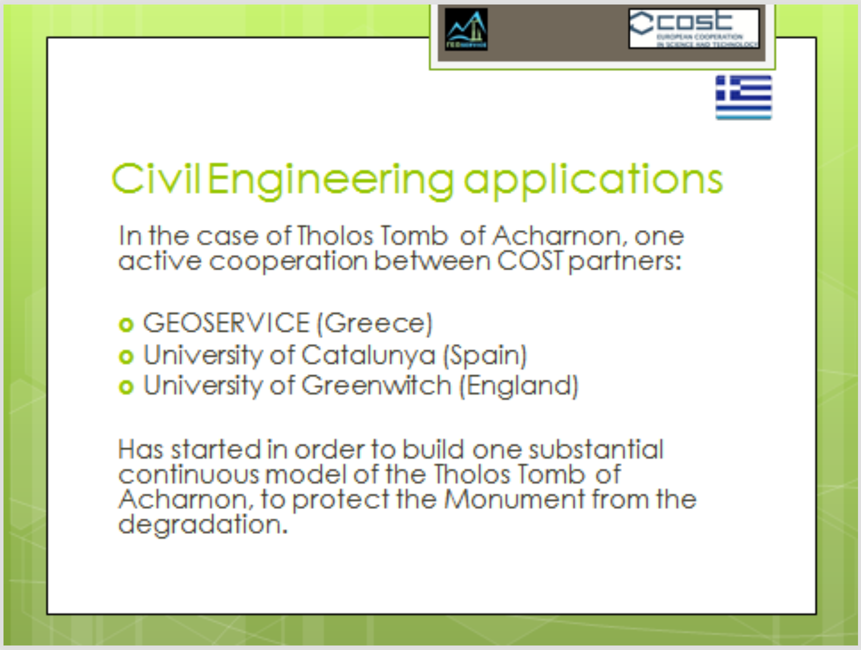
Civil Engineering applications
In the case of Tholos Tomb of Acharnon, one active cooperation between COST partners:
GEOSERVICE (Greece)
University of Catalunya (Spain)
University of Greenwitch (England)
Has started in order to build one substantial continuous model of the Tholos Tomb of Acharnon, to protect the Monument from the degradation.

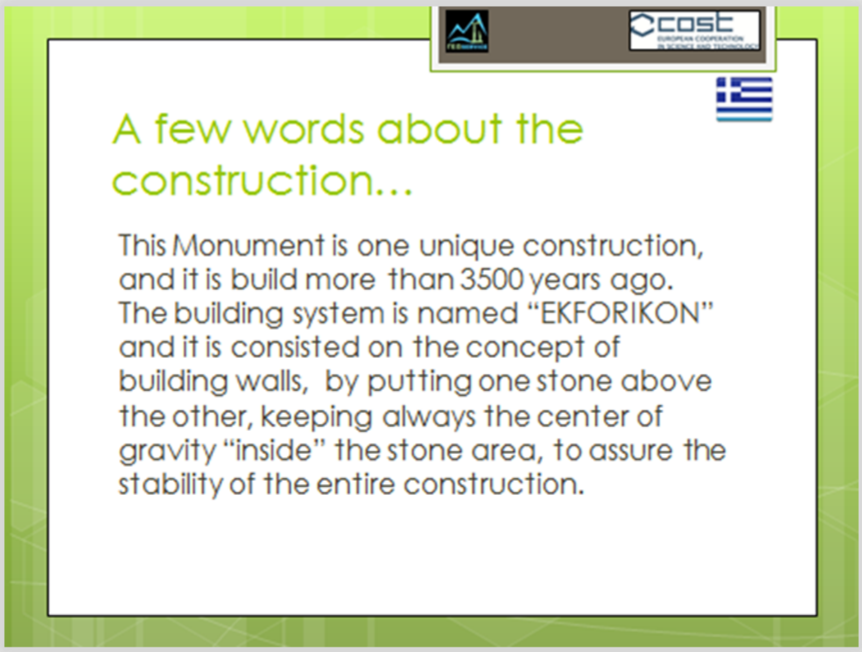
A few words about the construction…
This Monument is one unique construction, and it is build more than 3500 years ago. The building system is named "EKFORIKON" and it is consisted on the concept of building walls, by putting one stone above the other, keeping always the center of gravity "inside" the stone area, to assure the stability of the entire construction.

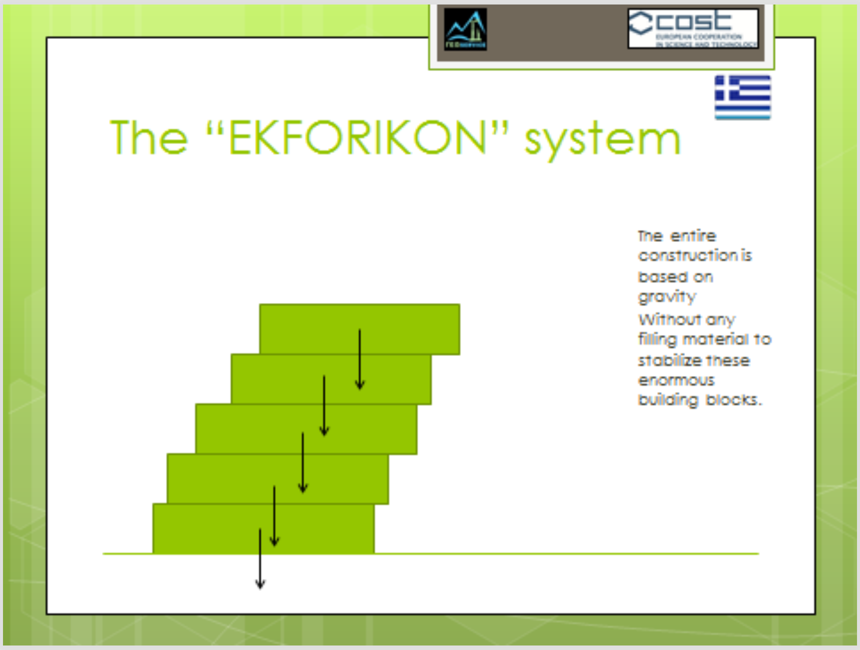
The "EKFORIKON" system
The entire construction is based on gravity
Without any filling material to stabilize these enormous building blocks.

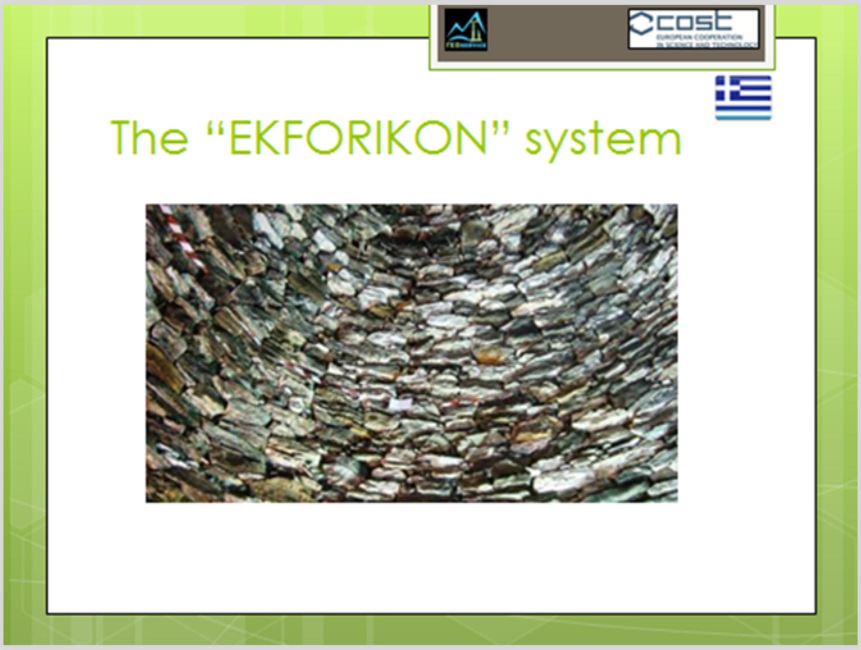
The "EKFORIKON" system

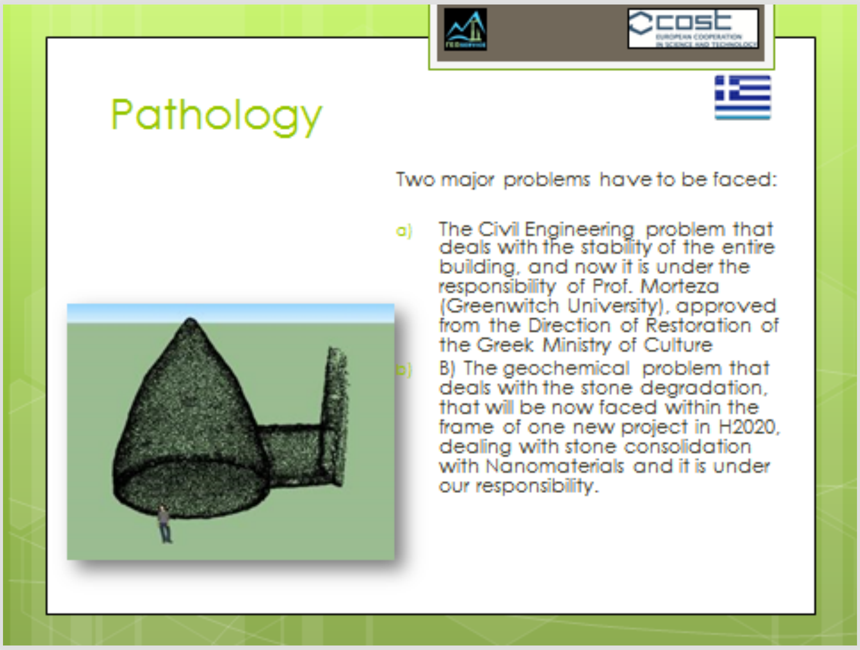
Pathology
Two major problems have to be faced:
a) The Civil Engineering problem that deals with the stability of the entire building, and now it is under the responsibility of Prof. Morteza (Greenwitch University), approved from the Direction of Restoration of the Greek Ministry of Culture
B) The geochemical problem that deals with the stone degradation, that will be now faced within the frame of one new project in H2020, dealing with stone consolidation with Nanomaterials and it is under our responsibility.


Building material consolidation using nanotechnologies
Today's condition of the building material of the grave: Altered and weathered stone from ageing and the deterioration of salts, existing in the soil at extreme concentrations.

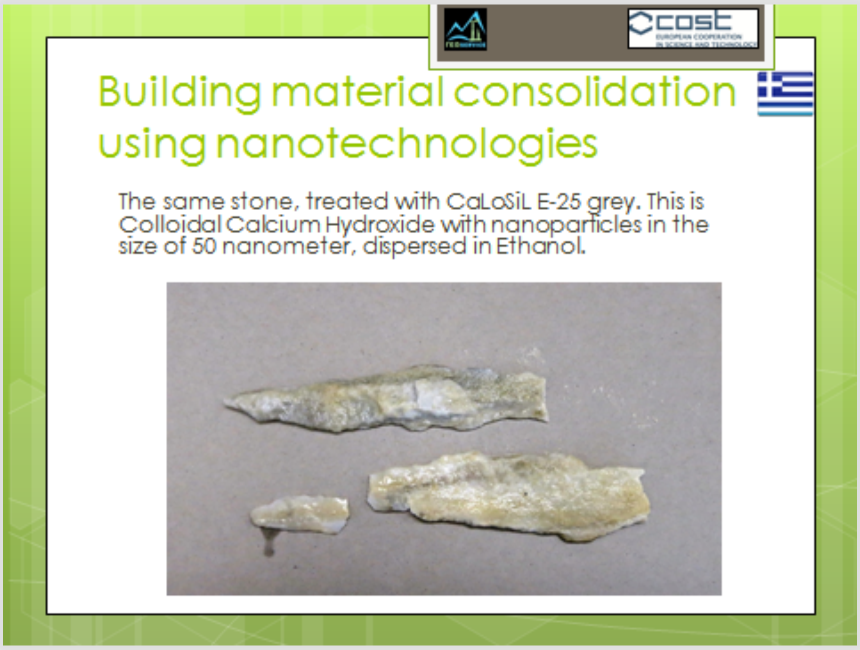
Building material consolidation using nanotechnologies
The same stone, treated with CaLoSiL E-25 grey. This is Colloidal Calcium Hydroxide with nanoparticles in the size of 50 nanometer, dispersed in Ethanol.

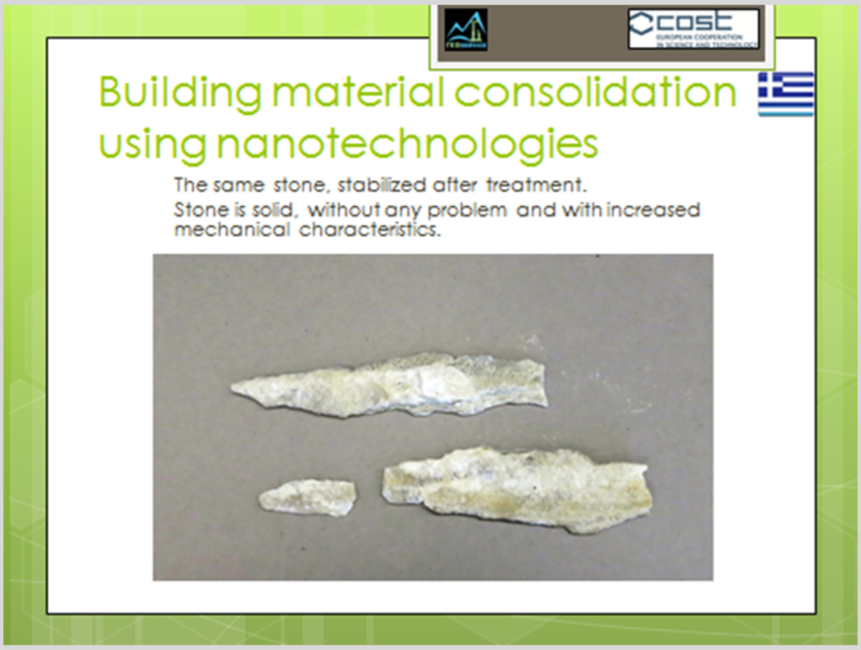
Building material consolidation using nanotechnologies
The same stone, stabilized after treatment.
Stone is solid, without any problem and with increased mechanical characteristics.

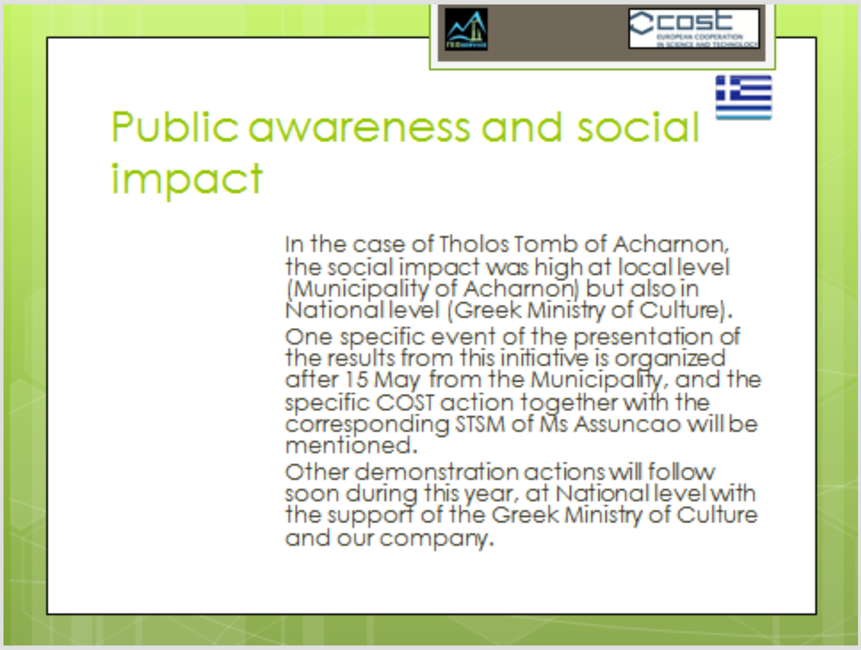
Public awareness and social impact
In the case of Tholos Tomb of Acharnon, the social impact was high at local level (Municipality of Acharnon) but also in National level (Greek Ministry of Culture).
One specific event of the presentation of the results from this initiative is organized after 15 May from the Municipality, and the specific COST action together with the corresponding STSM of Ms Assuncao will be mentioned.
Other demonstration actions will follow soon during this year, at National level with the support of the Greek Ministry of Culture and our company.

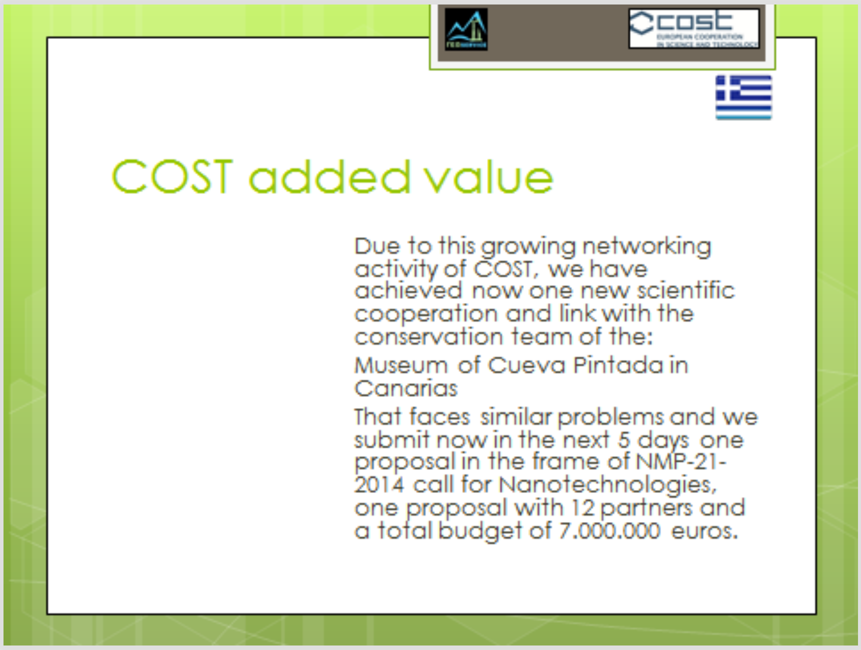
COST added value
Due to this growing networking activity of COST, we have achieved now one new scientific cooperation and link with the conservation team of the:
Museum of Cueva Pintada in Canarias
That faces similar problems and we submit now in the next 5 days one proposal in the frame of NMP-21-2014 call for Nanotechnologies, one proposal with 12 partners and a total budget of 7.000.000 euros.

Progress Report of Project 4.5

"Development of other advanced electric and electromagnetic methods for the characterization of construction materials"

Marc Van Meirvenne (BE) - *marc.vanmeirvenne@ugent.be*

Participants (18 → 37)
At Rome meeting (July 2013): appointment of leader; no report.
No report at Nantes meeting.

Actions:
1. Establishment of participant list
2. Questionnaire prior to EGU2014

1. Which, other than GPR, electric and electromagnetic methods do you use for the characterization of construction materials (including soil)?

- EMI: EM31, EM34, EM38, EM61, Dualem1, Dualem12, Dualem421
- ERT: electrical resistivity tomography, sounding and profiling, CVES/IP (Circular Vertical Electrical Sounding/Induced Polarization with multi electrode arrays)
- Transient EM (helicopter)
- MRS (Magnetic Resonance Sounding: hydraulic permeability and porosity)
- Borehole logging : electrical-, EM-, radioactive-probes, CS616, CS650, HydraProbe
- TDR (time domain reflectometry)

Other non-E or -EM methods mentioned:
- Magnetometry
- Seismic (refraction seismic, surface wave seismic and high resolution, reflection seismic)
- seismic, video and acoustic probes

Other E or EM methods not mentioned:
- gamma ray
- vis-NIR spectrometry

2. For which purpose do you use these methods ?

- Soil characterization over large scales (agriculture, environmental management..)
- Soil Volumetric Water Content, hydraulic conductivity
- Porosity, compaction
- Frost, snow
- Soil deformation
- For ground investigation for infrastructure work. It can be early in the site investigation to map at a larger geological scale or in the detailed geotechnical investigation to map with high resolution or to solve specific geotechnical problems.
- To map aquifers or aquifer protection
- Utility and UXO (on-shore and off-shore)
- Archaeological prospection
- Waste detection and characterization (Landfill Mining)

3. Do you combine or integrate the results of these methods with GPR measurements, or do you use each method independently? Please explain further.

- EMI data and GPR data are jointly interpreted whenever possible, but not quantitatively merged.
- ERT is used to calibrate the EMI data and to obtain quantitative EMI data at large scales and to invert for layered subsurface conductivities.
- We combine the data when possible, e.g. electrical conductivity results of surface GPR full-waveform inversion are successfully combined with EMI and ERT.
- We use TDR measurements to validate GPR measurements.
- Normally we do independent geophysical interpretation first, followed by integrated geological interpretation. If we have boreholes we use these in the integrated interpretation.
- EM31 -38 are used mainly in soil studies to get the EC profile of soil.

4. If you do not use any other method besides GPR, do you intent to expand your actions into another E or EM method in the near future (i.e. within the time window of the COST action) ? If so, which method do you intend to acquire ?

No reactions.

5. Any other information you want to provide in the frame of this project (like why you joined this project)?

- "For characterizing soil, or identifying subsurface features, GPR alone is not sufficient at all. Other sensors need to be taken in account, but merging these datasets is a big challenge."
- "Recent improvements of EMI equipment and the development of quantitative multi-layer inversion software enables the lateral and vertical characterization of the subsurface over large scales. Until now most of these developments are used for soil characterization, I see huge opportunities of this method in the civil-engineering area."
- "We joined this project to gain knowledge on GPR, especially on 3D-radar systems that we recently started to use. We also want to share the experience we have with our integrated use of many methods. Based on our marine work we also use advanced solutions for positioning, navigation and not least for efficient reporting and here we also feel that we can share some experience."
- "I know that GPR is good method to find out moisture changes in media, but it is poor to classify changes in conductivity. There are better methods for conductivity classification. I know the probes for monitoring purposes and some EM methods, but I am sure there are new better ways as well. "

Conclusion of questionnaire

- Several E- and EM-methods are used besides GPR, mainly EMI and ERT.
- Wide range of applications: from soil and infrastructure characterization to utility and UXO detection).
- GPR and the other methods are mostly integrated or combined in some way, but full quantitative fusion remains a challenge.
- Members expect two-way interactions: share expertise and learn about new approaches.

Plans for the future

- Relaunch questionnaire with more directed questions to P4.5.
- List more extensively available methods, application fields, expectations and expertises.
- Disseminate results among all COST TU1208 to facilitate interactions and collaborations.

Acknowledgement - The author acknowledges the COST Action TU1208 "Civil Engineering Applications of GPR", supporting this work.

"COMBINING GROUND PENETRATING RADAR AND ELECTROMAGNETIC INDUCTION FOR INDUSTRIAL SITE CHARACTERIZATION"
(CONTRIBUTION TO PROJECT 4.5)

Marc Van Meirvenne (BE), Ellen Van De Vijver(BE), Timothy Saey (BE), Philippe De Smedt (BE), Samuël Delefortrie (BE), Piet Seuntjens (BE)
marc.vanmeirvenne@ugent.be

The abstract is published in *Geophysical Research Abstracts*, Vol. 16, EGU2014-1886, 2014 and is available on *www.egu2014.eu*

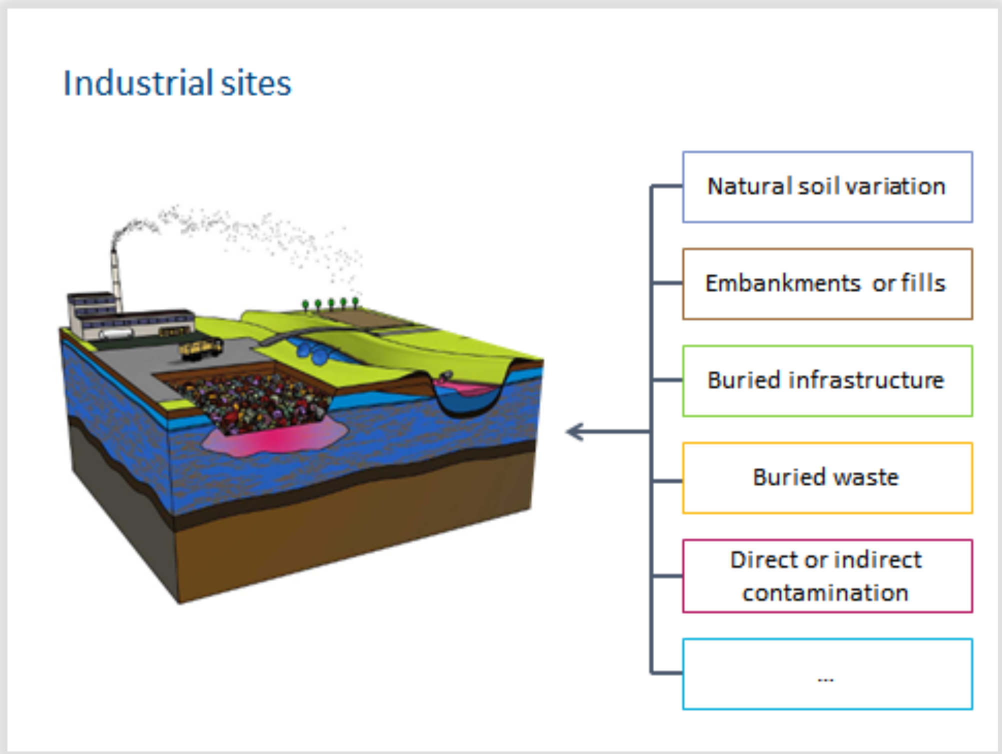

A multi-sensor approach is adopted: Electromagnetic induction & GPR

Electromagnetic induction (EMI)

- DUALEM-21S

4 transmitter-receiver coil pairs ➔ 4 depths of exploration

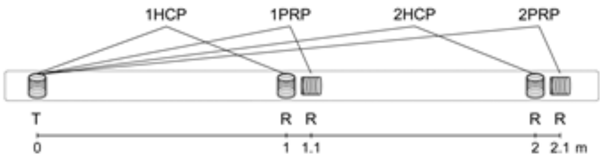

- Mobile set-up:

Ground penetrating radar (GPR)

- 3d-Radar
  - stepped-frequency continuous wave (100 MHz – 3 GHz)
  - 13 transmitter-receiver antenna pairs

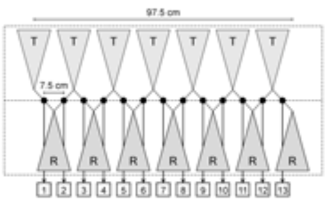

- Mobile set-up:

Case study: a former manufactured gas plant

- Belgian coastal plain
- Prior-info through environmental assessments

Study area: former phosphate production unit

- now: lawn
- 3400 m²

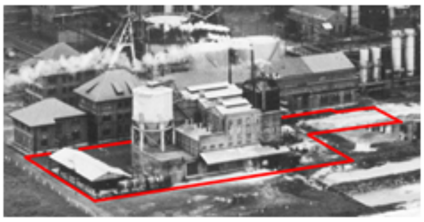

1959

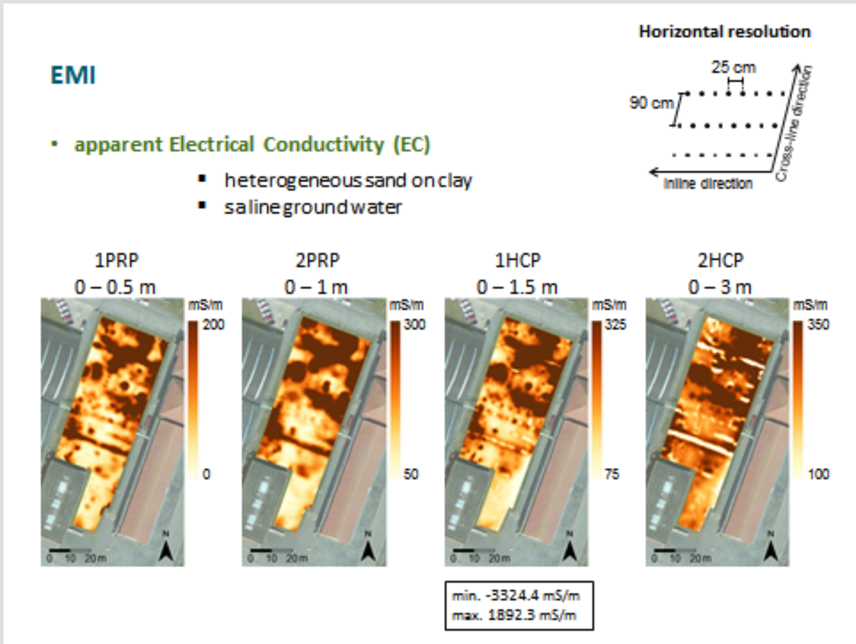
EMI
Horizontal resolution
25 cm
90 cm
inline direction
Cross-line direction
• apparent Electrical Conductivity (EC)
▪ heterogeneous sand on clay
▪ saline groundwater
1PRP
0 – 0.5 m
mS/m
200
0
2PRP
0 – 1 m
mS/m
300
50
1HCP
0 – 1.5 m
mS/m
325
75
2HCP
0 – 3 m
mS/m
350
100
min. -3324.4 mS/m
max. 1892.3 mS/m

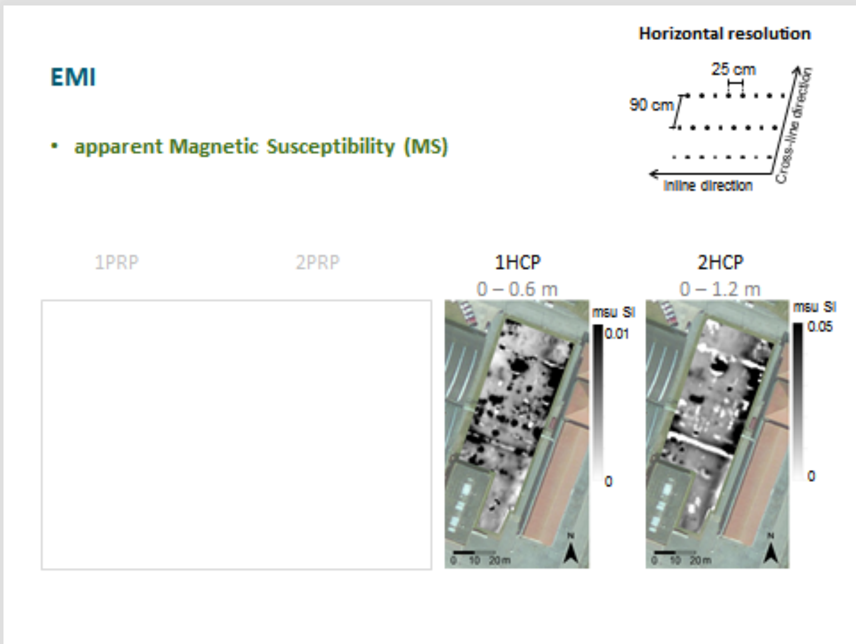
EMI
Horizontal resolution
25 cm
90 cm
inline direction
Cross-line direction
• apparent Magnetic Susceptibility (MS)
1PRP
2PRP
1HCP
0 – 0.6 m
msu SI
0.01
0
2HCP
0 – 1.2 m
msu SI
0.05
0

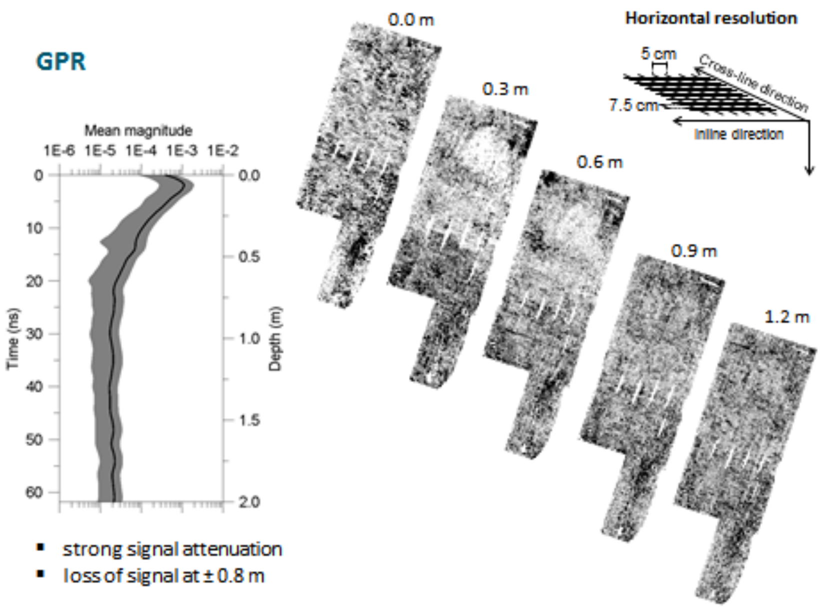

- strong signal attenuation
- loss of signal at ± 0.8 m

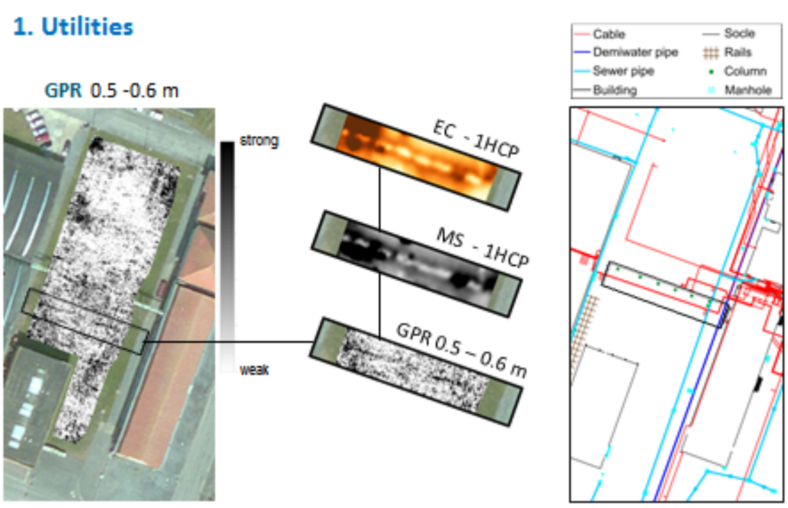

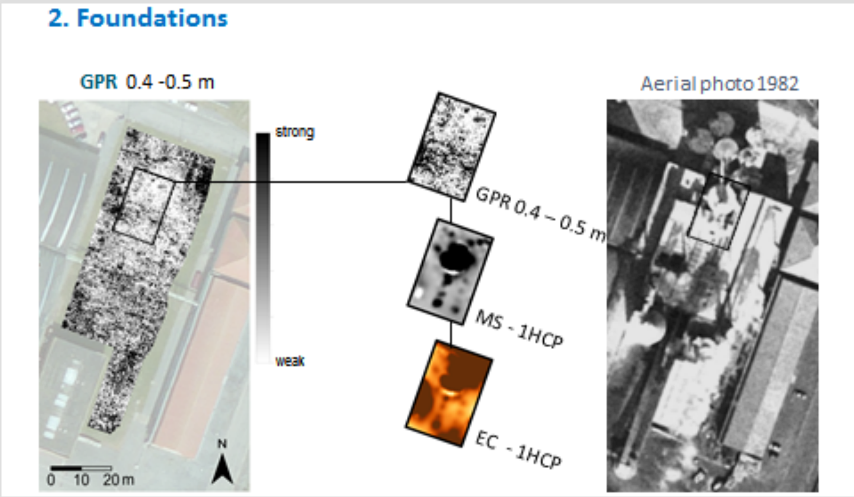

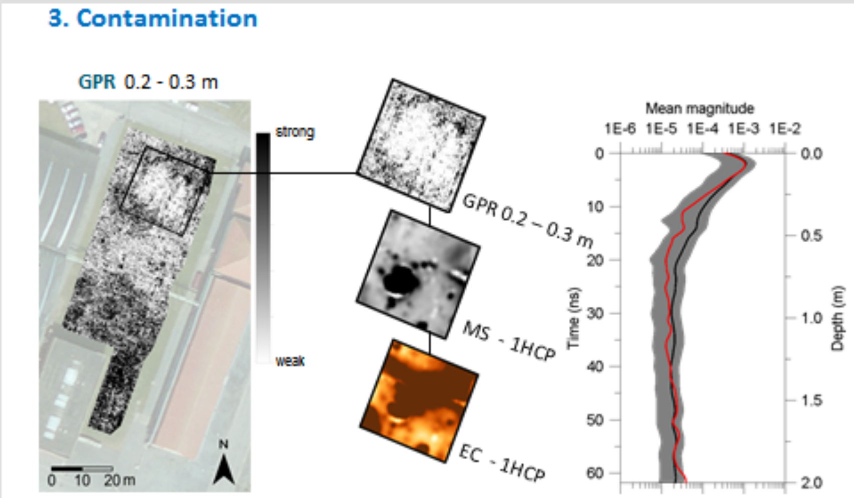

CONCLUSIONS

Both EMI and GPR allow to produce detailled subsurface images. Their combination gives a good representation of the general organisation of the soil and allows the detection, identification and localisation of different types of subsurface features. Although ground truthing remains required for anambiguous interpretation, EMI + GPR represent a powerful combination for industrial site characterisation.

"Submerged Prehistoric Archaeology and Landscapes of the Continental Shelf – Perspective for the TU1208 COST Action"

Dragos Ene (RO) - *dragos@inoe.inoe.ro*

Overview

Cost Action SPLASHCOS - Submerged Prehistoric Archaeology and Landscapes of the Continental Shelf begun in 2009, with the aim to reunite specialists from different domains (marine scientists, geologists, archaeologists, engineers aso) and different types of organization in the field of marine sciences, with interest in the drowned prehistoric landscapes of the European continental shelf, and to disseminate that knowledge to a wider audience. During the Ice Ages, the sea level oscillated around of 50 meters below present level.

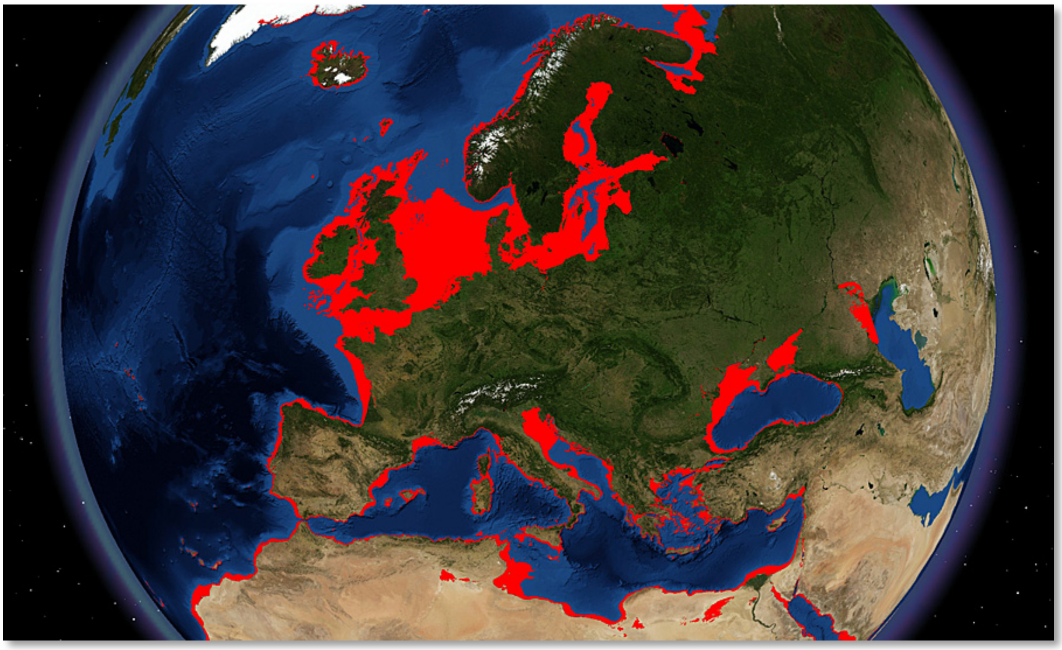

European continental shelf with maximum extent in red of exposed land 20,000 years ago

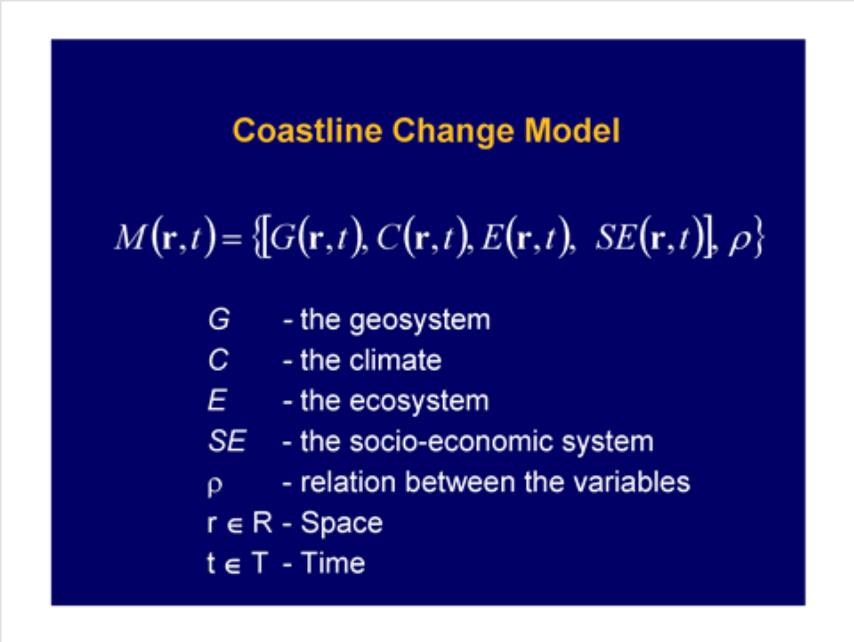
Coastline Change Model
$M(\mathbf{r},t) = \{[G(\mathbf{r},t), C(\mathbf{r},t), E(\mathbf{r},t), SE(\mathbf{r},t)], \rho\}$
G - the geosystem
C - the climate
E - the ecosystem
SE - the socio-economic system
ρ - relation between the variables
r ∈ R - Space
t ∈ T - Time

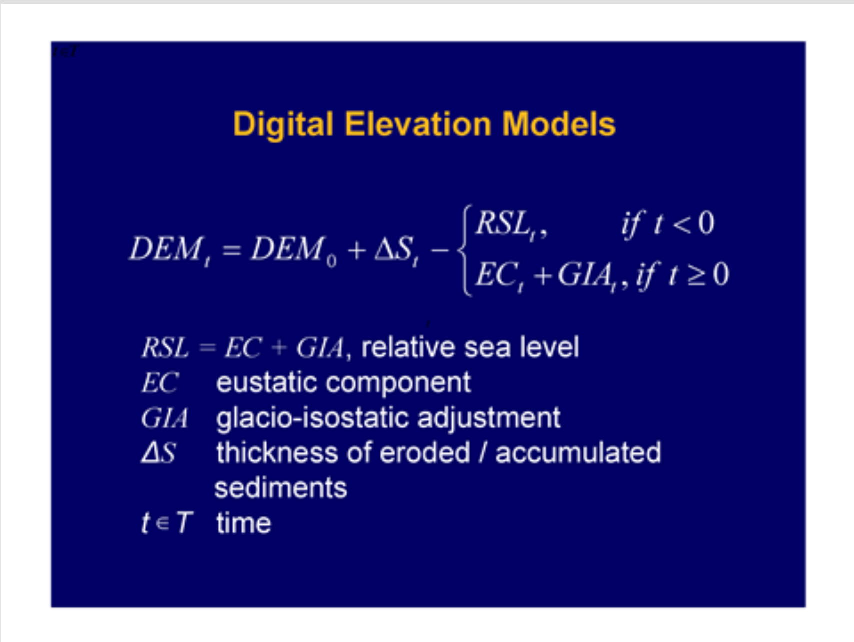
Digital Elevation Models
$DEM_t = DEM_0 + \Delta S_t - \begin{cases} RSL_t, & if\ t < 0 \\ EC_t + GIA_t, & if\ t \geq 0 \end{cases}$
$RSL = EC + GIA$, relative sea level
EC eustatic component
GIA glacio-isostatic adjustment
ΔS thickness of eroded / accumulated sediments
$t \in T$ time

Methods for location & detailed investigation of submerged sites and relevant environments		Type of data	Sub-divisions
Remote sensing			
	Acoustic	Bathymetric - maps of bottom 'topography'	Sidescanners
			Multibeams
		Subbottom - one or two sensor based 2D or 3D representations of the bottom stratigraphy	Conventional echo-sounders
			Chirp
			Parametric
			Boomer
			Sparker
			3D systems
	Photographic	Surface of bottom - photographic documentation of the exposed surface	Camera - remotely operated
			Videocamera - remotely operated
	Electric, electromagnetic & magnetic	Subbottom - representations of the bottom stratigraphy or of features embedded in the bottom	Ground penetrating Radar (GPR)
			Resistivity
			Magnetic Gradiometry
Direct sampling/ investigation			
	Coring from surface	Geological/archaeological/ environmental	Different types of coring devices
	Diving	Geological/archaeological/ environmental	Survey by divers
			Excavation by divers
			Coring by divers
Platforms for investigation		Wide spectre - depends on techniques employed	Submersibles
			ROVs
			AUVs

Principal Objectives of the COST Action SPLASHCOS

Not Research as such, but: collection of information, development of contacts/ collaborations, sharing of ideas, formulation of research programmes (to be funded elsewhere).

The main focus was on archaeology – how to find it, and how to preserve & manage it. This includes geology, oceanography, environment – the cultural landscape. But excludes shipwrecks and historical data (except for methodological overlap).

RESEARCH TASKS

1. Audit current state of knowledge on known Stone Age (pre-6000) underwater sites
2. Factors affecting survival and visibility of sites and terrestrial features
3. Environment & topography of submerged terrestrial landscape
4. Centres of expertise, laboratories etc.
5. Collaboration with industry and commerce
6. Communication and outreach
7. Impact on understanding of European & World Prehistory

WORKING GROUPS

4 WGs. Up to 2 (MC) + 8 participants from each country at 2 per WG (preferably not more than 6 in total)!

WG1. Archaeological Data and Interpretation (RTs 1, 2 & 7)

WG2. Environmental Data and Interpretation (RT 3)

WG3. Technology, techniques, training (RT 4)

WG4. Commercial collaboration, outreach (RTs 5 & 6)

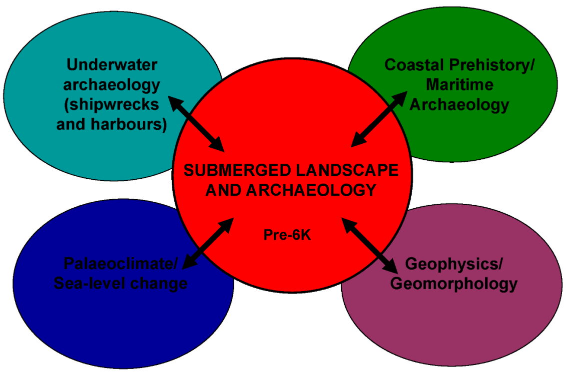

QUESTIONS

What do we currently know? What would we like to know? – WG1 and WG2

How do we recover new information from the seabed? – Technical issues, equipment, resources, training – WG3

Collaboration with industry and commerce - WG4

How do we communicate the importance of all of this to a wider constituency? - WG4

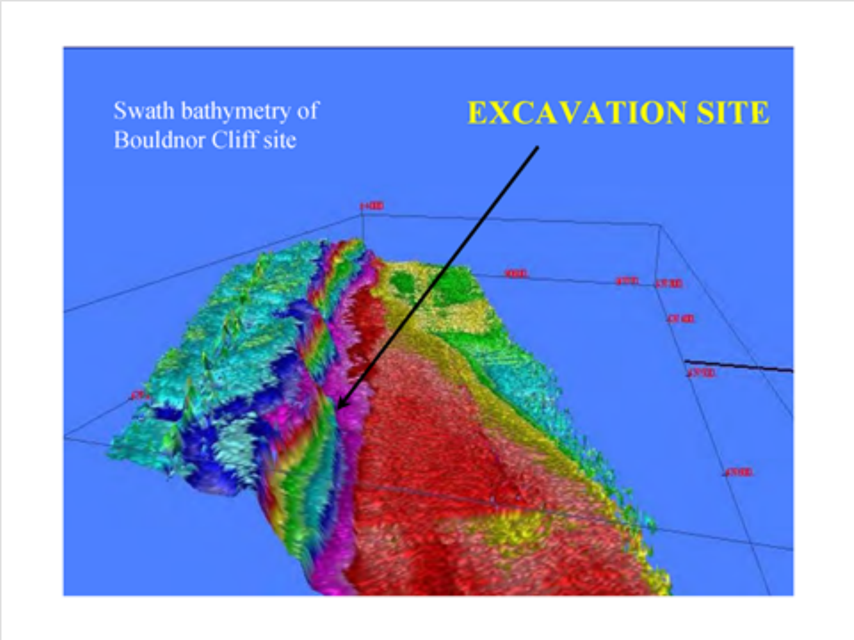
Swath bathymetry of
Bouldnor Cliff site
EXCAVATION SITE

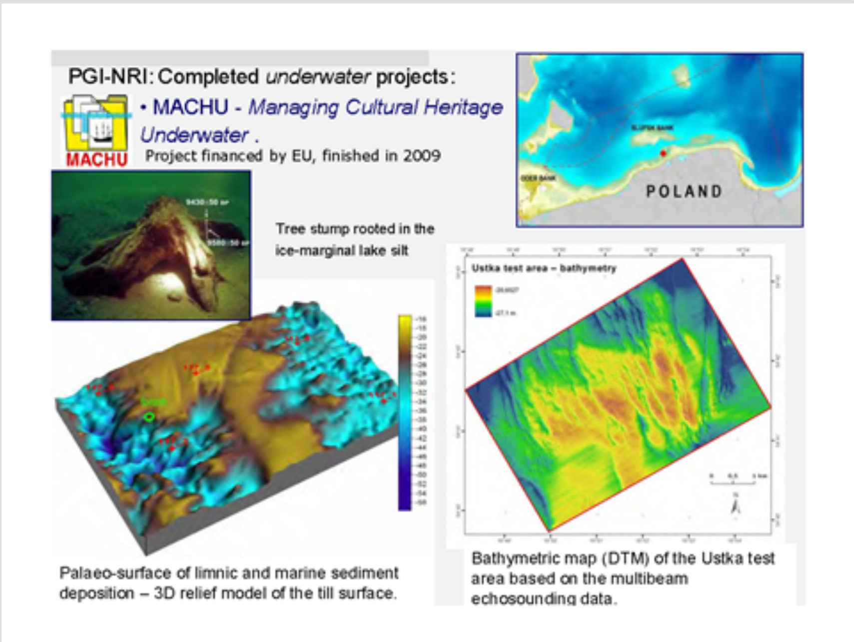
PGI-NRI: Completed underwater projects:
• MACHU - Managing Cultural Heritage Underwater .
MACHU
Project financed by EU, finished in 2009
POLAND
Tree stump rooted in the ice-marginal lake silt
Ustka test area – bathymetry
Palaeo-surface of limnic and marine sediment deposition – 3D relief model of the till surface.
Bathymetric map (DTM) of the Ustka test area based on the multibeam echosounding data.

"A MULTIDISCIPLINARY APPROACH TO INVESTIGATE ROCK SPREADING, ROCK SLIDING AND CULTURAL HERITAGE SITES ON THE MALTESE ARCHIPELAGO"

Sebastiano D'Amico (IT)
sebdamico@gmail.com

ABSTRACT

Landslides are widespread along the north-western coast of the Island of Malta and are strictly linked to the structural setting. Lateral spreading phenomena and rockfalls are due to Limestones overlying a clayey formation, representing the shallower lithotypes that characterize the superficial layer. In this study we propose a a multidisciplinary and multitechnical approach in order to investigate the kinematics and the evolution of these types of coastal landslides.

1. INTRODUCTION

The Maltese Archipelago is situated in the Mediterranean Sea, about 290 km northeast of Tunisia and 90 km south of Sicily. It consists of three major islands: Malta, Gozo, and Comino, which lies in the Comino Straits separating the two largest islands. The Maltese economy is mainly based on the tourism industry with a high degree of coastal urban settlements. In order to better preserve the historical heritage, landscapes, and coastal areas and to promote tourism activities, it has been proposed that the archipelago might be considered as an open air laboratory. In this context multidisciplinary studies integrating geology, engineering, geomorphology as well as history and archeology may be undertaken in order to develop and test methodologies for the assessment of the relationship between the physical environment and cultural heritage sites. In this study we propose a a multidisciplinary and multitechnical approach in order to investigate the kinematics and the evolution of coastal landslides and the conservation of historical sites.

2. METHOD

In Fig. 1 is reported an example of typical situation of lateral spreading and rock fall on the Maltese archipelago. In order to investigate the mass movement and the influence of the fractures in the Upper Coralline

Limestone (UCL) formation we recorded ambient noise time series at several locations using a portable 3-component seismograph. The time series are processed to give both horizontal-to-vertical spectral ratio graphs (H/V) as well as frequency-dependent polarisation analysis.

.

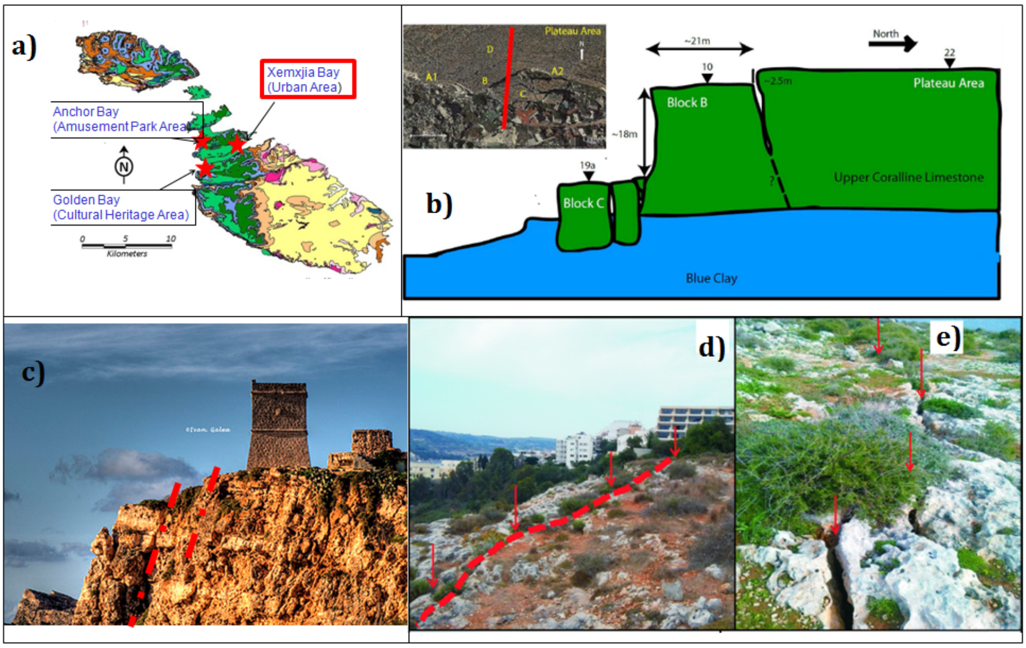

FIG. 1– *a) Location of the test sites in the Maltese Archipelago (colours represent the surface geology) b) cartoon sketch of cross section across the edge of the cliff, illustrating vertical displacements of Blocks B and C, and approximate positions of measurement sites 22, 10 and 19. The approximate transect is shown on the inset map. This is a typical situation of lateral spreading and rock fall on the Maltese archipelago. c) d) e). Fractures at the selected sites. It is evident that the fractures are effecting historical sites as well as modern urban areas.*

The H/V graphs illustrate and quantify aspects of site resonance effects due both to underlying geology as well as to mechanical resonance of partly or wholly detached blocks [1]. The polarization diagrams indicate predominant directions of vibrational effects. Results from this study show an unambiguous distinction between the behaviour of the inland plateau areas, away from the cliff edges, the region of the unstable cliff

edge and the actual rockfall areas. However, it has not be possible to evaluate the extension of the fractures and the depth they reach. This is the reason why we propose the use of other engineering techniques such as Ground Penetrating radar which can help to identify buried structures as well as have a measurements of the extention of potentially hazardous fractures presents in area of high density buildings and/or historical monuments.

3. Conclusion

Ambient vibration time series have been shown to contain information that is relevant to the behaviour of coastal features at different stages of destabilisation. Using polarisation analysis, it has been possible to distinguish unambiguously between H/V peaks that arise from resonances in the shallow crustal layering, including low-velocity layers in this particular case, and peaks that arise from whole-block mechanical vibrational modes. Where blocks are only partly detached from the mainland, and are limited in their degrees of freedom, the dominant direction of polarization is generally normal to the cliff edge, or to the large scale fractures. Where blocks are fully detached, the polarization directions appear to indicate the existence of more degrees of freedom. Finally we propose that the orientation, persistency and width of the discontinuity sets of calcareous rock masses can be reconstructed by means of a Ground Penetrating Radar (GPR) campaign.

Acknowledgement

The authors acknowledge the COST Action TU1208 "Civil Engineering Applications of Ground Penetrating Radar", supporting this work.

References

[1] F. Panzera, S. D'Amico, A. Lotteri, P. Galea, G. Lombardo, "Seismic site response of unstable steep slope using noise measurements: the case study of Xemxija Bay area, Malta," *Nat. Hazards Earth Syst. Sci.*, vol. 12, pp. 3421–3431, 2012.

A Test Study to Display Buried Anti-Tank Landmines with GPR and Research Soil Characteristics with CRS

Selma Kadioglu (TR), Yusuf Kagan Kadioglu (TR)
kadioglu@eng.ankara.edu.tr

The abstract is published in *Geophysical Research Abstracts*, Vol. 16, EGU2014-10131, 2014 and is available on *www.egu2014.eu*

Electrical Resistivity Tomography and Ground Penetrating Radar for locating buried petrified wood sites: a case study in the natural monument of the Petrified Forest of Evros, Greece

Nectaria Diamanti (GR), George Vargemezis (GR),
Panagiotis Tsourlos (GR), Ilias Fikos (GR)
ndiamant@geo.auth.gr

The abstract is published in *Geophysical Research Abstracts*, Vol. 16, EGU2014-14298, 2014 and is available on *www.egu2014.eu*

These contributions were presented as posters.

TABLE OF CONTENTS

COST - European Cooperation in Science and Technology is an intergovernmental framework aimed at facilitating the collaboration and networking of scientists and researchers at European level. It was established in 1971 by 19 member countries and currently includes 35 member countries across Europe, and Israel as a cooperating state.

COST funds pan-European, bottom-up networks of scientists and researchers across all science and technology fields. These networks, called 'COST Actions', promote international coordination of nationally-funded research. By fostering the networking of researchers at an international level, COST enables break-through scientific developments leading to new concepts and products, thereby contributing to strengthening Europe's research and innovation capacities.

COST's mission focuses in particular on: building capacity by connecting high quality scientific communities throughout Europe and worldwide; providing networking opportunities for early career investigators; increasing the impact of research on policy makers, regulatory bodies and national decision makers as well as the private sector.

Through its inclusiveness, COST supports the integration of research communities, leverages national research investments and addresses issues of global relevance. Every year thousands of European scientists benefit from being involved in COST Actions, allowing the pooling of national research funding to achieve common goals.

As a precursor of advanced multidisciplinary research, COST anticipates and complements the activities of EU Framework Programmes, constituting a "bridge" towards the scientific communities of emerging countries. In particular, COST Actions are also open to participation by non-European scientists coming from neighbour countries (for example Albania, Algeria, Armenia, Azerbaijan, Belarus, Egypt, Georgia, Jordan, Lebanon, Libya, Moldova, Montenegro, Morocco, the Palestinian Authority, Russia, Syria, Tunisia and Ukraine) and from a number of international partner countries.

COST's budget for networking activities has traditionally been provided by successive EU RTD Framework Programmes. COST is currently executed by the European Science Foundation (ESF) through the COST Office on a mandate by the European Commission, and the framework is governed by a Committee of Senior Officials (CSO) representing all its 35 member countries.

More information about COST is available at www.cost.eu.

The scientific activities of the COST Action TU1208 are carried out within four Working Groups (WGs). The effectiveness of this scheme will be checked after the first year of activities and will eventually be modified, considering the actual number of active participants in each WG. The structure of each WG will always be kept as flexible as possible, in order to enable new participants to join. All the participants, when joining the Action, are invited to provide basic information on their experience, interests, and current research projects, as well as WGs and Projects preferences. Each participant can belong to two WGs and an arbitrary number of projects within the chosen WGs.

The four TU1208 WGs are: WG1 – Novel GPR instrumentation; WG2 – GPR surveying of pavements, bridges, tunnels and buildings; underground utility and void sensing; WG3 – EM methods for near-field scattering problems by buried structures and data processing techniques; WG4 – Different applications of GPR and other NDT technologies in civil engineering. The WG meetings constitute an opportunity to present activities, results and plans for the future. Between meetings, the WG members regularly interact.

COST ACTION TU1208

CIVIL ENGINEERING APPLICATIONS OF GROUND PENETRATING RADAR

2014 Second Action's General Meeting - Proceedings

Vienna, Austria, April 30 – May 2, 2014

The COST Action TU1208 focuses on the exchange of scientific-technical knowledge and experience of Ground Penetrating Radar (GPR) techniques in Civil Engineering (CE). The project is being developed within the frame of a unique approach based on the integrated contribution of University researchers, software developers, geophysics experts, Non-Destructive Testing equipment designers and producers, end users from private companies and public agencies. In this interdisciplinary Action, advantages and limitations of GPR will be highlighted leading to the identification of gaps in knowledge and technology. Protocols and guidelines for EU Standards will be developed, for effective application of GPR in CE. A novel GPR will be designed and realized: a multi-static system, with dedicated software and calibration procedures, able to construct real-time lane 3D high resolution images of investigated areas. Advanced electromagnetic-scattering and data-processing techniques will be developed. The understanding of relationships between geophysical parameters and CE needs will be improved. Freeware software will be released, for inspection and monitoring of structures and infrastructures, buried-object localization, shape reconstruction and estimation of useful parameters. A high level training program will be organized. Mobility of early career researchers will be encouraged. The project has already received the interest of key end users and excellent EU Institutions.

www.GPRadar.eu
www.cost.eu/domains_actions/tud/Actions/TU1208

This publication is supported by COST